

**Diverse Mechanistic Approaches to [4 + 2] and [2 + 2] Cycloadditions by
Transition Metal Photosensitization**

By

Anna Elise Hurtley

A dissertation submitted in partial fulfillment
of the requirements for the degree of

Doctor of Philosophy

(Chemistry)

at the

UNIVERSITY OF WISCONSIN–MADISON

2014

Date of final oral examination: 06/26/2014

The dissertation is approved by the following members of the Final Oral Committee:

Tehshik P. Yoon, Professor, Chemistry

Steven D. Burke, Professor, Chemistry

Clark R. Landis, Professor, Chemistry

Jennifer M. Schomaker, Assistant Professor, Chemistry

Eric R. Strieter, Assistant Professor, Chemistry

Diverse Mechanistic Approaches to [4 + 2] and [2 + 2] Cycloadditions by Transition Metal Photosensitization

By

Anna Elise Hurlley

Under the supervision of Professor Tehshik P. Yoon
at the University of Wisconsin–Madison

Abstract

Organic photochemistry enables the rapid synthesis of complex structures that are often difficult to access by other reaction types. The work described herein has capitalized on three mechanistically distinct modes of photoactivation for the synthesis of a variety of heterocyclic and carbocyclic scaffolds. Chapter 2 describes the development of a hetero-Diels–Alder cycloaddition of bis(enone) substrates that operates under visible light photoredox catalysis. Single-electron reduction inverts the polarity of one of the enone coupling partners to facilitate the electronically mismatched cycloaddition. In all cases, the reaction generates a single constitutional isomer with high diastereoselectivity. Chapter 3 describes the development of a visible light promoted [2+2] cycloaddition of conjugated 1,3-dienes that operates by energy transfer sensitization. The scope of the reaction is broad and complementary to the radical ion cycloadditions previously developed in our group. The synthetic utility of this method was illustrated in a concise synthesis of the cyclobutane-containing natural product epiraihovenal. Chapter 4 describes preliminary efforts towards the development of an enantioselective copper-catalyzed [2+2] cycloaddition. Our strategy involves the use of chiral, non-coordinating

counterions to mimic the electronic and photophysical properties of the highly cationic copper catalysts typically employed in the racemic reaction. Although the levels of enantioselectivity achieved to date are modest, these proof-of-concept results represent the first catalytic, asymmetric approach to this class of reactions.

Acknowledgements

I thank my advisor Professor Tehshik Yoon for all of his guidance throughout the course of my graduate studies. I have been greatly inspired by his limitless creativity, passionate commitment to education, and unwavering generosity in always setting aside what he is working on to talk about science and research goals.

I thank the members of my thesis committee, Professors Steven Burke, Clark Landis, Jennifer Schomaker, and Eric Strieter for their many insights and contributions to my development as a scientist over the years. I thank Drs. Charlie Fry, Monika Ivancic, Bob Shanks, Martha Vestling, and Ilia Guzei for maintaining exquisite instrument facilities, which have contributed immensely to my research studies. I also thank all of the faculty and staff in the chemistry department for creating an academically rigorous yet truly collegial environment.

Finally, I would especially like to express my gratitude to all of the amazing colleagues I have had the opportunity to work with in the Yoon group. I deeply appreciate your warm support, sense of humor, and dedication to science. I have been profoundly influenced by each of you over the years and would be delighted to cross paths again as we move forward in our careers.

Anna E. Hurtley
June 18, 2014

Table of Contents

Abstract	i
Acknowledgements	iii
Table of Contents	iv
List of Schemes	viii
List of Figures	xi
List of Tables/Charts	xii
Chapter 1. <i>Lewis Acid Catalysis in Organic Photochemistry</i>	1
1.1 Introduction	2
1.2 Use of Lewis acids to manipulate the redox potentials of organic substrates in photoinduced electron-transfer reactions	3
1.3 Use of Lewis acids to manipulate the absorption properties and photochemical reactivity of organic chromophores	8
1.4 Lewis acidic metal centers as catalysts for photoinduced organometallic processes	15
1.4.1 Photoinduced copper-catalyzed [2 + 2] cycloaddition reactions	15
1.4.2 Photoinduced copper-catalyzed cross-coupling reactions	21
1.5 Conclusions and Outlook	26
1.6 References	26
Chapter 2. <i>Visible Light Photocatalysis of Radical Anion Hetero-Diels–Alder Cycloadditions</i>	31
2.1 Introduction	32
2.2 Results and Discussion	33
2.3 Conclusions	39
2.4 Contributions	39

2.5 Experimental	40
2.5.1 General experimental information	40
2.5.2 Preparation of bis(enone) substrates	40
2.5.3 Experimental details for the hetero Diels–Alder cyclization of bis(enone) substrates	48
2.5.4 Experimental details for the functionalization of cycloadduct 3.4	56
2.5.5 Stereochemical determinations	59
2.6 References	59
Chapter 3. [2+2] Cycloaddition of 1,3-Dienes by Visible Light Photocatalysis	62
3.1 Introduction	63
3.2 Results and Discussion	64
3.3 Conclusions	72
3.4 Experimental	72
3.4.1 General experimental information	72
3.4.2 Synthesis of cycloaddition substrates	73
3.4.3 [2+2] Photocycloadditions	93
3.4.4 Verification of the relative stereochemistry of cycloadducts 3.9 and 3.14	110
3.4.5 Verification of the relative stereochemistry of cycloadduct 3.21 : comparison of iridium and ruthenium-catalyzed experiments	112
3.4.6 Synthetic elaboration of vinylcyclobutane products	113
3.4.7 Synthesis of epiraikovenal	117
3.4.8 Representative NOE data	120
3.5 References	120

Chapter 4. <i>Enantioselective Copper-Catalyzed [2+2] Photocycloaddition Reactions</i>	124
4.1 Introduction	125
4.2 Results and Discussion	127
4.3 Outlook and Future Directions	132
4.4 Contributions	134
4.5 Experimental	134
4.5.1 General experimental information	134
4.5.2 General procedure for the asymmetric [2+2] photocycloaddition	134
4.5.3 Synthesis of chiral acids	135
4.6 References	140
Appendix A. <i>Intermolecular [2+2] Cycloaddition Reactions of Styrenes and 1,3-Dienes by Visible Light Photocatalysis</i>	142
A.1 Introduction	143
A.2 Results and Discussion	144
A.3 Outlook and Future Directions	147
A.4 Experimental	149
A.4.1 General experimental information	149
A.4.2 [2+2] Photocycloadditions	150
A.4.3 Representative NOE data	154
A.5 References	154
Appendix B. ^1H and ^{13}C NMR spectra for new compounds	155
List of compounds from Chapter 2	156
List of compounds from Chapter 3	181

List of compounds from Chapter 4	241
List of compounds from Appendix A	245
Appendix C. X-Ray crystallographic data	251
Compound 2.14	253
Compound C.1	264

List of Schemes**Chapter 1**

Scheme 1-1.	Visible light photoredox catalysis of [2+2] enone cycloadditions	4
Scheme 1-2.	Expanding the synthetic utility of [2+2] enone cycloadditions	5
Scheme 1-3.	Inherent challenges associated with enantioselective photochemical reactions	6
Scheme 1-4.	Complementary selectivity in asymmetric [2+2] photocycloaddition reactions	6
Scheme 1-5.	Diverse reactivity of photochemically generated radical anion intermediates	7
Scheme 1-6.	Effect of Lewis acids on the photostationary state of conjugated alkenes	9
Scheme 1-7.	Lewis acid catalysis of photochemical [2+2] coumarin dimerizations	10
Scheme 1-8.	Lewis acid catalysis of crossed [2+2] photocycloaddition reactions of coumarin	10
Scheme 1-9.	Chiral Lewis acid-catalyzed enantioselective [2+2] photocycloaddition of coumarins	11
Scheme 1-10.	Chiral Lewis acid-catalyzed enantioselective [2+2] photocycloaddition of 5,6-dihydro-4-pyridones	13
Scheme 1-11.	Synthetic applications of [2+2] cycloadduct products	14
Scheme 1-12.	Charge transfer mechanisms in copper-catalyzed [2+2] cycloadditions	16
Scheme 1-13.	Tridentate coordination in diene-copper complexes	16
Scheme 1-14.	Copper-catalyzed [2+2] cycloadditions in the preparation of diverse carbocycles	17
Scheme 1-15.	Copper-catalyzed [2+2] cycloadditions in the preparation of diverse heterocycles	18
Scheme 1-16.	Chiral auxiliary approach to enantioselective [2+2] cycloadditions	18

Scheme 1-17. Copper-catalyzed [2+2] cycloaddition of carbohydrate-embedded scaffolds	19
Scheme 1-18. Oxidative desymmetrization of [2+2] cycloadducts	19
Scheme 1-19. Synthesis of α - and β -panasinsene	20
Scheme 1-20. Synthesis of (\pm)-kelsoene	20
Scheme 1-21. Synthesis of (–)-grandisol	21
Scheme 1-22. Radical mechanisms in photochemical Ullmann C-N coupling reactions	22
Scheme 1-23. Evidence for radical intermediates in photoinduced Ullmann C-N coupling reactions	23
Scheme 1-24. Catalytic variant of the photoinduced Ullmann C-N coupling reaction	23
Scheme 1-25. Expanding the synthetic utility of photoinduced, copper-catalyzed C-N cross-coupling reactions	24
Scheme 1-26. Proposed mechanism for photoinduced, copper-catalyzed C-N cross-coupling reactions	25
Scheme 1-27. Viability of oxygen and sulfur nucleophiles in photoinduced copper-catalyzed cross-coupling reactions	25
Chapter 2	
Scheme 2-1. Photocatalytic [2+2] and [4+2] cycloadditions	33
Scheme 2-2. Proposed mechanism for regioselective hetero-Diels–Alder cycloaddition of unsymmetrical bis(enone) 2.19	37
Scheme 2-3. Diastereoselective functionalization of 2.4	38
Chapter 3	
Scheme 3-1. [2+2] Cycloaddition of higher-order polyenes	68
Scheme 3-2. Limitations in the scope of the visible light promoted [2+2] cycloaddition	69

Scheme 3-3.	Synthetic elaboration of vinylcyclobutane products	71
Scheme 3-4.	Modular synthesis of epiraikovenal	72
Chapter 4		
Scheme 4-1.	Copper(I)-catalyzed alkene photocycloadditions	125
Scheme 4-2.	Inherent limitation of chiral ligand approach	126
Scheme 4-3.	Investigation of privileged chiral phosphoric acids	129
Scheme 4-4.	pKa values of chiral Brønsted acids	130
Scheme 4-5.	Synthesis of novel chiral sulfonic acid frameworks	131
Scheme 4-6.	Survey of chiral acids of varying pKa	132
Appendix A		
Scheme A-1.	Intermolecular [2 + 2] photocycloaddition reactions: reactivity and selectivity issues	143
Scheme A-2.	Homodimerization of indene by visible light photosensitization	144
Scheme A-3.	Homodimerization of 1,3-cyclohexadiene by energy transfer photosensitization	146
Scheme A-4.	Crossed intermolecular [2+2] cycloadditions of 1,3-cyclohexadiene	146
Scheme A-5.	Crossed [2+2] cycloadditions of indene by energy transfer photosensitization: project goals	148

List of Figures**Chapter 1**

- Figure 1-1.** Effect of Lewis acid complexation on coumarin UV/Vis absorption spectra 12
- Figure 1-2.** Extensive bathochromic shift of 5,6-dihydro-4-pyridones upon Lewis acid complexation 13

Chapter 3

- Figure 3-1.** [2+2] Cycloadditions of 1,3-dienes provide access to synthetically versatile vinylcyclobutanes 64

List of Tables/Charts

Chapter 2

Table 2-1.	Optimization of [4+2] cycloaddition of 3.3	34
Table 2-2.	Scope of the photocatalytic [4+2] cycloaddition	36

Chapter 3

Table 3-1.	Control studies for visible light promoted diene-olefin [2+2] cycloadditions	65
Table 3-2.	Investigation of structural diversity in the visible light promoted [2+2] cycloaddition of 1,3-dienes	67

Chapter 4

Table 4-1.	Chiral anion approach to enantioselective copper-catalyzed [2+2] cycloadditions	127
Table 4-2.	Investigation of chiral BINOL-derived phosphoric acids	128
Table 4-3.	Alternative substrate design	129
Chart 4-1.	Future directions: explore new counteranion frameworks	133
Chart 4-2.	Future directions: explore new substrate designs	133

Appendix A

Table A-1.	Crossed intermolecular [2+2] cycloadditions of indene	145
Table A-2.	Crossed [2+2] cycloaddition of indene and methyl acrylate: effect of relative substrate equivalents on selectivity	147
Table A-3.	Crossed [2+2] cycloaddition of indene and methyl acrylate: effect of Lewis and Brønsted acids	149

Chapter 1. Lewis Acid Catalysis in Organic Photochemistry

1.1 Introduction

Lewis acid activation has been widely employed as a strategy to accelerate and control a variety of synthetically valuable reactions.¹ A number of notable features of Lewis acids have contributed to their transformative role in organic synthesis. First and foremost, Lewis acid activation alters the relative electronic properties of the reaction partners to enable transformations that are often otherwise challenging in the absence of an additive. Lewis acid complexation also provides structural pre-organization of the reagents, which often profoundly impacts the regiochemistry and stereochemistry of the ensuing bond-forming steps. Due to the availability of a vast number of Lewis acidic reagents with varying electronic and steric parameters, this mode of activation is highly tunable to the demands of a particular class of substrates or desired transformation. Finally, Lewis acids can be further tailored with a wide variety of chiral ligands to provide entry into highly selective asymmetric methods.

Given the many appealing fundamental features of Lewis acid activation and its documented success in promoting highly selective thermal reactions, it is somewhat surprising that this strategy has historically been largely underexplored in the context of organic photochemistry. In general, few strategies for catalytically influencing the reactivity of photochemical transformations are known, and even fewer still that involve inner sphere coordination of a catalyst and a substrate. As a result, the regiochemistry and stereochemistry of photochemical reactions are generally dictated by the inherent reactivity profiles of the organic substrates, which constitute a significant synthetic limitation. Nonetheless, many photochemical reactions proceed on scaffolds with polarized Lewis basic functional groups that are amenable to Lewis acid coordination, which suggests that these processes have the potential to widely benefit from the many advantages of Lewis acid catalysis.

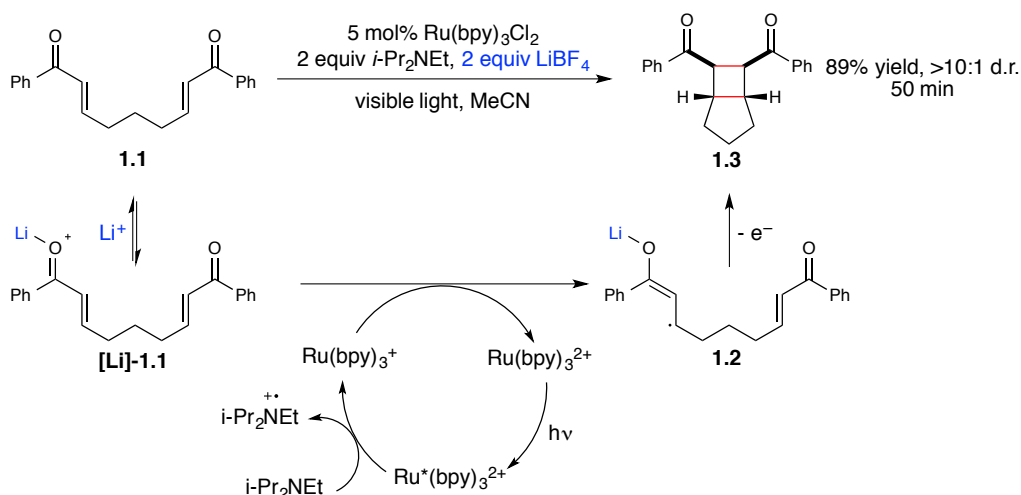
The following review will address leading contributions in which Lewis acidic metal centers have been successfully employed to control the selectivity or rate of photochemical reactions. Several distinct mechanistic roles for the Lewis acid have been described, from which three dominant themes emerge. Section 1.2 of this review illustrates the use of Lewis acid additives to modulate the reduction potentials of enone substrates in the context of visible light photoredox reactions. In these cases, Lewis acid activation is critical to the success of the reaction but not directly involved in the photoactivation step. In section 1.3, the use of Lewis acids to manipulate the inherent ultraviolet absorption properties of organic chromophores is documented. Finally, section 1.4 summarizes the use of Lewis acidic transition metal catalysts for photoinduced organometallic processes. In these examples, complexation of the Lewis acid and organic substrate creates a new chromophore and thereby provides entry into a unique mode of reactivity. The following discussion will highlight the distinctive mechanistic features and synthetic utility of each body of work under review.

1.2. Use of Lewis acids to manipulate the redox potentials of organic substrates in photoinduced electron-transfer reactions

Our group has a longstanding interest in developing synthetically valuable organic transformations that utilize visible light. A leading study in this research area demonstrated that aryl bis(enone) substrates undergo efficient intramolecular [2+2] cycloaddition reactions upon visible light irradiation in the presence of the photocatalyst $\text{Ru}(\text{bpy})_3\text{Cl}_2$ and *i*- Pr_2NEt and LiBF_4 as stoichiometric additives (Scheme 1-1).² In the proposed mechanism, photoexcitation of $\text{Ru}(\text{bpy})_3^{2+}$ with visible light followed by reductive quenching with *i*- Pr_2NEt generates $\text{Ru}(\text{bpy})_3^+$, the catalytically relevant reductant in this reaction. Although the reduction potential of $\text{Ru}(\text{bpy})_3^+$ is insufficient to enable direct reduction of phenyl bis(enone) substrate **1.1**, this

event is facilitated by Lewis acid activation of the enone by LiBF_4 . Stepwise cyclization of the resulting radical anion intermediate (**1.2**) and loss of an electron then generates the cyclobutane product (**1.3**). In addition to modulating the reduction potential of the aryl enone substrate, the Lewis acid additive also likely stabilizes the radical anion intermediates to allow productive reactivity.

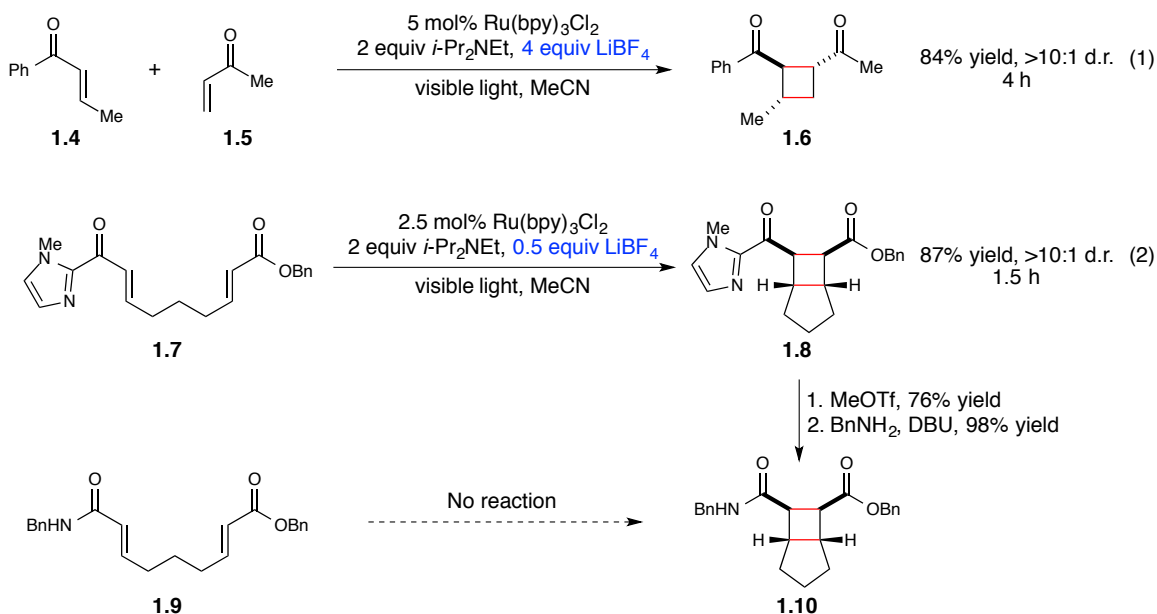
Scheme 1-1. Visible light photoredox catalysis of [2+2] enone cycloadditions.



The synthetic utility of visible light [2+2] photocycloadditions was further explored in crossed intermolecular reactions (Scheme 1-2, eq 1).³ In this system, one of the reaction partners is restricted to an aryl enone to ensure efficient reduction by the photocatalyst, but a variety of electronically diverse Michael acceptors readily serve as the coupling partner. The [2+2] cycloaddition reactions of α,β -unsaturated 2-acylimidazole substrates were also investigated (Scheme 1-2, eq 2).⁴ In line with the aryl enone system, these substrates are sufficiently electron-deficient in conjunction with Lewis acid activation by LiBF_4 to undergo reduction and productive reactivity. However, following the cycloaddition, the imidazole ring also serves as a "redox auxiliary" that undergoes facile cleavage with a variety of nucleophiles to generate the corresponding amides, esters and carboxylic acids. The direct linear precursors to these

cycloadducts (e.g. **1.9**) are not amenable to [2+2] cycloaddition under the standard reaction conditions due to their prohibitively high reduction potentials, yet the desired cyclobutane products can be easily accessed by the two-step procedure.

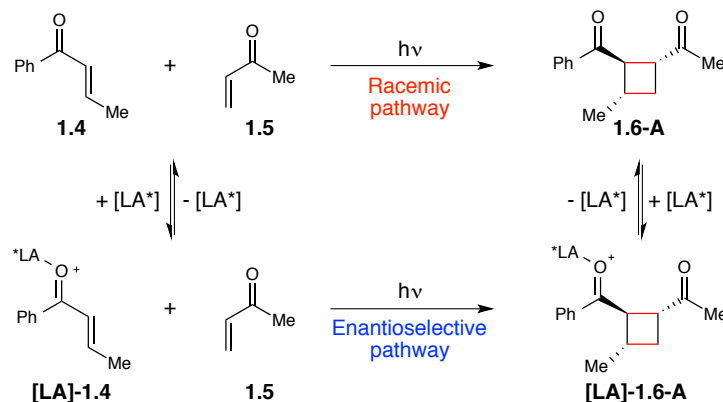
Scheme 1-2. Expanding the synthetic utility of [2+2] enone cycloadditions.



Given the critical role of Lewis acid additives in the photoredox reactions of enones developed by our group, we have recently become interested in tailoring this strategy to asymmetric catalysis through the use of chiral ligands. The development of enantioselective photochemical processes that operate with substoichiometric quantities of a chiral controller represents a historically difficult area of catalysis.¹⁴ A principle challenge stems from competitive background racemic reactions that occur upon direct absorption of ultraviolet light by the organic substrate in the absence of a chiral catalyst (Scheme 1-3). The photocatalytic [2+2] cycloaddition of enones developed in our group, however, provides an ideal model system for asymmetric catalysis due to the inherent absence of a background reaction. The reaction is initiated upon selective photoexcitation of the Ru(bpy)₃²⁺ catalyst with visible light, wavelengths at which organic chromophores do not absorb. Furthermore, Lewis acid activation of the enone is

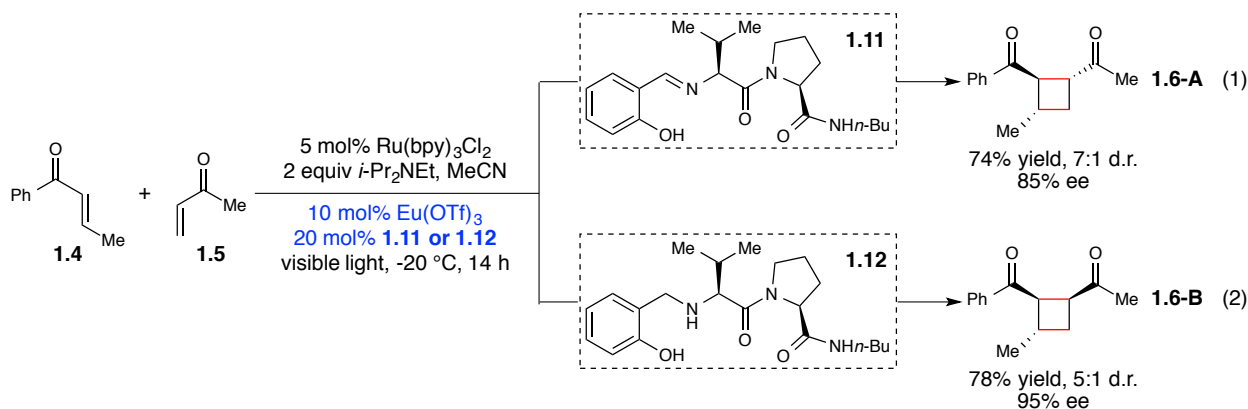
necessary for efficient reduction by the photocatalyst and therefore, despite the reversible nature of Lewis acid coordination, the reaction cannot occur on the uncomplexed substrate. These combined factors ensure that the cycloaddition proceeds exclusively via the enantioselective pathway.

Scheme 1-3. Inherent challenges associated with enantioselective photochemical reactions.



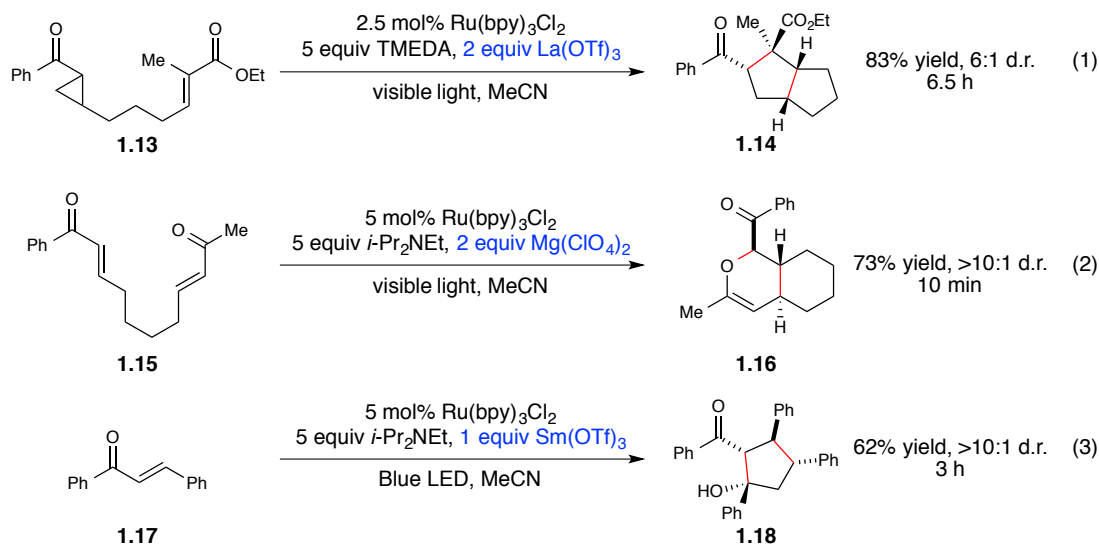
An empirical screen of a variety of Lewis acids and chiral ligands revealed that 10 mol% $\text{Eu}(\text{OTf})_3$ and 20 mol% of the Schiff base dipeptide ligand **1.11** provide cycloadduct **1.6** in good yield and enantioselectivity (Scheme 1-4, eq 1). Subsequent studies demonstrated that the analogous secondary amine ligand **1.12** produces the cycloadduct in similarly high yield and enantioselectivity, but with complete reversal of the diastereoselectivity (Scheme 1-4, eq 2).

Scheme 1-4. Complementary selectivity in asymmetric [2+2] photocycloaddition reactions.



Key to the successful development of a dual-catalysis strategy for asymmetric [2+2] enone cycloadditions was the independent nature of the Lewis acid and the transition metal photocatalyst. The Lewis acid therefore serves as a highly tunable additive that can be altered without impacting the photoactivation step. The versatility of the Lewis acid co-catalyst has also contributed to the discovery of a variety of additional photoredox transformations.

Scheme 1-5. Diverse reactivity of photochemically generated radical anion intermediates.



The use of $\text{La}(\text{OTf})_3$ as the Lewis acid in combination with TMEDA as the reductant enabled the reductive ring-opening and [3+2] cycloaddition of aryl cyclopropyl ketones (Scheme 1-5, eq 1).⁵ Notably, the optimized conditions, with LiBF_4 and $i\text{-Pr}_2\text{NEt}_2$ as additives, failed to produce any desired product. A photocatalytic hetero-Diels–Alder cycloaddition of aryl bis(enone) substrates was also investigated (Scheme 1-5, eq 2).⁶ In this system, $\text{Mg}(\text{ClO}_4)_2$ was identified as the optimal Lewis acid for unsymmetrical substrates such as **1.15**, and provided greater rate acceleration and chemoselectivity than LiBF_4 (refer to chapter 3 herein for a complete discussion of these results). Xia studied the reductive aldol dimerization of chalcones and found that the highest-yielding reactions occurred in the presence of $\text{Sm}(\text{OTf})_3$ (Scheme 1-5, eq 3).⁷ In each of

these examples, the tunable nature of the Lewis acid additive was critical to the successful optimization of the reaction.

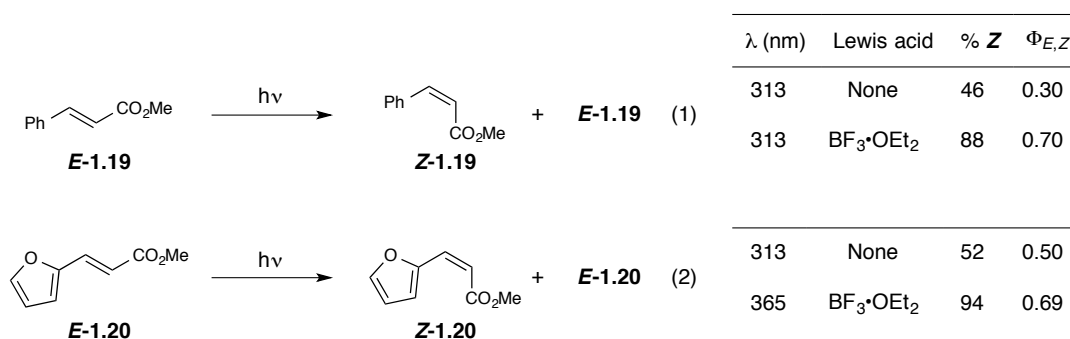
The use of Lewis acid additives in visible light photoredox transformations serves to both modulate the reduction potential of the organic substrate and stabilize the reactive radical anion intermediates. Importantly, because the role of the Lewis acid is completely decoupled from the photoactivation step, it can be independently optimized without perturbing the photophysical properties of the transition metal chromophore. This combined approach to substrate activation is thus uniquely poised to facilitate the rapid discovery of new organic transformations that operate via single-electron transfer, as well as new chiral catalyst combinations in pursuit of highly stereoselective processes.

1.3 Use of Lewis acids to manipulate the absorption properties and photochemical reactivity of organic chromophores

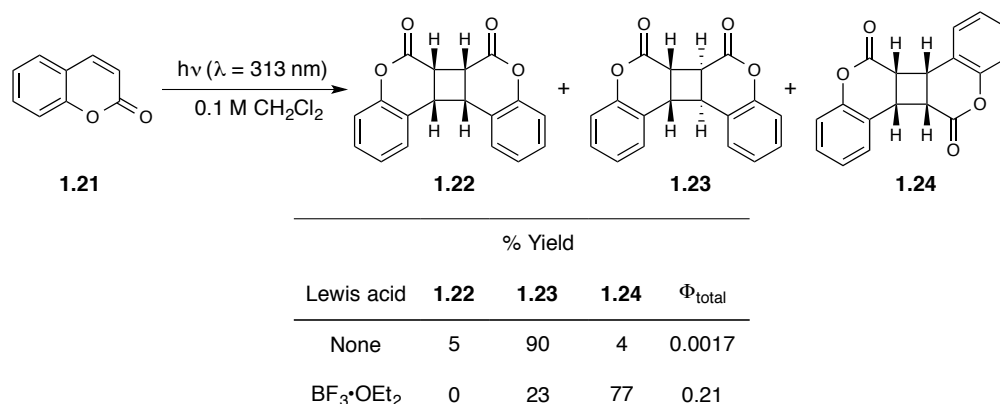
Photoactivation of enones to their electronically excited states can be achieved through the direct irradiation of these organic chromophores with ultraviolet light. The use of Lewis acids to accelerate and control the reactivity of this highly versatile substrate class is an emerging synthetic strategy. In a series of pioneering contributions, Lewis demonstrated that the spectroscopic properties and photochemical behavior of a variety of α,β -unsaturated esters can be dramatically altered by the presence of strongly coordinating Lewis acids. Among a number of examples,⁸ complexation of Lewis acids to methyl cinnamate (**1.19**)⁹ and methyl furylacrylate (**1.20**)¹⁰ was shown to significantly impact the *E/Z* photoisomerization of these organic chromophores (Scheme 1-6). Irradiation of *E*-**1.19** and *E*-**1.20** with 313-nm light in the absence of Lewis acid resulted in photostationary states comprised of 46% and 52% *Z* isomer, respectively. In both systems, coordination of $\text{BF}_3 \cdot \text{OEt}_2$ induced a significant bathochromic shift

in the absorption spectra, and judicious selection of the excitation wavelength provided access to photostationary states greatly enriched in the *Z* isomers. The origin of the observed selectivity was attributed to the preferable formation of Lewis acid complexes with the *E* isomer, as well as the selective photoexcitation and greater quantum yield ($\Phi_{E,Z}$) for isomerization observed with this complex. These studies thus provided the first examples of Lewis acids being used to influence a photochemical transformation, as well as a viable approach to the selective preparation of thermodynamically unfavorable *Z* alkenes.

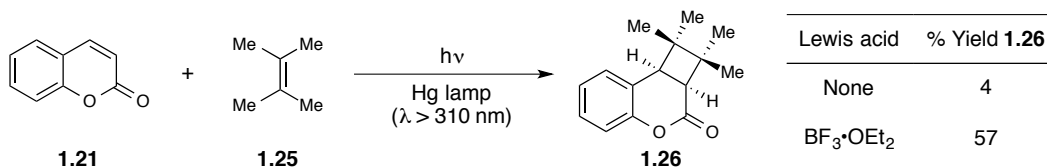
Scheme 1-6. Effect of Lewis acids on the photostationary state of conjugated alkenes.



The effect of Lewis acids on [2+2] photocycloaddition reactions of a variety of enone chromophores was also investigated.¹¹ For example, the dimerization of coumarin¹² occurred upon direct irradiation at 313 nm and exhibited good selectivity for the anti head-to-head isomer **1.23** (Scheme 1-7). Irradiation in the presence of $\text{BF}_3 \cdot \text{OEt}_2$, however, resulted in a dramatic change in the selectivity and provided syn head-to-tail isomer **1.24** as the major product. A significant increase in the overall quantum yield (Φ_{total}) was also observed.

Scheme 1-7. Lewis acid catalysis of photochemical [2+2] coumarin dimerizations.

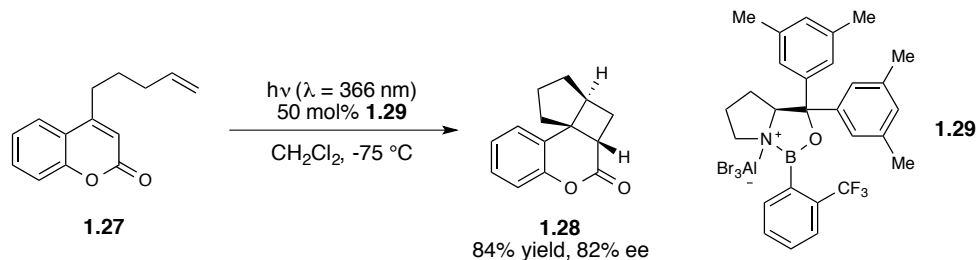
Lewis acid complexation was also shown to accelerate the crossed [2+2] cycloaddition of coumarin with a variety of simple alkenes. Although the direct photocycloaddition of coumarin and tetramethylethylene is highly inefficient in the absence of a Lewis acid additive,¹³ the reaction was greatly enhanced by the presence of $\text{BF}_3 \cdot \text{OEt}_2$ (Scheme 1-8).^{12a} The observed rate acceleration was attributed to the increased singlet-state lifetime and electrophilicity of the Lewis acid-coumarin complex. Collectively, these observations demonstrated that Lewis acid additives serve to vastly alter the photophysical properties of organic chromophores, which in turn can impact both the efficiency and selectivity of the desired photochemical transformation.

Scheme 1-8. Lewis acid catalysis of crossed [2+2] photocycloaddition reactions of coumarin.

The insights garnered from these fundamental studies have been recently exploited in the context of asymmetric [2+2] photocycloaddition reactions. As highlighted in the previous section, enantioselective photochemical transformations are often difficult to achieve due to the propensity of organic chromophores to undergo racemic background reactions in the absence of

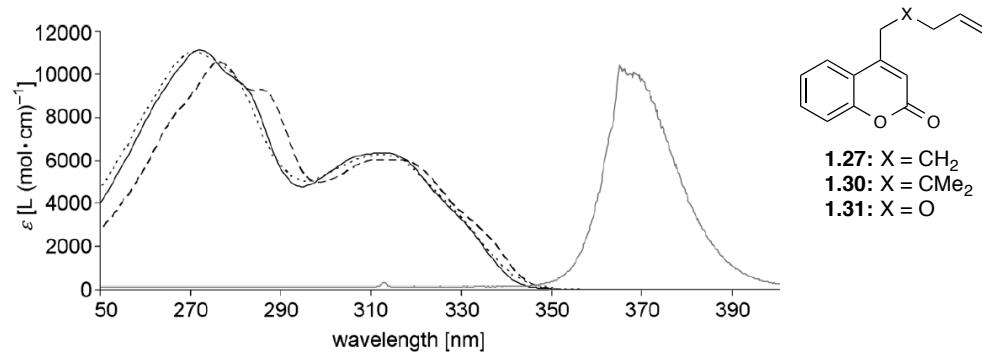
a chiral catalyst.¹⁴ Bach demonstrated, however, that AlBr₃-activated chiral oxazaborolidine **1.29** serves as a competent catalyst for the intramolecular cycloaddition of coumarin derivative **1.27** upon irradiation with 366 nm light to afford the cyclobutane product **1.28** in 84% yield and 82% ee (Scheme 1-9).¹⁵

Scheme 1-9. Chiral Lewis acid-catalyzed enantioselective [2+2] photocycloaddition of coumarins.

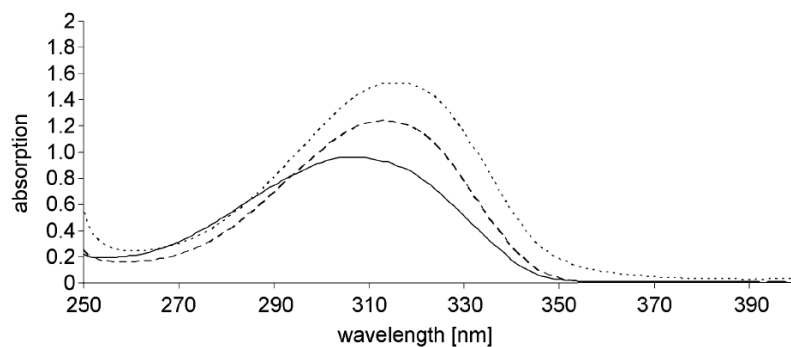


To rationalize the high enantioselectivity, the authors obtained UV/Vis absorption spectra of a variety of coumarin substrates in the absence and presence of Lewis acids. A superimposition of the absorption spectra of the uncomplexed coumarin substrates with the emission spectrum of the light source ($\lambda_{\text{max}} = 366$ nm) indicates little spectral overlap (Figure 1-1, a). In line with this observation, low conversion to cyclobutane was observed upon direct irradiation of the substrates at this wavelength under standard reaction conditions (<25% conversion after 5 hours). On the other hand, the absorption spectra of coumarin **1.27** exhibit a bathochromic shift upon complexation with a variety of Lewis acids and partial overlap with the emission band of the lamp (Figure 1-1, b). Selective photoexcitation of the chiral Lewis acid-coumarin complex with 366 nm light therefore favors the enantioselective reaction pathway. In line with observations made previously by Lewis, fluorescence measurements for this system also indicated a significant increase in the singlet state lifetime of coumarin in the presence of Lewis acids. Both factors likely contributed to the success of this strategy in achieving high levels of asymmetric induction.

Figure 1-1. Effect of Lewis acid complexation on coumarin UV/Vis absorption spectra.^a



(a) UV/Vis spectra of representative coumarins **1.27** (—), **1.30** (---), and **1.31** (···) in dichloromethane solution ($c = 0.8$ mM). The normalized emission spectrum of the light source with $\lambda_{\text{max}} = 366$ nm (—) is superimposed.

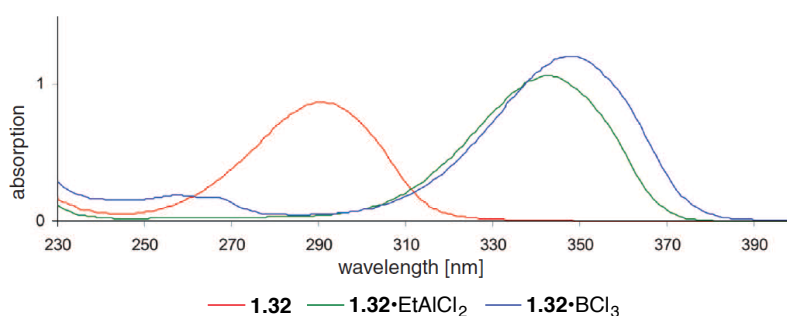


(b) UV/Vis spectra of coumarin **1.27** dichloromethane solution ($c = 0.8$ mM) upon addition of 20 equiv BF₃ (—), EtAlCl₂ (---), or AlBr₃ (···).

^a Figures reproduced from reference 15a

Bach also investigated chiral Lewis acid catalysts in the enantioselective [2+2] photocycloaddition of 5,6-dihydro-4-pyridones.¹⁶ The absorption spectra of this class of substrates were shown to exhibit an extensive shift (>50 nm) in the presence of Lewis acids such as EtAlCl₂ and BCl₃ (Figure 1-2). By analogy to the coumarin system, selective photoexcitation of chiral Lewis acid-complexed substrate **1.32** afforded the desired cyclobutane **1.33** in 84% yield and 88% ee. Although Lewis acid coordination did not affect fluorescence in this case, the large bathochromic shift alone proved sufficient to control the selectivity.

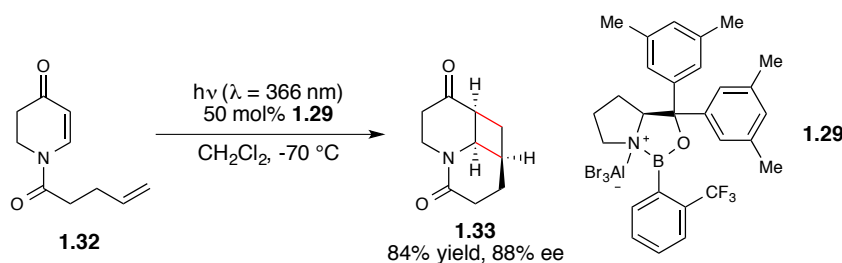
Figure 1-2. Extensive bathochromic shift of 5,6-dihydro-4-pyridones upon Lewis acid complexation.^a



UV/Vis spectra of substrate **1.32** in the presence of Lewis acids.

^a Figure reproduced from reference 16.

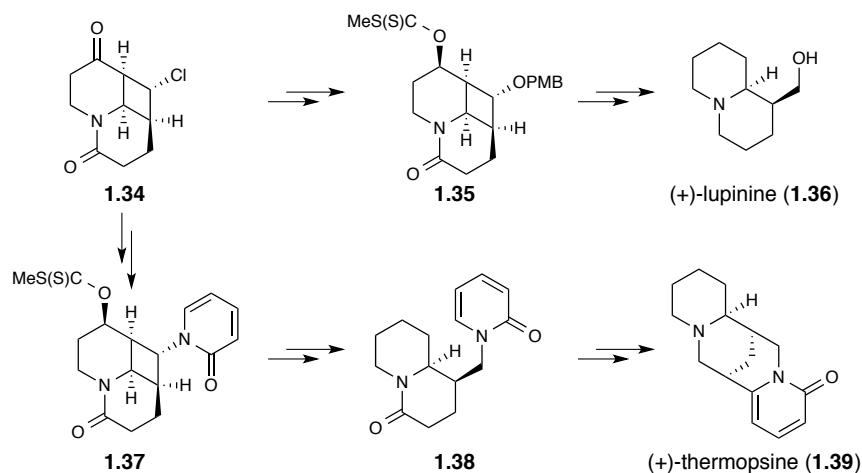
Scheme 1-10. Chiral Lewis acid-catalyzed enantioselective [2+2] photocycloaddition of 5,6-dihydro-4-pyridones.



The utility of this class of cyclobutane products was demonstrated by the synthesis of the lupin alkaloids (+)-lupinine and (+)-thermopsine (Scheme 1-11). The quinolizidine core structure of these natural products (**1.34**) was readily accessed by the enantioselective [2+2] cycloaddition. The chloride substituent provided a synthetic handle to introduce the requisite functionality,

while the cyclobutane underwent a reductive ring-opening reaction to generate the desired scaffolds.

Scheme 1-11. Synthetic applications of [2+2] cycloadduct products.



Photoactivation of enones to their electronically excited states is one of the most synthetically versatile and widely exploited areas of organic photochemistry. The design of generalizable strategies to exert catalyst control over these photochemical processes is therefore a highly important goal. The prominent contributions described above demonstrate the viability of Lewis acid catalysis in governing the efficiency, chemoselectivity, and stereoselectivity of reactions initiated by direct photoexcitation of organic chromophores. In these systems, the Lewis acid modulates the innate photophysical properties of the substrates and thereby introduces mechanistic pathways that diverge from the background reaction. This approach stands in contrast to the use of Lewis acids in photoredox reactions in which substrate activation is completely distinct from the photoinitiation step. Nonetheless, both strategies benefit from the ability to easily tune the identity of the Lewis acid and its surrounding ligand environment.

1.4. Lewis acidic metal centers as catalysts for photoinduced organometallic processes

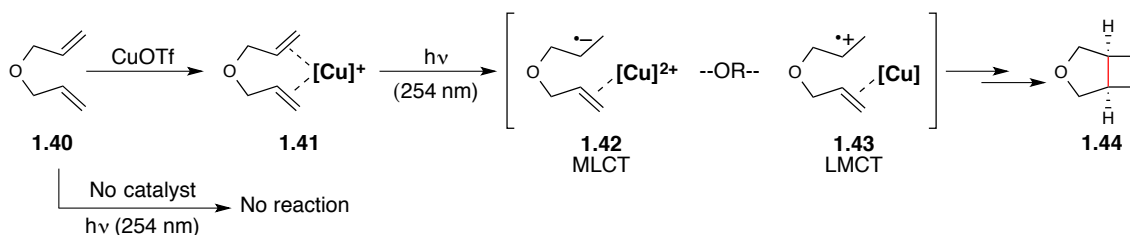
A vast number of well-characterized organometallic complexes exhibit notable photophysical properties upon absorption of light.¹⁷ For example, ruthenium and iridium polypyridyl complexes have been widely studied in the context of solar energy conversion¹⁸ as well as the sensitization of organic reactions¹⁹ (the topic of section 1.2 and chapters 2 and 3 of this thesis). The following discussion is specifically focused, however, on the reactivity of coordinatively unsaturated Lewis acidic metal centers that form photoactive complexes with organic substrates to provide entry into new reactive intermediates as well as guide the ensuing organic transformation.

1.4.1 Photoinduced copper-catalyzed [2+2] cycloaddition reactions

Lewis acidic copper(I) salts have been widely used as catalysts to promote [2+2] cycloaddition reactions of non-conjugated alkenes (Scheme 1-12).²⁰ While leading contributions investigated intermolecular dimerization reactions of cyclic alkenes,²¹ intramolecular cyclization reactions have been subsequently extensively developed as a valuable synthetic strategy for the preparation of complex bicyclic structures. Notably, this mode of activation represents the only known method to achieve photocycloadditions of non-conjugated alkenes, which absorb at prohibitively high-energy wavelengths of light (~190 nm) in the absence of a catalyst. These cycloaddition reactions proceed through well-defined 2:1 alkene:copper complexes that undergo charge transfer excitation upon irradiation with ultraviolet light.²² The absorption spectra of the copper-alkene complexes typically exhibit two bands corresponding to metal-to-ligand (MLCT) and ligand-to-metal charge transfer (LMCT) and it remains unknown which event induces cycloaddition.²³ Although a variety of copper(I) salts serve as competent catalysts, CuOTf

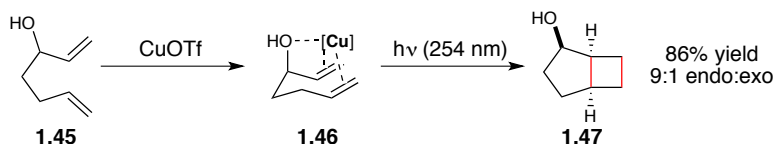
generally provides the greatest reaction rates due to its highly cationic nature and tight binding interactions with the olefin substrate.²⁴

Scheme 1-12. Charge transfer mechanisms in copper-catalyzed [2+2] cycloadditions.



In addition to modulating the photophysical properties of olefin substrates, the scaffolding ability of Lewis acidic copper catalysts often translates to high levels of diastereoselectivity in the cycloaddition. For example, diene substrate **1.45**, which bears an additional coordinating group in the tether, undergoes cycloaddition with good selectivity for *endo* diastereomer **1.47**. Although the *exo* diastereomer is thermodynamically more favorable, tridentate coordination of the diene-copper complex (**1.46**) strongly dictates the stereochemical outcome.

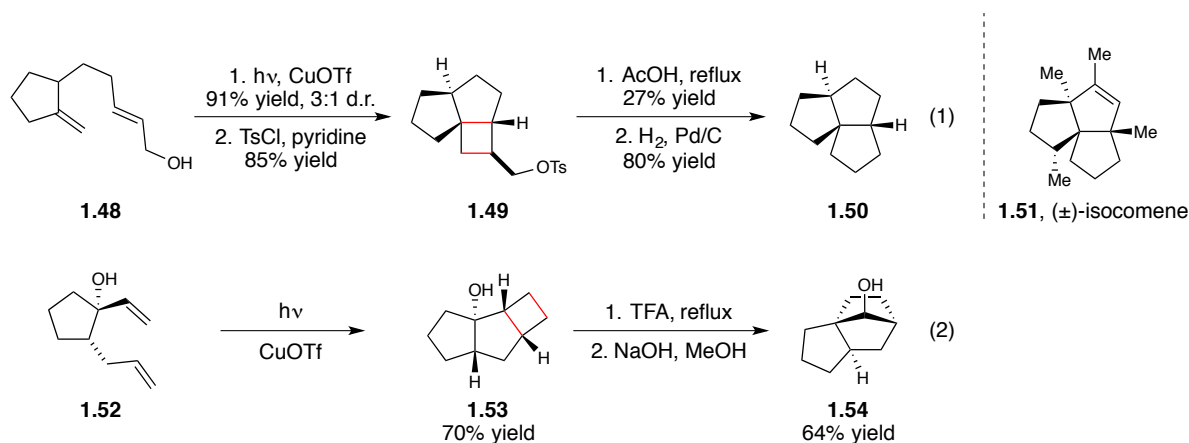
Scheme 1-13. Tridentate coordination in diene-copper complexes.



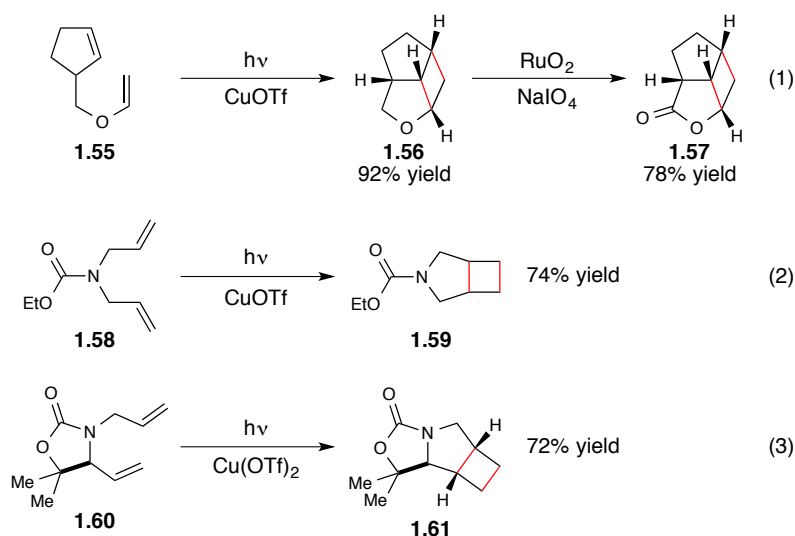
Due to the many valuable features of copper-catalyzed photocycloadditions, a number of research groups have explored the diverse utility of this transformation in organic synthesis. Salomon investigated photocycloadditions as part of a two-step strategy for constructing complex carbocyclic scaffolds. For example, he demonstrated that diene **1.48** undergoes efficient [2+2] cycloaddition to afford cyclobutane **1.49** in excellent yield (Scheme 1-14, eq 1).²⁵ The resulting cyclobutane is then amenable to a ring-rearrangement reaction upon loss of a tosylate leaving group to generate tricyclic product **1.50**. Ring systems of this type are prevalent in

sesquiterpene natural products such as (\pm)-isocomene (**1.51**). Salomon also developed an efficient [2+2] cycloaddition of diene **1.52** followed by a ring-rearrangement reaction to afford hydroxynorbornane **1.54** (Scheme 1-14, eq 2).²⁶

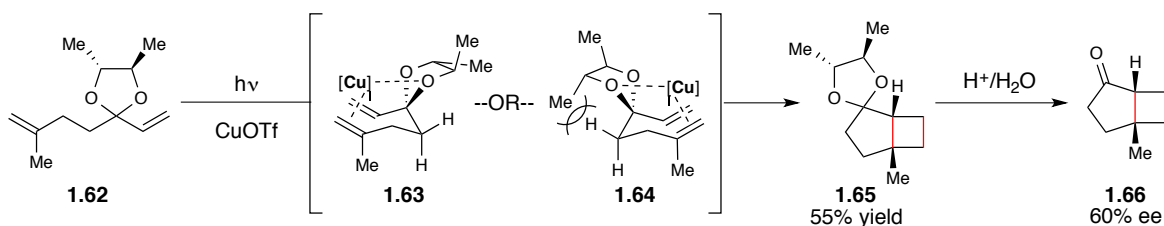
Scheme 1-14. Copper-catalyzed [2+2] cycloadditions in the preparation of diverse carbocycles.



Copper-catalyzed [2+2] photocycloadditions also serve as a valuable tool for the construction of diverse heterocyclic scaffolds. Irradiation of vinyl ether **1.55** in the presence of CuOTf provides tricyclic product **1.56**, which can be further functionalized to lactone **1.57** through a regioselective oxidation reaction with ruthenium tetroxide (Scheme 1-15, eq 1). Nitrogen heterocycles have been prepared by photocycloaddition of *N,N*-diallyl carbamates (eq 2)²⁷ and *N*-allyl-4-vinyloxazolidinones (eq 3).²⁸

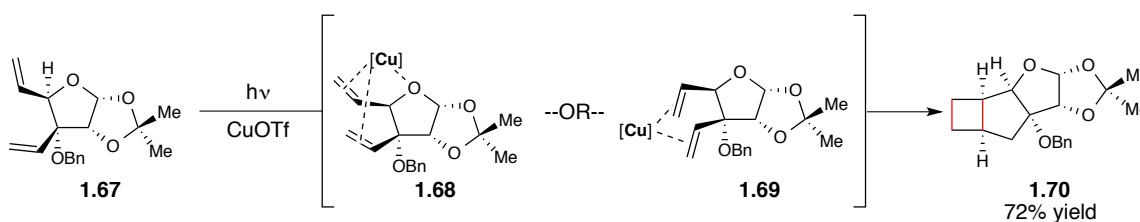
Scheme 1-15. Copper-catalyzed [2+2] cycloadditions in the preparation of diverse heterocycles.

Copper-catalyzed [2+2] photocycloadditions have been investigated in the synthesis of enantioenriched cyclobutanes. In the context of developing an asymmetric synthesis of cyclobutane-containing natural product grandisol, Mattay considered a variety of strategies for achieving asymmetric induction in this class of reactions.²⁹ The use of chiral starting materials and chiral catalysts proved quite challenging, and ultimately the best results were achieved with removable chiral ketal auxiliaries. Diene **1.62** undergoes [2+2] cycloaddition in the presence of CuOTf to give cyclobutane product **1.66** in 60% ee following cleavage of the auxiliary (Scheme 1-16). The authors proposed that tridentate coordination of the Lewis acidic copper center to the substrate dictates the observed selectivity; an unfavorable methyl group/hydrogen interaction occurs in complex **1.64**, while complex **1.63** does not exhibit this constraint.

Scheme 1-16. Chiral auxiliary approach to enantioselective [2+2] cycloadditions.

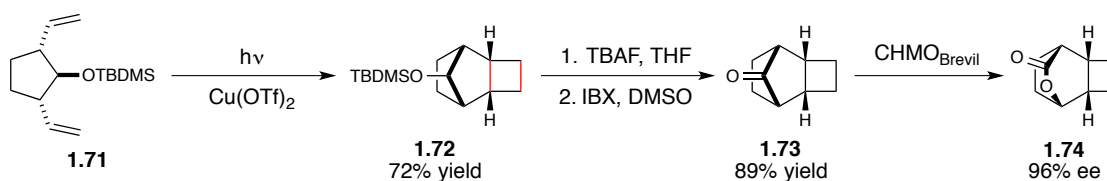
Ghosh has investigated the [2+2] cycloaddition reactions of diene substrates incorporated into carbohydrate templates.³⁰ For example, diene **1.67** undergoes copper-catalyzed cycloaddition in good yield with high selectivity for the thermodynamically unfavorable *cis*-syn-*cis* diastereomer **1.70** (Scheme 1-17).³¹ This result was rationalized by preferential preorganization of the substrate by the copper center through tridentate coordination (**1.68**) over bidentate coordination (**1.69**).

Scheme 1-17. Copper-catalyzed [2+2] cycloaddition of carbohydrate-embedded scaffolds.



Bach demonstrated that cyclobutane adducts obtained by photocycloaddition reactions serve as excellent substrates for asymmetric Baeyer–Villiger oxidation reactions (Scheme 1-18).³² Diene **1.71** undergoes efficient cycloaddition to **1.72**, which can then be deprotected and oxidized to give prochiral cyclic ketone **1.73**. Oxidative desymmetrization of **1.73** by cyclohexanone monooxygenase (CHMO) delivers the tricyclic lactone **1.74** with excellent enantioselectivity.

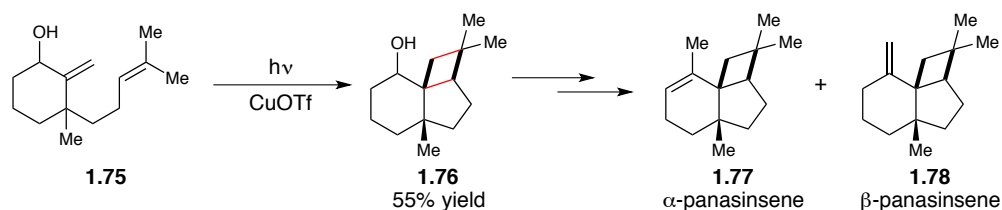
Scheme 1-18. Oxidative desymmetrization of [2+2] cycloadducts.



Copper-catalyzed photocycloadditions of non-conjugated dienes have also been employed as a strategy-level tool for natural product synthesis. In 1980, McMurray demonstrated that irradiation of diene **1.75** in the presence of CuOTf provides entry into tricyclic scaffold **1.76**

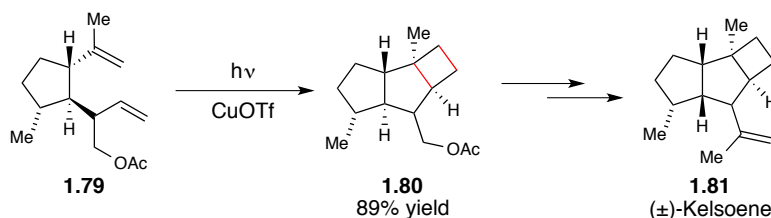
(Scheme 1-19).³³ The alcohol functional group was then further manipulated to deliver a mixture of the sesquiterpene natural products α - and β -panasinsene.

Scheme 1-19. Synthesis of α - and β -panasinsene.

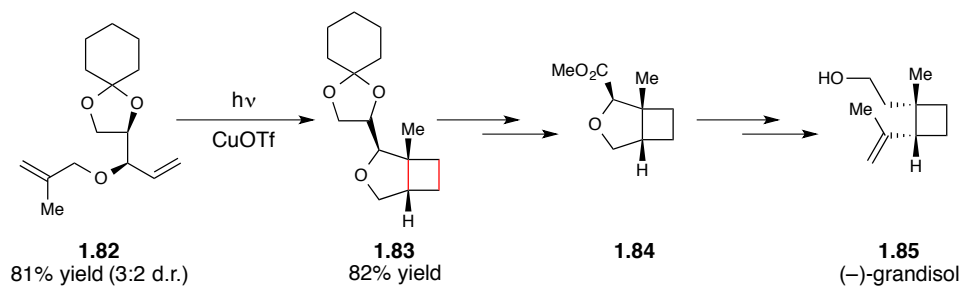


More recently, Bach developed a synthesis of sesquiterpene (\pm)-kelsoene that also involved a strategic copper-catalyzed [2+2] cycloaddition reaction (Scheme 1-20).³⁴ This study presented an alternative to prior synthetic routes that relied on enone photocycloadditions. These examples thus demonstrate how photocycloaddition reactions of non-conjugated alkenes can be employed to rapidly prepare complex carbocyclic scaffolds from minimally functionalized hydrocarbon starting materials.

Scheme 1-20. Synthesis of (\pm)-kelsoene.



In 2004, Ghosh described the copper-catalyzed photocycloaddition reactions of a variety of chiral glyceraldehyde-derived substrates (Scheme 1-21).³⁵ Diene **1.82** underwent smooth photocycloaddition followed by cleavage of the chiral auxiliary to generate **1.84**, which was carried forward to complete a short formal synthesis of (–)-grandisol.

Scheme 1-21. Synthesis of (–)-grandisol.

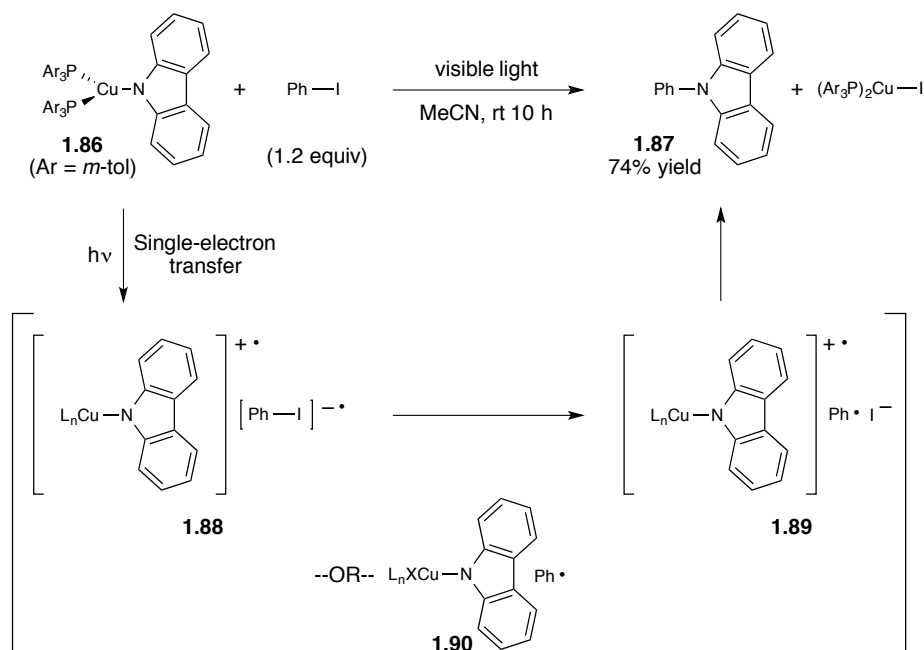
In summary, copper catalysis enables efficient [2+2] photocycloaddition reactions of non-conjugated alkenes, which are otherwise challenging to achieve due to the high-energy wavelengths of light required for the direct photoactivation of these substrates. The copper catalyst plays two significant roles in these reactions. First, it forms a photoactive complex with the diene substrate and induces cycloaddition via single-electron transfer. Second, the highly Lewis acidic copper center tightly pre-organizes the substrate which often thereby profoundly impacts the stereoselectivity of the bond-forming steps. Given the rigidity of the copper-alkene complex and the lack of an inherent background reaction, it is perhaps surprising that, to date, there exists no catalytic, asymmetric variant of this synthetically powerful transformation. A full discussion of this limitation and our proposed approach towards the development of an enantioselective method is the focus of Chapter 4 of this thesis.

1.4.2 Photoinduced copper-catalyzed cross-coupling reactions

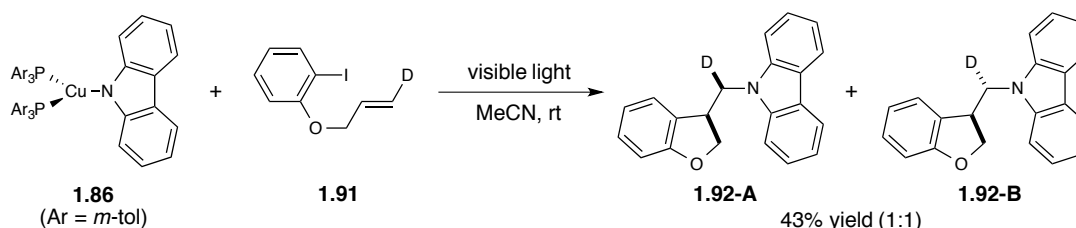
The research groups of Fu and Peters recently described a photoinduced Ullmann C–N coupling of luminescent copper carbazolidine complex (**1.86**)³⁶ with phenyl iodide upon visible light irradiation at room temperature (Scheme 1-22).³⁷ Notably, this study established exceedingly mild reaction conditions compared to conventional Ullmann cross-coupling reactions, as well as provided strong evidence that single electron-transfer serves as a viable mechanistic pathway for

this type of transformation. In the proposed mechanism, photoexcitation of the copper complex initiates single-electron transfer to the phenyl iodide to generate the radical anion (**1.88**), which then undergoes facile fragmentation to a halide anion and phenyl radical (**1.89**). The phenyl radical could alternatively result from direct halogen atom transfer to the copper complex (**1.90**). The copper complex and phenyl radical then react to afford the C-N cross-coupled product.

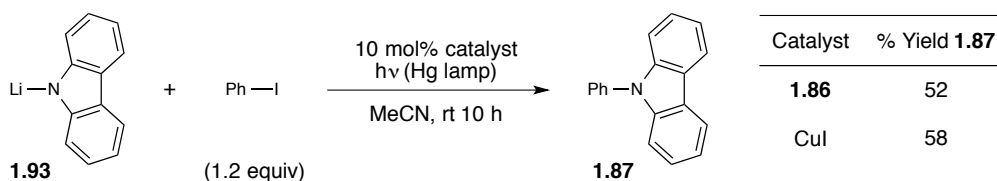
Scheme 1-22. Radical mechanisms in photochemical Ullmann C-N coupling reactions.



This mechanistic proposal was interrogated with deuterium-labeled radical probe substrate **1.91** (Scheme 1-23). Irradiation of the two reaction partners under the standard conditions resulted in the formation of a 1:1 mixture of cyclized products **1.92A** and **1.92B**, which is consistent with the intermediacy of a phenyl radical. In addition, EPR studies conducted on irradiated reaction mixtures were consistent with the formation of a copper-containing radical species.

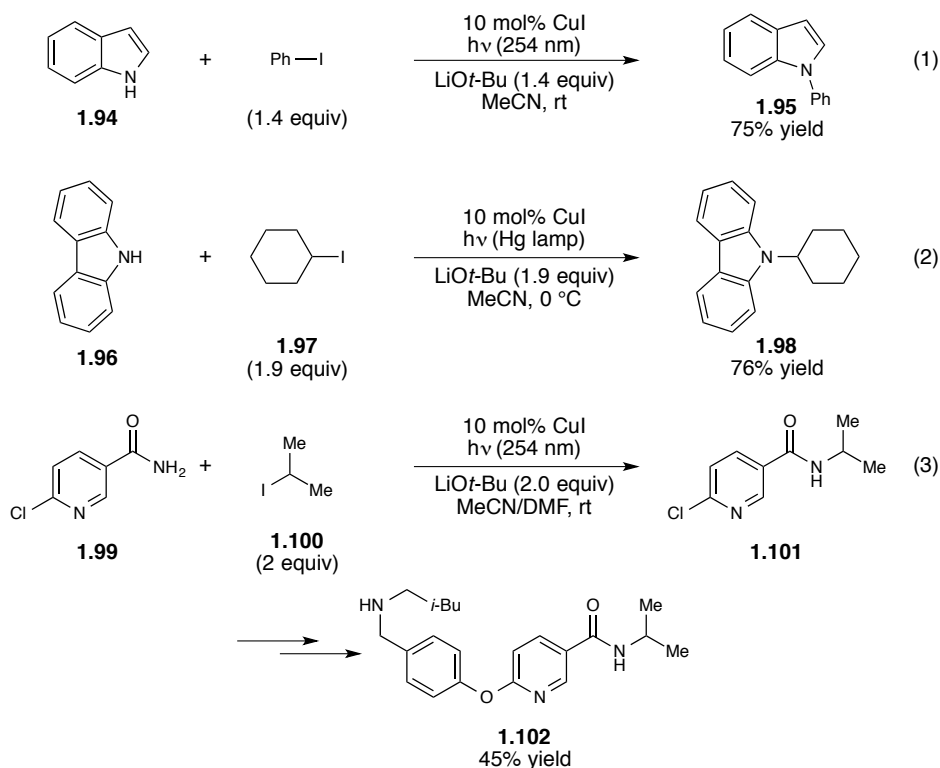
Scheme 1-23. Evidence for radical intermediates in photoinduced Ullmann C-N coupling reactions.

A catalytic variant of the photoinduced Ullmann cross-coupling reaction was also explored (Scheme 1-24). Irradiation of a mixture of lithium carbazolidine and phenyl iodide in the presence of either copper complex **1.86** or CuI provided the cross-coupled product in moderate yield.

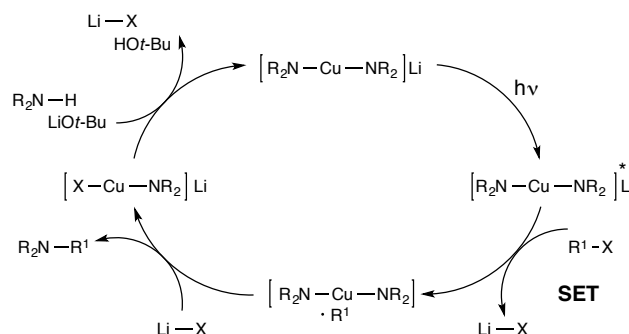
Scheme 1-24. Catalytic variant of the photoinduced Ullmann C-N coupling reaction.

Fu and Peters subsequently explored the versatility of this catalyst system for a variety of additional C-N bond forming reactions (Scheme 1-25). The N-arylation of an array of synthetically valuable heterocycles was achieved under ultra-violet irradiation in the presence of 10 mol% CuI as the catalyst (eq 1).³⁸ The N-alkylation of carbazole (eq 2)³⁹ and benzamides (eq 3)⁴⁰ with alkyl iodides was also accommodated under these reaction conditions. Alkylation of benzamide **1.99** followed by further elaboration of the 2-chloropyridyl group enabled the synthesis of opioid receptor agonist **1.102**.

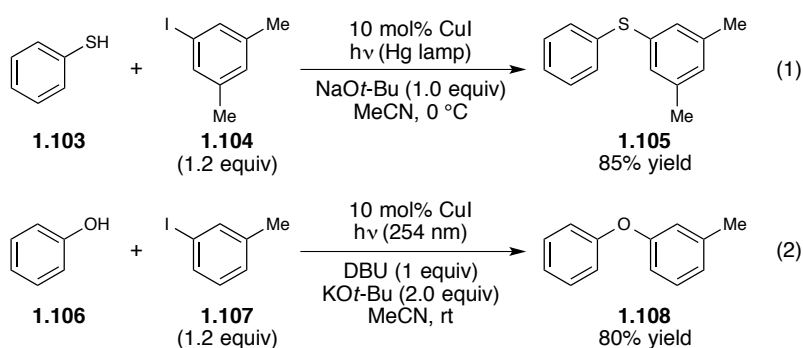
Scheme 1-25. Expanding the synthetic utility of photoinduced, copper-catalyzed C-N cross-coupling reactions.



A proposed catalytic cycle to account for the photoinduced C-N cross-coupling reaction is depicted in Scheme 1-26. Photoexcitation of an anionic copper carbazolidate complex induces single-electron transfer to generate the reactive radical species, which then undergoes C-N bond formation with the copper complex. In support of this mechanism, the N-alkylation reaction of carbazole (Scheme 1-25, eq 2) was monitored by electrospray mass spectrometry and peaks consistent with the formation of $[\text{Cu}(\text{carbazolidate})_2]^-$ were observed. Furthermore, complex $[\text{Li}(\text{MeCN})_4][\text{Cu}(\text{carbazolidate})_2]$ was independently synthesized and shown to catalyze the alkylation reaction under otherwise standard reaction conditions.

Scheme 1-26. Proposed mechanism for photoinduced, copper-catalyzed C-N cross-coupling reactions.

Fu and Peters have recently demonstrated that sulfur⁴¹ and oxygen⁴² nucleophiles also serve as competent coupling partners in photoinduced copper-catalyzed cross-coupling reactions under mild conditions (Scheme 1-27). The irradiation wavelength was optimized in each case, yet a wide range of reaction partners are accommodated under otherwise similar reaction conditions. These collective studies demonstrate that photoactivation of copper-bound nucleophiles provides a simple and generalizable platform for the development of many new carbon-heteroatom bond-forming reactions. More broadly, the rapid success of this strategy suggests that photochemistry has the power to introduce new mechanistic insights and viable synthetic alternatives to classes of reactions that are not conventionally conducted with photochemical activation.

Scheme 1-27. Viability of oxygen and sulfur nucleophiles in photoinduced copper-catalyzed cross-coupling reactions.

1.5 Conclusions and Outlook

Although Lewis acid catalysis is a widely applied strategy for controlling thermal reactions, it has received much less attention in the context of organic photochemistry. The prominent contributions described above demonstrate the viability of Lewis acid additives in governing the efficiency, chemoselectivity, and stereoselectivity of a number of photochemical processes. As illustrated in many of these examples, organic photochemistry is uniquely poised to forge complex and often highly strained architectures that are otherwise unfavorable upon thermal activation. The application of Lewis acids to photochemistry capitalizes on the synthetic versatility of photoactivated organic intermediates, yet also provides a powerful platform for manipulating known transformations and uncovering mechanistically novel modes of reactivity. The unique intersection of these two powerful fields of organic chemistry will likely prove an active area of research well into the future.

1.6 References

1. *Lewis Acids in Organic Synthesis* ed. H. Yamamoto, Wiley–CVH, Weinheim, **2000**.
2. Ischay, M. A.; Anzovino, M. E.; Du, J.; Yoon, T. P. "Efficient Visible Light Photocatalysis of [2+2] Enone Cycloadditions" *J. Am. Chem. Soc.* **2008**, *130*, 12886–12887.
3. Du, J.; Yoon, T. P. "Crossed Intermolecular [2+2] Cycloadditions of Acyclic Enones via Visible Light Photocatalysis" *J. Am. Chem. Soc.* **2009**, *131*, 14604–14605.
4. Tyson, E. L.; Farney, E. P.; Yoon, T. P. "Photocatalytic [2+2] Cycloadditions of Enones with Cleavable Redox Auxiliaries" *Org. Lett.* **2012**, *14*, 1110–1113.
5. Lu, Z.; Shen, M. H.; Yoon, T. P. "[3+2] Cycloadditions of Aryl Cyclopropyl Ketones by Visible Light Photocatalysis" *J. Am. Chem. Soc.* **2011**, *133*, 1162–1164.
6. Hurtley, A. E.; Cismesia, M. A.; Ischay, M. A.; Yoon, T. P. "Visible Light Photocatalysis of Radical Anion Hetero-Diels–Alder Cycloadditions" *Tetrahedron* **2011**, *67*, 4442–4448.

-
7. Zhao, G.; Yang, C.; Guo, L.; Sun, H.; Lin, R.; Xia, W. "Reactivity Insight into Reductive Coupling and Aldol Cyclization of Chalcones by Visible Light Photocatalysis" *J. Org. Chem.* **2012**, *77*, 6302–6306.
 8. (a) Lewis, F. D.; Elbert, J. E.; Upthagrove, A. L.; Hale, P. D. "Structure and Photoisomerization of (*E*)-Cinnamamides and (*Z*)-Cinnamamides and Their Lewis Acid Complexes" *J. Org. Chem.* **1991**, *56*, 553–561. (b) Lewis, F. D.; Howard, D. K.; Barancyk, S. V.; Oxman, J. D. "Lewis Acid Catalysis of Photochemical Reactions. 5. Selective Isomerization of Conjugated Butenoic and Dienoic Esters" *J. Am. Chem. Soc.* **1986**, *108*, 3016–3023. (c) Lewis, F. D.; Oxman, J. D. "Lewis Acid Enhancement of Photochemical Trans-Cis Isomerization of α,β -Unsaturated Esters" *J. Am. Chem. Soc.* **1981**, *103*, 7345–7347. (d) Childs, R. F.; Duffey, B.; Mika-Gibala, A. "Use of Solid Acids to Catalyze the Cis/Trans Photoisomerization of α,β -Unsaturated Carbonyl Compounds" *J. Org. Chem.* **1984**, *49*, 4352–4358.
 9. Lewis, F. D.; Oxman, J. D.; Gibson, L. L.; Hampsch, H. L.; Quillen, S. L. "Lewis Acid Catalysis of Photochemical Reactions. 4. Selective Isomerization of Cinnamic Esters" *J. Am. Chem. Soc.* **1986**, *108*, 3005–3015.
 10. Lewis, F. D.; Howard, D. K.; Oxman, J. D.; Upthagrove, A. L.; Quillen, S. L. "Lewis Acid Catalysis of Photochemical Reactions. 6. Selective Isomerization of β -Furylacrylic and Urocanic Esters" *J. Am. Chem. Soc.* **1986**, *108*, 5964–5968.
 11. (a) Lewis, F. D.; Reddy, G. D.; Elbert, J. E.; Tillberg, B. E.; Meltzer, J. A.; Kojima, M. "Spectroscopy and Photochemistry of 2-Quinolones and Their Lewis Acid Complexes" *J. Org. Chem.* **1991**, *56*, 5311–5318. (b) Lewis, F. D.; Quillen, S. L.; Hale, P. D.; Oxman, J. D. "Lewis Acid Catalysis of Photochemical Reactions. 7. Photodimerization and Cross-Cycloaddition of Cinnamic Esters" *J. Am. Chem. Soc.* **1988**, *110*, 1261–1267. (c) Lewis, F. D.; Oxman, J. D.; Huffman, J. C. "Photodimerization of Lewis Acid Complexes of Cinnamate Esters in Solution and the Solid State" *J. Am. Chem. Soc.* **1984**, *106*, 466–468. (d) Ogawa, T.; Masui, Y.; Ojima, S.; Suzuki, H. "Influences of Lewis Acids on the Photochemical Cyclodimerization of Cyclopentenone" *Bull. Chem. Soc. Jpn.* **1987**, *60*, 423–425.
 12. (a) Lewis, F. D.; Barancyk, S. V. "Lewis Acid Catalysis of Photochemical Reactions. 8. Photodimerization and Cross-Cycloaddition of Coumarin" *J. Am. Chem. Soc.* **1989**, *111*, 8653–8661. (b) Lewis, F. D.; Howard, D. K.; Oxman, J. D. "Lewis Acid Catalysis of Coumarin Photodimerization" *J. Am. Chem. Soc.* **1983**, *105*, 3344–3345.
 13. Wells, P. P.; Morrison, H. "Photocycloaddition of Coumarin to Tetramethyleneethylene. A Photoreaction Associated with the Apparent Interception of the Coumarin Singlet Excimer" *J. Am. Chem. Soc.* **1975**, *97*, 154–159.
 14. (a) Inoue, Y. "Asymmetric Photochemical Reactions in Solution" *Chem. Rev.* **1992**, *92*, 741–770. (b) Rau, H. "Asymmetric Photochemistry in Solution" *Chem. Rev.* **1983**, *83*, 535–547.

-
15. (a) Brimioulle, R.; Guo, H.; Bach, T. "Enantioselective Intramolecular [2+2] Photocycloaddition Reactions of 4-Substituted Coumarins Catalyzed by a Chiral Lewis Acid" *Chem. Eur. J.* **2012**, *18*, 7552–7560. (b) Guo, H.; Herdtweck, E.; Bach, T. "Enantioselective Lewis Acid Catalysis in Intramolecular [2+2] Photocycloaddition Reactions of Coumarins" *Angew. Chem. Int. Ed.* **2010**, *49*, 7782–7785.
16. Brimioulle, R.; Bach, T. "Enantioselective Lewis Acid Catalysis of Intramolecular Enone [2+2] Photocycloaddition Reactions" *Science* **2013**, *342*, 840–843.
17. Hennig, H.; Rehorek, D. "Photocatalytic Systems with Light-Sensitive Coordination Compounds and Possibilities of their Spectroscopic Sensitization—An Overview" *Coord. Chem. Rev.* **1985**, *61*, 1–53.
18. (a) Kalyanasundaram, K. "Photophysics, photochemistry and Solar Energy Conversion with Tris(bipyridyl)ruthenium(II) and its Analogues" *Coord. Chem. Rev.* **1982**, *46*, 159–244. (b) Flamigni, L.; Barbieri, A.; Sabatini, C.; Ventura, B.; Barigelletti, F. "Photochemistry and Photophysics of Coordination Compounds: Iridium" *Top. Curr. Chem.* **2007**, *281*, 143–203.
19. Prier, C. K.; Rankic, D. A.; MacMillan, D. W. C. "Visible Light Photoredox Catalysis with Transition Metal Complexes: Applications in Organic Synthesis" *Chem. Rev.* **2013**, *113*, 5322–5363.
20. General review: (a) Salomon, R. G. "Homogeneous Metal-Catalysis in Organic Photochemistry" *Tetrahedron* **1983**, *39*, 485–575. Transformation depicted in Scheme 2-x: (b) Ghosh, S.; Raychaudhuri, S. R.; Salomon, R. G. "Synthesis of Cyclobutanated Butyrolactones via Copper(I)-Catalyzed Intermolecular Photocycloadditions of Homoallyl Vinyl or Diallyl Ethers" *J. Am. Chem. Soc.* **1987**, *52*, 83–90.
21. (a) Salomon, R. G.; Kochi, J. K. "Copper(I) Catalysis in Photocycloadditions. I. Norbornene." *J. Am. Chem. Soc.* **1974**, *96*, 1137–1144. (b) Salomon, R. G.; Folting, K.; Streib, W. E.; Kochi, J. K. "Copper(I) Catalysis in Photocycloadditions. II. Cyclopentene, Cyclohexene, and Cycloheptene" *J. Am. Chem. Soc.* **1974**, *96*, 1145–1152.
22. Salomon, R.G.; Kochi, J.K. "Cationic Olefin Complexes of Copper(I). Structure and Bonding in Group 1b Metal-Olefin Complexes" *J. Am. Chem. Soc.* **1973**, *95*, 1889–1897.
23. Discussion of MLCT pathway: (a) Budzelaar, P. H. M. "Bonding in the Ground State and Excited States of Copper-Alkene Complexes" *J. Organomet. Chem.* **1987**, *331*, 397–407. (b) Geiger, D.; Ferraudi, G. "Photochemistry of Cu–Olefin Complexes: a Flash Photochemical Investigation of the Reactivity of Cu(ethylene)⁺ and Cu(*cis,cis*-1,5-cyclooctadiene)₂⁺" *Inorg. Chim. Acta.* **1985**, *101*, 197–210. Discussion of LMCT pathway: (c) Salomon, R. G.; Sinha, A.; Salomon, M. F. "Copper(I) Catalysis of Olefin Photoreactions. Photorearrangement and Photofragmentation of Methylene cyclopropanes" *J. Am. Chem. Soc.* **1978**, *100*, 520–526. (d) Salomon, R. G.; Salomon, M. F. "Copper(I) Catalysis of Olefin Photoreactions.

-
- Photorearrangements and Photofragmentation of 7-Methyleneorcarane" *J. Am. Chem. Soc.* **1976**, *98*, 7454–7456.
24. Salomon, R. G.; Kochi, J. K. "Copper(I) Triflate: A Superior Catalyst for Olefin Photodimerization" *Tetrahedron Lett.* **1973**, *14*, 2529–2532.
25. Salomon, R. G.; Ghosh, S.; Zagorski, M. G.; Reitz, M. "Copper(I) Catalysis of Olefin Photoreactions. 10. Synthesis of Multicyclic Carbon Networks by Photobicyclization" *J. Org. Chem.* **1982**, *47*, 829–836.
26. Avasthi, K.; Salomon, R. G. "A Copper(I)-Catalyzed Photobicyclization Route to exo-1,2-Polymethylene- and 7-Hydroxynorbornanes. Nonclassical 2-Bicyclo[3.2.0]heptyl and 7-Norbornyl Carbenium Ion Intermediates" *J. Org. Chem.* **1986**, *51*, 2556–2562.
27. Salomon, R. G.; Ghosh, S.; Raychaudhuri, S. R.; Miranti, T. S. "Synthesis of Multicyclic Pyrrolidines via Copper(I) Catalyzed Photobicyclization of Ethyl *N,N*-Diallyl Carbamates" *Tetrahedron Lett.* **1984**, *25*, 3167–3170.
28. Bach, T.; Kruger, C.; Harms, K. "The Stereoselective Synthesis of 2-Substituted 3-Azabicyclo[3.2.0]heptanes by Intramolecular [2+2]-Photocycloaddition Reactions" *Synthesis* **2000**, *2*, 305–320.
29. Langer, K.; Mattay, J. "Stereoselective Intramolecular Copper(I)-Catalyzed [2 + 2]-Photocycloadditions. Enantioselective Synthesis of (+)- and (–)-Grandisol" *J. Org. Chem.* **1995**, *60*, 7256–7266.
30. Holt, D. J.; Barker, W. D.; Jenkins, P. R.; Ghosh, S.; Russell, D. R.; Fawcett, J. "The Copper(I) Catalysed [2+2] Intramolecular Photoannulation of Carbohydrate Derivatives" *Synlett* **1999**, *SI*, 1003–1005.
31. Banerjee, S.; Ghosh, S. "Intramolecular [2 + 2] Photocycloaddition of Alkenes Incorporated in a Carbohydrate Template. Synthesis of Enantiopure Bicyclo[3.2.0]heptanes and -[6.3.0]undecanes" *J. Org. Chem.* **2003**, *68*, 3981–3989.
32. Braun, I.; Rudroff, F.; Mihovilovic, M. D.; Bach, T. "Synthesis of Enantiomerically Pure Bicyclo[4.2.0]octanes by Cu-Catalyzed [2+2] Photocycloaddition and Enantiotopos-Differentiating Ring Opening" *Angew. Chem. Int. Ed.* **2006**, *45*, 1–5.
33. McMurry, J. E.; Choy, W. "Total Synthesis of α - and β -Panasinsene" *Tetrahedron Lett.* **1980**, *21*, 2477–2480.
34. Bach, T.; Spiegel, A. "Stereoselective Total Synthesis of the Tricyclic Sesquiterpene (\pm)-Kelsoene by an Intramolecular Cu(I)-Catalyzed [2+2]-Photocycloaddition Reaction" *Synlett* **2002**, *8*, 1305–1307.

-
35. Sarkar, N.; Nayek, A.; Ghosh, S. "Copper(I)-Catalyzed Intramolecular Asymmetric [2 + 2] Photocycloaddition. Synthesis of Both Enantiomers of Cyclobutane Derivatives" *Org. Lett.* **2004**, *6*, 1903–1095.
 36. Lotito, K. J.; Peters, J. C. "Efficient Luminescence from Easily Prepared Three-Coordinate Copper(I) Arylamidophosphines" *Chem. Commun.* **2010**, *46*, 3690–3692.
 37. Creutz, S. E.; Lotito, K. J.; Fu, G. C.; Peters, J. C. "Photoinduced Ullmann C-N Coupling: Demonstrating the Viability of a Radical Pathway" *Science* **2012**, *338*, 647–651.
 38. Ziegler, D. T.; Choi, J.; Munoz-Molina, J. M.; Bissember, A. C.; Peters, J. C.; Fu, G. C. "A Versatile Approach to Ullmann C-N Couplings at Room Temperature: New Families of Nucleophiles and Electrophiles for Photoinduced, Copper-Catalyzed Processes" *J. Am. Chem. Soc.* **2013**, *135*, 13107–13112.
 39. Bissember, A. C.; Lundgren, R. J.; Creutz, S. E.; Peters, J. C.; Fu, G. C. "Transition-Metal-Catalyzed Alkylations of Amines with Alkyl Halides: Photoinduced, Copper-Catalyzed Couplings of Carbazoles" *Angew. Chem. Int. Ed.* **2013**, *52*, 5129–5133.
 40. Do, H. Q.; Bachman, S.; Bissember, A. C.; Peters, J. C.; Fu, G. C. "Photoinduced, Copper-Catalyzed Alkylation of Amides with Unactivated Secondary Alkyl Halides at Room Temperature" *J. Am. Chem. Soc.* **2014**, *136*, 2162–2167.
 41. Uyeda, C.; Tan, Y. C.; Fu, G. C.; Peters, J. C. "A New Family of Nucleophiles for Photoinduced, Copper-Catalyzed Cross-Couplings via Single-Electron Transfer: Reactions of Thiols with Aryl Halides Under Mild Conditions (0 °C)" *J. Am. Chem. Soc.* **2013**, *135*, 9548–9552.
 42. Tan, Y.; Muñoz-Molina, J. M.; Fu, G. C.; Peters, J. C. "Oxygen Nucleophiles as Reaction Partners in Photoinduced, Copper-Catalyzed Cross-Couplings: *O*-Arylations of Phenols at Room Temperature" *Chem. Sci.* **2014**, DOI: 10.1039/c4sc00368c.

Chapter 2. Visible Light Photocatalysis of Radical Anion Hetero-Diels–Alder Cycloadditions

Portions of this work have been previously published:

Hurtley, A. E.; Cismesia, M. A.; Ischay, M. A.; Yoon, T. P. "Visible Light Photocatalysis of Radical Anion Hetero-Diels–Alder Cycloadditions" *Tetrahedron* **2011**, *67*, 4442–4448.

2.1 Introduction

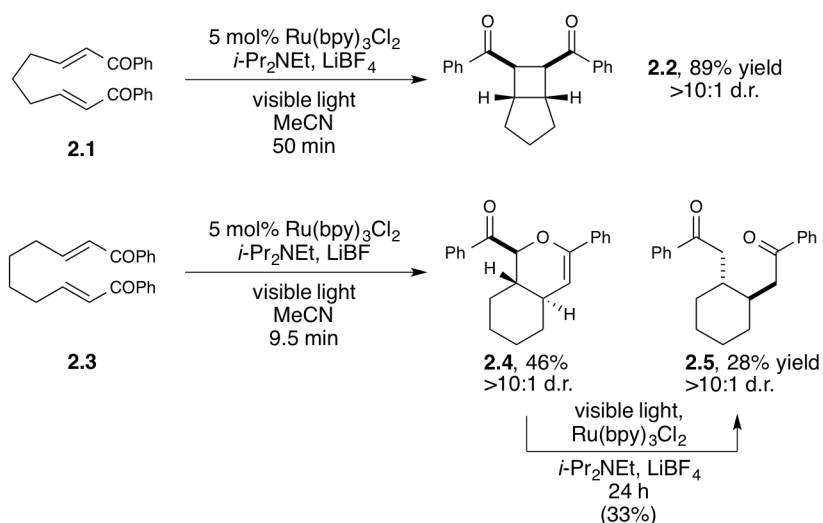
Tetrahydropyrans and related six-membered heterocycles are ubiquitous substructures found in a variety of carbohydrates, polyketide natural products, and other bioactive compounds. Among the most powerful methods for the rapid construction of densely functionalized six-membered oxaheterocycles are formal hetero-Diels–Alder cycloadditions. These methods have been the subject of numerous reviews¹ and have been extensively utilized as key steps in the synthesis of many complex organic structures.² Nevertheless, hetero-Diels–Alder cycloadditions proceed efficiently under mild conditions only when the components are electronically well matched, which involves the reaction of either electron-rich dienes with electron-deficient carbonyl compounds or electron-poor heterodienes with electron-rich olefins. Electronically mismatched hetero-Diels–Alder cycloadditions between two electron-deficient components typically require forcing conditions that limit their utility in synthesis.³

We,⁴ along with several other research groups,⁵ have recently begun to explore the ability of metal polypyridyl photocatalysts to promote a variety of synthetically useful transformations upon irradiation with visible light.⁶ In particular, our lab has become interested in exploiting the ability of $\text{Ru}(\text{bpy})_3^{2+}$ and related photoredox catalysts to initiate one-electron transfer processes without the need for strong stoichiometric reductants or oxidants. The facility with which radical cations and radical anions can be generated under photocatalytic conditions has enabled us to explore the chemistry of these reactive intermediates, whose utility in synthesis has been underdeveloped in comparison to that of neutral radicals. In this chapter, we describe high-yielding and highly diastereoselective radical anion hetero-Diels–Alder cycloadditions between electronically mismatched enones can be conducted using our group's strategy for visible light photocatalysis.

2.2 Results and Discussion

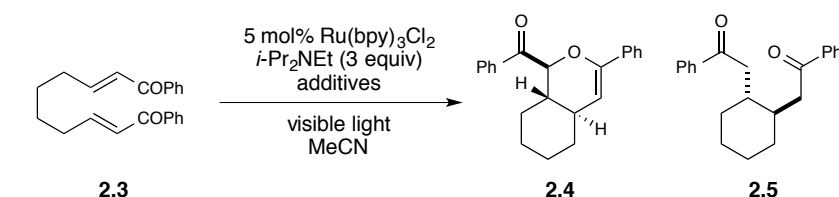
Our discovery of the hetero-Diels–Alder cycloaddition arose during an exploration of the scope of the photocatalytic intramolecular [2+2] enone cycloaddition developed in our labs. We observed that the length of the aliphatic tethering group had a dramatic influence on the intrinsic reactivity of the system (Scheme 2-1). Bis(enone) **2.1** bearing a three-carbon tether undergoes efficient [2+2] cycloaddition upon irradiation with visible light in the presence of $\text{Ru}(\text{bpy})_3^{2+}$ with LiBF_4 and $i\text{-Pr}_2\text{NEt}$ as additives.^{4a} However, when bis(enone) **2.3**, in which the tether length was increased by one methylene unit, was subjected to the same conditions, the expected [2+2] cycloadduct was not formed. Instead, the major products are the hetero-Diels–Alder cycloadduct **2.4** and the product of reductive monocyclization (**2.5**). Both products are formed with high diastereoselectivity. While analogous compounds were reported to be side products in the electrochemically induced [2+2] cycloadditions of **2.1** reported by Bauld and Krische,⁷ we did not observe their formation in our studies of the photocatalytic cycloaddition of **2.1**. Intrigued by this unexpected reactivity, we elected to initiate an examination of this hetero-Diels–Alder process by developing conditions that allow selective access to [4+2] cycloadduct **2.4**.

Scheme 2-1. Photocatalytic [2+2] and [4+2] cycloadditions.



We noted that under our initial conditions the selectivity for formation of **2.4** over the undesired reductive cyclization product **2.5** was high at relatively low conversions but steadily decreased over the course of the reaction. We hypothesized, therefore, that **2.5** might be a decomposition product arising from over-reduction and reductive cleavage of **2.4**. Indeed, when **2.4** was isolated and resubjected to the reaction conditions for 24 h, we observed formation of **2.5** in 33% yield, which suggested that the long reaction times were in part responsible for the formation of **2.5**. We therefore sought conditions that would accelerate the overall rate of conversion and limit the formation of this undesired side product.

Table 2-1. Optimization of [4+2] cycloaddition of **2.2**.^a

			
2.3		2.4	2.5
Entry	Additives	Time	% Yield (2.4/2.5) ^{b,c}
1	LiBF ₄ (2 equiv)	9.5 h	28/41
2	LiBF₄ (2 equiv), H₂O (10 equiv)	1 h	86^d/<5
3	LiBF ₄ (2 equiv), MeOH (10 equiv)	1 h	25/19 ^e
4	LiBF ₄ (2 equiv), CF ₃ CH ₂ OH (10 equiv)	1 h	61/25
5	H ₂ O (10 equiv)	1 h	0/0
6	Bu ₄ N ⁺ BF ₄ ⁻ (2 equiv), H ₂ O (10 equiv)	1 h	0/0

^a Reactions conducted in degassed MeCN (0.1 M) under irradiation with a 200 W tungsten filament light bulb at a distance of 30 cm.

^b Yield determined by ¹H NMR spectroscopy against an internal standard unless otherwise noted.

^c The products were formed in >10:1 d.r. unless otherwise noted.

^d Isolated yield.

^e **2.5** was formed as a 2:1 mixture of diastereomers in this experiment.

In an initial screen of solvents, we found that the presence of water had a profound influence on the rate of the reaction. Upon addition of 10 equiv of water, the reaction time decreased dramatically from 9.5 h to 1 h (Table 2-1, entries 1 and 2). Importantly, very little of the undesired over-reduction product **2.5** was formed, and the hetero-Diels–Alder cycloadduct

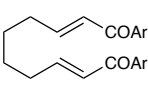
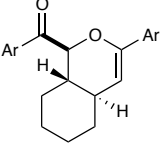
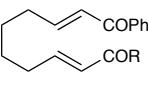
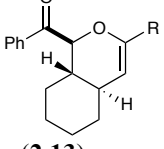
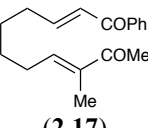
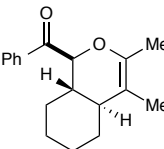
could be isolated in 86% yield. Water proved to be a uniquely effective protic additive;⁸ while both methanol and trifluoroethanol also afforded an increase in the rate of the reaction, neither provided good yields of the desired [4+2] cycloadduct. Control studies indicated that LiBF₄ was an essential additive. No consumption of the starting bis(enone) occurred when LiBF₄ was either omitted from the reaction or was replaced by Bu₄N⁺BF₄⁻. This indicates that the Lewis acidity of the lithium cation is crucial for successful cycloaddition,⁹ as it is in the analogous [2+2] cycloaddition reactions reported by our group.^{4a}

We next conducted a survey of the scope of the hetero-Diels–Alder cycloaddition, and the results are summarized in Table 2-2. A number of symmetrical aryl bis(enones) were found to be excellent substrates for this reaction. Both electron-deficient (entries 2–3) and electron-rich (entry 4) aryl enones react in high yield and diastereoselectivity, as do polyaromatic (entry 5) and heteroaryl enones (entry 6). Fluoride substitution at the ortho position is well tolerated (entry 7), although larger groups at this position significantly hinder reactivity (entry 8). In all cases, the desired [4+2] cycloadduct was formed with excellent diastereoselectivity.

We also became interested in exploring the cycloadditions of unsymmetrical bis(enones) in which two possible constitutional isomers could reasonably be formed. We examined the reactions of a number of substrates bearing one aryl enone and one aliphatic enone under our optimized reaction conditions. An α -benzyloxy enone underwent efficient cycloaddition to afford a single regioisomer of the hetero-Diels–Alder product (entry 9). Other substrates were less successful. A methyl enone required significantly longer reaction times and consequently afforded lower yields of the desired cycloadduct, although the regioselectivity of this process was also excellent (entry 10). Upon careful optimization, we were able to increase the efficiency of this reaction to 73% by removing water and replacing the LiBF₄ additive with

Mg(ClO₄)₂ (entry 11). Other aliphatic enones also underwent cycloaddition under these conditions, although the yields of these reactions decreased with increasing steric demand (entries 12–14). Reactions involving enoates and α,β -unsaturated thioesters were unsuccessful under both sets of conditions.

Table 2-2. Scope of the photocatalytic [4+2] cycloaddition.^a

Entry	Method ^b	Substrate	Product	Time	% Yield ^c
<div style="display: flex; align-items: center; justify-content: center;"> <div style="text-align: center;">  </div> <div style="text-align: center;">  </div> </div>					
1	A	Ar = Ph (2.4)		1 h	86
2	A	Ar = 4-Cl-C ₆ H ₄ (2.6)		30 min	70
3	A	Ar = 4-CF ₃ -C ₆ H ₄ (2.7)		30 min	83 ^d
4	A	Ar = 4-AcO-C ₆ H ₄ (2.8)		1 h	76
5	A	Ar = 2-naphthyl (2.9)		1.5 h	77
6	A	Ar = 2-furyl (2.10)		30 min	77
7	A	Ar = 2-F-C ₆ H ₄ (2.11)		30 min	84
8	A	Ar = 2-Me-C ₆ H ₄ (2.12)		6 h	5 ^e
<div style="display: flex; align-items: center; justify-content: center;"> <div style="text-align: center;">  </div> <div style="text-align: center;">  </div> </div>					
9	A	R = CH ₂ OBn (2.13)		20 min	76
10	A	R = Me (2.14)		2 h	39
11	B	R = Me (2.14)		10 min	73
12	B	R = <i>i</i> -Pr (2.15)		1.5 h	58
13	B	R = <i>t</i> -Bu (2.16)		6 h	12 ^e
<div style="display: flex; align-items: center; justify-content: center;"> <div style="text-align: center;">  <p>(2.17)</p> </div> <div style="text-align: center;">  <p>(2.18)</p> </div> </div>					
14	B			5 h	17 ^e

^a All reactions were irradiated with a 200 W tungsten filament light bulb at a distance of 30 cm.

^b Method A: Bis(enone) substrate (1 equiv), Ru(bpy)₃Cl₂ (0.05 equiv), LiBF₄ (2 equiv), *i*-Pr₂NEt (3 equiv), and H₂O (10 equiv) in degassed MeCN (0.1 M). Method B: Bis(enone) substrate (1 equiv), Ru(bpy)₃Cl₂ (0.05 equiv), Mg(ClO₄)₂ (2 equiv), and *i*-Pr₂NEt (5 equiv) in degassed MeCN (0.025 M).

^c Data represent the average isolated yields from two reproducible experiments, unless otherwise noted.

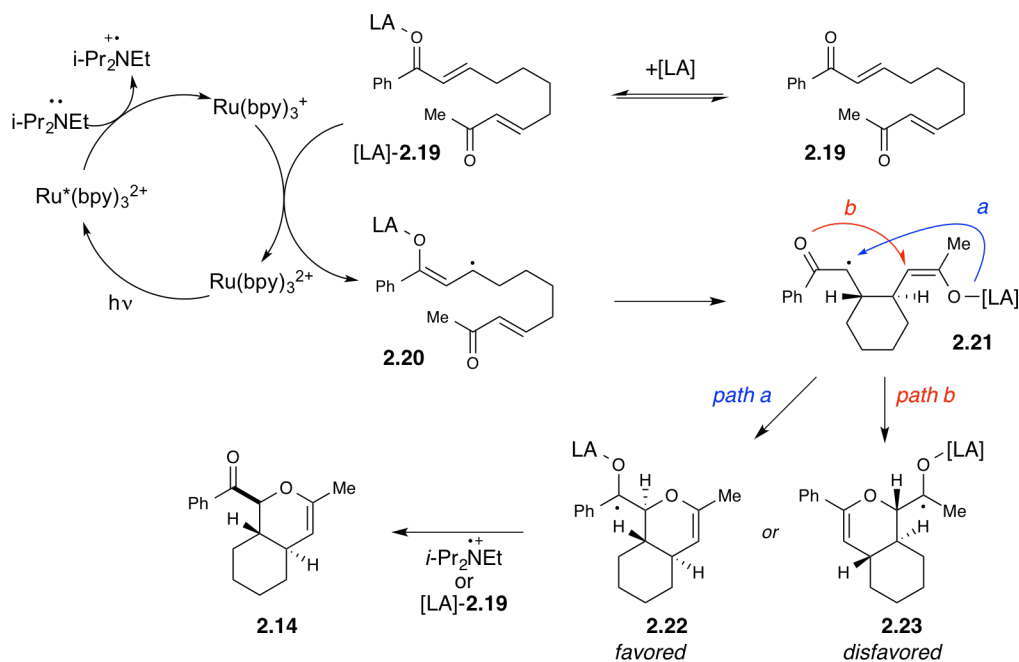
^d Isolated yield of a single experiment.

^e Yield of a single experiment, determined by ¹H NMR spectroscopy against an internal standard.

The high level of regioselectivity observed in the cycloaddition of unsymmetrical bis(enones) (e.g., **2.19**) can be rationalized by the mechanism outlined in Scheme 2-2, which is

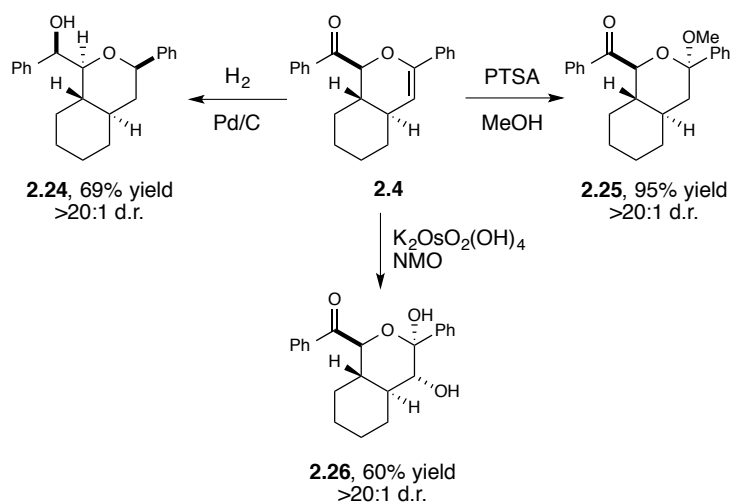
based upon Krische and Bauld's proposal that radical anion cycloadditions proceed in a step-wise fashion.⁷ Photoexcitation of $\text{Ru}(\text{bpy})_3^{2+}$ with visible light affords an excited state that can undergo efficient reductive quenching by $i\text{-Pr}_2\text{NEt}$. The Lewis acid-activated enone complex ([LA]-**2.19**) can then accept an electron from the resulting $\text{Ru}(\text{bpy})_3^+$ reductant to afford an activated radical anion intermediate (**2.20**) that should undergo β - β coupling to afford a monocyclized distonic radical anion intermediate (**2.21**). Formation of the carbon-oxygen bond could proceed to form two possible isomeric ketyl radicals (**2.22** and **2.23**). We speculate that the greater stabilization of the aryl ketyl radical may then serve as a driving force for selective formation of **2.22**. Finally, the neutral hetero-Diels-Alder cycloadduct is produced upon loss of one electron, either to another equivalent of enone in a chain propagation step or to the photogenerated amine radical cation in a chain termination step.

Scheme 2-2. Proposed mechanism for regioselective hetero-Diels-Alder cycloaddition of unsymmetrical bis(enone) **2.19**.



The dihydropyrans formed in this study can be synthetically elaborated in a number of ways (Scheme 2-3). The enol ether functionality of **2.4** can be converted to an acetal (**2.25**) upon treatment with methanol and catalytic PTSA in excellent yield and diastereoselectivity. Dihydroxylation of the olefin under Upjohn conditions¹⁰ similarly provides the corresponding diol (**2.26**) with high stereochemical purity. Finally, catalytic hydrogenation of **2.4** reduces both the enol ether and the aryl ketone, introducing two new stereocenters with very high diastereoselectivity in the doubly reduced product (**2.24**).

Scheme 2-3. Diastereoselective functionalization of **3.4**.



The origins of the chemoselectivity for [2+2] vs [4+2] pathways in these radical anion processes are not clear at this time, but the length of the aliphatic tether appears to be critical. Subjecting the three-carbon tethered bis(enone) **2.1** to the optimized conditions in Table 2 produced only [2+2] cycloadduct and none of the hetero-Diels–Alder product. Five- and six-carbon tethers that would afford medium-sized rings produced neither cycloadduct. We speculate that the initial bond-forming event in the stepwise cycloaddition of **2.1** has a kinetic preference for formation of the *cis* cyclopentane isomer. Subsequent coupling of the α,α carbons would afford the [3.2.0] bicycloheptane ring structure observed in the intramolecular

cyclobutanation.^{4a} On the other hand, we speculate that the initial carbon-carbon bond formation in the cycloaddition of **2.3** produces a *trans*-substituted cyclohexane intermediate. Coupling of the a positions would afford a *trans* [4.2.0] ring system that we would expect to be prohibitively strained, while formation of a new C–O bond would produce a conformationally reasonable *trans* oxadecalin bicycle.

2.3 Conclusions

Our group's investigations of visible light photocatalysis have led to the discovery of an interesting intramolecular hetero-Diels–Alder cycloaddition. This reactivity is notable for a number of reasons. First, the intermediacy of an enone radical anion facilitates the efficient coupling of a dienophile and heterodiene that are both electron-deficient, which enables the construction of a cycloadduct that is difficult to access upon thermal activation. Second, the diastereoselectivity of the process is high, and the products are amenable to a variety of further synthetic manipulations. Finally, one of the most intriguing unanswered questions is how the effect of the tether length controls the chemoselectivity for [4+2] vs. [2+2] cycloaddition. Studies to elucidate the origins of this divergent reactivity are underway in our laboratory, and these investigations provide a promising framework for further studies of the chemistry of photogenerated radical anions.

2.4 Contributions

Megan Cismesia conducted the experiments depicted in **Scheme 2-4** and characterized hydrogenation product **2.24** by derivatization and X-ray crystallography (refer to Appendix C for experimental details).

2.5 Experimental

2.5.1 General experimental information

Acetonitrile, dichloromethane and tetrahydrofuran were purified by elution through alumina on a glass contour solvent system as described by Grubbs.¹¹ Diisopropylethylamine was purified by distillation from CaH_2 immediately prior to use. $\text{Ru}(\text{bpy})_3\text{Cl}_2 \cdot 6\text{H}_2\text{O}$ was purchased from Strem and used without purification. LiBF_4 and $\text{Mg}(\text{ClO}_4)_2$ were purchased from Sigma-Aldrich and Strem, respectively, and stored in a glove box under an atmosphere of nitrogen. Millipore water was used in all photochemical reactions depicted in tables 2, 3 and 6 and prepared as a stock solution in acetonitrile. Diastereomeric ratios for all products were determined by ^1H NMR spectroscopic analysis of the isolated products after flash column chromatography. Flash column chromatography was performed with Silicycle 40-63Å silica (230-400 mesh).¹² All glassware was oven-dried prior to use. ^1H and ^{13}C NMR data for all previously uncharacterized compounds were obtained using Varian Unity-500 spectrometers and are referenced to TMS (0.0 ppm) and CDCl_3 (77.0 ppm), respectively. Mass spectrometry was performed with a Waters (Micromass) AutoSpec®. These facilities are funded by the NSF (CHE-9974839, CHE-9304546) and the University of Wisconsin.

2.5.2 Preparation of bis(enone) substrates

General procedure: A dry 3-neck round-bottomed flask was charged with cyclohexene (1 equiv) and CH_2Cl_2 (0.3-0.4 M) and cooled to $-78\text{ }^\circ\text{C}$. The reaction mixture was stirred while a stream of ozone was passed through the solution until a blue color persisted. The excess ozone was removed by a flow of oxygen and the ozonide was quenched with dimethyl sulfide (3

equiv). The ylide (2.5 equiv) was added in a solution of CH_2Cl_2 and the reaction mixture was then allowed to warm slowly to room temperature and stirred under N_2 for 24-48 hours. The reaction mixture was concentrated *in vacuo* and purified by flash column chromatography on silica gel.

(2E,8E)-1,10-bis(4-chlorophenyl)deca-2,8-diene-1,10-dione (2.27): Prepared according to the

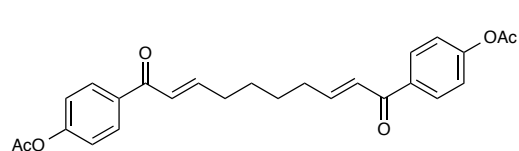
general procedure with 1.2 mL cyclohexene (12.2 mmol), 30 mL CH_2Cl_2 , 2.7 mL DMS (36.6 mmol), and 12.7 g 1-(4-chloro-phenyl)-2-(triphenylphosphoranylidene)-ethanone¹³ (30.5 mmol). Following ozonolysis, the Wittig reaction was allowed to stir for 36 hours at room temperature and then concentrated *in vacuo*. The residue was purified by flash column chromatography on silica gel (6:1 hexanes:ethyl acetate) and recrystallization in ethyl acetate/hexanes to afford the product (0.828 g, 2.14 mmol, 18%) as a white, crystalline solid. ¹H NMR: (500 MHz, CDCl_3) δ 7.87 (dt, J = 8.6, 1.9 Hz, 4H), 7.44 (dt, J = 8.6, 1.9 Hz, 4H), 7.07 (dt, J = 15.3, 7.0 Hz, 2H), 6.86 (dt, J = 15.3, 1.5 Hz, 2H), 2.37 (tdd, J = 6.7, 6.3, 1.2 Hz, 4H), 1.61 (m, 4H); ¹³C NMR: (125 MHz, CDCl_3) δ 189.3, 149.7, 139.1, 136.2, 129.9, 128.9, 125.7, 32.6, 27.7. HRMS (EI) calculated for $[\text{C}_{22}\text{H}_{20}\text{Cl}_2\text{O}_2]^+$ requires m/z 386.0835, found 386.0821.

(2E,8E)-1,10-bis(4-(trifluoromethyl)phenyl)deca-2,8-diene-1,10-dione (2.28): Prepared

according to the general procedure with 0.140 mL cyclohexene (1.34 mmol), 3.5 mL CH_2Cl_2 , 0.3 mL DMS (4.00 mmol), and 1.5 g 1-(4-(trifluoromethyl)phenyl)-2-(triphenylphosphoranylidene)-ethanone¹³ in a solution of 2 mL

CH₂Cl₂. Following ozonolysis, the Wittig reaction was allowed to stir for 48 hours at room temperature and then concentrated *in vacuo*. The residue was purified by flash column chromatography on silica gel (6:1 hexanes:ethyl acetate) to afford the product (90.5 mg, 0.200 mmol, 30%) as a white solid. ¹H NMR: (500 MHz, CDCl₃) δ 8.01 (d, J = 8.2 Hz, 4H), 7.74 (d, J = 8.2 Hz, 4H), 7.09 (dt, J = 15.2, 7.0 Hz, 2H), 6.87 (dt, J = 15.2, 1.3 Hz, 2H), 2.39 (tdd, J = 6.8, 6.8, 1.3 Hz, 4H), 1.63 (m, 4H); ¹³C NMR: (125 MHz, CDCl₃) δ 192.5, 153.3, 143.4, 136.7 (q, ²J_{CF} = 33 Hz), 131.5, 128.6, 128.3 (q, ³J_{CF} = 3.5 Hz), 126.3 (q, ¹J_{CF} = 273 Hz), 35.3, 30.3. HRMS (EI) calculated for [C₂₄H₂₀F₆O₂]⁺ requires 454.1362, found 454.1367.

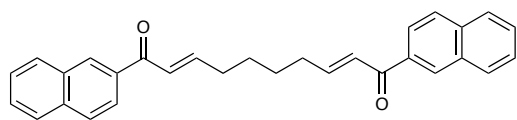
((2E,8E)-deca-2,8-dienedioyl)bis(4,1-phenylene)diacetate (2.29): Prepared according to the



general procedure with 0.3 mL (3.01 mmol) cyclohexene, 10 mL CH₂Cl₂, 0.7 mL DMS (9 mmol), and 3.3 g 1-(4-acetoxy-phenyl)-2-

(triphenylphosphoranylidene)-ethanone¹⁴ (2.7 mmol) in a solution of 5 mL CH₂Cl₂. Following ozonolysis, the Wittig reaction was allowed to stir for 48 hours at room temperature and then concentrated *in vacuo*. The residue was purified by flash column chromatography (3:1 hexanes:acetone) and recrystallization in EtOAc/hexanes to afford the product (0.435 g, 1.00 mmol, 33%) as a white crystalline solid. ¹H NMR: (500 MHz, CDCl₃) δ 7.97 (dt, J = 8.6, 1.8 Hz, 2H), 7.20 (dt, J = 8.6, 1.8 Hz, 2H), 7.07 (dt, J = 15.3, 6.8 Hz, 2H), 6.88 (dt, J = 15.3, 1.3 Hz, 2H), 2.36 (m, 4H), 2.33 (s, 6H), 1.61 (m, 4H); ¹³C NMR: (125 MHz, CDCl₃) δ 189.5, 168.9, 154.1, 149.4, 135.5, 130.1, 125.9, 121.7, 32.5, 27.7, 21.1. HRMS (EI) calculated for [C₂₆H₂₆O₆]⁺ requires *m/z* 434.1724, found 434.1725.

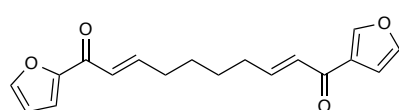
(2E,8E)-1,10-di(naphthalen-2-yl)deca-2,8-diene-1,10-dione (2.30): Prepared according to the



general procedure with 0.86 mL cyclohexene (8.5 mmol), 21 mL CH₂Cl₂, 2 mL DMS (25.5 mmol), and

9.17 g 1-(2-naphthalenyl)-2-(triphenylphosphoranylidene)-ethanone¹⁵ (21.3 mmol) in a solution of 20 mL CH₂Cl₂. Following ozonolysis, the Wittig reaction was allowed to stir for 36 hours at room temperature and then concentrated *in vacuo*. The residue was purified by flash column chromatography (8:1 hexanes:acetone) to afford the product (0.720 g, 1.72 mmol, 20%) as a pale yellow solid. ¹H NMR: (500 MHz, CDCl₃) δ 8.45 (bs, 2H), 8.03 (dd, J = 8.7, 1.7 Hz, 2H), 7.95 (d, J = 8.1 Hz, 2H), 7.90 (d, J = 8.7 Hz, 2H), 7.86 (d, J = 8.1 Hz, 2H), 7.59 (dt, J = 7.0, 1.2 Hz, 2H), 7.54 (dt, J = 7.0, 1.2 Hz, 2H), 7.15 (dt, J = 15.3, 6.7 Hz, 2H), 7.08 (d, J = 15.3 Hz, 2H), 2.43 (td, J = 6.3, 6.1 Hz, 4H), 1.67 (m, 4H); ¹³C NMR: (125 MHz, CDCl₃) δ 190.5, 149.1, 135.4, 135.2, 132.5, 130.0, 129.5, 128.5, 128.3, 127.8, 126.7, 126.1, 124.5, 32.6, 27.9. HRMS (EI) calculated for [C₃₀H₂₆O₂]⁺ requires *m/z* 418.1928, found 418.1925.

(2E,8E)-1-(furan-2-yl)-10-(furan-3-yl)deca-2,8-diene-1,10-dione (2.31): Prepared according

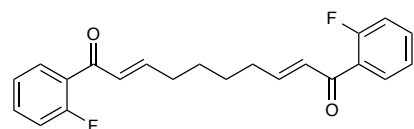


to the general procedure with 0.41 mL cyclohexene (4.05 mmol), 10 mL CH₂Cl₂, 1.47 mL DMS (2.00 mmol), and 3.7 g

1-furan-2-yl-2-(triphenylphosphoranylidene)-ethanone¹⁶ in a solution of 25 mL CH₂Cl₂. Following ozonolysis, the Wittig reaction was allowed to stir for 48 hours at room temperature and then concentrated *in vacuo*. The residue was purified by flash column chromatography on silica gel (2:1 hexanes:ethyl acetate) to afford the product (0.290 g, 0.972 mmol, 24%) as a white solid. ¹H NMR: (500 MHz, CDCl₃) δ 7.62 (dd, J = 1.5, 0.6 Hz, 2H), 7.25 (dd, J = 3.7, 0.6 Hz, 2H), 7.15 (dt, J = 15.5, 7.0 Hz, 2H), 6.82 (dt, J = 15.5, 1.5 Hz, 2H), 6.56 (dd, J = 3.7, 1.5 Hz,

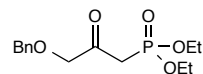
2H), 2.35 (tdd, $J = 6.1, 6.1, 1.3$ Hz, 4H), 1.60 (m, 4H); ^{13}C NMR: (125 MHz, CDCl_3) δ 178.1, 153.3, 148.5, 146.5, 125.2, 117.6, 112.4, 32.4, 27.6. HRMS (EI) calculated for $[\text{C}_{18}\text{H}_{18}\text{O}_4]^+$ requires m/z 298.1200, found 298.1211.

(2E,8E)-1,10-bis(2-fluorophenyl)deca-2,8-diene-1,10-dione (2.32): Prepared according to the



general procedure with 0.6 mL cyclohexene (5.9 mmol), 20 mL CH_2Cl_2 , 1.6 mL DMS (17.7 mmol), and 1-(2-fluorophenyl)-2-(triphenylphosphoranylidene)-ethanone in a solution of 15 mL CH_2Cl_2 . Following ozonolysis, the Wittig reaction was allowed to stir for 48 hours at room temperature and then concentrated in vacuo. The residue was purified by flash column chromatography (4:1 hexanes:acetone) to afford the product (0.235 g, 0.663 mmol, 11%) as a white solid. ^1H NMR: (500 MHz, CDCl_3) δ 7.71 (td, $J = 7.6, 1.8$ Hz, 2H), 7.49 (m, 2H), 7.23 (td, $J = 7.6, 0.8$ Hz, 2H), 7.12 (ddd, $J = 10.6, 8.2, 0.7$ Hz, 2H), 6.97 (dtd, $J = 15.5, 7.0, 1.8$ Hz, 2H), 6.73 (ddt, $J = 15.5, 2.8, 1.5$ Hz, 2H), 2.33 (m, 4H), 1.58 (m, 4H); ^{13}C NMR: (125 MHz, CDCl_3) δ 189.6 (d, $J = 2.1$ Hz), 161.0 (d, $J = 253.6$ Hz), 149.7, 133.7 (d, $J = 8.6$ Hz), 130.8 (d, $J = 2.5$ Hz), 129.8 (d, $J = 5.9$ Hz), 127.0 (d, $J = 13.6$ Hz), 124.4 (d, $J = 3.1$ Hz), 116.4 (d, $J = 23.1$ Hz), 32.3, 27.5. HRMS (EI) calculated for $[\text{C}_{22}\text{H}_{20}\text{F}_2\text{O}_2]^+$ requires m/z 354.1426, found 354.1409.

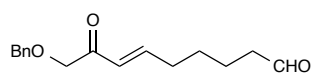
Diethyl (3-(benzyloxy)-2-oxopropyl)phosphonate (2.33): A dry 3-neck round-bottomed flask



was charged with *n*-BuLi (1.6 M solution in hexanes, 7.05 mL, 11.28 mmol) and dry THF (12 mL) under N_2 and cooled to -78°C . Diethyl methylphosphonate (1.5 mL, 10.25 mmol) in dry THF (1 mL) was added dropwise to the reaction mixture and allowed to stir for 30 min. CuBr (1.62 g, 11.28 mmol) was then added as a

solid and the reaction mixture was warmed to -50 °C. After stirring for 1.5 hours at that temperature, benzyloxyacetyl chloride (1.6 mL, 10.25 mmol) in dry Et₂O (4.5 mL) was added dropwise and the reaction mixture warmed to -40 °C and allowed to stir at that temperature overnight. The reaction was then quenched with approximately 3 mL H₂O and passed across a plug of silica gel with EtOAc. The eluent was concentrated *in vacuo* and the residue purified by flash column chromatography on silica gel (1.5:1 hexanes:acetone) to afford the product (1.89 g, 6.29 mmol, 61%) as a clear liquid. ¹H NMR: (500 MHz, CDCl₃) δ 7.4-7.29 (m, 5H), 4.61 (s, 2H), 4.21 (s, 2H), 4.18-4.10 (m, 4H), 3.16 (d, J = 22.7 Hz, 2H), 1.32 (t, J = 7.1 Hz, 6H); ¹³C NMR: (125 MHz, CDCl₃) δ 200.0 (d, ³J_{C-P} = 7.5 Hz), 137.1, 128.5, 128.1, 128.0, 75.1, 73.4, 62.7 (d, ²J_{C-P} = 6.1 Hz), 38.5 (d, ¹J_{C-P} = 129.7 Hz), 16.2 (d, ³J_{C-P} = 6.1 Hz). HRMS (EI) calculated for [C₁₄H₂₁O₅P + H]⁺ requires *m/z* 301.1200, found 301.1208.

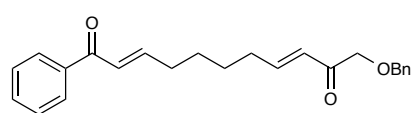
(E)-9-(benzyloxy)-8-oxonon-6-enal: A dry 100 mL 3-neck round-bottomed flask was charged



with NaH (240 mg, 5.99 mmol) and dry THF (23 mL) under N₂ and cooled to 0 °C. Diethyl (3-(benzyloxy)-2-oxopropyl)phosphonate (1.8 g, 5.99 mmol) in dry THF (2 mL) was added dropwise to the reaction mixture and allowed to stir for 25 minutes. 6,6-dimethoxyhexanal¹⁷ (0.8 g, 4.99 mmol) in dry THF (2 mL) was added dropwise and the reaction mixture was stirred at 0 °C for 3 hours. The reaction mixture was then diluted in CH₂Cl₂ and quenched with H₂O. The phases were separated and the aqueous phase was washed an additional 2 times with CH₂Cl₂. The combined organic phases were dried over Na₂SO₄, concentrated *in vacuo*, and the resulting residue was purified by flash column chromatography on silica gel (3:1 hexanes:acetone) to afford the desired acetal as an impure mixture. The crude material was then transferred to a 50 mL round-bottomed flask and stirred in

a mixture of THF (7 mL) and 1 M HCl (7 mL) for 30 minutes at room temperature at which point it was diluted with CH₂Cl₂ and H₂O. The phases were separated and the aqueous layer washed an additional 2 times with CH₂Cl₂. The combined organic phases were dried over Na₂SO₄, concentrated *in vacuo*, and the resulting residue was purified by flash column chromatography on silica gel (3:1 hexanes:acetone) to afford the desired aldehyde (0.606 g, 2.33 mmol, 47% over 2 steps) as a clear oil, which was carried on immediately in the synthesis of (2E,8E)-11-(benzyloxy)-1-phenylundeca-2,8-diene-1,10-dione.

(2E,8E)-11-(benzyloxy)-1-phenylundeca-2,8-diene-1,10-dione (2.34): A dry 25 mL round-

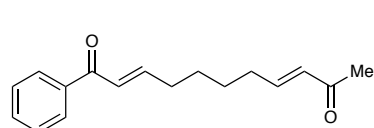


bottomed flask was charged with (E)-9-(benzyloxy)-8-oxonon-6-enal (606 mg, 2.33 mmol),

(benzoylmethylene)triphenylphosphorane (1.77 g, 4.66 mmol), and CH₂Cl₂ (6 mL). The reaction mixture was stirred at room temperature under N₂ for 36 hours at which point an additional portion of (benzoylmethylene)triphenylphosphorane (0.300 g, 0.790 mmol) was added. The reaction mixture was allowed to stir for an additional 12 hours and then concentrated *in vacuo*. The residue was purified by flash column chromatography on silica gel (3:1 hexanes:ethyl acetate) to afford the product (0.609 g, 1.68 mmol, 72%) as a pale yellow oil. ¹H NMR: (500 MHz, CDCl₃) δ7.92 (dt, J = 7.5, 1.5 Hz, 2H), 7.56 (tt, J = 7.5, 1.5 Hz, 1H), 7.47 (tt, J = 7.5, 1.5 Hz, 2H), 7.38-7.28 (m, 5H), 7.03 (dt, J = 15.5, 6.7 Hz, 1H), 6.96 (dt, J = 15.8, 6.8 Hz, 1H), 6.88 (dt, J = 15.5, 1.5 Hz, 1H), 6.31 (dt, J = 15.8, 1.5 Hz, 1H), 4.61 (s, J = Hz, 2H), 4.21 (s, J = Hz, 2H), 2.33 (td, J = 6.6, 6.6 Hz, 2H), 2.26 (td, J = 6.6, 6.6, 2H), 1.55 (m, 4H); ¹³C NMR: (125 MHz, CDCl₃) δ199.6, 193.4, 151.8, 150.8, 140.6, 139.9, 135.3, 131.2, 131.2, 130.7, 130.6,

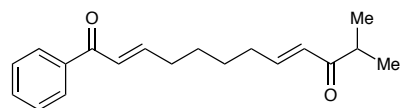
128.9, 128.9, 76.8, 76.0, 35.2, 35.0, 30.4, 30.2. HRMS (EI) calculated for $[C_{24}H_{26}O_3]^+$ requires m/z 362.1877, found 362.1868.

(*E,E*)-8-acetyl-1-benzoyl-1,7-octadiene (2.19): A dry 50 mL round-bottomed flask was charged



with 7-benzoyl-6-heptenal ¹⁸ (1.18 g, 5.4 mmol), 1-(triphenylphosphoranylidene)-2-propanone (5.2 g, 16.3 mmol), and CH_2Cl_2 (13.5 mL). The reaction mixture was stirred under N_2 for 48 hours and then concentrated *in vacuo*. The residue was purified by flash column chromatography on silica gel (4:1 hexanes:ethyl acetate) to afford the product (1.00 g, 3.9 mmol, 73%) as a clear oil. 1H NMR: (500 MHz, $CDCl_3$) δ 7.93 (dt, J = 7.6, 1.3 Hz, 2H), 7.56 (tt, J = 7.6, 1.3 Hz, 1H), 7.47 (tt, J = 7.6, 1.3 Hz, 2H), 7.05 (dt, J = 15.3, 6.9 Hz, 1H), 6.89 (dt, J = 15.3, 1.4 Hz, 1H), 6.79 (dt, J = 16.0, 6.8 Hz, 1H), 6.09 (dt, J = 16.0, 1.4 Hz, 1H), 2.35 (tdd, J = 7.0, 7.0, 1.4 Hz, 2H), 2.27 (dtd, J = 7.1, 6.8, 1.4 Hz, 2H), 2.24 (s, 3H); ^{13}C NMR: (125 MHz, $CDCl_3$) δ 198.6, 190.7, 149.1, 147.7, 137.9, 132.7, 131.5, 128.5, 128.5, 126.2, 32.5, 32.2, 27.7, 27.7, 26.9. HRMS (EI) calculated for $[C_{17}H_{20}O_2]^+$ requires m/z 256.1458, found 256.1451.

(*E,E*)-8-isopropanoyl-1-benzoyl-1,7-octadiene (2.35): A dry 50 ml round-bottomed flask was



charged with 7-benzoyl-6-heptenal (0.863 g, 3.97 mmol), 1-(triphenylphosphoranylidene)-3-methyl-2-butanone (2.03 g, 5.87 mmol), and benzene (10 mL). The reaction flask was fitted to a cold water condensor and allowed to reflux with stirring under N_2 for 18 hours. The reaction mixture was then cooled to room temperature and passed across a plug of silica gel (2:1 hexanes:acetone). The eluent was concentrated *in vacuo* and the resulting residue purified by flash column chromatography on

silica gel (5:1 hexanes:acetone) to afford the product (588 mg, 2.07 mmol, 52%) as a white solid. ^1H NMR: (500 MHz, CDCl_3) δ 7.93 (dt, $J = 7.6, 1.2$ Hz, 2H), 7.56 (tt, $J = 7.6, 1.2$ Hz, 1H), 7.47 (t, $J = 7.6$ Hz, 2H), 7.05 (dt, $J = 15.5, 6.9$ Hz, 1H), 6.89 (d, $J = 15.5$ Hz, 1H), 6.87 (dt, $J = 15.7, 7.1$ Hz, 1H), 6.18 (d, $J = 15.7$ Hz, 1H), 2.82 (sept, $J = 7.0$ Hz, 1H), 2.35 (td, $J = 6.7, 6.3$ Hz, 2H), 2.26 (td, $J = 7.1, 6.7$ Hz, 2H), 1.56 (m, 4H), 1.10 (d, $J = 7.0$ Hz, 6H); ^{13}C NMR: (125 MHz, CDCl_3) δ 204.0, 190.8, 149.2, 146.5, 137.9, 132.7, 128.6, 128.5, 128.5, 126.2, 38.5, 32.5, 32.2, 27.7, 18.4. HRMS (EI) calculated for $[\text{C}_{19}\text{H}_{24}\text{O}_2]^+$ requires m/z 284.1771, found 284.1766.

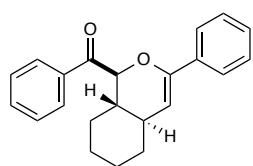
2.5.3 Experimental details for the hetero Diels–Alder cyclization of bis(enone) substrates

General procedure A: To an oven-dried 25 mL Schlenk tube equipped with a magnetic stir bar was added bis(enone) (1 equiv), $\text{Ru}(\text{bpy})_3\text{Cl}_2\cdot\text{H}_2\text{O}$ (0.05 equiv), LiBF_4 (2 equiv), MeCN (0.1 M), H_2O (10 equiv) as a stock solution in MeCN, and *i*- Pr_2NEt (3 equiv). The tube was sealed and degassed by 3 freeze-pump-thaw cycles under nitrogen in the absence of light. The reaction mixture was then stirred in a water bath at room temperature and irradiated with a 200 W light bulb at a distance of 30 cm. Upon consumption of the bis(enone), the reaction mixture was passed across a short plug of silica with a mixture of either hexanes:EtOAc or hexanes: Et_2O , concentrated *in vacuo* to approximately 4 mL and then purified immediately by flash column chromatography on silica gel.

General procedure B: To an oven-dried 50 mL Schlenk tube equipped with a magnetic stir bar was added $\text{Ru}(\text{bpy})_3\text{Cl}_2\cdot\text{H}_2\text{O}$ (0.05 equiv), $\text{Mg}(\text{ClO}_4)$ (2 equiv), and MeCN (0.025 M). The mixture was stirred until homogenous and then charged with the bis(enone) (1 equiv) and *i*- Pr_2NEt (3 equiv). The tube was sealed and degassed by 3 freeze-pump-thaw cycles under

nitrogen in the absence of light. The reaction mixture was then stirred in a water bath at room temperature and irradiated with a 200 W light bulb at a distance of 30 cm. Upon consumption of the bis(enone), the reaction mixture was passed across a 6 inch plug of silica with a mixture of hexanes:Et₂O. The reaction mixture was then concentrated in vacuo to approximately 4 mL and purified immediately by silica gel flash column chromatography.

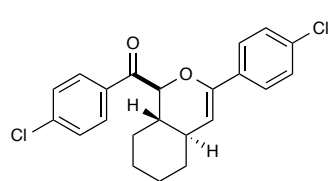
(Table 2-2, entry 1, 2.4): Experiment 1: Prepared according to general procedure A with 100.1



mg (0.314 mmol) bis(enone), 11.9 mg (0.016 mmol) Ru(bpy)₃Cl₂·6H₂O, 59.8 mg (0.638 mmol) LiBF₄, 57 μL (3.14 mmol) H₂O, 164 μL (0.942 mmol) *i*-Pr₂NEt, and 3.14 mL MeCN and an irradiation time of 60 min.

Purification by flash column chromatography (20:1 hexanes:EtOAc) afforded 85 mg cycloadduct (0.267 mmol, 85%). Experiment 2: 100.2 mg (0.315 mmol) bis(enone), 12.2 mg (0.163 mmol) Ru(bpy)₃Cl₂·6H₂O, 59.2 mg (0.631 mmol) LiBF₄, 57 μL (3.14 mmol) H₂O, 164 μL *i*-Pr₂NEt, and 3.14 mL MeCN. Isolated 86 mg cycloadduct (0.270 mmol, 86%) as a white solid. ¹H NMR: (500 MHz, CDCl₃) δ 8.13 (ddd, *J* = 8.1, 1.3, 1.3 Hz, 2H), 7.59 (tt, *J* = 7.4, 1.3 Hz, 1H), 7.54 (ddd, *J* = 7.8, 1.3, 1.3 Hz, 2H), 7.31-7.23 (m, 3H), 5.31 (d, *J* = 1.7 Hz, 1H), 4.93 (d, *J* = 10.4 Hz, 1H), 2.17 (dddd, *J* = 10.5, 10.5, 2.2, 2.2 Hz, 1H), 1.95-1.74 (m, 4H), 1.56 (dddd, *J* = 11.9, 2.2, 2.2, 2.2 Hz, 1H), 1.39 (qt, *J* = 12.8, 3.3 Hz, 1H), 1.29 (qt, *J* = 12.8, 3.3 Hz, 1H), 1.21 (qd, *J* = 12.8, 3.3 Hz, 1H), 1.07 (qd, *J* = 12.6, 3.5 Hz, 1H); ¹³C NMR: (125 MHz, CDCl₃) δ 196.9, 149.6, 135.7, 135.1, 133.5, 129.4, 128.6, 128.1, 128.0, 124.4, 102.5, 83.1, 41.3, 38.4, 32.7, 27.7, 26.0, 25.9. HRMS (EI) calculated for [C₂₂H₂₂O₂]⁺ *m/z* requires 318.1615, found 318.1599.

(Table 2-2, entry 2, 2.6): Experiment 1: Prepared according to general procedure A with 99.3



mg (0.256 mmol) bis(enone), 10.0 mg (0.0134 mmol) Ru(bpy)₃Cl₂·6H₂O, 49.3 mg (0.526 mmol) LiBF₄, 46 μL (2.58 mmol) H₂O, 135 μL (0.774 mmol) *i*-Pr₂NEt, and 2.6 mL MeCN and an

irradiation time of 30 min. Purification by flash column chromatography (20:1 hexanes:EtOAc)

afforded 69 mg cycloadduct (0.178 mmol, 69%) as a white crystalline solid. Experiment 2: 100

mg (0.258 mmol) bis(enone), 9.7 mg (0.0129 mmol) Ru(bpy)₃Cl₂·6H₂O, 48.4 mg (0.516 mmol)

LiBF₄, 46 μL (2.58 mmol) H₂O, 135 μL (0.774 mmol) *i*-Pr₂NEt, and 2.6 mL MeCN. Isolated 71

mg cycloadduct (0.183 mmol, 71%). ¹H NMR: (500 MHz, CDCl₃) δ8.05 (dt, *J* = 8.7, 2.0 Hz,

2H), 7.44 (dt, *J* = 8.7, 2.0 Hz, 4H), 7.25 (dt, *J* = 8.7, 2.0 Hz, 2H), 5.30 (d, *J* = 1.8 Hz, 1H), 4.86

(d, *J* = 10.5 Hz, 1H), 2.15 (dddd, *J* = Hz, 10.8, 10.8, 2.3, 2.3H), 1.90 (dddd, *J* = 13.0, 2.5, 2.5,

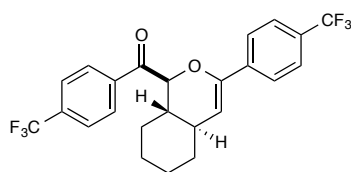
2.5 Hz, 1H), 1.85-1.75 (m, 3H), 1.54 (dddd, *J* = 13.0, 2.5, 2.5, 2.5 Hz, 1H), 1.44-1.15 (m, 3H),

1.065 (dddd, *J* = 12.7, 12.7, 12.7, 3.8 Hz, 1H); ¹³C NMR: (125 MHz, CDCl₃) δ195.5, 148.5,

140.1, 133.8, 133.4, 130.8, 129.0, 128.3, 125.7, 103.0, 83.3, 41.2, 38.4, 32.6, 27.6, 26.0, 25.8.

HRMS (EI) calculated for *m/z* [C₂₂H₂₀Cl₂O₂]⁺ requires 386.0835, found 386.0848.

(Table 2-2, entry 3, 2.7): Experiment 1: Prepared according to general procedure A with 81.4



mg (0.179 mmol) bis(enone), 7.7 mg (1.01 mmol) Ru(bpy)₃Cl₂·6H₂O, 36.7 mg (0.391 mmol) LiBF₄, 32 μL (1.76 mmol) H₂O, 92 μL (0.528 mmol) *i*-Pr₂NEt, and 1.76 mL MeCN

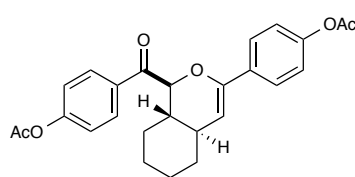
and an irradiation time of 30 min. Purification by flash column chromatography (30:1

hexanes:EtOAc) afforded 68 mg cycloadduct (0.150 mmol, 83%) as a white solid. ¹H NMR:

(500 MHz, CDCl₃) δ8.22 (d, *J* = 8.3 Hz, 2H), 7.75 (d, *J* = 8.3 Hz, 2H), 7.62 (d, *J* = 8.3 Hz, 2H),

7.54 (d, $J = 8.3$ Hz, 2H), 5.44 (d, $J = 1.7$ Hz, 1H), 4.93 (d, $J = 10.4$ Hz, 1H), 2.20 (dddd, $J = 10.4$, 10.4, 2.3, 2.3 Hz, 1H), 1.94 (dd, $J = 12.5$, 2.4 Hz, 1H), 1.87-1.77 (m, $J =$ Hz, 3H), 1.56 (dq, $J = 10.1$, 2.7 Hz, 1H), 1.47-1.18 (m, 3H), 1.10 (qd, $J = 12.4$, 3.7 Hz, 1H). HRMS (EI) calculated for m/z $[C_{24}H_{20}F_6O_2]^+$ requires 454.1362, found 454.1352.

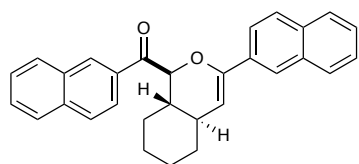
(Table 2-2, entry 4, 2.8): Experiment 1: Prepared according to general procedure A with 101.0



mg (0.232 mmol) bis(enone), 9.1 mg (0.0122 mmol) $Ru(bpy)_3Cl_2 \cdot 6H_2O$, 42.1 mg (0.449 mmol) $LiBF_4$, 41 μL (2.30 mmol) H_2O , 121 μL (0.690 mmol) $i\text{-}Pr_2NEt$, and 2.3 mL MeCN

and an irradiation time of 30 min. Purification by flash column chromatography (5:1 hexanes:acetone) afforded 77 mg cycloadduct (0.177 mmol, 76%) as a white solid. Experiment 2: 92.0 mg (0.212 mmol) bis(enone), 8.2 mg (0.0109 mmol) $Ru(bpy)_3Cl_2 \cdot 6H_2O$, 41.0 mg (0.437 mmol) $LiBF_4$, 39 μL (2.19 mmol) H_2O , 114 μL (0.651 mmol) $i\text{-}Pr_2NEt$, and 2.19 mL MeCN. Isolated 70 mg cycloadduct (0.161 mmol, 76%). 1H NMR: (500 MHz, $CDCl_3$) δ 8.17 (dt, $J = 8.8$, 1.9 Hz, 2H), 7.54 (dt, $J = 8.8$, 1.9 Hz, 2H), 7.20 (dt, $J = 8.8$, 1.9 Hz, 2H), 7.01 (dt, $J = 8.8$, 1.9 Hz, 2H), 5.28 (d, $J = 1.9$ Hz, 1H), 4.86 (d, $J = 10.4$ Hz, 1H), 2.33 (s, 3H), 2.28 (s, 3H), 2.15 (dddd, $J = 10.6$, 10.6, 2.5, 2.5 Hz, 1H), 1.90 (dddd, $J = 12.7$, 2.3, 2.3, 2.3 Hz, 1H), 1.86-1.75 (m, 3H), 1.54 (dddd, $J = 12.7$, 2.3, 2.3, 2.3 Hz, 1H), 1.45-1.15 (m, 3H), 1.07 (qd, $J = 12.7$, 3.9 Hz, 1H); ^{13}C NMR: (125 MHz, $CDCl_3$) δ 195.5, 169.4, 168.8, 154.6, 150.5, 148.8, 133.1, 132.8, 131.2, 125.6, 121.8, 121.3, 102.7, 83.6, 41.2, 38.4, 32.6, 27.6, 26.0, 25.8, 21.1, 21.1. HRMS (EI) calculated for $[C_{26}H_{26}O_6]^+$ requires m/z 434.1724, found 434.1714.

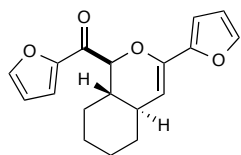
(Table 2-2, entry 5, 2.9): Experiment 1: Prepared according to general procedure A with 100.6



mg (0.240 mmol) bis(enone), 9.3 mg (0.0124 mmol) Ru(bpy)₃Cl₂·6H₂O, 43.9 mg (0.468 mmol) LiBF₄, 43 μL (2.39 mmol) H₂O, 125 μL (0.717 mmol) *i*-Pr₂NEt, and 2.39 mL MeCN

and an irradiation time of 1.5 hours. Purification by flash column chromatography (20:1 hexanes:Et₂O) afforded 75 mg cycloadduct (0.177 mmol, 75%). Experiment 2: 99.7 mg (0.238 mmol) bis(enone), 9.3 mg (0.0124 mmol) Ru(bpy)₃Cl₂·6H₂O, 44.5 mg (0.475 mmol) LiBF₄, 43 μL (2.39 mmol) H₂O, 125 μL (0.717 mmol) *i*-Pr₂NEt, and 2.39 mL MeCN. Isolated 79 mg cycloadduct (0.189 mmol, 79%) as a colorless oil. ¹H NMR: (500 MHz, CDCl₃) δ8.75 (s, 1H), 8.19 (dd, *J* = 8.8, 1.7 Hz, 1H), 8.03 (s, 1H), 7.93 (t, *J* = 7.9 Hz, 2H), 7.89 (d, *J* = 8.1 Hz, 1H), 7.80-7.67 (m 4H), 7.61 (td, *J* = 7.9, 0.9 Hz, 1H), 7.52 (td, *J* = 7.9, 0.9 Hz, 1H), 7.43-7.37 (m, 2H), 5.49 (d, *J* = 1.7 Hz, 1H), 5.16 (d, *J* = 10.4 Hz, 1H), 2.27 (dddd, *J* = 10.4, 10.4, 1.5, 1.5 Hz, 1H), 1.96 (qd, *J* = 10.5, 3.1 Hz, 2H), 1.82 (dt, *J* = 12.4, 2.4 Hz, 1H), 1.77 (dt, *J* = 12.4, 2.4 Hz, 1H), 1.61 (dd, *J* = 12.2, 2.4 Hz, 1H), 1.49-1.22 (m, 3H), 1.12 (qd, *J* = 13.0, 3.7 Hz, 1H); ¹³C NMR: (125 MHz, CDCl₃) δ196.9, 149.7, 135.8, 133.2, 133.2, 133.1, 132.5, 132.4, 131.5, 129.9, 128.8, 128.5, 128.4, 127.8, 127.7, 127.5, 126.8, 126.1, 125.9, 124.8, 123.4, 122.6, 103.4, 83.1, 41.6, 38.7, 32.7, 27.8, 26.1, 25.9. HRMS (EI) calculated for [C₃₀H₂₆O₂]⁺ requires *m/z* 418.1928, found 418.1936.

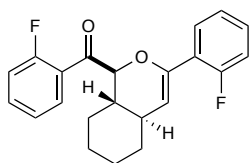
(Table 2-2, entry 6, 2.10): Experiment 1: Prepared according to general procedure A with 102.0



mg (0.342 mmol) bis(enone), 13.4 mg (0.0179 mmol) $\text{Ru}(\text{bpy})_3\text{Cl}_2 \cdot 6\text{H}_2\text{O}$, 61.5 mg (0.656 mmol) LiBF_4 , 60 μL (3.35 mmol) H_2O , 175 μL (1.01 mmol) *i*- Pr_2NEt , and 3.35 mL MeCN and an irradiation time of 30 min.

Purification by flash column chromatography (15:1 hexanes:EtOAc) afforded 79 mg cycloadduct (0.258 mmol, 77%) as a colorless oil. Experiment 2: 101.5 mg (0.340 mmol) bis(enone), 12.5 mg (0.0167 mmol) $\text{Ru}(\text{bpy})_3\text{Cl}_2 \cdot 6\text{H}_2\text{O}$, 62.3 mg (0.665 mmol) LiBF_4 , 60 μL (3.35 mmol) H_2O , 175 μL (1.01 mmol) *i*- Pr_2NEt , and 3.35 mL MeCN. Isolated 77 mg cycloadduct (0.258, 76%). ^1H NMR: (500 MHz, CDCl_3) δ 7.67 (dd, $J = 1.6, 0.6$ Hz, 1H), 7.40 (dd, $J = 3.7, 0.6$ Hz, 1H), 7.36 (dd, $J = 1.4, 1.4$ Hz, 1H), 6.55 (dd, $J = 3.7, 1.6$ Hz, 1H), 6.39-6.36 (m, 2H), 5.29 (d, $J = 1.8$ Hz, 1H), 4.86 (d, $J = 10.6$ Hz, 1H), 2.14 (dddd, $J = 10.6, 10.6, 2.2, 2.2$ Hz, 1H), 1.90 (dddd, $J = 13.0, 1.3, 1.3, 1.3$ Hz, 1H), 1.79 (dddd, $J = 12.4, 2.2, 2.2, 2.2$ Hz, 1H), 1.69 (dddd, $J = 10.5, 10.5, 10.5, 3.0$ Hz, 1H), 1.60-1.53 (m, 1H), 1.44-1.08 (m, 4H); ^{13}C NMR: (125 MHz, CDCl_3) δ 185.6, 150.8, 149.5, 147.4, 142.7, 142.0, 120.4, 112.3, 111.1, 105.9, 101.7, 83.3, 42.1, 38.0, 32.5, 27.2, 25.9, 25.8. HRMS (EI) calculated for m/z $[\text{C}_{18}\text{H}_{18}\text{O}_4]^+$ requires 298.1200, found 298.1187.

(Table 2-2, entry 7, 2.11): Experiment 1: Prepared according to general procedure A with 99.7

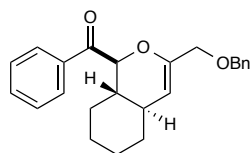


mg (0.281 mmol) bis(enone), 10.5 mg (0.0140 mmol) $\text{Ru}(\text{bpy})_3\text{Cl}_2 \cdot 6\text{H}_2\text{O}$, 52.1 mg (0.556 mmol) LiBF_4 , 51 μL (2.82 mmol) H_2O , 148 μL (0.847 mmol) *i*- Pr_2NEt , and 2.8 mL MeCN and an irradiation time of 30 min.

Purification by flash column chromatography (20:1 hexanes:Et₂O) afforded 84 mg cycloadduct (0.237 mmol, 84%) as a white solid. Experiment 2: 99.8 mg (0.282 mmol) bis(enone), 11.2 mg (0.0150 mmol) $\text{Ru}(\text{bpy})_3\text{Cl}_2 \cdot 6\text{H}_2\text{O}$, 51.9 mg (0.554 mmol) LiBF_4 , 51 μL (2.82 mmol) H_2O , 148

μL (0.847 mmol) *i*-Pr₂NEt, and 2.8 mL MeCN. Isolated 84 mg cycloadduct (0.237 mmol, 84%).
¹H NMR: (500 MHz, CDCl₃) δ 7.86 (td, *J* = 7.6, 1.7 Hz, 1H), 7.54 (m, 1H), 7.45 (td, *J* = 7.9, 1.7 Hz, 1H), 7.25 (td, *J* = 7.8, 1.1 Hz, 1H), 7.21-7.12 (m, 2H), 7.04-6.98 (m, 2H), 5.39 (bs, 1H), 5.01 (d, *J* = 10.4 Hz, 1H), 2.19 (dddd, *J* = 11.0, 11.0, Hz, 1H), 1.91-1.75 (m, 4H), 1.70 (dddd, *J* = 12.6, 2.7, 2 Hz, 1H), 1.45-1.08 (m, 4H); ¹³C NMR: (125 MHz, CDCl₃) δ 196.9 (d, *J* = 3.2), 161.4 (d, *J* = 254.0), 159.8 (d, *J* = 251.2), 144.7 (d, *J* = 3.5), 134.6 (d, *J* = 9.8), 130.9 (d, *J* = 2.3), 128.9 (d, *J* = 8.6), 128.1 (d, *J* = 2.2), 125.8 (d, *J* = 13.1), 124.5 (d, *J* = 3.2), 123.8 (d, *J* = 3.6), 123.3 (d, *J* = 10.8), 116.7 (d, *J* = 23.2), 115.8 (d, *J* = 23.2), 107.9 (d, *J* = 12.1), 83.4 (d, *J* = 5.0), 40.9, 38.5, 27.4, 26.1, 25.9, 32.6. HRMS (EI) calculated for [C₂₂H₂₀F₂O₂]⁺ *m/z* requires 354.1426, found 354.1423.

(Table 2-2, entry 9, 2.13): Experiment 1: Prepared according to general procedure A with 99.7

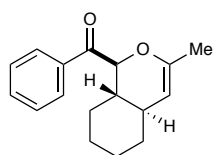


mg (0.275 mmol) bis(enone), 10.8 mg (0.0144 mmol) Ru(bpy)₃Cl₂·6H₂O, 52 mg (0.555 mmol) LiBF₄, 50 μL (2.76 mmol) H₂O, 144 μL (0.828 mmol) *i*-Pr₂NEt, and 2.76 mL MeCN and an irradiation time of 20 min.

Purification by flash column chromatography (10:1 hexanes:Et₂O) afforded 75 mg cycloadduct (0.207 mmol, 75%) as a colorless oil. Experiment 2: 100.2 mg (0.276 mmol) bis(enone), 10.3 mg (0.0138 mmol) Ru(bpy)₃Cl₂·6H₂O, 52 mg (0.555 mmol) LiBF₄, 50 μL (2.76 mmol) H₂O, 144 μL (0.828 mmol) *i*-Pr₂NEt, and 2.76 mL MeCN. Isolated 76 mg cycloadduct (0.210 mmol, 76%). ¹H NMR: (500 MHz, CDCl₃) δ 8.07 (dt, *J* = 7.5, 1.2 Hz, 2H), 7.57 (tt, *J* = 7.5, 1.2 Hz, 1H), 7.43 (td, *J* = 7.5, 1.2 Hz, 2H), 7.36-7.25 (m, 5H), 4.84 (d, *J* = 10.4 Hz, 1H), 4.80 (s, 1H), 4.57 (s, 2H), 3.96 (ABq, *J* = 12.0 Hz, 2H), 2.03 (dddd, *J* = 11.0, 11.0, 1.4, 1.4 Hz, 1H), 1.84-1.69 (m, 4H), 1.49 (ddd, *J* = 12.8, 2.3, 2.3 Hz, 1H), 1.39-1.19 (m, 2H), 1.12 (dddd, *J* = 12.8, 12.8, 12.8, 3.2 Hz, 1H),

1.00 (dddd, $J = 12.8, 12.8, 12.8, 3.7$ Hz, 1H); ^{13}C NMR: (125 MHz, CDCl_3) δ 197.0, 149.0, 138.2, 135.8, 133.4, 129.3, 128.5, 128.3, 127.8, 127.6, 104.9, 82.6, 72.3, 69.9, 41.4, 37.8, 32.4, 27.7, 26.0, 25.9. HRMS (EI) calculated for $[\text{C}_{24}\text{H}_{26}\text{O}_3]^+$ requires m/z 362.1877, found 362.1869.

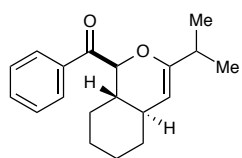
(Table 2-2, entry 10, 2.14): Experiment 1: Prepared according to general procedure B with



101.0 mg (0.394 mmol) bis(enone), 14.4 mg (0.0192 mmol) $\text{Ru}(\text{bpy})_3\text{Cl}_2 \cdot 6\text{H}_2\text{O}$, 173.9 mg (0.779 mmol) $\text{Mg}(\text{ClO}_4)_2$, 340 μL (1.95 mmol) $i\text{-Pr}_2\text{NEt}$, and 15.6 mL MeCN and an irradiation time of 10 min. Purification

by flash column chromatography (20:1 hexanes:EtOAc) afforded 75 mg cycloadduct (0.293 mmol, 74%) as a colorless oil. Experiment 2: 98.9 mg (0.386 mmol) bis(enone), 14.4 mg (0.0192 mmol) $\text{Ru}(\text{bpy})_3\text{Cl}_2 \cdot 6\text{H}_2\text{O}$, 172.9 mg (0.775 mmol) $\text{Mg}(\text{ClO}_4)_2$, 340 μL (1.95 mmol) $i\text{-Pr}_2\text{NEt}$, and 15.6 mL MeCN. Isolated 72 mg cycloadduct (0.281, 72%). ^1H NMR: (500 MHz, CDCl_3) δ 8.05 (dt, $J = 7.7, 1.3$ Hz, 2H), 7.58 (tt, $J = 7.7, 1.3$ Hz, 1H), 7.47 (tt, $J = 7.7, 1.3$ Hz, 2H), 4.82 (d, $J = 10.3$ Hz, 1H), 4.43 (s, 1H), 1.95 (dddd, $J = 11.3, 11.3, 1.8, 1.8$ Hz, 1H), 1.79 (dd, $J = 2.0, 0.8$ Hz, 3H), 1.77-1.64 (m, 4H), 1.44 (dddd, $J = 12.4, 2.7, 2.7, 2.7$ Hz, 1H), 1.37-1.18 (m, 2H), 1.07 (dddd, $J = 12.4, 12.4, 12.4, 2.7$ Hz, 1H), 0.97 (dddd, $J = 12.6, 12.6, 12.6, 3.6$ Hz, 1H); ^{13}C NMR: (125 MHz, CDCl_3) δ 197.5, 149.2, 136.0, 133.4, 129.2, 128.5, 128.5, 101.5, 82.3, 41.7, 38.1, 32.7, 27.7, 25.9, 25.9, 19.7. HRMS (EI) calculated for $[\text{C}_{17}\text{H}_{20}\text{O}_2]^+$ requires m/z 256.1458, found 256.1455.

(Table 2-2, entry 12, 2.15): Experiment 1: Prepared according to general procedure B with

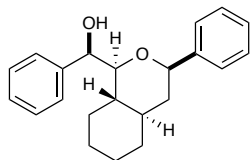


100.2 mg (0.353 mmol) bis(enone), 13.6 mg (0.0182 mmol) $\text{Ru}(\text{bpy})_3\text{Cl}_2 \cdot 6\text{H}_2\text{O}$, 158.5 mg (0.710 mmol) $\text{Mg}(\text{ClO}_4)_2$, 307 μL (1.76 mmol) *i*- Pr_2NEt , and 14.1 mL MeCN and an irradiation time of 1.5 hours.

Purification by flash column chromatography (20:1 hexanes: Et_2O) afforded 58 mg cycloadduct (0.204 mmol, 58%) as a colorless oil. Experiment 2: 100.6 mg (0.354 mmol) bis(enone), 13.7 mg (0.0183 mmol) $\text{Ru}(\text{bpy})_3\text{Cl}_2 \cdot 6\text{H}_2\text{O}$, 158.0 mg (0.708 mmol) $\text{Mg}(\text{ClO}_4)_2$, 307 μL (1.76 mmol) *i*- Pr_2NEt , and 14.1 mL MeCN. Isolated 58 mg cycloadduct (0.204 mmol, 58%). ^1H NMR: (500 MHz, CDCl_3) δ 8.07 (ddd, $J = 7.8, 1.2, 1.0$ Hz, 2H), 7.57 (tt, $J = 7.8, 1.2, 1.0$ Hz, 1H), 7.46 (ddd, $J = 7.8, 7.8, 1.0$ Hz, 2H), 4.70 (d, $J = 10.4$ Hz, 1H), 4.42 (s, $J = 1.0$ Hz, 1H), 2.27 (sept, $J = 6.8$ Hz, 1H), 1.95 (dddd, $J = 10.5, 10.5, 1.0$ Hz, 1H), 1.80-1.59 (m, 4H), 1.47 (dddd, $J = 13.0, 3.0, 3.0$ Hz, 1H), 1.38-1.16 (m, 2H), 1.24-0.92 (m, 8H); ^{13}C NMR: (125 MHz, CDCl_3) δ 197.5, 157.6, 135.7, 133.3, 129.4, 128.4, 98.4, 83.2, 41.7, 37.9, 32.9, 32.0, 27.6, 26.0, 26.0, 20.5. HRMS (EI) calculated for $[\text{C}_{19}\text{H}_{24}\text{O}_2]^+$ requires m/z 284.1771, found 284.1780.

2.5.4 Experimental details for the functionalization of cycloadduct 2.4

(Scheme 2-3, 2.24): To an oven-dried 500 ml pressure flask equipped with a magnetic stir bar

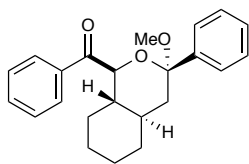


was added 10% Pd/C (62 mg) followed by cycloadduct **2.4** (100 mg, 0.314 mmol) in dichloromethane (8.0 mL) under an atmosphere of nitrogen. The flask was fitted with a regulator and filled with H_2 and evacuated twice,

then filled with 20 psi of H_2 . The reaction was allowed to stir at room temperature for 3 hours and then the excess H_2 was vented. The reaction was filtered over wet Celite and concentrated *in vacuo*. The residue was purified by flash column chromatography on silica gel (8:1

hexanes:ethyl acetate) to afford the product (70 mg, 0.217 mmol, 69%) as a clear oil. IR(thin film): 3553, 3432, 2926, 2852 cm^{-1} . ^1H NMR: (500 MHz, CDCl_3) δ 7.46 (dt, $J = 7.0, 1.5$ Hz, 2H), 7.39-7.26 (m, 8H), 4.80 (dd, $J = 9.4, 3.2$ Hz, 1H), 4.49 (dd, $J = 11.3, 2.2$ Hz, 1H), 3.70 (dd, $J = 10.1, 3.3$ Hz, 1H), 3.40 (d, $J = 9.6$ Hz, 1H, (OH)), 1.80 (dddd, $J = 12.4, 2.8, 2.8, 2.8$ Hz, 1H), 1.73 (m, 1H), 1.67 (tt, $J = 12.4, 2.8$ Hz, 2H), 1.56 (dddd, $J = 12.9, 2.8, 2.8, 2.8$ Hz, 1H), 1.40 (tt, $J = 11.7, 3.3$ Hz, 1H), 1.27 (qt, $J = 13.0, 3.7$ Hz, 1H), 1.16 (q, $J = 12.3$ Hz, 1H), 1.12 (qt, $J = 13.0, 3.7$ Hz, 1H), 1.00 (qd, $J = 12.1, 3.3$ Hz, 1H), 0.89 (qd, $J = 12.8, 3.7$ Hz, 1H), 0.76 (qd, $J = 10.2, 3.2$ Hz, 1H); ^{13}C NMR: (125 MHz, CDCl_3) δ 143.2, 140.62, 128.3, 128.0, 127.9, 127.5, 127.3, 125.8, 84.5, 80.1, 73.8, 42.4, 41.7, 41.1, 32.7, 27.2, 25.9, 25.6. HRMS (EI) calculated for $[\text{C}_{22}\text{H}_{26}\text{O}_2 + \text{Na}]^+$ requires m/z 345.1825, found 345.1835.

(Scheme 2-3, 2.25): To an oven-dried 10 mL round bottom flask equipped with a magnetic stir

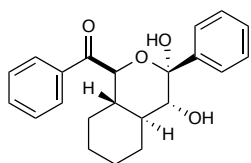


bar was added cycloadduct **2.4** (100 mg, 0.314 mmol), *p*-toluenesulfonic acid monohydrate (6 mg, 0.032 mmol), and methanol (3.2 mL). The reaction was allowed to stir at room temperature for 3.5 hours and then

concentrated *in vacuo*. The residue was purified by flash column chromatography on silica gel (8:1 hexanes:ethyl acetate) to afford the product (104 mg, 0.297 mmol, 95%) as a white solid. IR(thin film): 3059, 2924, 2854, 1679 cm^{-1} . ^1H NMR: (500 MHz, CDCl_3) δ 8.21 (ddd, $J = 7.5, 1.0, 1.0$ Hz, 2H), 7.61 (tt, $J = 7.5, 1.0$ Hz, 1H), 7.51 (t, $J = 7.8$ Hz, 2H), 7.49 (d, $J = 7.3$ Hz, 2H), 7.34 (td, $J = 7.4, 1.0$ Hz, 2H), 7.28 (tt, $J = 7.3, 1.0$ Hz, 1H), 4.73 (d, $J = 10.6$ Hz, 1H), 3.05 (s, 3H), 2.09 (dd, $J = 13.6, 3.6$ Hz, 1H), 1.94 (qt, $J = 11.8, 3.5$ Hz, 1H), 1.70 (m, 4H), 1.51 (t, $J = 13.0$ Hz, 1H), 1.44 (dt, $J = 12.8, 2.2$ Hz, 1H), 1.35 (qt, $J = 12.7, 3.5$ Hz, 1H), 1.23 (qt, $J = 12.8, 3.5$ Hz, 1H), 1.07 (qd, $J = 12.2, 3.5$ Hz, 1H), 1.00 (qd, $J = 12.2, 3.5$ Hz, 1H); ^{13}C NMR: (125

MHz, CDCl₃) δ 197.8, 142.0, 136.2, 133.3, 129.4, 128.5, 128.2, 127.8, 125.9, 100.8, 78.5, 49.5, 44.8, 43.2, 36.0, 32.8, 27.4, 25.9, 25.7; HRMS (EI) calculated for [C₂₃H₂₆O₃ -MeO]⁺ requires m/z 319.1693, found 319.1689.

(Scheme 2-3, 2.26): A 1.5 dram vial was charged with potassium osmate (VI) dihydrate (2 mg,



0.005 mmol) and sealed with a teflon cap. To the vial was added cycloadduct **2.4** (100 mg, 0.314 mmol), *N*-methylmorpholine *N*-oxide (54 mg, 0.461 mmol), citric acid (60 mg, 0.312 mmol) and a magnetic stir bar,

followed by *tert*-butanol (0.93 mL) and distilled water (0.31 mL). The reaction was then resealed and allowed to stir at room temperature for 23 hours. Sodium sulfite (40 mg, 0.317 mmol) was then added and the reaction was stirred another 30 minutes. The reaction was diluted with water and extracted twice with ethyl acetate. The combined organic extracts were dried over sodium sulfate, filtered and concentrated *in vacuo* to a white solid. The solid was purified by flash column chromatography on silica gel (10:1 toluene:acetone) then recrystallized in hexanes and ethyl acetate to afford the product (65 mg, 0.184 mmol, 60%) as a white crystalline solid. IR(thin film): 3447, 2931, 2856, 1684 cm⁻¹. ¹H NMR: (500 MHz, Acetone-*d*₆) δ 8.14 (dt, *J* = 8.5, 1.5 Hz, 2H), 7.61 (dd, *J* = 8.5, 1.5 Hz, 1H), 7.60 (qt, *J* = 6.7, 1.3 Hz, 2H), 7.48 (tt, *J* = 7.8, 1.5 Hz, 2H), 7.29-7.21 (m, 3H), 5.63 (s, 1H, (OH)), 5.13 (d, *J* = 10.4 Hz, 1H), 3.40 (d, *J* = 9.3 Hz, 1H, (OH)), 3.29 (t, *J* = 9.3 Hz, 1H), 2.24 (m, 1H), 1.98 (qd, *J* = 11.0, 3.2 Hz, 1H), 1.86 (qd, *J* = 11.0, 3.2 Hz, 1H), 1.81 (m, 1H), 1.72 (m, 1H), 1.57 (m, 1H), 1.38-1.24 (m, 2H), 1.13-0.94 (m, 2H); ¹³C NMR: (125 MHz, Acetone-*d*₆) δ 196.1, 143.8, 136.4, 133.1, 129.2, 128.5, 127.5, 127.2, 126.6, 98.7, 76.7, 74.8, 42.7, 41.7, 28.4, 27.2, 25.7, 25.2. HRMS (EI) calculated for [C₂₂H₂₄O₄ + Na]⁺ requires m/z 375.1567, found 375.1583.

2.5.5 Stereochemical determinations

NOE correlations were used to verify the relative stereochemistry of acetal **2.25** and dihydroxylation product **2.26**, as well as the regiochemistry of cycloadduct **2.14**. X-ray crystallography was used to verify the relative stereochemistry in cycloadduct **2.4** and hydrogenation product **2.24** (refer to Appendix C for the experimental details). Subsequent assignments were made by analogy.

2.6 References

- For recent reviews, see: (a) Tietze, L. F.; Kettschau, G. *Top. Curr. Chem.* **1997**, *189*, 1–120. (b) Tietze, L. F.; Kettschau, G.; Gewert, J. A.; Schuffenhauer, A. *Curr. Org. Chem.* **1998**, *2*, 19–62. (c) Boger, D. L.; Weinreb, S. M. *Hetero-Diels–Alder Methodology in Organic Synthesis*; Wasserman, H. H., Ed.; Academic Press: San Diego, 1987. (d) Jørgensen, K. A. *Eur. J. Org. Chem.* **2004**, 2093–2102. (e) Pellissier, H. *Tetrahedron* **2009**, *65*, 2839–2877.
- For seminal examples, see: (a) Thompson, C. F.; Jamison, T. F.; Jacobsen, E. N. *J. Am. Chem. Soc.* **2000**, *122*, 10482–10483. (b) Liu, P.; Jacobsen, E. J. *J. Am. Chem. Soc.* **2001**, *123*, 10772–10773. (c) Chavez, D. E.; Jacobsen, E. N. *Angew. Chem., Int. Ed.* **2001**, *40*, 3667–3670. (d) Paterson, I.; De Savi, C.; Tudge, M. *Org. Lett.* **2001**, *3*, 3149–3152. (e) Evans, D. A.; Starr, J. T. *Angew. Chem., Int. Ed.* **2002**, *41*, 1787–1790. (f) Paterson, I.; Tudge, M. *Angew. Chem., Int. Ed.* **2003**, *42*, 343–347. (g) Voight, E. A.; Seradj, H.; Roethle, P. A.; Burke, S. D. *Org. Lett.* **2004**, *6*, 4045–4048. (h) Tietze, L. F.; Rackelmann, N.; Müller, I. *Chem.–Eur. J.* **2004**, *10*, 2722–2731. (i) Lucas, B. S.; Luther, L. M.; Burke, S. D. *J. Org. Chem.* **2005**, *70*, 3757–3760. (j) Majumder, U.; Cox, J. M.; Johnson, H. W. B.; Rainier, J. D. *Chem.–Eur. J.* **2006**, *12*, 1736–1746. (k) Louis, I.; Hungerford, N. L.; Humphries, E. J.; McLeod, M. D.; *Org. Lett.* **2006**, *8*, 1117–1120. (l) Lucas, B. S.; Gopalsamuthiram, V.; Burke, S. D. *Angew. Chem., Int. Ed.* **2007**, *46*, 769–772. (m) Ghosh, A. K.; Gong, G. *Org. Lett.* **2007**, *9*, 1437–1440. (n) Bonazzi, S.; Güttinger, S.; Zemp, I.; Kutay, U.; Gademann, K. *Angew. Chem., Int. Ed.* **2007**, *46*, 8707–8710. (o) Dilger, A. K.; Gopalsamuthiram, V.; Burke, S. D. *J. Am. Chem. Soc.* **2007**, *129*, 16273–16277.
- (a) Desimoni, G.; Tacconi, G. *Chem. Rev.* **1975**, *75*, 651–692. (b) Schmidt, J. A.; Jorgensen, W. L. *J. Org. Chem.* **1983**, *48*, 3923–3941. (c) Jun, J.-G.; Shin, D. G.; Lee, C. K.; Sin, K. S. *Bull. Korean Chem. Soc.* **1990**, *11*, 307–309.
- (a) Ischay, M. A.; Anzovino, M. E.; Du, J.; Yoon, T. P. *J. Am. Chem. Soc.* **2008**, *130*, 12886–12887. (b) Du, J.; Yoon, T. P. *J. Am. Chem. Soc.* **2009**, *131*, 14604–14605. (c) Ischay, M. A.; Lu, Z.; Yoon, T. P. *J. Am. Chem. Soc.* **2010**, *132*, 8572–8574. (d) Lu, Z.; Shen, M.; Yoon, T. P. *J. Am. Chem. Soc.* **2011**, *133*, 1162–1164. (e) Hurlley, A. E.; Cismesia, M. A.; Ischay, M.

-
- A.; Yoon, T. P. *Tetrahedron* **2011**, *67*, 4442–4448. (f) Lin, S.; Ischay, M. A.; Fry, C. G.; Yoon, T. P. *J. Am. Chem. Soc.* **2011**, *133*, 19350–19353. (g) Tyson, E. L.; Farney, E. P.; Yoon, T. P. *Org. Lett.* **2012**, *14*, 1110–1113. (h) Ischay, M. A.; Ament, M. S.; Yoon, T. P. *Chem. Sci.* **2012**, *3*, 2807–2811.
5. For leading contributions, see: (a) Nicewicz, D.; MacMillan, D. W. C. *Science* **2008**, *322*, 70–80. (b) Narayanam, J. M. R.; Tucker, J. W.; Stephenson, C. R. J. *J. Am. Chem. Soc.* **2009**, *131*, 8756–8757.
 6. For reviews on recent developments in transition metal photoredox catalysis in organic synthesis, see: (a) Zeitler, K. *Angew. Chem. Int. Ed.* **2009**, *48*, 9785–9789. (b) Yoon, T. P.; Ischay, M. A.; Du, J. *Nature Chem.* **2010**, *2*, 527–532. (c) Narayanam, J. M. R.; Stephenson, C. R. J. *Chem. Soc. Rev.* **2011**, *40*, 102–113. (d) Prier, C. K.; Rankic, D. A.; MacMillan, D. W. C. *Chem. Rev.* **2013**, *113*, 5322–5363. (e) Yoon, T. P. *ACS Catal.* **2013**, *3*, 895–902. (f) Schultz, D. M.; Yoon, T. P. *Science* **2014**, *343*, 1239176.
 7. (a) Roh, Y.; Jang, H. Y.; Lynch, V.; Bauld, N. L.; Krische, M. J. *Org. Lett.* **2002**, *4*, 611–613. (b) Yang, J.; Felton, G. A. N.; Bauld, N. L.; Krische, M. J. *J. Am. Chem. Soc.* **2004**, *126*, 1634–1635. (c) Felton, G. A. N.; Bauld, N. L. *Tetrahedron Lett.* **2004**, *45*, 8465–8469. (d) Felton, G. A. N.; Bauld, N. L. *Tetrahedron* **2004**, *60*, 10999–11010.
 8. The origin of this effect is not clear at this time, but given the polar nature of the intermediates and the step-wise mechanism proposed for radical anion cycloadditions, the hydrophobic effect proposed by Breslow for the rate acceleration of thermal Diels–Alder reactions in water is most likely not operational: Breslow, R. *Acc. Chem. Res.* **1991**, *24*, 159–164.
 9. Fournier, F.; Fournier, M. *Can. J. Chem.* **1986**, *64*, 881–890.
 10. VanRheenen, V.; Kelly, R. C.; Cha, D. Y. *Tetrahedron Lett.* **1976**, *17*, 1973–1976.
 11. Pangborn, A. B.; Giardello, M. A.; Grubbs, R. H.; Rosen, R. K.; Timmers, F. T. *Organometallics* **1996**, *15*, 1518–1520.
 12. Still, W. C.; Kahn, M.; Hong, P. C.; Lu, L. *J. Org. Chem.* **1978**, *43*, 2923–2925.
 13. Blank, B.; DiTullio, N.W.; Deviney, L.; Roberts, J.T.; Saunders, H.L. *J. Med. Chem.* **1975**, *18*, 952–954.
 14. Bravo, P.; Ticozzi, C.; Cezza, A. *Gazzetta Chimica Italiana.* **1975**, *105*, 109–15.
 15. Marques-Lopez, E.; Herrera, R. P.; Marks, T.; Jacobs, W. C.; Konning, D.; de Figueiredo, R. M.; Christmann, M. *Org. Lett.* **2009**, *11*, 4116–4119.
 16. Hayashi, Y.; Gotoh, H.; Tamura, T.; Yamaguchi, H.; Masui, R.; Shoji, M. *J. Am. Chem. Soc.* **2005**, *127*, 16028–16029.

-
17. Nakamura, H.; Aoyagi, K.; Shim, J-G.; Yamamoto, Y. *J. Am. Chem. Soc.* **2001**, *123*, 372–377.
18. Claus, R.E.; Schreiber, S.L. *Org. Synth.* **1968**, *64*, 150.

Chapter 3. [2+2] Cycloaddition of 1,3-Dienes by Visible Light Photocatalysis

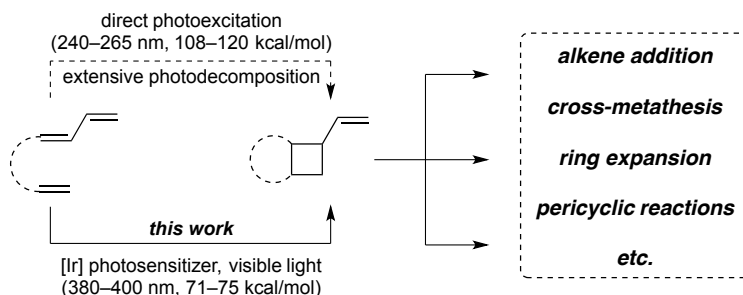
Portions of this work have been previously published:

Hurtley, A. E.; Lu, Z; Yoon, T. P "[2+2] Cycloaddition of 1,3-Dienes by Visible Light Photocatalysis" *Angew. Chem. Int. Ed.* **2014**, DOI: 10.1002/anie.201405359.

3.1 Introduction

Photochemical reactions provide uniquely direct access to complex, highly strained molecular structures that are often difficult to synthesize using other reaction types.¹ The utility of photochemical [2+2] cycloaddition reactions, in particular, has become widely appreciated by synthetic chemists both because of the prevalence of cyclobutanes in a diverse family of bioactive natural products² and because of the utility of strain-releasing fragmentation reactions in the assembly of structurally complex larger-ring systems.³ Over the past several years, our research group has taken advantage of the unique properties of transition metal chromophores to develop a variety of photocycloaddition reactions that can be accomplished with visible light.^{4,5} In examining synthetic targets to demonstrate the utility of visible light induced photocycloadditions, we came to realize that [2+2] cycloadditions of 1,3-dienes would afford facile access to versatile vinylcyclobutanes that are ideally poised for diverse synthetic elaborations via manipulation of their alkenyl substituents (Figure 3-1). Notably, only a few examples of [2+2] diene-olefin photocycloadditions have been reported in the context of total synthesis.^{6,7} This stands in sharp contrast to the multitude of syntheses that feature analogous [2+2] enone-olefin photocycloadditions. One important reason for this surprising discrepancy might be that the direct photoexcitation of dienes requires irradiation with very high-energy UVC light (ca. 240–265 nm).⁸ These high-energy photons (108–120 kcal/mol) are incompatible with the highly functionalized organic substrates generally required for late-stage synthetic applications. The ability to promote the [2+2] cycloaddition of dienes with low-energy visible light (<75 kcal/mol) would thus greatly increase the versatility of this vastly underexploited transformation and facilitate its use in the synthesis of complex organic targets.

Figure 3-1. [2+2] Cycloadditions of 1,3-dienes provide access to synthetically versatile vinylcyclobutanes.



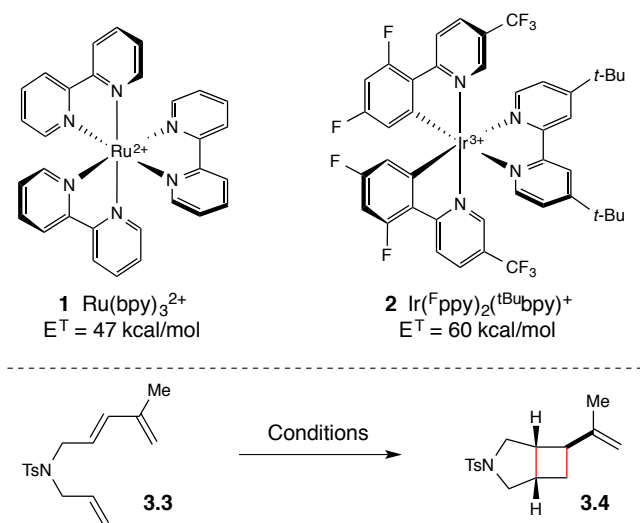
Most of the recent interest in visible light mediated photochemical reactions has focused on photoinduced redox activation of organic functional groups using transition metal photocatalysts such as $\text{Ru}(\text{bpy})_3^{2+}$ (**1**).⁵ We have reported a complementary approach that uses iridium complex **2** to perform the [2+2] cycloaddition of a variety of electronically diverse styrenes via an energy transfer mechanism.⁹ We speculated that this strategy might also be capable of activating dienes towards [2+2] cycloaddition reactions using visible light. Although dienes are more resistant to one-electron oxidation than styrenes,¹⁰ their lowest-lying triplet states are quite similar in energy (ca. 55–60 kcal/mol).¹¹ We reasoned, therefore, that the same visible light-activated photocatalysts that proved to be effective for sensitization of styrenes might also activate simple 1,3-dienes and could thus provide access to a wide range of synthetically valuable vinylcyclobutane products.

3.2 Results and Discussion

Triene **3.3** was selected as a model substrate for our preliminary investigations (Table 3-1). The direct photoexcitation of this compound requires short-wavelength UVC light, and as expected, irradiation in a Rayonet reactor at 254 nm resulted in rapid and complete decomposition after 30 min (entry 1), consistent with the destructive nature of these high-energy photons. No trace of the desired [2+2] cycloadduct could be observed even at partial

conversion (entry 2). On the other hand, we were pleased to find that vinylcyclobutane **3.4** was formed in high yield upon irradiation of **3.3** with a household CFL bulb in the presence of 1 mol% iridium complex **2** (entry 3).¹² Importantly, we did not observe any products arising from competitive electrocyclicization or [4+2] cycloaddition events under these conditions. The observation that $\text{Ru}(\text{bpy})_3^{2+}$ (**1**), which possesses a substantially lower triplet energy (47 kcal/mol),¹³ fails to promote this reaction (entry 4) is consistent with the proposed role of **2** as a triplet sensitizer rather than a photoredox catalyst. Finally, no reaction occurred in the absence of either light or the photocatalyst (entries 5 and 6), in line with our observations in studies of similar systems.

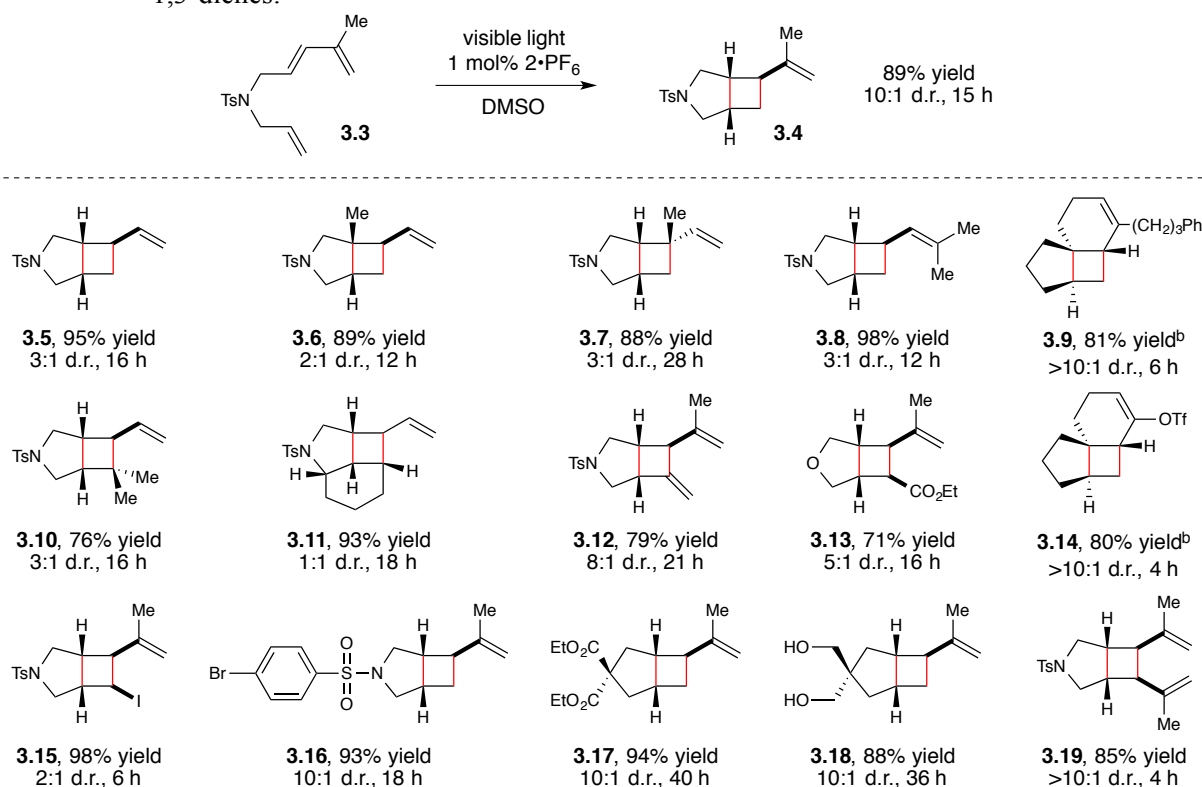
Table 3-1. Control studies for visible light promoted diene-olefin [2+2] cycloadditions.^a



Entry	Conditions	% Conversion	% Yield 3.4 ^a
1 ^b	hν (UVC), 30 min	100	0
2 ^b	hν (UVC), 10 min	63	0
3	1 mol% 2 •PF ₆ , hν (visible), 15 h	100	89
4	1 mol% 1 •(PF ₆) ₂ , hν (visible), 15 h	12	0
5	hν(visible), 15 h	6	0
6	1 mol% 2 •PF ₆ , no light, 15 h	0	0

^a Yield determined by ¹H NMR spectroscopic analysis of the unpurified reaction mixture against an internal standard. Reactions conducted in DMSO unless otherwise noted. ^b Reactions conducted in MeCN.

Table 3-2 summarizes experiments probing the effect of substrate modifications on the [2+2] cycloaddition. Collectively, these studies demonstrate that the scope of this reaction is gratifyingly broad. Substrates bearing substitution at each position of the diene underwent smooth reaction (**3.4**, **3.6–3.9**, and **3.14**), including systems that produce cyclobutanes bearing all-carbon quaternary centers (**3.6**, **3.7**, **3.9** and **3.14**). Similarly, a wide range of structurally varied alkenes served as suitable partners in this cycloaddition, and their reactions proved to be relatively insensitive to their electronic and steric properties (**3.10–3.13**, **3.15**). Although we focused on sulfonamide-tethered substrates due to their ease of synthesis, ether-containing and all-carbon tethers provide good yields as well (**3.9**, **3.13**, **3.14**, **3.17**, and **3.18**). The reactions of cyclic dienes occurred at somewhat faster rates (**3.9** and **3.14**), consistent with the prevention of energy-wasting *cis-trans* diene isomerizations, although a small amount of an inseparable Diels–Alder side product was also produced in these reactions.

Table 3-2. Investigation of structural diversity in the visible light promoted [2+2] cycloaddition of 1,3-dienes.

^a Unless otherwise noted, the isolated yields reported are averaged values from two reproducible experiments.

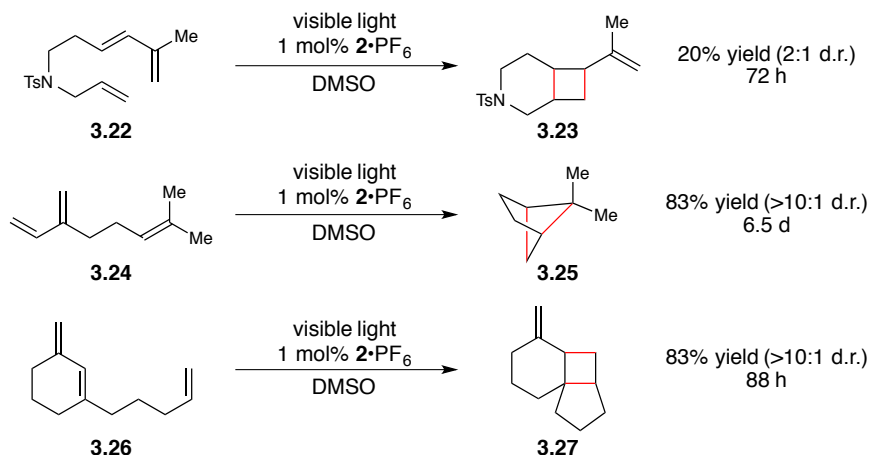
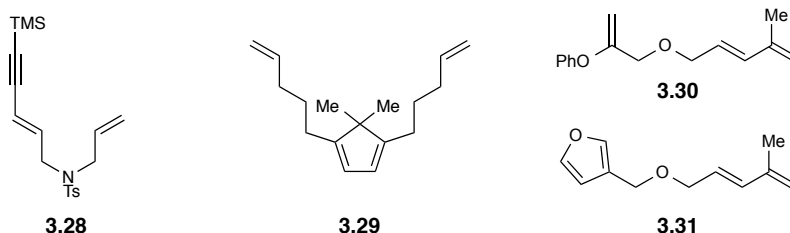
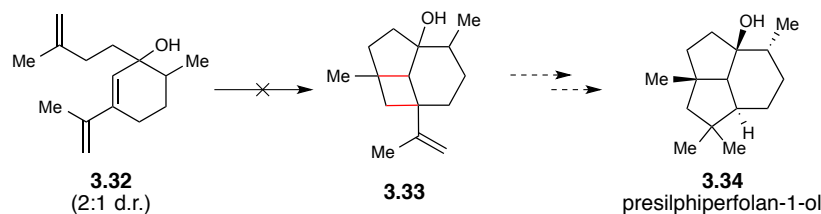
Diastereomeric ratios were determined by ¹H NMR spectroscopic analysis of the unpurified reaction mixtures.

^b Yields of [2+2] cycloadduct determined by ¹H NMR spectroscopic analysis using an internal standard.

Most notably, and in good accord with our central motivation for this study, the visible light induced cycloaddition was quite tolerant of a wide range of functional groups, including vinyl iodide and aryl bromide bonds that could be sensitive to either direct photodecomposition or photoredox-induced reductive dehalogenation¹⁴ (**3.15** and **3.16**). Other functional groups that are easily tolerated include esters, triflates, and unprotected alcohols (**3.13**, **3.14**, **3.17**, **3.18**), all of which provide useful synthetic handles for further elaboration of these cyclobutane-containing scaffolds.

Ru conditions: 1 mol% **1**•(PF₆)₂, 4 h: 93% yield, >10:1 E:Z, 2:1 d.r.

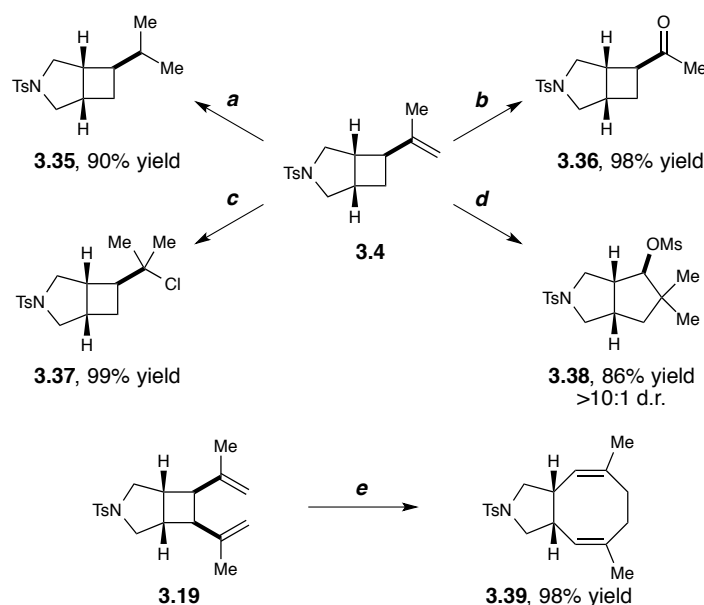
We also investigated the sensitization of higher-order conjugated polyenes (Scheme 3-1). Substrate **3.20** underwent high-yielding cycloaddition to **3.21** upon irradiation in the presence of **2**•PF₆, although the product was formed as a 1:1 mixture of *E* and *Z* isomers. The poor geometric selectivity is attributable to unproductive photosensitization and subsequent isomerization of the product diene. Speculating that a photocatalyst possessing a lower-energy triplet state might be able to selectively activate the more conjugated triene but not the higher-energy diene, we conducted a photocycloaddition in the presence of Ru(bpy)₃²⁺ (**1**). Indeed, under these conditions, the cycloaddition proceeds with excellent geometric selectivity. These studies highlight the versatility of energy transfer as a mode of photoactivation; the availability of a vast number of well-characterized transition metal photocatalysts¹⁵ with long-lived excited states spanning a wide range of triplet excited state energies is a distinct advantage of this approach.

Scheme 3-2. Limitations in the scope of the visible light promoted [2+2] cycloaddition.**(a) Require long reactions times to reach full conversion:****(b) No [2 + 2] cycloadduct observed:****(c) Proposed route to the natural product presilphiperfolan-1-ol:**

A number of limitations in the substrate scope were identified throughout the course of these studies (Scheme 3-2). Six-membered ring formation was prohibitively slow (**3.22**), as were the cyclizations of myrcene (**3.24**) and an exocyclic cyclohexadiene substrate (**3.26**), although all of these reactions proceeded with good mass balance. A conjugated enyne substrate (**3.28**) proved to be unstable under the reaction conditions and resulted in no formation of the [2+2] cycloadduct. A cyclopentadiene substrate (**3.29**) and analogues of the parent diene substrate bearing furan (**3.31**) and vinyl ether (**3.30**) coupling partners did not react under the standard conditions, although the starting material was recovered in these cases.

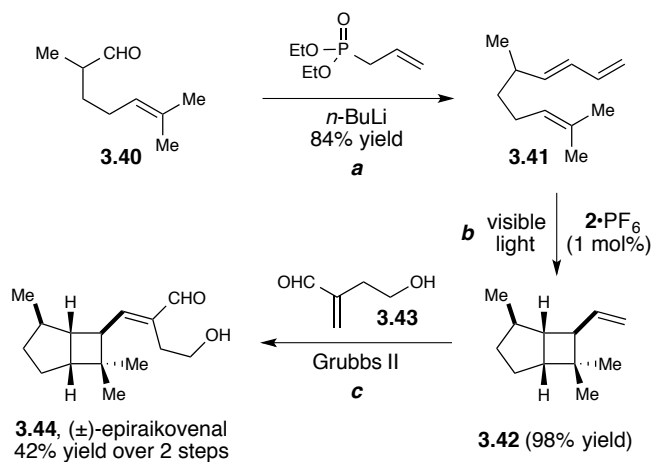
We also prepared triene **3.32** as a precursor to the natural product presilphiperfolan-1-ol, which we envisioned accessing through a [2+2] cycloaddition followed by an acid-catalyzed cationic ring rearrangement of the vinylcyclobutane (**3.33**). Unfortunately, we did not observe any productive reactivity of this substrate under our standard photochemical conditions.

The vinylcyclobutane motif readily accessible by [2+2] cycloadditions of dienes is amenable to a diverse set of high-yielding functionalization and rearrangement reactions (Scheme 3-3). For example, cycloadduct **3.4** undergoes hydrogenation to afford **3.35** as well as ozonolysis to give cyclobutyl methyl ketone **3.36**. The vinylcyclobutane can be elaborated via a variety of acid-promoted processes as well. The addition of HCl across the alkene occurs in quantitative yield (**3.37**) without fragmentation of the cyclobutane. On the other hand, methanesulfonic acid initiates a cationic ring expansion that generates a corresponding cyclopenta[*c*]pyrrole ring system (**3.38**). Finally, the divinylcyclobutane **3.19** provides access to ring-expanded cyclooctadiene **3.39** in excellent yield via a facile thermal Cope rearrangement.

Scheme 3-3. Synthetic elaboration of vinylcyclobutane products.

Conditions: (a) H_2 , 10% Pd/C, MeOH, rt. (b) 1. O_3 , CH_2Cl_2 , -78°C 2. DMS (c) HCl (2 M Et₂O), CH_2Cl_2 , rt. (d) MeSO_3H , CH_2Cl_2 , rt. (e) Benzene, 80°C .

The availability of these and similar complexity-building reactions of vinylcyclobutanes suggests that the ability to perform [2+2] cycloadditions of a structurally diverse set of dienes should be an enabling strategy in the synthesis of many complex organic targets. In order to highlight this feature, we designed a concise and modular synthesis of the cyclobutane-containing natural product (\pm)-epiraikovenal¹⁶ (Scheme 3-4). The diene precursor (**3.41**) to the key photochemical step is accessible by Horner-Wadsworth-Emmons olefination of aldehyde **3.40**. Subsequent photocycloaddition proceeds in high yield to generate the cyclobutane-containing carbocyclic core of the natural product (**3.42**). The unpurified product of the cycloaddition was then subjected to cross-metathesis with enal **3.43** to deliver fully functionalized (\pm)-epiraikovenal in 42% yield over these two steps.

Scheme 3-4. Modular synthesis of epiraikovenal.

Conditions: (a) THF/HMPA, -78 °C to rt (b) 1 mol, 0.1 M CDCl_3 (c) 7 mol% Grubbs II, 1 equiv **3.43**, 5 Å MS

3.3 Conclusions

Iridium photocatalyst **2** enables the efficient [2+2] photocycloaddition of a structurally diverse range of 1,3-diene substrates using visible light irradiation. The low-energy photons involved in this process are tolerant of a variety of common functional groups that would be prone to decomposition by the significantly higher-energy UVC wavelengths required for the direct photoexcitation of 1,3-dienes. We expect that this greater functional group compatibility coupled with the range of diversification reactions available to vinylcyclobutanes will facilitate the exploration of [2+2] diene-olefin cycloadditions in the context of complex target-oriented organic synthesis.

3.4 Experimental

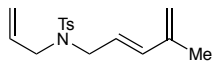
3.4.1 General experimental information

$[\text{Ir}(\text{dF}(\text{CF}_3)\text{ppy})_2(\text{dtbbpy})](\text{PF}_6)$ was prepared as previously described by Malliaras and Bernard.¹⁷ Diethyl ether, toluene, THF, and CH_2Cl_2 were purified by elution through alumina

as described by Grubbs.¹⁸ A 23 W (1380 lumen) compact fluorescent bulb was used for all photochemical reactions. Flash column chromatography was performed with Sigma-Aldrich silica gel (pore size 60 Å, 230–400 mesh particle size) using the method of Still.¹⁹ Diastereomeric ratios for all compounds were determined by ¹H NMR spectroscopic analysis of the crude reaction mixture. ¹H and ¹³C NMR data for all previously uncharacterized compounds were obtained using a Bruker Avance III 500 MHz spectrometer and are referenced to TMS (0.0 ppm) and CDCl₃ (77.16 ppm), respectively. ¹⁹F and ³¹P data were obtained using a Bruker Avance III 400 MHz spectrometer and are referenced externally to the corresponding ¹H spectra. The NMR facilities at UW-Madison are funded by the NSF (CHE-1048642) and a generous gift from Paul J. Bender. IR spectral data were obtained using a Bruker Platinum-ATR spectrometer (neat). Melting points were obtained using a Stanford Research Systems DigiMelt apparatus. Mass spectrometry was performed with a Waters (Micromass) AutoSpec. These facilities are funded by the NSF (CHE-9974839, CHE-9304546) and the University of Wisconsin.

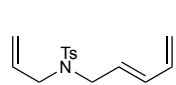
3.4.2 Synthesis of cycloaddition substrates.

(*E*)-*N*-allyl-4-methyl-*N*-(4-methylpenta-2,4-dien-1-yl)benzenesulfonamide (3.3): A flame-

 dried 250 mL round-bottomed flask was charged with PPh₃ (1.4 equiv, 8.50 mmol, 2.22 g) and *N*-allyl-4-methyl-benzenesulfonamide²⁰ (1 equiv, 6.1 mmol, 1.3 g) and then purged with N₂. Dry THF (120 mL) and (*E*)-4-methylpenta-2,4-diene-1-ol²¹ (1 equiv, 6.10 mmol, 600 mg) were added via syringe, and the reaction mixture was stirred and cooled to 0 °C. Diisopropyl azodicarboxylate (DIAD, 1.4 equiv, 8.50 mmol, 1.67 mL) was added dropwise, and the reaction was slowly warmed to room temperature. After 36 h, the solvent

was removed *in vacuo* and the residue purified by flash column chromatography on silica gel (8:1 hexanes: EtOAc) to afford the product as a clear oil (999 mg, 3.43 mmol, 55%). IR (neat): 2922, 1341, 1156, 734 cm^{-1} . ^1H NMR (500 MHz, CDCl_3) δ 7.71 (d, J = 8.2 Hz, 2H), 7.30 (d, J = 8.0 Hz, 2H), 6.14 (d, J = 15.7 Hz, 1H), 5.62 (ddt, J = 17.4, 9.3, 6.3 Hz, 1H), 5.37 (dt, J = 15.5, 6.8 Hz, 1H), 5.17–5.11 (m, 2H), 4.96 (s, 1H), 4.91 (s, 1H), 3.86 (d, J = 6.8 Hz, 2H), 3.80 (d, J = 6.2 Hz, 2H), 2.43 (s, 3H), 1.72 (s, 3H). ^{13}C NMR (126 MHz, CDCl_3) δ 143.4, 141.2, 137.6, 137.0, 132.9, 129.8, 127.4, 123.8, 119.0, 117.2, 49.6, 48.9, 21.6, 18.5. HRMS (ESI) calculated for $[\text{C}_{16}\text{H}_{21}\text{NO}_2\text{S} + \text{NH}_4]^+$ requires m/z 309.1632, found 309.1614.

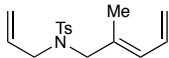
(*E*)-*N*-Allyl-4-methyl-*N*-(penta-2,4-dien-1-yl)benzenesulfonamide (3.45): A flame-dried



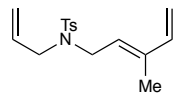
100 mL round-bottomed flask was charged with PPh_3 (1.2 equiv, 2.50 mmol, 656 mg) and (*E*)-*N*-(penta-2,4-dien-1-yl)-4-methylbenzenesulfonamide²² (1 equiv, 2.10 mmol, 500 mg) and then purged with N_2 . Dry THF (42 mL) and allyl alcohol (1 equiv, 2.10 mmol, 145 μL) were added via syringe, and the reaction mixture was stirred and cooled to 0 $^\circ\text{C}$. Diisopropyl azodicarboxylate (DIAD, 1.2 equiv, 2.50 mmol, 492 μL) was added dropwise, and the reaction was slowly warmed to room temperature. After 24 h, an additional portion of allyl alcohol (0.25 equiv, 0.50 mmol, 36 μL), PPh_3 (0.25 equiv, 0.50 mmol, 164 mg) and DIAD (0.25 equiv, 0.5 mmol, 123 μL) were added, and the reaction was stirred for an additional 24 h. The solvent was then removed *in vacuo* and the residue purified by flash column chromatography on silica gel (8:1 hexanes: EtOAc) to afford the product as a clear oil (308 mg, 1.11 mmol, 53%). IR (neat): 3018, 2925, 1345, 1159, 1046 cm^{-1} . ^1H NMR (500 MHz, CDCl_3) δ 7.70 (d, J = 8.0 Hz, 2H), 7.30 (d, J = 8.0 Hz, 2H), 6.24 (dt, J = 16.9, 10.3 Hz, 1H), 6.07 (dd, J = 15.3, 10.5 Hz, 1H), 5.61 (ddt, J = 17.7, 9.5, 6.3 Hz, 1H), 5.46 (dt, J =

15.1, 6.7 Hz, 1H), 5.19–5.11 (m, 3H), 5.08 (d, $J = 10.2$ Hz, 1H), 3.83 (d, $J = 6.7$ Hz, 2H), 3.79 (d, $J = 6.4$ Hz, 2H), 2.43 (s, 3H). ^{13}C NMR (126 MHz, CDCl_3) δ 143.3, 137.4, 135.9, 134.8, 132.8, 129.8, 127.8, 127.3, 119.0, 118.0, 49.5, 48.5, 21.6. HRMS (ESI) calculated for $[\text{C}_{15}\text{H}_{19}\text{NO}_2\text{S} + \text{H}]^+$ requires m/z 278.1210, found 278.1200.

(*E*)-*N*-Allyl-4-methyl-*N*-(2-methylpenta-2,4-dien-1-yl)benzenesulfonamide (3.46): A

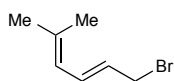
 flame-dried 100 mL round-bottomed flask was charged with PPh_3 (1.2 equiv, 2.45 mmol, 643 mg) and *N*-allyl-4-methyl-benzenesulfonamide²⁰ (1 equiv, 2.04 mmol, 431 mg) and then purged with N_2 . Dry THF (40 mL) and (*E*)-2-methylpenta-2,4-diene-1-ol²³ (1 equiv, 2.04 mmol, 200 mg) were added via syringe, and the reaction mixture was stirred and cooled to 0 °C. Diisopropyl azodicarboxylate (DIAD, 1.2 equiv, 2.45 mmol, 482 μL) was added dropwise, and the reaction was slowly warmed to room temperature. After 36 hours, the solvent was removed *in vacuo* and the residue purified by flash column chromatography on silica gel (8:1 hexanes: EtOAc) to afford the product as a clear oil (319 mg, 1.09 mmol, 54%). IR (neat): 3089, 2986, 1470, 1347, 1162 cm^{-1} . ^1H NMR (500 MHz, CDCl_3) δ 7.70 (d, $J = 8.1$ Hz, 2H), 7.30 (d, $J = 8.0$ Hz, 2H), 6.54 (dt, $J = 16.8, 10.5$ Hz, 1H), 5.88 (d, $J = 10.9$ Hz, 1H), 5.51 (ddt, $J = 16.8, 10.3, 6.5$ Hz, 1H), 5.18–5.03 (m, 4H), 3.74 (d, $J = 6.8$ Hz, 2H), 3.73 (s, 2H), 2.43 (s, 3H), 1.72 (s, 3H). ^{13}C NMR (126 MHz, CDCl_3) δ 143.3, 137.5, 133.1, 132.5, 132.5, 129.8, 129.4, 127.3, 119.3, 117.6, 54.6, 49.6, 21.7, 14.7. HRMS (ESI) calculated for $[\text{C}_{16}\text{H}_{21}\text{NO}_2\text{S} + \text{NH}_4]^+$ requires m/z 309.1632, found 309.1617.

(*E*)-*N*-Allyl-4-methyl-*N*-(3-methylpenta-2,4-dien-1-yl)benzenesulfonamide (3.47): A



flame-dried 25 mL round-bottomed flask was charged with PPh₃ (1.4 equiv, 3.50 mmol, 918 mg) and *N*-allyl-4-methyl-benzenesulfonamide²⁰ (1 equiv, 2.50 mmol, 538 mg) and then purged with N₂. Dry THF (5 mL) and (*E*)-3-methylpenta-2,4-diene-1-ol²⁴ (1 equiv, 2.50 mmol, 250 mg) were added via syringe, and the reaction mixture was stirred and cooled to 0 °C. Diisopropyl azodicarboxylate (DIAD, 1.4 equiv, 3.50 mmol, 690 μL) was added dropwise, and the reaction was slowly warmed to room temperature. After 36 h, the solvent was removed *in vacuo* and the residue purified by flash column chromatography on silica gel (8:1 hexanes: EtOAc) to afford the product as a clear oil (526 mg, 1.81 mmol, 72%). IR (neat): 2926, 1340, 1157, 732 cm⁻¹. ¹H NMR (500 MHz, CDCl₃) δ 7.70 (d, *J* = 8.3 Hz, 2H), 7.30 (d, *J* = 8.0 Hz, 2H), 6.25 (dd, *J* = 17.4, 10.7 Hz, 1H), 5.64 (ddt, *J* = 17.9, 9.7, 6.3 Hz, 1H), 5.27 (t, *J* = 7.1 Hz, 1H), 5.19–5.10 (m, 3H), 5.02 (d, *J* = 10.7 Hz, 1H), 3.93 (d, *J* = 7.0 Hz, 2H), 3.78 (d, *J* = 6.4 Hz, 2H), 2.43 (s, 3H), 1.70 (s, 3H). ¹³C NMR (126 MHz, CDCl₃) δ 143.3, 140.5, 137.5, 137.5, 133.1, 129.8, 127.3, 126.2, 118.9, 113.1, 49.8, 44.5, 21.6, 11.9. HRMS (ESI) calculated for [C₁₆H₂₁NO₂S + H]⁺ requires *m/z* 292.1366, found 292.1366.

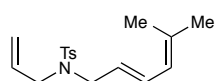
(*E*)-1-Bromo-5-methylhexa-2,4-diene: A stirred solution of (*E*)-5-methylhexa-2,4-dien-1-ol²⁵



(3.2 mmol, 360 mg) in dry Et₂O (3 mL) was cooled to 0 °C under N₂ in a flame-dried 25 mL round-bottomed flask. A solution of PBr₃ (2.7 mmol, 254 μL) in dry Et₂O (3 mL) was added dropwise via syringe pump, and the reaction mixture continued to stir at 0 °C for an additional 60 min. The reaction was quenched by the dropwise addition of saturated aqueous NaHCO₃ and then diluted with water and Et₂O. The layers were separated, and the aqueous layer further extracted with Et₂O (2x). The combined organic layers

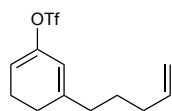
were washed with brine, dried over MgSO_4 , filtered, and concentrated *in vacuo*. The crude bromide was used immediately in the synthesis of (*E*)-*N*-allyl-4-methyl-*N*-(5-methylhexa-2,4-dien-1-yl)benzenesulfonamide without further purification.

(*E*)-*N*-Allyl-4-methyl-*N*-(5-methylhexa-2,4-dien-1-yl)benzenesulfonamide (3.48): A stirred



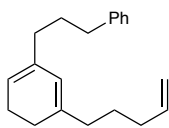
suspension of NaH (60% dispersion in mineral oil, 2.4 mmol, 96 mg) in freshly distilled DMF (2.5 mL) was cooled to 0 °C under N_2 in a flame-dried 25 mL round-bottomed flask. A solution of *N*-allyl-4-methyl-benzenesulfonamide²⁰ (1.6 mmol, 338 mg) in DMF (2.5 mL) was added dropwise, and the reaction mixture was warmed to room temperature for 20 min before being cooled again to 0 °C. The crude bromide (*E*)-1-bromo-5-methylhexa-2,4-diene was added dropwise in DMF (3 mL), and the reaction mixture was slowly warmed to room temperature. After 16 h, the reaction was quenched with saturated aqueous NH_4Cl and extracted into Et_2O (3x). The combined organic layers were dried over MgSO_4 , filtered, and concentrated *in vacuo*. The residue was purified by flash column chromatography on silica gel (8:1 hexanes:EtOAc) to afford the product as a clear oil (>10:1 *E*:*Z*, 1.49 mmol, 456 mg, 93%). IR (neat): 2978, 1336, 1154, 663 cm^{-1} . ^1H NMR (500 MHz, CDCl_3) δ 7.70 (d, J = 8.3 Hz, 2H), 7.29 (d, J = 8.0 Hz, 2H), 6.25 (dd, J = 14.9, 11.1 Hz, 1H), 5.72 (d, J = 10.9 Hz, 1H), 5.67–5.58 (m, 1H), 5.26 (dt, J = 14.5, 6.9 Hz, 1H), 5.17–5.11 (m, 2H), 3.85 (d, J = 6.9 Hz, 2H), 3.79 (d, J = 6.3 Hz, 2H), 2.43 (s, 3H), 1.75 (s, 3H), 1.70 (s, 3H). ^{13}C NMR (126 MHz, CDCl_3) δ 143.2, 137.7, 136.6, 133.1, 131.2, 129.8, 127.3, 124.1, 124.0, 118.9, 49.2, 49.0, 26.1, 21.7, 18.4. HRMS (ESI) calculated for $[\text{C}_{17}\text{H}_{23}\text{NO}_2\text{S} + \text{H}]^+$ requires m/z 306.1523, found 306.1536.

5-(Pent-4-en-1-yl)cyclohexa-1,5-dien-1-yl trifluoromethanesulfonate (3.49): A solution of



LDA was freshly prepared by the dropwise addition of *n*-BuLi (1.6 M in hexanes, 3.10 mmol, 1.9 mL) to *i*-Pr₂NH₂ (3.10 mmol, 435 μ L) at $-78\text{ }^{\circ}\text{C}$ under N₂ in dry THF (5 mL) in a flame-dried 100 mL round-bottomed flask. The reaction mixture was allowed to stir for 20 minutes at $-78\text{ }^{\circ}\text{C}$, at which point a nitrogen-purged solution of 3-(pent-4-en-1-yl)cyclohex-2-enone²⁶ (2.9 mmol, 480 mg) in THF (10 mL) was added dropwise. The reaction was allowed to stir for an additional 30 min and was then warmed to $0\text{ }^{\circ}\text{C}$. A nitrogen-purged solution of *N*-phenyl-bis(trifluoromethanesulfonimide) (2.9 mmol, 1.0 g) in THF (4 mL) was added dropwise, and after stirring at $0\text{ }^{\circ}\text{C}$ for an additional 3 h, the reaction was quenched with water and extracted into Et₂O (3x). The combined organic layers were washed with brine, dried over MgSO₄, filtered, and concentrated *in vacuo*. The resulting residue was purified by flash column chromatography under N₂ on silica gel (2x, hexanes to 20:1 hexanes:Et₂O) to afford the product as a clear oil (1.85 mmol, 547 mg, 64%). This material was used immediately as a substrate for the [2+2] photocycloaddition and in the synthesis of (3-(5-(pent-4-en-1-yl)cyclohexa-1,5-dien-1-yl)propyl)benzene. IR (neat): 2939, 1420, 1216, 1145 cm^{-1} . ¹H NMR (500 MHz, CDCl₃) δ 5.80 (ddt, $J = 16.9, 10.2, 6.7\text{ Hz}$, 1H), 5.59–5.52 (m, 2H), 5.02 (ddt, $J = 17.2, 1.5, 1.5\text{ Hz}$, 1H), 5.00–4.96 (m, 1H), 2.37 (td, $J = 9.7, 4.7\text{ Hz}$, 2H), 2.16 (t, $J = 9.8\text{ Hz}$, 2H), 2.14 (t, $J = 7.8\text{ Hz}$, 2H) 2.07 (dt, $J = 7.2, 7.2\text{ Hz}$, 2H), 1.60–1.52 (m, 2H). ¹³C NMR (126 MHz, CDCl₃) δ 146.8, 146.3, 138.3, 118.7 (q, $J = 320.5\text{ Hz}$), 115.3, 115.2, 111.8, 36.3, 33.3, 26.4, 26.2, 22.2. HRMS (ESI) calculated for [C₁₂H₁₅F₃O₃·S + NH₄]⁺ requires m/z 314.1033, found 314.1031.

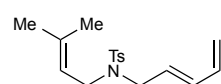
(3-(5-(Pent-4-en-1-yl)cyclohexa-1,5-dien-1-yl)propyl)benzene (3.50): A solution of (3-



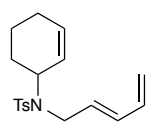
phenylpropyl)magnesium bromide was freshly prepared by the dropwise addition of 1-bromo-3-phenylpropane (2.53 mmol, 385 μ L) to a suspension of magnesium (3.80 mmol, 92 mg) in Et₂O (5 mL) in a 25 mL flame-dried 3-neck flask fitted to a reflux condenser under N₂. The solution was heated occasionally with a heat gun during the addition to initiate the reaction, and then allowed to stir at room temperature for an additional 2 h. Meanwhile, a solution of Ni(dppp)Cl₂ (0.05 equiv, 0.085 mmol, 45 mg) and 5-(pent-4-en-1-yl)cyclohexa-1,5-dien-1-yl trifluoromethanesulfonate (1 equiv, 1.69 mmol, 500 mg) in Et₂O (8.5 mL) was cooled to -78°C under N₂ in an oven-dried 50 mL Schlenk flask. The Grignard solution was then added dropwise, the flask sealed with a glass stopper, and the reaction mixture stirred at 0°C for 18 h. The reaction was quenched with water and extracted into Et₂O (3x). The combined organic layers were washed with brine, dried over MgSO₄, filtered and concentrated *in vacuo*. The resulting residue was purified by flash column chromatography on silica gel (hexanes) and then again on silica gel containing 10% AgNO₃²⁷ (20:1 hexanes:Et₂O to 5:1 hexanes:Et₂O). The combined clean fractions were taken up in Et₂O and washed with saturated aqueous NH₄OH and brine, dried over MgSO₄, filtered and concentrated *in vacuo*. The resulting residue was purified on silica gel (hexanes) to afford the product as a clear oil (0.856 mmol, 228 mg, 51%). IR (neat): 3026, 2927, 1454, 910, 698 cm^{-1} . ¹H NMR (500 MHz, CDCl₃) δ 7.30–7.23 (m, 2H), 7.20–7.14 (m, 3H), 5.82 (ddt, J = 16.9, 10.2, 6.6 Hz, 1H), 5.56 (s, 1H), 5.36 (t, J = 4.4 Hz, 1H), 5.01 (ddt, J = 17.3, 1.7, 1.7 Hz, 1H), 4.96 (dd, J = 10.1, 1.7 Hz, 1H), 2.60 (t, J = 7.7 Hz, 2H), 2.18–1.97 (m, 10H), 1.73 (tt, J = 7.7, 7.7 Hz, 2H), 1.54 (tt, J = 7.4, 7.4 Hz, 2H). ¹³C NMR (126 MHz, CDCl₃) δ 142.8, 140.2, 139.0, 136.2, 128.6, 128.4,

125.7, 121.7, 117.8, 114.7, 36.9, 35.6, 35.3, 33.6, 30.3, 27.0, 27.0, 23.4. HRMS (EI) calculated for $[C_{20}H_{26}]^+$ requires m/z 266.2030, found 266.2034.

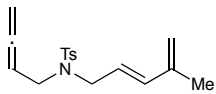
(*E*)-4-Methyl-*N*-(3-methylbut-2-en-1-yl)-*N*-(penta-2,4-dien-1-yl)benzenesulfonamide



(3.51): A flame-dried 100 mL round-bottomed flask was charged with PPh_3 (1.4 equiv, 2.45 mmol, 643 mg) and (*E*)-*N*-(penta-2,4-dien-1-yl)-4-methylbenzenesulfonamide²² (1 equiv, 1.75 mmol, 415 mg) and then purged with N_2 . Dry THF (35 mL) and 3-methyl-2-buten-1-ol (1 equiv, 1.75 mmol, 180 μ L) were added via syringe, and the reaction mixture was stirred and cooled to 0 °C. Diisopropyl azodicarboxylate (DIAD, 1.4 equiv, 2.45 mmol, 482 μ L) was added dropwise, and the reaction was slowly warmed to room temperature. After 36 h, the solvent was removed *in vacuo* and the residue purified by flash column chromatography on silica gel (8:1 hexanes: EtOAc) to afford the product as a clear oil (370 mg, 1.21 mmol, 69%). IR (neat): 2917, 1337, 1154, 904, 739 cm^{-1} . 1H NMR (500 MHz, $CDCl_3$) δ 7.69 (d, J = 8.0 Hz, 2H), 7.29 (d, J = 8.0 Hz, 2H), 6.25 (dt, J = 16.9, 10.3 Hz, 1H), 6.07 (dd, J = 15.2, 10.5 Hz, 1H), 5.49 (dt, J = 15.2, 6.6 Hz, 1H), 5.15 (d, J = 16.9 Hz, 1H), 5.07 (d, J = 10.1 Hz, 1H), 5.01–4.94 (m, 1H), 3.80 (d, J = 6.6 Hz, 2H), 3.77 (d, J = 7.1 Hz, 2H), 2.42 (s, 3H), 1.65 (s, 3H), 1.57 (s, 3H). ^{13}C NMR (126 MHz, $CDCl_3$) δ 143.1, 137.7, 137.1, 136.1, 134.5, 129.7, 128.4, 127.3, 118.9, 117.8, 48.5, 44.6, 25.9, 21.6, 18.0. HRMS (ESI) calculated for $[C_{17}H_{23}NO_2S + H]^+$ requires m/z 306.1523, found 306.1529.

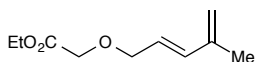
(E)-N-(Cyclohex-2-en-1-yl)-4-methyl-N-(penta-2,4-dien-1-yl)benzenesulfonamide (3.52):

A flame-dried 250 mL round-bottomed flask was charged with PPh₃ (1.2 equiv, 5.10 mmol, 1.34 g) and (E)-N-(penta-2,4-dien-1-yl)-4-methylbenzenesulfonamide²² (1 equiv, 4.20 mmol, 1.00 g) and then purged with N₂. Dry THF (84 mL) and 2-cyclohexen-1-ol (1 equiv, 4.20 mmol, 412 μ L) were added via syringe, and the reaction mixture was stirred and cooled to 0 °C. Diisopropyl azodicarboxylate (DIAD, 1.2 equiv, 5.10 mmol, 1.00 mL) was added dropwise and the reaction was slowly warmed to room temperature. After 24 h, an additional portion of PPh₃ (0.25 equiv, 1.05 mmol, 335 mg) and DIAD (0.25 equiv, 1.05 mmol, 250 μ L) were added and the reaction was stirred for an additional 24 h. The solvent was then removed *in vacuo* and the residue purified by flash column chromatography on silica gel (8:1 hexanes: EtOAc) to afford the product as a clear oil (997 mg, 3.14 mmol, 75%). IR (neat): 2933, 1355, 1157, 1090, 662 cm⁻¹. ¹H NMR (500 MHz, CDCl₃) δ 7.71 (d, *J* = 8.1 Hz, 2H), 7.28 (d, *J* = 8.2 Hz, 2H), 6.28 (dt, *J* = 16.9, 10.2 Hz, 1H), 6.15 (dd, *J* = 15.2, 10.5 Hz, 1H), 5.84–5.75 (m, 1H), 5.69 (dt, *J* = 15.1, 6.2 Hz, 1H), 5.17 (d, *J* = 16.8 Hz, 1H), 5.10 (d, *J* = 10.3 Hz, 1H), 5.07 (d, *J* = 10.3 Hz, 1H), 4.57–4.49 (m, 1H), 3.89 (dd, *J* = 16.7, 5.7 Hz, 1H), 3.66 (dd, *J* = 16.7, 6.7 Hz, 1H), 2.42 (s, 3H), 1.97–1.89 (m, 2H), 1.89–1.80 (m, 1H), 1.80–1.69 (m, 1H), 1.64–1.49 (m, 2H). ¹³C NMR (126 MHz, CDCl₃) δ 143.1, 138.5, 136.4, 132.8, 132.6, 131.9, 129.7, 127.6, 127.2, 117.3, 55.5, 45.7, 29.0, 24.6, 21.8, 21.6. HRMS (ESI) calculated for [C₁₈H₂₃NO₂S +H]⁺ requires *m/z* 318.1523, found 318.1526.

(E)-N-(Buta-2,3-dien-1-yl)-4-methyl-N-(4-methylpenta-2,4-dien-1-yl)benzenesulfonamide

(3.53): A flame-dried 25 mL round-bottomed flask was charged with PPh₃ (1.2 equiv, 2.10 mmol, 551 mg) and then purged with N₂. Dry THF (9

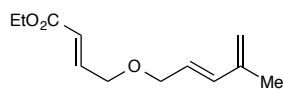
mL), *N*-(buta-2,3-dien-1-yl)-4-methylbenzenesulfonamide²⁸ (1 equiv, 1.79 mmol, 400 mg), and (*E*)-4-methylpenta-2,4-diene-1-ol²¹ (1 equiv, 1.79 mmol, 176 mg) were added via syringe and the reaction mixture was stirred and cooled to 0 °C. Diisopropyl azodicarboxylate (DIAD, 1.2 equiv, 2.10 mmol, 413 μL) was added dropwise, and the reaction was slowly warmed to room temperature. After 20 h, the solvent was removed *in vacuo* and the residue purified by flash column chromatography on silica gel (8:1 hexanes: EtOAc) to afford the product as a clear oil (408 mg, 1.34 mmol, 75%). IR (neat): 2923, 1337, 1156, 734 cm⁻¹. ¹H NMR (500 MHz, CDCl₃) δ 7.71 (d, *J* = 8.3 Hz, 2H), 7.30 (d, *J* = 8.0 Hz, 2H), 6.18 (d, *J* = 15.6 Hz, 1H), 5.42 (dt, *J* = 15.6, 6.8 Hz, 1H), 4.99–4.86 (m, 3H), 4.70 (t, *J* = 2.5 Hz, 1H), 4.69 (t, *J* = 2.5 Hz, 1H), 3.90 (d, *J* = 6.8 Hz, 2H), 3.85 (dt, *J* = 7.1, 2.5 Hz, 2H), 2.42 (s, 3H), 1.75 (s, 3H). ¹³C NMR (126 MHz, CDCl₃) δ 209.7, 143.4, 141.2, 137.6, 137.1, 129.8, 127.3, 123.7, 117.2, 85.8, 76.3, 48.8, 45.9, 21.6, 18.6. HRMS (ESI) calculated for [C₁₇H₂₁NO₂S + H]⁺ requires *m/z* 304.1366, found 304.1361.

(E)-Ethyl 2-((4-methylpenta-2,4-dien-1-yl)oxy)acetate (3.54):

sodium hydride (60% dispersion in mineral oil, 1.4 equiv, 30.0 mmol, 1.20 g) in dry THF (42 mL) was cooled to 0 °C under N₂ in a flame-dried 250 mL round-bottomed flask. A solution of (*E*)-4-methylpenta-2,4-penta-2,4-dien-1-ol⁵ (1 equiv, 21.4 mmol, 2.10 g) in dry THF (21 mL) was added dropwise over 30 min. The reaction mixture was warmed to room temperature and stirred for an additional 30 min before being cooled again to

0 °C. A solution of ethyl bromoacetate (1.4 equiv, 30.0 mmol, 3.30 mL) in dry THF (11 mL) was then added and the reaction mixture slowly warmed to room temperature. After 15 h, the reaction was quenched with water and extracted with Et₂O (3x). The combined organic layers were washed with brine, dried over MgSO₄, and concentrated *in vacuo*. The residue was purified by flash column chromatography on silica gel (8:1 hexanes:EtOAc) to afford the product as a clear liquid (2.35 g, 12.8 mmol, 60%). IR (neat): 2984, 1749, 1210, 1127 cm⁻¹. ¹H NMR (500 MHz, CDCl₃) δ 6.35 (d, *J* = 15.8 Hz, 1H), 5.74 (dt, *J* = 15.6, 6.4 Hz, 1H), 5.01 (s, 1H), 5.00 (s, 1H), 4.23 (q, *J* = 7.1 Hz, 2H), 4.17 (d, *J* = 6.3 Hz, 2H), 4.08 (s, 2H), 1.86 (s, 3H), 1.29 (t, *J* = 7.1 Hz, 3H). ¹³C NMR (126 MHz, CDCl₃) δ 170.5, 141.3, 136.6, 124.9, 117.5, 72.0, 67.3, 61.0, 18.6, 14.3. HRMS (ESI) calculated for [C₁₀H₁₆O₃ + NH₄]⁺ requires *m/z* 202.1438, found 202.1430.

(*E*)-Ethyl-4-(((*E*)-4-methylpenta-2,4-dien-1-yl)oxy)but-2-enoate (3.55): A solution of (*E*)-



Ethyl 2-((4-methylpenta-2,4-dien-1-yl)oxy)acetate (1 equiv, 4.10 mmol, 755 mg) in dry Et₂O (135 mL) was cooled to -78 °C under N₂

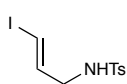
in a flame-dried 500 mL round-bottomed flask. DIBAL (1.0 M in hexanes, 1.5 equiv, 6.2 mL) was added dropwise via syringe pump. After stirring for an additional 60 minutes, the reaction mixture was warmed to 0 °C, quenched with saturated Rochelle's salt, and stirred at room temperature for 45 min. The mixture was then extracted with Et₂O (3x), dried over Na₂SO₄, filtered, and concentrated *in vacuo*. The crude aldehyde was added in CH₂Cl₂ (2 mL) to a stirred solution of (carbethoxymethylene)triphenylphosphorane (1.5 equiv, 6.15 mmol, 2.14 g) in CH₂Cl₂ (10 mL) in a flame-dried 50 mL round bottom flask under N₂ at room temperature. After stirring for 12 h, an additional portion of the ylide (0.53 equiv, 2.15 mmol, 0.75 g) was

added and the reaction mixture continued to stir for 6 h, at which point it was concentrated *in vacuo*. The crude residue was purified by flash column chromatography (10:1 hexanes:EtOAc) to afford the product as a clear oil (pure *E* isomer: 267 mg, 1.27 mmol, 31%). IR (neat): 2981, 1719, 1177, 981 cm^{-1} . ^1H NMR (500 MHz, CDCl_3) δ 6.97 (dt, $J = 15.7, 4.4$ Hz, 1H), 6.35 (d, $J = 15.7$ Hz, 1H), 6.09 (dt, $J = 15.7, 1.9$ Hz, 1H), 5.73 (dt, $J = 15.7, 6.2$ Hz, 1H), 5.01 (s, 1H), 5.00 (s, 1H), 4.21 (q, $J = 7.1$ Hz, 2H), 4.15 (dd, $J = 4.4, 2.0$ Hz, 2H), 4.10 (d, $J = 6.0$ Hz, 2H), 1.86 (s, 3H), 1.29 (t, $J = 7.1$ Hz, 3H). ^{13}C NMR (126 MHz, CDCl_3) δ 166.5, 144.4, 141.4, 135.9, 125.4, 121.5, 117.3, 71.4, 68.7, 60.5, 18.7, 14.4. HRMS (ESI) calculated for $[\text{C}_{12}\text{H}_{18}\text{O}_3 + \text{H}]^+$ requires m/z 211.1329, found 211.1321.

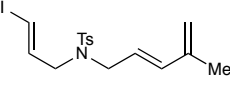
(*E*)-*tert*-Butyl-(3-iodoallyl)(tosyl)carbamate (3.56): A stirred solution of (*E*)-ethyl 3-iodoacrylate²⁹ (10.2 mmol, 2.3 g) in 20 mL dry THF was cooled to -78 $^{\circ}\text{C}$ under N_2 in an oven-dried 250 mL round-bottomed flask. DIBAL (1.0 M in hexanes, 2.5 equiv, 25 mL) was added dropwise. After stirring for an additional 2 hours at -78 $^{\circ}\text{C}$, the reaction mixture was warmed to 0 $^{\circ}\text{C}$, quenched with saturated Rochelle's salt and stirred at room temperature for 45 min. The mixture was then extracted into Et_2O (3x), dried over MgSO_4 , filtered, and partially concentrated *in vacuo* to a volume of approximately 10 mL. The crude alcohol (*E*)-3-iodoprop-2-en-1-ol thus obtained was added to a stirred mixture of *N*-(*tert*-butoxycarbonyl)-*p*-toluenesulfonamide (1 equiv, 10.2 mmol, 2.76 g), PPh_3 (1.2 equiv, 12.2 mmol, 3.2 g), and THF (100 mL) in an oven-dried 250 mL round-bottomed flask under N_2 at 0 $^{\circ}\text{C}$. Diisopropyl azodicarboxylate (DIAD, 1.2 equiv, 12.2 mmol, 2.4 mL) was then added dropwise, and the reaction mixture was allowed to slowly warm to room temperature. After 20 h, the solvent was removed *in vacuo*, and the resulting residue purified by flash column

chromatography on silica gel (5:1 hexanes:EtOAc) to afford the product as a white solid (4.1 g, 9.4 mmol, 93%). Melting point: 112–114 °C. IR (neat): 1722, 1349, 1151, 668 cm^{-1} . ^1H NMR (500 MHz, CDCl_3) δ 7.81–7.71 (d, J = 8.4 Hz, 2H), 7.32 (d, J = 8.4 Hz, 2H), 6.64 (dt, J = 14.5, 6.4 Hz, 1H), 6.51 (dt, J = 14.5, 1.2 Hz, 1H), 4.37 (dd, J = 6.5, 1.2 Hz, 2H), 2.45 (s, 3H), 1.35 (s, 9H). ^{13}C NMR (126 MHz, CDCl_3) δ 150.6, 144.6, 140.5, 137.0, 129.4, 128.3, 84.9, 81.6, 50.0, 28.0, 21.8. HRMS (ESI) calculated for $[\text{C}_{15}\text{H}_{20}\text{INO}_4\text{S} + \text{H}]$ requires m/z 438.0231, found 438.0230.

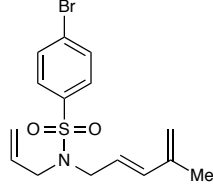
(*E*)-*N*-(3-Iodoallyl)-4-methylbenzenesulfonamide (3.57): A solution of (*E*)-*tert*-butyl-(3-iodoallyl)(tosyl)carbamate (2 g, 4.6 mmol) in CH_2Cl_2 (23 mL) was cooled to 0 °C under N_2 in a flame-dried 100 mL round-bottomed flask. TFA (9 mL) was added dropwise, and the solution was warmed to room temperature. After 60 min, the reaction was quenched with saturated aqueous NaHCO_3 and extracted into EtOAc (3x). The combined organic layers were dried with Na_2SO_4 , filtered, and concentrated *in vacuo*. The resulting residue was purified by flash column chromatography on silica gel (4:1 hexanes:EtOAc) to afford the product as a white solid (1.4 g, 4.2 mmol, 95%). Melting point: 92–95 °C. IR (neat): 3258, 1429, 1156, 1034, 673, 546 cm^{-1} . ^1H NMR (500 MHz, CDCl_3) δ 7.73 (d, J = 8.3 Hz, 2H), 7.33 (d, J = 8.1 Hz, 2H), 6.38 (dt, J = 14.5, 6.0 Hz, 1H), 6.29 (dt, J = 14.5, 1.2 Hz, 1H), 4.53 (t, J = 6.4 Hz, NH), 3.56 (ddd, J = 6.2, 6.2, 1.2 Hz, 2H), 2.44 (s, 3H). ^{13}C NMR (126 MHz, CDCl_3) δ 144.0, 140.4, 136.9, 130.0, 127.3, 79.9, 47.4, 21.7. HRMS (ESI) calculated for $[\text{C}_{10}\text{H}_{12}\text{INO}_2\text{S} + \text{H}]$ requires m/z 337.9707, found 337.9708.



***N*-((*E*)-3-Iodoallyl)-4-methyl-*N*-((*E*)-4-methylpenta-2,4-dien-1-yl)benzenesulfonamide**

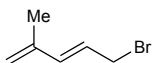
 **(3.58)**: A flame-dried 25 mL round-bottomed flask was charged with PPh₃ (1.3 equiv, 4.6 mmol, 1.2 g) and (*E*)-*tert*-butyl (3-iodoallyl)(tosyl)carbamate (1 equiv, 3.6 mmol, 1.2 g) and then purged with N₂. (*E*)-4-Methylpenta-2,4-diene-1-ol⁵ (1 equiv, 3.6 mmol, 350 mg) and dry THF (70 mL) were added, and the stirred reaction mixture was cooled to 0 °C. Diisopropyl azodicarboxylate (DIAD, 1.3 equiv, 4.6 mmol, 910 µL) was added dropwise, and the reaction was slowly warmed to room temperature. After 14 h, the solvent was removed in vacuo, and the residue was purified by flash column chromatography on silica gel (8:1 hexanes:EtOAc) to afford the product as a white solid (1.1 g, 2.7 mmol, 77%). Melting point: 65–67 °C. IR (neat): 2970, 1332, 1154, 889, 554 cm⁻¹. ¹H NMR (500 MHz, CDCl₃) δ 7.68 (d, *J* = 8.3 Hz, 2H), 7.32 (d, *J* = 8.0 Hz, 2H), 6.33 (dt, *J* = 14.4, 6.3 Hz, 1H), 6.25 (d, *J* = 14.6 Hz, 1H), 6.14 (d, *J* = 15.2 Hz, 1H), 5.37 (dt, *J* = 15.5, 6.8 Hz, 1H), 4.98 (s, 1H), 4.94 (s, 1H), 3.85 (d, *J* = 6.8 Hz, 2H), 3.74 (d, *J* = 6.2 Hz, 2H), 2.44 (s, 3H), 1.74 (s, 3H). ¹³C NMR (126 MHz, CDCl₃) δ 143.7, 141.0, 140.4, 137.3, 137.2, 129.9, 127.4, 123.5, 117.7, 80.3, 50.8, 49.5, 21.7, 18.6. HRMS (ESI) calculated for [C₁₆H₂₀INO₂S + H] requires *m/z* 418.0333, found 418.0318.

***(E)*-*N*-Allyl-4-bromo-*N*-(4-methylpenta-2,4-dien-1-yl)benzenesulfonamide (3.59)**: A flame-

 dried 50 mL round-bottomed flask was charged with PPh₃ (1.4 equiv, 4.13 mmol, 290 mg) and *N*-allyl-4-bromo-benzenesulfonamide²⁰ (1 equiv, 2.95 mmol, 815 mg) and then purged with N₂. Dry THF (6 mL) and (*E*)-4-methylpenta-2,4-dien-1-ol²¹ (1 equiv, 2.95 mmol, 290 mg) were added via syringe, and the reaction mixture was cooled to 0 °C. Diisopropyl azodicarboxylate (DIAD, 1.4 equiv, 4.13

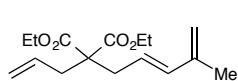
mmol, 813 μ L) was added dropwise, and the reaction mixture was then slowly warmed to room temperature. After 20 h, the solvent was removed *in vacuo* and the residue purified by flash column chromatography on silica gel (8:1 hexanes:EtOAc) to afford the product as a clear oil (2.51 mmol, 894 mg, 85%). IR (neat): 2915, 1335, 1161, 1067, 888 cm^{-1} . ^1H NMR (500 MHz, CDCl_3) δ 7.71–7.62 (m, 4H), 6.15 (d, J = 15.6 Hz, 1H), 5.62 (ddt, J = 16.7, 10.2, 6.3 Hz, 1H), 5.37 (dt, J = 15.5, 6.7 Hz, 1H), 5.19–5.13 (m, 2H), 4.99 (s, 1H), 4.93 (s, 1H), 3.87 (d, J = 6.7 Hz, 2H), 3.82 (d, J = 6.4 Hz, 2H), 1.74 (s, 3H). ^{13}C NMR (126 MHz, CDCl_3) δ 141.0, 139.7, 137.4, 132.5, 132.4, 128.9, 127.5, 123.2, 119.4, 117.6, 49.6, 48.9, 18.5. HRMS (ESI) calculated for $[\text{C}_{15}\text{H}_{18}\text{BrNO}_2\text{S} + \text{Na}]^+$ requires m/z 378.0134, found 378.0148.

(*E*)-5-Bromo-2-methylpenta-1,3-diene.²¹ A solution of (*E*)-4-methylpenta-2,4-dien-1-ol (7.69



mmol, 755 mg) in dry Et_2O (8 mL) was cooled to 0 $^\circ\text{C}$ under N_2 in a flame-dried 50 mL round-bottomed flask. A solution of PBr_3 (6.41 mmol, 608 μ L) in dry Et_2O (8 mL) was added dropwise via syringe pump, and the reaction mixture continued to stir at 0 $^\circ\text{C}$ for an additional 2 h. The reaction was quenched by the dropwise addition of saturated aqueous NaHCO_3 , and then diluted with water and Et_2O . The layers were separated, and the aqueous layer further extracted with Et_2O (2x). The combined organic layers were washed with brine, dried over MgSO_4 , filtered, and concentrated *in vacuo*. The crude bromide was used immediately in the synthesis of (*E*)-diethyl 2-allyl-2-(4-methylpenta-2,4-dien-1-yl)malonate without further purification.

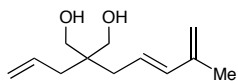
(E)-Diethyl 2-allyl-2-(4-methylpenta-2,4-dien-1-yl)malonate (3.60): A stirred suspension of



NaH (60% dispersion in mineral oil, 7.69 mmol, 310 mg) in dry THF (9 mL) was cooled to 0 °C under N₂ in a flame-dried 50 mL round-

bottomed flask. Diethyl allylmalonate³⁰ (5.49 mmol, 1.10 g) was added dropwise, and the reaction mixture was warmed to room temperature for 20 min before being cooled again to 0 °C. Unpurified (*E*)-5-Bromo-2-methylpenta-1,3-diene was added dropwise in THF (1 mL), and the reaction mixture was slowly warmed to room temperature. After 16 h, the reaction was quenched with water and extracted into Et₂O (3x). The combined organic layers were washed with brine, dried over MgSO₄, filtered, and concentrated *in vacuo*. The residue was purified by flash column chromatography on silica gel (10:1 hexanes:EtOAc) to afford the product as a clear oil (2.83 mmol, 794 mg, 53%). IR (neat): 2984, 1726, 1472, 1382, 1096 cm⁻¹. ¹H NMR (500 MHz, CDCl₃) δ 6.17 (d, *J* = 15.8 Hz, 1H), 5.67 (ddt, *J* = 16.4, 10.6, 7.4 Hz, 1H), 5.47 (dt, *J* = 15.4, 7.6 Hz, 1H), 5.12 (d, *J* = 16.4 Hz, 1H), 5.11 (d, *J* = 10.6 Hz, 1H), 4.90 (s, 1H), 4.88 (s, 1H), 4.18 (q, *J* = 7.1 Hz, 4H), 2.68 (d, *J* = 7.6 Hz, 2H), 2.64 (d, *J* = 7.4 Hz, 2H), 1.80 (s, 3H), 1.24 (t, *J* = 7.1 Hz, 6H). ¹³C NMR (126 MHz, CDCl₃) δ 170.9, 141.8, 137.1, 132.5, 123.7, 119.3, 115.9, 61.4, 57.8, 37.2, 36.0, 18.7, 14.3. HRMS (ESI) calculated for [C₁₆H₂₄O₄ + Na]⁺ requires *m/z* 303.1567, found 303.1559.

(E)-2-Allyl-2-(4-methylpenta-2,4-dien-1-yl)propane-1,3-diol (3.61): A stirred suspension of

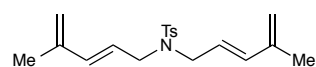


LiAlH₄ (2.5 equiv, 5.0 mmol, 190 mg) in dry Et₂O (2.5 mL) was cooled to 0 °C under N₂ in a flame-dried 25 mL round-bottomed flask. A

solution of (*E*)-diethyl 2-allyl-2-(4-methylpenta-2,4-dien-1-yl)malonate (1 equiv, 2.0 mmol, 560 mg) in Et₂O (1.3 mL) was added dropwise via syringe pump. The reaction mixture was

warmed to room temperature and allowed to stir for 4 h, at which point it was cooled again to 0 °C and quenched by the dropwise addition of water. The mixture was diluted with 10% H₂SO₄ and EtOAc, the layers were separated, and the aqueous layer was further extracted with EtOAc (4x). The combined organic layers were dried over Na₂SO₄, filtered, and concentrated *in vacuo*. The residue was purified by flash column chromatography on silica gel (1:1 hexanes:EtOAc) to afford the product as a clear oil (1.95 mmol, 383 mg, 97%). IR (neat): 3388, 2920, 1710, 1026, 734 cm⁻¹. ¹H NMR (500 MHz, CDCl₃) δ 6.20 (d, *J* = 15.5 Hz, 1H), 5.86 (ddt, *J* = 16.4, 10.6, 7.5 Hz, 1H), 5.66 (dt, *J* = 15.5, 7.7 Hz, 1H), 5.12 (d, *J* = 16.4 Hz, 1H), 5.11 (d, *J* = 10.6 Hz, 1H), 4.91 (s, 1H), 4.90 (s, 1H), 3.59 (s, 4H), 2.32 (bs, 2H), 2.14 (d, *J* = 7.6 Hz, 2H), 2.09 (d, *J* = 7.5 Hz, 2H), 1.84 (s, 3H). ¹³C NMR (126 MHz, CDCl₃) δ 141.9, 136.3, 134.1, 125.4, 118.3, 115.4, 68.5, 42.8, 36.5, 35.1, 18.9. HRMS (ESI) calculated for [C₁₂H₂₀O₂ + H]⁺ requires *m/z* 197.1537, found 197.1538.

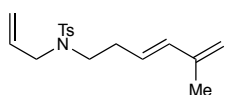
4-Methyl-*N,N*-bis((*E*)-4-methylpenta-2,4-dien-1-yl)benzenesulfonamide (3.62): Dienyl



bromide (*E*)-5-bromo-2-methylpenta-1,3-diene was freshly prepared with the procedure described above using (*E*)-4-methylpenta-2,4-dien-1-ol (12.7 mmol, 1.25 g) in Et₂O (12.7 mL) and PBr₃ (10.6 mmol, 1.00 mL) in Et₂O (1 mL). Meanwhile, a stirred suspension of NaH (60% dispersion in mineral oil, 12.2 mmol, 490 mg) in freshly distilled DMF (7.5 mL) was cooled to 0 °C under N₂ in a flame-dried 50 mL round-bottomed flask. A solution of *p*-toluenesulfonamide (5.1 mmol, 870 mg) in DMF (7.5 mL) was added dropwise, and the reaction mixture was warmed to room temperature for 20 min before being cooled again to 0 °C. The crude bromide was added dropwise in DMF (4 mL), and the reaction mixture slowly warmed to room temperature. After 18 h, the reaction

was quenched with water and extracted into Et₂O (3x). The combined organic layers were dried over MgSO₄, filtered, and concentrated *in vacuo*. The residue was purified by flash column chromatography on silica gel (8:1 hexanes:EtOAc) and then on silica gel containing 10% AgNO₃²⁷ (8:1 to 4:1 hexanes:EtOAc). The combined clean fractions were taken up in Et₂O and washed with saturated aqueous NH₄OH and brine, dried over MgSO₄, filtered, and concentrated *in vacuo*. The resulting residue was purified again on silica gel (8:1 hexanes:EtOAc) to afford the product as a white solid (1.41 mmol, 467 mg, 28%). Melting point: 58–61 °C. IR (neat): 2942, 1329, 1154, 962, 739 cm⁻¹. ¹H NMR (500 MHz, CDCl₃) δ 7.71 (d, *J* = 8.3 Hz, 2H), 7.30 (d, *J* = 8.2 Hz, 2H), 6.14 (d, *J* = 15.7 Hz, 2H), 5.38 (dt, *J* = 15.6, 6.7 Hz, 2H), 4.96 (s, 2H), 4.91 (s, 2H), 3.85 (d, *J* = 6.7 Hz, 4H), 2.43 (s, 3H), 1.73 (s, 6H). ¹³C NMR (126 MHz, CDCl₃) δ 143.3, 141.2, 137.6, 136.9, 129.7, 127.4, 124.0, 117.2, 49.1, 21.6, 18.5. HRMS (ESI) calculated for [C₁₉H₂₅NO₂S + H]⁺ requires *m/z* 332.1679, found 332.1677.

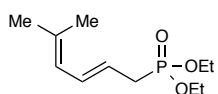
(*E*)-*N*-Allyl-4-methyl-*N*-(5-methylhexa-3,5-dien-1-yl)benzenesulfonamide (3.63): A flame-



dried 50 mL round-bottomed flask was charged with PPh₃ (1.6 equiv, 1.07 mmol, 281 mg) and *N*-allyl-4-methyl-benzenesulfonamide²⁰ (1 equiv, 0.67 mmol, 142 mg) and then purged with N₂. Dry THF (13 mL) and (*E*)-5-methylhexa-3,5-dien-1-ol³¹ (1 equiv, 0.67 mmol, 75 mg) were added via syringe, and the reaction mixture was cooled to 0 °C. Diisopropyl azodicarboxylate (DIAD, 1.4 equiv, 0.94 mmol, 185 μL) was added dropwise, and the reaction mixture was then slowly warmed to room temperature. After 22 h, the solvent was removed *in vacuo*, and the resulting residue was purified by flash column chromatography on silica gel (8:1 hexanes:EtOAc) to afford the product as a clear oil (0.462 mmol, 141 mg, 69%). IR (neat): 2923, 1337, 1154, 659 cm⁻¹. ¹H NMR (500 MHz, CDCl₃) δ

7.70 (d, $J = 8.2$ Hz, 2H), 7.30 (d, $J = 8.0$ Hz, 2H), 6.12 (d, $J = 15.7$ Hz, 1H), 5.65 (ddt, $J = 16.7, 10.1, 6.4$ Hz, 1H), 5.51 (dt, $J = 15.6, 7.1$ Hz, 1H), 5.19 (dd, $J = 16.7, 1.2$ Hz, 1H), 5.15 (dd, $J = 10.1, 1.2$ Hz, 1H), 4.90 (s, 1H), 4.87 (s, 1H), 3.82 (d, $J = 6.4$ Hz, 2H), 3.19 (t, $J = 7.6$ Hz, 2H), 2.43 (s, 3H), 2.34 (dt, $J = 7.1, 7.1$ Hz, 2H), 1.80 (s, 3H). ^{13}C NMR (126 MHz, CDCl_3) δ 143.3, 141.9, 137.3, 135.2, 133.4, 129.8, 127.3, 126.3, 118.9, 115.5, 50.9, 47.1, 32.1, 21.7, 18.7. HRMS (ESI) calculated for $[\text{C}_{17}\text{H}_{23}\text{NO}_2\text{S} + \text{H}]^+$ requires m/z 306.1523, found 306.1524.

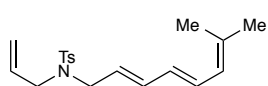
(*E*)-Diethyl (5-methylhexa-2,4-dien-1-yl)phosphonate (3.64): Dienyl bromide (*E*)-1-bromo-



5-methylhexa-2,4-diene was freshly prepared with the procedure described above using (*E*)-5-methylhexa-2,4-dien-1-ol (6.06 mmol, 680 mg) in Et_2O (6 mL) and PBr_3 (5.05 mmol, 475 μL) in Et_2O (6 mL). The crude bromide was transferred in toluene (12 mL) to an oven-dried 100 mL 3-neck flask fitted to a reflux condenser under N_2 . Freshly distilled and sparged $\text{P}(\text{OEt})_3$ (12 mL) was added, and the reaction mixture was heated to 110°C for 12 h. After cooling to room temperature, the solvent was removed *in vacuo* and then further concentrated by high vacuum distillation at 40°C . The resulting residue was purified by flash column chromatography on silica gel (Et_2O to EtOAc) and then heated to 75°C under high vacuum for 90 min to remove any triethyl phosphate to afford the product as a clear liquid (10:1 E:Z, 0.237 mmol, 557 mg, 40%). IR (neat): 2982, 1244, 1020, 960, 732 cm^{-1} . ^1H NMR (500 MHz, CDCl_3) δ 6.37 (ddd, $J = 15.7, 10.9, 5.1$ Hz, 1H), 5.82 (d, $J = 10.9$ Hz, 1H), 5.48 (ddt, $J = 15.0, 7.5, 7.5$ Hz, 1H), 4.16–4.04 (m, 4H), 2.64 (dd, $J = 22.3, 7.6$ Hz, 2H), 1.76 (s, 3H), 1.74 (s, 3H), 1.32 (t, $J = 7.1$ Hz, 6H). ^{13}C NMR (126 MHz, CDCl_3) δ 135.27 (d, $J = 4.5$ Hz), 131.76 (d, $J = 15.0$ Hz), 124.56 (d, $J = 4.8$ Hz), 118.87 (d, $J = 12.7$ Hz), 62.06 (d, $J = 6.7$ Hz), 31.01 (d, $J = 139.8$ Hz), 26.09 (d, $J = 1.6$ Hz), 18.43 (d, $J = 1.4$ Hz), 16.60 (d, $J =$

6.0 Hz). ^{13}P NMR (162 MHz, CDCl_3): δ 27.4. HRMS (ESI) calculated for $[\text{C}_{11}\text{H}_{21}\text{O}_3\text{P} + \text{H}]^+$ requires m/z 233.1302, found 233.1307.

***N*-Allyl-4-methyl-*N*-((2*E*,4*E*)-7-methylocta-2,4,6-trien-1-yl)benzenesulfonamide (3.20):** A



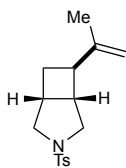
stirred solution of (*E*)-diethyl (5-methylhexa-2,4-dien-1-yl)phosphonate (1.26 equiv, 2.26 mmol, 525 mg) in dry THF (6 mL) was cooled to -78

$^{\circ}\text{C}$ under N_2 in a flame-dried 25 mL round-bottomed flask; *n*-BuLi (1.6 M hexanes, 1.2 equiv, 1.35 mL) was added dropwise, and the resulting mixture was allowed to stir an additional 20 min. A solution of *N*-allyl-4-methyl-*N*-(2-oxoethyl)benzenesulfonamide³² (1 equiv, 1.79 mmol, 453 mg) in HMPA (2.4 equiv, 4.3 mmol, 741 μL) and THF (2 mL) was added dropwise, and the mixture was allowed to slowly warm to room temperature. After 14 h, the reaction was quenched with saturated aqueous NH_4Cl and extracted into Et_2O (3x). The combined organic layers were washed with brine, dried over MgSO_4 , filtered, and concentrated *in vacuo*. The resulting residue was purified by flash column chromatography on silica gel (8:1 hexanes:EtOAc) to afford the product as a pale yellow semisolid (10:1 *E*:*Z*, 0.706 mmol, 234 mg, 39%). IR (neat): 2921, 1344, 1157, 991, 547 cm^{-1} . ^1H NMR (500 MHz, CDCl_3) δ 7.70 (d, $J = 8.2$ Hz, 2H), 7.29 (d, $J = 7.9$ Hz, 2H), 6.36 (dd, $J = 14.8, 11.2$ Hz, 1H), 6.11 (dd, $J = 15.1, 10.7$ Hz, 1H), 5.99 (dd, $J = 14.7, 10.7$ Hz, 1H), 5.83 (d, $J = 11.1$ Hz, 1H), 5.61 (ddt, $J = 19.3, 9.8, 6.3$ Hz, 1H), 5.36 (dt, $J = 14.4, 6.9$ Hz, 1H), 5.20–5.07 (m, 2H), 3.84 (d, $J = 6.9$ Hz, 2H), 3.79 (d, $J = 6.2$ Hz, 2H), 2.43 (s, 3H), 1.80 (s, 3H), 1.77 (s, 3H). ^{13}C NMR (126 MHz, CDCl_3) δ 143.3, 137.7, 137.4, 135.2, 132.9, 130.3, 129.8, 128.8, 127.4, 125.6, 125.1, 119.0, 49.4, 48.8, 26.3, 21.7, 18.6. HRMS (ESI) calculated for $[\text{C}_{19}\text{H}_{25}\text{NO}_2\text{S} + \text{NH}_4]^+$ requires m/z 349.1945, found 349.1954.

3.4.3 [2 + 2] Photocycloadditions.

General Procedure: A solution of 1 equiv of substrate and 1 mol% $[\text{Ir}(\text{dF}(\text{CF}_3)\text{ppy})_2(\text{dtbbpy})](\text{PF}_6)$ in DMSO (0.05 M) was placed in an oven-dried 25 mL Schlenk tube and degassed by 4 freeze-pump-thaw cycles in the dark. The reaction mixture was then stirred at room temperature and irradiated with a 23 W (1380 lumen) compact fluorescent light bulb at a distance of 10 cm. Upon full consumption of the starting material as determined by TLC or GC analysis, the reaction mixture was diluted with Et_2O (20 mL) and water (20 mL). The aqueous layer was separated and further extracted with Et_2O (20 mL x 2). The combined organic layers were dried with MgSO_4 , filtered, and concentrated *in vacuo*. The resulting residue was purified by flash column chromatography on silica gel.

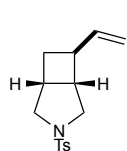
(1*R,5*S**,6*R**)-6-(Prop-1-en-2-yl)-3-tosyl-3-azabicyclo[3.2.0]heptane (3.4):** Experiment 1:



Prepared according to the general procedure with (*E*)-*N*-allyl-4-methyl-*N*-(4-methylpenta-2,4-dien-1-yl)benzenesulfonamide (0.346 mmol, 100.9 mg), $[\text{Ir}(\text{dF}(\text{CF}_3)\text{ppy})_2(\text{dtbbpy})](\text{PF}_6)$ (3.4 μmol , 3.9 mg), DMSO (6.9 mL) and an irradiation time of 15 h. Purification on silica gel (8:1 hexanes:EtOAc) afforded 89.6 mg of product (0.307 mmol, 89%, 10:1 d.r.) as a white solid. Experiment 2: (*E*)-*N*-allyl-4-methyl-*N*-(4-methylpenta-2,4-dien-1-yl)benzenesulfonamide (0.344 mmol, 100.4 mg), $[\text{Ir}(\text{dF}(\text{CF}_3)\text{ppy})_2(\text{dtbbpy})](\text{PF}_6)$ (3.4 μmol , 3.9 mg), and DMSO (6.9 mL). Isolated: 88.8 mg (0.305 mmol, 88%, 10:1 d.r.). Melting point: 100–102 °C. IR (neat): 2968, 1341, 1166, 576 cm^{-1} . ^1H NMR (500 MHz, CDCl_3) δ 7.71 (d, J = 8.2 Hz, 2H), 7.33 (d, J = 7.9 Hz, 2H), 4.74 (q, J = 1.4 Hz, 1H), 4.67 (s, 1H), 3.46 (d, J = 9.5 Hz, 2H), 2.80–2.59 (m, 5H), 2.44 (s, 3H), 2.13 (ddd, J = 12.0, 8.0, 8.0 Hz, 1H), 1.97 (ddd, J = 12.1, 9.4, 3.1 Hz, 1H), 1.67 (s, 3H). ^{13}C NMR

(126 MHz, CDCl₃) δ 147.3, 143.7, 132.1, 129.7, 128.2, 108.1, 54.6, 54.4, 43.3, 42.6, 33.7, 28.7, 21.7, 20.3. HRMS (ESI) calculated for [C₁₆H₂₁NO₂S + H]⁺ requires m/z 292.1366, found 292.1363.

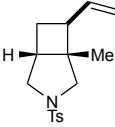
3-Tosyl-6-vinyl-3-azabicyclo[3.2.0]heptane (3.5): Experiment 1: Prepared according to the



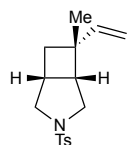
general procedure with (*E*)-*N*-allyl-4-methyl-*N*-(penta-2,4-dien-1-yl)benzenesulfonamide (0.361 mmol, 100.2 mg), [Ir(dF(CF₃)ppy)₂(dtbbpy)](PF₆) (3.6 μ mol, 4.1 mg), DMSO (7.2 mL) and an irradiation time of 16 h. Purification on silica gel (8:1 hexanes:EtOAc) afforded 93.9 mg of product (0.339 mmol, 94%, 3:1 d.r.) as a white solid. Experiment 2: (*E*)-*N*-allyl-4-methyl-*N*-(penta-2,4-dien-1-yl)benzenesulfonamide (0.363 mmol, 100.7 mg), [Ir(dF(CF₃)ppy)₂(dtbbpy)](PF₆) (3.6 μ mol, 4.1 mg), and DMSO (7.2 mL). Isolated: 96.6 mg (0.348 mmol, 96%, 3:1 d.r.). **(1*R**,5*S**,6*S**) Diastereomer (3.5-A, major):** IR (neat): 2971, 2849, 1342, 1154, 662 cm⁻¹. ¹H NMR (500 MHz, CDCl₃) δ 7.71 (d, J = 7.8 Hz, 2H), 7.34 (d, J = 7.8 Hz, 2H), 5.92 (ddd, J = 17.2, 10.4, 7.2 Hz, 1H), 4.95 (d, J = 17.3 Hz, 1H), 4.94 (d, J = 10.4 Hz, 1H), 3.48 (d, J = 9.4 Hz, 1H), 3.45 (d, J = 9.6 Hz, 1H), 2.80 (app p, J = 7.5 Hz, 1H), 2.72 (app p, J = 7.0 Hz, 1H), 2.67–2.55 (m, 3H), 2.44 (s, 3H), 2.10–1.99 (m, 2H). ¹³C NMR (126 MHz, CDCl₃) δ 143.7, 141.8, 131.7, 129.7, 128.2, 112.9, 54.5, 54.2, 43.4, 40.4, 34.0, 29.8, 21.7. HRMS (ESI) calculated for [C₁₅H₁₉NO₂S + H]⁺ requires m/z 278.1210, found 278.1214. **(1*R**,5*S**,6*R**) Diastereomer (3.5-B, minor):** IR (neat): 2975, 2849, 1344, 1165, 665 cm⁻¹. ¹H NMR (500 MHz, CDCl₃) δ 7.70 (d, J = 8.0 Hz, 2H), 7.33 (d, J = 7.9 Hz, 2H), 5.98 (ddd, J = 17.7, 10.2, 7.8 Hz, 1H), 5.08 (d, J = 10.3 Hz, 1H), 4.99 (d, J = 17.2 Hz, 1H), 3.59 (d, J = 10.2 Hz, 1H), 3.36 (d, J = 9.4 Hz, 1H), 3.04 (app p, J = 8.7 Hz, 1H), 2.89 (app q, J = 7.8 Hz, 1H), 2.83–2.75 (m, 1H), 2.55–2.47 (m, 2H), 2.44 (s, 3H), 2.40–2.32

(m, 1H), 1.89–1.82 (m, 1H). ^{13}C NMR (126 MHz, CDCl_3) δ 143.6, 137.8, 131.8, 129.6, 128.2, 116.2, 54.3, 49.3, 41.6, 36.3, 34.5, 29.6, 21.7. HRMS (ESI) calculated for $[\text{C}_{15}\text{H}_{19}\text{NO}_2\text{S} + \text{H}]^+$ requires m/z 278.1210, found 278.1205.

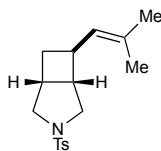
1-Methyl-3-tosyl-7-vinyl-3-azabicyclo[3.2.0]heptane (3.6): Experiment 1: Prepared


 according to the general procedure with (*E*)-*N*-allyl-4-methyl-*N*-(2-methylpenta-2,4-dien-1-yl)benzenesulfonamide (0.348 mmol, 101.3 mg), $[\text{Ir}(\text{dF}(\text{CF}_3)\text{ppy})_2(\text{dtbbpy})](\text{PF}_6)$ (3.4 μmol , 3.9 mg), DMSO (6.9 mL) and an irradiation time of 12 h. Purification on silica gel (8:1 hexanes:EtOAc) afforded 89.8 mg of product (0.308 mmol, 89%, 2:1 d.r.) as a white solid. Experiment 2: (*E*)-*N*-allyl-4-methyl-*N*-(2-methylpenta-2,4-dien-1-yl)benzenesulfonamide (0.342 mmol, 99.6 mg), $[\text{Ir}(\text{dF}(\text{CF}_3)\text{ppy})_2(\text{dtbbpy})](\text{PF}_6)$ (3.4 μmol , 3.9 mg), and DMSO (6.9 mL). Isolated: 89.4 mg (0.307 mmol, 89%, 2:1 d.r.). (**1S*,5R*,7S***) (**3.6-A**, major) and (**1S*,5R*,7R***) (**3.6-B**, minor) diastereomers as an inseparable mixture: IR (neat): 2954, 1343, 1157, 662 cm^{-1} . ^1H NMR (500 MHz, CDCl_3) δ 7.72–7.67 (m, 2H), 7.36–7.30 (m, 2H), 5.98 (ddd, $J = 17.1, 10.2, 7.9$ Hz, 0.37H), 5.83 (ddd, $J = 17.5, 10.3, 7.6$ Hz, 0.63H), 5.10–4.90 (m, 2H), 3.55 (d, $J = 10.0$ Hz, 0.37H), 3.44 (d, $J = 9.8$ Hz, 0.63H), 3.39 (d, $J = 9.4$ Hz, 0.63H), 3.32 (d, $J = 9.5$ Hz, 0.37H), 2.97 (app q, $J = 8.3$ Hz, 0.63H), 2.79 (dd, $J = 9.8, 7.0$ Hz, 0.63H), 2.71–2.60 (m, 0.74H), 2.44 (s, 3H), 2.34–2.25 (m, 1.37H), 2.22–2.16 (m, 1H), 2.11 (ddd, $J = 12.3, 8.6, 8.6$ Hz, 0.63H), 1.90 (ddd, $J = 12.4, 9.2, 3.2$ Hz, 0.63H), 1.72–1.63 (m, 0.37H), 1.10 (s, 1.11H), 0.99 (s, 1.89H). ^{13}C NMR (126 MHz, CDCl_3) δ 143.7, 143.6, 138.9, 137.8, 132.3, 132.2, 129.7, 129.6, 128.2, 128.2, 116.1, 115.3, 60.8, 55.4, 54.6, 54.1, 49.1, 48.7, 44.5, 43.0, 40.8, 40.6, 27.1, 26.6, 24.9, 21.7, 21.7, 18.3. HRMS (ESI) calculated for $[\text{C}_{16}\text{H}_{21}\text{NO}_2\text{S} + \text{H}]^+$ requires m/z 292.1366, found 292.1367.

6-Methyl-3-tosyl-6-vinyl-3-azabicyclo[3.2.0]heptane (3.7): Experiment 1: Prepared



according to the general procedure with (*E*)-*N*-allyl-4-methyl-*N*-(3-methylpenta-2,4-dien-1-yl)benzenesulfonamide (0.342 mmol, 99.6 mg), [Ir(dF(CF₃)ppy)₂(dtbbpy)](PF₆) (3.4 μmol, 3.9 mg), DMSO (6.9 mL) and an irradiation time of 28 h. Purification on silica gel (3:1 hexanes:EtOAc) afforded 87.0 mg of product (0.299 mmol, 87%, 3:1 d.r.) as a white solid. Experiment 2: (*E*)-*N*-allyl-4-methyl-*N*-(3-methylpenta-2,4-dien-1-yl)benzenesulfonamide (0.346 mmol, 100.8 mg), [Ir(dF(CF₃)ppy)₂(dtbbpy)](PF₆) (3.4 μmol, 3.9 mg), and DMSO (6.9 mL). Isolated: 90.9 mg (0.312 mmol, 90%, 3:1 d.r.). **(1*R**,5*R**,6*R**) Diastereomer (3.7-A, major):** IR (neat): 2926, 1344, 1159, 598 cm⁻¹. ¹H NMR (500 MHz CDCl₃) δ 7.69 (d, *J* = 8.0 Hz, 2H), 7.32 (d, *J* = 7.9 Hz, 2H), 5.91 (dd, *J* = 17.4, 10.7 Hz, 1H), 5.11 (d, *J* = 10.7 Hz, 1H), 4.98 (d, *J* = 17.4 Hz, 1H), 3.54 (d, *J* = 10.3 Hz, 1H), 3.35 (d, *J* = 9.3 Hz, 1H), 2.83 (app p, *J* = 6.9 Hz, 1H), 2.57–2.48 (m, 2H), 2.43 (s, 3H), 2.39 (dd, *J* = 7.5, 7.5 Hz, 1H), 2.03 (dd, *J* = 12.2, 6.5 Hz, 1H), 1.87 (ddd, *J* = 11.5, 8.7, 1.9 Hz, 1H), 1.24 (s, 3H). ¹³C NMR (126 MHz, CDCl₃) δ 143.6, 142.0, 132.3, 129.6, 128.2, 113.8, 53.8, 49.9, 48.4, 38.6, 35.4, 32.2, 28.0, 21.7. HRMS (ESI) calculated for [C₁₆H₂₁NO₂S + H]⁺ requires *m/z* 292.1366, found 292.1357. **(1*R**,5*R**,6*S**) Diastereomer (3.7-B, minor):** IR (neat): 2925, 1343, 1156, 662 cm⁻¹. ¹H NMR (500 MHz, CDCl₃) δ 7.71 (d, *J* = 8.2 Hz, 2H), 7.33 (d, *J* = 8.0 Hz, 2H), 5.99 (dd, *J* = 17.3, 10.5 Hz, 1H), 4.96 (d, *J* = 17.3 Hz, 1H), 4.94 (d, *J* = 10.5 Hz, 1H), 3.64 (d, *J* = 9.9 Hz, 1H), 3.36 (d, *J* = 9.4 Hz, 1H), 2.79–2.69 (m, 1H), 2.57–2.46 (m, 3H), 2.44 (s, 3H), 2.22 (ddd, *J* = 12.3, 8.9, 1.9 Hz, 1H), 1.73 (dd, *J* = 12.3, 6.4 Hz, 1H), 1.14 (s, 3H). ¹³C NMR (126 MHz, CDCl₃) δ 147.9, 143.7, 131.9, 129.6, 128.3, 109.5, 53.8, 49.4, 45.5, 38.5, 36.5, 32.1, 21.7, 20.9. HRMS (ESI) calculated for [C₁₆H₂₁NO₂S + NH₄]⁺ requires *m/z* 309.1632, found 309.1639.

6-(2-Methylprop-1-en-1-yl)-3-tosyl-3-azabicyclo[3.2.0]heptane (3.8): Experiment 1:

Prepared according to the general procedure with (*E*)-*N*-allyl-4-methyl-*N*-(5-methylhexa-2,4-dien-1-yl)benzenesulfonamide (0.326 mmol, 99.7 mg),

[Ir(dF(CF₃)ppy)₂(dtbbpy)](PF₆) (3.3 μmol, 3.7 mg), DMSO (6.5 mL) and an

irradiation time of 12 h. Purification on silica gel (7:1 hexanes:EtOAc) afforded 96.3 mg of

product (0.315 mmol, 97%, 3:1 d.r.) as a white solid. Experiment 2: (*E*)-*N*-allyl-4-methyl-*N*-(5-

methylhexa-2,4-dien-1-yl)benzenesulfonamide (0.324 mmol, 99.0 mg),

[Ir(dF(CF₃)ppy)₂(dtbbpy)](PF₆) (3.3 μmol, 3.7 mg), and DMSO (6.5 mL). Isolated: 97.6 mg

(0.320 mmol, 99%, 3:1 d.r.). (**1*R**,5*S**,6*S****) **diastereomer (3.8-A, major)**: IR (neat): 2926,

1345, 1170, 664, 550 cm⁻¹. ¹H NMR (500 MHz, CDCl₃) δ 7.71 (d, *J* = 8.1 Hz, 2H), 7.33 (d, *J* =

8.0 Hz, 2H), 5.25 (d, *J* = 8.9 Hz, 1H), 3.47 (d, *J* = 9.7 Hz, 1H), 3.43 (d, *J* = 9.5 Hz, 1H), 2.92

(app p, *J* = 8.4 Hz, 1H), 2.75–2.63 (m, 2H), 2.60 (dd, *J* = 9.7, 6.0 Hz, 1H), 2.50 (app q, *J* = 6.2

Hz, 1H), 2.43 (s, 3H), 2.08 (ddd, *J* = 13.0, 9.3, 3.9 Hz, 1H), 1.91 (ddd, *J* = 12.3, 8.1, 8.1 Hz,

1H), 1.67 (s, 3H), 1.54 (s, 3H). ¹³C NMR (126 MHz, CDCl₃) δ 143.6, 132.1, 131.7, 129.8,

129.6, 128.2, 54.7, 54.5, 45.3, 35.9, 34.1, 31.9, 25.7, 21.7, 18.4. HRMS (ESI) calculated for

[C₁₇H₂₃NO₂S + H]⁺ requires *m/z* 306.1523, found 306.1520. (**1*R**,5*S**,6*R****) **diastereomer**

(3.8-B, minor): IR (neat): 2921, 1343, 1169, 664, 550 cm⁻¹. ¹H NMR (500 MHz, CDCl₃) δ 7.71

(d, *J* = 8.2 Hz, 2H), 7.32 (d, *J* = 7.8 Hz, 2H), 5.29 (d, *J* = 8.6 Hz, 1H), 3.56 (d, *J* = 10.1 Hz,

1H), 3.35 (d, *J* = 9.4 Hz, 1H), 3.19 (app p, *J* = 8.9 Hz, 1H), 2.88 (app q, *J* = 7.9 Hz, 1H), 2.80–

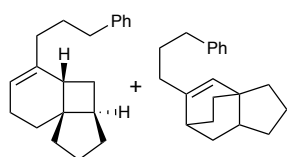
2.71 (m, 1H), 2.56 (dd, *J* = 9.5, 5.7 Hz, 1H), 2.50 (dd, *J* = 10.1, 7.5 Hz, 1H), 2.46–2.37 (m,

1H), 2.43 (s, 3H), 1.72–1.65 (m, 1H), 1.71 (s, 3H), 1.51 (d, *J* = 1.3 Hz, 3H). ¹³C NMR (126

MHz, CDCl₃) δ 143.5, 133.5, 132.4, 129.6, 128.3, 125.4, 54.6, 49.3, 42.1, 34.7, 32.1, 31.1,

25.7, 21.7, 18.3. HRMS (ESI) calculated for $[C_{17}H_{23}NO_2S + H]^+$ requires m/z 306.1523, found 306.1526.

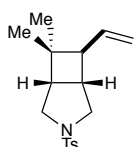
(3a*R,4a*S**,8a*S**)-5-(3-phenylpropyl)-1,2,3,3a,4,4a,7,8-octahydrocyclopenta[1,4]cyclobuta[1,2]benzene (3.9)** ([2+2] cycloadduct, major) **and 5-(3-phenylpropyl)-1,2,3,6,7,7a-hexahydro-3a,6-ethanoindene (3.65)** ([4+2] cycloadduct, minor):



(A) Yields determined by 1H NMR spectroscopy: A solution of (3-(5-(pent-4-en-1-yl)cyclohexa-1,5-dien-1-yl)propyl)benzene (0.0750 mmol, 20.1 mg), $[Ir(dF(CF_3)ppy)_2(dtbbpy)](PF_6)$ (0.8 μ mol, 0.8 mg), PhTMS (internal standard, 0.142 mmol, 21.4 mg) and DMSO- d_6 (1.5 mL) was placed in an oven-dried 25 mL Schlenk tube and degassed by 4 freeze-pump-thaw cycles in the dark. The reaction mixture was stirred at room temperature and irradiated per the general procedure for 1.5 h. Yields determined by 1H NMR spectroscopy with respect to PhTMS as the internal standard: 81% [2+2] cycloadduct (>20:1 d.r.) and 13% [4+2] cycloadduct. (B) Isolated yield studies: Experiment 1: Prepared according to the general procedure with (3-(5-(pent-4-en-1-yl)cyclohexa-1,5-dien-1-yl)propyl)benzene (0.377 mmol, 100.4 mg), $[Ir(dF(CF_3)ppy)_2(dtbbpy)](PF_6)$ (3.8 μ mol, 4.2 mg), DMSO (7.5 mL) and an irradiation time of 6 hours. Purification on silica gel (hexanes) afforded 92.8 mg of product (0.348 mmol, 92%, 6:1 mixture of [2 + 2] (>20:1 d.r) and [4+2] cycloadducts) as a clear oil. Experiment 2: (3-(5-(pent-4-en-1-yl)cyclohexa-1,5-dien-1-yl)propyl)benzene (0.378 mmol, 100.7 mg), $[Ir(dF(CF_3)ppy)_2(dtbbpy)](PF_6)$ (3.8 μ mol, 4.2 mg), and DMSO (7.5 mL). Isolated: 89.0 mg (0.334 mmol, 88%, 6:1 mixture of products). **[2+2] cycloadduct (3.9, major)**: IR (neat): 2923, 1447, 744, 696 cm^{-1} . 1H NMR (500 MHz, $CDCl_3$) δ 7.30–7.24 (m, 2H), 7.19–7.14 (m, 3H),

5.53 (d, $J = 4.5$ Hz, 1H), 2.63–2.52 (m, 2H), 2.28 (ddd, $J = 10.7, 5.9, 5.9$ Hz, 1H), 2.20–2.04 (m, 3H), 1.98–1.85 (m, 3H), 1.82–1.45 (m, 8H), 1.39 (ddd, $J = 13.1, 5.0, 3.3$ Hz, 1H), 1.34–1.23 (m, 2H). ^{13}C NMR (126 MHz, CDCl_3) δ 143.2, 143.0, 128.6, 128.4, 125.7, 120.6, 47.9, 41.1, 38.7, 38.0, 36.1, 36.0, 33.1, 32.9, 31.1, 29.9, 25.0, 23.9. HRMS (EI) calculated for $[\text{C}_{20}\text{H}_{26}]^+$ requires m/z 266.2030, found 266.2022. The relative stereochemistry of this compound was verified by an alternative synthesis from a previously characterized starting material (see section IV below for details). **[4+2] cycloadduct (3.52, minor):** ^1H NMR (500 MHz, CDCl_3) δ 7.31–7.21 (m, 2H), 7.21–7.12 (m, 3H), 5.47 (s, 1H), 2.63–2.58 (m, 2H), 2.35–2.31 (m, 1H), 2.12 (t, $J = 7.2$ Hz, 2H), 1.86–1.44 (m, 9H), 1.41–1.13 (m, 4H), 0.99 (ddt, $J = 12.1, 5.4, 2.5$ Hz, 1H), 0.91–0.81 (m, 1H). ^{13}C NMR (126 MHz, CDCl_3) δ 146.0, 142.9, 129.6, 128.6, 128.4, 125.8, 46.2, 44.4, 35.8, 35.7, 34.8, 34.7, 34.3, 33.5, 32.8, 29.8, 25.1, 23.6. HRMS (EI) calculated for $[\text{C}_{20}\text{H}_{26}]^+$ requires m/z 266.2030, found 266.2029.

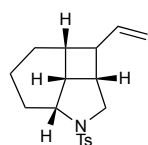
(1*S,5*S**,7*S**)-6,6-Dimethyl-3-tosyl-7-vinyl-3-azabicyclo[3.2.0]heptane (3.10):** Experiment



1: Prepared according to the general procedure with (*E*)-4-methyl-*N*-(3-methylbut-2-en-1-yl)-*N*-(penta-2,4-dien-1-yl)benzenesulfonamide (0.330 mmol, 100.9 mg), $[\text{Ir}(\text{dF}(\text{CF}_3)\text{ppy})_2(\text{dtbbpy})](\text{PF}_6)$ (3.3 μmol , 3.7 mg), DMSO (6.5 mL) and an irradiation time of 16 h. Purification on silica gel (6:1 hexanes:EtOAc) afforded 76.0 mg of product (0.249 mmol, 75%, 4:1 d.r.) as a white solid. Experiment 2: (*E*)-4-methyl-*N*-(3-methylbut-2-en-1-yl)-*N*-(penta-2,4-dien-1-yl)benzenesulfonamide (0.330 mmol, 100.8 mg), $[\text{Ir}(\text{dF}(\text{CF}_3)\text{ppy})_2(\text{dtbbpy})](\text{PF}_6)$ (3.3 μmol , 3.7 mg), and DMSO (6.5 mL). Isolated: 78.0 mg (0.255 mmol, 77%, 4:1 d.r.). IR (neat): 2955, 1343, 1185, 733 cm^{-1} . ^1H NMR (500 MHz, CDCl_3) δ 7.71 (d, $J = 7.9$ Hz, 2H), 7.33 (d, $J = 7.9$ Hz, 2H), 5.81 (ddd, $J = 17.6, 10.4, 7.9$ Hz,

1H), 4.99 (d, $J = 10.3$ Hz, 1H), 4.94 (d, $J = 17.1$ Hz, 1H), 3.61 (d, $J = 10.5$ Hz, 1H), 3.37 (d, $J = 9.4$ Hz, 1H), 2.65 (app q, $J = 6.9$ Hz, 1H), 2.56–2.42 (m, 3H), 2.44 (s, 3H), 2.18 (dd, $J = 7.8$, 7.8 Hz, 1H), 1.02 (s, 3H), 0.98 (s, 3H). ^{13}C NMR (126 MHz, CDCl_3) δ 143.6, 137.5, 132.1, 129.6, 128.2, 115.4, 52.8, 50.8, 49.1, 45.3, 38.1, 37.1, 26.0, 23.7, 21.7. HRMS (ESI) calculated for $[\text{C}_{17}\text{H}_{23}\text{NO}_2\text{S} + \text{H}]^+$ requires m/z 306.1523, found 306.1511.

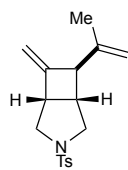
1-Tosyl-3-vinyldecahydrocyclobuta[cd]indole (3.11): Experiment 1: Prepared according to



the general procedure with (*E*)-*N*-(cyclohex-2-en-1-yl)-4-methyl-*N*-(penta-2,4-dien-1-yl)benzenesulfonamide (0.316 mmol, 100.2 mg), $[\text{Ir}(\text{dF}(\text{CF}_3)\text{ppy})_2(\text{dtbbpy})](\text{PF}_6)$ (3.2 μmol , 3.5 mg), DMSO (6.3 mL) and an irradiation time of 18 h. Purification on silica gel (10:1 hexanes:EtOAc) afforded 91.0 mg of product (0.287 mmol, 91%, 1:1 d.r.) as a clear oil. Experiment 2: (*E*)-*N*-(cyclohex-2-en-1-yl)-4-methyl-*N*-(penta-2,4-dien-1-yl)benzenesulfonamide (0.314 mmol, 99.8 mg), $[\text{Ir}(\text{dF}(\text{CF}_3)\text{ppy})_2(\text{dtbbpy})](\text{PF}_6)$ (3.2 μmol , 3.5 mg), and DMSO (6.3 mL). Isolated: 94.0 mg (0.296 mmol, 94%, 1:1 d.r.). **(2a*S**,2a¹*R**,3*R**,3a*R**,6a*R**) Diastereomer (3.11-A):** IR (neat): 2929, 1340, 1160, 666 cm^{-1} . ^1H NMR (500 MHz, CDCl_3) δ 7.68 (d, $J = 8.0$ Hz, 2H), 7.33 (d, $J = 8.0$ Hz, 2H), 5.82 (ddd, $J = 17.3$, 10.2, 7.2 Hz, 1H), 4.96 (d, $J = 17.3$ Hz, 1H), 4.91 (d, $J = 10.2$ Hz, 1H), 3.59 (d, $J = 9.7$ Hz, 1H), 3.05 (d, $J = 8.6$ Hz, 1H), 2.80 (app q, $J = 7.5$ Hz, 1H), 2.75 (dd, $J = 9.7$, 5.2 Hz, 1H), 2.65 (d, $J = 13.2$ Hz, 1H), 2.54 (app q, $J = 8.2$ Hz, 1H), 2.44 (s, 3H), 2.38 (app q, $J = 6.8$ Hz, 1H), 2.22 (app q, $J = 8.6$ Hz, 1H), 1.98 (app qt, $J = 13.6$, 3.3 Hz, 1H), 1.53–1.40 (m, 2H), 1.40–1.23 (m, 2H). ^{13}C NMR (126 MHz, CDCl_3) δ 143.6, 141.1, 131.9, 129.6, 128.3, 113.6, 57.4, 55.9, 43.0, 38.4, 37.3, 34.0, 27.1, 25.5, 21.7, 15.0. HRMS (ESI) calculated for $[\text{C}_{18}\text{H}_{23}\text{NO}_2\text{S} + \text{H}]^+$ requires m/z 318.1523, found 318.1519.

(2a*S,2a¹*R**,3*S**,3a*R**,6a*R**) Diastereomer (3.11-B):** IR (neat): 2925, 1339, 1159, 680 cm⁻¹. ¹H NMR (500 MHz, CDCl₃) δ 7.68 (d, *J* = 8.1 Hz, 2H), 7.33 (d, *J* = 7.9 Hz, 2H), 6.54 (ddd, *J* = 16.9, 10.2, 10.2 Hz, 1H), 5.13 (dd, *J* = 10.1, 2.6 Hz, 1H), 5.00 (dd, *J* = 17.0, 2.5 Hz, 1H), 3.68 (d, *J* = 10.1 Hz, 1H), 3.12 (app q, *J* = 10.1 Hz, 1H), 3.07–3.02 (m, 1H), 2.84–2.66 (m, 4H), 2.62 (app dq, *J* = 14.0, 3.5 Hz, 1H), 2.44 (s, 3H), 1.91 (app qdd, *J* = 13.3, 4.7, 2.6 Hz, 1H), 1.58–1.52 (m, 1H), 1.47–1.24 (m, 3H). ¹³C NMR (126 MHz, CDCl₃) δ 143.6, 135.3, 131.7, 129.6, 128.4, 118.7, 57.9, 53.5, 43.3, 40.0, 36.2, 30.3, 26.1, 23.4, 21.7, 17.2. HRMS (ESI) calculated for [C₁₈H₂₃NO₂S + H]⁺ requires *m/z* 318.1523, found 318.1525.

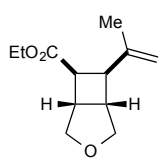
(1*S,5*S**,7*R**)-6-Methylene-7-(prop-1-en-2-yl)-3-tosyl-3-azabicyclo[3.2.0]heptane (3.12):**



Experiment 1: Prepared according to the general procedure with (*E*)-*N*-(buta-2,3-dien-1-yl)-4-methyl-*N*-(4-methylpenta-2,4-dien-1-yl)benzenesulfonamide (0.332 mmol, 100.6 mg), [Ir(dF(CF₃)ppy)₂(dtbbpy)](PF₆) (3.3 μmol, 3.7 mg), DMSO (6.6 mL) and an irradiation time of 21 h. Purification on silica gel (6:1 hexanes:EtOAc) afforded 79.3 mg of product (0.261 mmol, 79%, 8:1 d.r.) as a white solid. Experiment 2: (*E*)-*N*-(buta-2,3-dien-1-yl)-4-methyl-*N*-(4-methylpenta-2,4-dien-1-yl)benzenesulfonamide (0.333 mmol, 101.1 mg), [Ir(dF(CF₃)ppy)₂(dtbbpy)](PF₆) (3.3 μmol, 3.7 mg), and DMSO (6.6 mL). Isolated: 80.9 mg (0.267 mmol, 80%, 8:1 d.r.). Melting point: 82–84 °C. IR (neat): 2967, 1338, 1161, 1005, 548 cm⁻¹. ¹H NMR (500 MHz, CDCl₃) δ 7.70 (d, *J* = 8.1 Hz, 2H), 7.33 (d, *J* = 7.9 Hz, 2H), 4.99 (dd, *J* = 2.1, 2.1 Hz, 1H), 4.90 (dd, *J* = 2.1, 2.1 Hz, 1H), 4.84 (s, 1H), 4.75 (s, 1H), 3.60 (d, *J* = 9.5 Hz, 1H), 3.55 (d, *J* = 9.4 Hz, 1H), 3.37–3.32 (m, 1H), 3.29–3.23 (m, 1H), 2.72–2.62 (m, 3H), 2.44 (s, 3H), 1.71 (s, 3H). ¹³C NMR (126 MHz, CDCl₃) δ 150.1, 144.3, 143.8,

132.0, 129.7, 128.2, 110.4, 109.9, 54.8, 54.0, 53.9, 44.6, 40.6, 21.7, 20.2. HRMS (ESI) calculated for $[\text{C}_{17}\text{H}_{21}\text{NO}_2\text{S} + \text{H}]^+$ requires m/z 304.1366, found 304.1360.

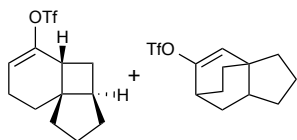
(1*S,5*S**,6*S**,7*S**)-Ethyl 7-(prop-1-en-2-yl)-3-oxabicyclo[3.2.0]heptane-6-carboxylate**



(3.13): Experiment 1: Prepared according to the general procedure with (*E*)-ethyl-4-(((*E*)-4-methylpenta-2,4-dien-1-yl)oxy)but-2-enoate (0.479 mmol, 100.8 mg), $[\text{Ir}(\text{dF}(\text{CF}_3)\text{ppy})_2(\text{dtbbpy})](\text{PF}_6)$ (4.8 μmol , 5.3 mg), DMSO (9.6 mL) and

an irradiation time of 16 h. Purification on silica gel (5:1 hexanes:EtOAc) afforded 73.4 mg of product (0.349 mmol, 73%, 4:1 d.r.) as a clear oil. Experiment 2: (*E*)-ethyl-4-(((*E*)-4-methylpenta-2,4-dien-1-yl)oxy)but-2-enoate (0.478 mmol, 100.6 mg), $[\text{Ir}(\text{dF}(\text{CF}_3)\text{ppy})_2(\text{dtbbpy})](\text{PF}_6)$ (4.8 μmol , 5.3 mg), and DMSO (9.6 mL). Isolated: 68.9 mg (0.328 mmol, 69%, 4:1 d.r.). IR (neat): 2919, 2850, 1728, 1157, 889 cm^{-1} . ^1H NMR (500 MHz, CDCl_3) δ 4.91–4.89 (m, 1H), 4.82 (s, 1H), 4.15–4.03 (m, 2H), 3.94 (d, $J = 9.6$ Hz, 1H), 3.84 (d, $J = 9.4$ Hz, 1H), 3.58 (dd, $J = 9.6, 6.0$ Hz, 1H), 3.50 (dd, $J = 9.4, 4.9$ Hz, 1H), 3.21–3.14 (m, 1H), 3.12–3.05 (m, 2H), 2.95 (dd, $J = 10.2, 6.3$ Hz, 1H), 1.70 (s, 3H), 1.23 (t, $J = 7.1$ Hz, 3H). ^{13}C NMR (126 MHz, CDCl_3) δ 173.2, 143.9, 111.4, 73.6, 73.2, 60.5, 45.9, 45.8, 41.2, 37.7, 22.5, 14.4. HRMS (ESI) calculated for $[\text{C}_{12}\text{H}_{18}\text{O}_3 + \text{H}]^+$ requires m/z 211.1329, found 211.1328.

(3a*R,4a*R**,8a*S**)-1,2,3,3a,4,4a,7,8-Octahydrocyclopenta[1,4]cyclobuta[1,2]benzen-5-yl trifluoromethanesulfonate (3.14)** ([2+2] cycloadduct, major) and **1,2,3,6,7,7a-hexahydro-3a,6-ethanoinden-5-yl trifluoromethanesulfonate** ([4+2] cycloadduct, minor): (A) Yields

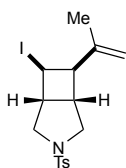


determined by ^1H NMR spectroscopy: A solution of 5-(pent-4-en-1-yl)cyclohexa-1,5-dien-1-yl trifluoromethanesulfonate (0.0496 mmol, 14.7 mg), $[\text{Ir}(\text{dF}(\text{CF}_3)\text{ppy})_2(\text{dtbbpy})](\text{PF}_6)$ (0.5 μmol , 0.6 mg),

PhTMS (internal standard, 0.0858 mmol, 12.9 mg) and DMSO-d_6 (1 mL) was placed in an oven-dried 25 mL Schlenk tube and degassed by 4 freeze-pump-thaw cycles in the dark. The reaction mixture was stirred at room temperature and irradiated per the general procedure for 1.5 h. Yields determined by ^1H NMR spectroscopy with respect to PhTMS as the internal standard: 80% [2+2] cycloadduct **3.14** (>20:1 d.r.) and 14% [4+2] cycloadduct. (B) Isolated yield studies: Experiment 1: Prepared according to the general procedure with 5-(pent-4-en-1-yl)cyclohexa-1,5-dien-1-yl trifluoromethanesulfonate (0.341 mmol, 101.0 mg), $[\text{Ir}(\text{dF}(\text{CF}_3)\text{ppy})_2(\text{dtbbpy})](\text{PF}_6)$ (3.4 μmol , 3.8 mg), DMSO (6.7 mL) and an irradiation time of 4 hours. Purification on silica gel (hexanes) afforded 91.6 mg of product (0.309 mmol, 91%, 6:1 mixture of [2 + 2] (>20:1 d.r.) and [4 + 2] cycloadducts) as a clear oil. Experiment 2: 5-(pent-4-en-1-yl)cyclohexa-1,5-dien-1-yl trifluoromethanesulfonate (0.338 mmol, 100.2 mg), $[\text{Ir}(\text{dF}(\text{CF}_3)\text{ppy})_2(\text{dtbbpy})](\text{PF}_6)$ (3.4 μmol , 3.8 mg), and DMSO (6.7 mL). Isolated: 90.3 mg (0.305 mmol, 90%, 6:1 mixture of [2 + 2] and [4 + 2]). **[2+2] cycloadduct (3.14)** (major): IR (neat): 2933, 1413, 1200, 1139, 610 cm^{-1} . ^1H NMR (500 MHz, CDCl_3) δ 5.84 (dd, J = 4.7, 4.7 Hz, 1H), 2.47–2.42 (m, 1H), 2.40–2.29 (m, 3H), 2.00–1.80 (m, 4H), 1.68 (dd, J = 12.9, 6.7 Hz, 1H), 1.62–1.52 (m, 2H), 1.49–1.36 (m, 3H). ^{13}C NMR (126 MHz, CDCl_3) δ 154.4, 118.5 (q, J = 320.9 Hz), 117.5, 50.2, 40.5, 38.2, 38.0, 32.8, 30.8, 29.6, 24.8, 23.2. ^{19}F NMR (377 MHz,

CDCl_3) δ -74.2. HRMS (ASAP) calculated for $[\text{C}_{12}\text{H}_{15}\text{F}_3\text{O}_3\text{S}]^+$ requires m/z 296.0689, found 296.0688. The relative stereochemistry of this compound was verified by an alternative synthesis from a previously characterized starting material (see section IV below for details).

6-Iodo-7-(prop-1-en-2-yl)-3-tosyl-3-azabicyclo[3.2.0]heptane (3.15): Experiment 1:

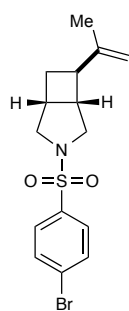


Prepared according to the general procedure with *N*-((*E*)-3-iodoallyl)-4-methyl-*N*-((*E*)-4-methylpenta-2,4-dien-1-yl)benzenesulfonamide (0.238 mmol, 99.4 mg), $[\text{Ir}(\text{dF}(\text{CF}_3)\text{ppy})_2(\text{dtbbpy})](\text{PF}_6)$ (2.4 μmol , 2.7 mg), DMSO (4.8 mL) and an irradiation time of 5.5 h. Purification on silica gel (8:1 hexanes:EtOAc) afforded 96.9 mg of product (0.232 mmol, 97%, 2:1 d.r.). Experiment 2: *N*-((*E*)-3-iodoallyl)-4-methyl-*N*-((*E*)-4-methylpenta-2,4-dien-1-yl)benzenesulfonamide (0.240 mmol, 100.0 mg), $[\text{Ir}(\text{dF}(\text{CF}_3)\text{ppy})_2(\text{dtbbpy})](\text{PF}_6)$ (2.4 μmol , 2.7 mg), and DMSO (4.8 mL). Isolated: 99.3 mg (0.238 mmol, 99%, 2:1 d.r.). **(1*S**,5*R**,6*S**,7*R**) diastereomer (3.15-A, major)**: Melting point: 151-153 °C (decomp). IR (neat): 2973, 1336, 1161, 808, 547 cm^{-1} . ^1H NMR (500 MHz, CDCl_3) δ 7.69 (d, J = 8.2 Hz, 2H), 7.34 (d, J = 8.1 Hz, 2H), 5.07 (q, J = 1.2 Hz, 1H), 4.76 (s, 1H), 4.57 (dd, J = 8.5, 2.9 Hz, 1H), 3.60 (d, J = 10.6 Hz, 1H), 3.45 (d, J = 9.9 Hz, 1H), 3.18–3.08 (m, 2H), 2.93–2.88 (m, 1H), 2.67–2.57 (m, 2H), 2.44 (s, 3H), 1.68 (s, 3H). ^{13}C NMR (126 MHz, CDCl_3) δ 145.5, 144.1, 131.8, 129.8, 128.2, 112.2, 53.4, 53.2, 49.0, 48.7, 39.7, 27.8, 21.7, 21.7. HRMS (ESI) calculated for $[\text{C}_{16}\text{H}_{20}\text{INO}_2\text{S} + \text{H}]^+$ requires m/z 418.0333, found 418.0338. **(1*S**,5*R**,6*R**,7*R**) diastereomer (3.15-B, minor)**: Melting point: 133-134 °C. IR (neat): 2969, 1337, 1162, 812, 549 cm^{-1} . ^1H NMR (500 MHz, CDCl_3) δ 7.76 (d, J = 8.2 Hz, 2H), 7.35 (d, J = 8.2 Hz, 2H), 4.82 (q, J = 1.4 Hz, 1H), 4.71 (s, 1H), 4.60–4.55 (m, 1H), 3.84 (dd, J = 10.8, 1.5 Hz, 1H), 3.47 (d, J = 9.8 Hz, 1H), 3.10 (dd, J = 7.9, 7.9 Hz, 1H), 3.01 (dd, J

= 10.8, 8.1 Hz, 1H), 2.95 (ddd, J = 6.8, 6.8, 5.0 Hz, 1H), 2.84–2.77 (m, 1H), 2.74 (dd, J = 9.7, 5.0 Hz, 1H), 2.44 (s, 3H), 1.73 (s, 3H). ^{13}C NMR (126 MHz, CDCl_3) δ 143.9, 143.8, 132.6, 129.8, 128.2, 110.1, 55.9, 55.0, 54.3, 42.8, 40.9, 24.1, 21.7, 20.1. HRMS (ESI) calculated for $[\text{C}_{16}\text{H}_{20}\text{INO}_2\text{S} + \text{H}]^+$ requires m/z 418.0333, found 418.0323.

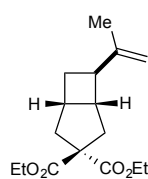
(1*R,5*S**,6*R**)-3-((4-Bromophenyl)sulfonyl)-6-(prop-1-en-2-yl)-3-**

azabicyclo[3.2.0]heptane (3.16): Experiment 1: Prepared according to the general procedure

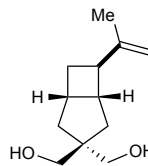


with (*E*)-*N*-allyl-4-bromo-*N*-(4-methylpenta-2,4-dien-1-yl)benzenesulfonamide (0.283 mmol, 100.7 mg), $[\text{Ir}(\text{dF}(\text{CF}_3)\text{ppy})_2(\text{dtbbpy})](\text{PF}_6)$ (2.8 μmol , 3.1 mg), DMSO (5.6 mL) and an irradiation time of 18 h. Purification on silica gel (7:1 hexanes:EtOAc) afforded 93.2 mg of product (0.262 mmol, 93%, 10:1 d.r.) as a white solid. Experiment 2: (*E*)-*N*-allyl-4-bromo-*N*-(4-methylpenta-2,4-dien-1-

yl)benzenesulfonamide (0.282 mmol, 100.3 mg), $[\text{Ir}(\text{dF}(\text{CF}_3)\text{ppy})_2(\text{dtbbpy})](\text{PF}_6)$ (2.8 μmol , 3.1 mg), and DMSO (5.6 mL). Isolated: 93.7 mg (0.263 mmol, 93%, 10:1 d.r.). Melting point: 96–99 °C. IR (neat): 2968, 1341, 1166, 575 cm^{-1} . ^1H NMR (500 MHz, CDCl_3) δ 7.69 (s, 4H), 4.75 (s, 1H), 4.68 (s, 1H), 3.48 (d, J = 9.1 Hz, 1H), 3.47 (d, J = 9.7 Hz, 1H), 2.79–2.62 (m, 5H), 2.19–2.11 (m, 1H), 1.97 (ddd, J = 11.9, 8.9, 2.7 Hz, 1H), 1.67 (s, 3H). ^{13}C NMR (126 MHz, CDCl_3) δ 147.1, 134.2, 132.4, 129.6, 128.0, 108.3, 54.6, 54.5, 43.3, 42.6, 33.7, 28.8, 20.3. HRMS (ESI) calculated for $[\text{C}_{15}\text{H}_{18}\text{BrNO}_2\text{S} + \text{H}]^+$ requires m/z 356.0315, found 356.0300.

((1*S,5*R**,6*R**)-Diethyl 6-(prop-1-en-2-yl)bicyclo[3.2.0]heptane-3,3-dicarboxylate (3.17):**

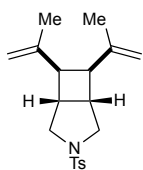
Experiment 1: Prepared according to the general procedure with (*E*)-diethyl 2-allyl-2-(4-methylpenta-2,4-dien-1-yl)malonate (0.359 mmol, 100.6 mg), [Ir(dF(CF₃)ppy)₂(dtbbpy)](PF₆) (3.6 μmol, 4.0 mg), DMSO (7.1 mL) and an irradiation time of 40 h. Purification on silica gel (10:1 hexanes:EtOAc) afforded 93.2 mg of product (0.332 mmol, 93%, 10:1 d.r.) as a clear oil. Experiment 2: (*E*)-diethyl 2-allyl-2-(4-methylpenta-2,4-dien-1-yl)malonate (0.356 mmol, 99.8 mg), [Ir(dF(CF₃)ppy)₂(dtbbpy)](PF₆) (3.6 μmol, 4.0 mg), and DMSO (7.1 mL). Isolated: 94.8 mg (0.338 mmol, 95%, 10:1 d.r.). IR (neat): 2977, 1727, 1246, 1064, 883 cm⁻¹. ¹H NMR (500 MHz, CDCl₃) δ 4.71 (q, *J* = 1.5 Hz, 1H), 4.67 (s, 1H), 4.23 (q, *J* = 7.1 Hz, 2H), 4.16 (q, *J* = 7.1 Hz, 2H), 2.74–2.61 (m, 2H), 2.55 (app q, *J* = 7.7 Hz, 1H), 2.52–2.41 (m, 2H), 2.36 (dd, *J* = 13.7, 5.2 Hz, 1H), 2.28 (dd, *J* = 13.9, 2.8 Hz, 1H), 2.05 (ddd, *J* = 12.1, 8.2, 8.2 Hz, 1H), 1.82 (ddd, *J* = 11.9, 9.0, 3.1 Hz, 1H), 1.67 (s, 3H), 1.28 (t, *J* = 7.1 Hz, 3H), 1.24 (t, *J* = 7.1 Hz, 3H). ¹³C NMR (126 MHz, CDCl₃) δ 172.6, 172.5, 148.4, 107.6, 64.5, 61.6, 61.5, 45.7, 44.3, 41.3, 41.2, 35.1, 28.4, 20.4, 14.2, 14.2. HRMS (ESI) calculated for [C₁₆H₂₄O₄ + H]⁺ requires *m/z* 281.1748, found 281.1749.

((1*S,5*R**,6*R**)-6-(Prop-1-en-2-yl)bicyclo[3.2.0]heptane-3,3-diyl)dimethanol (3.18):**

Experiment 1: Prepared according to the general procedure with (*E*)-2-allyl-2-(4-methylpenta-2,4-dien-1-yl)propane-1,3-diol (0.507 mmol, 99.6 mg), [Ir(dF(CF₃)ppy)₂(dtbbpy)](PF₆) (5.1 μmol, 5.7 mg), DMSO (10.2 mL) and an irradiation time of 36 h. Purification on silica gel (2:1 to 1:2 hexanes:EtOAc) afforded 87.8 mg of product (0.447 mmol, 88%, 10:1 d.r.) as a white solid. Experiment 2: (*E*)-2-allyl-2-(4-methylpenta-2,4-dien-1-yl)propane-1,3-diol (0.511 mmol, 100.3 mg),

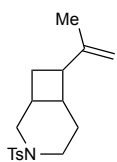
[Ir(dF(CF₃)ppy)₂(dtbbpy)](PF₆) (5.1 μmol, 5.7 mg), and DMSO (10.2 mL). Isolated: 89.4 mg (0.455 mmol, 89%, 10:1 d.r.). Melting point: 73–75 °C. IR (neat): 3255, 2930, 1016, 882, 667 cm⁻¹. ¹H NMR (500 MHz, CDCl₃) δ 4.71 (s, 1H), 4.67 (s, 1H), 3.83 (d, *J* = 4.9 Hz, 2H), 3.47 (d, *J* = 5.1 Hz, 2H), 2.61–2.57 (m, 3H), 2.38–2.28 (m, 1H), 2.25–2.16 (m, 1H), 2.11–2.02 (m, 2H), 1.89–1.77 (m, 2H), 1.68 (s, 3H), 1.48 (dd, *J* = 13.3, 6.8 Hz, 1H), 1.43 (dd, *J* = 13.7, 3.0 Hz, 1H). ¹³C NMR (126 MHz, CDCl₃) δ 148.7, 107.5, 72.0, 69.2, 54.7, 48.1, 44.0, 39.3, 39.2, 34.5, 29.4, 20.5. HRMS (ESI) calculated for [C₁₂H₂₀O₂ + Na]⁺ requires *m/z* 219.1356, found 219.1359.

(1*R,5*S**,6*R**,7*S**)-6,7-Di(prop-1-en-2-yl)-3-tosyl-3-azabicyclo[3.2.0]heptane (3.19):**



Experiment 1: Prepared according to the general procedure with 4-methyl-*N,N*-bis((*E*)-4-methylpenta-2,4-dien-1-yl)benzenesulfonamide (0.305 mmol, 101.0 mg), [Ir(dF(CF₃)ppy)₂(dtbbpy)](PF₆) (3.0 μmol, 3.4 mg), DMSO (6.0 mL) and an irradiation time of 3.5 h. Purification on silica gel (8:1 hexanes:EtOAc) afforded 85.4 mg of product (0.258 mmol, 85%, >10:1 d.r.) as a white solid. Experiment 2: 4-methyl-*N,N*-bis((*E*)-4-methylpenta-2,4-dien-1-yl)benzenesulfonamide (0.301 mmol, 99.7 mg), [Ir(dF(CF₃)ppy)₂(dtbbpy)](PF₆) (3.0 μmol, 3.4 mg), and DMSO (6.0 mL). Isolated: 84.4 mg (0.255 mmol, 85%, >10:1 d.r.). Melting point: 80–84 °C. IR (neat): 2967, 2863, 1339, 1154, 813, 598 cm⁻¹. ¹H NMR (500 MHz, CDCl₃) δ 7.71 (d, *J* = 8.2 Hz, 2H), 7.34 (d, *J* = 8.0 Hz, 2H), 4.81 (s, 2H), 4.67 (s, 2H), 3.48 (d, *J* = 9.7 Hz, 2H), 3.03 (d, *J* = 3.9 Hz, 2H), 2.81–2.70 (m, 4H), 2.44 (s, 3H), 1.67 (s, 6H). ¹³C NMR (126 MHz, CDCl₃) δ 145.4, 143.7, 132.1, 129.7, 128.2, 111.0, 54.1, 48.0, 38.9, 21.9, 21.7. HRMS (ESI) calculated for [C₁₉H₂₅NO₂S + H]⁺ requires *m/z* 332.1679, found 332.1676.

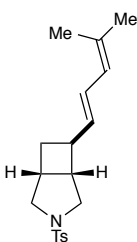
7-(Prop-1-en-2-yl)-3-tosyl-3-azabicyclo[4.2.0]octane (3.23): Experiment 1: A solution of



(*E*)-*N*-allyl-4-methyl-*N*-(5-methylhexa-3,5-dien-1-yl)benzenesulfonamide (0.0809 mmol, 24.7 mg), [Ir(dF(CF₃)ppy)₂(dtbbpy)](PF₆) (0.8 μmol, 0.9 mg), PhTMS (internal standard, 0.122 mmol, 18.4 mg) and DMSO-d₆ (1.6 mL) was placed in an

oven-dried 25 mL Schlenk tube and degassed by 4 freeze-pump-thaw cycles in the dark. The reaction mixture was then stirred at room temperature and irradiated per the general procedure for 72 h. Yields determined by ¹H NMR spectroscopy with respect to PhTMS as the internal standard: 23% [2 + 2] cycloadduct (2:1 d.r.), 74% remaining starting material (2:1 *E*:*Z*).

Experiment 2: (*E*)-*N*-allyl-4-methyl-*N*-(5-methylhexa-3,5-dien-1-yl)benzenesulfonamide (0.0864 mmol, 26.4 mg), [Ir(dF(CF₃)ppy)₂(dtbbpy)](PF₆) (0.8 μmol, 0.9 mg), PhTMS (internal standard, 0.125 mmol, 18.8 mg) and DMSO-d₆ (1.6 mL). ¹H NMR yield: 20% [2+2] cycloadduct (2:1 d.r.), 79% remaining starting material (2:1 *E*:*Z*). Purification on silica gel (8:1 hexanes:EtOAc) afforded the product as an inseparable mixture of diastereomers (relative stereochemistry could not be assigned unambiguously). IR (neat): 2929, 1344, 1164, 549 cm⁻¹. ¹H NMR (500 MHz, CDCl₃) δ 7.67 (d, *J* = 8.2 Hz, 1.4H), 7.64 (d, *J* = 8.2 Hz, 0.6H), 7.34 (d, *J* = 8.0 Hz, 1.4H), 7.31 (d, *J* = 8.0 Hz, 0.6H), 4.69 (q, *J* = 1.5 Hz, 0.7H), 4.64 (q, *J* = 1.5 Hz, 0.3H), 4.60 (s, 0.7H), 4.55 (s, 0.3H), 3.97–3.91 (m, 0.6H), 3.76 (ddd, *J* = 11.8, 7.4, 1.8 Hz, 0.7H), 3.53–3.46 (m, 0.7H), 2.72–2.60 (m, 1.4H), 2.55–2.28 (m, 5.8H), 2.18–2.12 (ddd, *J* = 9.2, 6.2, 6.2, 0.3H), 1.95–1.83 (m, 1.4H), 1.82–1.75 (app dq, *J* = 12.1, 3.0 Hz, 0.3H), 1.73–1.48 (m, 5.7H), 1.25–1.15 (m, 0.3H). ¹³C NMR (126 MHz, CDCl₃) δ 147.4, 147.3, 143.3, 143.2, 134.4, 133.8, 129.7, 129.6, 127.6, 127.4, 108.4, 108.2, 52.3, 49.0, 48.8, 47.4, 46.7, 43.4, 41.3, 36.5, 35.2, 32.1, 30.5, 28.6, 28.3, 25.5, 21.6, 21.5, 20.9, 20.6. HRMS (ESI) calculated for [C₁₇H₂₃NO₂S + H]⁺ requires *m/z* 306.1523, found 306.1520.

6-(4-Methylpenta-1,3-dien-1-yl)-3-tosyl-3-azabicyclo[3.2.0]heptane (3.21) (Ru conditions):

Experiment 1: Prepared according to the general procedure with *N*-allyl-4-methyl-*N*-((2*E*,4*E*)-7-methylocta-2,4,6-trien-1-yl)benzenesulfonamide (0.224 mmol, 74.1 mg), Ru(bpy)₃(PF₆)₂ (2.2 μmol, 1.9 mg), DMSO (4.5 mL) and an irradiation time of 4 h. Purification on silica gel (7:1 hexanes:EtOAc) afforded

69.4 mg of product (0.209 mmol, 94%, >10:1 *E*:*Z*, 2:1 d.r.) as a white semisolid. Experiment 2:

N-allyl-4-methyl-*N*-((2*E*,4*E*)-7-methylocta-2,4,6-trien-1-yl)benzenesulfonamide (0.230 mmol, 76.1 mg), Ru(bpy)₃(PF₆)₂ (2.2 μmol, 1.9 mg), and DMSO (4.5 mL). Isolated: 69.6 mg (0.210

mmol, 91%, >10:1 *E*:*Z*, 2:1 d.r.). The mixture of products was carried on to 6-(4-methylpentyl)-3-tosyl-3-azabicyclo[3.2.0]heptane to confirm the assigned stereochemistry (see

section V below for details). **(1*R**,5*S**,6*S**) diastereomer (3.21-A, major):** ¹H NMR (500

MHz, CDCl₃) δ 7.71 (d, *J* = 8.2 Hz, 2H), 7.33 (d, *J* = 8.0 Hz, 2H), 6.15 (dd, *J* = 14.9, 10.9 Hz, 1H), 5.77 (d, *J* = 10.7 Hz, 1H), 5.63 (dd, *J* = 15.0, 8.0 Hz, 1H), 3.48 (d, *J* = 8.7 Hz, 1H), 3.45

(d, *J* = 9.4 Hz, 1H), 2.89–2.78 (m, 1H), 2.76–2.50 (m, 4H), 2.43 (s, 3H), 2.08–2.00 (m, 2H), 1.76 (s, 3H), 1.74 (s, 3H). ¹³C NMR (126 MHz, CDCl₃) δ 143.7, 134.7, 134.6, 132.1, 129.7,

128.2, 125.6, 124.7, 54.6, 54.2, 44.4, 40.2, 34.0, 30.8, 26.1, 21.7, 18.4. HRMS (ESI) calculated for [C₁₉H₂₅NO₂S + H]⁺ requires *m/z* 332.1679, found 332.1671. **(1*R**,5*S**,6*R**) diastereomer**

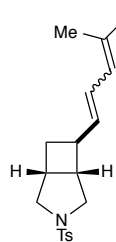
(3.21-B, minor): ¹H NMR (500 MHz, CDCl₃) δ 7.71 (d, *J* = 8.2 Hz, 2H), 7.32 (d, *J* = 8.0 Hz, 2H), 6.17 (dd, *J* = 15.1, 10.9 Hz, 1H), 5.83 (d, *J* = 10.9 Hz, 1H), 5.69 (dd, *J* = 15.1, 8.7 Hz,

1H), 3.58 (d, *J* = 10.0 Hz, 1H), 3.36 (d, *J* = 9.4 Hz, 1H), 3.05 (app p, *J* = 9.0 Hz, 1H), 2.89 (app q, *J* = 7.9 Hz, 1H), 2.81–2.73 (m, 1H), 2.57 (dd, *J* = 9.5, 5.7 Hz, 1H), 2.53 (dd, *J* = 10.2, 7.5

Hz, 1H), 2.45–2.35 (m, 1H), 2.43 (s, 3H), 1.84–1.72 (m, 1H), 1.77 (s, 3H), 1.74 (s, 3H). ¹³C NMR (126 MHz, CDCl₃) δ 143.6, 134.4, 132.4, 130.6, 129.6, 128.3, 128.3, 125.1, 54.4, 49.4,

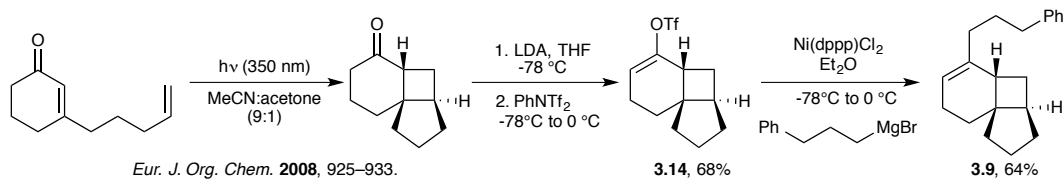
42.3, 36.0, 34.5, 30.9, 26.1, 21.7, 18.4. HRMS (ESI) calculated for $[\text{C}_{19}\text{H}_{25}\text{NO}_2\text{S} + \text{H}]^+$ requires m/z 332.1679, found 332.1673.

6-(4-Methylpenta-1,3-dien-1-yl)-3-tosyl-3-azabicyclo[3.2.0]heptane (3.21) (Ir conditions):



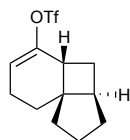
Experiment 1: A solution of *N*-allyl-4-methyl-*N*-((2*E*,4*E*)-7-methylocta-2,4,6-trien-1-yl)benzenesulfonamide (0.0772 mmol, 25.6 mg), $[\text{Ir}(\text{dF}(\text{CF}_3)\text{ppy})_2(\text{dtbbpy})](\text{PF}_6)$ (0.8 μmol , 0.9 mg), PhTMS (internal standard, 0.145 mmol, 21.8 mg) and DMSO-d_6 (1.5 mL) was placed in an oven-dried 25 mL Schlenk tube and degassed by 4 freeze-pump-thaw cycles in the dark. The reaction mixture was then stirred at room temperature and irradiated per the general procedure for 18 h. Yield determined by ^1H NMR spectroscopy with respect to PhTMS as the internal standard: 95% yield [2 + 2] cycloadduct **3.21** (1:1 *E*:*Z*, 2:1 d.r.). Experiment 2: *N*-allyl-4-methyl-*N*-((2*E*,4*E*)-7-methylocta-2,4,6-trien-1-yl)benzenesulfonamide (0.0754 mmol, 25.0 mg), $[\text{Ir}(\text{dF}(\text{CF}_3)\text{ppy})_2(\text{dtbbpy})](\text{PF}_6)$ (0.8 μmol , 0.9 mg), PhTMS (internal standard, 0.141 mmol, 21.2 mg) and DMSO-d_6 (1.5 mL). ^1H NMR yield: 97% yield [2+2] cycloadduct **3.21** (1:1 *E*:*Z*, 2:1 d.r.). The mixture of products was purified as described above for the ruthenium-catalyzed experiment and then carried on to 6-(4-methylpentyl)-3-tosyl-3-azabicyclo[3.2.0]heptane to confirm the assigned stereochemistry (see section 4.4.5 below for details).

3.4.4 Verification of the relative stereochemistry of cycloadducts 3.9 and 3.14:



(3aR*,4aR*,8aS*)-1,2,3,3a,4,4a,7,8-Octahydrocyclopenta[1,4]cyclobuta[1,2]benzen-5-yl

trifluoromethanesulfonate (3.14): A solution of LDA was freshly prepared by the dropwise

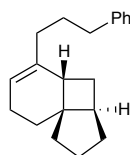


addition of *n*-BuLi (1.6 M in hexanes, 1.07 equiv, 0.521 mmol, 325 μ L) to a solution of *i*-Pr₂NH₂ (1.07 equiv, 0.521 mmol, 73 μ L) in dry THF (0.8 mL) at -78 $^{\circ}$ C under N₂ in a flame-dried 25 mL round-bottomed flask. The reaction mixture

was allowed to stir for 20 min at -78 $^{\circ}$ C at which point a solution of (3aR*,4aR*,8aS*)-octahydrocyclopenta[1,4]cyclobuta[1,2]benzen-5(6*H*)-one²⁶ (1 equiv, 0.487 mmol, 80.0 mg) in THF (1.6 mL) was added dropwise and then allowed to stir for an additional 30 min. A solution of *N*-phenyl-bis(trifluoromethanesulfonimide) (1.09 equiv, 0.530 mmol, 189 mg) in THF (0.7 mL) was then added dropwise. After stirring at 0 $^{\circ}$ C for an additional 3 h, the reaction was quenched with water and extracted into Et₂O (3x). The combined organic layers were washed with brine, dried over MgSO₄, filtered and concentrated *in vacuo*. The residue was purified by flash column chromatography on silica gel (2x) (gradient, hexanes to 20:1 hexanes:Et₂O) to afford the product as a clear oil (0.331 mmol, 98.0 mg, 68%). All spectroscopic data for this compound matched those previously obtained for the major product of the iridium-catalyzed photocycloaddition of 5-(pent-4-en-1-yl)cyclohexa-1,5-dien-1-yl trifluoromethanesulfonate.

(3aR*,4aS*,8aS*)-5-(3-Phenylpropyl)-1,2,3,3a,4,4a,7,8-

octahydrocyclopenta[1,4]cyclobuta[1,2]benzene (3.9): A solution of (3-

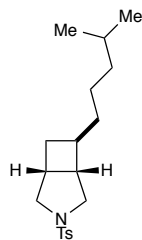


phenylpropyl)magnesium bromide was freshly prepared by the dropwise addition of 1-bromo-3-phenylpropane (1.02 mmol, 155 μ L) to a suspension of magnesium (1.53 mmol, 37 mg) in Et₂O (2 mL) in a 25 mL flame-dried 3-neck flask fitted to a

reflux condenser under N₂. The solution was heated occasionally with a heat gun during the addition to initiate the reaction and was then allowed to stir at room temperature for an additional 2 h. Meanwhile, a solution of Ni(dppp)Cl₂ (0.05 equiv, 0.0085 mmol, 4.4 mg), (3*aR**,4*aR**,8*aS**)-1,2,3,3*a*,4,4*a*,7,8-octahydrocyclopenta[1,4]cyclobuta[1,2]benzen-5-yl trifluoromethanesulfonate **3.14** (1 equiv, 0.169 mmol, 50.0 mg) in Et₂O (0.85 mL) was cooled to -78 °C under N₂ in an oven-dried 25 mL Schlenk flask. The Grignard solution was then added dropwise, the flask was sealed with a glass stopper, and the reaction mixture was stirred at 0 °C for 16 h. The reaction was quenched with water and extracted into Et₂O (3x). The combined organic layers were washed with brine, dried over MgSO₄, filtered and concentrated *in vacuo*. The resulting residue was purified by flash column chromatography on silica gel (pentanes) to afford the product as a clear oil (0.107 mmol, 28.6 mg, 64%). All spectroscopic data for this compound matched those previously obtained for the major product of the iridium-catalyzed photocycloaddition of (3-(5-(pent-4-en-1-yl)cyclohexa-1,5-dien-1-yl)propyl)benzene.

3.4.5 Verification of the relative stereochemistry of cycloadduct **3.21**: comparison of iridium and ruthenium-catalyzed experiments.

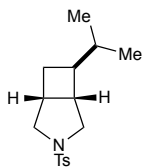
6-(4-Methylpentyl)-3-tosyl-3-azabicyclo[3.2.0]heptane (3.66): A septum-capped oven-dried 3-dram vial was charged with a magnetic stir bar, 10% Pd/C (10 mg) and MeOH (1.2 mL). The stirred solution was fitted with a hydrogen balloon and purged for 20 min. Dienylcyclobutane 6-(4-methylpenta-1,3-dien-1-yl)-3-tosyl-3-azabicyclo[3.2.0]heptane (**3.21**) (>10:1 E:Z, 2:1 d.r. from the iridium-catalyzed experiment) (0.060 mmol, 20 mg) was then added, and the reaction was stirred at room



temperature for 5 h, at which point it was passed across a Celite plug (Et₂O). The solvent was removed *in vacuo*, and the resulting residue was purified by flash column chromatography on silica gel (8:1 hexanes:EtOAc) to afford the product as a white semisolid (0.060 mmol, 20 mg, quantitative). The experiment was repeated with vinylcyclobutane 6-(4-methylpenta-1,3-dien-1-yl)-3-tosyl-3-azabicyclo[3.2.0]heptane (**3.21**) (1:1 E:Z, 2:1 d.r. from the iridium-catalyzed experiment) to afford a spectroscopically identical diastereomeric mixture of products. (**1R*,5S*,6R***) (**3.66-A**, major) and (**1R*,5S*,6S***) (**3.66-B**, minor) diastereomers as an inseparable mixture: IR (neat): 2921, 1344, 1166, 661, 548 cm⁻¹. ¹H NMR (500 MHz, CDCl₃) δ 7.74–7.66 (m, 2H), 7.32 (d, *J* = 8.0 Hz, 2H), 3.59 (d, *J* = 10.2 Hz, 0.3H), 3.41 (d, *J* = 9.6 Hz, 0.7H), 3.40 (d, *J* = 9.5 Hz, 0.7H), 3.30 (d, *J* = 9.4 Hz, 0.3H), 2.81–2.66 (m, 1.30H), 2.63 (dd, *J* = 9.5, 6.8 Hz, 0.7H), 2.58 (dd, *J* = 9.6, 6.2 Hz, 0.7H), 2.54–2.46 (m, 0.6H), 2.43 (s, 3H), 2.36 (app q, *J* = 6.0 Hz, 0.7H), 2.34–2.22 (m, 0.6H), 2.10–2.01 (m, 0.7H), 1.92 (ddd, *J* = 12.4, 8.8, 3.9 Hz, 0.7H), 1.73 (ddd, *J* = 12.3, 8.9, 6.6 Hz, 0.7H), 1.56–1.28 (m, 3.30H), 1.22–1.03 (m, 4H), 0.85 (d, *J* = 6.6 Hz, 6H). ¹³C NMR (126 MHz, CDCl₃) δ 143.6, 143.5, 132.1, 132.1, 129.6, 129.6, 128.3, 128.2, 54.7, 54.6, 54.2, 48.7, 43.6, 40.1, 39.0, 37.5, 37.0, 34.6, 34.2, 32.6, 30.9, 30.4, 30.4, 28.1, 28.1, 24.8, 24.6, 22.8, 22.7, 22.7, 21.7, 21.7. HRMS (ESI) calculated for [C₁₉H₂₉NO₂S + H]⁺ requires *m/z* 336.1992, found 336.1986.

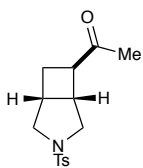
3.4.6 Synthetic elaboration of vinylcyclobutane products

(**1R*,5S*,6S***)-6-Isopropyl-3-tosyl-3-azabicyclo[3.2.0]heptane (**3.35**): A septum-capped, oven-dried 3-dram vial was charged with a magnetic stir bar, 10% Pd/C (37 mg), and MeOH (1.7 mL). The stirred solution was fitted with a hydrogen balloon and purged for 20 min. Vinylcyclobutane (**1R*,5S*,6R***)-6-(prop-1-en-2-yl)-3-tosyl-



3-azabicyclo[3.2.0]heptane (**3.4**) (0.17 mmol, 50 mg) was then added, and the reaction was stirred at room temperature for 2 h, at which point it was passed across a Celite plug (Et₂O). The solvent was removed *in vacuo* and the resulting residue was purified by flash column chromatography on silica gel (8:1 hexanes:EtOAc) to afford the product as a white solid (0.169 mmol, 49.7 mg, 98%). Melting point: 82–83 °C. IR (neat): 2953, 1342, 1154, 811, 662, 549 cm⁻¹. ¹H NMR (500 MHz, CDCl₃) δ 7.70 (d, *J* = 8.1 Hz, 2H), 7.32 (d, *J* = 8.0 Hz, 2H), 3.41 (d, *J* = 9.3 Hz, 1H), 3.37 (d, *J* = 9.5 Hz, 1H), 2.68–2.56 (m, 3H), 2.49–2.39 (m, 4H), 1.90–1.71 (m, 3H), 1.53–1.41 (m, 1H), 0.79 (d, *J* = 6.6 Hz, 3H), 0.78 (d, *J* = 6.7 Hz, 3H). ¹³C NMR (126 MHz, CDCl₃) δ 143.6, 132.1, 129.6, 128.2, 54.9, 54.7, 45.0, 42.1, 33.8, 33.5, 28.9, 21.7, 19.3, 19.2. HRMS (ESI) calculated for [C₁₆H₂₃NO₂S + H]⁺ requires *m/z* 294.1523, found 294.1531.

(1*R,5*R**,6*R**)-1-(3-Tosyl-3-azabicyclo[3.2.0]heptan-6-yl)ethanone (3.36):** A stirred

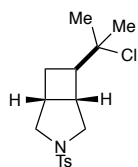


solution of vinylcyclobutane (1*R**,5*S**,6*R**)-6-(prop-1-en-2-yl)-3-tosyl-3-azabicyclo[3.2.0]heptane (**3.4**) (1 equiv, 0.172 mmol, 50.0 mg) in CH₂Cl₂ (1.7 mL) was cooled to -78 °C in an oven-dried 25 mL 3-neck flask. The solution

was purged with oxygen for 10 minutes, then with ozone until a blue color appeared and persisted (<5 minutes). Oxygen was passed through the solution until it was clear again, and the reaction was quenched with DMS (10 equiv, 1.72 mmol, 215 μL) and allowed to slowly warm to room temperature over 4 h. The solvent was then removed *in vacuo*, and the resulting residue was purified by flash column chromatography on silica gel (3:2 hexanes:EtOAc) to afford the product as a white solid (0.154 mmol, 45.3 mg, 90%). Melting point: 115–117 °C. IR (neat): 2968, 1700, 1338, 1151, 662, 547 cm⁻¹. ¹H NMR (500 MHz, CDCl₃) δ 7.70 (d, *J* = 8.2 Hz, 2H), 7.34 (d, *J* = 7.9 Hz, 2H), 3.49 (d, *J* = 9.9 Hz, 1H), 3.48 (d, *J* = 9.8 Hz, 1H), 3.17–

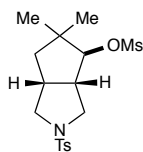
3.10 (m, 1H), 3.06 (ddd, $J = 6.1, 6.1, 6.1$ Hz, 1H), 2.72–2.64 (m, 1H), 2.62–2.54 (m, 2H), 2.44 (s, 3H), 2.40–2.30 (m, 1H), 2.09 (s, 3H), 2.10–2.02 (m, 1H). ^{13}C NMR (126 MHz, CDCl_3) δ 208.3, 144.0, 131.6, 129.8, 128.3, 54.3, 54.1, 48.0, 39.2, 34.0, 27.5, 26.7, 21.7. HRMS (ESI) calculated for $[\text{C}_{15}\text{H}_{19}\text{NO}_3\text{S} + \text{H}]^+$ requires m/z 294.1159, found 294.1150.

(1*R,5*R**,6*R**)-6-(2-Chloropropan-2-yl)-3-tosyl-3-azabicyclo[3.2.0]heptane (3.37):**



Anhydrous HCl in Et_2O (2 M, 5 equiv, 0.86 mmol, 430 μL) was added dropwise to a stirred solution of vinylcyclobutane (1*R**,5*S**,6*R**)-6-(prop-1-en-2-yl)-3-tosyl-3-azabicyclo[3.2.0]heptane (**3.4**) (1 equiv, 0.172 mmol, 50.0 mg) in CH_2Cl_2 (1.7 mL) in an oven-dried 3-dram vial. The vial was sealed with a Teflon cap and stirred at room temperature for 7 h. The reaction was then quenched with saturated aqueous NaHCO_3 and extracted into CH_2Cl_2 (3x). The combined organic layers were washed with brine, dried over Na_2SO_4 , filtered, and concentrated *in vacuo*. The resulting residue was purified by flash column chromatography on silica gel (7:1 hexanes:EtOAc) to afford the product as a white solid (0.171 mmol, 56.0 mg, 99%). Melting point: 68–72 $^\circ\text{C}$. IR (neat): 2932, 1340, 1153, 809, 590 cm^{-1} . ^1H NMR (500 MHz, CDCl_3) δ 7.70 (d, $J = 8.1$ Hz, 2H), 7.34 (d, $J = 7.9$ Hz, 2H), 3.45 (d, $J = 9.4$ Hz, 1H), 3.43 (d, $J = 9.8$ Hz, 1H), 2.82 (ddd, $J = 6.1, 6.1, 6.1$ Hz, 1H), 2.68–2.52 (m, 3H), 2.44 (s, 3H), 2.39–2.28 (m, 1H), 2.25–2.17 (m, 1H), 1.87 (ddd, $J = 13.0, 9.4, 3.8$ Hz, 1H), 1.47 (s, 3H), 1.45 (s, 3H). ^{13}C NMR (126 MHz, CDCl_3) δ 143.8, 131.7, 129.7, 128.3, 73.2 (4 $^\circ\text{C}$), 54.6, 54.4, 49.3, 40.5, 33.2, 29.8, 29.2, 26.8, 21.7. HRMS (ESI) calculated for $[\text{C}_{16}\text{H}_{22}\text{ClNO}_2\text{S} + \text{H}]^+$ requires m/z 328.1133, found 328.1137.

(3aS*,4S*,6aR*)-5,5-Dimethyl-2-tosyloctahydrocyclopenta[c]pyrrol-4-yl

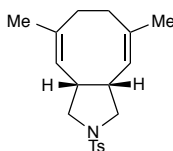


methanesulfonate (3.38): Methanesulfonic acid (5 equiv, 0.86 mmol, 56 μ L) was added dropwise to a stirred solution of vinylcyclobutane (1*R**,5*S**,6*R**)-6-(prop-1-en-2-yl)-3-tosyl-3-azabicyclo[3.2.0]heptane (**3.4**) (1 equiv, 0.172 mmol,

50.0 mg) in CH_2Cl_2 (1.7 mL) in an oven-dried 3-dram vial. The vial was sealed with a Teflon cap and stirred at room temperature for 2 h. The reaction was then quenched with saturated aqueous NaHCO_3 and extracted into CH_2Cl_2 (3x). The combined organic layers were washed with brine, dried over Na_2SO_4 , filtered, and concentrated *in vacuo*. The resulting residue was purified by flash column chromatography (3:2 hexanes:EtOAc) to afford the product as white solid (0.150 mmol, 58.0 mg, 87%). Melting point: 178–181 $^\circ\text{C}$. IR (neat): 2963, 1337, 1160, 962, 664, 527 cm^{-1} . ^1H NMR (500 MHz, CDCl_3) δ 7.68 (d, J = 8.3 Hz, 2H), 7.34 (d, J = 7.9 Hz, 2H), 4.38 (d, J = 5.0 Hz, 1H), 3.68 (d, J = 8.5 Hz, 1H), 3.16 (d, J = 9.4 Hz, 1H), 3.03 (s, 3H), 2.77–2.64 (m, 3H), 2.61 (dd, J = 9.3, 6.0 Hz, 1H), 2.44 (s, 3H), 1.82 (dd, J = 12.8, 7.7 Hz, 1H), 1.38 (dd, J = 13.0, 8.5 Hz, 1H), 1.09 (s, 3H), 0.93 (s, 3H). ^{13}C NMR (126 MHz, CDCl_3) δ 144.0, 131.5, 129.7, 128.4, 93.1, 53.7, 52.2, 47.3, 43.6, 43.3, 38.6, 38.2, 25.7, 21.7, 20.9. HRMS (ESI) calculated for $[\text{C}_{17}\text{H}_{25}\text{NO}_5\text{S}_2 + \text{NH}_4]^+$ requires m/z 405.1513, found 405.1522.

(3aR*,4Z,8Z,9aS*)-5,8-Dimethyl-2-tosyl-2,3,3a,6,7,9a-hexahydro-1H-cycloocta[c]pyrrole

(3.39): An oven-dried 3-dram vial was charged with vinylcyclobutane (1*R**,5*S**,6*R**)-6-(prop-1-en-2-yl)-3-tosyl-3-azabicyclo[3.2.0]heptane (**3.19**) (0.172 mmol, 50.0 mg) and benzene (1.5 mL). The vial was sealed with a Teflon cap and heated to 80 $^\circ\text{C}$ for 3 h. After it was allowed to cool to room temperature, the solvent was

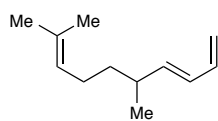


removed *in vacuo*, and the resulting residue was purified by flash column chromatography on

silica gel (8:1 hexanes:EtOAc) to afford the product as a white solid (0.145 mmol, 48.0 mg, 96%). Melting point: 96–99 °C. IR (neat): 2955, 1339, 1159, 807, 665, 548 cm^{-1} . ^1H NMR (500 MHz, CDCl_3) δ 7.74 (d, J = 8.2 Hz, 2H), 7.34 (d, J = 7.9 Hz, 2H), 4.70 (s, 2H), 3.47 (dd, J = 9.6, 6.3 Hz, 2H), 3.20–3.07 (m, 2H), 3.01 (dd, J = 9.7, 5.6 Hz, 2H), 2.65–2.55 (m, 2H), 2.44 (s, 3H), 1.90–1.78 (m, 2H), 1.57 (s, 6H). ^{13}C NMR (126 MHz, CDCl_3) δ 143.5, 137.0, 134.0, 129.8, 127.7, 122.4, 53.9, 42.4, 32.2, 25.5, 21.7. HRMS (ESI) calculated for $[\text{C}_{19}\text{H}_{25}\text{NO}_2\text{S} + \text{H}]^+$ requires m/z 332.1679, found 332.1676.

3.4.7 Synthesis of epiraikovenal

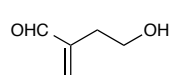
(±)-(E)-5,9-Dimethyldeca-1,3,8-triene (3.41): A solution of diethyl allylphosphonate (1.2



equiv, 11.1 mmol, 1.9 mL) in dry THF (30 mL) was cooled to -78 °C under N_2 in a flame-dried 100 mL round-bottomed flask; $n\text{-BuLi}$ (1.6 M hexanes, 1.2 equiv, 11.1 mmol, 6.9 mL) was added dropwise and the reaction mixture was allowed to stir for an additional 15 min. A solution of (±)-2,6-dimethyl-5-heptenal (1 equiv, 9.2 mmol, 1.3 g) in HMPA (2.4 equiv, 22.1 mmol, 3.8 mL) and THF (1 mL) was added dropwise and the mixture was allowed to slowly warm to room temperature. After 12 h, the reaction was quenched with saturated aqueous NH_4Cl and extracted into Et_2O (3x). The combined organic layers were washed with brine, dried over MgSO_4 , filtered, and concentrated *in vacuo*. The resulting residue was purified by flash column chromatography on silica gel (pentanes) to afford the product as a clear oil ($>20:1$ E:Z, 7.9 mmol, 1.3 g, 84%). IR (neat): 2965, 2913, 1453, 1001, 895 cm^{-1} . ^1H NMR (500 MHz, CDCl_3) δ 6.31 (ddd, J = 17.0, 10.2, 10.2 Hz, 1H), 6.01 (dd, J = 15.3, 10.4 Hz, 1H), 5.58 (dd, J = 15.3, 7.9 Hz, 1H), 5.15–5.01 (m, 3H), 4.95 (dd, J = 10.1, 1.8 Hz, 1H), 2.17 (dtq, J = 7.0, 7.0, 7.0 Hz, 1H), 1.95 (dt, J = 7.4, 7.4 Hz, 2H), 1.68

(d, $J = 1.3$ Hz, 3H), 1.59 (s, 3H), 1.33 (dt, $J = 7.1, 7.1$ Hz, 2H), 1.00 (d, $J = 6.7$ Hz, 3H). ^{13}C NMR (126 MHz, CDCl_3) δ 141.3, 137.6, 131.5, 129.4, 124.7, 114.8, 37.1, 36.4, 26.0, 25.9, 20.5, 17.8. HRMS (EI) calculated for $[\text{C}_{12}\text{H}_{20}]^+$ requires m/z 164.1560, found 164.1563.

4-Hydroxy-2-methylenebutanal (3.43): A solution of dimethyl itaconate (1 equiv, 11.4

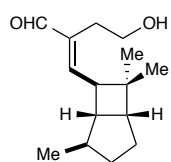


mmol, 1.80 g) in dry THF (75 mL) was cooled to -78 °C under N_2 in a flame-dried 250 mL round-bottomed flask. DIBAL (1.0 M hexanes, 4.4 equiv, 50 mL)

was added dropwise via an addition funnel and the reaction mixture was allowed to slowly warm to room temperature over 4 h, at which point it was quenched by the dropwise addition of water, diluted with saturated aqueous Rochelle's salt and stirred for 60 minutes. The mixture was then extracted with EtOAc (5x), dried over Na_2SO_4 , filtered, and concentrated. The crude diol was transferred to an oven-dried 500 mL round-bottomed flask containing CH_2Cl_2 (230 mL) and activated MnO_2 (10 equiv, 114 mmol, 9.9 g) and allowed to stir at room temperature for 3 h. The reaction mixture was filtered over Celite (CH_2Cl_2), concentrated *in vacuo*, and purified by flash column chromatography on silica gel (1:1 pentanes: Et_2O) to afford the product as a clear liquid (4.73 mmol, 474 mg, 42% yield). The spectroscopic data for this compound were consistent with the previously reported values.³³

(±)-(E)-4-Hydroxy-2-(((1S*,4S*,5R*,6R*)-4,7,7-trimethylbicyclo[3.2.0]heptan-6-yl)

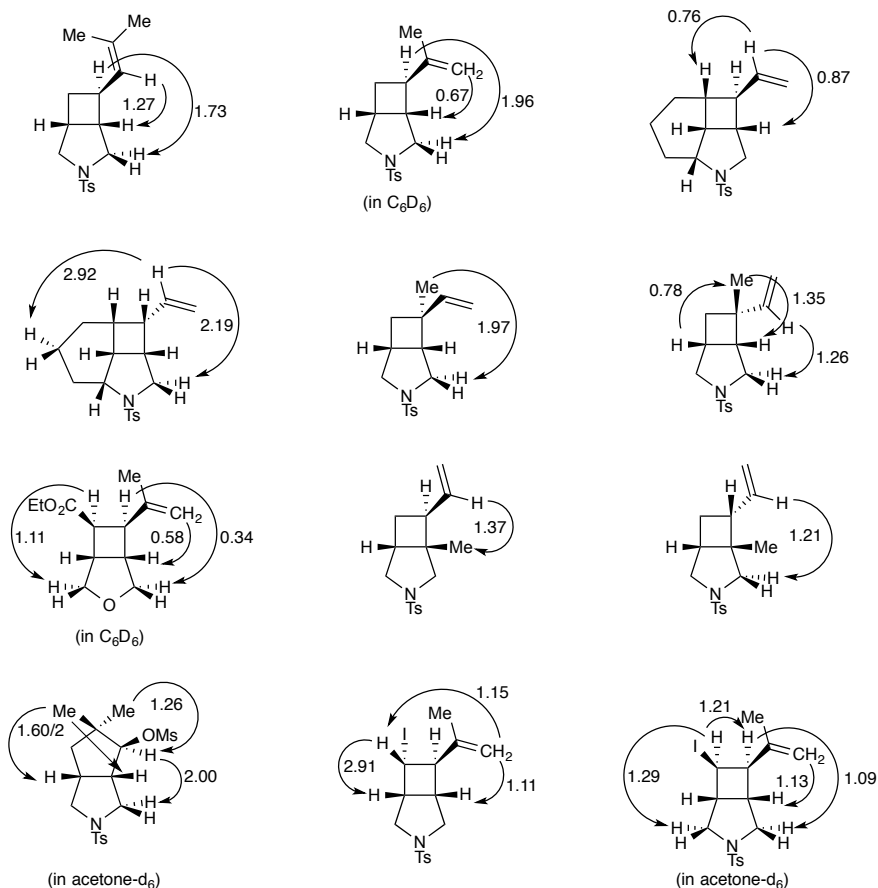
methylene)butanal (3.44, Epiraikovenal):¹⁶ An oven-dried 25 mL Schlenk tube was charged



with (*E*)-5,9-dimethyldeca-1,3,8-triene (1 equiv, 0.369 mmol, 60.6 mg), $[\text{Ir}(\text{dF}(\text{CF}_3)\text{ppy})_2(\text{dtbbpy})](\text{PF}_6)$ (3.7 μmol , 4.1 mg) and dry CDCl_3 (2.8 mL) and degassed by 4 freeze-pump-thaw cycles in the dark. The reaction mixture

was stirred at room temperature and irradiated with a 23 W (1380 lumen) compact fluorescent light bulb at a distance of 10 centimeters for 72 hours. The reaction mixture was then treated with dry 5 Å molecular sieves (120 mg), 4-hydroxy-2-methylenebutanal (1 equiv, 0.365 mmol, 36.5 mg) in CDCl₃ (0.4 mL) and the Grubbs Catalyst 2nd generation (0.07 equiv, 22 mg) in CDCl₃ (0.4 mL) under N₂ in the given order. The reaction mixture was allowed to stir for an additional 24 hours at room temperature in the dark at which point it was purified directly by flash column chromatography on silica gel (1:1 hexanes:Et₂O) to afford the product as a clear oil (>10:1 d.r., 6:1 E:Z, 0.155 mmol, 36.7 mg, 42%). IR (neat): 2949, 2867, 1681, 1042, 736 cm⁻¹. ¹H NMR (500 MHz, CDCl₃) δ 9.41 (s, 1H), 6.71 (d, *J* = 10.1 Hz, 1H), 3.60 (dt, *J* = 6.0, *J* = 6.0 Hz, 2H), 2.55 (dd, *J* = 10.2, 6.6 Hz, 1H), 2.49 (td, *J* = 6.5, 2.5 Hz, 2H), 2.34 (ddd, *J* = 7.4, 7.4, 2.6 Hz, 1H), 2.31–2.25 (m, 1H), 2.03–1.85 (m, 3H, includes OH), 1.75–1.64 (m, 2H), 1.56–1.50 (m, 1H), 1.13 (s, 3H), 0.93 (s, 3H), 0.79 (d, *J* = 7.0 Hz, 3H). ¹³C NMR (126 MHz, CDCl₃) δ 196.2, 159.2, 140.0, 62.2, 48.1, 46.8, 46.0, 38.1, 38.1, 33.7, 28.4, 27.3, 24.7, 24.5, 19.8. HRMS (EI) calculated for [C₁₅H₂₄O₂]⁺ requires *m/z* 236.1771, found 236.1776.

3.4.8 Representative NOE data



3.5 References

- For leading reviews on the use of photocycloaddition in synthesis, see: (a) Bach, T.; Hehn J. P. *Angew. Chem.* **2011**, *123*, 1032–1077; *Angew. Chem. Int. Ed.* **2011**, *50*, 1000–1045. (b) Hoffman, N. *Chem. Rev.* **2008**, *108*, 1052–1103.
- For reviews on cyclobutane natural products, see: (a) Hansen, T. V.; Stenstrom, Y. in *Organic Synthesis: Theory and Applications*, Vol. 5 (Ed. T. Hudlicky) Elsevier, Oxford, UK, **2001**, pp. 1–38. (b) Dembitsky, V. M. *J. Nat. Med.* **2008**, *62*, 1–33.
- For reviews on the use of cyclobutane intermediates in synthesis, see: (a) Namyslo, J. C.; Kaufmann, D. E. *Chem. Rev.* **2003**, *103*, 1485–1538. (b) Seiser, T.; Saget, T.; Tran, D. N.; Cramer, N. *Angew. Chem. Int. Ed.* **2011**, *50*, 7740–7752.
- (a) Ischay, M. A.; Anzovino, M. E.; Du, J.; Yoon, T. P. *J. Am. Chem. Soc.* **2008**, *130*, 12886–12887. (b) Du, J.; Yoon, T. P. *J. Am. Chem. Soc.* **2009**, *131*, 14604–14605 (c)

- Ischay, M. A.; Lu, Z.; Yoon, T. P. *J. Am. Chem. Soc.* **2010**, *132*, 8572–8574. (d) Lu, Z.; Shen, M.; Yoon, T. P. *J. Am. Chem. Soc.* **2011**, *133*, 1162–1164. (e) Hurtley, A. E.; Cismesia, M. A.; Ischay, M. A.; Yoon, T. P. *Tetrahedron* **2011**, *67*, 4442–4448. (f) Lin, S.; Ischay, M. A.; Fry, C. G.; Yoon, T. P. *J. Am. Chem. Soc.* **2011**, *133*, 19350–19353. (g) Tyson, E. L.; Farney, E. P.; Yoon, T. P. *Org. Lett.* **2012**, *14*, 1110–1113. (h) Ischay, M. A.; Ament, M. S.; Yoon, T. P. *Chem. Sci.* **2012**, *3*, 2807–2811.
5. For recent comprehensive reviews on visible light photocatalysis, see: (a) Tepley, F. *Collect. Czech. Chem. Commun.* **2011**, *76*, 859–917. (b) Prier, C. K.; Rankic, D. A.; MacMillan, D. W. C. *Chem. Rev.* **2013**, *113*, 5322–5363.
6. (a) Wender, P. A.; Correia, C. R. D. *J. Am. Chem. Soc.* **1987**, *109*, 2523–2525. (b) Corey, E. J.; Cane, D. E.; Libit, L. *J. Am. Chem. Soc.* **1971**, *93*, 7016–7021. (c) Bülow, N.; König, W. A. *Phytochemistry* **2000**, *55*, 141–168. (d) Yoshihara, K.; Ohta, Y.; Sakai, T.; Hirose, Y. *Tetrahedron Lett.* **1969**, *10*, 2263–2264.
7. For reviews of diene and polyene photochemistry, see: (a) Srinivasan, R. in *Advances in Photochemistry*, Vol. 4 (Eds. W. A. Noyes, G. Hammond, J. N. Pitts) John Wiley and Sons, **1966**, pp. 113–142. (b) Dilling, W. L. *Chem. Rev.* **1969**, 845–877. (c) Liu, R. S. H.; Hammond, G. S. *Photochem. Photobiol. Sci.* **2003**, *2*, 835–844. (d) Sieburth, S. M. in *Molecular and Supramolecular Photochemistry, Synthetic Organic Photochemistry*, Vol. 12 (Eds. A. G. Griesbeck, J. Mattay) J. Marcel Decker, New York, New York, **2005**, pp. 239–268.
8. In contrast, the absorption spectra of simple enones possess a low-energy $n \rightarrow p^*$ transition that is accessible with relatively lower energy UVA irradiation (ca. 300–350 nm).
9. Lu, Z.; Yoon, T. P. *Angew. Chem. Int. Ed.* **2012**, *51*, 10329–10332.
10. Shono, T.; Kashimura, S.; Kise, N. in *The Chemistry of Dienes and Polyenes*, Vol. 1 (Ed: Z. Rappoport), J. Wiley & Sons, Chichester, **1997**, 753–774.
11. (a) Lamola, A. A.; Hammond, G. S. *J. Chem. Phys.* **1965**, *43*, 2129–2135 (b) Ni, T.; Caldwell, R. A.; Melton, L. A. *J. Am. Chem. Soc.* **1989**, *111*, 457–464. (c) Evans, D. F. *J. Chem. Soc.* **1960**, 1735–1745.
12. The reaction time can be significantly reduced by irradiation with a higher-intensity purple LED light source; under these conditions, **1** is converted to **2** in 90% yield (10:1 d.r.) after 7 h. However, household CFL bulbs were generally used to represent more readily accessible consumer light sources.
13. Rillema, D. P.; Allen, G.; Meyer, T. J.; Conrad, D. *Inorg. Chem.* **1983**, *22*, 1617–1622.

-
14. (a) Nguyen, J. D.; D'Amato, E. M.; Narayanam, J. M. R.; Stephenson, C. R. J. *Nature Chem.* **2012**, *4*, 854–859. (b) Kim, H.; Lee, C. *Angew. Chem. Int. Ed.* **2012**, *51*, 12303–12306.
 15. (a) Juris, A.; Balzani, V.; Barigelletti, F.; Campagna, S.; Belser, P.; von Zelewsky, A. *Coord. Chem. Rev.* **1988**, *84*, 85–277. (b) Flamigni, L.; Barbieri, A.; Sabatini, C.; Ventura, B.; Barigelletti, F. *Top. Curr. Chem.* **2007**, *281*, 143–203.
 16. (a) Guella, G.; Dini, F.; Pietra, F. *Helv. Chem. Acta.* **1995**, *78*, 1747–1754. (b) Snider, B. B.; Lu, Q. *Synth. Commun.* **1997**, *27*, 1583–1600. (c) Rosini, G.; Laffi, F.; Morotta, E.; Pagani, I.; Righi, P. *J. Org. Chem.* **1998**, *63*, 2389–2391. (d) Ko, C.; Feltenberger, J. B.; Ghosh, S. K.; Hsung, R. *Org. Lett.* **2008**, *10*, 1971–1974.
 17. Lowry, M. S.; Goldsmith, J. I.; Slinker, J. D.; Rohl, R.; Pascal, Jr., R. A.; Malliaras, G. G.; Bernhard, S. *Chem. Mater.* **2005**, *17*, 5712–5719.
 18. Pangborn, A. B.; Giardello, M. A.; Grubbs, R. H.; Rosen, R. K.; Timmers, F. T. *Organometallics* **1996**, *15*, 1518–1520.
 19. Still, W. C.; Kahn, M.; Hong, P. C.; Lu, L. *J. Org. Chem.* **1978**, *43*, 2923–2925.
 20. Brummond, K. M.; Chen, H.; Mitasev, B.; Casarez, A. D. *Org. Lett.* **2004**, *6*, 2161–2163.
 21. Laird, T.; Ollis, W. D.; Sutherland, I. O.; *J. Chem. Soc., Perkin Trans. I* **1980**, 2033–2048.
 22. Lei, A.; Lu, X. *Org. Lett.* **2000**, *2*, 2357–2360.
 23. Piers, E.; Jung, G. L.; Ruediger, E. H. *Can. J. Chem.* **1987**, *65*, 670–682.
 24. Yildizhan, S.; Schulz, S. *Synlett* **2011**, 2831–2833.
 25. DeBoef, B.; Counts, W. R.; Gilbertson, S. R.; *J. Org. Chem.* **2007**, *72*, 799–804.
 26. Lutteke, G.; AlHussainy, R.; Wrigstedt, P. J.; Hue, B. T. B.; de Gelder, R.; van Maarseveen, J. H.; Hiemstra, H. *Eur. J. Org. Chem.* **2008**, 925–933.
 27. Li, T-S.; Li, J-T.; Li, H-Z. *J. Chromatogr. A* **1995**, *715*, 372–375.
 28. Ohno, H.; Mizutani, T.; Kadoh, Y.; Aso, A.; Miyamura, K.; Fujii, N.; Tanaka, T. *J. Org. Chem.* **2007**, *72*, 4378–4389.
 29. Trost, B. M.; Papillon, J. P. N.; Nussbaumer, T. *J. Am. Chem. Soc.* **2005**, *127*, 17921–17937.

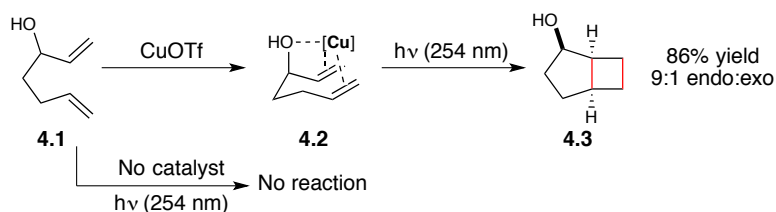
-
30. Lanners, S.; Norouzi-Arasi, H.; Khiri, N.; Hanquet, G. *Eur. J. Org. Chem.* **2007**, 4065–4075.
31. Fürstner, A.; Flügge, S.; Larionov, O.; Takahashi, Y.; Kubota, T.; Kobayashi, J. *Chem. Eur. J.* **2009**, *15*, 4011–4029.
32. Poornachandran, M.; Raghunathan, R. *Tetrahedron* **2000**, *64*, 6461–6474.
33. Batt, F.; Bourcet, E.; Kassab, Y.; Fache, F. *Synlett* **2007**, 1869–1872.

Chapter 4. Enantioselective Copper-Catalyzed [2+2] Photocycloaddition Reactions

4.1 Introduction

The development of catalytic, asymmetric methods is a longstanding goal in organic photochemistry.¹ A fundamental challenge in designing such methods is the general scarcity of photochemical processes in which the catalyst and substrate are closely associated throughout the key bond-forming steps. As a result, the traditional arsenal of privileged chiral catalysts developed for thermal reactions is not readily applicable to photochemical reactions. To address this challenge, we became interested in pursuing an asymmetric variant of the copper(I)-catalyzed [2+2] cycloaddition of non-conjugated alkenes developed largely by Salomon and co-workers (Scheme 4-1).² These cycloadditions occur through 2:1 alkene-copper complexes that undergo charge-transfer excitation upon absorption of ultraviolet light. Copper(I) triflate is the most effective catalyst as the triflate anion is highly non-coordinating and does not compete with the substrate for binding to the copper center.³ We hypothesized that these reactions should be amenable to asymmetric induction because they proceed through well-defined catalyst-substrate complexes. Although a number of highly diastereoselective copper-catalyzed [2+2] cycloadditions have been developed and successfully applied to total synthesis,⁴ this work would provide the first catalytic, asymmetric variant.

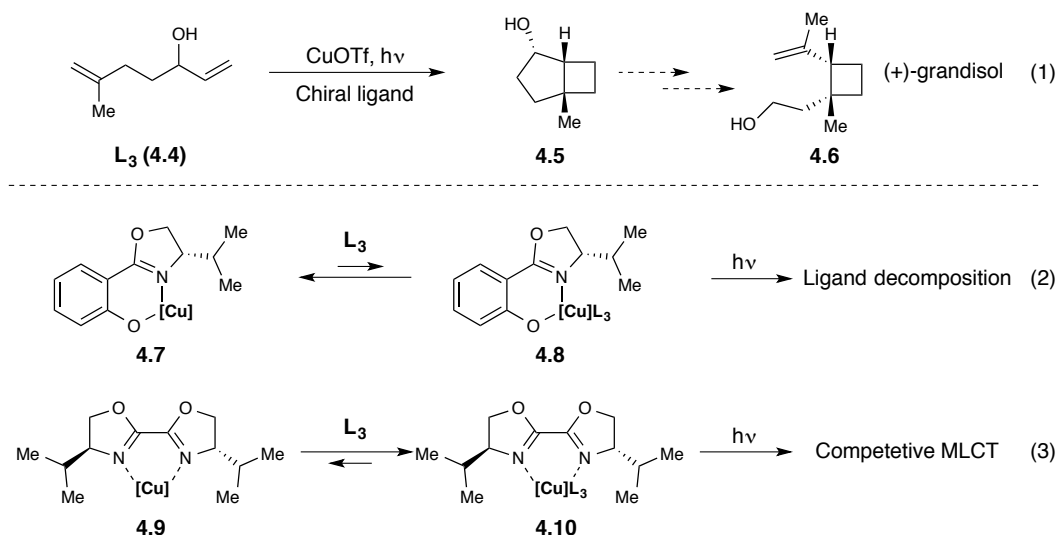
Scheme 4-1. Copper(I)-catalyzed alkene photocycloadditions.



While studying the asymmetric synthesis of the cyclobutane-containing natural product (+)-grandisol, Mattay and co-workers surveyed a variety of chiral copper-oxazoline complexes for the key [2+2] photocycloaddition step (Scheme 4-2).⁵ Unfortunately, they observed

drastically reduced reactivity and only marginal enantioselectivity (<5% ee) for all ligands examined. In particular, neutral copper complexes derived from strongly donating anionic ligands (e.g. **4.7**) prohibited binding of the olefin substrate, resulting in complete inhibition of the reaction and decomposition of the ligand upon irradiation. On the other hand, cationic complexes derived from neutral ligands (e.g. **4.9**) were shown to effectively bind to the olefin substrate and the poor reactivity observed in these cases was attributed to a competitive, unproductive metal-to-ligand charge-transfer between the copper center and the imine ligand.

Scheme 4-2. Inherent limitation of chiral ligand approach.

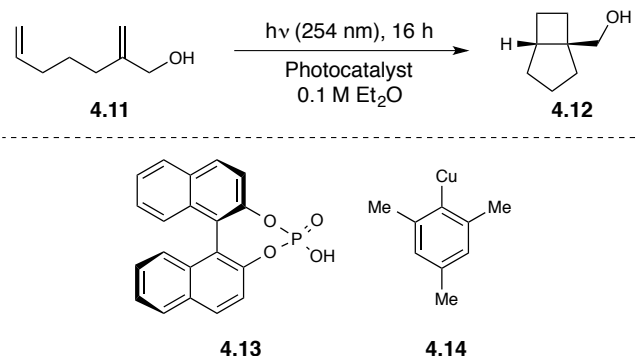


To circumvent these inherent challenges, we elected to alternatively study copper(I) complexes bearing chiral, non-coordinating counterions, which should more closely mimic the electronic and photophysical properties of the optimal CuOTf catalyst. We have largely focused our attention on chiral anions derived from BINOL (e.g. **4.13**). Although chiral Brønsted acids of this type have been most widely applied as organocatalysts,⁶ the use of these structures as counterions for transition metal catalysis has also been documented in a number of systems.⁷

4.2 Results and Discussion

The intramolecular [2+2] cycloaddition of prochiral diene **4.11** to cyclobutane **4.12** was selected as a model system for preliminary studies (Table 4-1). The racemic reaction proceeds in excellent yield in the presence of $(\text{CuOTf})_2 \cdot \text{C}_6\text{H}_6$ (entry 1).⁸ After some experimentation, we found that the desired copper phosphate catalysts were optimally generated *in situ* from mesityl copper and the free chiral phosphoric acid. We were pleased to observe that a 1:1 mixture of the acid and copper gave cyclobutane **4.12** in 29% yield and 20% ee (entry 2). The reaction conversion increased slightly with a higher acid to copper ratio (entries 3 and 4), although the overall catalyst loading did not have an effect (entry 5).

Table 4-1. Chiral anion approach to enantioselective copper-catalyzed [2+2] cycloadditions.



Entry	Photocatalyst	% Remaining 4.11 ^a	% Yield 4.12 ^a	% ee 4.12 ^b
1	2 mol% $(\text{CuOTf})_2 \cdot \text{C}_6\text{H}_6$	0	96	--
2	4 mol% 4.13 + 4 mol% 4.14	60	29	20
3	8 mol% 4.13 + 4 mol% 4.14	52	38	14
4	32 mol% 4.13 + 4 mol% 4.14	53	37	12
5	20 mol% 4.13 + 10 mol% 4.14	58	38	15

^a Yield determined by ¹H NMR spectroscopic analysis of the crude reaction mixture with respect to an internal standard.

^b Enantiomeric excess determined by SFC analysis of the corresponding 3,5-bis(nitro)benzoyl ester.

Following these proof-of-concept experiments, we next examined a variety of phosphate counterions bearing different substituents at the 3,3' positions in an attempt to optimize the enantioselectivity (Table 4-2). We were pleased to find that phosphate **4.15** (R = phenyl)

increased the enantiomeric excess to 28%, albeit with selectivity for the opposite enantiomer. The widely employed phosphates **4.16** ($R = 3,5-(CF_3)_2Ph$) and **4.17** (TRIP, $R = 2,4,6-(i\text{-}Pr)_3Ph$) resulted in poorer enantioselectivity (entries 3 and 4). Due to the unusual decrease in enantioselectivity with larger aryl groups and the reversal in the absolute selectivity, we were interested in studying catalysts with substituents of intermediate steric demand. Catalyst **4.19** ($R = Me$; entry 6) did indeed show some improvement over the parent phosphoric acid (entry 1). Unfortunately, limited reactivity was observed with catalysts bearing bromide (**4.18**), trimethylsilyl (**4.20**), or triphenylsilyl (**4.21**) groups (entries 5, 7-8).

Table 4-2. Investigation of chiral BINOL-derived phosphoric acids.

Entry	R (X^*H)	% Remaining 4.11 ^a	% Yield 4.12 ^a	% ee 4.12 ^b
1	H (4.13)	52	38	14
2	Ph (4.15)	56	20	-28
3	3,5-(CF_3) ₂ -Ph (4.16)	40	33	3
4	2,4,6-($i\text{-}Pr$) ₃ -Ph (4.17)	39	49	-10
5	Br (4.18)	--	0	--
6	Me (4.19)	59	25	25
7	TMS (4.20)	74	9	1
8	SiPh ₃ (4.21)	--	0	--

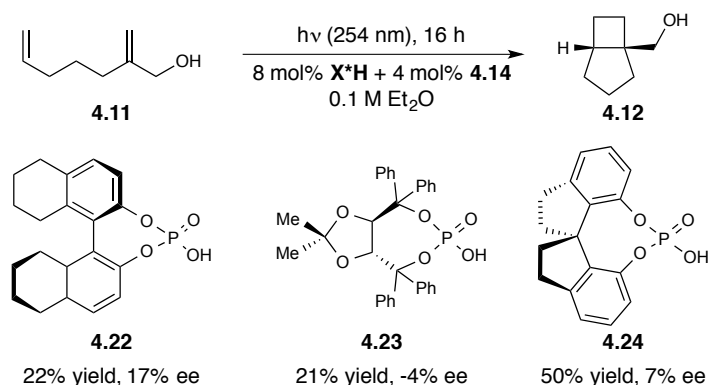
^a Yield determined by ¹H NMR spectroscopic analysis of the crude reaction mixture with respect to an internal standard.

^b Enantiomeric excess determined by SFC analysis of the corresponding 3,5-bis(nitro)benzoyl ester.

We also studied several other classes of privileged chiral phosphoric acid scaffolds (Scheme 4-3). The partially hydrogenated BINOL framework (**4.22**) gave comparable results to the parent

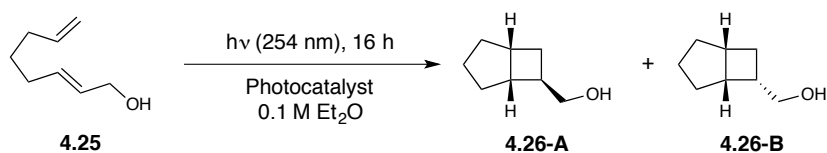
phosphoric acid (**4.13**), while TADDOL-derived phosphate **4.23** and SPINOL-derived phosphate **4.24** resulted in reduced enantioselectivity.

Scheme 4-3. Investigation of privileged chiral phosphoric acids.



Diene **4.25** was briefly examined as an alternative substrate design (Table 4-3). As the pendant hydroxyl group should be tightly bound to the copper center in the transition state, we thought that its relative position on the alkene might have a large impact on the observed selectivity. Unfortunately, the copper phosphate complex derived from **4.13** rendered cyclobutane **4.26** in only 18% yield with moderate diastereoselectivity and poor enantioselectivity (entry 2).

Table 4-3. Alternative substrate design.



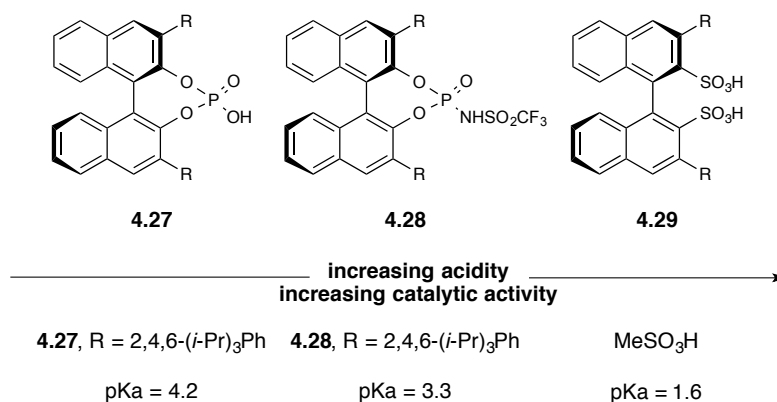
Entry	Photocatalyst	% Yield 4.26 (A + B) ^a	d.r. (A:B) ^a	% ee (A) ^b	% ee (B) ^b
1	2 mol% $(CuOTf)_2 \cdot C_6H_6$	93	3:1	--	--
2	8 mol% 4.13 + 4 mol% 4.14	18	4:1	~17	10

^a Yield and diastereomeric ratio determined by 1H NMR spectroscopic analysis of the crude reaction mixture with respect to an internal standard.

^b Enantiomeric excess determined by SFC analysis of the corresponding 3,5-bis(nitro)benzoyl ester.

Given the limited success of chiral copper-phosphate complexes with respect to both enantioselectivity and overall reactivity, we were interested in greatly expanding the scope of our catalyst studies. A key hypothesis was that the use of a less coordinating chiral anion would promote stronger metal-substrate binding and therefore greater reactivity in the photocycloaddition. The relative coordinating abilities of various chiral anions can be estimated from the pKa values of the corresponding conjugate acids (Scheme 4-4). A variety of BINOL-derived strong acids have been developed for Brønsted acid catalysis including *N*-triflyl phosphoramides (**4.28**)⁹ and disulfonic acids (**4.29**),¹⁰ which are significantly more acidic than the analogous phosphoric acids (**4.27**).¹¹

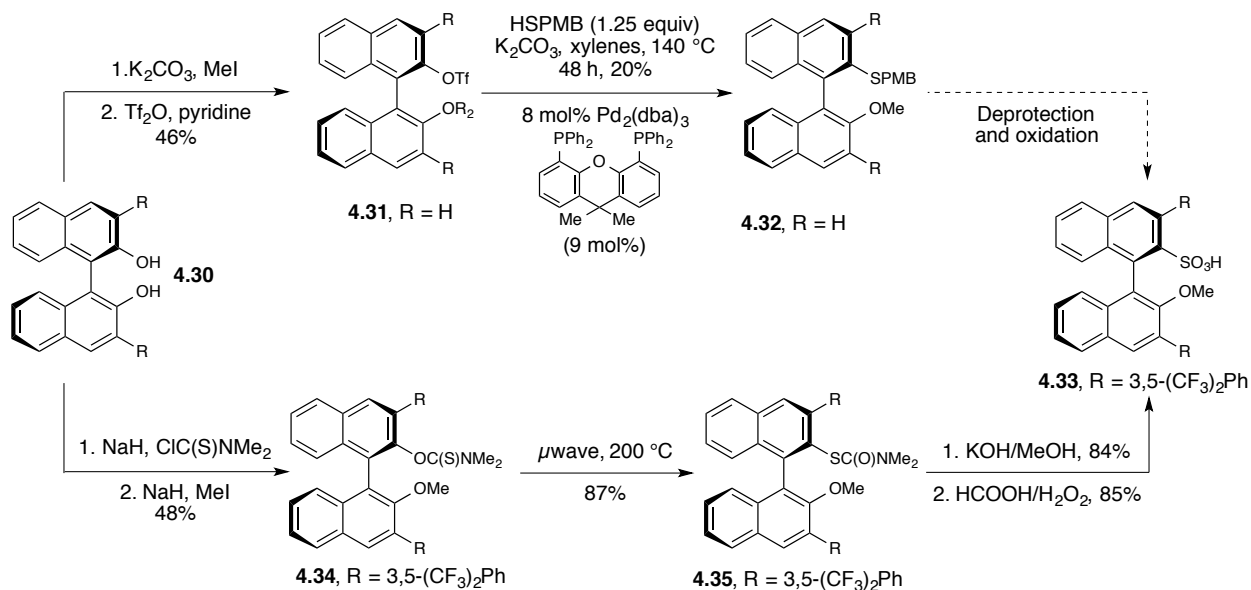
Scheme 4-4. pKa values of chiral Brønsted acids.



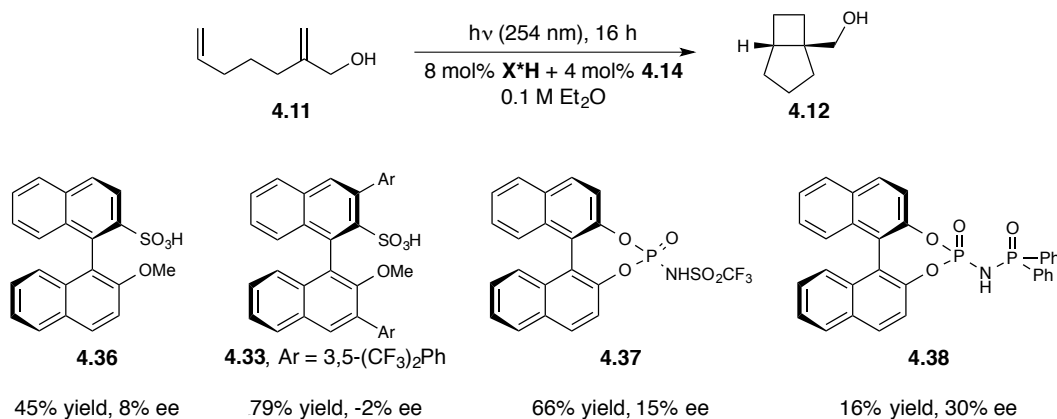
In order to test chiral acid structures across the full range of available pKa values, we undertook the synthesis of sulfonic acid **4.33** as an analogue of **4.29** that could readily serve as a precursor to 1:1 chiral anion:copper complexes (Scheme 4-5). Initial efforts focused on developing a novel cross-coupling route¹² to install the aryl-sulfur bond in **4.32** from the easily accessible triflate (**4.31**). However, only moderate yields of the desired product were achieved after extensive optimization of the reaction conditions. We therefore opted for a more conventional route and discovered efficient and high-yielding microwave conditions for the

Newman–Kwart rearrangement¹³ of *O*-aryl thiocarbamate **4.34** to *S*-aryl thiocarbamate **4.35**. Hydrolysis of the carbamate to the free thiol followed by performic acid oxidation and acidification generated the desired sulfonic acid **4.33** in high yield.

Scheme 4-5. Synthesis of novel chiral sulfonic acid frameworks: initial proposed route (top); successful second generation route (bottom).



In line with our hypothesis, the copper complexes derived from sulfonic acids greatly increased the reaction efficiency, albeit with low levels of enantioselectivity (Scheme 4-5). The 3,3'-disubstituted chiral sulfonic acid **4.33** promoted full conversion of the starting material to afford the cyclobutane in 79% yield. *N*-Triflyl phosphoramidate **4.37** also greatly accelerated the reaction and provided levels of enantioselectivity comparable to the structurally analogous phosphoric acid. *N*-Phosphinyl phosphoramidate **4.38**, the least acidic of all of the structures examined,¹⁴ provided the lowest conversion (16%). However, a very promising increase in the enantiomeric excess was also observed (30% ee).

Scheme 4-6. Survey of chiral acids of varying pKa.

4.3 Outlook and Future Directions

In summary, we have demonstrated that copper complexes bearing chiral counteranions serve as competent catalysts for [2+2] photocycloadditions. The levels of enantioselectivity achieved to date are modest, but highlight a fundamentally new approach to asymmetric induction for this class of reactions. These results also validate our hypothesis that less coordinating counteranions accelerate the reaction by enabling tighter binding of the diene substrate to the copper center. A number of interesting avenues remain to be explored with respect to catalyst design (Chart 4-1). The positive increase in enantioselectivity observed with *N*-phosphinyl phosphoramides (**4.39**) suggests that this chiral framework merits further optimization. Catalyst structures of this type are particularly appealing because the phosphinyl aryl groups provide an additional site at which the electronic nature and steric bulk surrounding the acidic moiety can be easily tuned. The novel sulfonic acid framework **4.40** we developed in the course of these studies is similarly highly tunable: the substituent on the aryl ether (R₂) provides a site of diversification at very close proximity to the sulfonate. These structural features can be studied in concert with modifications to the steric and electronic properties of the 3,3' substituents, the electronic properties of the 6,6' substituents, and the biaryl dihedral angle through partial hydrogenation of the ring system. An

alternative area of exploration might be to study 'confined' *N*-imidodiphosphoric acid structures, which were recently pioneered by List and co-workers (**4.41**) and designed to accommodate small and functionally unbiased substrates.¹⁵ For comparison, our sulfonic acid design should also provide entry into a 'confined' disulfonimide analogue (**4.42**).

Finally, the substrate design has been largely underexplored and merits further study (Chart 4-2). A number of structures could be synthesized to probe the effect of increasing the steric bulk on one of the olefin reaction partners (e.g. **4.43-4.45**). Alternatively, an additional Lewis basic coordination site could be introduced into the carbon tether, which could dramatically affect the nature of the catalyst-substrate complex (e.g. **4.46**).

Chart 4-1. Future directions: explore new counteranion frameworks.

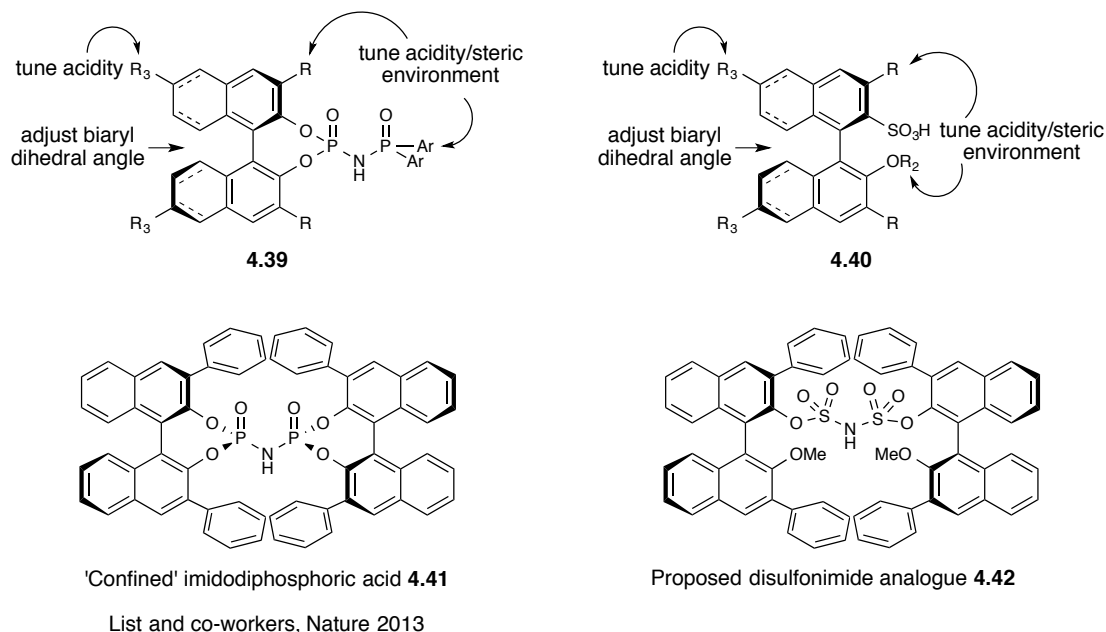
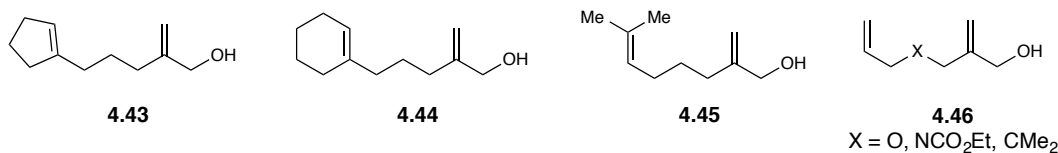


Chart 4-2. Future directions: explore new substrate designs.



4.4 Contributions

Matt Livingston contributed to the synthesis of phosphoric acid **4.15** and sulfonic acid **4.36**.

4.5 Experimental

4.5.1 General experimental information

Diethyl ether and dichloromethane were purified by elution through alumina on a glass contour solvent system as described by Grubbs.¹⁶ Pyridine was distilled from CaH₂ immediately before use. Mesityl copper was purchased from Strem, stored in a glove-box, and handled under inert gas. Flash column chromatography was performed with Sigma-Aldrich silica gel (pore size 60 Å, 230–400 mesh particle size) using the method of Still.¹⁷ ¹H and ¹³C NMR data for previously uncharacterized compounds were obtained using a Bruker Avance III 500 MHz spectrometer. ¹H NMR spectra are referenced to TMS (0.00 ppm) for CDCl₃, DMSO-*d*₆ (2.50 ppm), or Methanol-*d*₄ (3.31 ppm). ¹³C NMR spectra are referenced to CDCl₃ (77.16 ppm), DMSO-*d*₆ (39.52 ppm), or Methanol-*d*₄ (49.00). The NMR facilities at UW–Madison are funded by the NSF (CHE-1048642) and a generous gift from Paul J. Bender. Mass spectrometry was performed with a Waters (Micromass) AutoSpec. These facilities are funded by the NSF (CHE-9974839, CHE-9304546) and the University of Wisconsin. Enantiomeric ratios were determined by supercritical fluid chromatography (SFC) on a TharSFC investigator instrument equipped with a Waters 2996 photodiode array detector.

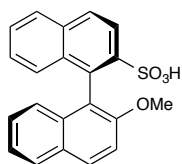
4.5.2 General procedure for the asymmetric [2+2] photocycloaddition

An oven-dried quartz vessel was charged with a stir bar and the chiral organic acid (0.08 equiv), fitted with a septum, and purged with nitrogen (3 cycles). Mesityl copper (0.04 equiv, 0.016 mmol, 2.9 mg) was then added as a stock solution in Et₂O (1 mL of a 0.016 mM solution) via an argon-purged syringe and the reaction mixture was allowed to stir at room temperature in the

dark for 3 hours. A solution of 2-(Hydroxymethyl)-1,6-heptadiene⁸ (1 equiv, 0.40 mmol, 50 mg) in Et₂O (3 mL) was added dropwise via an argon-purged syringe. The reaction vessel was sealed with a cold-water finger under a back-flow of nitrogen and irradiated in a Rayonet reactor at 254 nm with stirring and cooling for 16 hours. The solution was then diluted with CH₂Cl₂, quenched with 1 mL saturated NH₄OH, passed across a short plug of silica with Et₂O, and concentrated *in vacuo*. Trimethyl(phenyl)silane was added as an internal standard and the yield of the [2+2] cycloadduct was determined by ¹H NMR spectroscopic analysis (CDCl₃). The sample was then transferred to a 6-dram vial and treated with pyridine (2 mL), 4-(Dimethylamino)pyridine (0.12 equiv, 0.05 mmol, 6 mg) and 3,5-Dinitrobenzoyl chloride (4 equiv, 1.6 mmol, 370 mg). The vial was sealed with a Teflon cap and allowed to stir at room temperature for 2 hours at which point it was diluted with EtOAc and quenched with 1 N HCl. The organic layer was further washed with saturated NaHCO₃ (2x) and brine, dried over Na₂SO₄, and concentrated *in vacuo*. The residue was purified by flash column chromatography on silica gel (10:1 to 5:1 hexanes:Et₂O) to afford an inseparable mixture of the derivatized [2+2] cycloadduct (1*R**5*R**-bicyclo[3.2.0]heptan-1-ylmethyl 3,5-dinitrobenzoate) and the derivatized starting material (2-methylenehept-6-en-1-yl 3,5-dinitrobenzoate). The enantiomeric excess of the derivatized cycloadduct was determined by SFC analysis (Daicel CHIRALPAK[®] AD-H, 10% MeOH, 3 mL/min, t₁ = 10.14 min, t₂ = 10.80 min; derivatized starting material at t = 8.85 min).

4.5.3 Synthesis of chiral acids

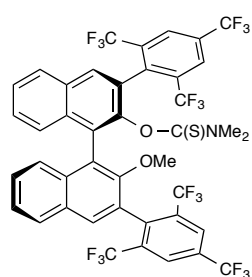
(*R*)-2'-methoxy-[1,1'-binaphthalene]-2-sulfonic acid (4.36): A solution of hydrogen peroxide (30 wt. % in water, 800 μL) was added dropwise at 0 °C to formic acid (8 mL) in a 6-dram vial. The stirred reaction mixture was allowed to slowly warm to room temperature over 60 minutes at which point a solution of (*R*)-2'-methoxy-



[1,1'-binaphthalene]-2-thiol¹³ (0.490 mmol, 155 mg) in CH₂Cl₂ (8 mL) was added dropwise. The reaction mixture was stirred vigorously for 2 hours, then cooled to 0 °C, quenched by the dropwise addition of dimethyl sulfide (7.3 mmol, 540 µL), and concentrated *in vacuo*. The residue was purified by flash column chromatography on silica gel (5:1 CH₂Cl₂:MeOH) then passed across a short plug of Amberlite[®] IR120 hydrogen form resin in MeOH. The eluent was concentrated *in vacuo* then dried at 30 °C under vacuum over night to afford the product as a brown solid (0.28 mmol, 103 mg, 58%). ¹H NMR (500 MHz, Methanol-*d*₄) δ 8.25 (d, *J* = 8.8 Hz, 1H), 8.05 – 7.91 (m, 3H), 7.83 (d, *J* = 8.2 Hz, 1H), 7.53 – 7.44 (m, 2H), 7.26 – 7.19 (m, 2H), 7.11 (ddd, *J* = 8.2, 6.7, 1.3 Hz, 1H), 7.03 (d, *J* = 8.6 Hz, 1H), 6.89 (d, *J* = 8.5 Hz, 1H), 3.75 (s, 3H). ¹³C NMR (126 MHz, Methanol-*d*₄) δ 156.2, 142.2, 135.8, 135.7, 134.8, 134.7, 130.6, 130.3, 128.9, 128.7, 128.6, 128.2, 128.1, 127.5, 127.0, 126.8, 126.0, 124.1, 122.0, 114.6, 56.6. HRMS (ESI) calculated for [C₂₁H₁₆O₄S + NH₄]⁺ requires *m/z* 382.1108, found 382.1101.

O-(*R*)-2'-methoxy-3,3'-bis(2,4,6-tris(trifluoromethyl)phenyl)-[1,1'-binaphthalen]-2-yl)

dimethylcarbamothioate (4.34): A flame-dried 100 mL round-bottomed flask fitted to a reflux



condensor was charged with (*R*)-3,3'-bis(2,4,6-tris(trifluoromethyl)phenyl)-[1,1'-binaphthalene]-2,2'-diol¹⁸ (5.77 mmol, 4.10 g) and freshly distilled

DMF (12 mL) and then cooled to 0 °C under nitrogen. NaH (60% dispersion in mineral oil, 6.35 mmol, 254 mg) was added portionwise and

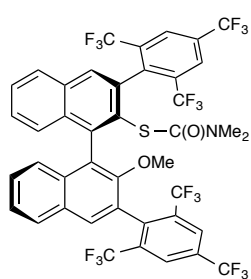
the reaction mixture was allowed to stir at 0 °C for an additional 60 minutes.

Dimethylthiocarbamoyl chloride (6.35 mmol, 785 mg) was then added and the reaction mixture heated to 85 °C for two hours at which point it was cooled again to 0 °C. NaH (60% dispersion in mineral oil, 6.92 mmol, 277 mg) was added portionwise and the reaction mixture was allowed

to stir at 0 °C for an additional 40 minutes. Methyl iodide (6.92 mmol, 430 μ L) was added and the reaction mixture heated to 85 °C overnight at which point it was cooled to room temperature and diluted with water and CH₂Cl₂. The layers were separated and the CH₂Cl₂ layer washed with water (2x), dried over Na₂SO₄, filtered and concentrated *in vacuo*. The crude residue was purified by flash column chromatography on silica gel (3:1 hexanes:CH₂Cl₂) to afford the product as a white solid (2.77 mmol, 2.25 g, 48%). ¹H NMR (300 MHz, CDCl₃) δ 8.21 (s, 2H), 8.15 (s, 2H), 8.12 – 7.83 (m, 4H), 7.66 – 7.32 (m, 4H), 7.31 – 7.22 (m, 2H), 3.12 (s, 3H), 2.99 (s, 3H), 2.81 (s, 3H).

***S*-((1*R*,3*r*)-2'-methoxy-3,3'-bis(2,4,6-tris(trifluoromethyl)phenyl)-[1,1'-binaphthalen]-2-yl)**

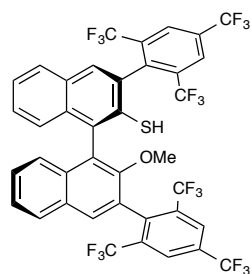
dimethylcarbamothioate (4.35): O-(*R*)-2'-methoxy-3,3'-bis(2,4,6-tris(trifluoromethyl)phenyl)-



[1,1'-binaphthalen]-2-yl) dimethylcarbamothioate (2.00 mmol, 1.62 g) was distributed evenly between 14 10 mL glass microwave reaction vessels (~115 mg each) which were then fitted with septa and heated to 200 °C at 300 W in a CEM Discover microwave reactor for 45 minutes. The

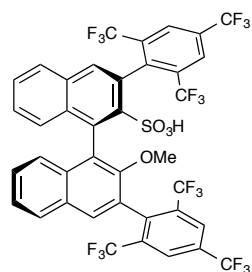
combined crude reaction mixtures were purified by flash column chromatography on silica gel (3:1 to 1:1 hexanes:CH₂Cl₂) to afford the product as a white solid (1.74 mmol, 1.41 g, 87%). ¹H NMR (300 MHz,) δ 8.28 – 8.20 (m, 2H), 8.14 – 8.07 (m, 2H), 8.04 – 7.85 (m, 4H), 7.58 (ddd, *J* = 8.1, 6.8, 1.3 Hz, 1H), 7.46 (ddd, *J* = 8.1, 6.8, 1.3 Hz, 1H), 7.42 – 7.27 (m, 3H), 7.25 – 7.19 (m, 1H), 3.11 (s, 3H), 2.48 (s, 6H).

(*R*)-2'-methoxy-3,3'-bis(2,4,6-tris(trifluoromethyl)phenyl)-[1,1'-binaphthalene]-2-thiol: A



solution of *S*-(*R*)-2'-methoxy-3,3'-bis(2,4,6-tris(trifluoromethyl)phenyl)-[1,1'-binaphthalen]-2-yl) dimethylcarbamothioate (1.72 mmol, 1.40 g) in MeOH (17 mL) was heated to reflux under N₂ in a flame-dried 100 mL round-bottomed flask fitted to a reflux condenser. A solution of KOH (9 mL, 10% in MeOH) was added slowly and the stirred reaction mixture continued to reflux for 45 hours at which point it was cooled to room temperature and quenched by the dropwise addition of 1 N HCl (~3 mL). The resulting precipitate was collected on a fritted filter and washed with water. The solid was dissolved in a small portion of CH₂Cl₂, dried over Na₂SO₄, filtered and concentrated *in vacuo* to afford the product as a pale yellow solid (1.44 mmol, 1.07 g, 84%). ¹H NMR (300 MHz, CDCl₃) δ 8.26 – 8.21 (m, 2H), 8.08 (s, 2H), 8.04 – 7.86 (m, 4H), 7.57 – 7.33 (m, 4H), 7.22 – 7.14 (m, 2H), 3.27 (s, 1H), 3.20 (s, 3H).

(*R*)-2'-methoxy-3,3'-bis(2,4,6-tris(trifluoromethyl)phenyl)-[1,1'-binaphthalene]-2-sulfonic

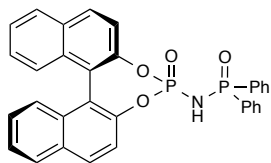


acid (4.33): A solution of hydrogen peroxide (30 wt. % in water, 1.1 mL) was added dropwise at 0 °C to formic acid (9.5 mL) in a 100 mL round-bottomed flask. The stirred reaction mixture was allowed to slowly warm to room temperature over 60 minutes at which point a solution of (*R*)-2'-methoxy-3,3'-bis(2,4,6-tris(trifluoromethyl)phenyl)-[1,1'-binaphthalene]-2-thiol (0.640 mmol, 475 mg) in CH₂Cl₂ (9.5 mL) was added dropwise. The reaction mixture was stirred vigorously for 3.5 hours, then eluted directly across a short silica plug (10:1 CH₂Cl₂:MeOH). The eluent was treated with saturated aqueous Na₂SO₃, the layers separated, and the aqueous layer further extracted with CH₂Cl₂ (2x). The combined organic layers were concentrated *in vacuo* and the residue purified by flash column chromatography on silica gel (10:1 CH₂Cl₂:MeOH). The

resulting product was dissolved in CH₂Cl₂, washed with 6 N HCl, and then passed across a short plug of Amberlite® IR120 hydrogen form resin in MeOH. The eluent was layered with toluene and concentrated *in vacuo* (3x) then dried at 30 °C under vacuum overnight to afford the product as a tan solid (0.56 mmol, 444 mg, 89%). ¹H NMR (500 MHz, CDCl₃) δ 8.14 (s, 2H), 7.99 – 7.83 (m, 6H), 7.65 (t, *J* = 7.5 Hz, 1H), 7.44 – 7.37 (m, 2H), 7.29 – 7.21 (m, 2H), 7.06 (d, *J* = 8.5 Hz, 1H), 3.07 (s, 1H). ¹³C NMR (126 MHz, CDCl₃) δ 151.5, 143.5, 140.4, 136.4, 135.4, 134.8, 134.0, 133.7, 133.0, 132.8, 132.4, 132.1, 131.9, 131.7, 131.6, 131.4, 131.0, 130.7, 130.6, 130.5, 130.1, 129.5, 128.5, 128.4, 128.4, 128.3, 127.8, 127.6, 126.8, 126.7, 126.0, 125.9, 124.6, 124.6, 122.5, 122.4, 121.5, 121.3, 120.3, 120.2, 61.1. (Note: Chemical shifts of ¹³C peaks reported directly; did not de-convolute C-F coupling). HRMS (ESI) calculated for [C₃₇H₂₀O₄SF₁₂ + NH₄]⁺ requires *m/z* 806.1229, found 806.1213.

***N*-(*R*)-4-oxidodinaphtho[2,1-*d*:1',2'-*f*][1,3,2]dioxaphosphepin-4-yl)-*P,P*-diphenylphosphinic**

amide (4.38): A flame-dried 25 mL round-bottomed flask fitted to a reflux condenser under N₂



was charged with (*R*)-(+)-1,1'-Bi(2-naphthol) (1.75 mmol, 500 mg) and freshly distilled pyridine (7 mL). Phosphorous oxychloride (5.24 mmol, 490 μL) was added dropwise and the stirred reaction mixture was heated to 60 °C for 3 hours and then to reflux for 15 minutes. The reaction was cooled to room temperature and the pyridine removed *in vacuo*. The residue was dissolved in EtOAc, filtered, and concentrated. The crude phosphoryl chloride thus obtained was dissolved in dry THF (14 mL) and added over 30 minutes to a stirred suspension of diphenyl phosphinamide (3.5 mmol, 760 mg) and NaH (60% dispersion in mineral oil, 5.25 mmol, 210 mg) in THF (17 mL) at room temperature under nitrogen. The reaction mixture was allowed to stir for 12 hours, then quenched

with water, extracted into CH₂Cl₂ and concentrated *in vacuo*. The residue was purified by flash column chromatography on silica gel (10:1 CH₂Cl₂:MeOH) and then dissolved in CH₂Cl₂, washed with 6 N HCl, and dried under vacuum overnight to afford the product as a pale yellow solid (0.42 mmol, 230 mg, 24%). ¹H NMR (500 MHz, DMSO-*d*₆) δ 8.16 (dd, *J* = 8.8, 5.2 Hz, 2H), 8.09 (dd, *J* = 8.2, 5.6 Hz, 2H), 7.75 (dd, *J* = 13.1, 7.5 Hz, 2H), 7.62 (dd, *J* = 13.0, 7.6 Hz, 2H), 7.58 – 7.43 (m, 8H), 7.41 – 7.28 (m, 4H), 7.23 (t, *J* = 8.2 Hz, 2H). ¹³C NMR (126 MHz, DMSO-*d*₆) δ 148.3, 148.2, 147.4, 147.4, 131.9, 131.9, 131.8, 131.7, 131.1, 131.0, 131.0, 130.9, 130.7, 130.7, 128.6, 128.5, 128.4, 128.3, 126.8, 126.7, 126.2, 126.1, 125.4, 125.3, 121.7, 121.6, 121.4, 121.4, 121.4, 121.3. (Note: Chemical shifts of ¹³C peaks reported directly; did not deconvolute C-P coupling). HRMS (ESI) calculated for [C₃₂H₂₃NO₄P₂ + H]⁺ requires *m/z* 548.1176, found 548.1179.

4.6 References:

1. (a) Inoue, Y. *Chem. Rev.* **1992**, 92, 741–770. (b) Rau, H. *Chem. Rev.* **1983**, 83, 535–547.
2. Salomon, R.G. *Tetrahedron*, **1983**, 39, 485–575.
3. (a) Salomon, R.G.; Kochi, J. K. *J. Am. Chem. Soc.* **1973**, 95, 1889–1897. (b) Salomon, R. G.; Kochi, J. K. *Tetrahedron Lett.* **1973**, 14, 2529–2532. (c) Salomon, R. G.; Kochi, J. K. *J. Am. Chem. Soc.* **1974**, 96, 1137–1144.
4. (a) McMurry, J.E.; Choy, W. *Tetrahedron Lett.* **1980**, 21, 2477–2480. (b) Bach, T.; Spiegel, A. *Synlett* **2002**, 1305–1307.
5. Langer, K.; Mattay, J. *J. Org. Chem.* **1995**, 60, 7256–7266.
6. (a) Akiyama, T. *Chem. Rev.* **2007**, 107, 5744–5758. (b) Terada, M. *Chem. Commun.* **2008**, 4097–4112.
7. (a) Lacour, J.; Hebbe-Viton, V. *Chem. Soc. Rev.* **2003**, 32, 373–382. (b) Llewellyn, D.B.; Adamson, D.; Arndtsen, B.A. *Org. Lett.* **2000**, 2, 4165–4168. (c) Mukherjee, S.; List, B. *J. Am. Chem. Soc.* **2007**, 129, 11336–11337. (c) Hamilton, G.L.; Kang, E.J.; Mba, M.; Toste, F.D. *Science* **2007**, 317, 496–499.

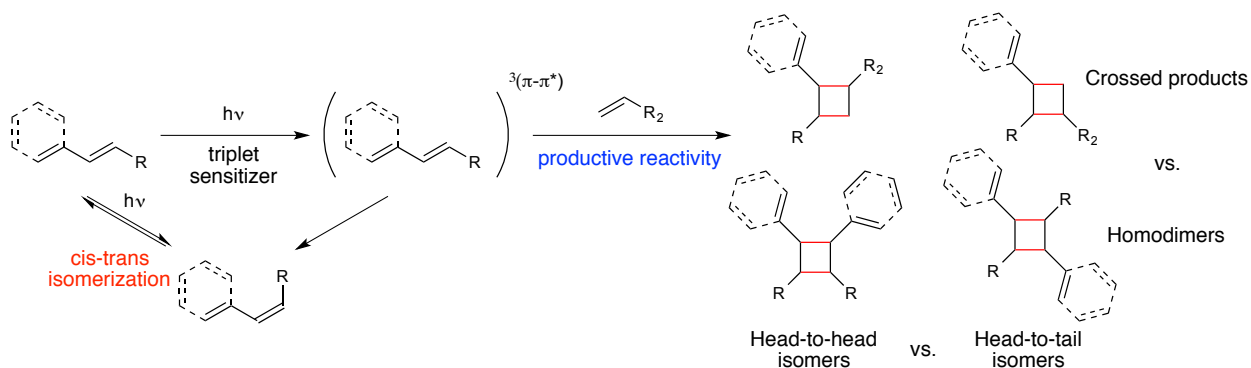
-
8. Salomon, R. G.; Coughlin, D. J.; Ghosh, S.; Zagorski, M. G. *J. Am. Chem. Soc.* **1982**, *104*, 998–1007.
 9. Nakashima, D.; Yamamoto, H. *J. Am. Chem. Soc.* **2006**, *128*, 9626–9627.
 10. Hatano, M.; Maki, T.; Moriyama, K.; Arinobe, M.; Ishihara, K. *J. Am. Chem. Soc.* **2008**, *130*, 16858–16860.
 11. pKa values of structures **5.27** and **5.28**: Christ, P.; Lindsay, A. G.; Vormittag, S. S.; Neudörfl, J.-M.; Berkessel, A.; O'Donoghue, A. C. *Chem. Eur. J.* 2011, *17*, 8524–8528; pKa value of MeSO₃H: Bordwell, F. G.; Algrim, D. *J. Org. Chem.* **1976**, *41*, 2507–2508.
 12. Mispelaere–Canivet, C.; Spindler, J.-F.; Perrio, S.; Beslin, P. *Tetrahedron* **2005**, *61*, 5253–5259.
 13. Fabbri, D.; Pulacchini, S.; Gladiali, S. *Synlett* **1996**, 1054–1056.
 14. Yang, C.; Xue, X.-S.; Li, X.; Cheng, J.-P. *J. Org. Chem.* **2014**, *79*, 4340–4351.
 15. Čorić, L.; List, B. *Nature* **2012**, *483*, 315–319.
 16. Pangborn, A. B.; Giardello, M. A.; Grubbs, R. H.; Rosen, R. K.; Timmers, F. T. *Organometallics* **1996**, *15*, 1518–1520.
 17. Still, W. C.; Kahn, M.; Hong, P. C.; Lu, L. *J. Org. Chem.* **1978**, *43*, 2923–2925.
 18. Akiyama, T.; Morita, H.; Itoh, J.; Fuchibe, K. *Org. Lett.* **2005**, *7*, 2583–2585.

Appendix A. Intermolecular [2+2] Cycloaddition Reactions of Styrenes and 1,3-Dienes by Visible Light Photocatalysis

A.1 Introduction

[2+2] Cycloadditions are among the most widely employed photochemical reactions in organic synthesis due to their ability to provide rapid access to densely functionalized cyclobutanes from simple olefin precursors.¹ Cyclobutanes are prominent substructures in an array of biologically active natural products,² and also serve as highly versatile synthetic intermediates.³ Our group has a longstanding interest in developing new cyclobutanation reactions that take advantage of visible light photocatalysis.⁴ In this context, we recently demonstrated that iridium complex **1**•PF₆ promotes the intramolecular cyclization of styrenes⁵ and conjugated 1,3-dienes (chapter 4)⁶ through an energy transfer photosensitization process. With the goal of increasing the broader utility of these reactions for natural product synthesis, we became interested in exploring the corresponding intermolecular cycloadditions.

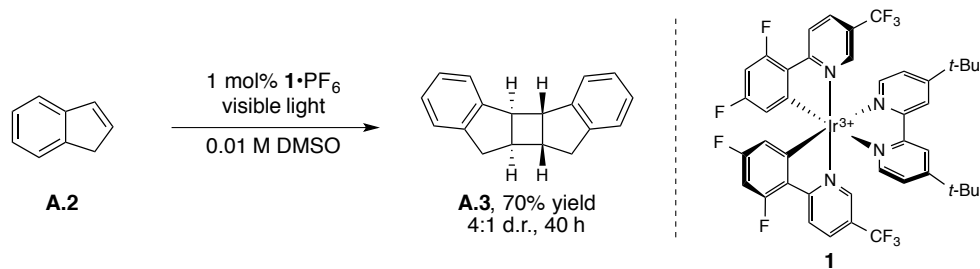
Scheme A-1. Intermolecular [2 + 2] photocycloaddition reactions: reactivity and selectivity issues.



While intramolecular photochemical [2+2] cycloadditions typically proceed with highly predictable and selective regiochemical outcomes, intermolecular reactions often suffer from a variety of reactivity and selectivity issues (Scheme A-1). First, the overall efficiency of these reactions can be limited by energy-wasting *cis-trans* isomerization from the triplet excited state that outcompetes productive reactivity. Furthermore, reactions involving two distinct olefin coupling partners can result in a mixture of crossed products and homodimers, each of which can

also exhibit head-to-tail or head-to-head constitutional isomers. Finally, the [2+2] cycloaddition sets up to four new stereocenters, resulting in many possible diastereomers of each of the products. Given these challenges, we elected to explore crossed [2+2] cycloaddition reactions of indene (**A.2**), which was previously shown to undergo homodimerization in good yield and diastereoselectivity in the presence of 1 mol% **1**•PF₆. (Scheme A-2). The constrained cyclic structure of indene prevents *cis-trans* isomerization and allows productive intermolecular reactivity in synthetically reasonable reaction times under standard catalyst conditions. We therefore thought indene would provide a good model system to probe for selectivity in crossed reactions.

Scheme A-2. Homodimerization of indene by visible light photosensitization.

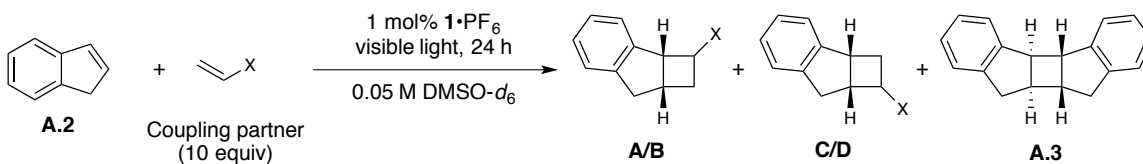


A.2 Results and Discussion

We initially explored the crossed [2+2] cycloaddition of indene with olefin coupling partners bearing a range of electronic properties. A select subset of these studies is depicted in Table A-1. A number of these systems did not exhibit any crossed reactivity, despite the large excess of olefin coupling partner employed (10 equiv). Non-conjugated aliphatic olefins, allenes, and vinyl ethers had been shown to be efficient coupling partners in the intramolecular [2+2] cycloaddition of styrenes, but gave only indene homodimerization in the corresponding intermolecular reactions (entries 2-4). However, electron-deficient alkenes such as acrylonitrile, methyl vinyl ketone, and methyl acrylate (entries 5-7) underwent cycloaddition with complete selectivity for

the cross-coupled product. These systems were also largely selective for the head-to-head isomers (**A/B**) over the head-to-tail isomers (**C/D**) (see experimental section for full details). The steric nature of the acrylate coupling partner was briefly examined to probe for any dominant changes in diastereoselectivity, but proved to have little effect on the reaction outcome (entry 8).

Table A-1. Crossed intermolecular [2+2] cycloadditions of indene.



Entry	Coupling partner	% Remaining indene (A.2) ^a	% Yield cycloadduct A/B (d.r.) ^a	% Yield A.3 ^a
1	None	16	--	65
2		31	0	64
3		15	0	73
4		33	0	52
5 ^b		0	91 (1.2:1) (A.4-A/B)	0
6 ^b		4	59 (2.5:1) (A.5-A/B)	0
7 ^b		0	83 (2.6:1) (A.6-A/B)	0
8		11	63 (3:1) (A.7-A/B)	0

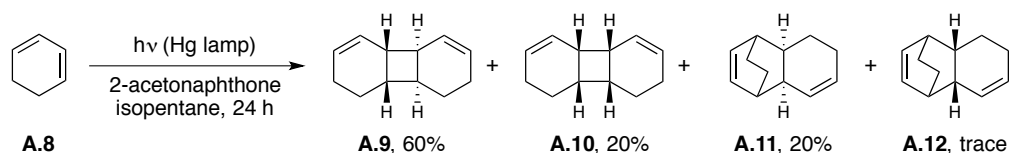
^a Yield and diastereomeric ratio determined by ^1H NMR spectroscopic analysis with respect to trimethyl(phenyl)silane as the internal standard.

^b Reaction performed in a J. Young NMR tube.

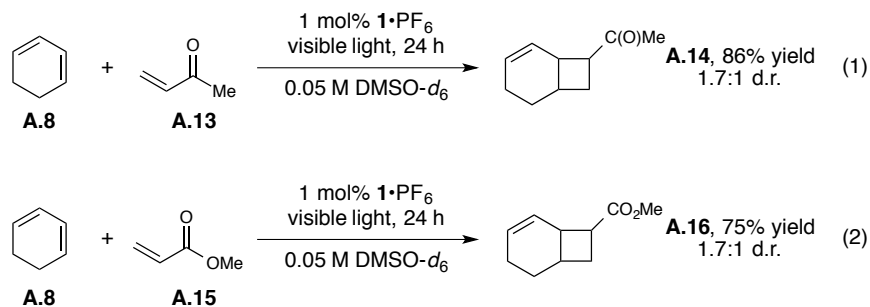
We also studied 1,3-cyclohexadiene as a substrate for intermolecular cycloaddition reactions, which is known to undergo homodimerization upon irradiation with UV light in the presence of a triplet sensitizer to generate a mixture of [2+2] and [4+2] cycloadducts (Scheme A-3). Again, we

found that electron-deficient alkenes underwent efficient crossed [2+2] cycloaddition reactions in the presence of **1**•PF₆ and visible light irradiation (Scheme A-4). We did not observe formation of any homodimers or corresponding Diels-Alder cycloadduct in these reactions.

Scheme A-3. Homodimerization of 1,3-cyclohexadiene by energy transfer photosensitization.



Scheme A-4. Crossed intermolecular [2+2] cycloadditions of 1,3-cyclohexadiene.



With these promising initial observations in hand, we elected to study the crossed [2+2] cycloaddition of indene and methyl acrylate in greater detail. In particular, we wanted to determine if these systems exhibit any inherent selectivity for crossed products upon lowering the equivalents of the coupling partner with respect to indene (Table A-2). Although the ratio of cross coupling to homodimerization events decreases slightly with loading of methyl acrylate, the crossed cycloadduct was indeed the major product across all experiments (entries 2-6).

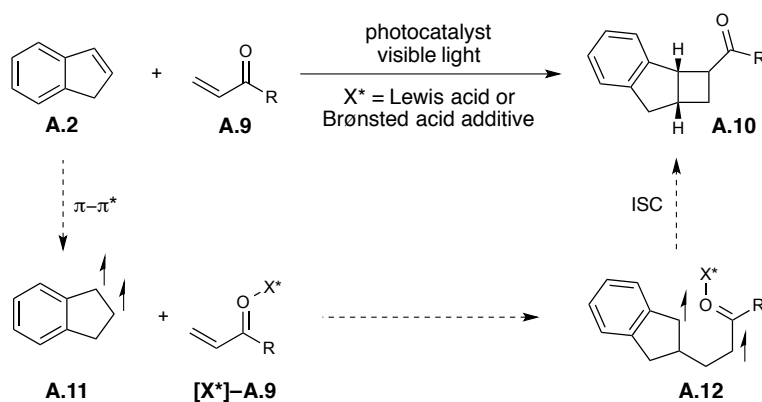
Table A-2. Crossed [2+2] cycloaddition of indene and methyl acrylate: effect of relative substrate equivalents on selectivity.

Entry	Solvent	Equivalents methyl acrylate (A.15)	% Remaining indene (A.2) ^a	% Yield A.6 (A/B/C/D) ^a	% Yield A.3 ^{a,b}	% Yield A.6-A/B (d.r.) ^c
1	DMSO- <i>d</i> ₆	10	52	45	1	29 (3.0:1)
2	MeCN	10	<1	94	2	73 (2.6:1)
3	MeCN	5	10	82	4	63 (2.6:1)
4	MeCN	2	13	77	6	59 (2.6:1)
5	MeCN	1	2	74	14	60 (2.6:1)
6	MeCN	0.5	8	47	34	39 (2.4:1)

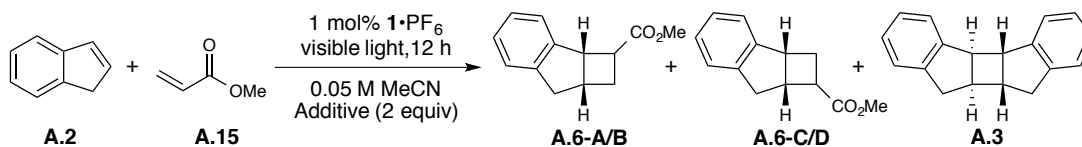
^a Yield determined by GC analysis with respect to biphenyl as the calibrated internal standard.^b Represents combined yield of all isomers.^c Yield and diastereomeric ratio determined by ¹H NMR spectroscopic analysis of the crude reaction mixture with respect to trimethyl(phenyl)silane as the internal standard.

A.3 Outlook and Future Directions

The goal of future work in this area will be to determine if Lewis or Brønsted acid additives can be used to impart control over the distribution of cycloadducts. The proposed mechanism of cycloadditions of this type involves photosensitization of the alkene to its first triplet excited state (A.11), addition to the coupling partner to generate a 1,4-diradical species (A.12), and subsequent ring closure to the final product. We aim to take advantage of the ability of enones to coordinate with Lewis or Brønsted acids to control the selectivity of these bond-forming steps. The observation that the electronic nature of the olefin coupling partner affects the distribution of homodimerization and heterodimerization products suggests that Lewis or Brønsted acid activation might further accelerate the crossed reaction. Achiral additives will be screened initially to probe for any positive effects on the reaction rate, chemoselectivity, and diastereoselectivity. Ultimately, we hope to identify a chiral catalyst system to achieve enantioselective [2+2] cycloadditions.

Scheme A-5. Crossed [2+2] cycloadditions of indene by energy transfer photosensitization: project goals.

Preliminary studies employing Lewis and Brønsted acid additives were unsuccessful and generally resulted in poor mass balance, reduced reactivity, and no change in the diastereoselectivity (Table A-3). Nonetheless, a wide variety of different reaction partners, conditions and additives remain to be explored to rigorously study this system.

Table A-3. Crossed [2+2] cycloaddition of indene and methyl acrylate: effect of Lewis and Brønsted acids.

Entry	Additive	% Remaining indene (A.2) ^a	% Yield A.6 (A/B/C/D) ^{a,c}	% Yield A.3 ^{a,b}
1	None	20	63	5
2	LiPF ₆	16	62	5
3	LiBF ₄	34	28	6
4	Mg(ClO ₄) ₂	22	36	4
5	Sc(OTf) ₃	20	16	2
6	Zn(OTf) ₂	30	50	6
7	La(OTf) ₃	50	22	9
8	Eu(OTf) ₃	61	7	2
9	Gd(OTf) ₃	43	22	4
10	PPTS	87	20	4
11	Acetic acid	32	26	3
12	Formic acid	41	16	3
13	Oxalic acid	30	46	6
14	TFA	41	19	3
15	CSA	25	35	5
16	p-TSA	25	29	5

^a Yield determined by GC analysis with respect to biphenyl as the calibrated internal standard.

^b Represents combined yield of all isomers.

^c Diastereomeric ratio of **A.6-A/B** determined by ¹H NMR spectroscopic analysis of the crude reaction mixtures; ~2.5:1 d.r. for all experiments.

A.4 Experimental

A.4.1 General experimental information

[Ir(dF(CF₃)ppy)₂(dtbbpy)](PF₆) was prepared as previously described by Malliaras and Bernard.⁷

Acetonitrile was purified by elution through alumina as described by Grubbs.⁸ Methyl acrylate, 1,3-cyclohexadiene, 1-octene, acrylonitrile and methyl vinyl ketone were purified by distillation immediately prior to use. Indene was passed across a short silica plug (neat) and distilled under full vacuum prior to use. A 23 W (1380 lumen) compact fluorescent bulb was used for all photochemical reactions. Flash column chromatography was performed with Sigma-Aldrich

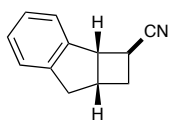
silica gel (pore size 60 Å, 230–400 mesh particle size) using the method of Still.⁹ Diastereomeric ratios for all compounds were determined by ¹H NMR spectroscopic analysis of the crude reaction mixture. ¹H and ¹³C NMR data for all previously uncharacterized compounds were obtained using a Bruker Avance III 500 MHz spectrometer and are referenced to TMS (0.0 ppm) and CDCl₃ (77.16 ppm), respectively. The NMR facilities at UW-Madison are funded by the NSF (CHE-1048642) and a generous gift from Paul J. Bender. IR spectral data were obtained using a Bruker Platinum-ATR spectrometer (neat). Melting points were obtained using a Stanford Research Systems DigiMelt apparatus. Mass spectrometry was performed with a Waters (Micromass) AutoSpec. These facilities are funded by the NSF (CHE-9974839, CHE-9304546) and the University of Wisconsin.

A.4.2 [2+2] Photocycloadditions

General Procedure A: A solution of 1 equivalent of substrate, 10 equivalents of the coupling partner, trimethyl(phenyl)silane as the internal standard, and 1 mol% [Ir(dF(CF₃)ppy)₂(dtbbpy)](PF₆) in DMSO-*d*₆ (0.05 M) was placed in an oven-dried 25 mL Schlenk tube and degassed by 3 freeze-pump-thaw cycles in the dark. The reaction mixture was then stirred at room temperature and irradiated with a 23 W (1380 lumen) compact fluorescent light bulb at a distance of 10 centimeters. After the noted reaction time, the yield of [2+2] cycloadduct was determined by ¹H NMR spectroscopic analysis with respect to trimethyl(phenyl)silane. The reaction mixture was then diluted with Et₂O and water, the layers separated, and the aqueous layer further extracted with Et₂O (2x). The combined organic layers were dried with MgSO₄, filtered, and concentrated *in vacuo*. The resulting residue was purified by flash column chromatography on silica gel.

General Procedure B: A solution of 1 equivalent of substrate, given equivalents of the coupling partner, and 1 mol% $[\text{Ir}(\text{dF}(\text{CF}_3)\text{ppy})_2(\text{dtbbpy})](\text{PF}_6)$ in MeCN (0.05 M) was placed in an oven-dried 25 mL Schlenk tube and degassed by 3 freeze-pump-thaw cycles in the dark. The reaction mixture was then stirred at room temperature and irradiated with a 23 W (1380 lumen) compact fluorescent light bulb at a distance of 10 centimeters. After the noted reaction time, biphenyl was added as an internal standard and the reaction progress determined by gas chromatography. The reaction mixture was then passed across a short plug of silica gel in diethyl ether and concentrated *in vacuo*. Trimethyl(phenyl)silane was added to the crude residue and the yield of determined by ^1H NMR spectroscopic analysis.

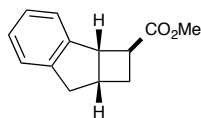
(2*R*,2*aS*,7*aR*)-2,2*a*,7,7*a*-tetrahydro-1*H*-cyclobuta[*a*]indene-2-carbonitrile (A.4): Prepared



according to general procedure A with indene (0.090 mmol, 10 mg), acrylonitrile (0.90 mmol, 55 μL), trimethyl(phenyl)silane (0.070 mmol, 10 mg), $[\text{Ir}(\text{dF}(\text{CF}_3)\text{ppy})_2(\text{dtbbpy})](\text{PF}_6)$ (0.0009 mmol, 1 mg) and $\text{DMSO-}d_6$ (1.7 mL). Reaction components were added from a 5 fold diluted stock solution in $\text{DMSO-}d_6$. Yield by ^1H NMR spectroscopic analysis at 24 hours: 91% yield (1.2:1 d.r.). Purified by preparative thin layer chromatography on silica gel. **(2*S**,2*aS**,7*aR**) Diastereomer (A.4-A, major):** ^1H NMR (500 MHz, CDCl_3) δ 7.37 – 7.13 (m, 4H), 4.10 – 4.06 (m, 1H), 3.51 – 3.42 (m, 1H), 3.21 (dd, J = 16.7, 8.1 Hz, 1H), 2.93 (dddd, J = 9.5, 4.2, 3.0, 1.3 Hz, 1H), 2.85 (d, J = 16.7 Hz, 1H), 2.66 – 2.57 (m, 1H), 2.19 (ddd, J = 12.7, 9.3, 7.5 Hz, 1H). ^{13}C NMR (126 MHz, CDCl_3) δ 143.7, 143.2, 128.2, 127.5, 125.9, 125.1, 123.1, 49.9, 39.6, 35.5, 30.8, 28.9. HRMS (ASAP) calculated for $[2(\text{C}_{12}\text{H}_{11}\text{N}) + \text{H}]^+$ requires m/z 339.1856, found 339.1858. **(2*R**,2*aS**,7*aR**) Diastereomer (A.4-B, minor):** ^1H NMR (500 MHz, CDCl_3) δ 7.50 – 7.20 (m, 4H), 4.03 – 3.97 (m, 1H), 3.55

(td, $J = 9.5, 8.0$ Hz, 1H), 3.23 – 3.10 (m, 3H), 2.81 (d, $J = 15.8$ Hz, 1H), 2.67 – 2.59 (m, 1H), 2.09 – 2.00 (m, 1H). ^{13}C NMR (126 MHz, CDCl_3) δ 143.8, 140.6, 128.4, 127.3, 126.8, 125.8, 120.0, 47.7, 39.5, 35.4, 31.1, 26.4.

Methyl 2,2a,7,7a-tetrahydro-1H-cyclobuta[a]indene-2-carboxylate (A.6): A solution of



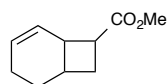
indene (0.86 mmol, 100 mg), methyl acrylate (8.6 mmol, 775 μL), $[\text{Ir}(\text{dF}(\text{CF}_3)\text{ppy})_2(\text{dtbbpy})](\text{PF}_6)$ (8.6 μmol , 10 mg) and DMSO (17 mL) was

transferred to two oven-dried 25 mL Schlenk tubes (~ 8.5 mL each) and degassed by 3 freeze-pump-thaw cycles in the dark. The reaction mixtures were stirred at room temperature and irradiated with a 23 W (1380 lumen) compact fluorescent light bulb at a distance of 10 centimeters for 36 hours at which point they were combined and diluted with Et_2O and water. The aqueous layer was separated and further extracted with Et_2O (2x). The combined organic layers were dried with MgSO_4 , filtered, and concentrated *in vacuo*. Trimethyl(phenyl)silane (0.23 mmol, 35.3 mg) was added as an internal standard and the yield of was determined by ^1H NMR spectroscopic analysis: 60% yield (2.5:1 d.r.). The residue was purified by flash column chromatography on silica gel (10:1 hexanes: EtOAc) to afford the product as a mixture of diastereomers and constitutional isomers (including Methyl 2,2a,7,7a-tetrahydro-1H-cyclobuta[a]indene-3-carboxylate, **A.6-C/D**) (135 mg, 78% yield). (**2S*,2aS*,7aR***)

Diastereomer (A.6-A, major): ^1H NMR (500 MHz, CDCl_3) δ 7.32 – 7.19 (m, 4H), 3.98 – 3.94 (m, 1H), 3.77 (s, 3H), 3.32 – 3.23 (m, 1H), 3.19 (dd, $J = 16.5, 8.3$ Hz, 1H), 2.95 (dddd, $J = 9.4, 4.2, 3.1, 1.0$ Hz, 1H), 2.84 (d, $J = 16.4$ Hz, 1H), 2.58 – 2.51 (m, 1H), 2.01 (dddd, $J = 12.6, 9.4, 6.6, 1.1$ Hz, 1H). ^{13}C NMR (126 MHz, CDCl_3) δ 176.3, 145.5, 144.2, 127.3, 127.1, 125.6, 125.0, 52.0, 49.1, 45.4, 40.0, 35.1, 29.6. HRMS (ESI) calculated for $[\text{C}_{13}\text{H}_{14}\text{O}_2 + \text{H}]^+$ requires m/z 203.1067, found 203.1072. (**2R*,2aS*,7aR***) **Diastereomer (A.6-B, minor):** ^1H NMR (500

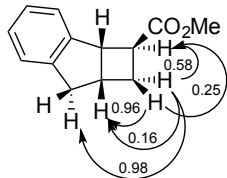
MHz, CDCl₃) δ 7.23 – 7.11 (m, 4H), 4.12 (t, J = 7.7 Hz, 1H), 3.56 (s, 3H), 3.18 – 2.96 (m, 3H), 2.81 (d, J = 15.7 Hz, 1H), 2.38 – 2.27 (m, 1H), 2.17 – 2.08 (m, 1H). ¹³C NMR (126 MHz, CDCl₃) δ 173.0, 144.7, 142.1, 127.6, 126.6, 125.9, 125.7, 51.3, 49.0, 41.7, 39.7, 33.4, 28.0.

Methyl bicyclo[4.2.0]oct-4-ene-7-carboxylate (A.16): Prepared according to the general



procedure with 1,3-cyclohexadiene (0.1 mmol, 8 mg), methyl acrylate (1.0 mmol, 90 μ L), trimethyl(phenyl)silane (0.04 mmol, 6 mg), [Ir(dF(CF₃)ppy)₂(dtbbpy)](PF₆) (0.001 mmol, 1 mg) and DMSO-*d*₆ (2 mL). Reaction components were added from a 10 fold diluted stock solution in DMSO-*d*₆. Yield by ¹H NMR spectroscopic analysis at 24 hours: 75% yield (1.7:1 d.r.). Purified by flash column chromatography on silica gel (10:1 pentanes:Et₂O). The relative stereochemistry of the diastereomeric products could not be assigned unambiguously. **Diastereomer (A.16-A, major):** ¹H NMR (500 MHz, CDCl₃) δ 5.91 – 5.86 (m, 1H), 5.76 (ddt, J = 10.1, 4.0, 1.9 Hz, 1H), 3.69 (s, 3H), 3.00 – 2.89 (m, 1H), 2.87 – 2.81 (m, 1H), 2.59 (dtd, J = 11.2, 8.1, 4.0 Hz, 1H), 2.32 – 2.24 (m, 1H), 2.21 – 1.86 (m, 3H), 1.74 – 1.67 (m, 1H), 1.53 (dtd, J = 13.2, 7.9, 5.2 Hz, 1H). ¹³C NMR (126 MHz, CDCl₃) δ 175.9, 129.0, 128.6, 51.7, 44.2, 36.7, 29.9, 26.7, 25.3, 22.0. **Diastereomer (A.16-B, minor):** ¹H NMR (500 MHz, CDCl₃) δ 5.98 – 5.91 (m, 1H), 5.64 (dt, J = 10.4, 3.6 Hz, 1H), 3.64 (s, 3H), 3.39 – 3.32 (m, 1H), 3.12 – 3.01 (m, 1H), 2.64 (app ddq, J = 12.1, 8.0, 3.8 Hz, 1H), 2.22 – 2.09 (m, 2H), 2.08 – 1.94 (m, 2H), 1.54 (app ddt, J = 13.8, 5.6, 2.6 Hz, 1H), 1.43 – 1.34 (m, 1H). ¹³C NMR (126 MHz, CDCl₃) δ 173.7, 130.3, 125.7, 51.3, 42.0, 36.3, 29.4, 23.7, 22.4, 21.0.

A.4.3 Representative NOE data

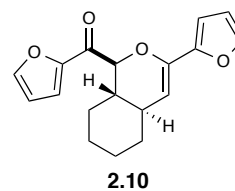
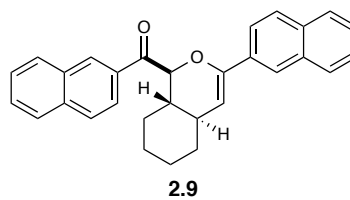
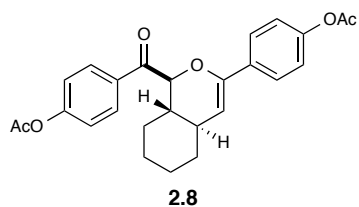
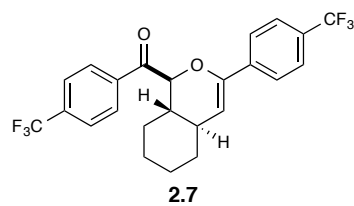
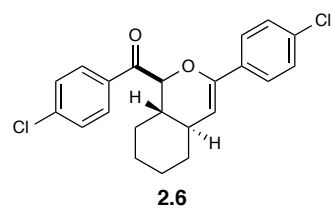
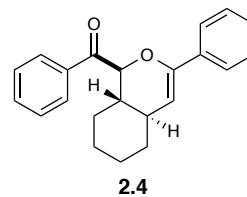
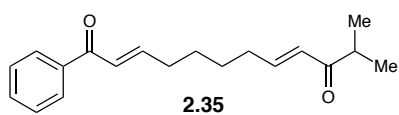
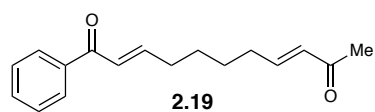
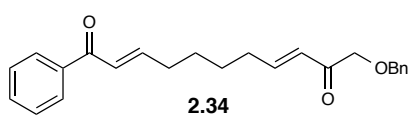
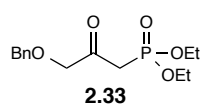
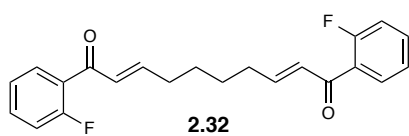
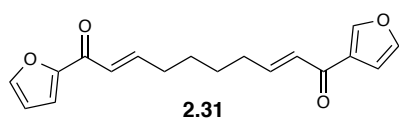
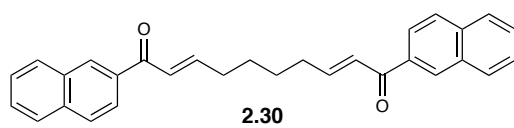
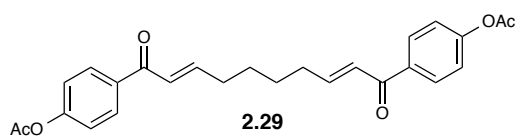
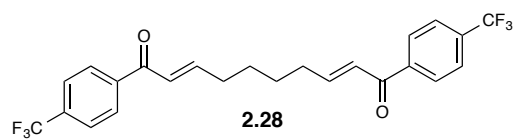
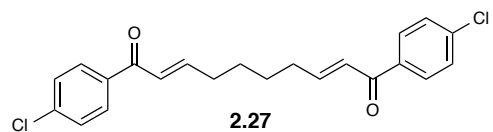


A.5 References

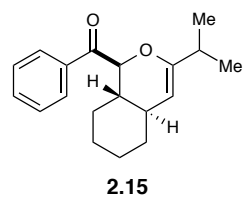
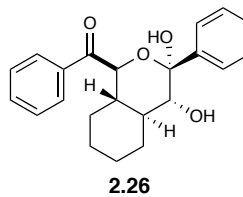
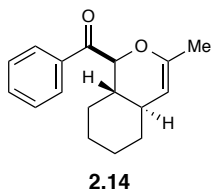
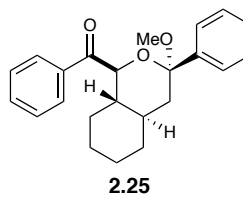
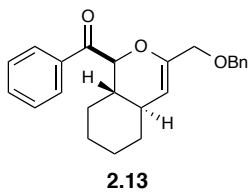
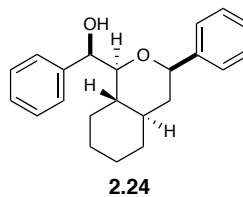
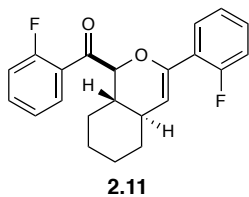
1. (a) Bach, T.; Hehn, J. P. *Angew. Chem. Int. Ed.* **2011**, *50*, 1000–1046. (b) Hoffman, N. *Chem. Rev.* **2008**, *108*, 1052–1103.
2. (a) Hansen, T. V.; Stenstrom, Y. in *Organic Synthesis: Theory and Applications*, Vol. 5 (Ed. T. Hudlicky) Elsevier, Oxford, UK, **2001**, pp. 1–38. (b) Dembitsky, V. M. *J. Nat. Med.* **2008**, *62*, 1–33.
3. (a) Namyslo, J. C.; Kaufmann, D. E. *Chem. Rev.* **2003**, *103*, 1485–1537. (b) Seiser, T.; Saget, T.; Tran, D. N.; Cramer, N. *Angew. Chem. Int. Ed.* **2011**, *50*, 7740–7752.
4. (a) Ischay, M. A.; Anzovino, M. E.; Du, J.; Yoon, T. P. *J. Am. Chem. Soc.* **2008**, *130*, 12886–12887. (b) Du, J.; Yoon, T. P. *J. Am. Chem. Soc.* **2009**, *131*, 14604–14605 (c) Ischay, M. A.; Lu, Z.; Yoon, T. P. *J. Am. Chem. Soc.* **2010**, *132*, 8572–8574. (d) Tyson, E. L.; Farney, E. P.; Yoon, T. P. *Org. Lett.* **2012**, *14*, 1110–1113. (e) Ischay, M. A.; Ament, M. S.; Yoon, T. P. *Chem. Sci.* **2012**, *3*, 2807–2811.
5. Lu, Z.; Yoon, T. P. *Angew. Chem. Int. Ed.* **2012**, *51*, 10329–10332.
6. Hurtley, A. E.; Lu, Z.; Yoon, T. P. *Angew. Chem. Int. Ed.* **2014**, DOI: 10.1002/anie.201405359.
7. Lowry, M. S.; Goldsmith, J. I.; Slinker, J. D.; Rohl, R.; Pascal, Jr., R. A.; Malliaras, G. G.; Bernhard, S. *Chem. Mater.* **2005**, *17*, 5712–5719.
8. Pangborn, A. B.; Giardello, M. A.; Grubbs, R. H.; Rosen, R. K.; Timmers, F. T. *Organometallics* **1996**, *15*, 1518–1520.
9. Still, W. C.; Kahn, M.; Hong, P. C.; Lu, L. *J. Org. Chem.* **1978**, *43*, 2923–2925.

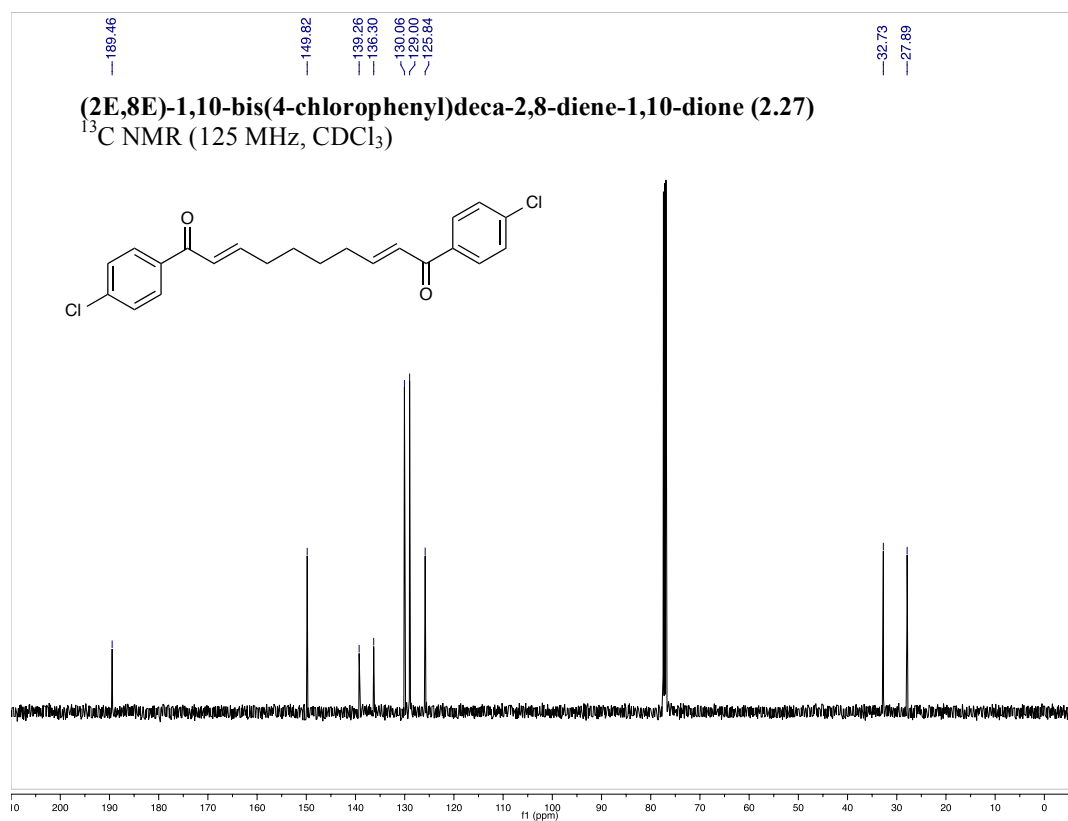
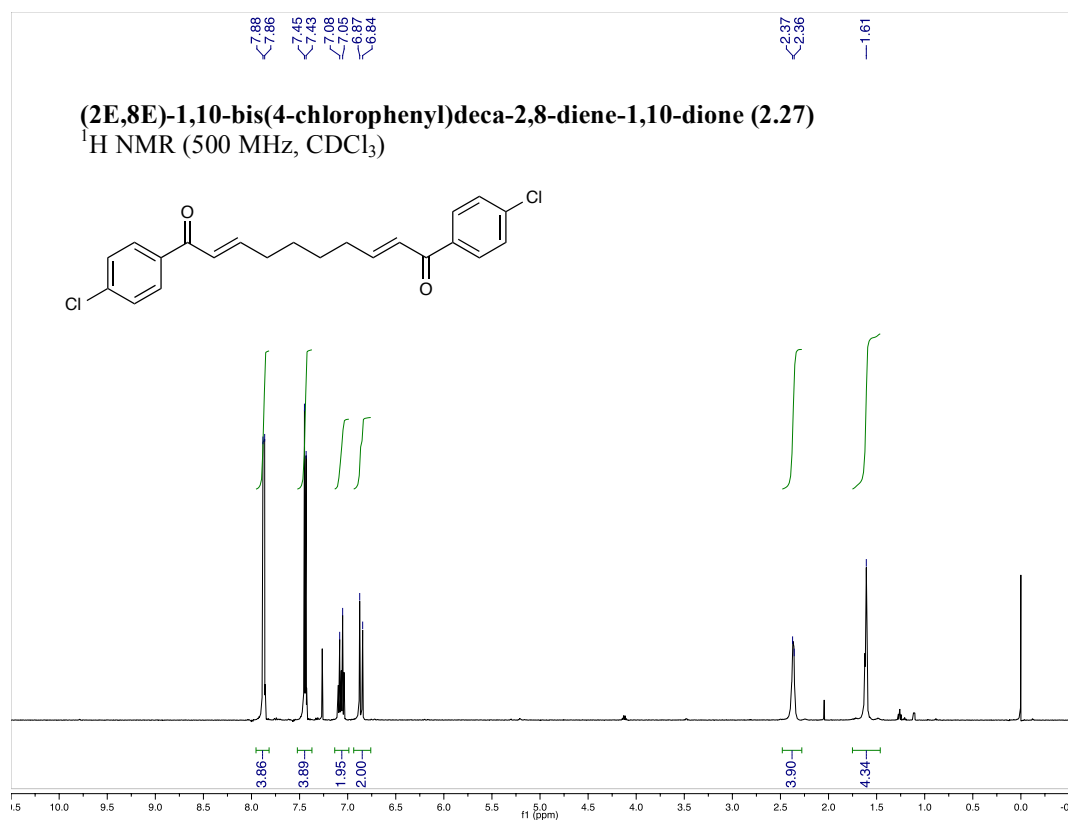
Appendix B. ^1H and ^{13}C NMR spectra for new compounds

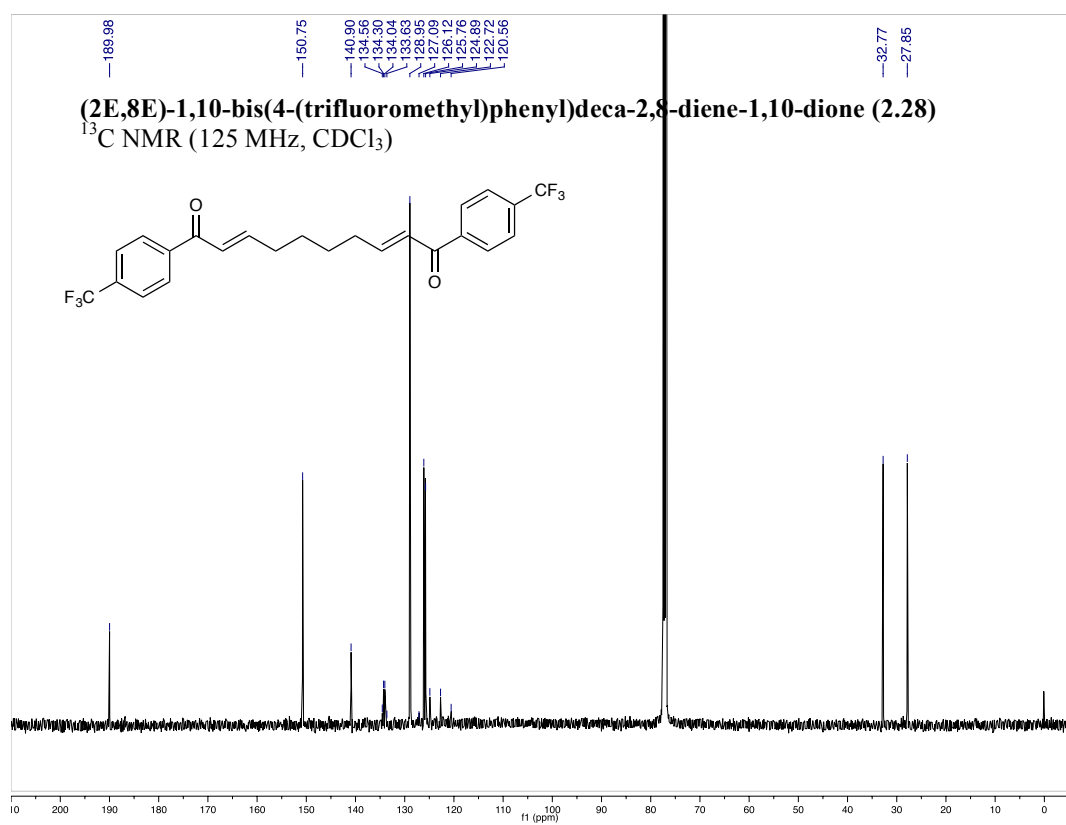
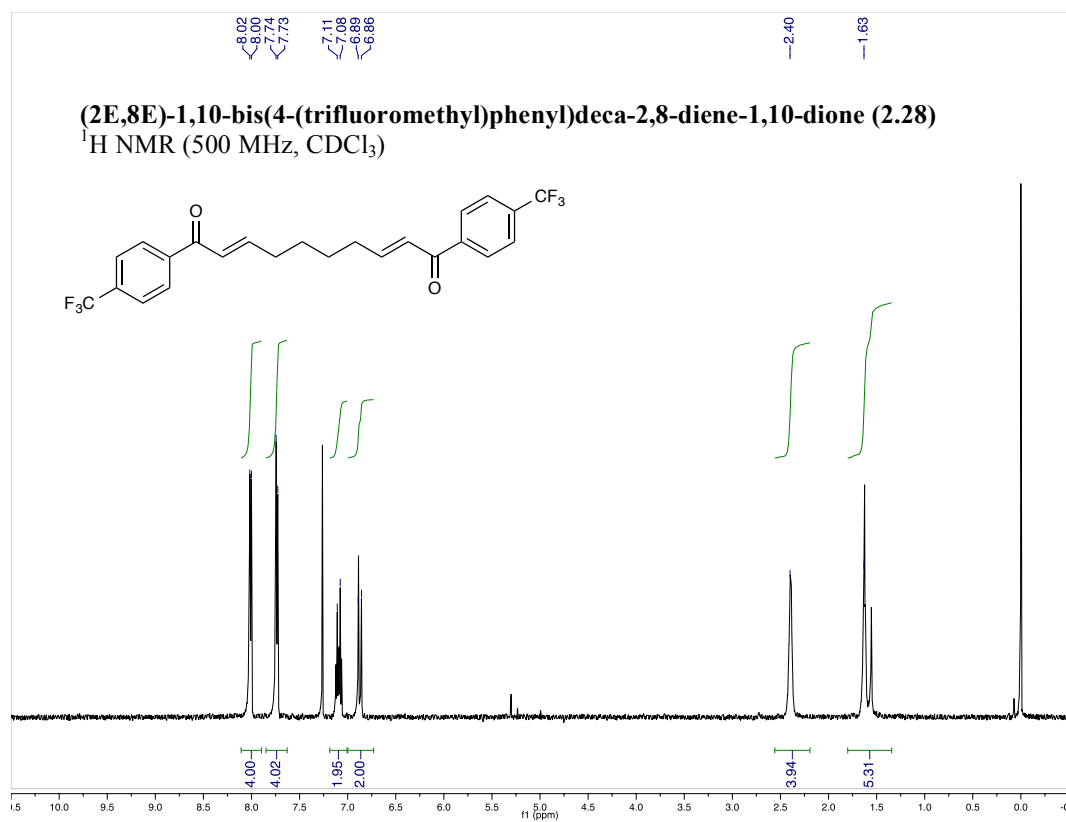
List of Compounds for Chapter 2

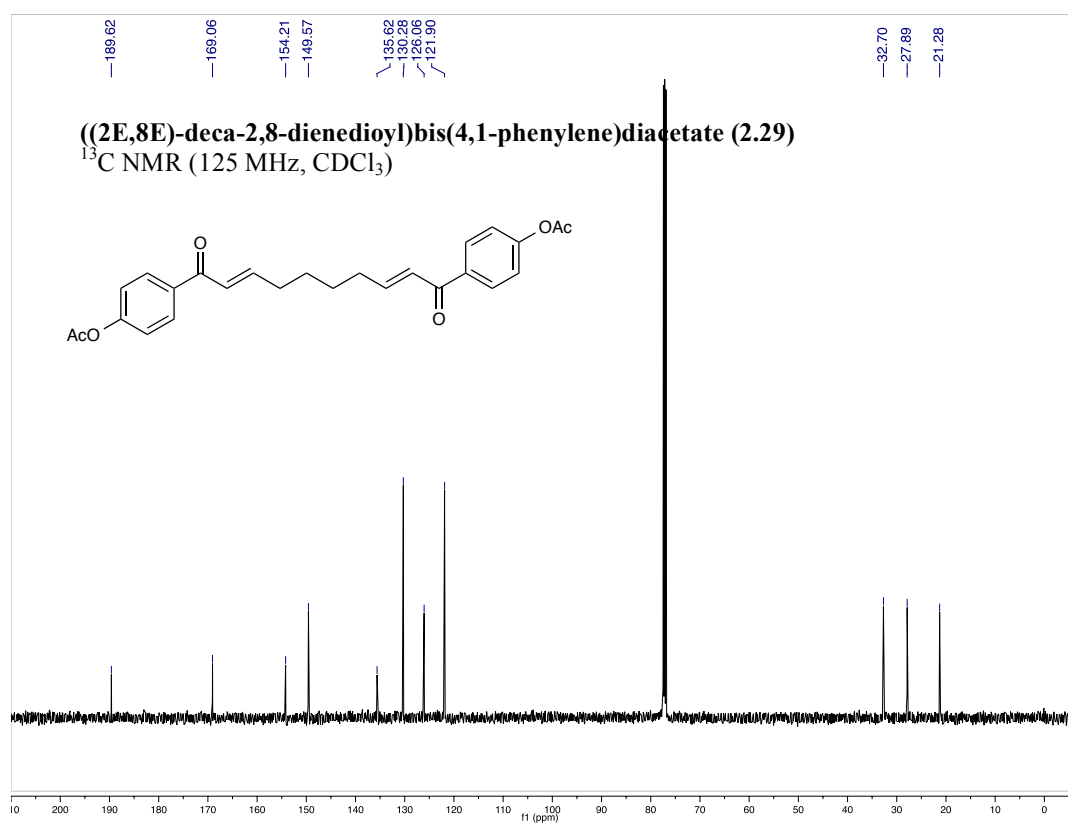
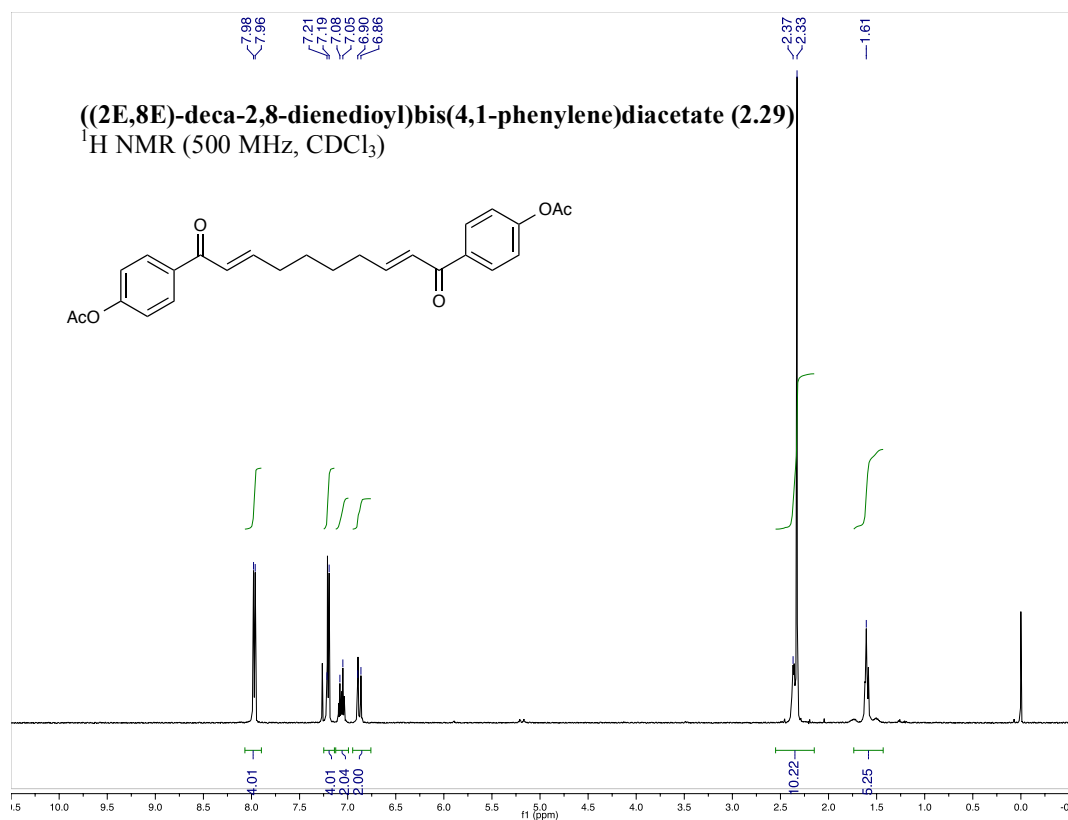


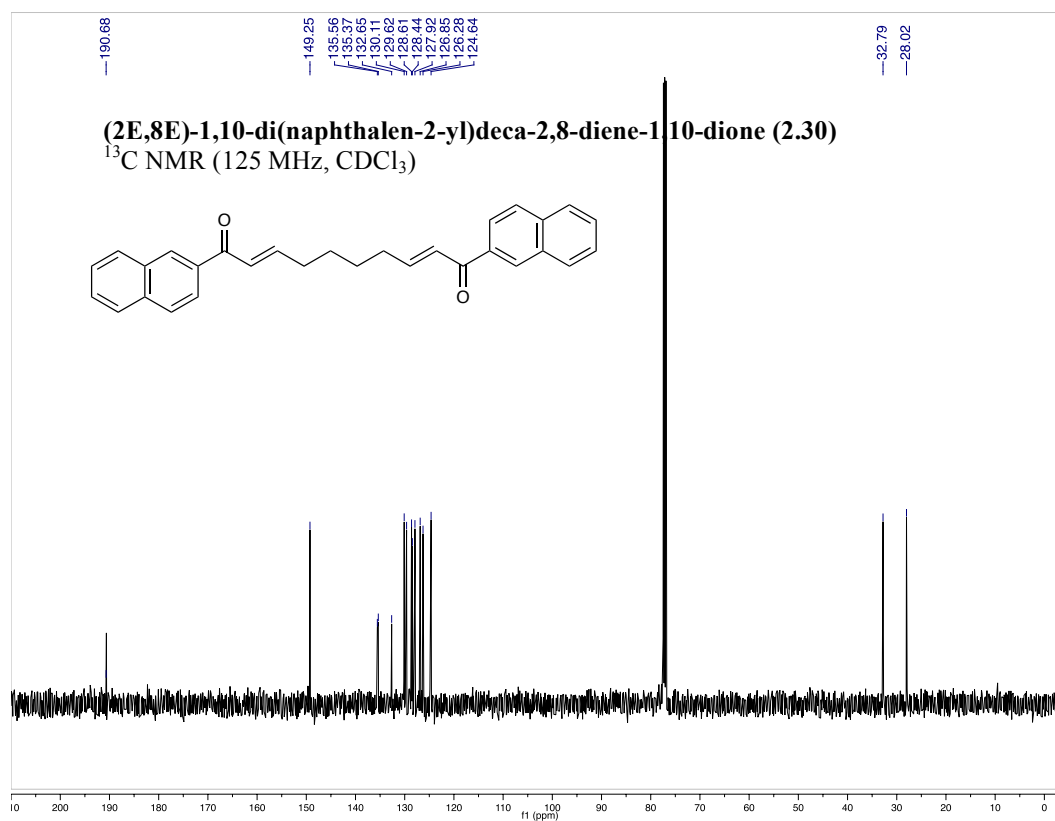
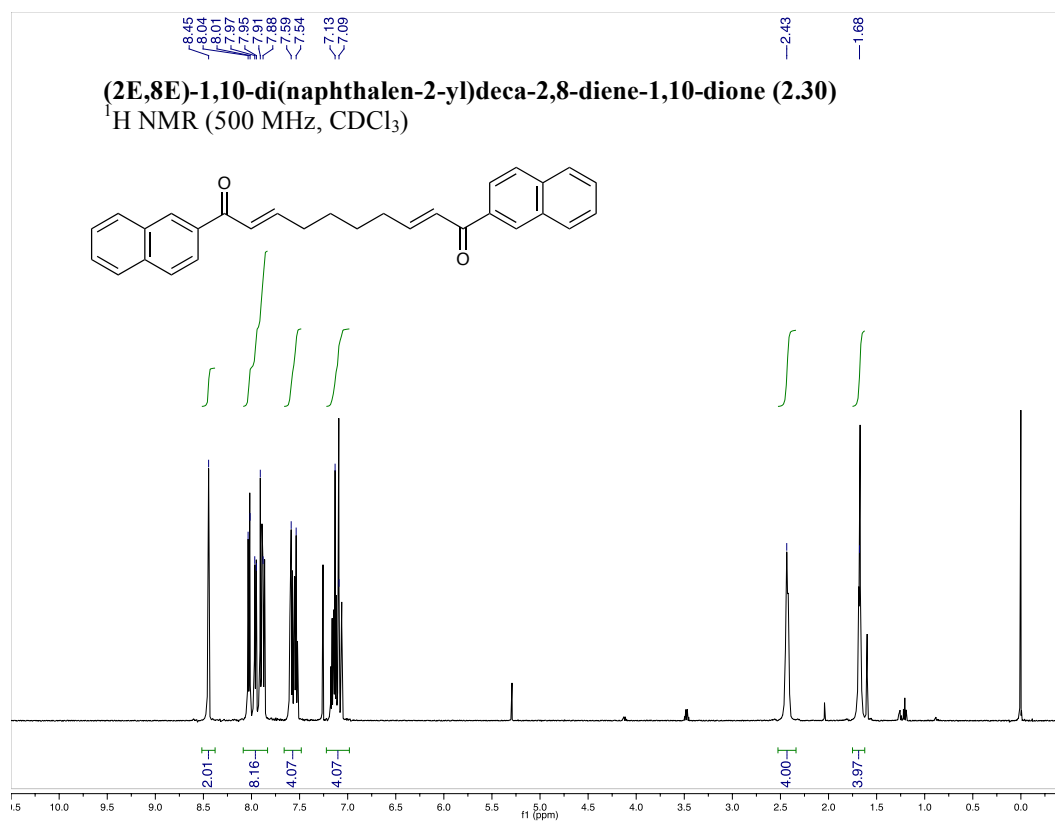
List of Compounds for Chapter 2

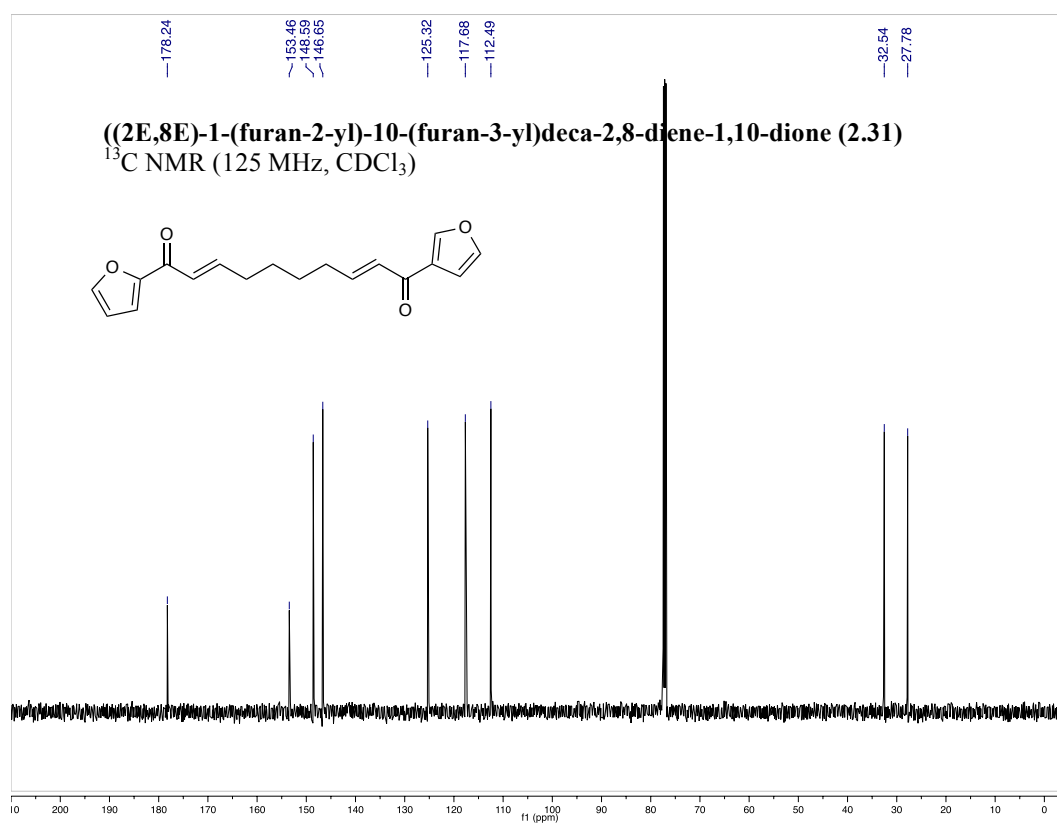
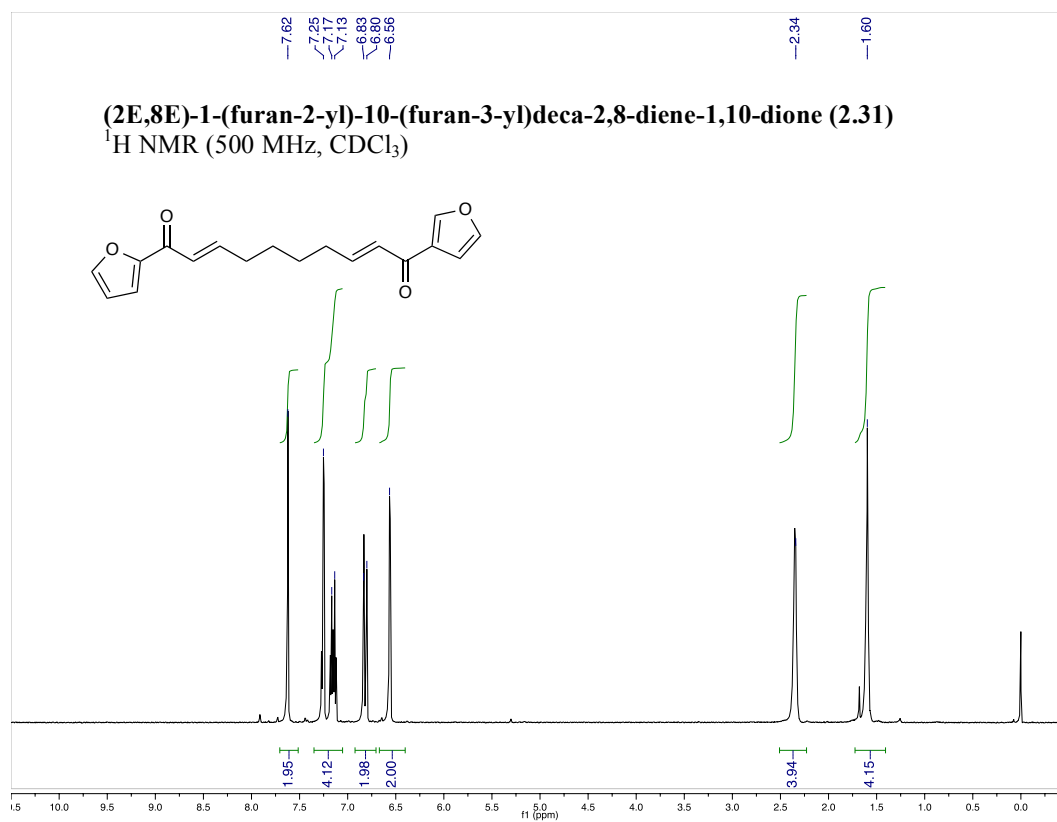


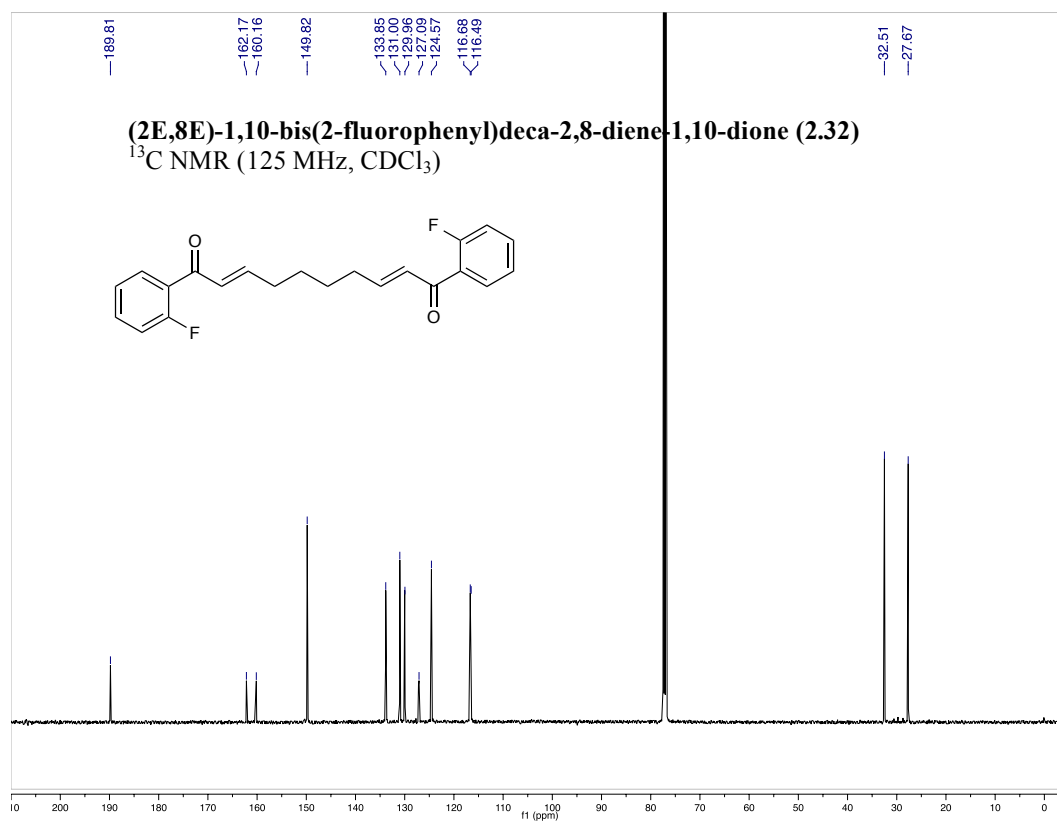
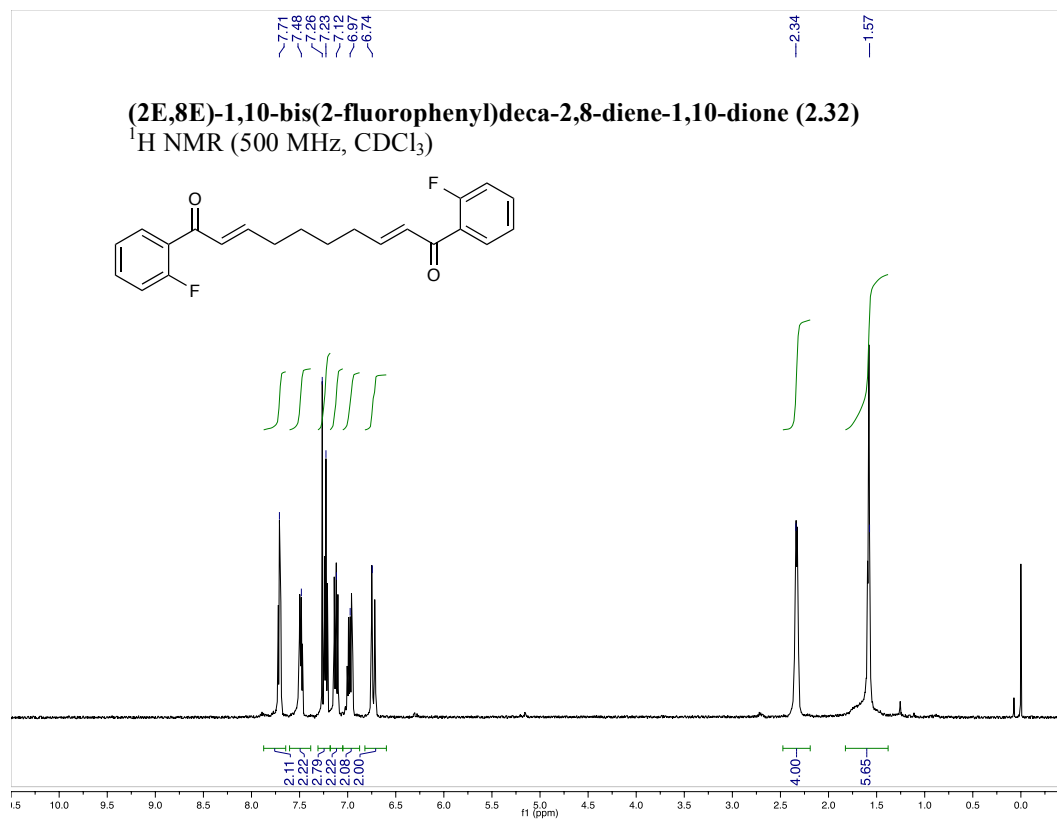


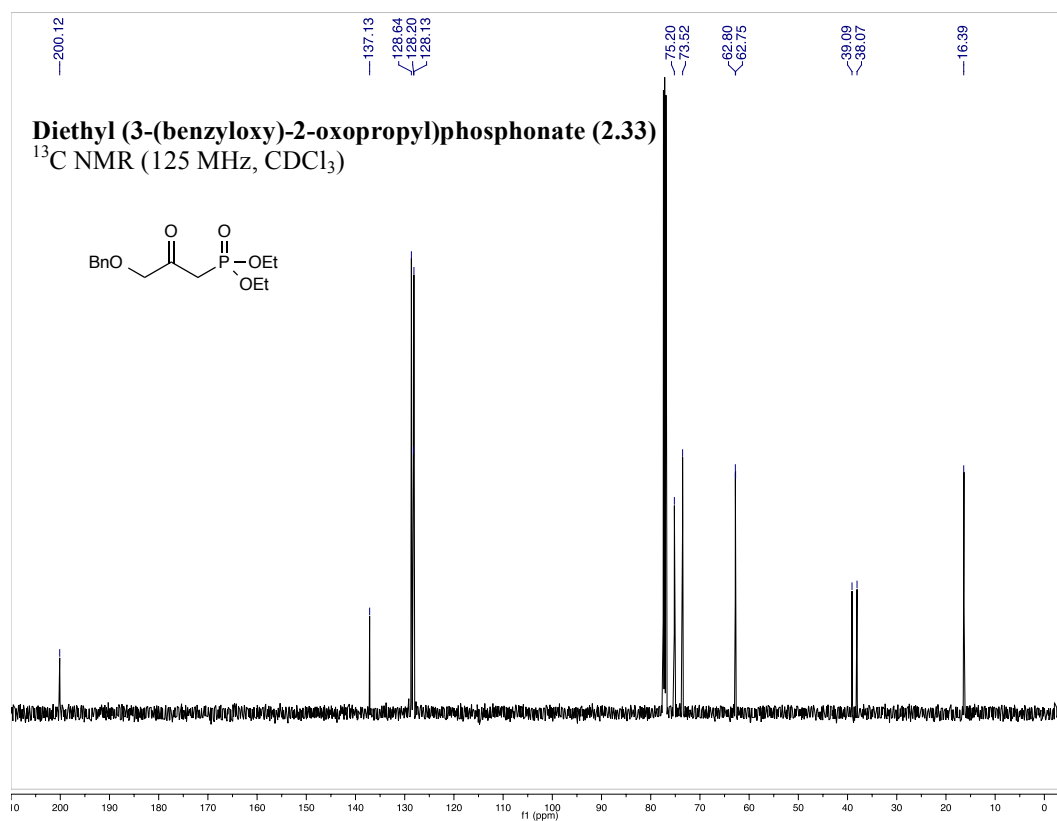
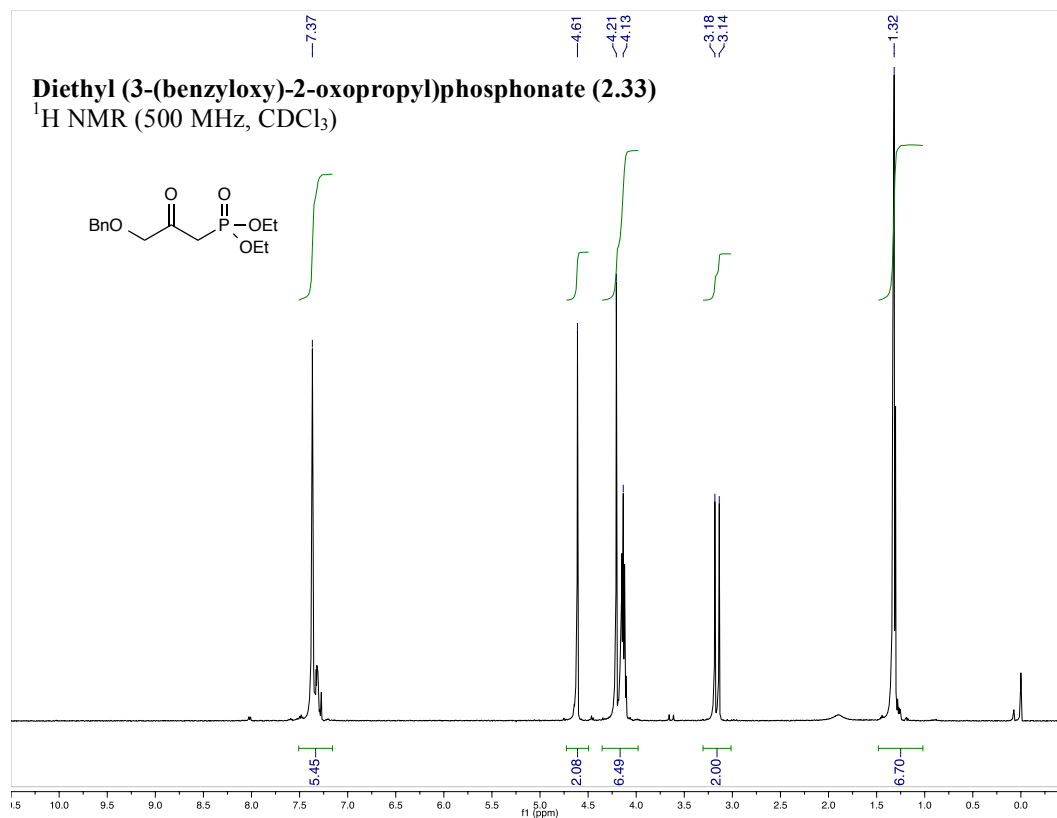


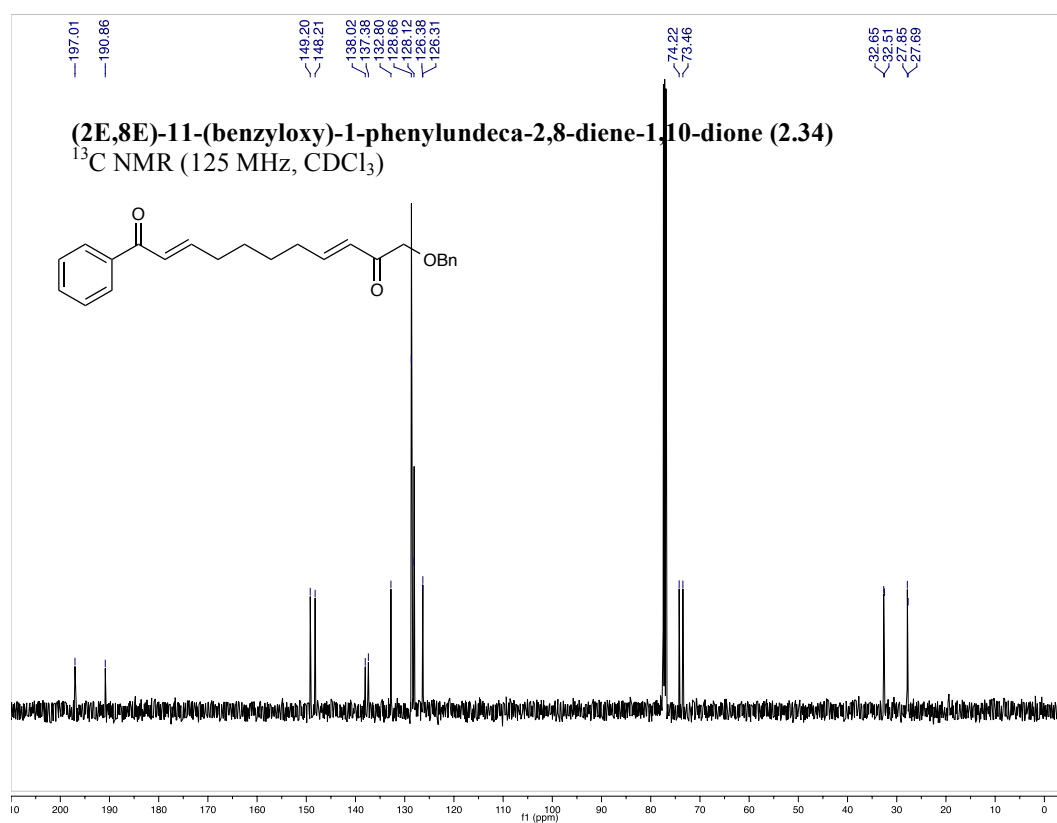
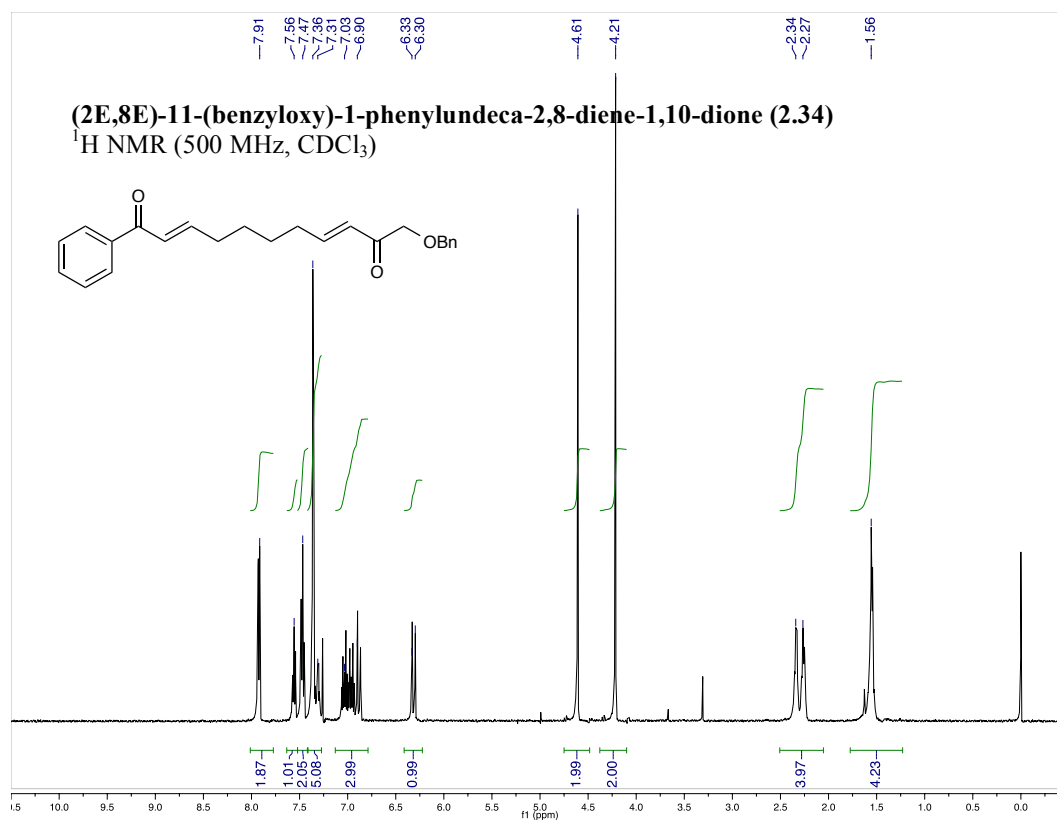


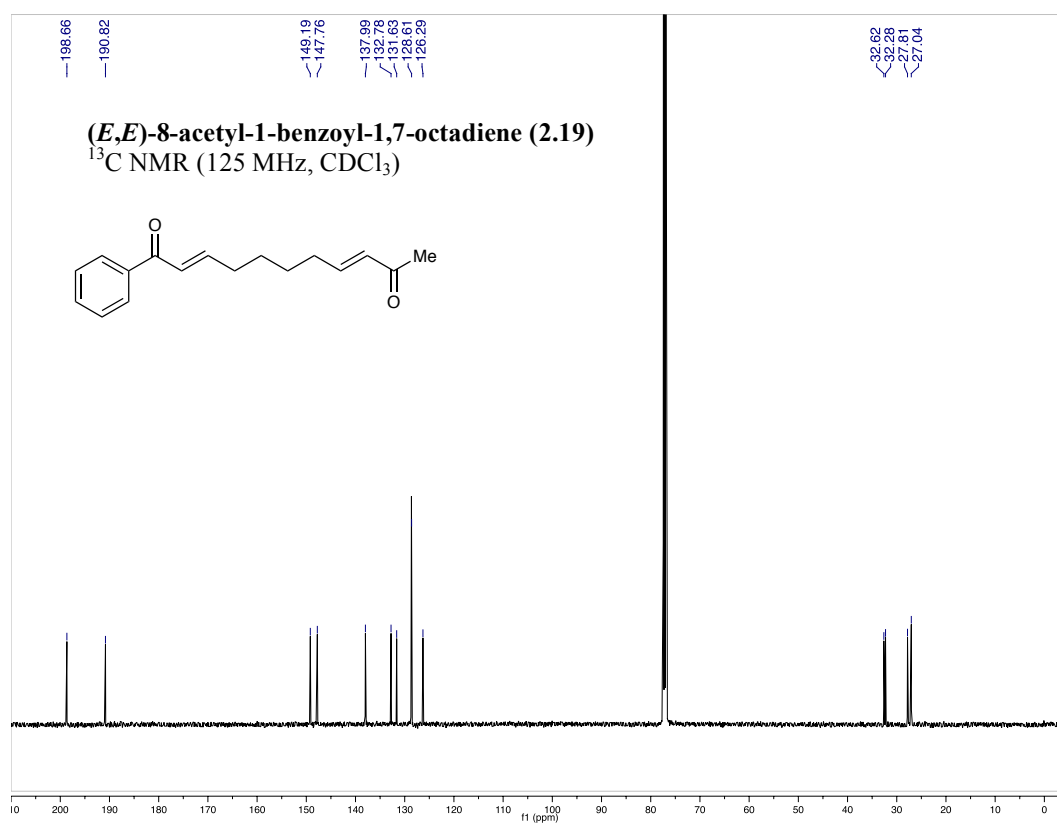
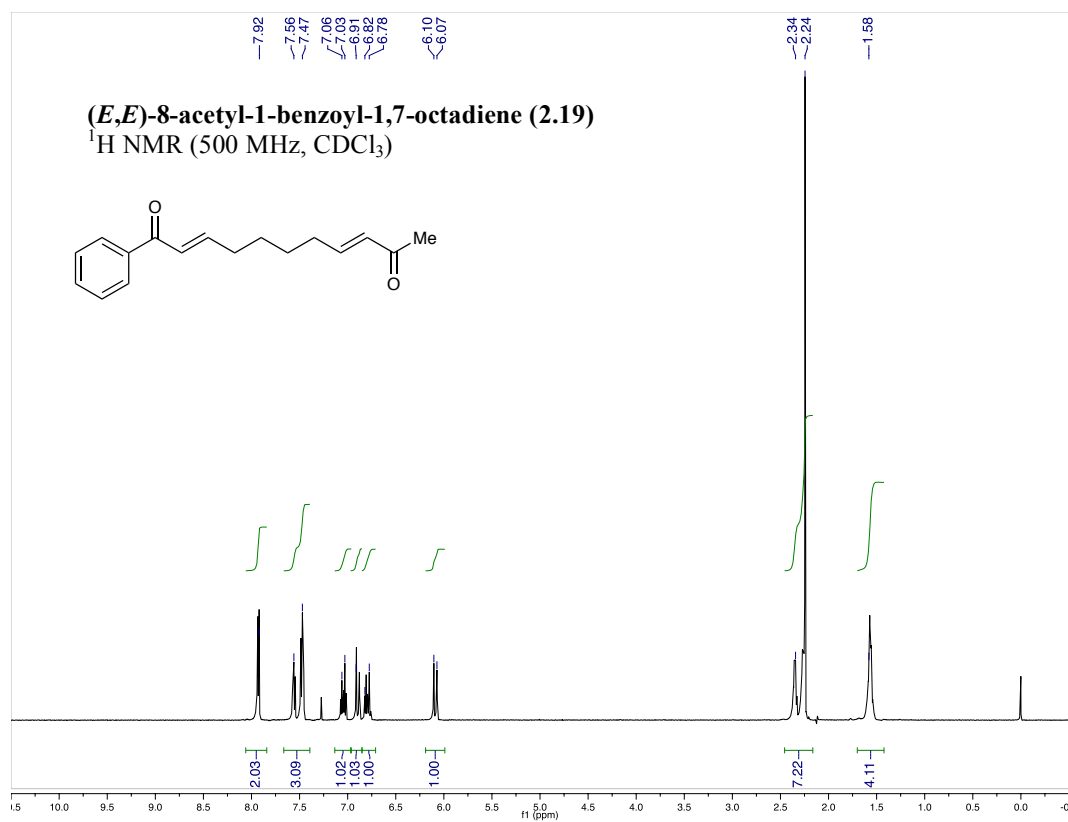


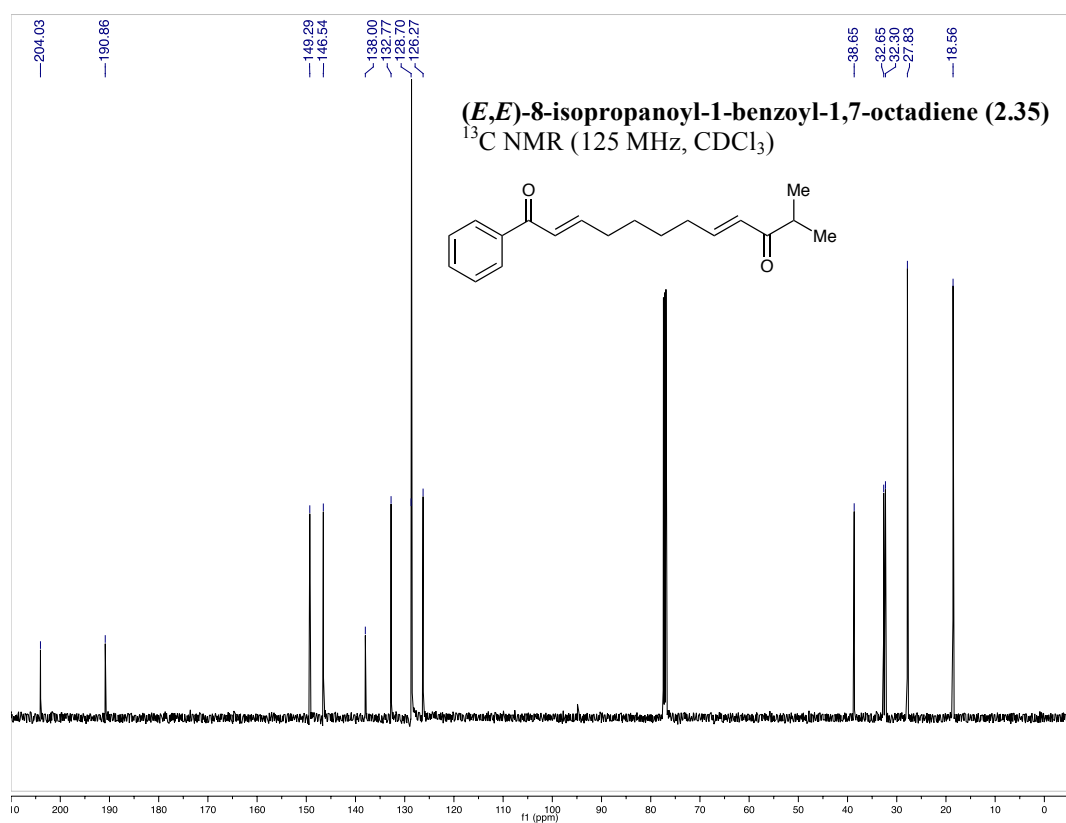
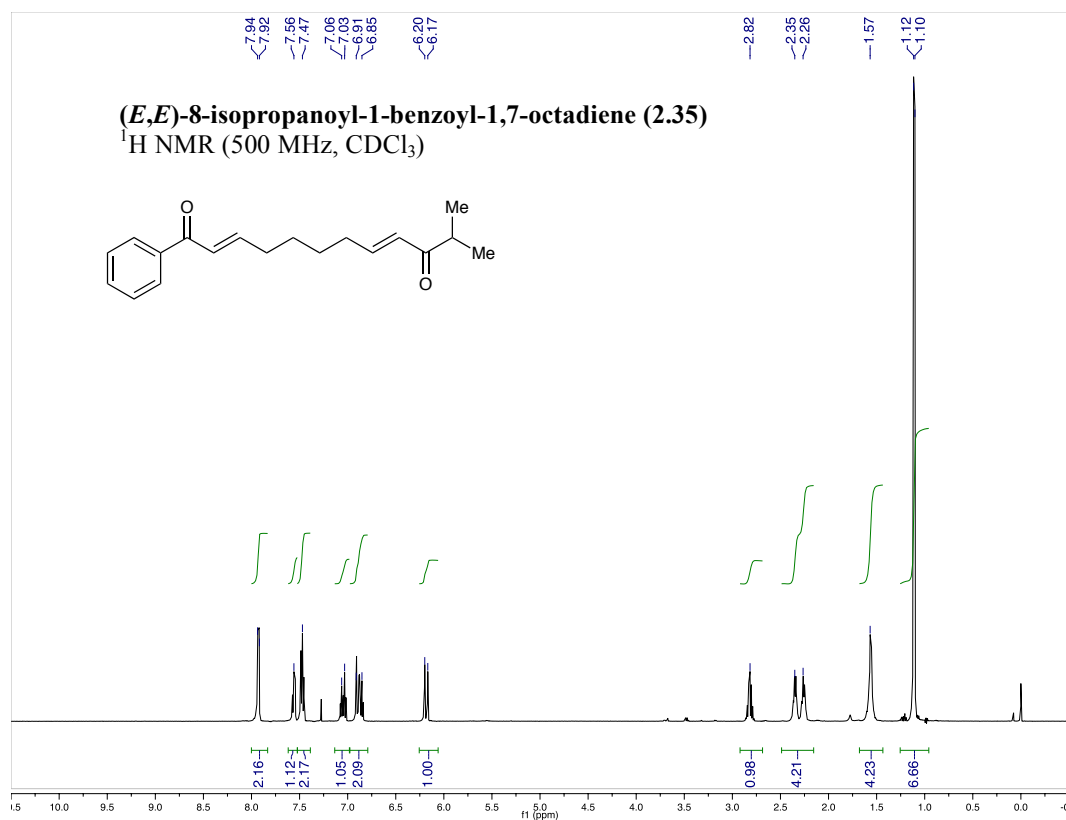


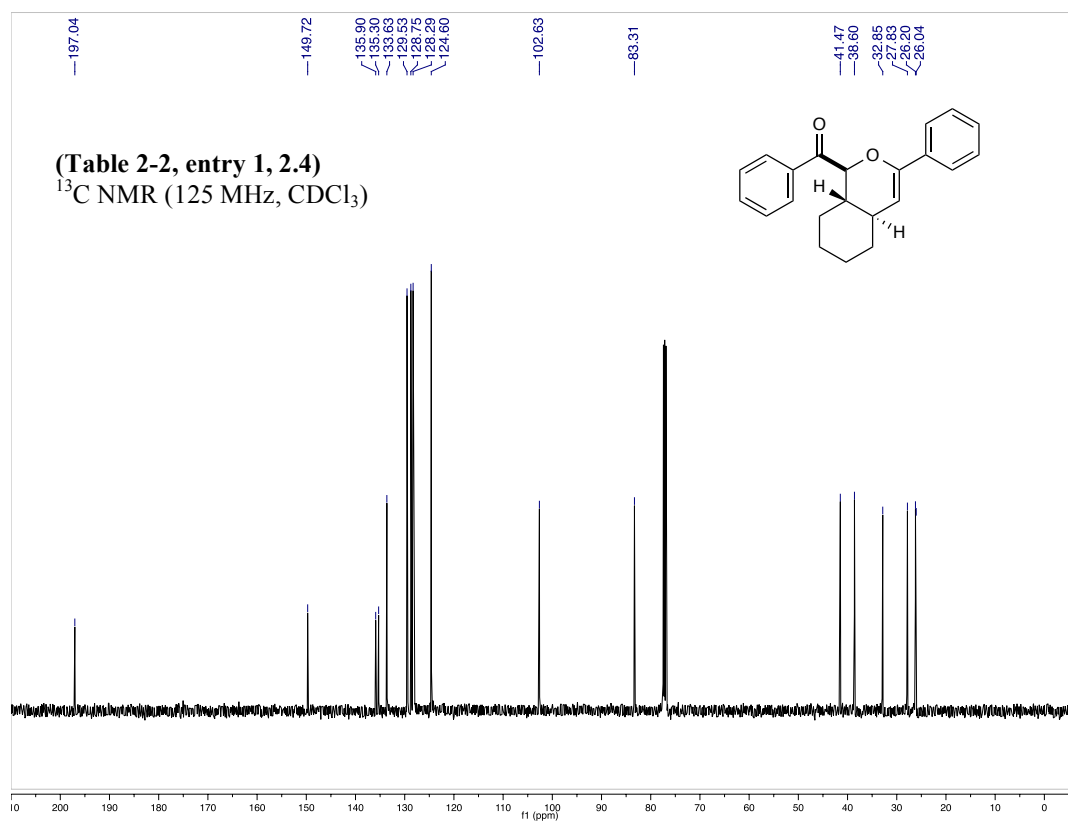
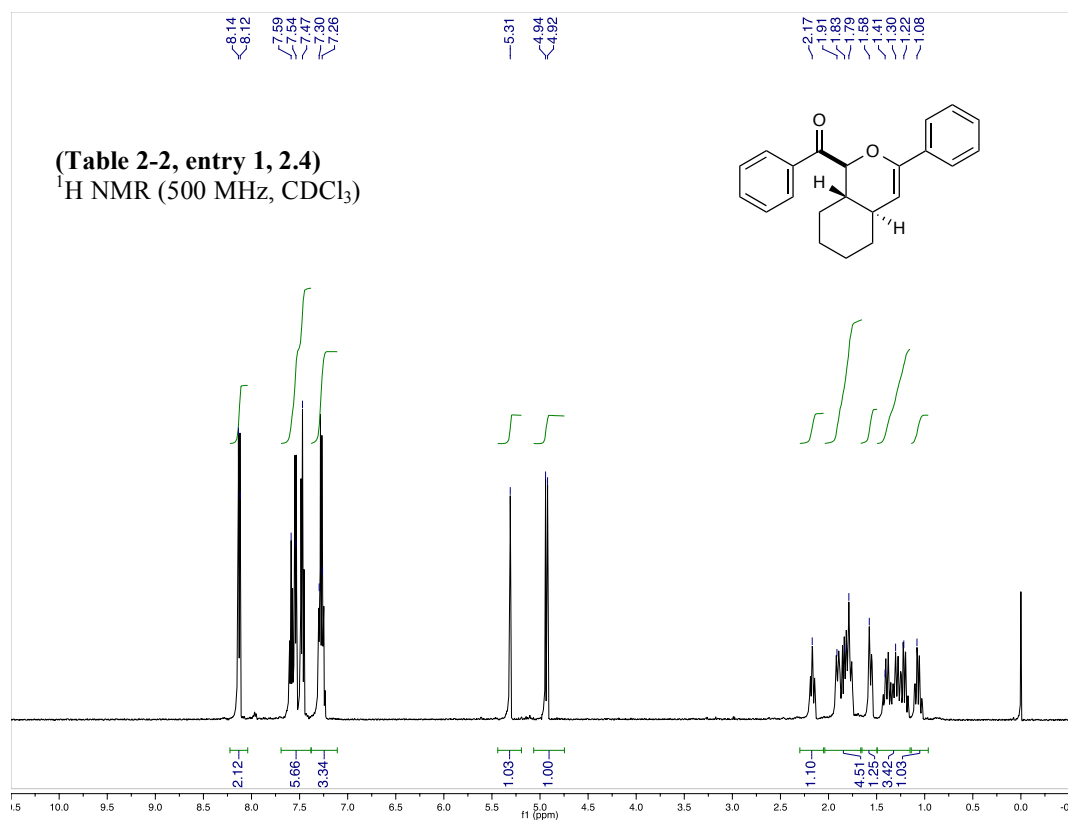


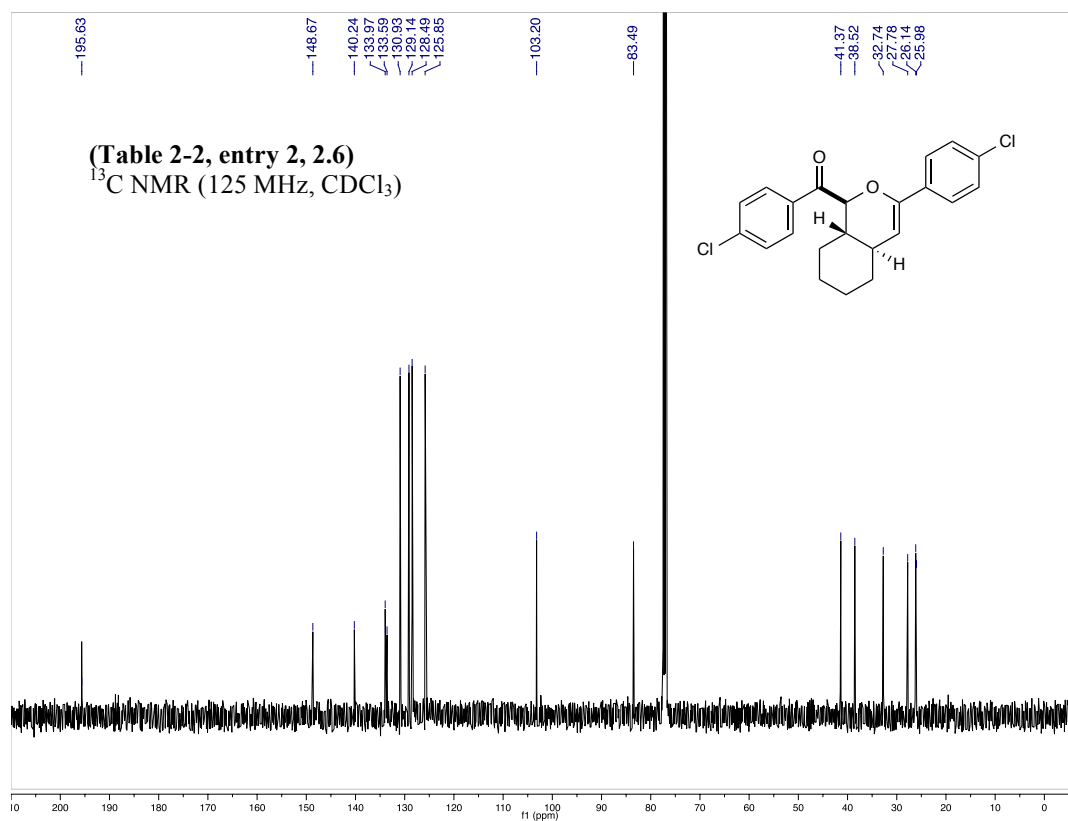
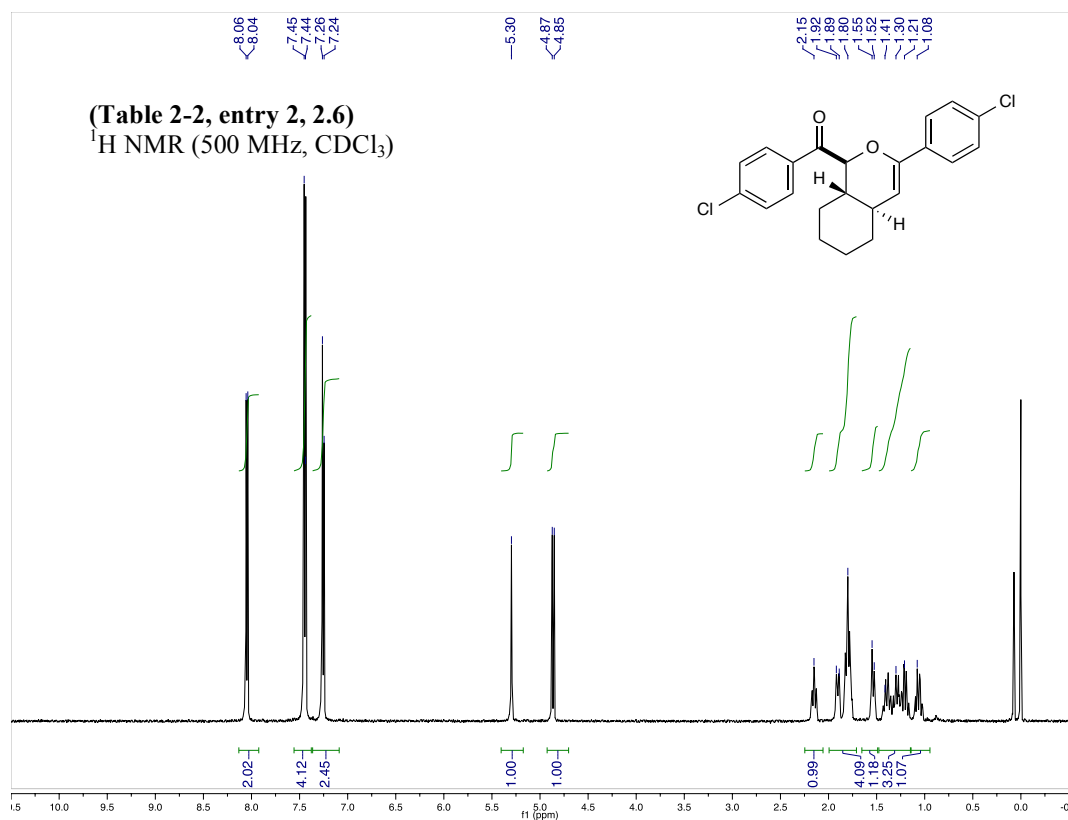


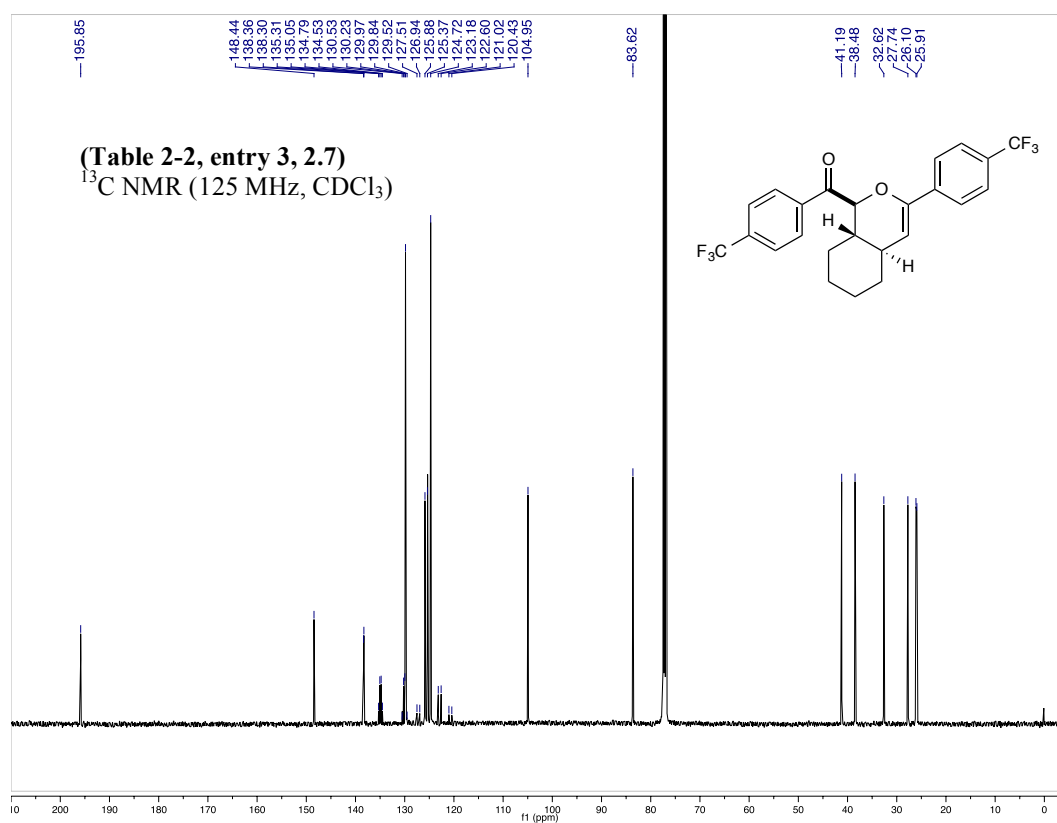
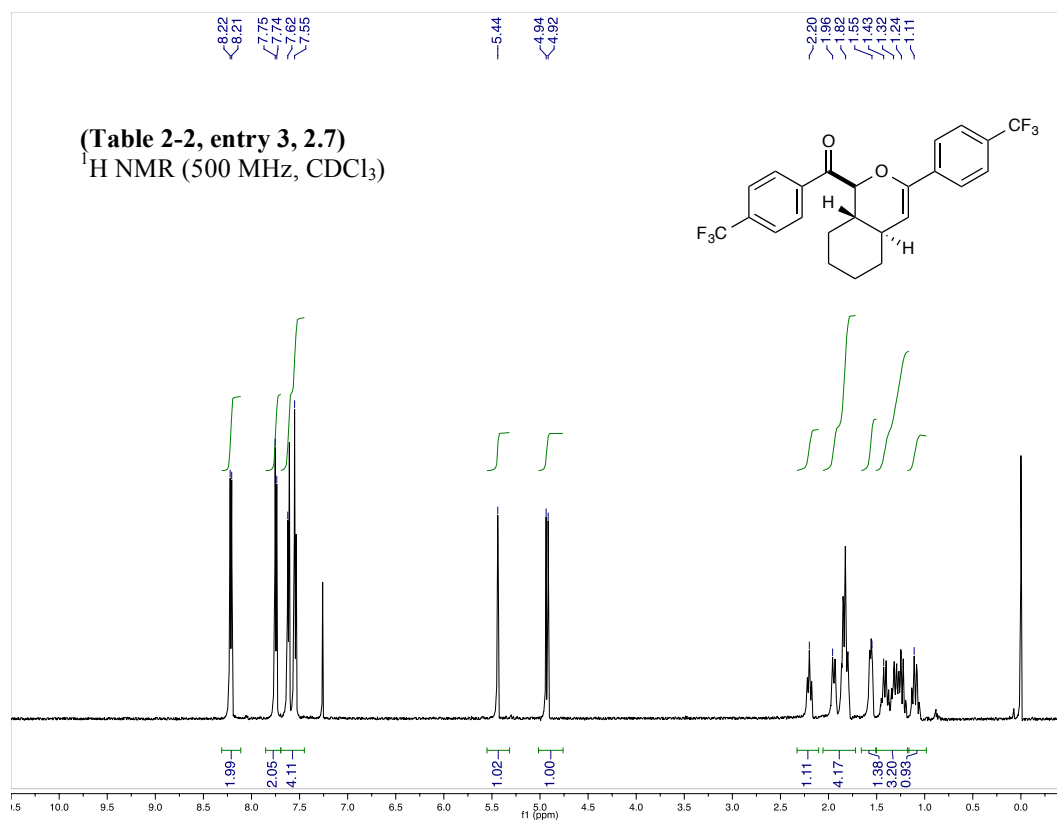


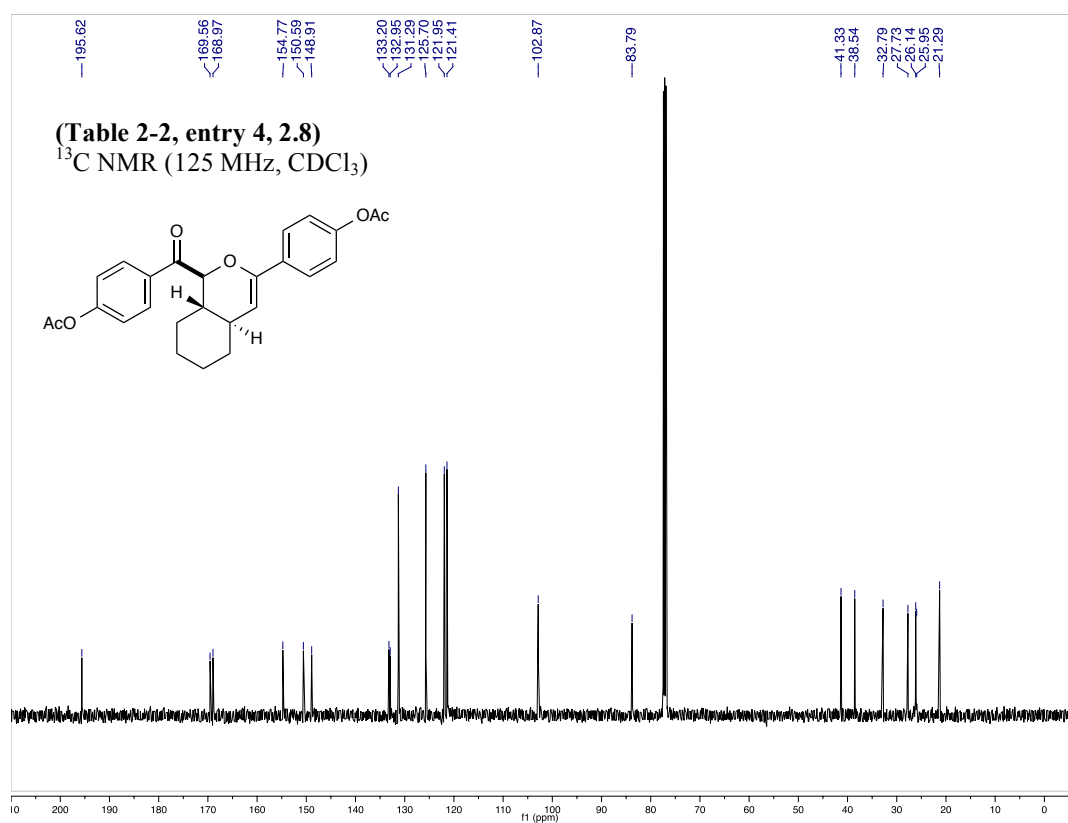
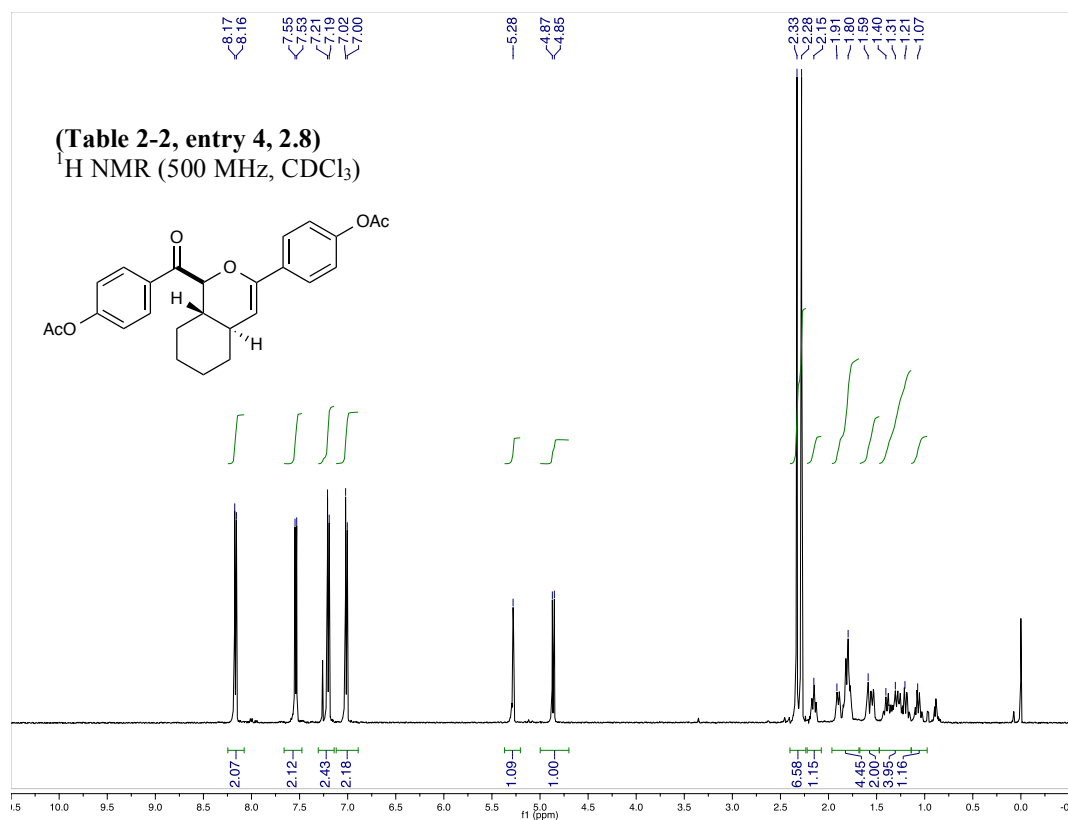


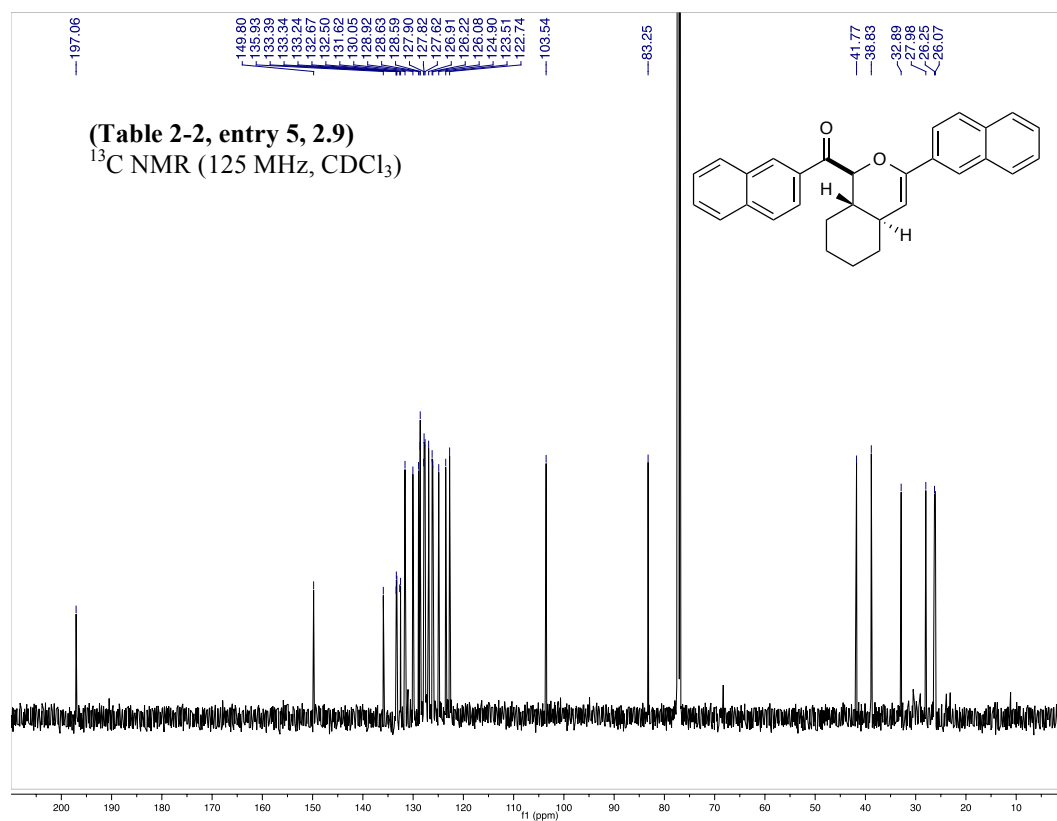
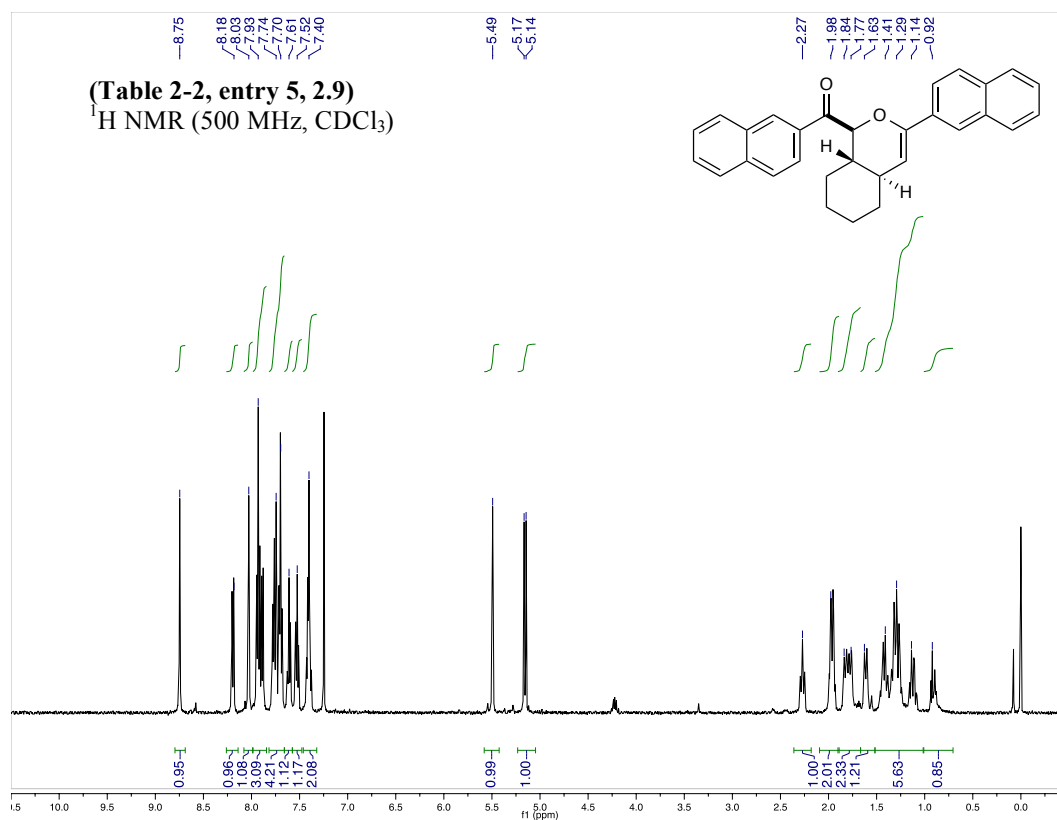


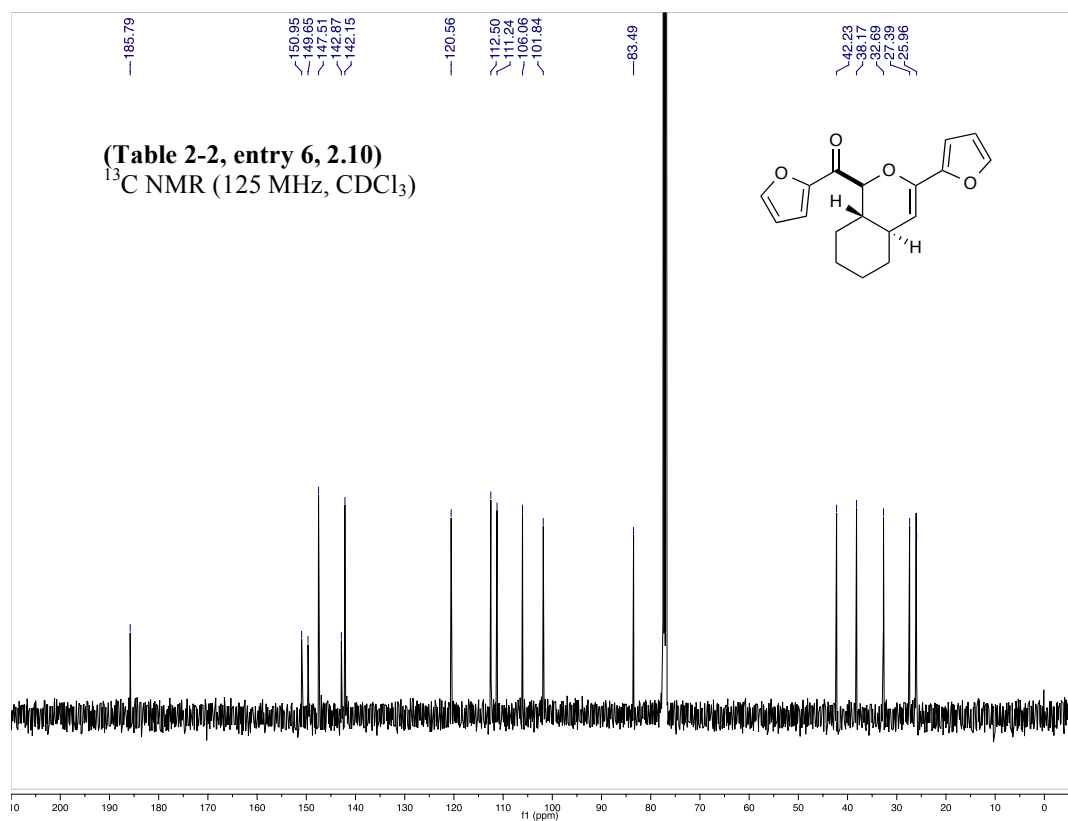
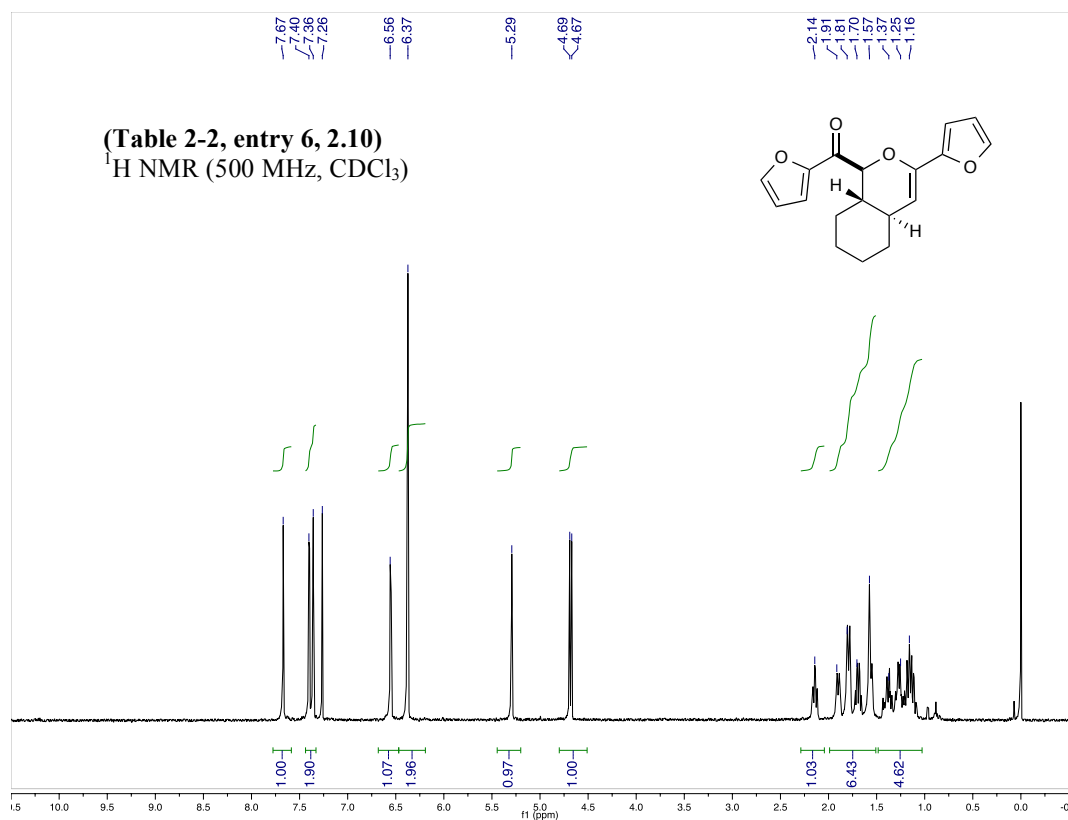


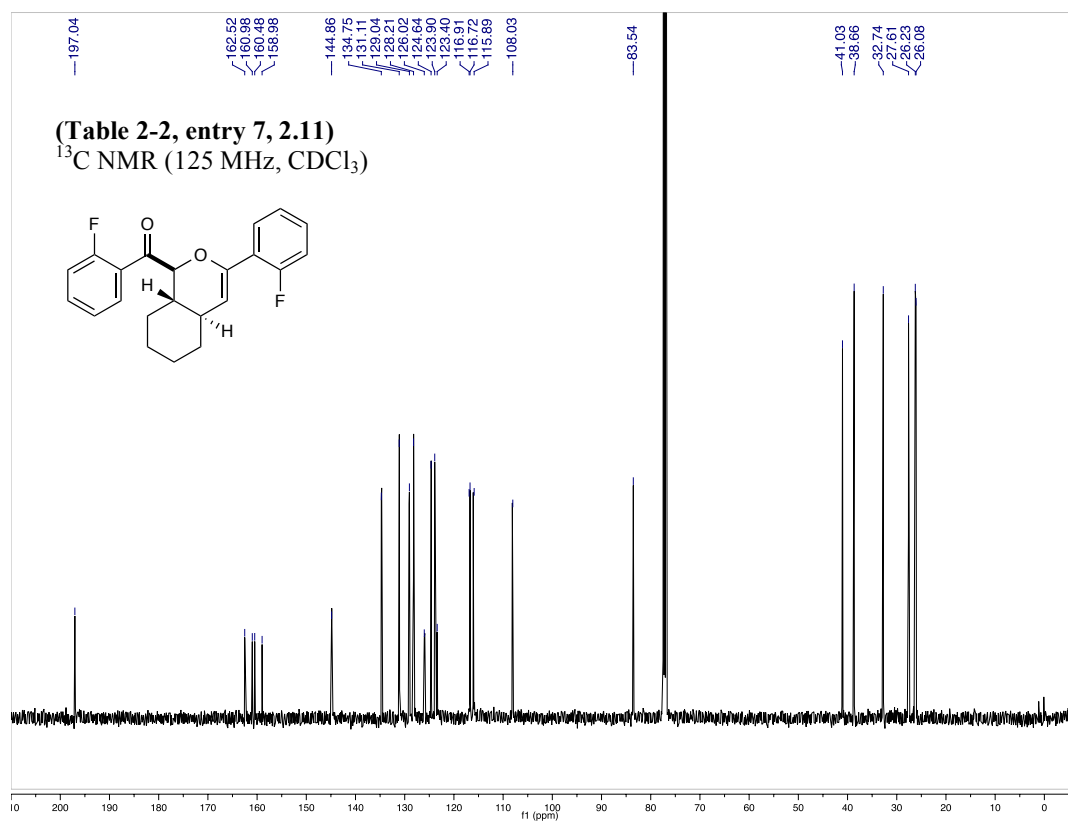
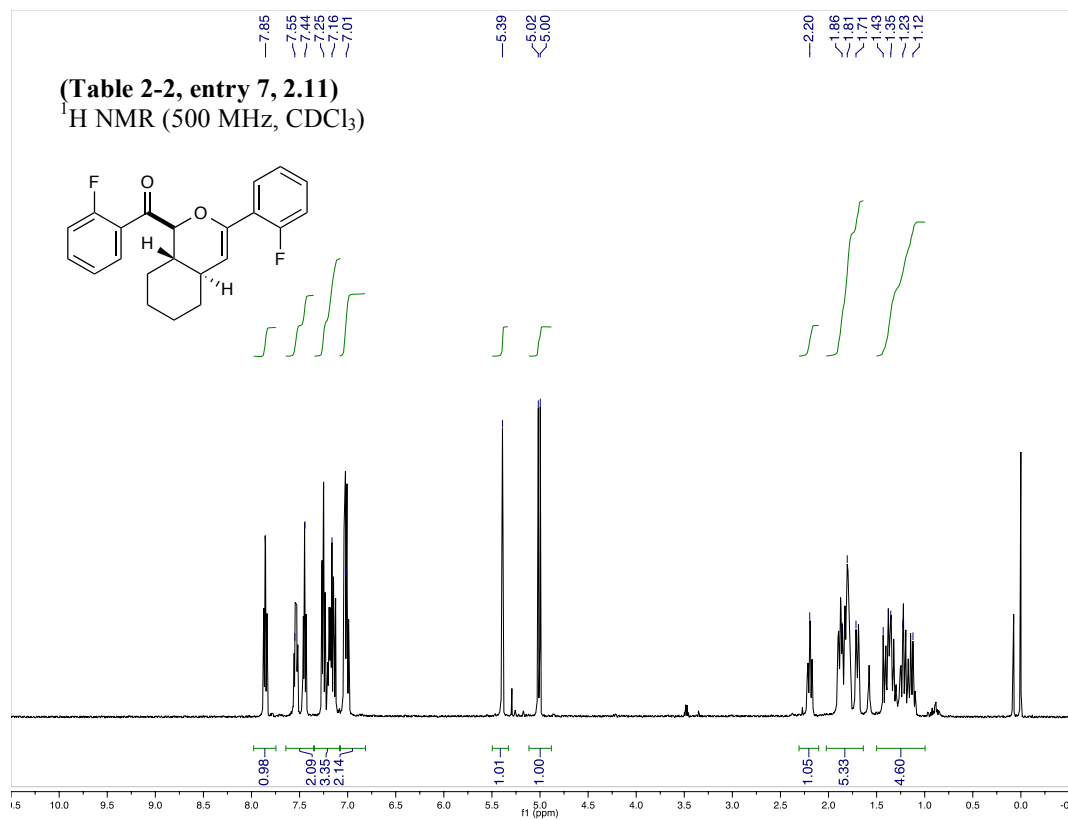


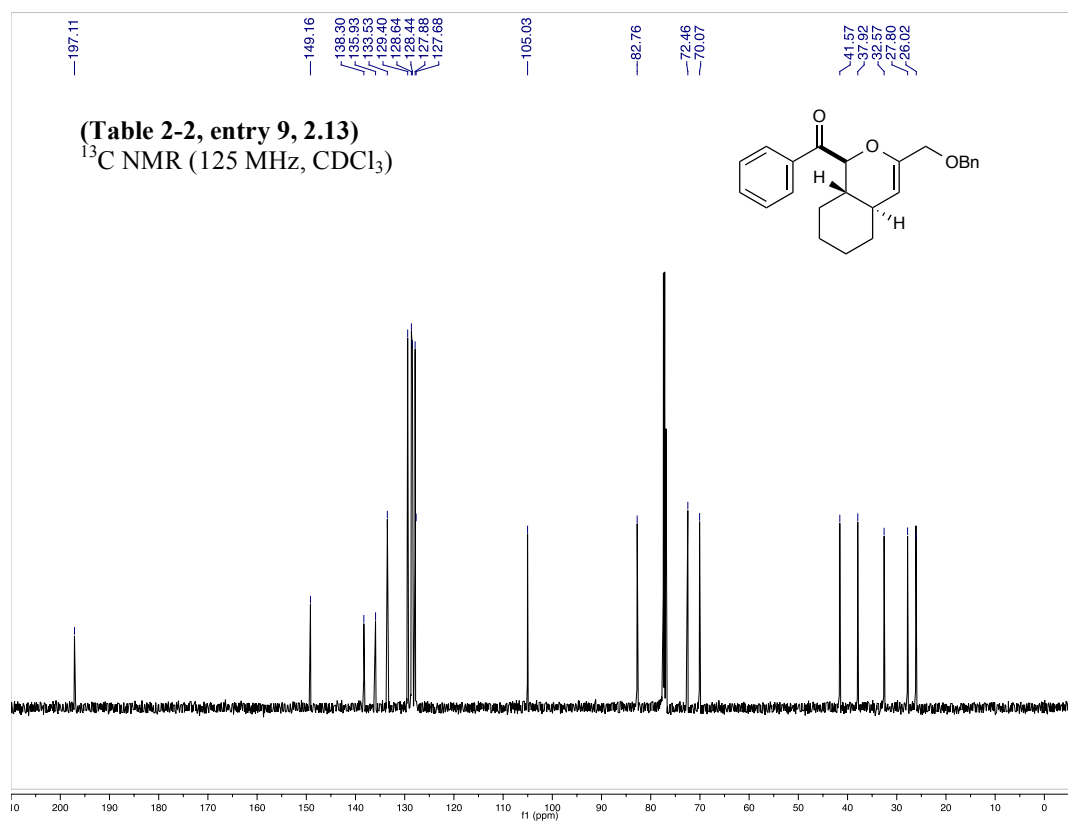
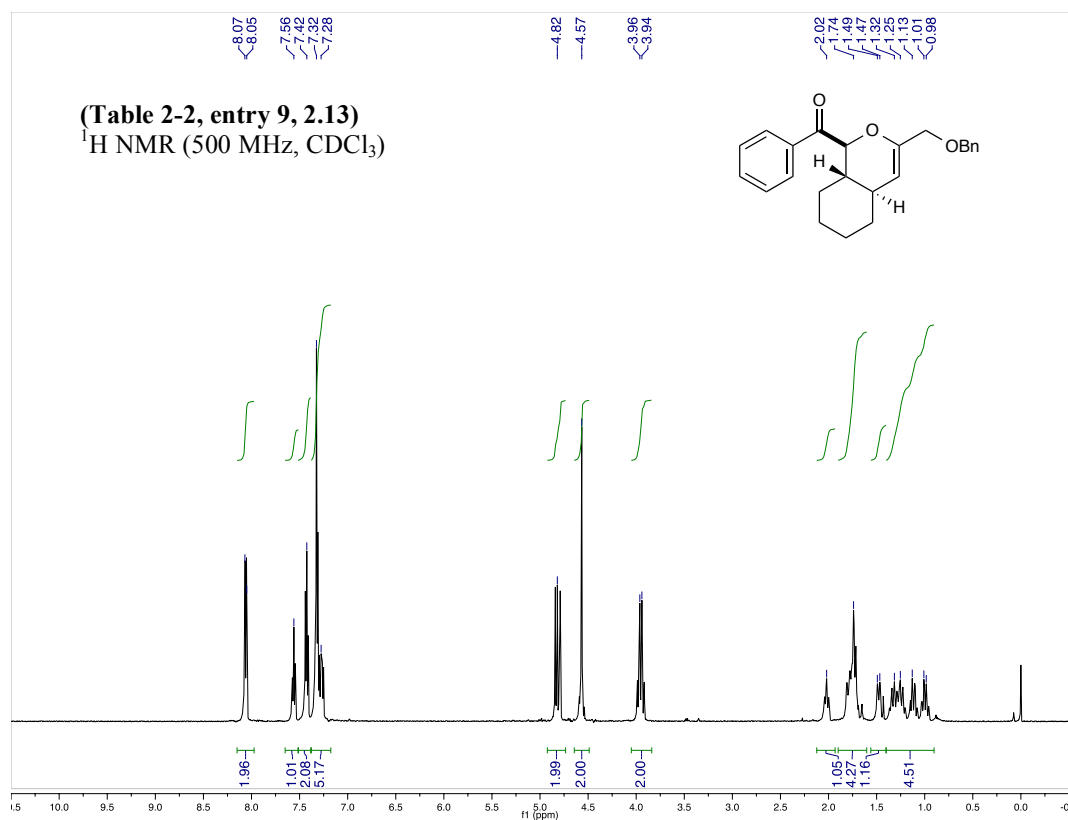


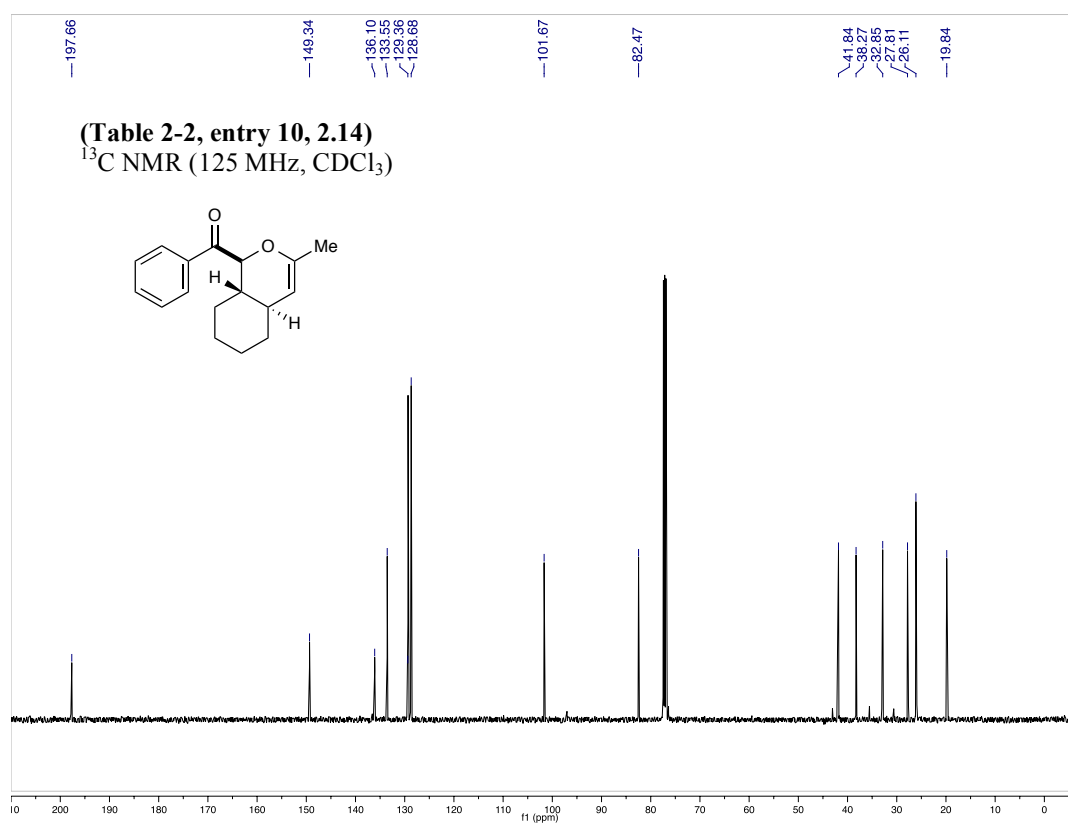
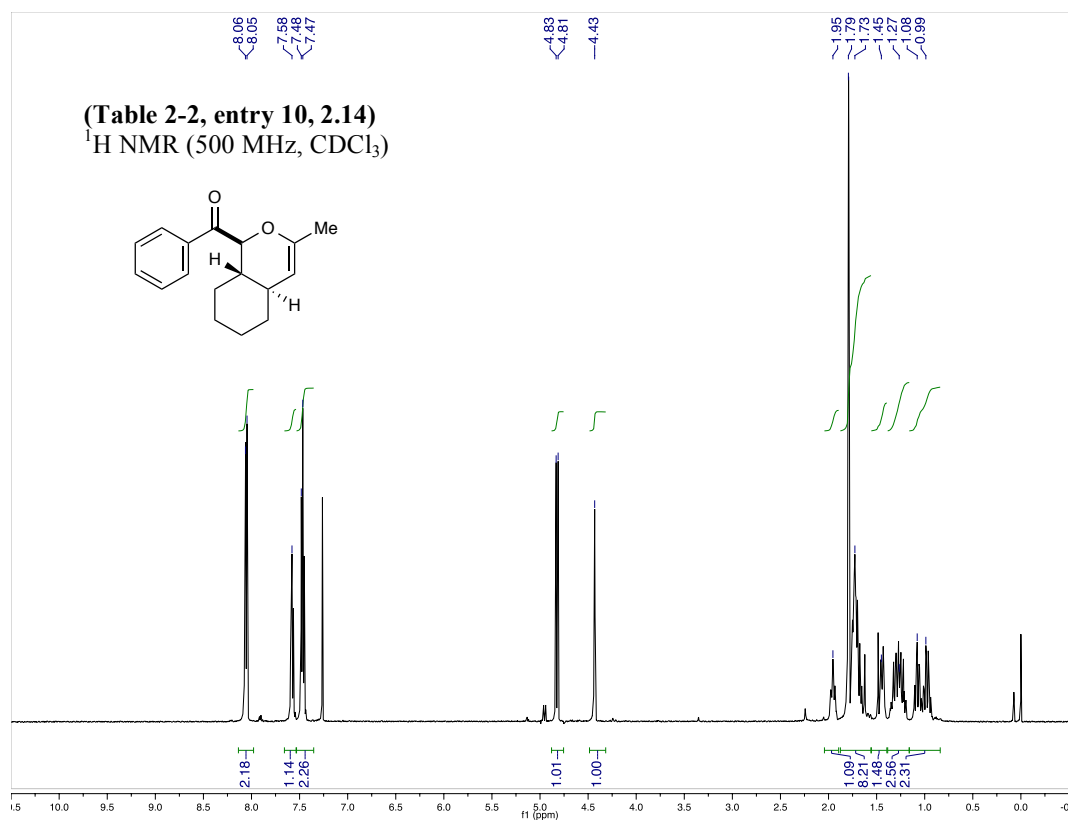


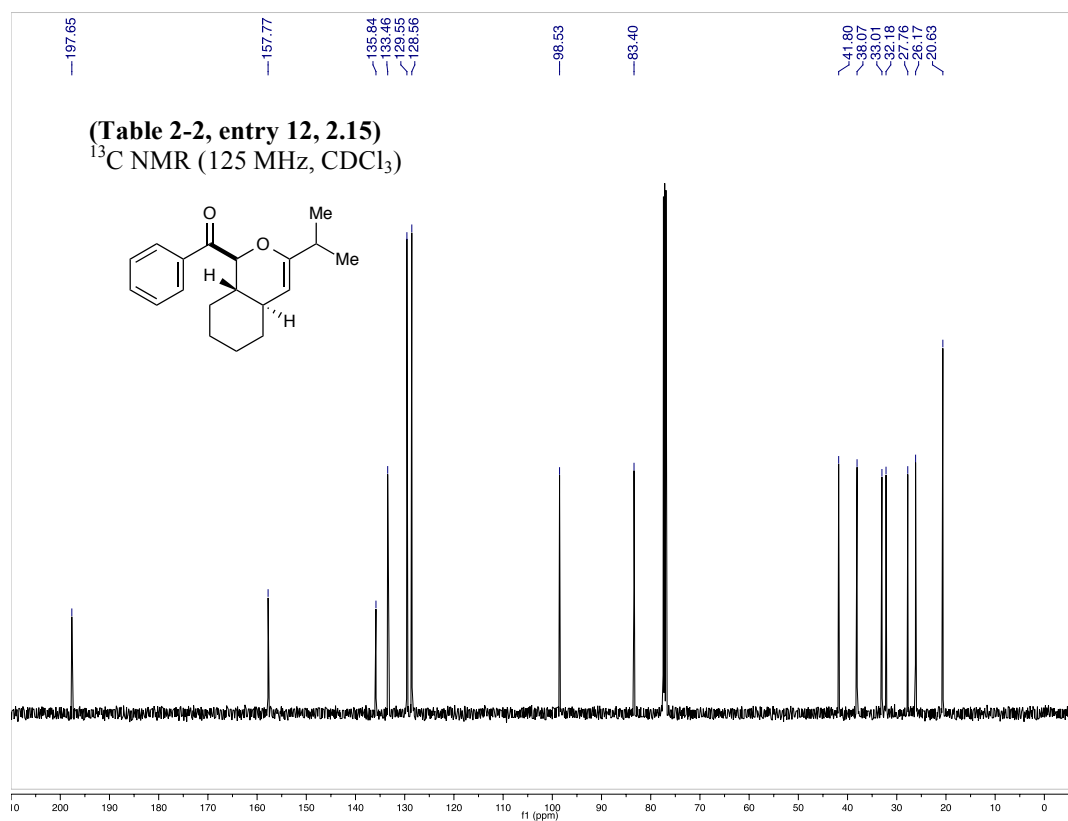
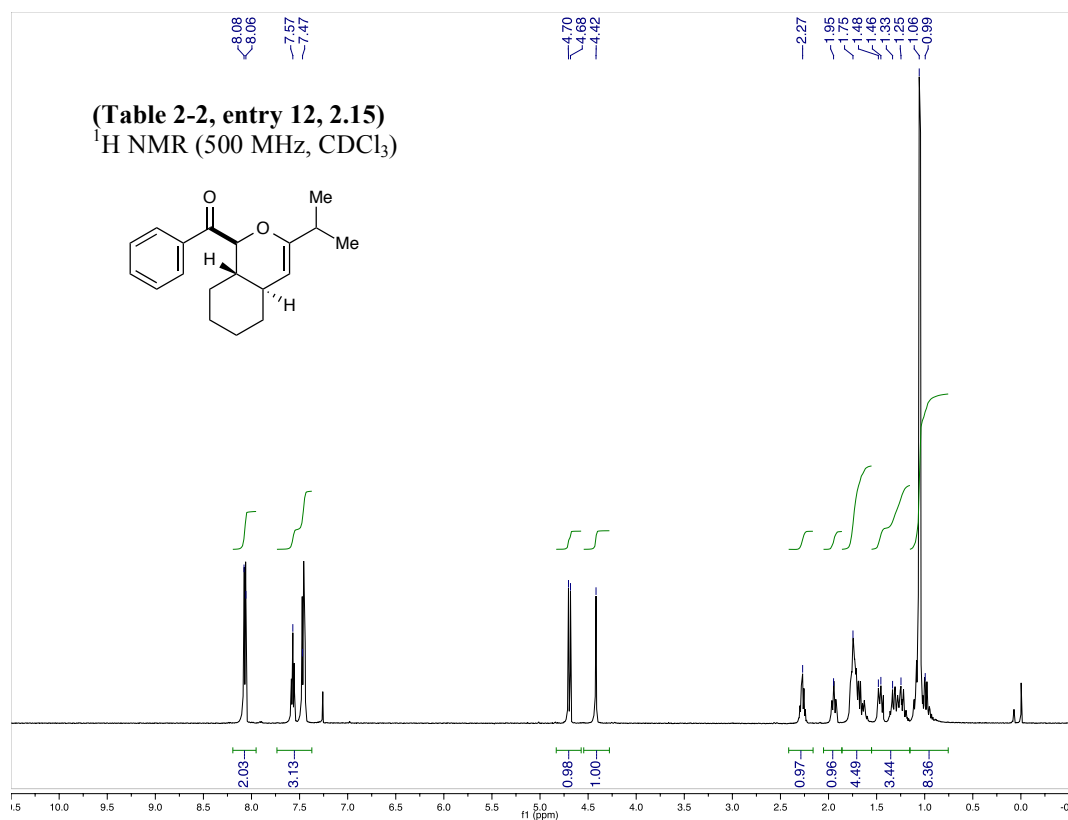


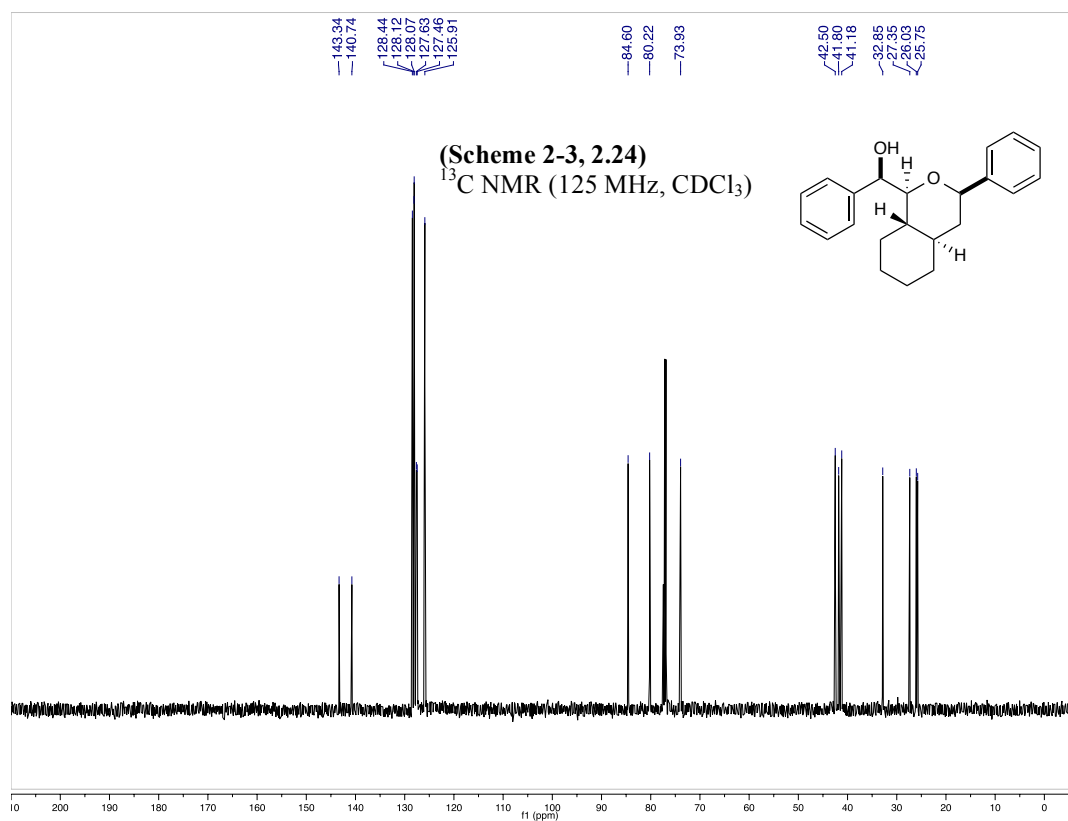
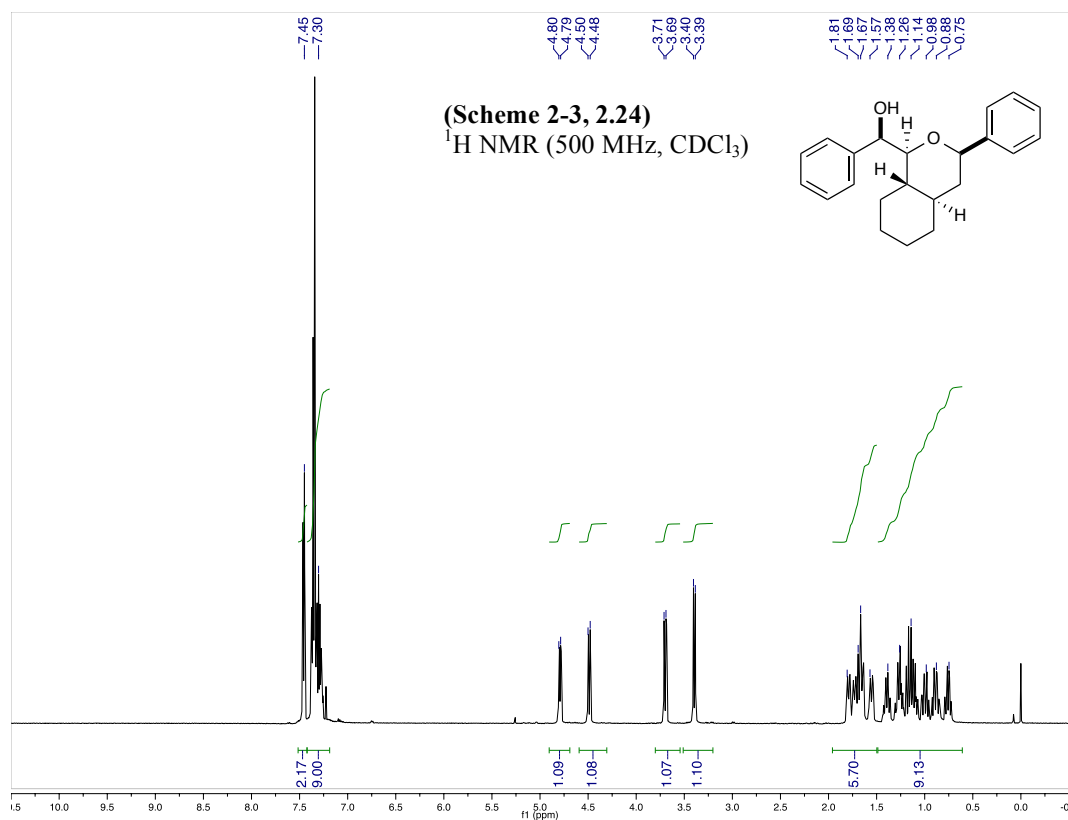


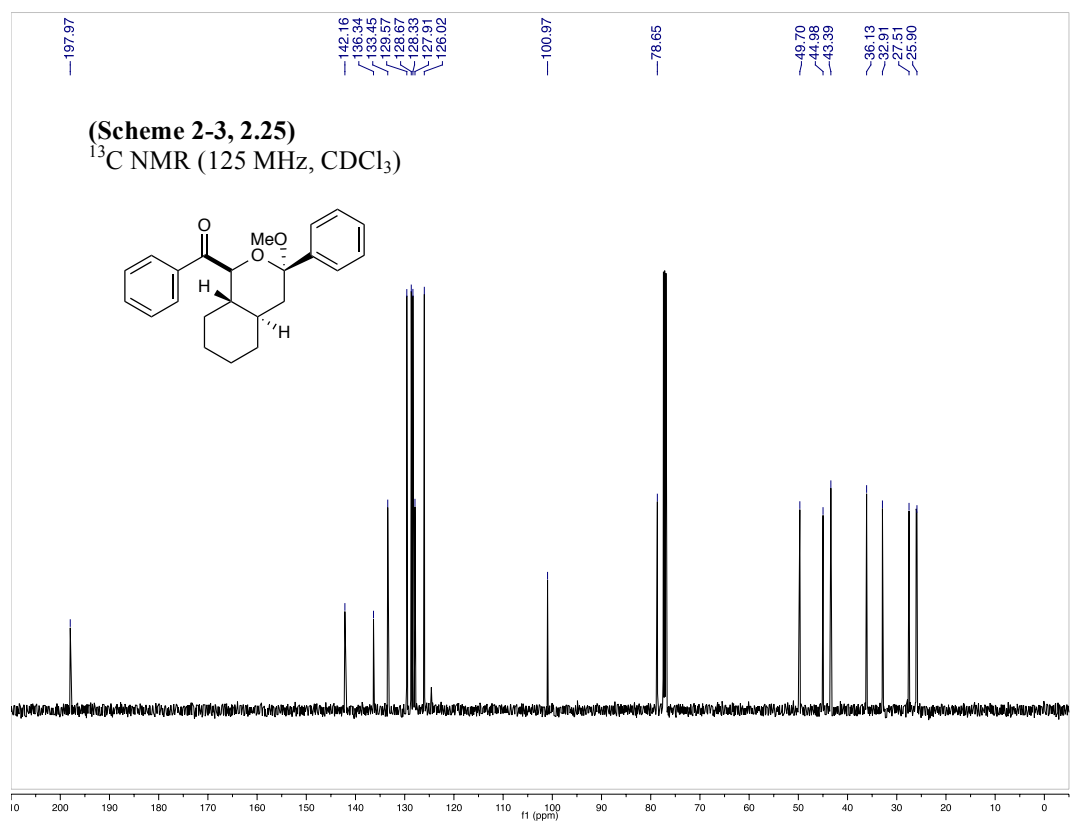
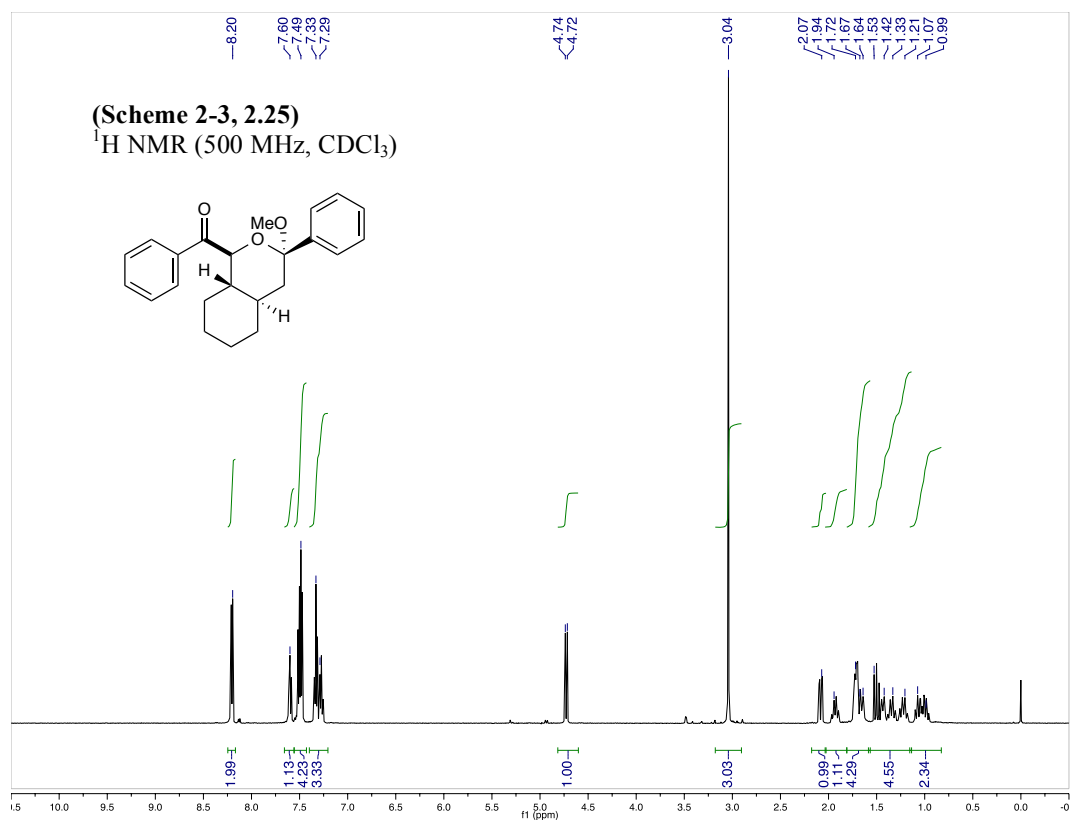


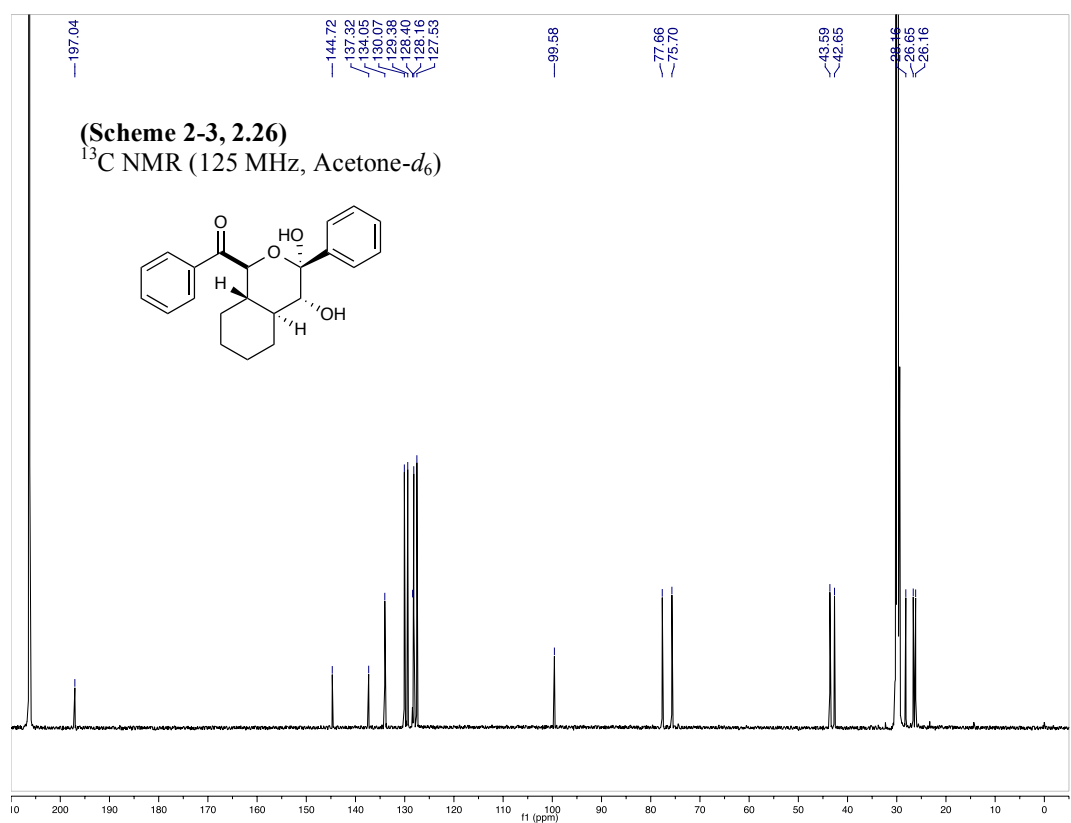
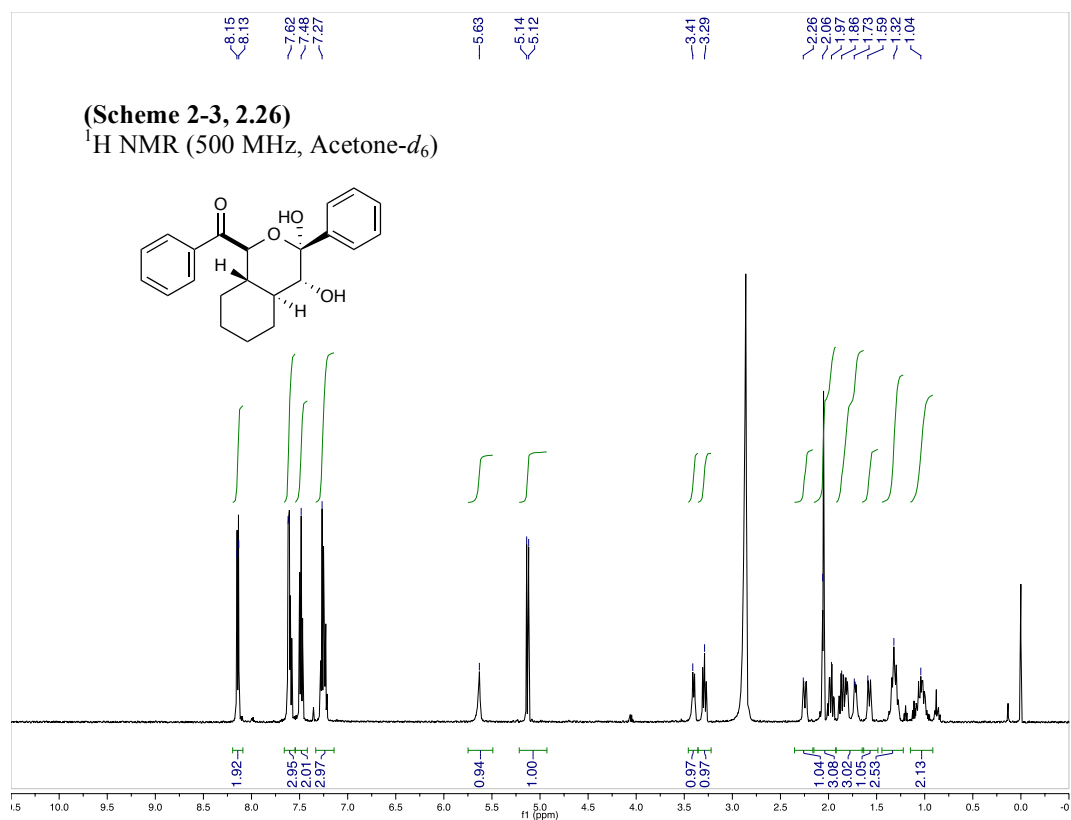




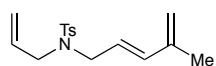




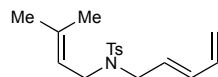




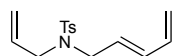
List of Compounds for Chapter 3



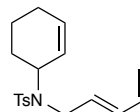
3.3



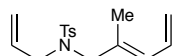
3.51



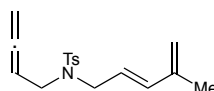
3.45



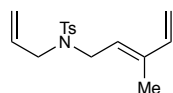
3.52



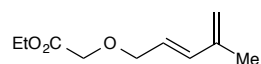
3.46



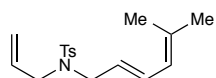
3.53



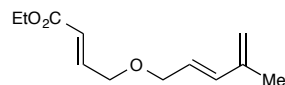
3.47



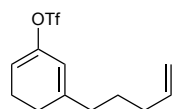
3.54



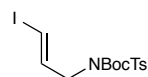
3.48



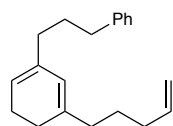
3.55



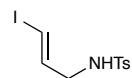
3.49



3.56

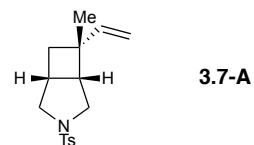
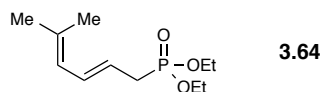
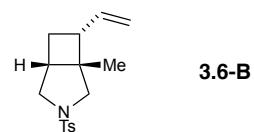
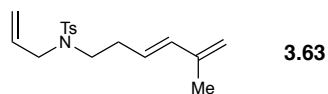
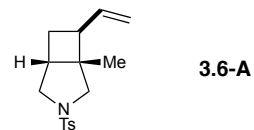
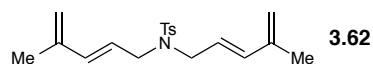
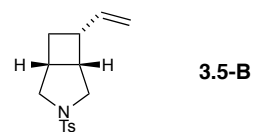
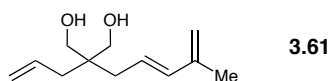
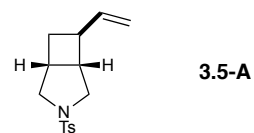
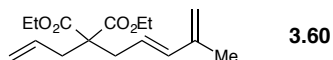
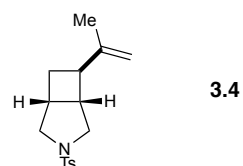
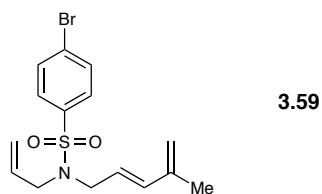
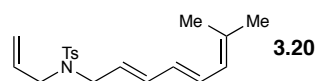
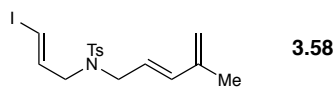


3.50

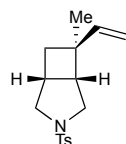


3.57

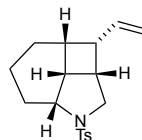
List of Compounds for Chapter 3



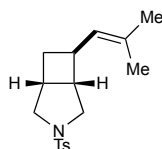
List of Compounds for Chapter 3



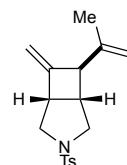
3.7-B



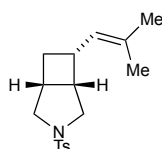
3.11-B



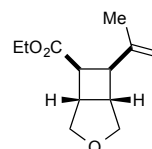
3.8-A



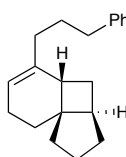
3.12



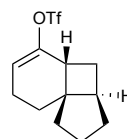
3.8-B



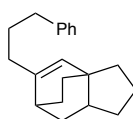
3.13



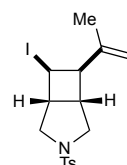
3.9



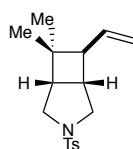
3.14



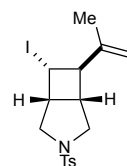
3.65



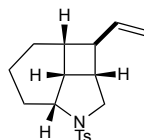
3.15-A



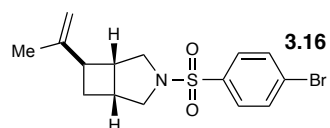
3.10



3.15-B

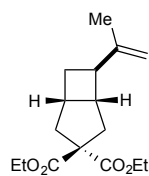


3.11-A

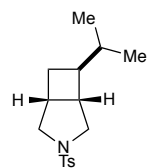


3.16

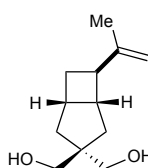
List of Compounds for Chapter 3



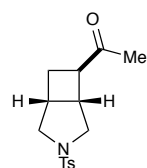
3.17



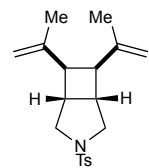
3.35



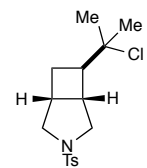
3.18



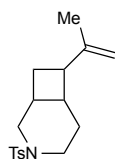
3.36



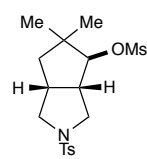
3.19



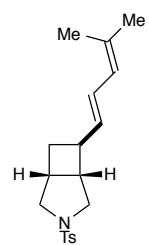
3.37



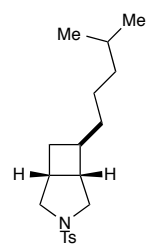
3.23



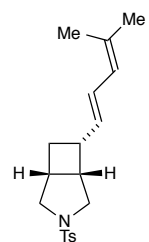
3.38



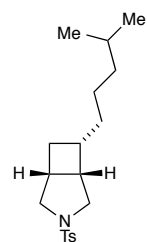
3.21-A



3.66-A

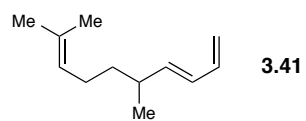
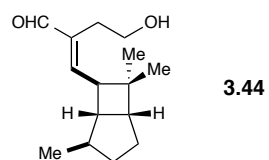
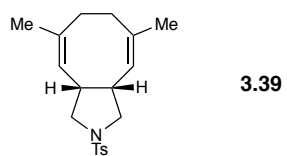


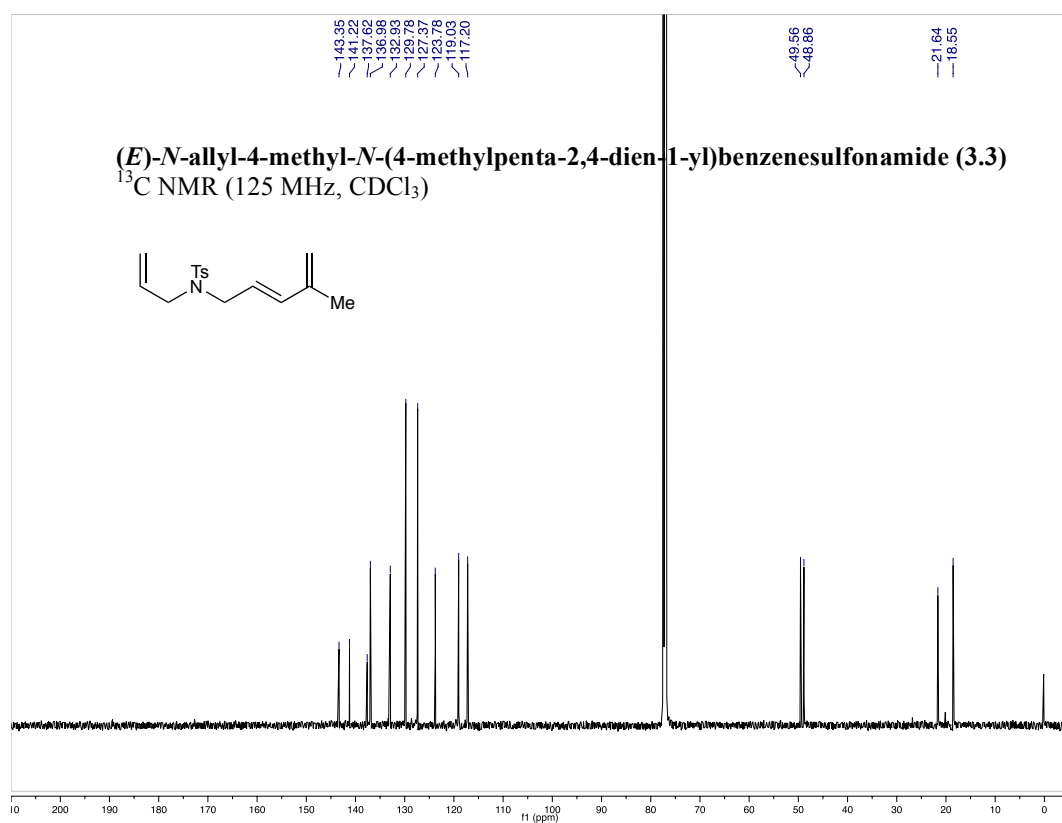
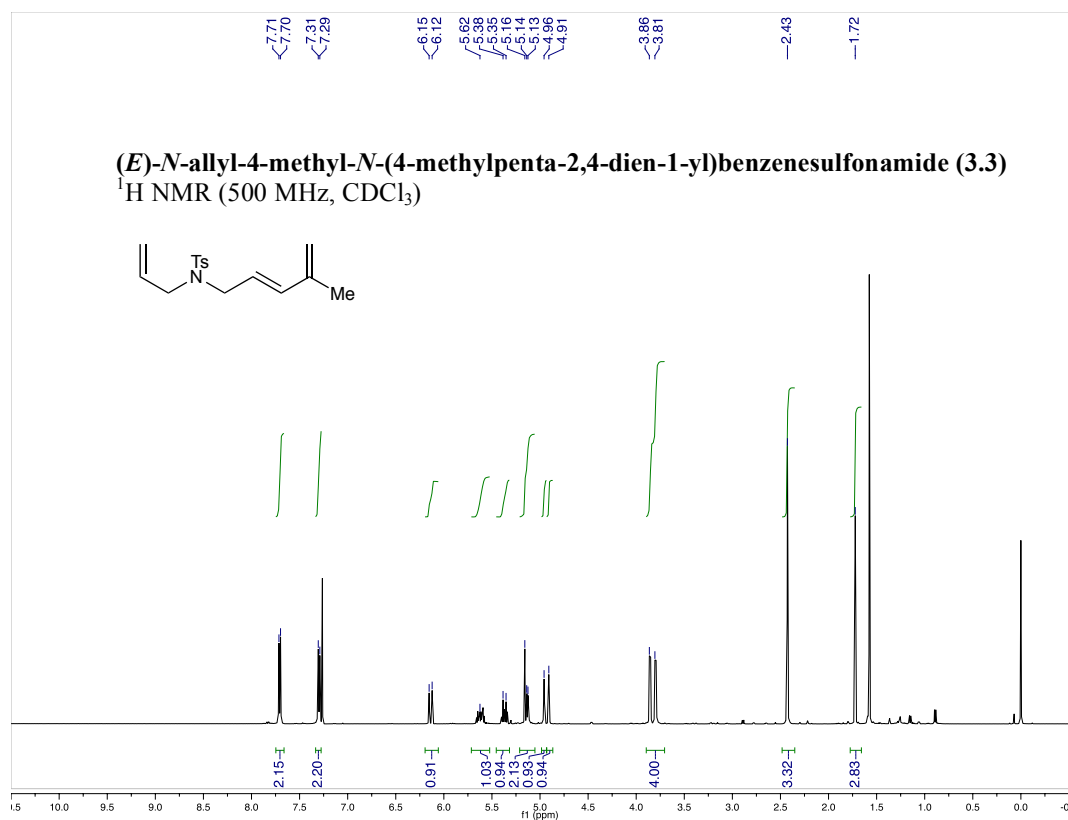
3.21-B

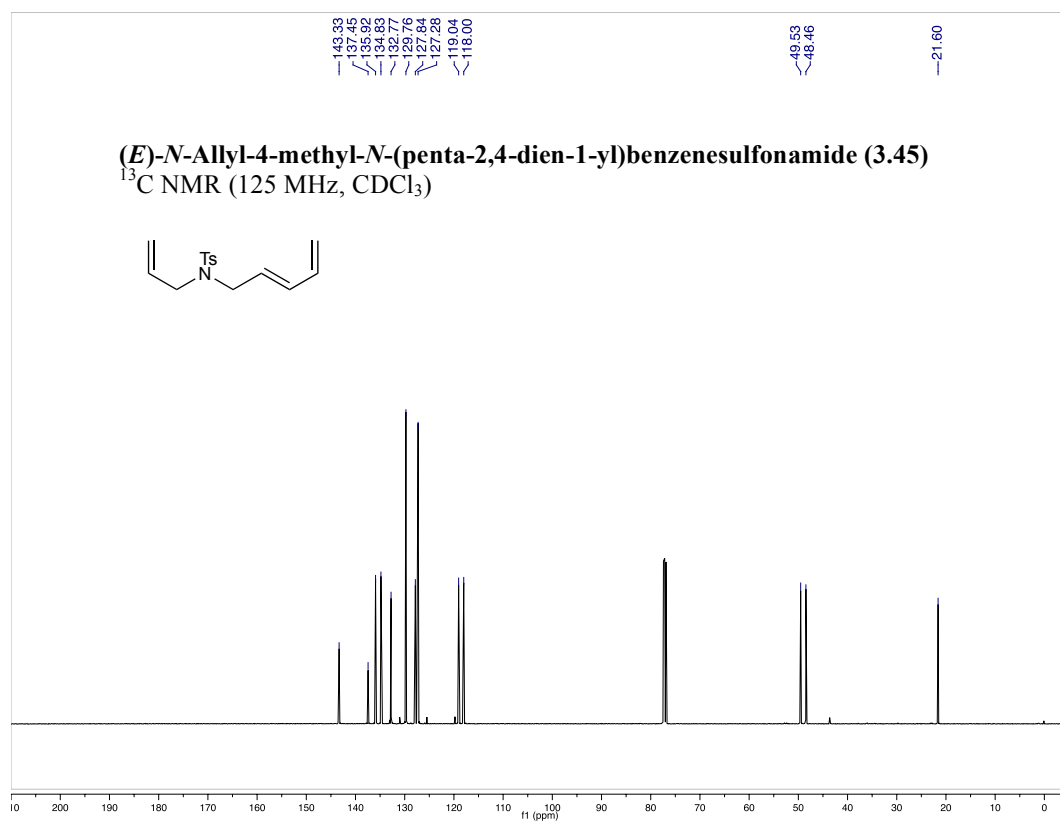
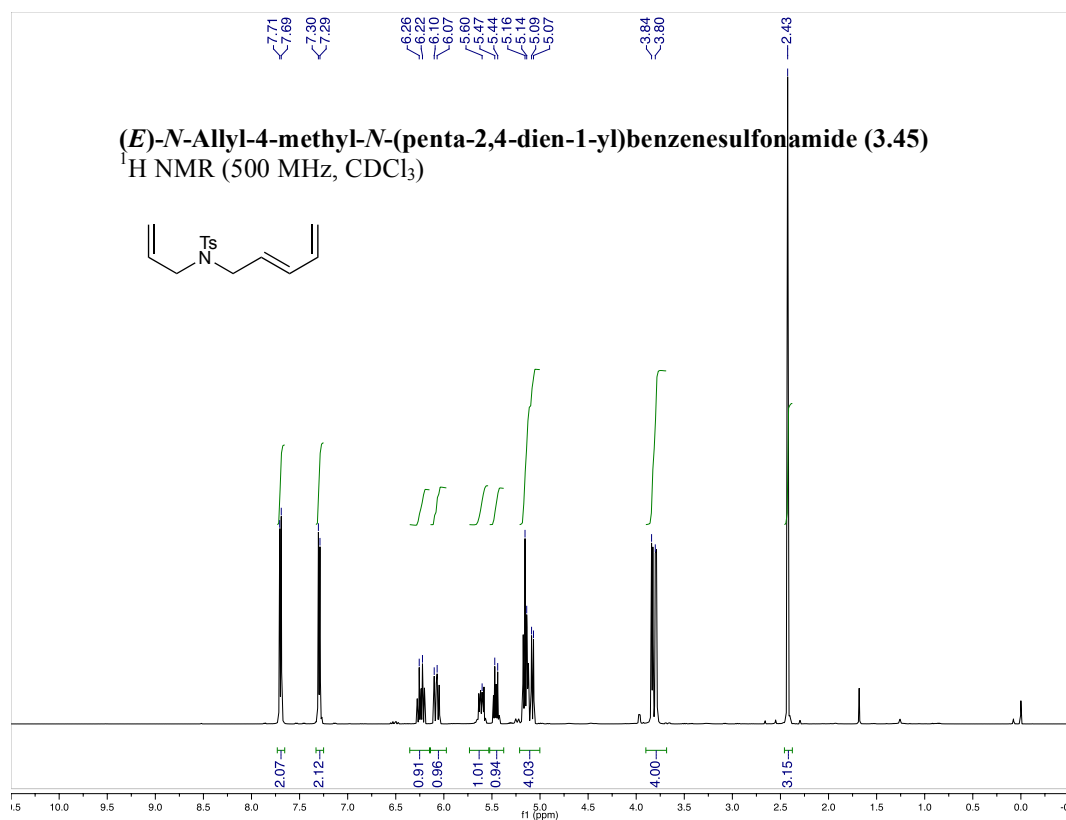


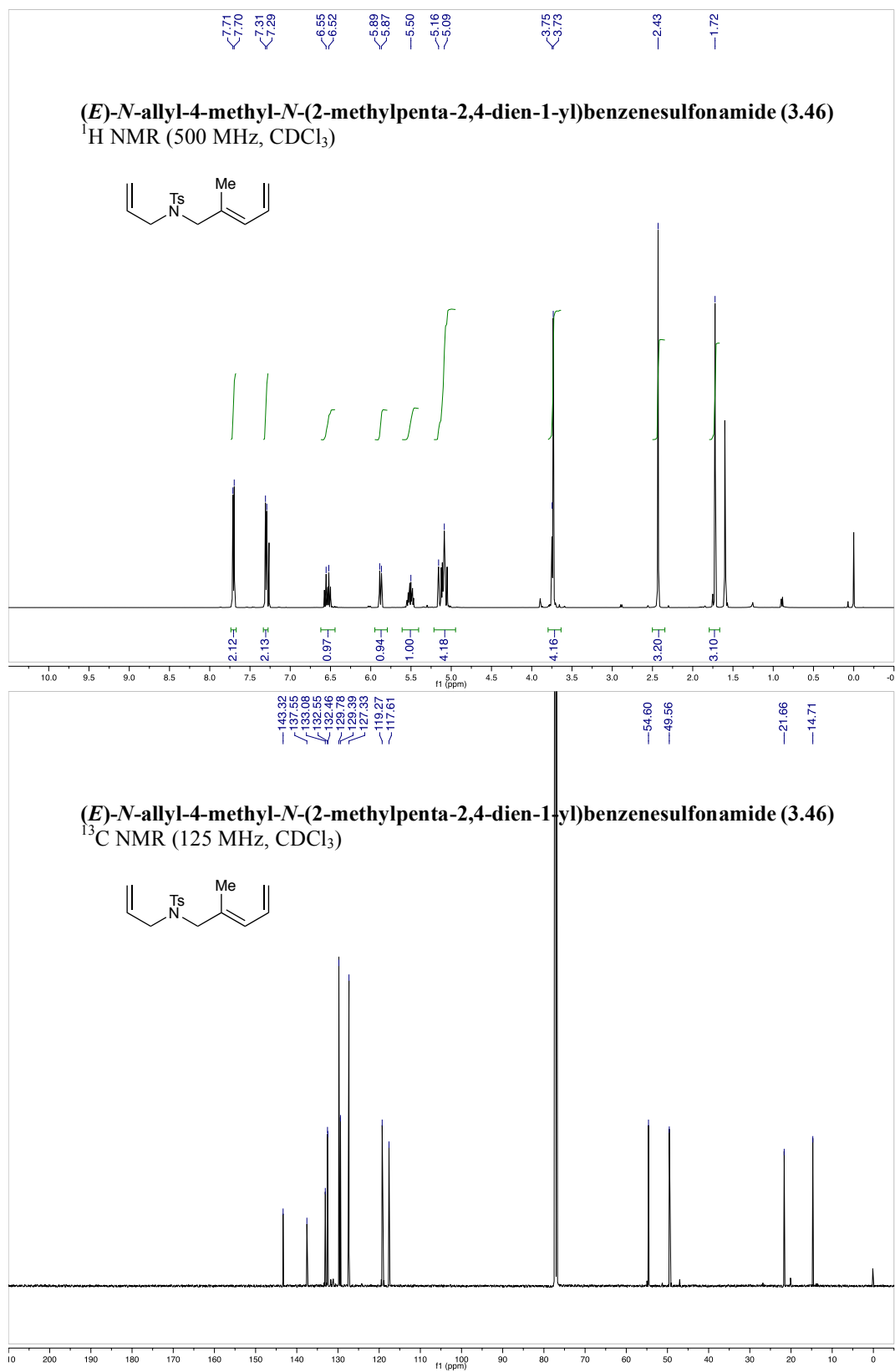
3.66-B

List of Compounds for Chapter 3

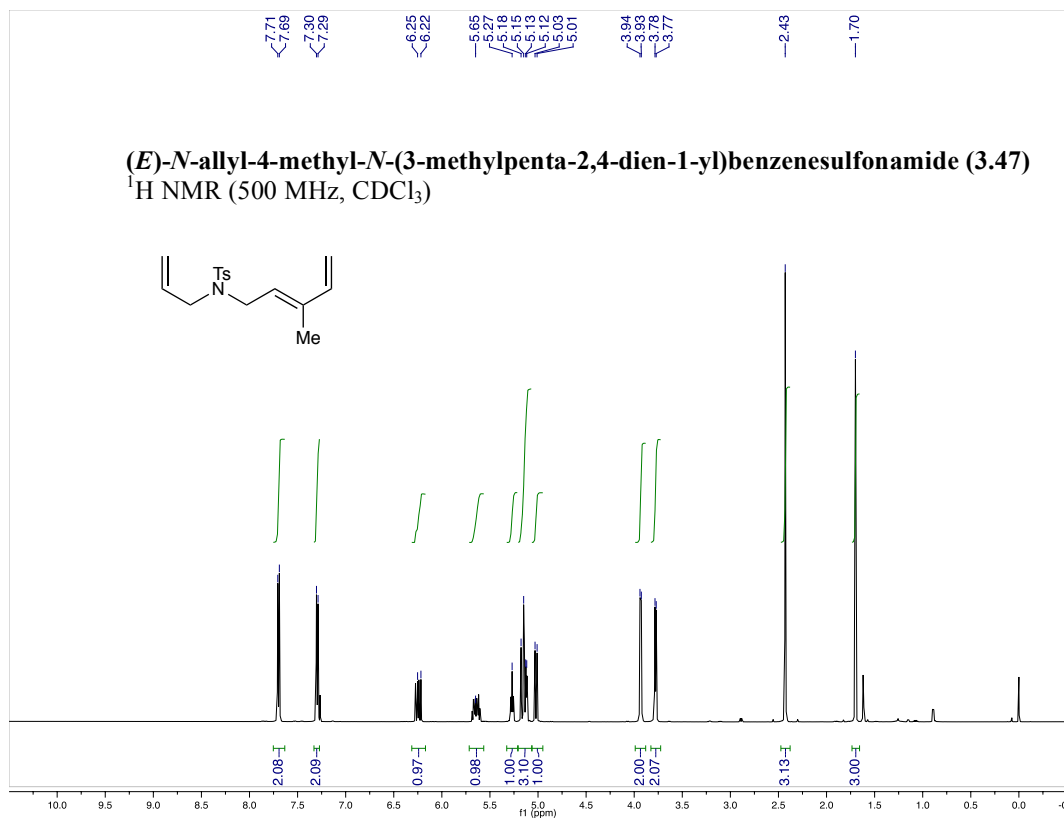




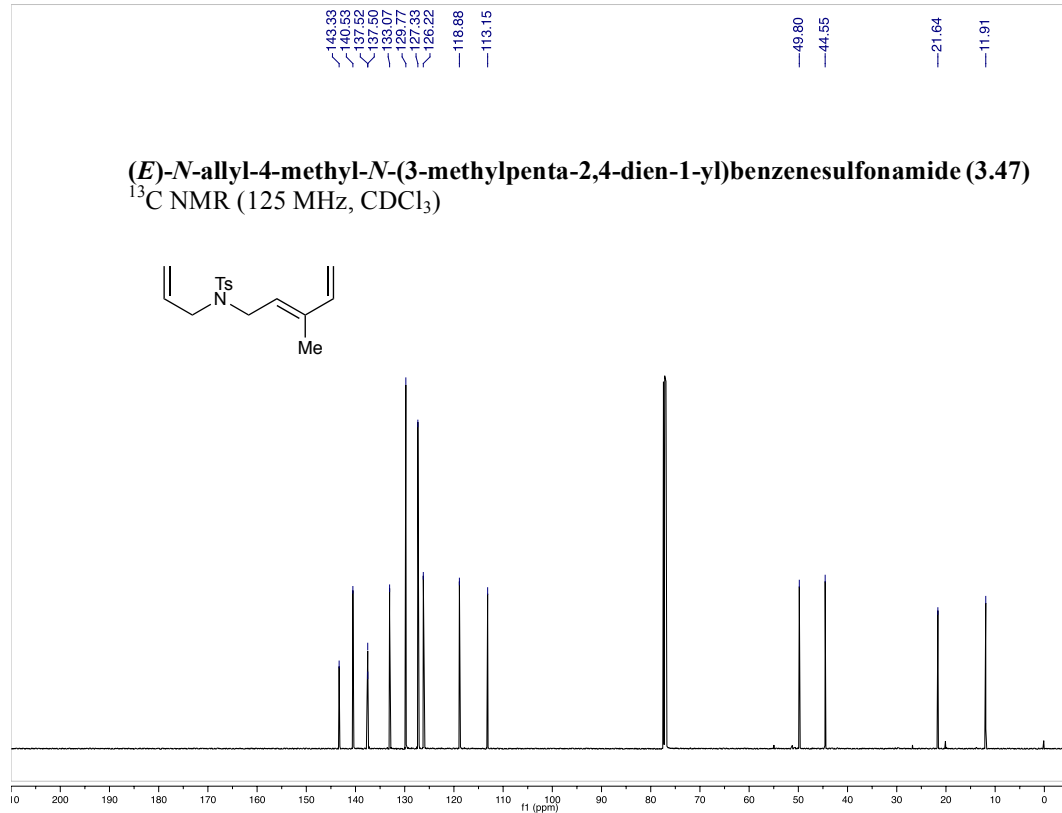


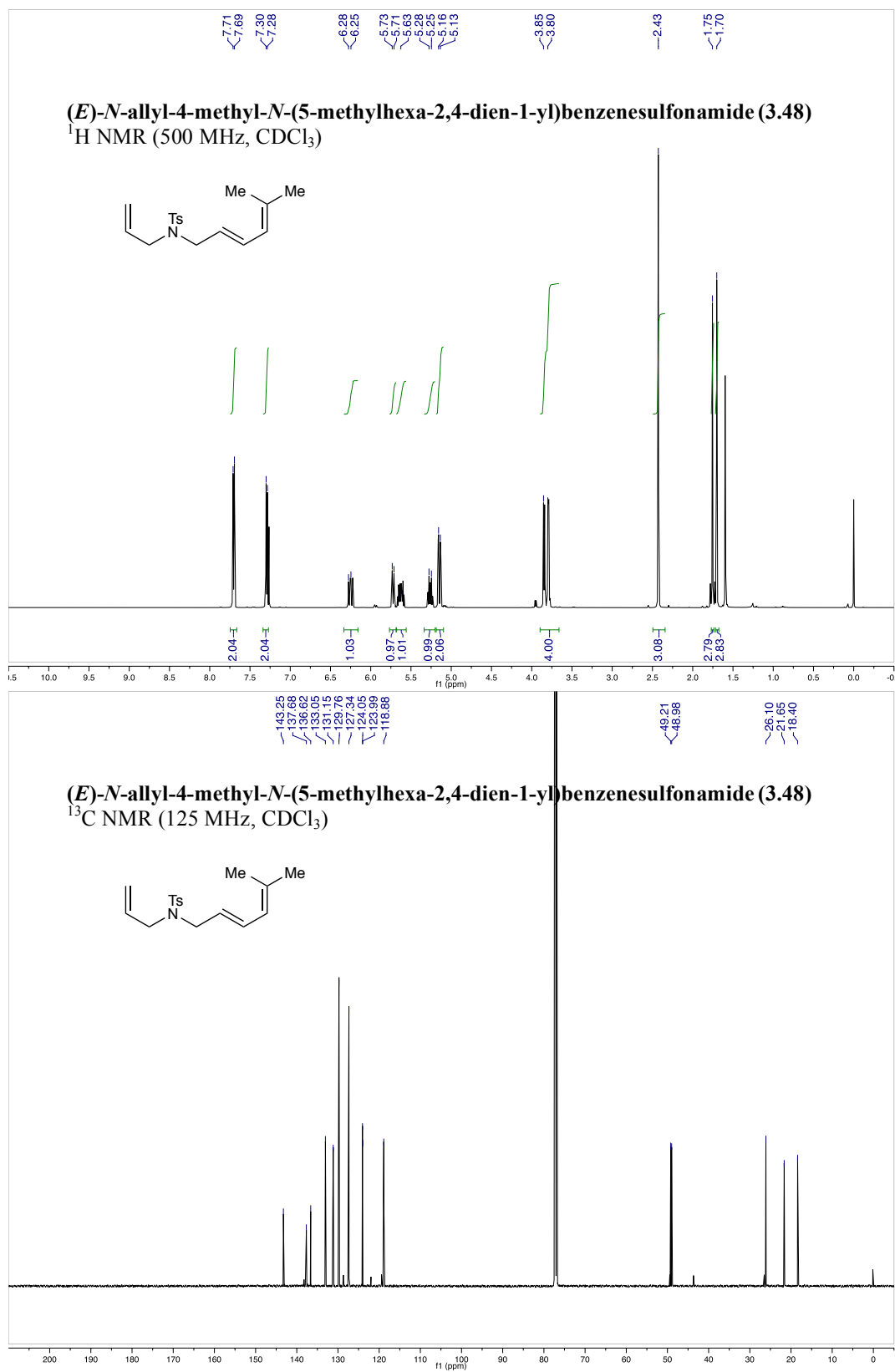


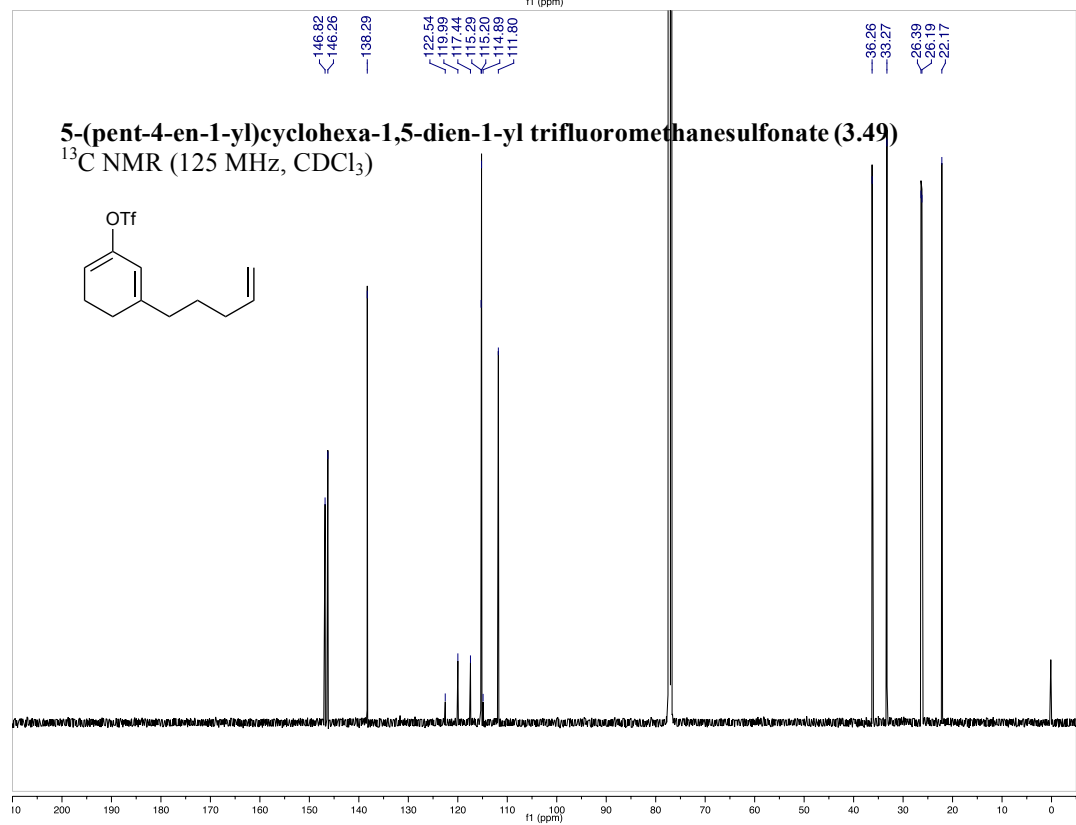
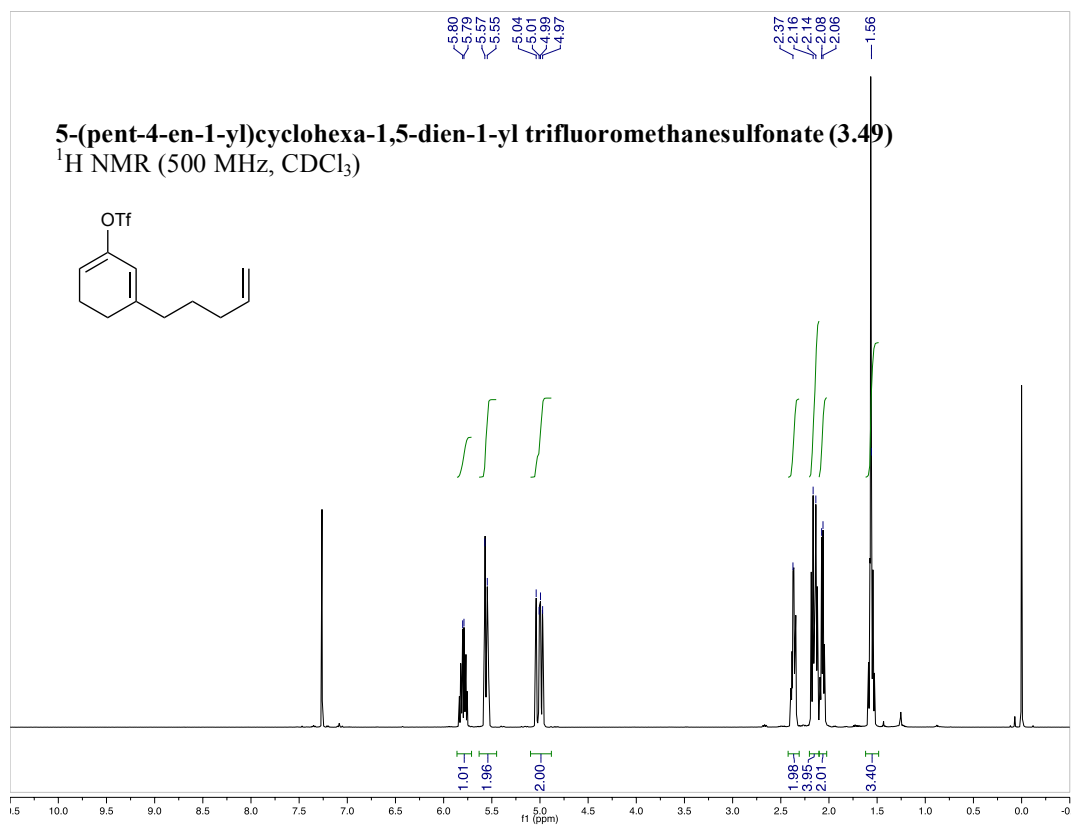
(*E*)-*N*-allyl-4-methyl-*N*-(3-methylpenta-2,4-dien-1-yl)benzenesulfonamide (3.47)
¹H NMR (500 MHz, CDCl₃)

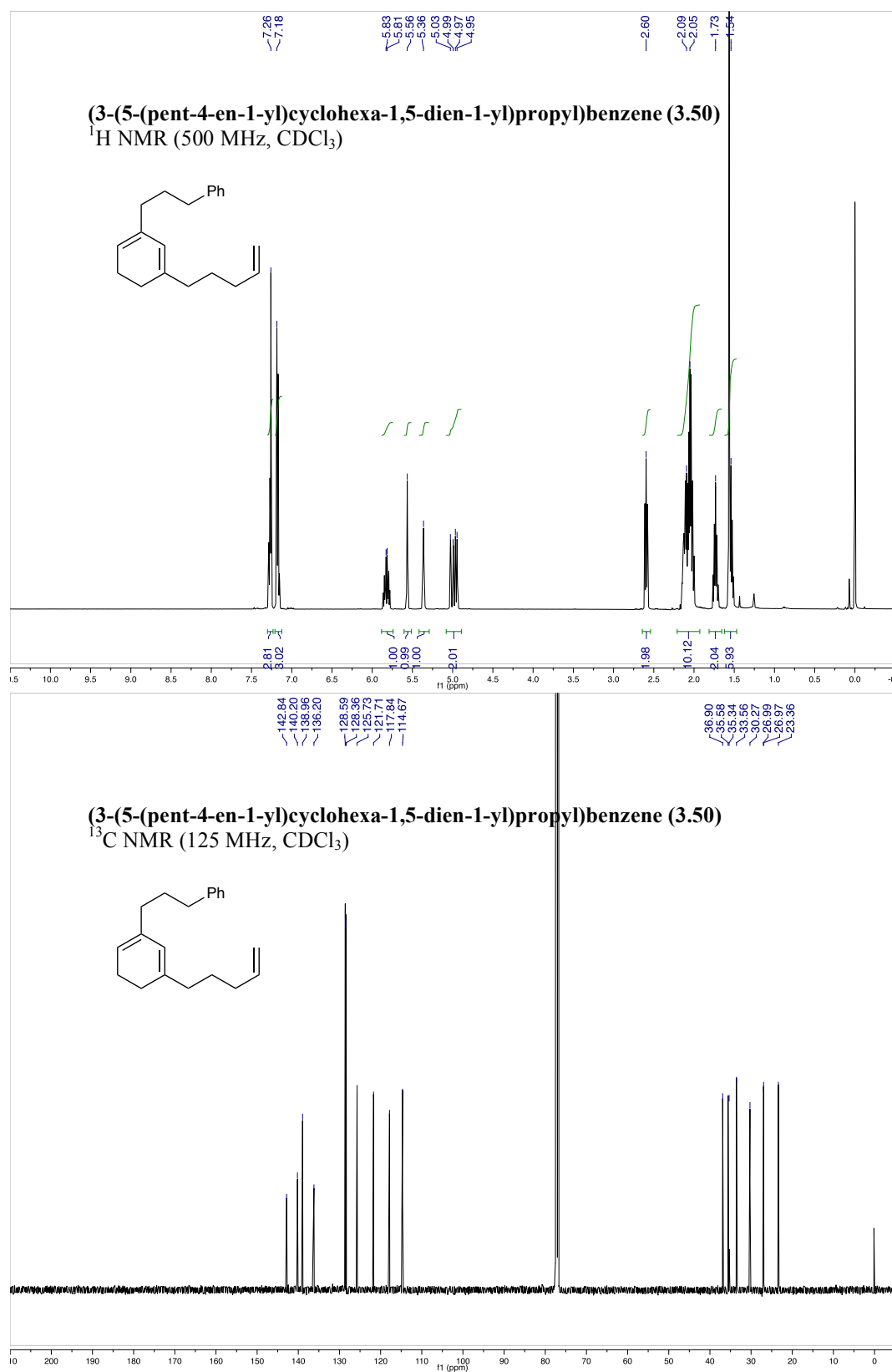


(*E*)-*N*-allyl-4-methyl-*N*-(3-methylpenta-2,4-dien-1-yl)benzenesulfonamide (3.47)
¹³C NMR (125 MHz, CDCl₃)

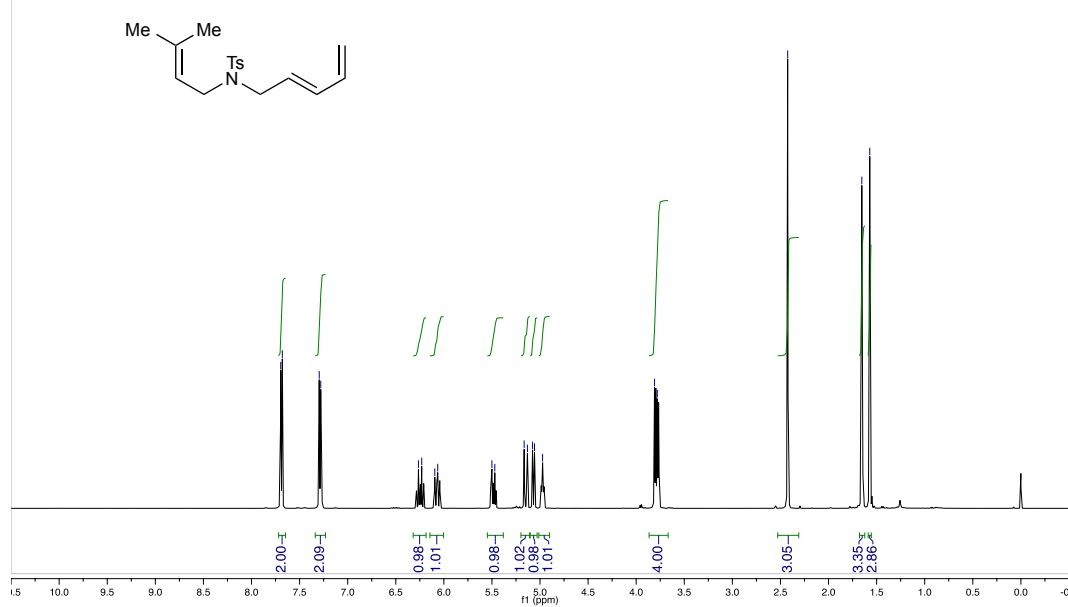




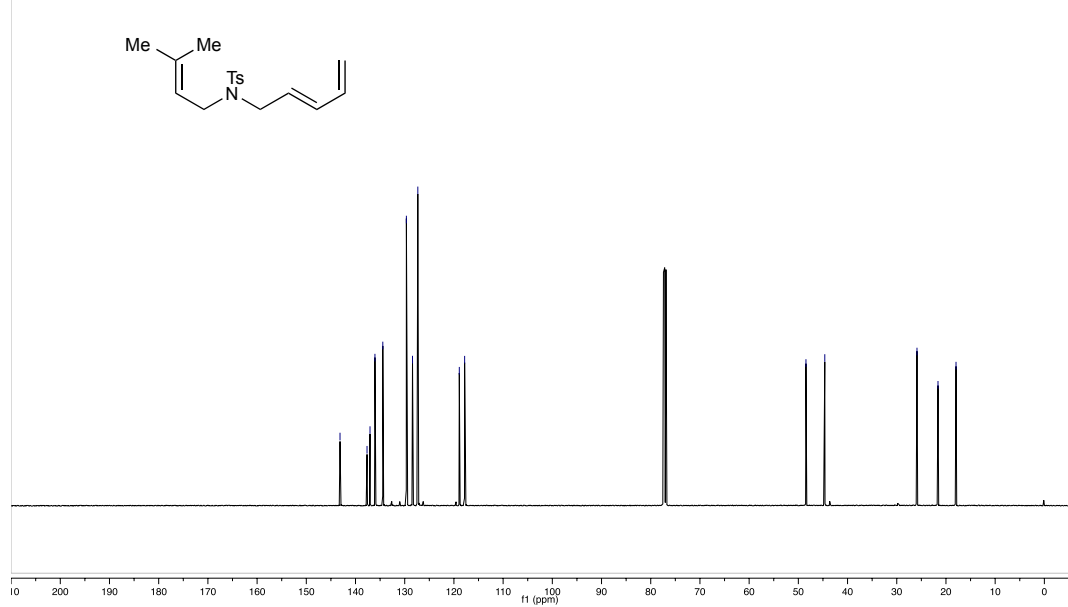




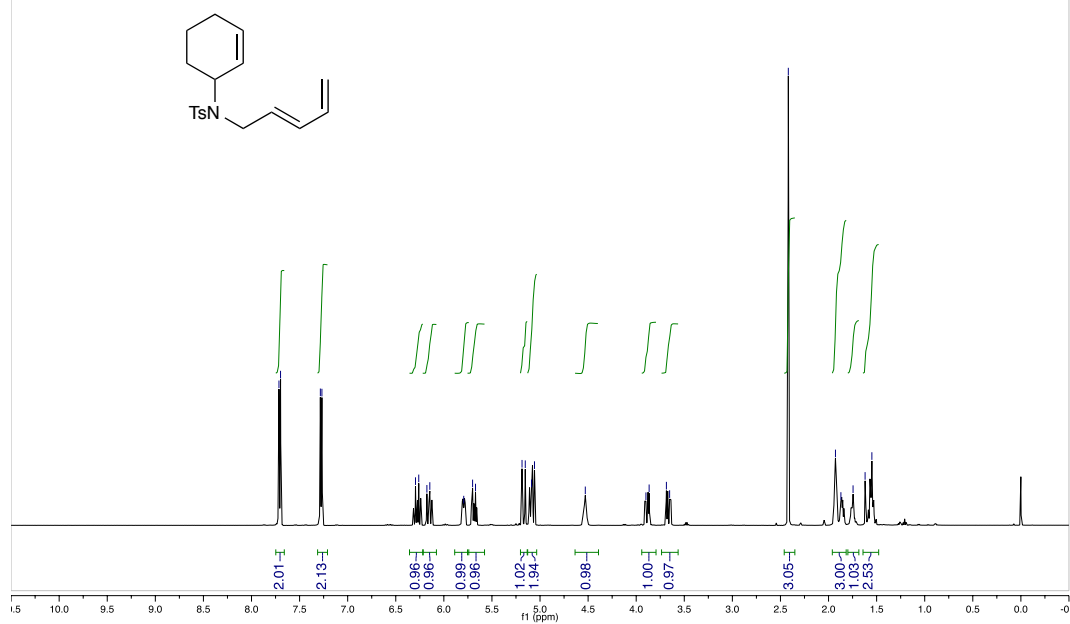
(*E*)-4-methyl-*N*-(3-methylbut-2-en-1-yl)-*N*-(penta-2,4-dien-1-yl)benzenesulfonamide (3.51)
¹H NMR (500 MHz, CDCl₃)



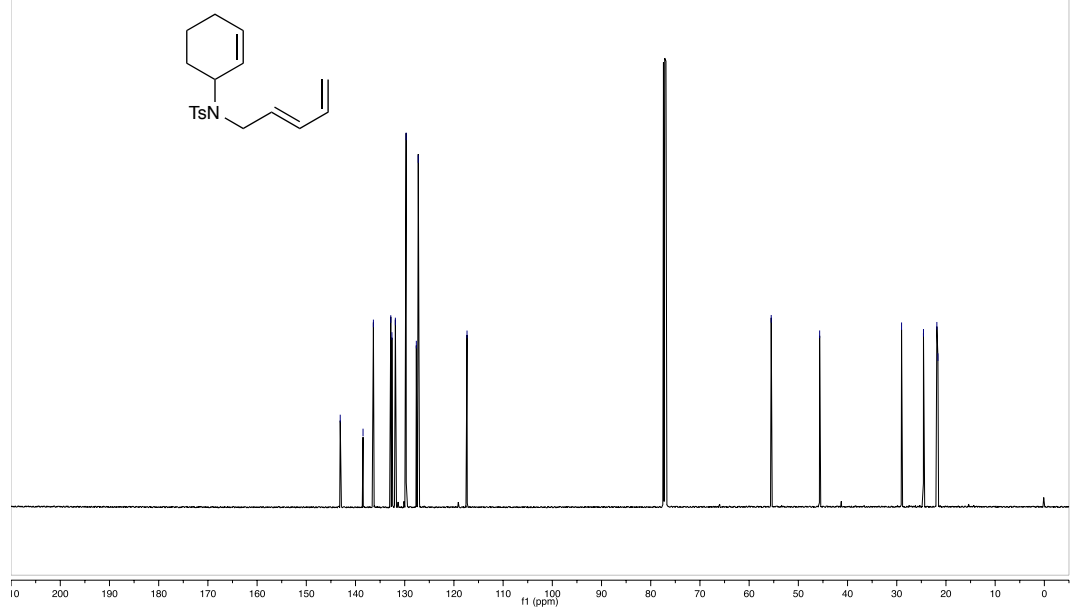
(*E*)-4-methyl-*N*-(3-methylbut-2-en-1-yl)-*N*-(penta-2,4-dien-1-yl)benzenesulfonamide (3.51)
¹³C NMR (125 MHz, CDCl₃)

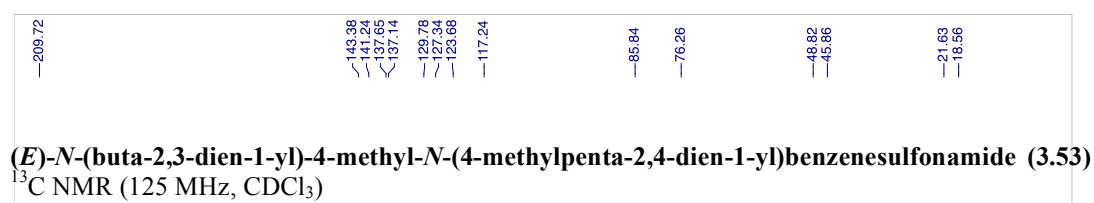
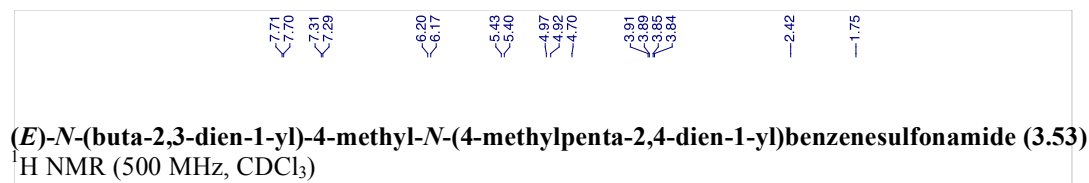


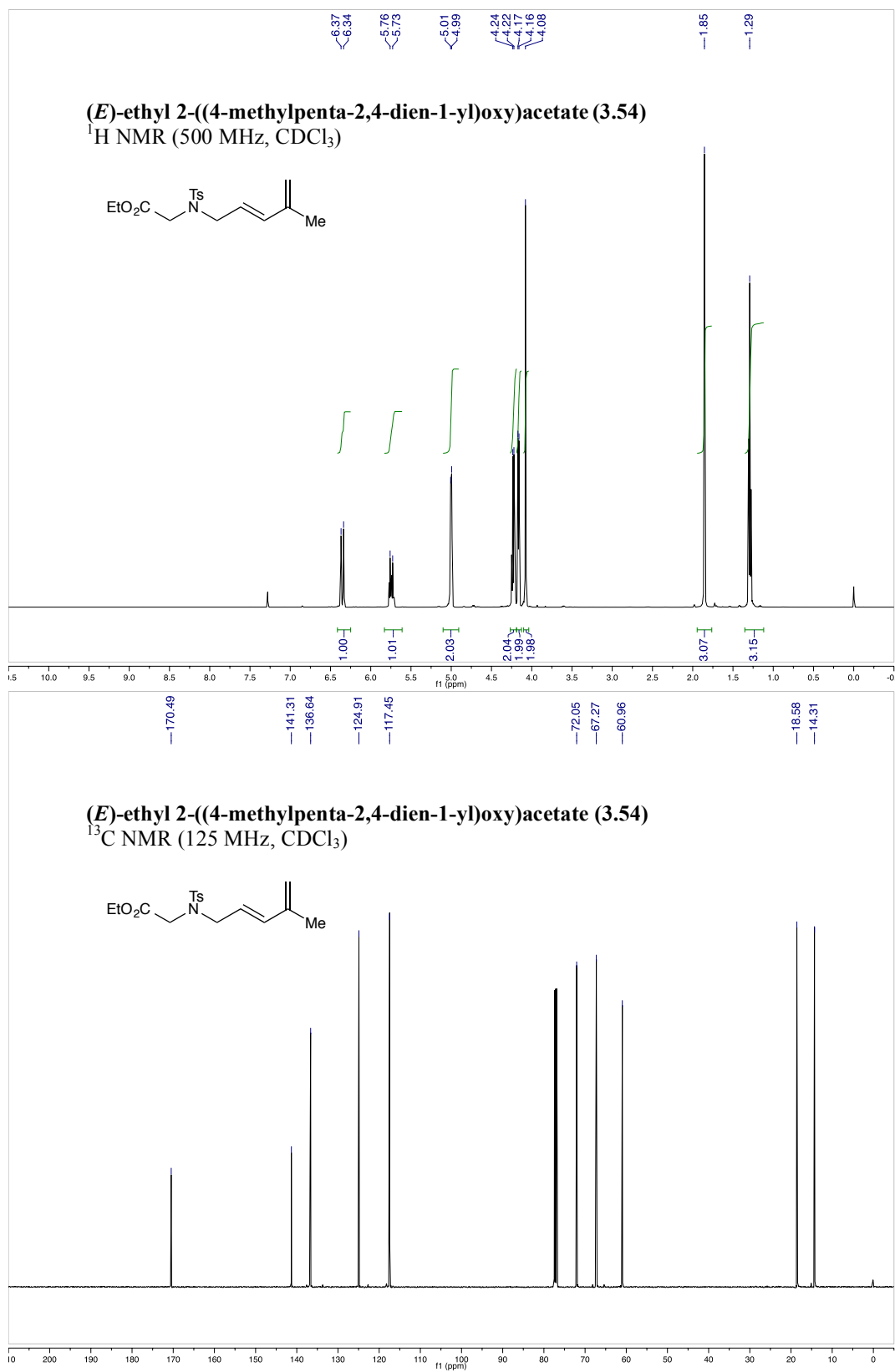
(*E*)-*N*-(cyclohex-2-en-1-yl)-4-methyl-*N*-(penta-2,4-dien-1-yl)benzenesulfonamide (3.52)
¹H NMR (500 MHz, CDCl₃)

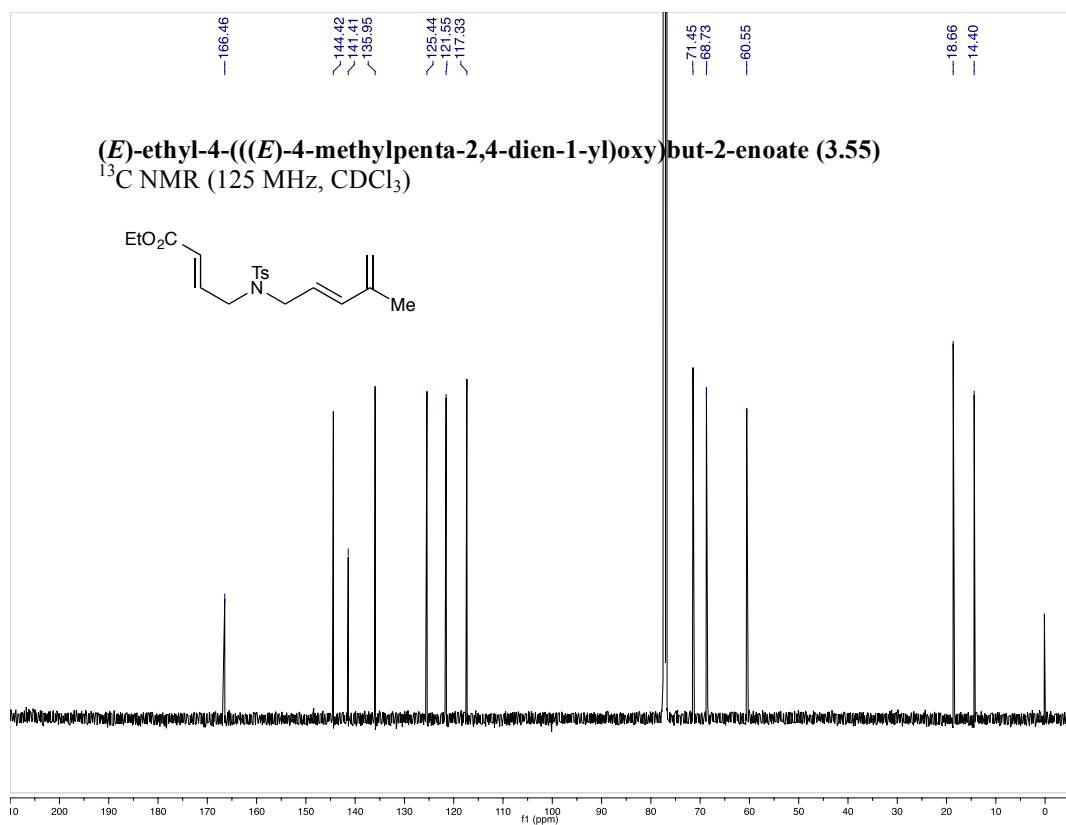
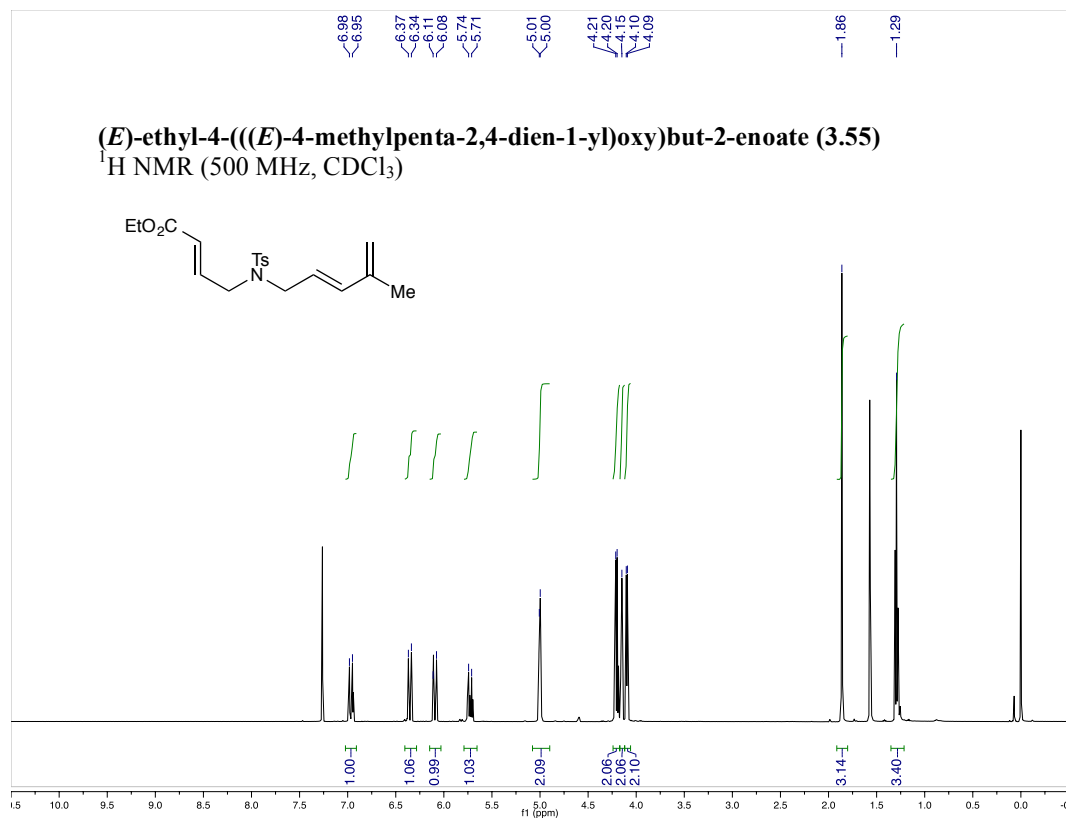


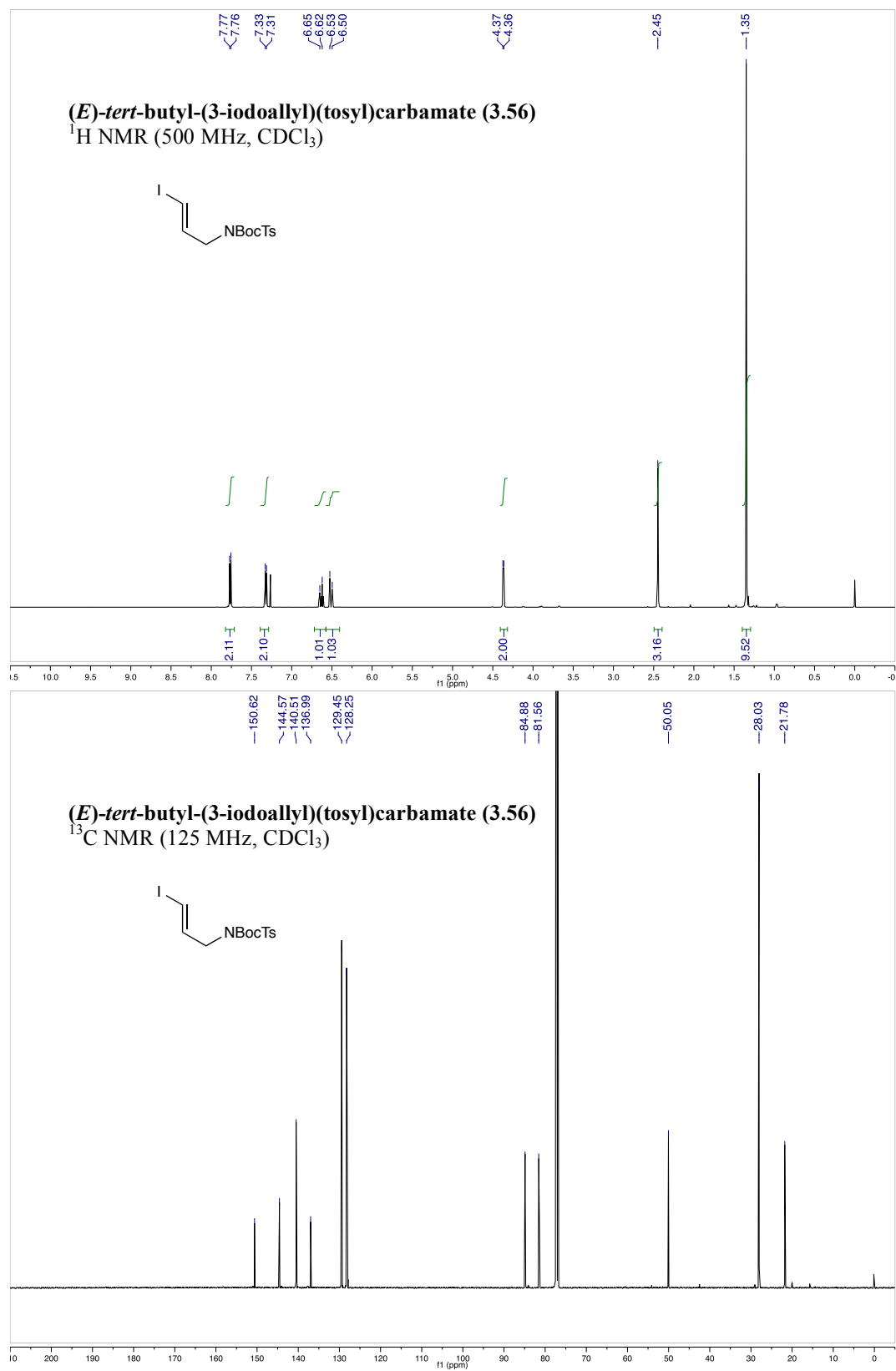
(*E*)-*N*-(cyclohex-2-en-1-yl)-4-methyl-*N*-(penta-2,4-dien-1-yl)benzenesulfonamide (3.52)
¹³C NMR (125 MHz, CDCl₃)

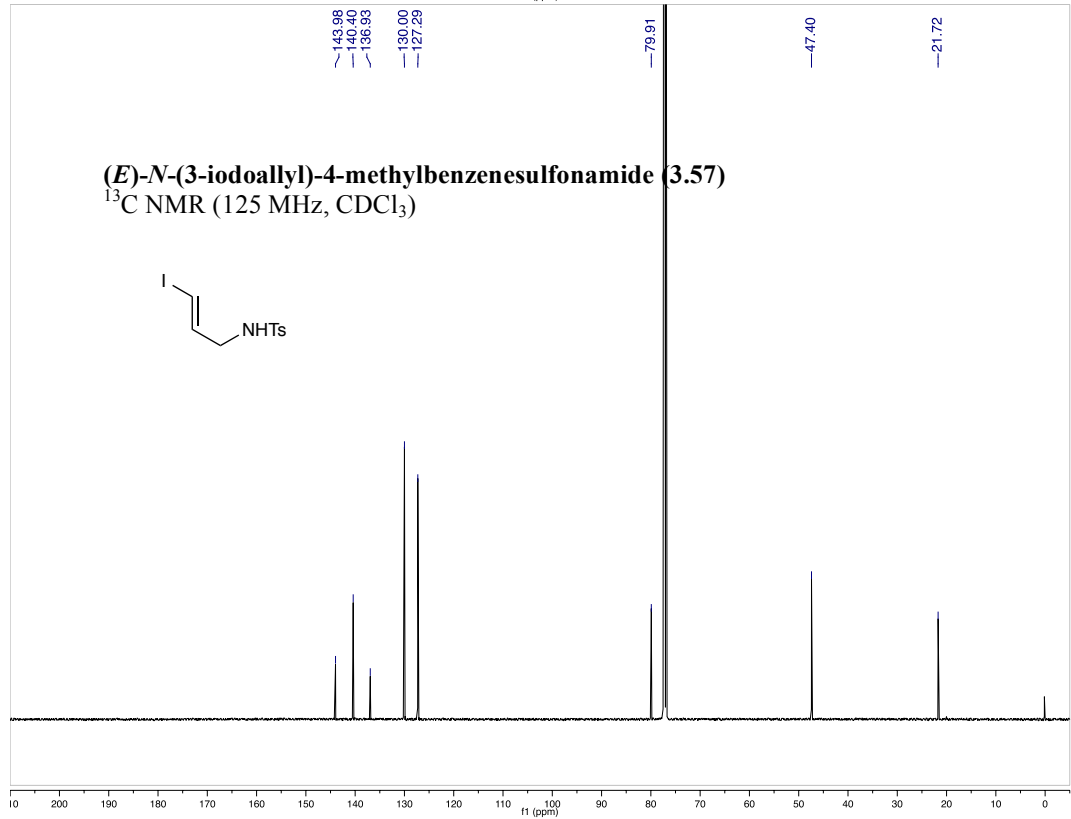
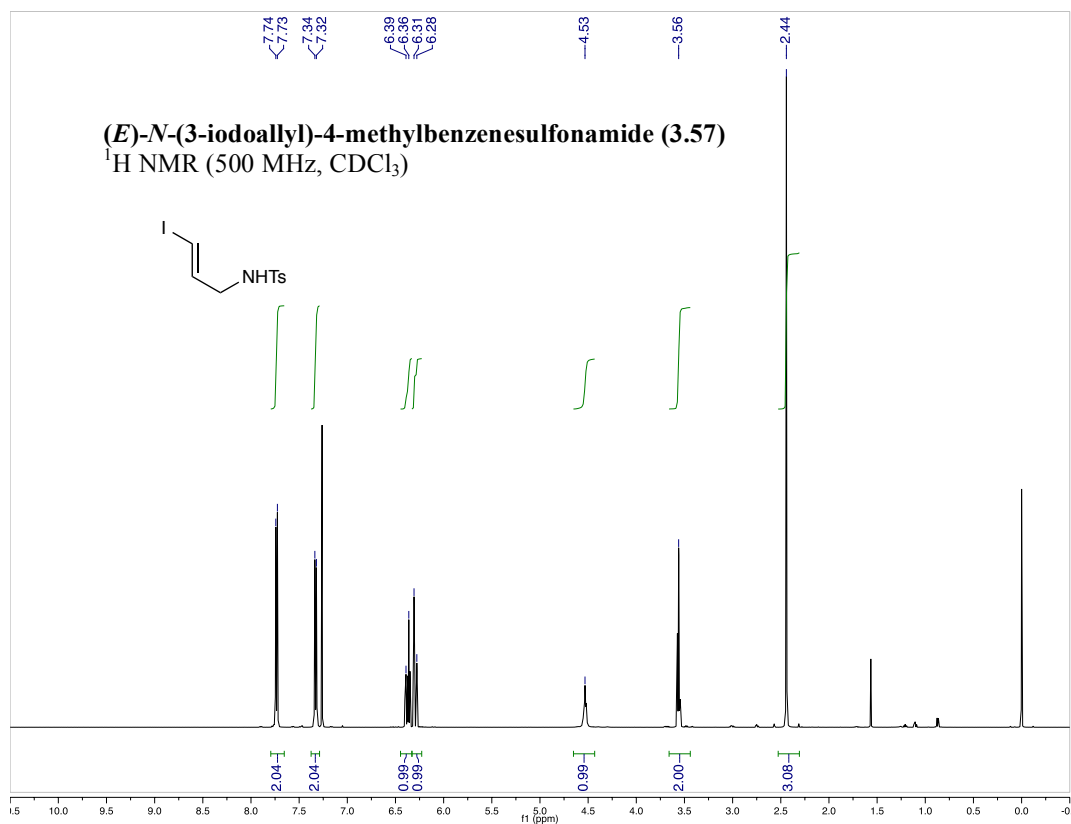


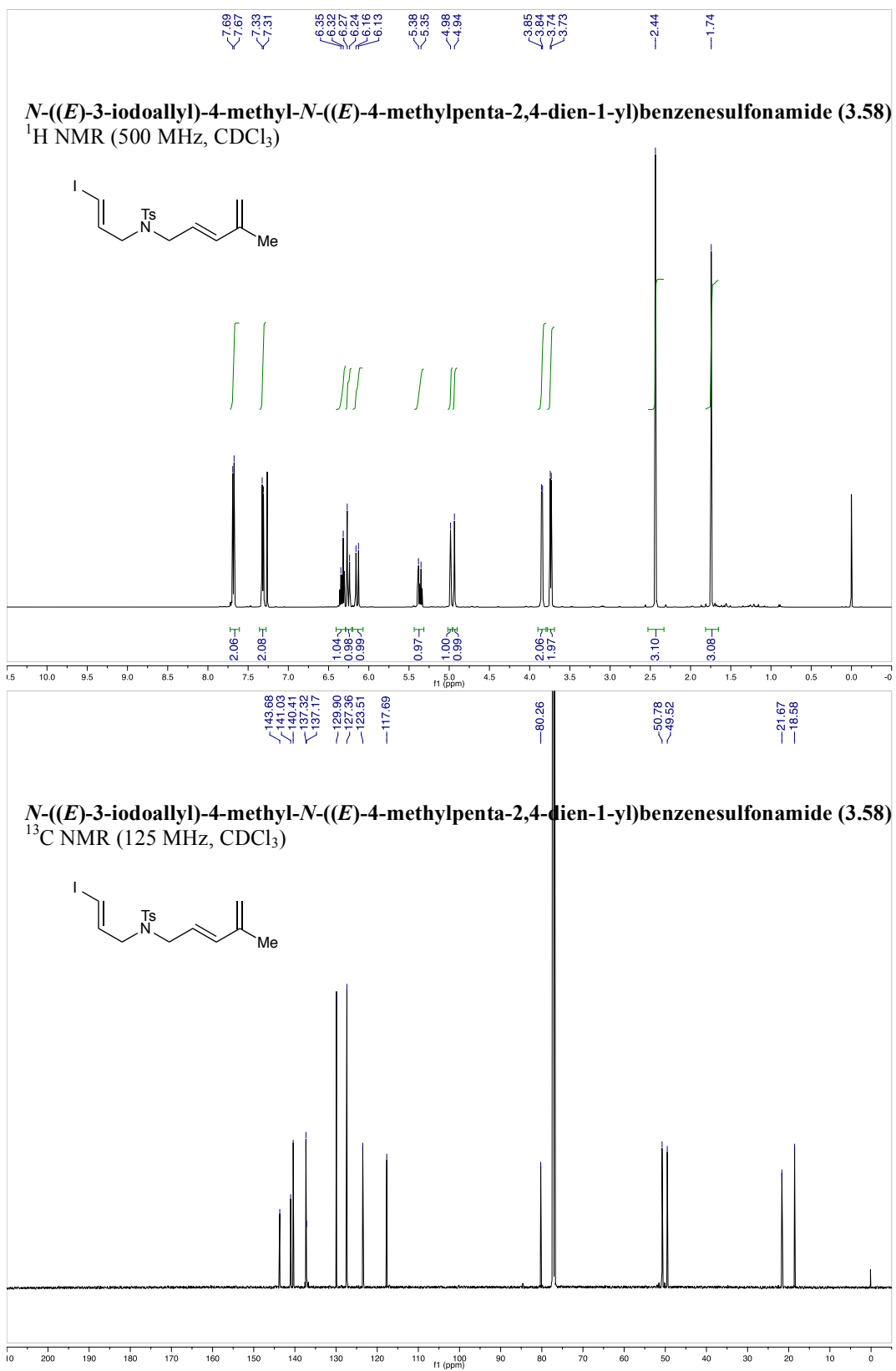


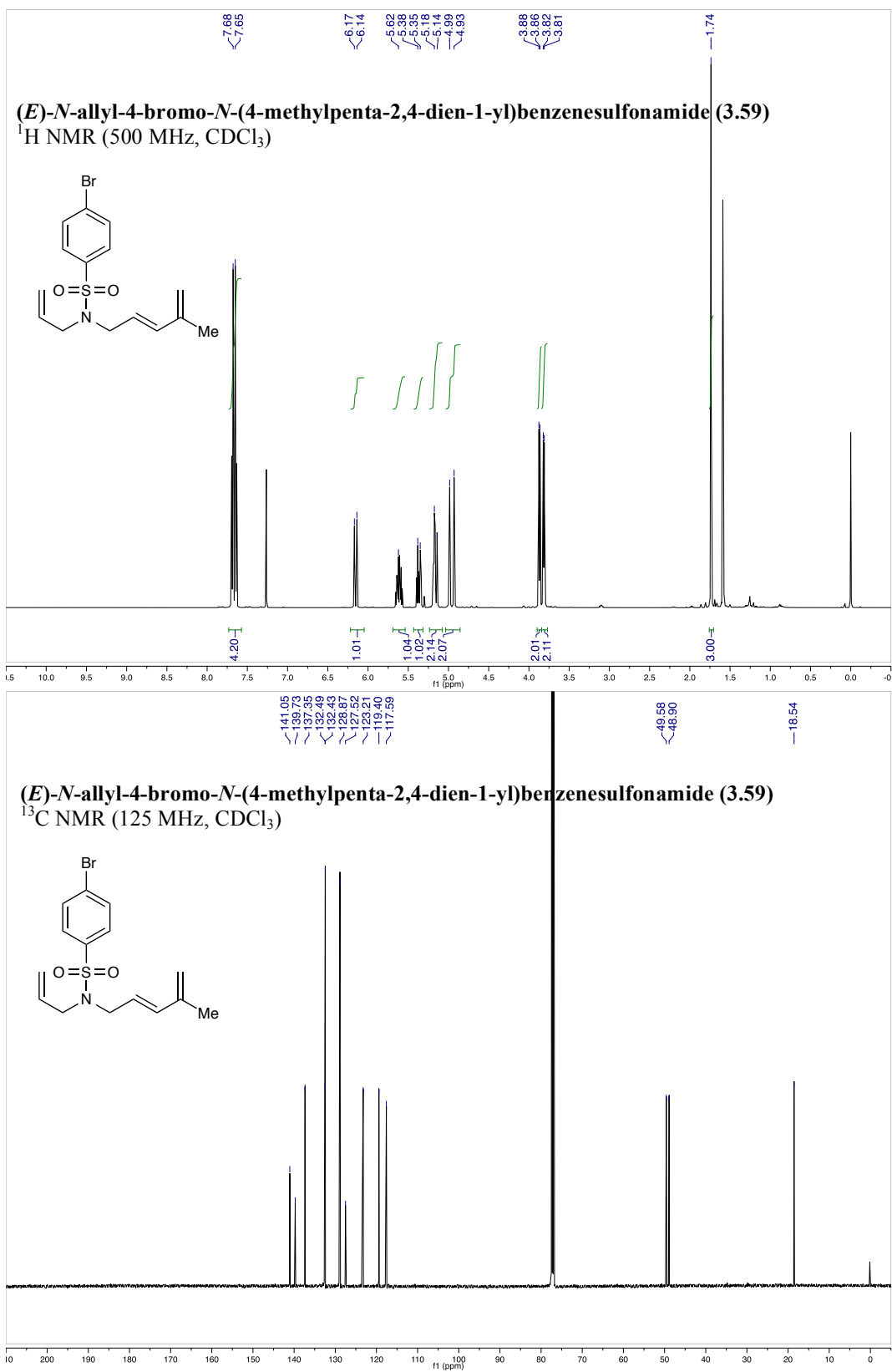


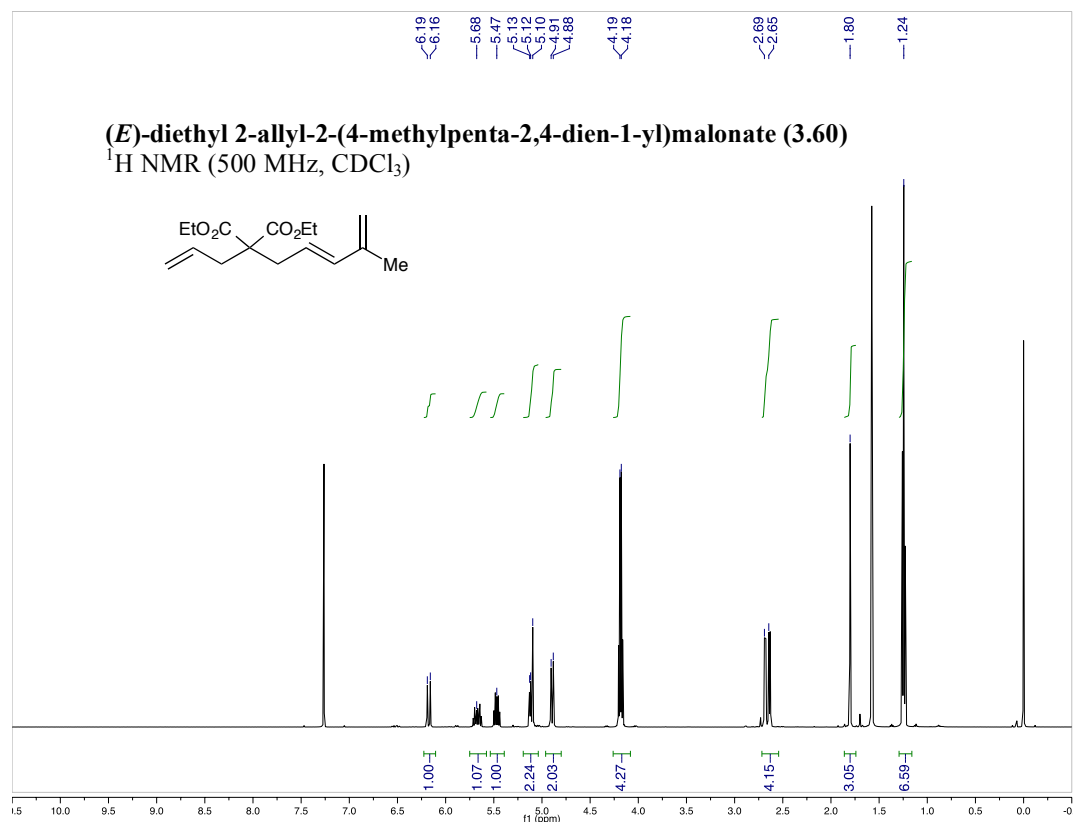
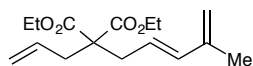
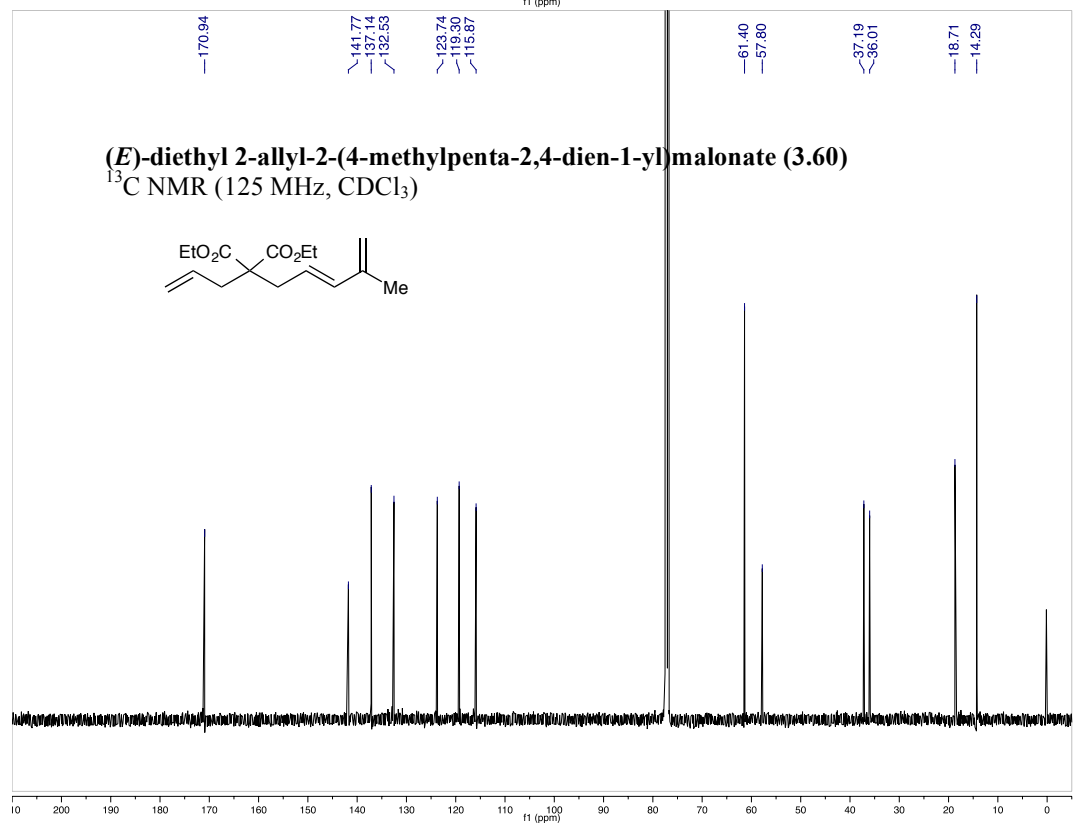
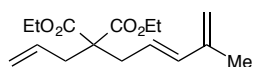


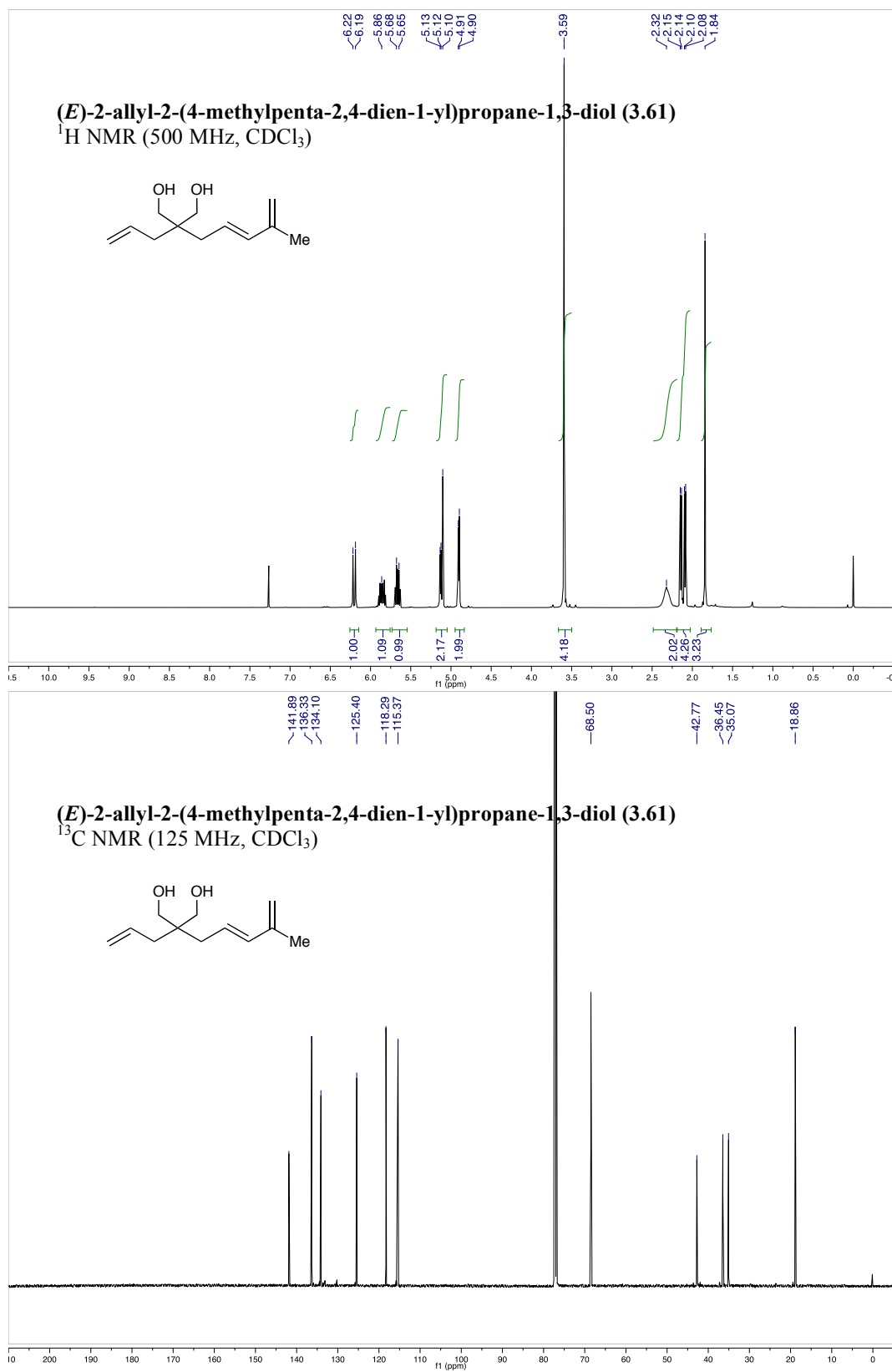


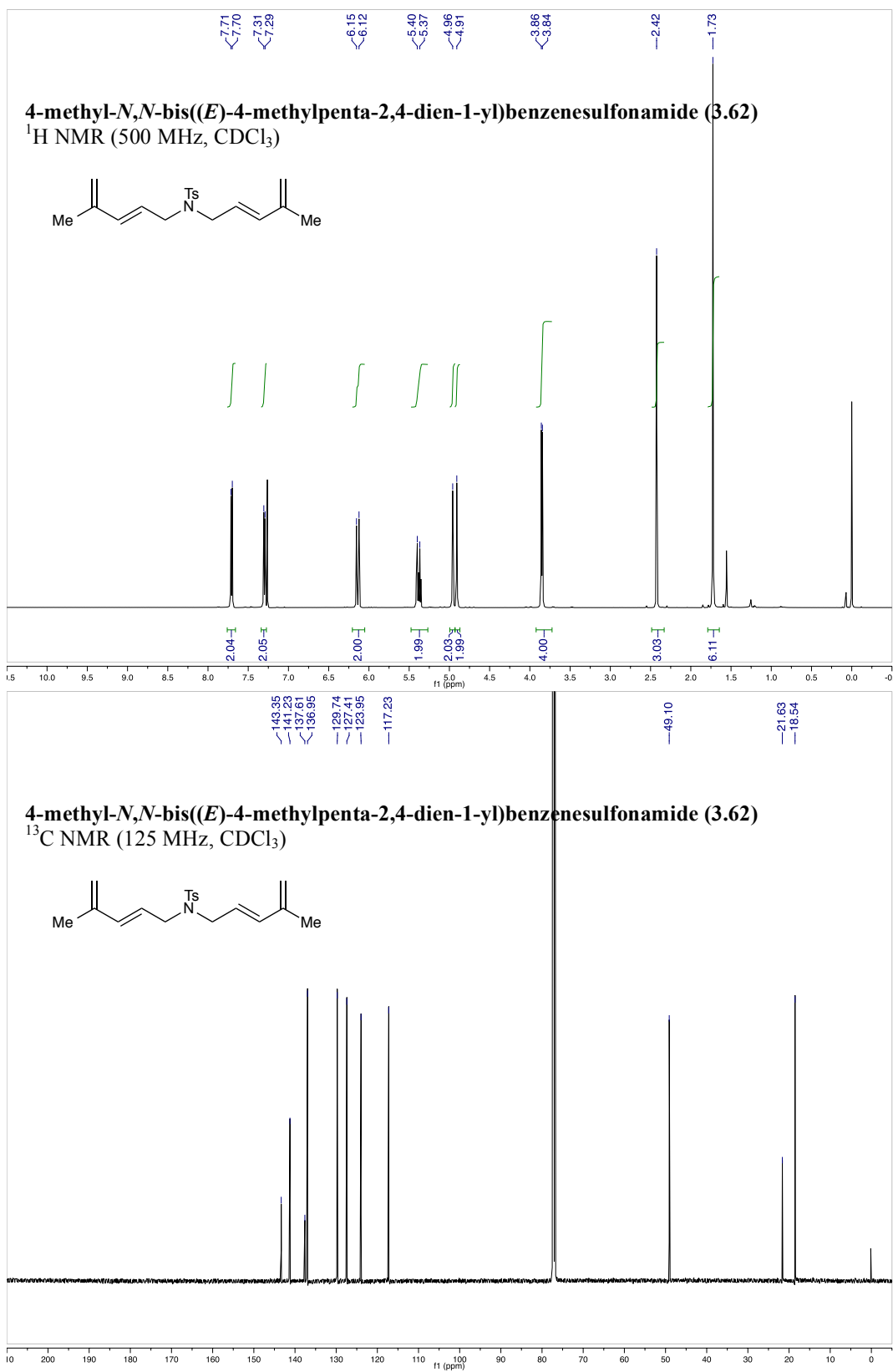


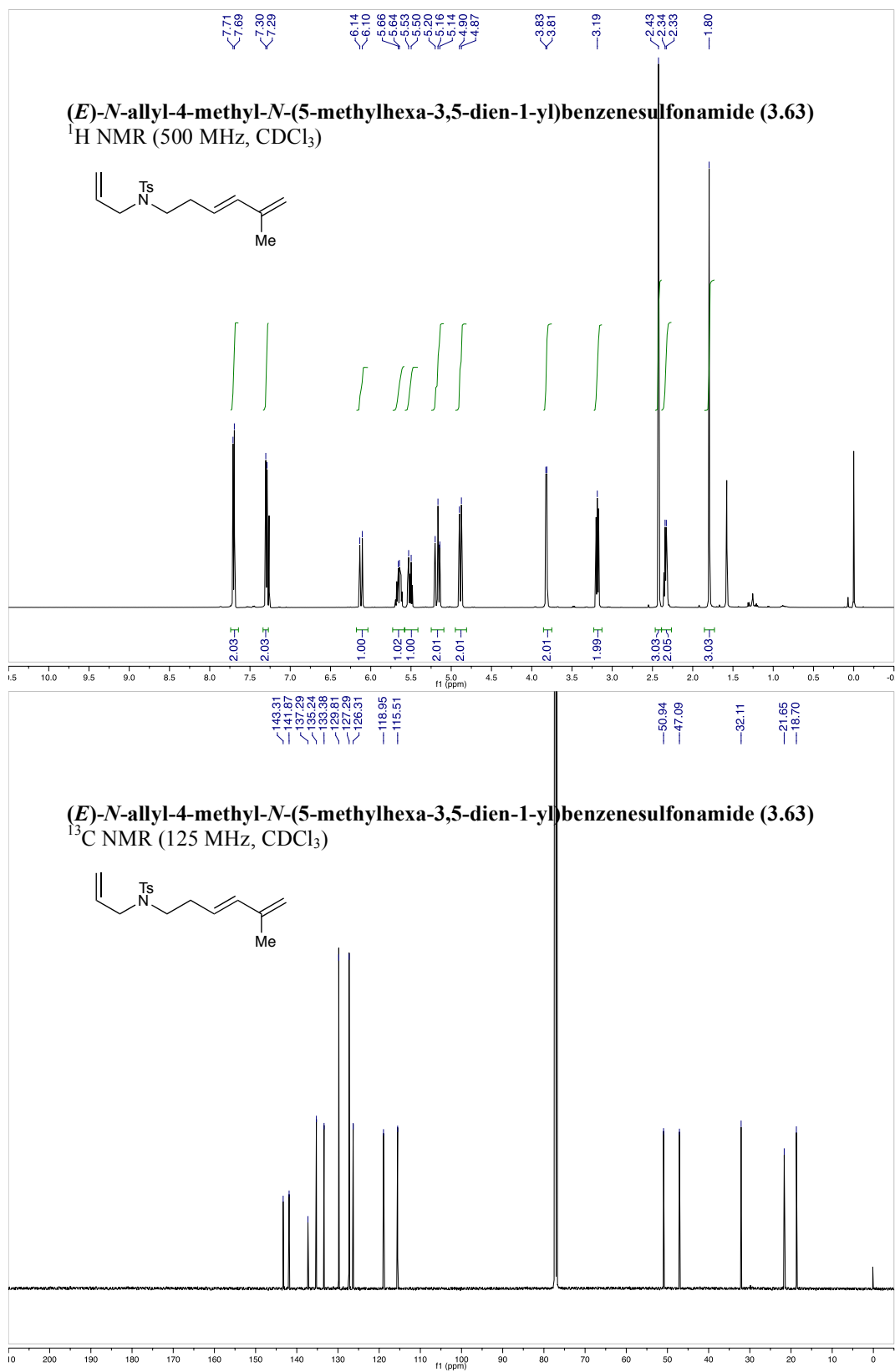


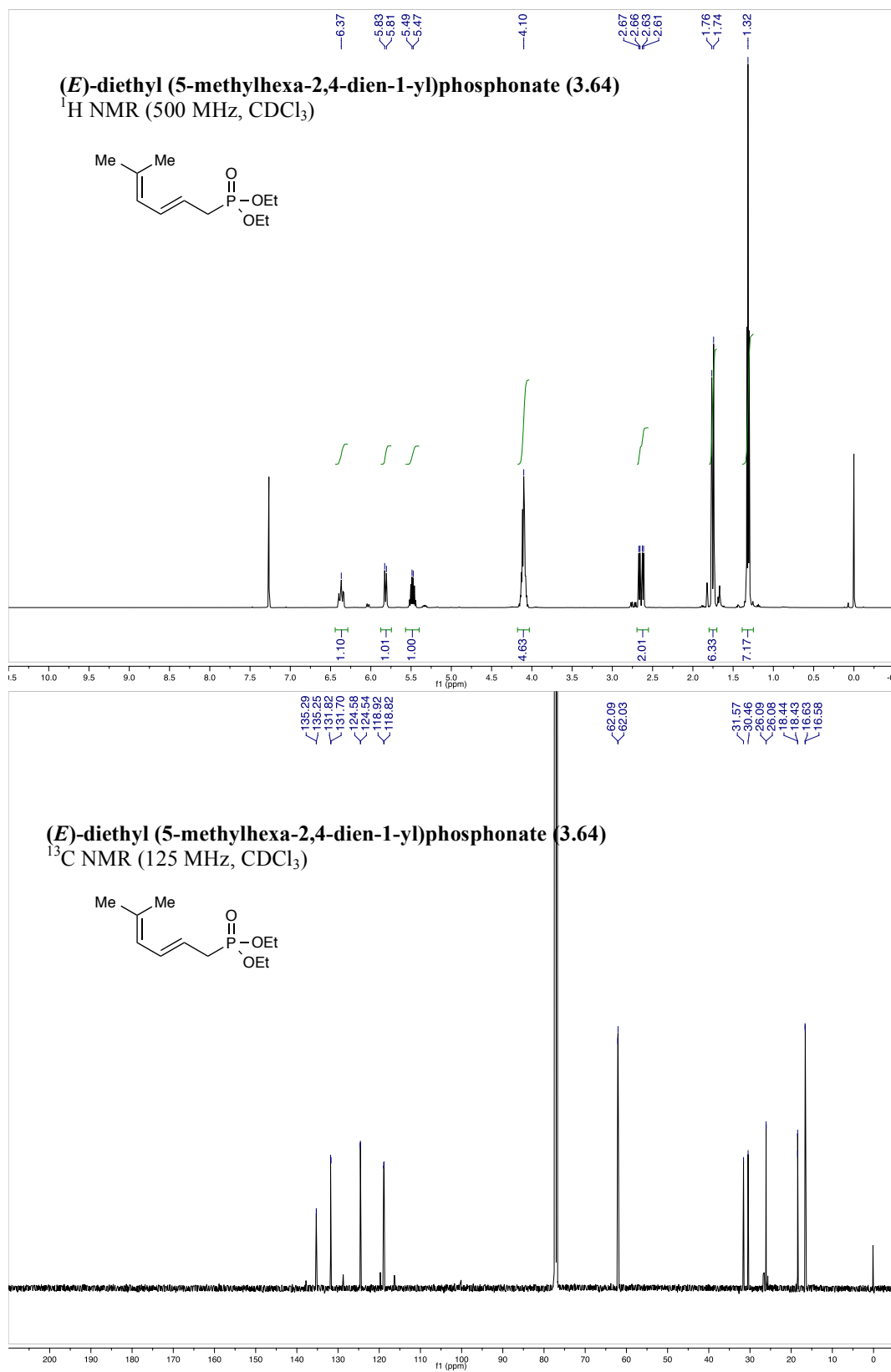


(E)-diethyl 2-allyl-2-(4-methylpenta-2,4-dien-1-yl)malonate (3.60)¹H NMR (500 MHz, CDCl₃)**(E)-diethyl 2-allyl-2-(4-methylpenta-2,4-dien-1-yl)malonate (3.60)**¹³C NMR (125 MHz, CDCl₃)

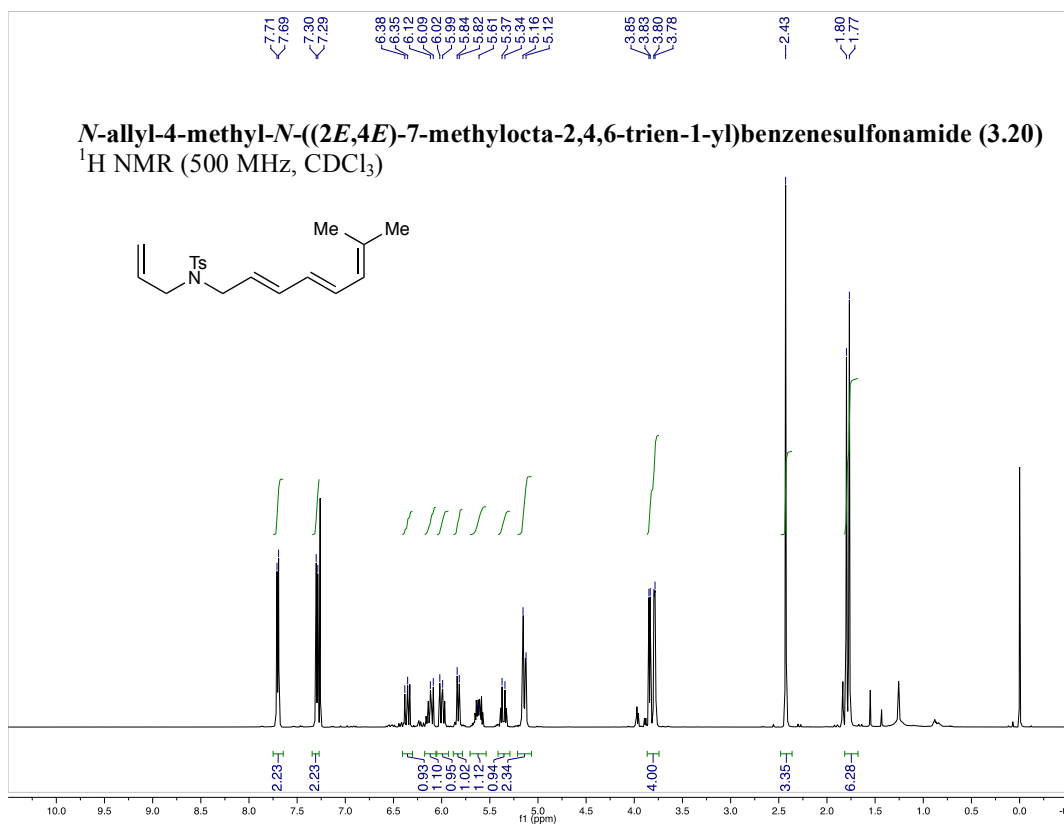




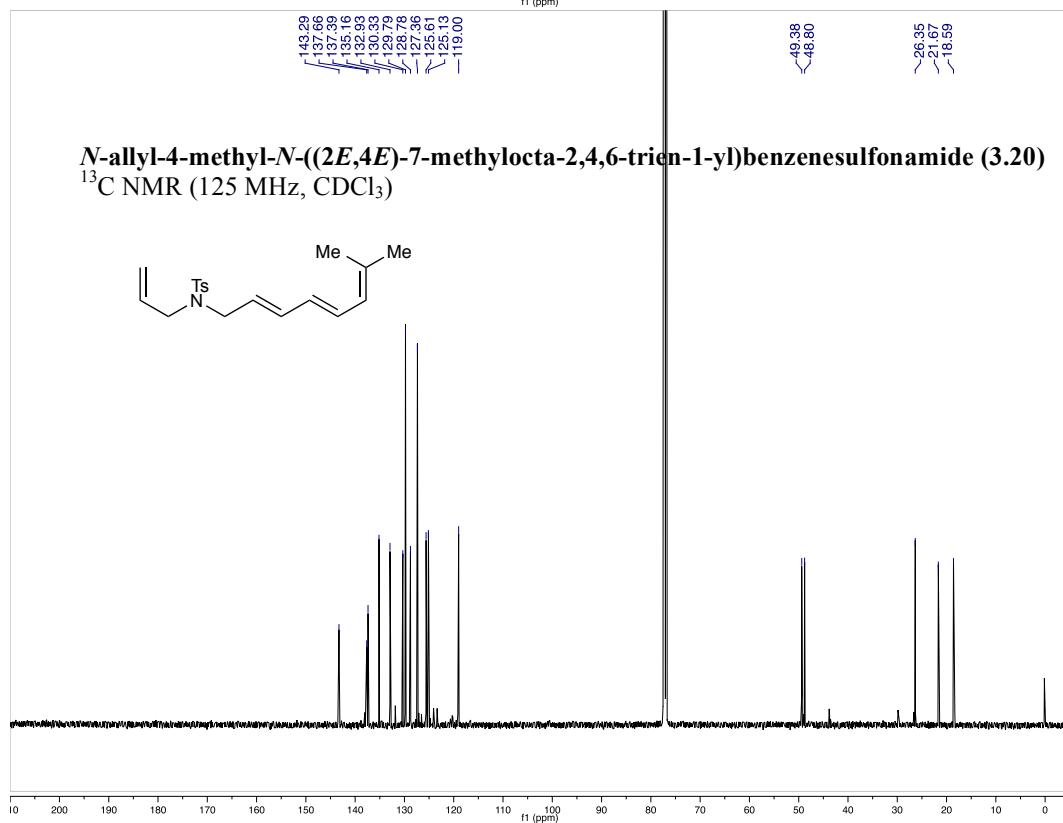


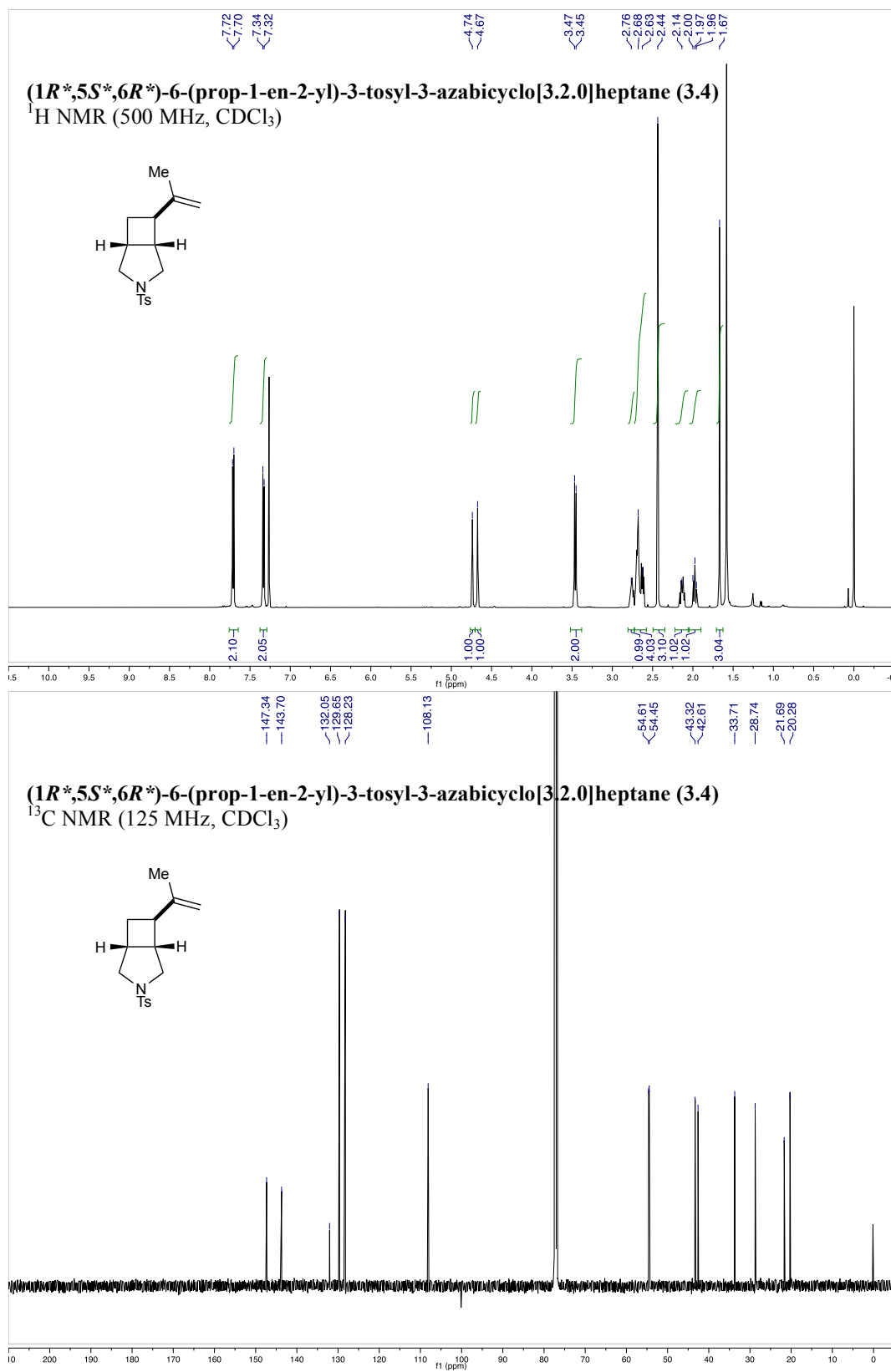


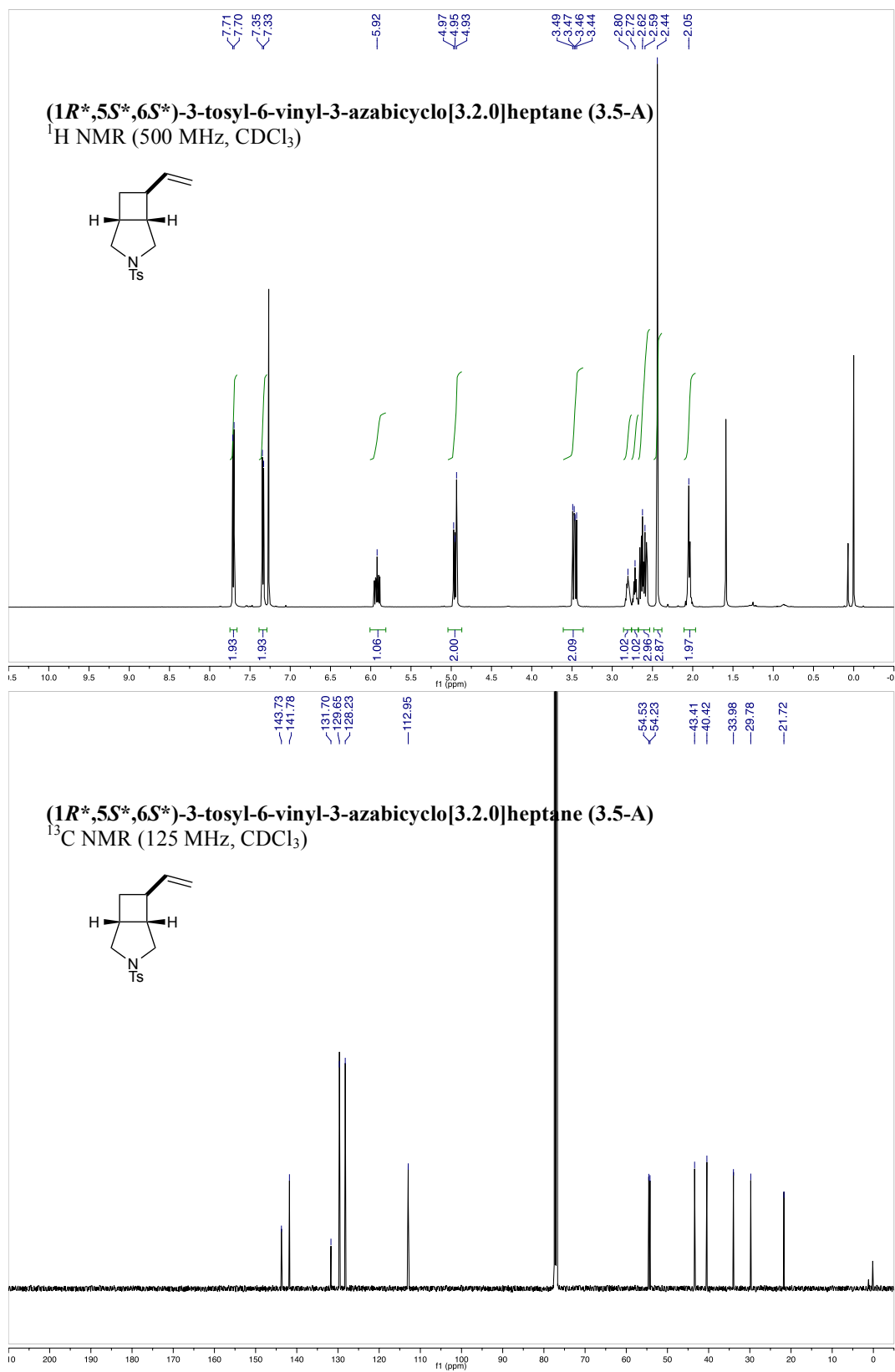
***N*-allyl-4-methyl-*N*-((2*E*,4*E*)-7-methylocta-2,4,6-trien-1-yl)benzenesulfonamide (3.20)**
¹H NMR (500 MHz, CDCl₃)

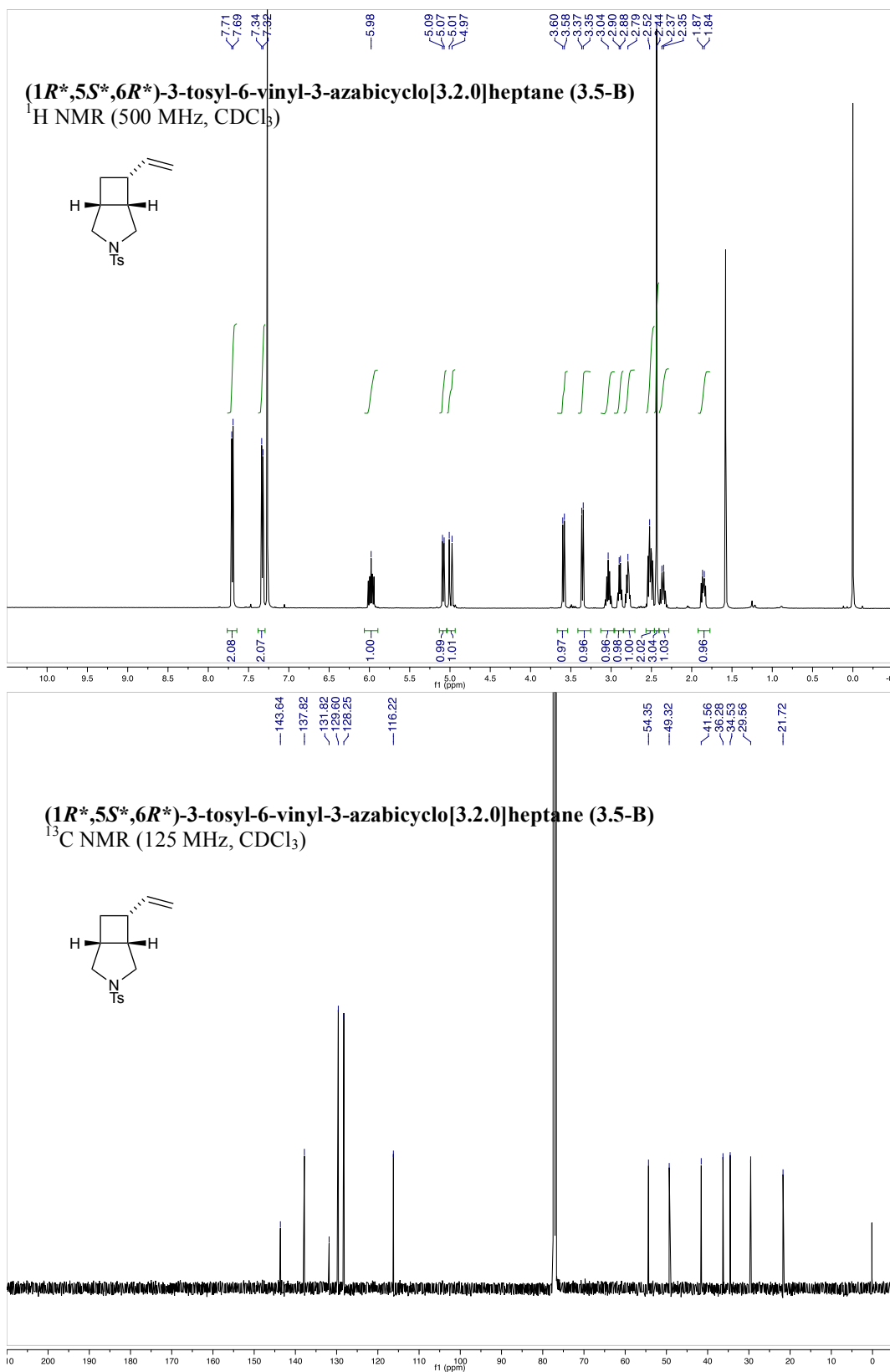


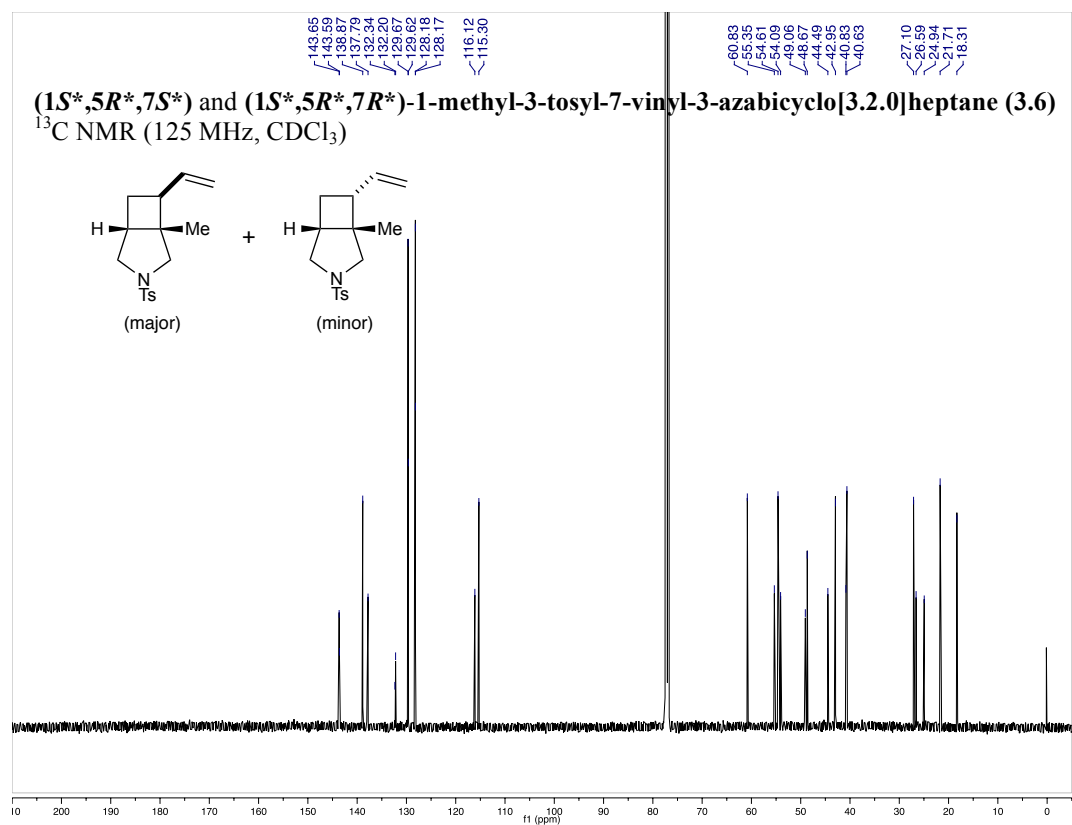
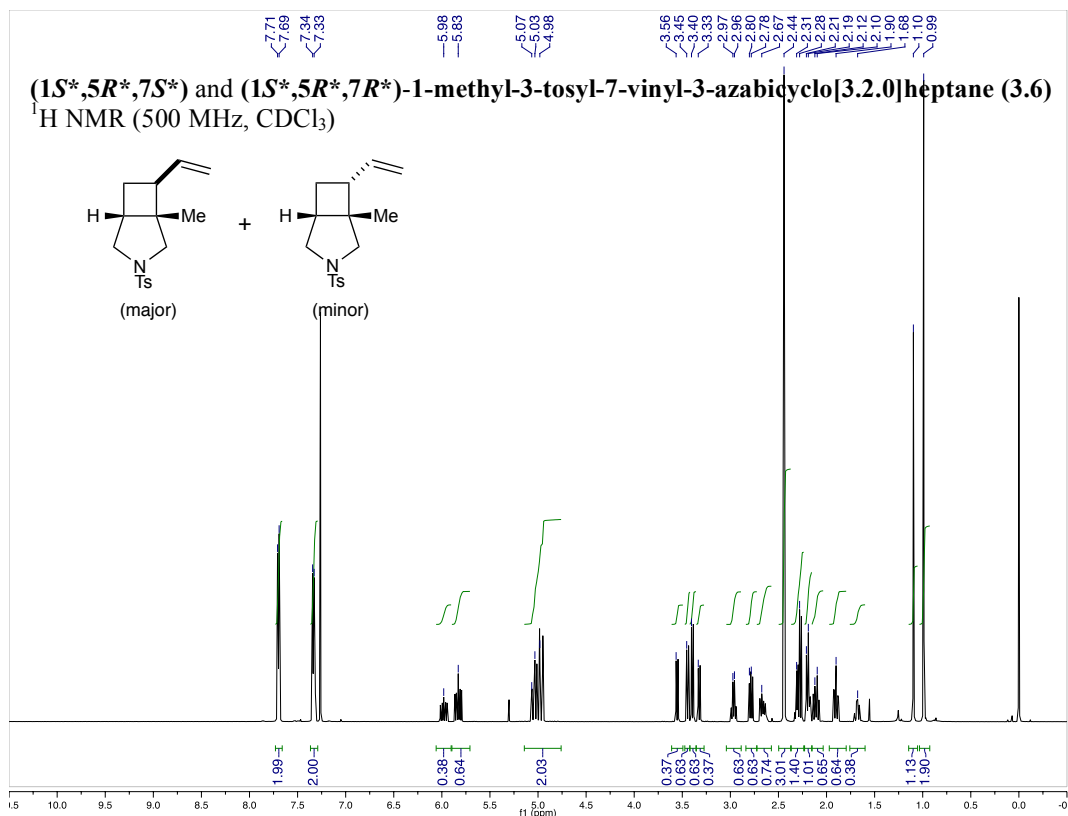
***N*-allyl-4-methyl-*N*-((2*E*,4*E*)-7-methylocta-2,4,6-trien-1-yl)benzenesulfonamide (3.20)**
¹³C NMR (125 MHz, CDCl₃)

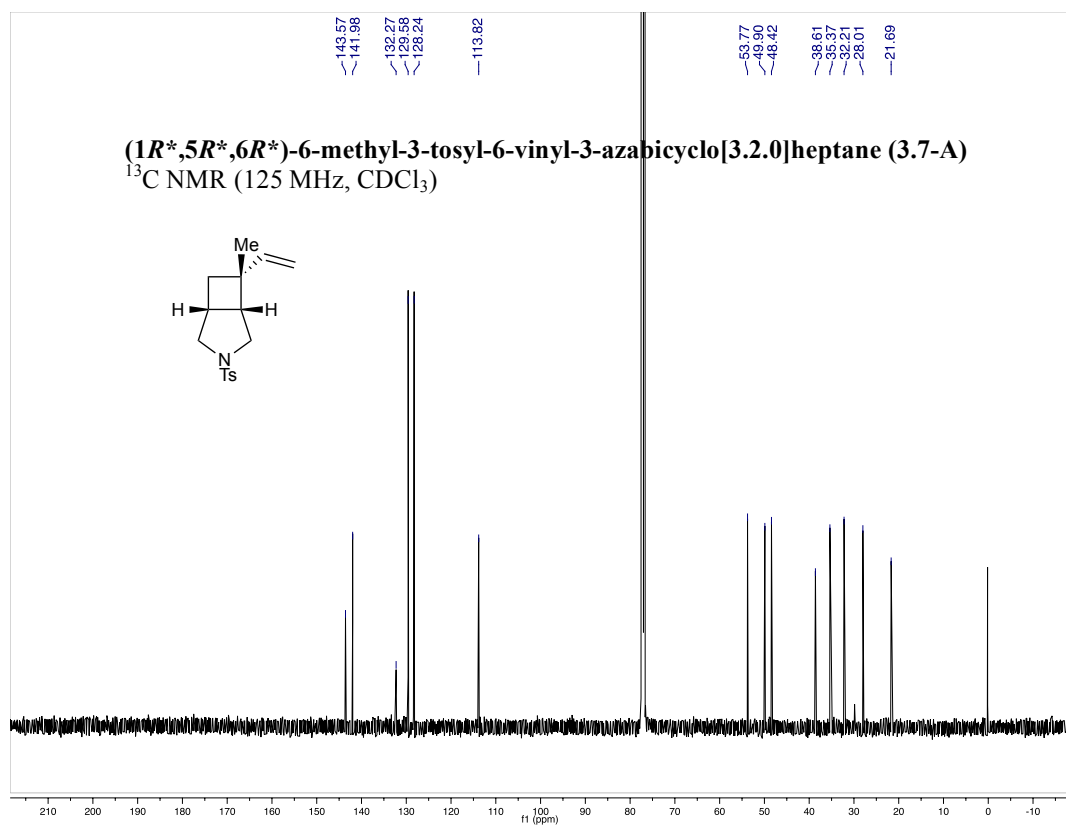
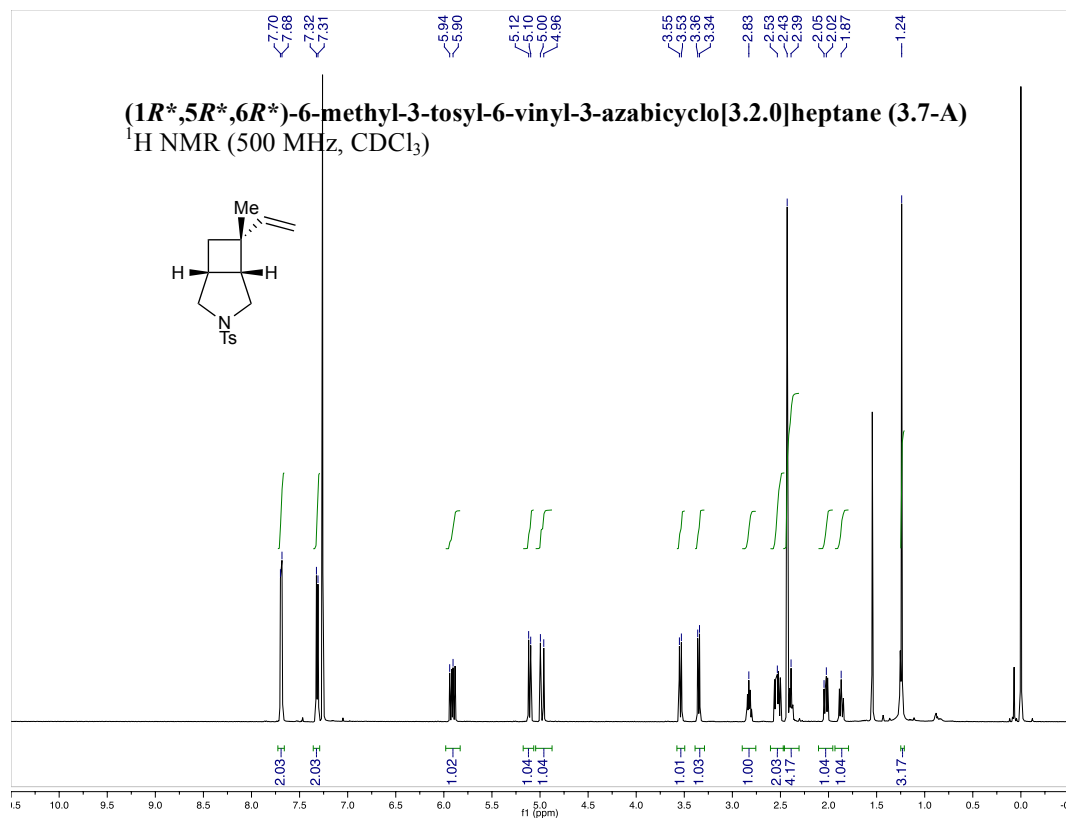


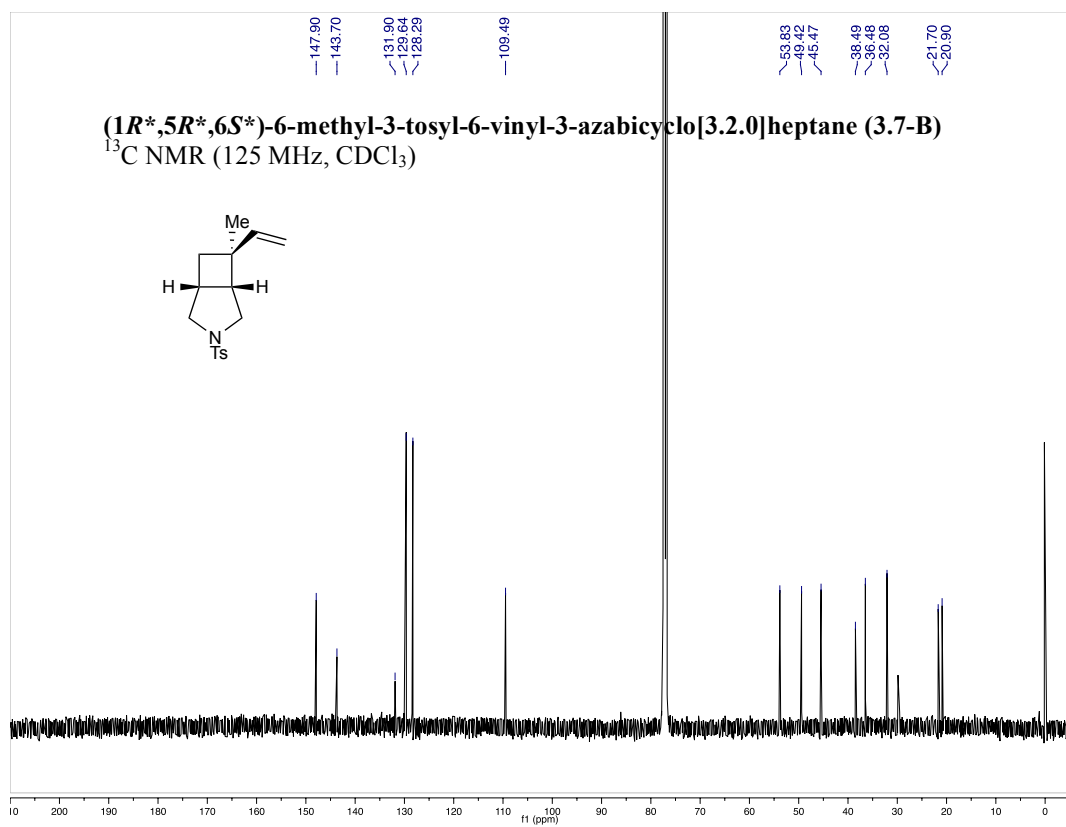
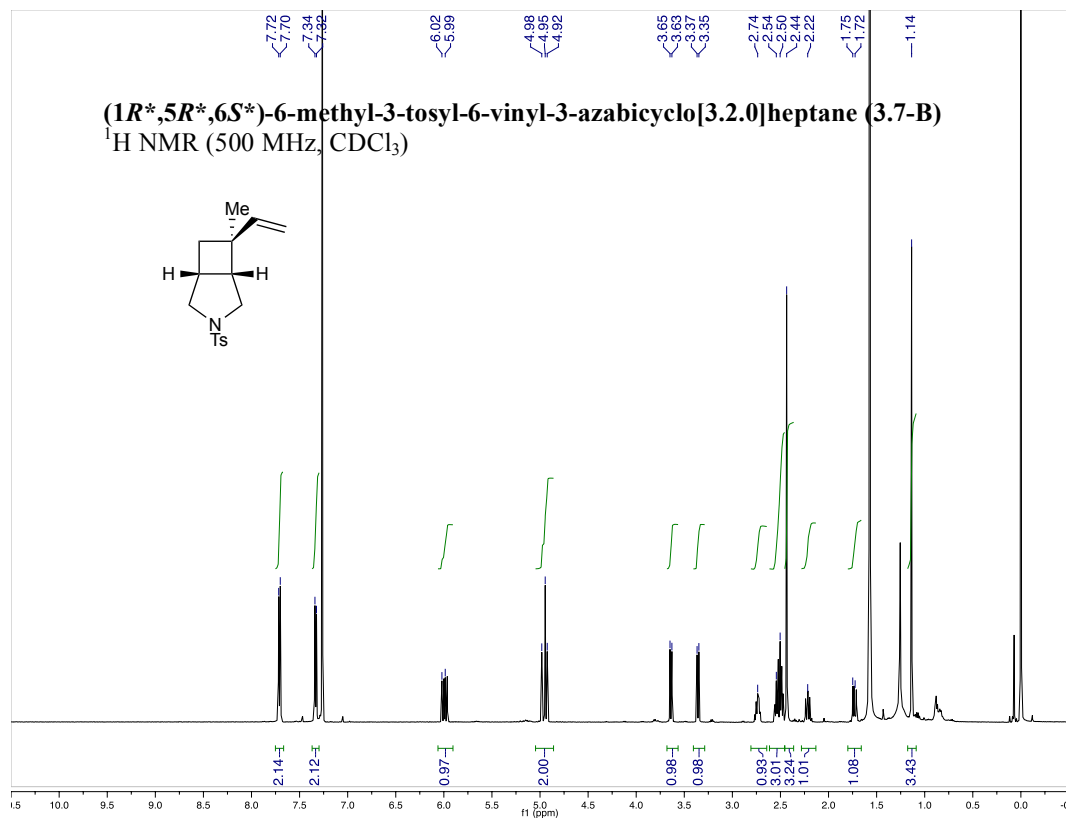


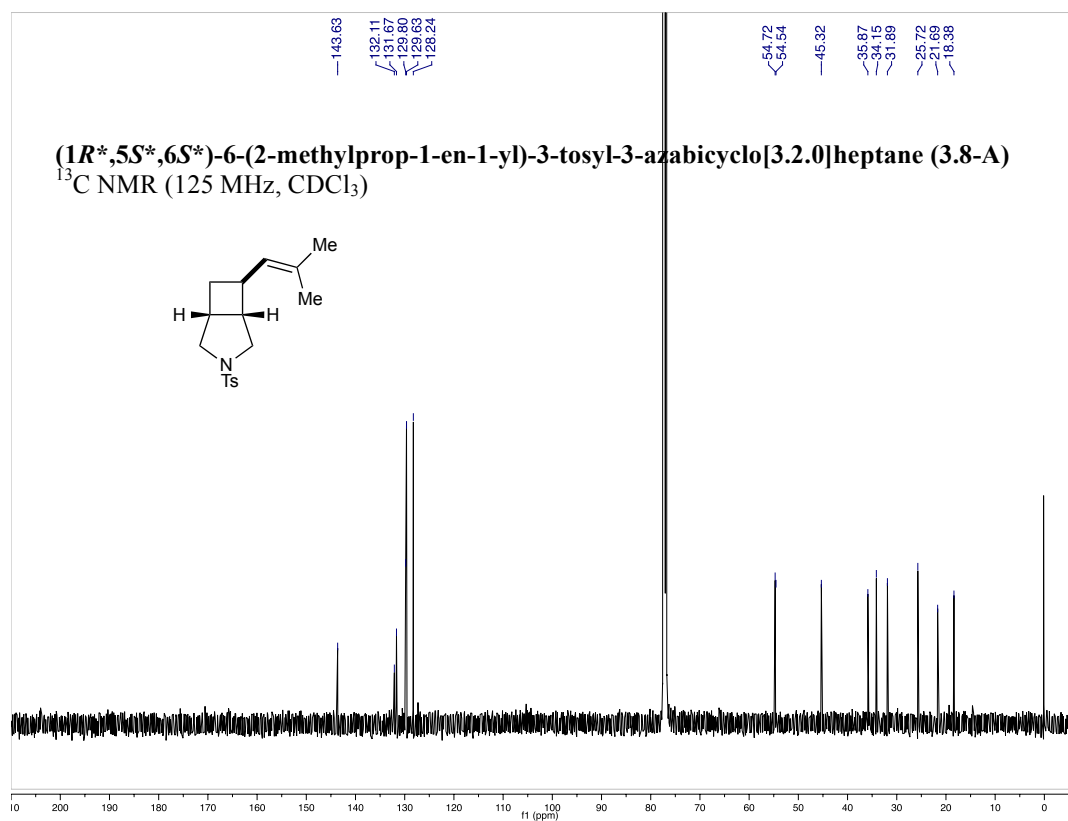
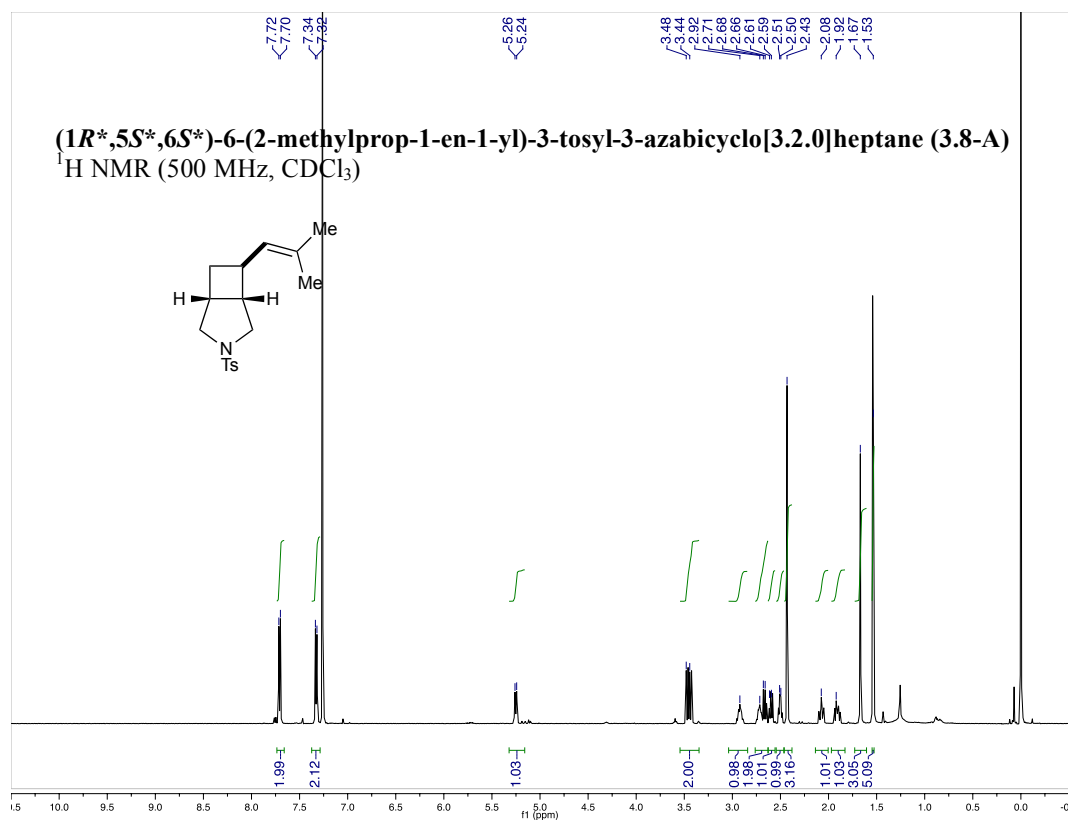


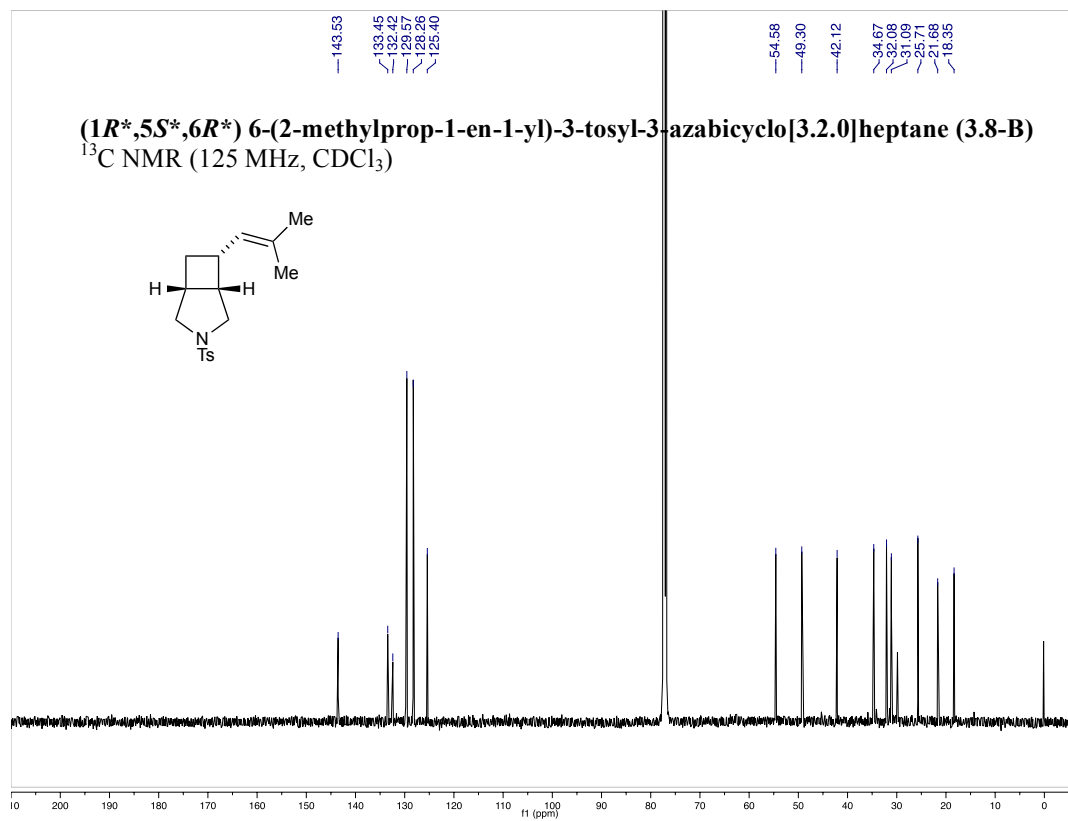
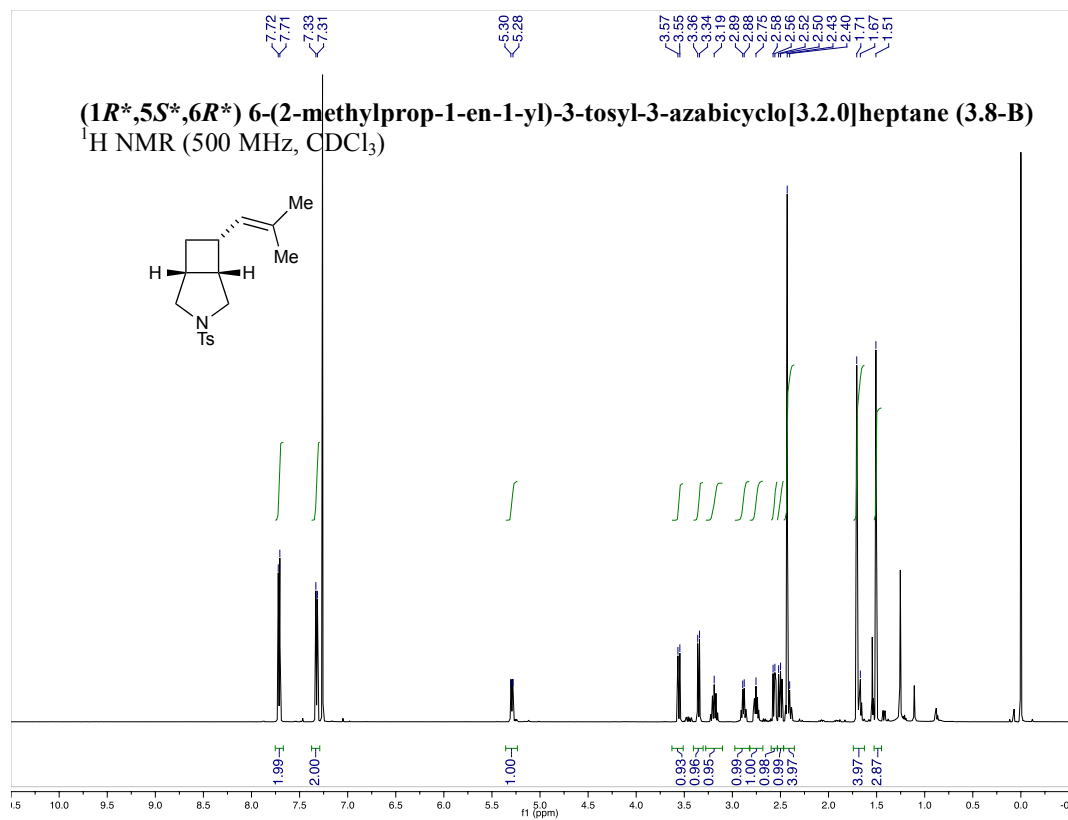


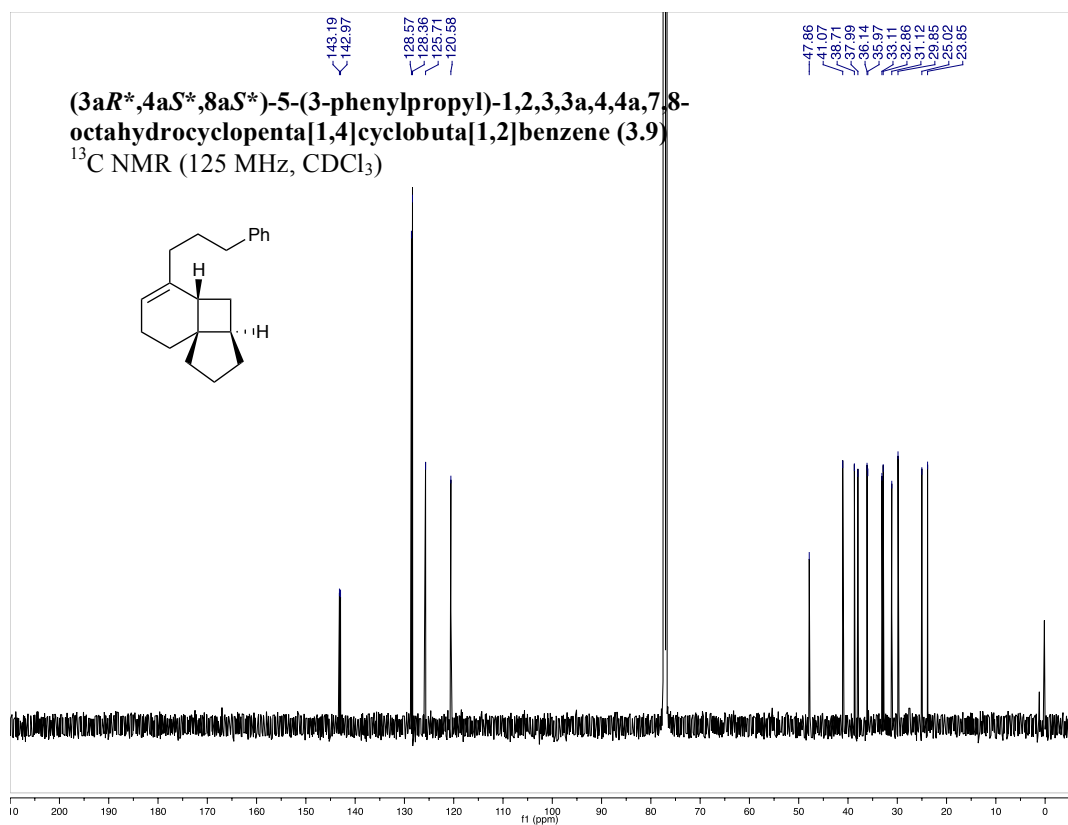
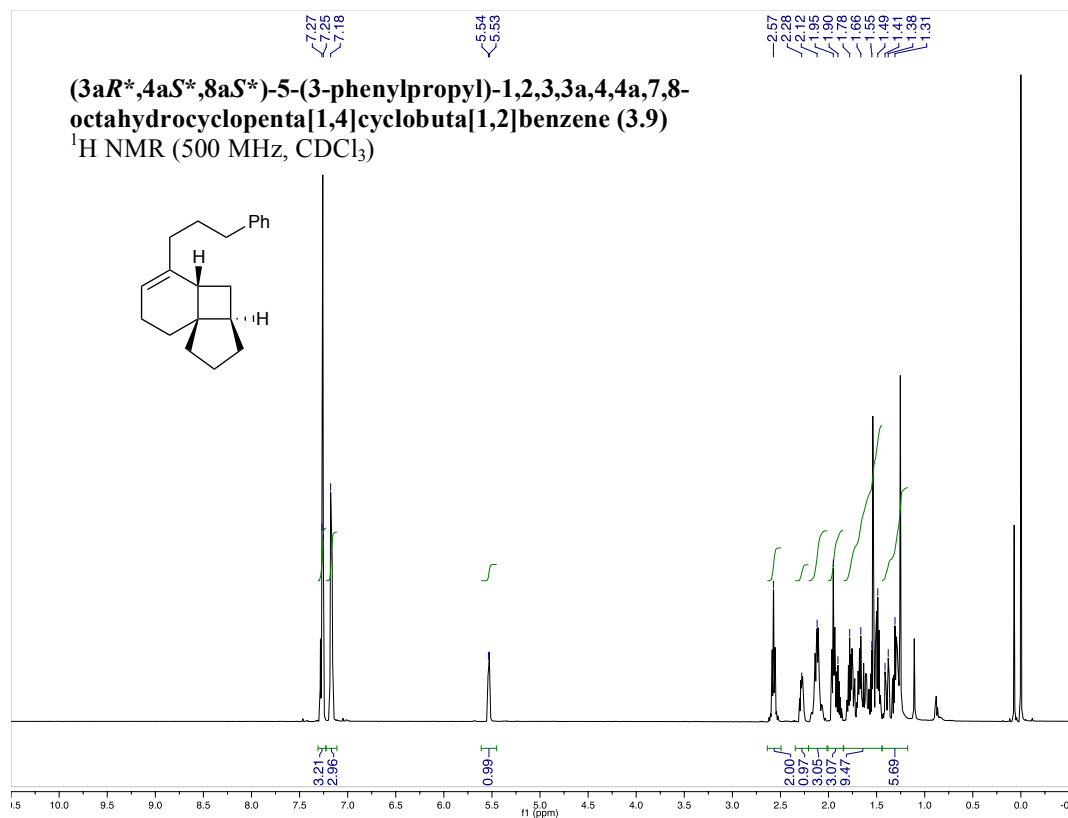


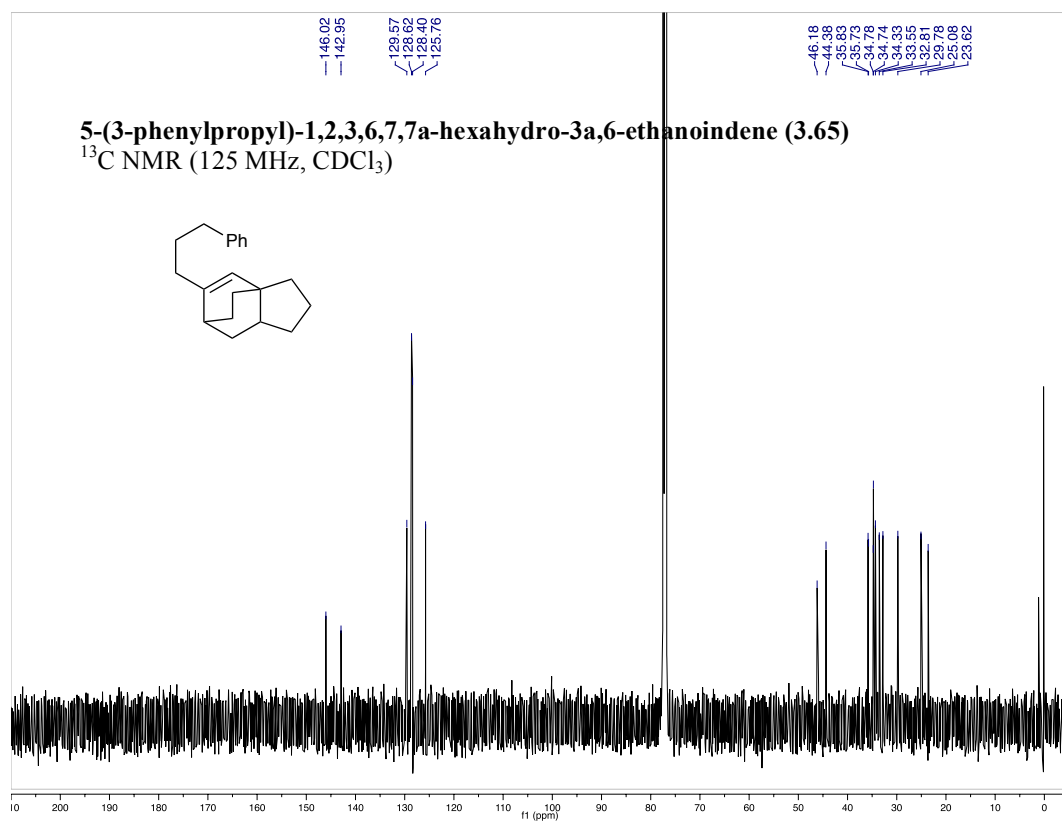
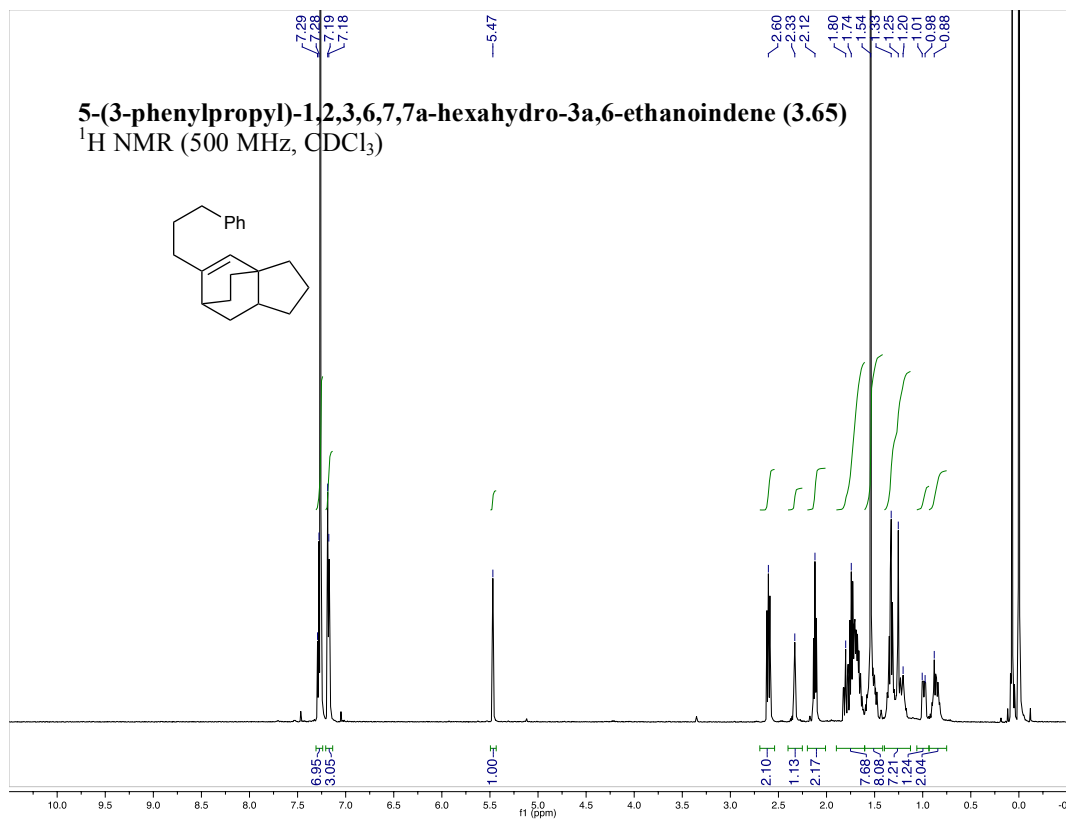


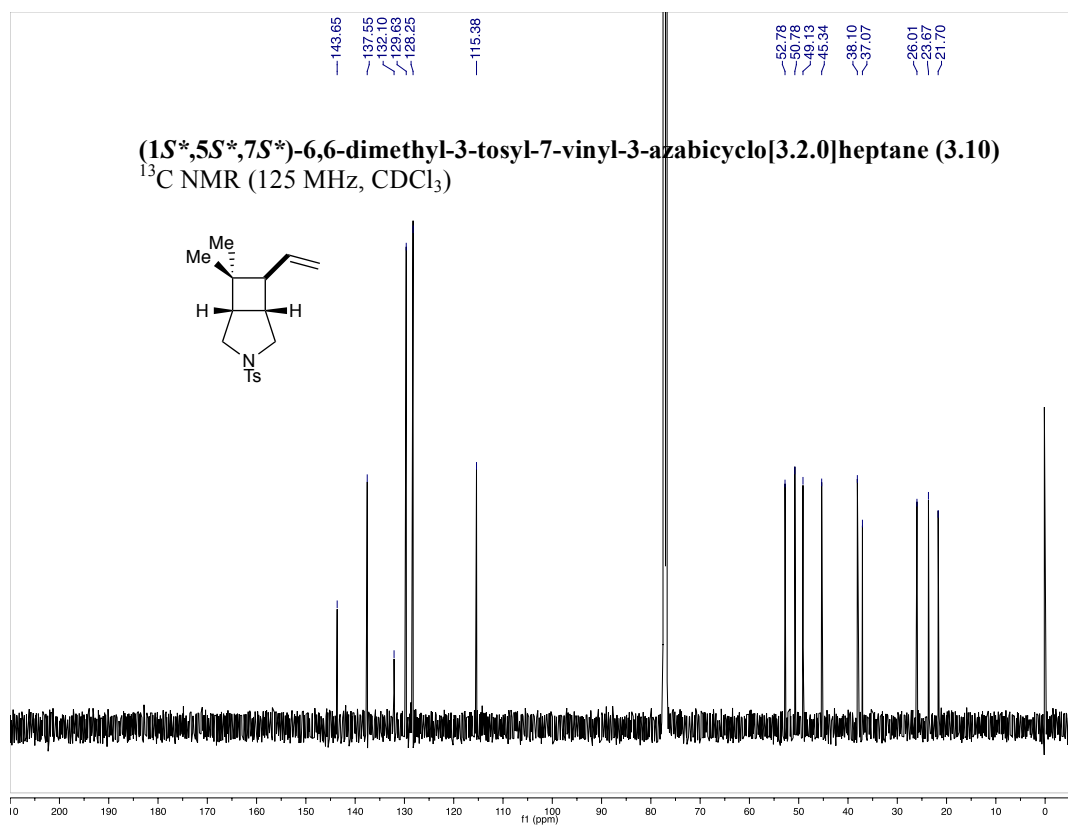
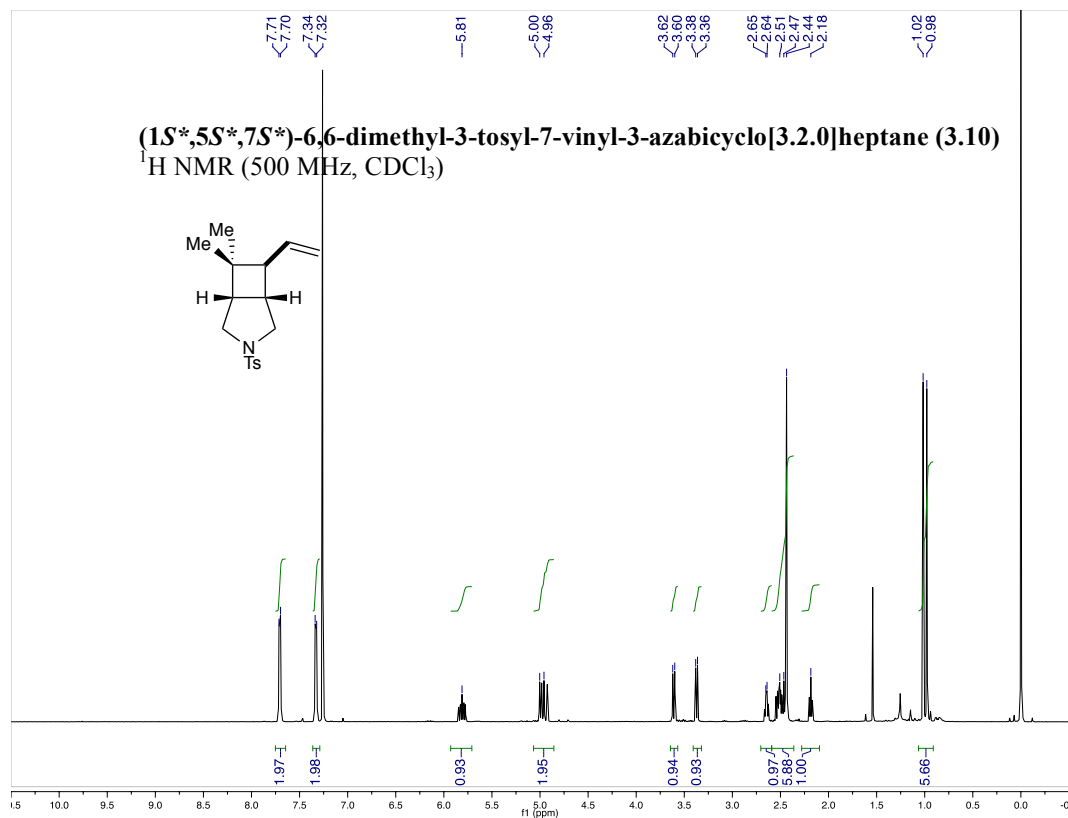


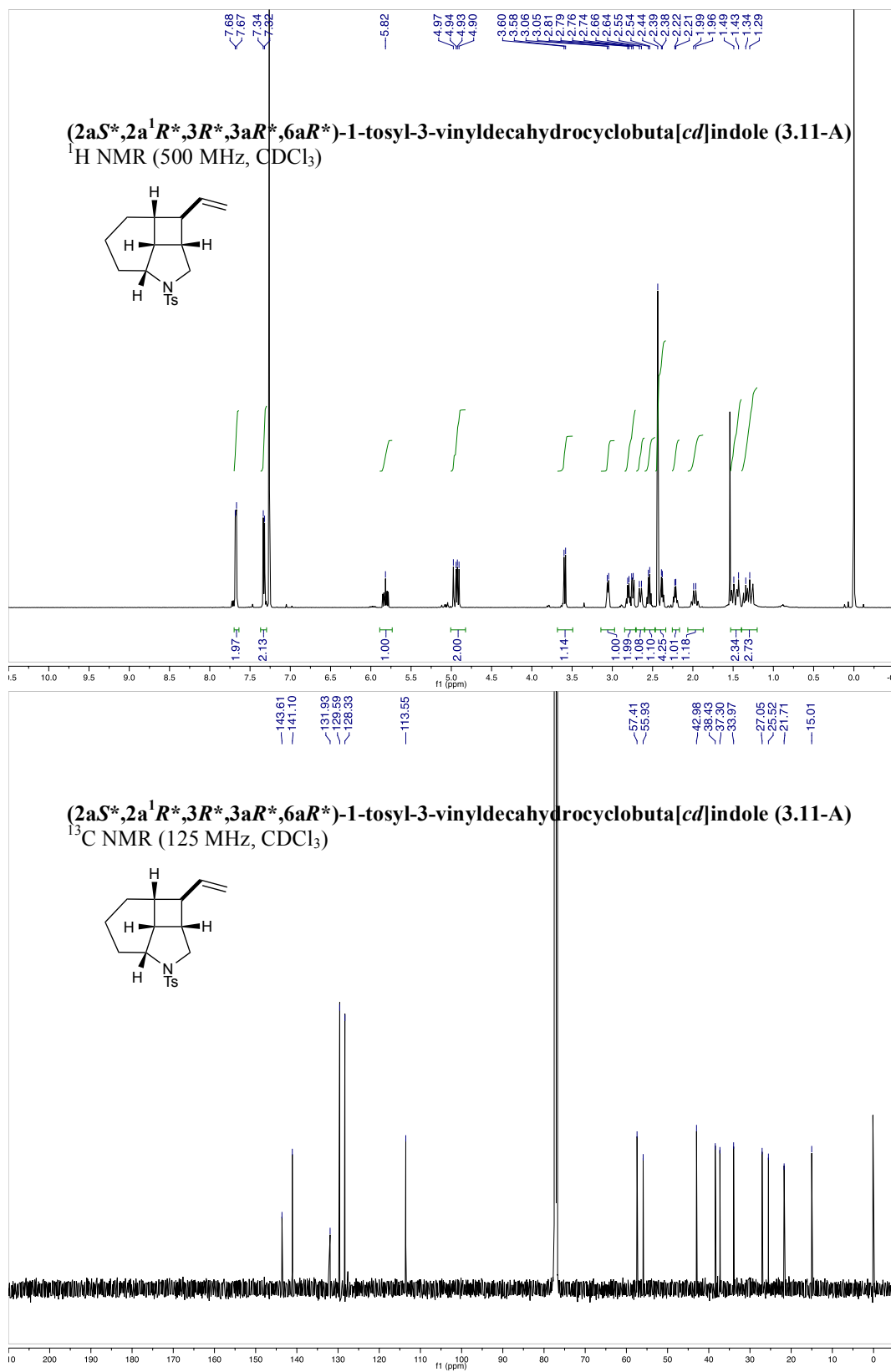


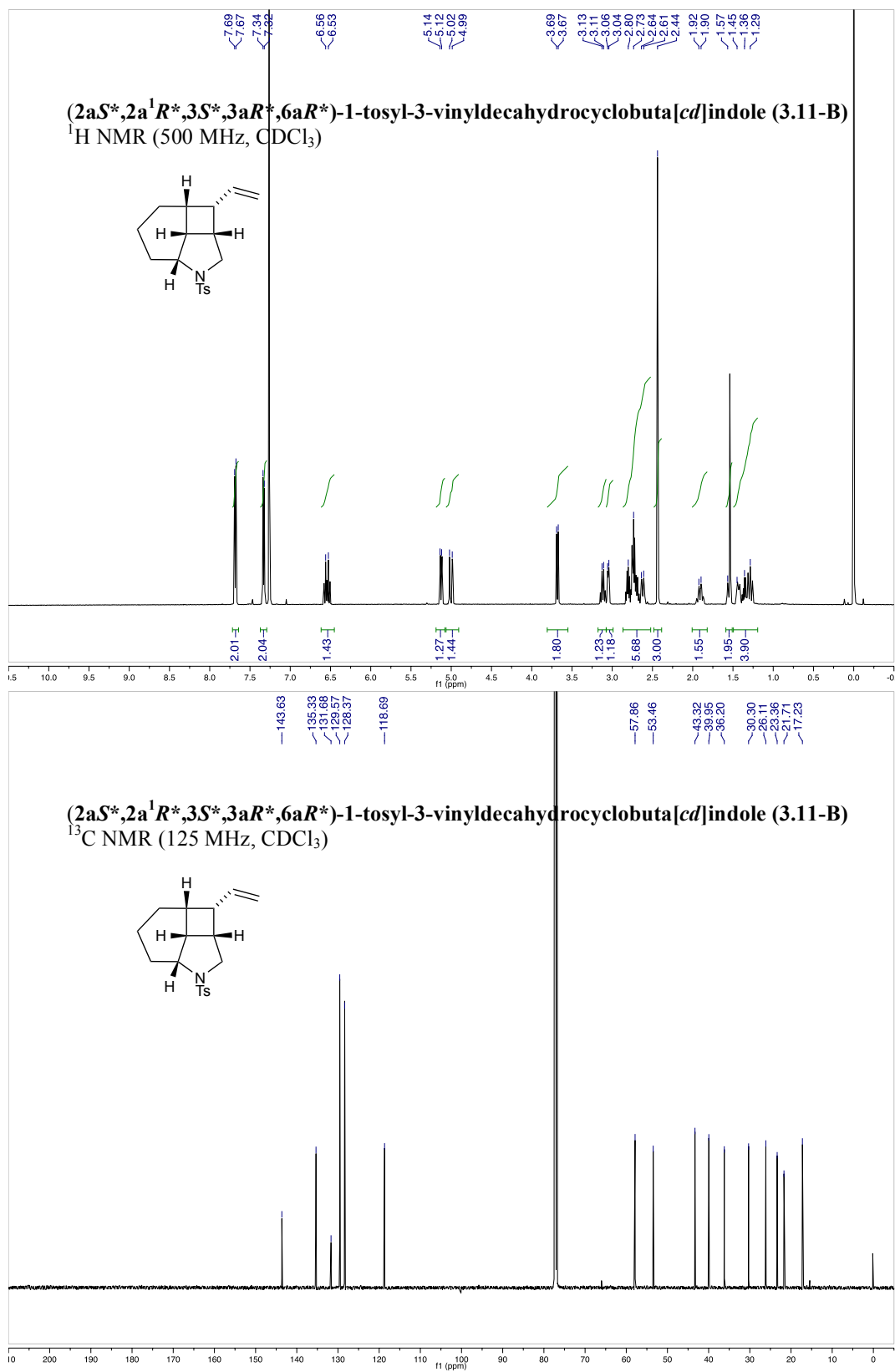


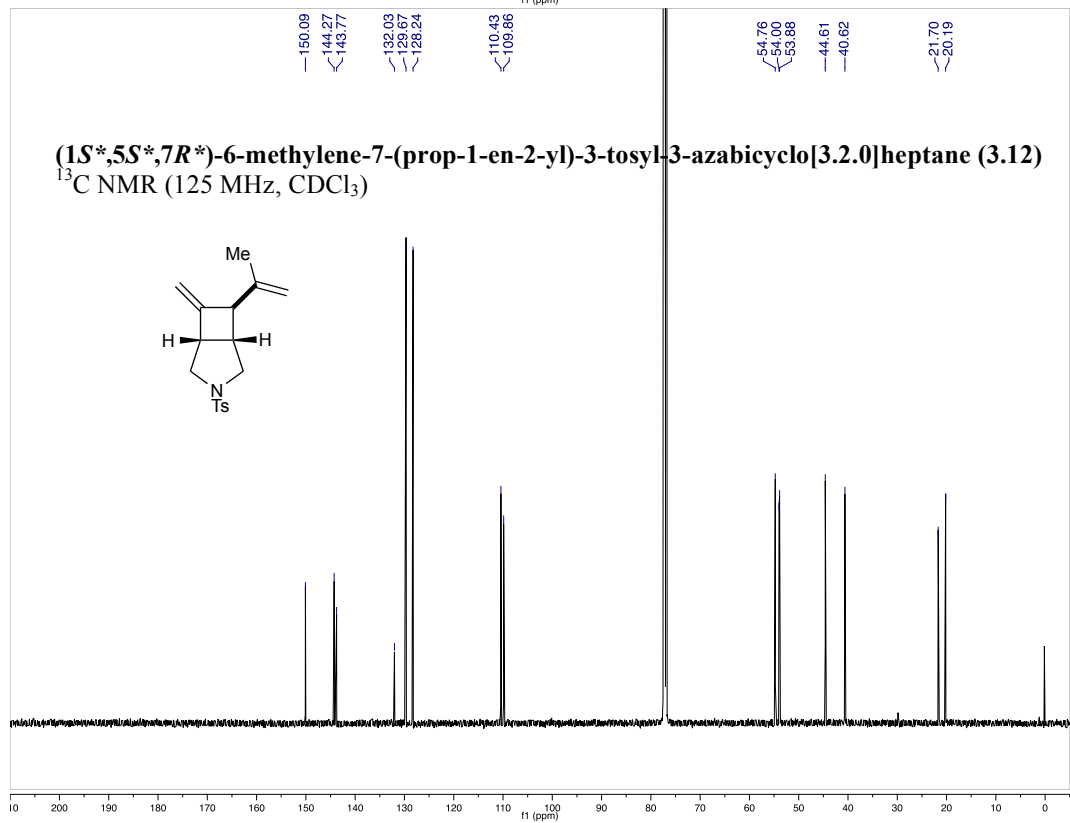
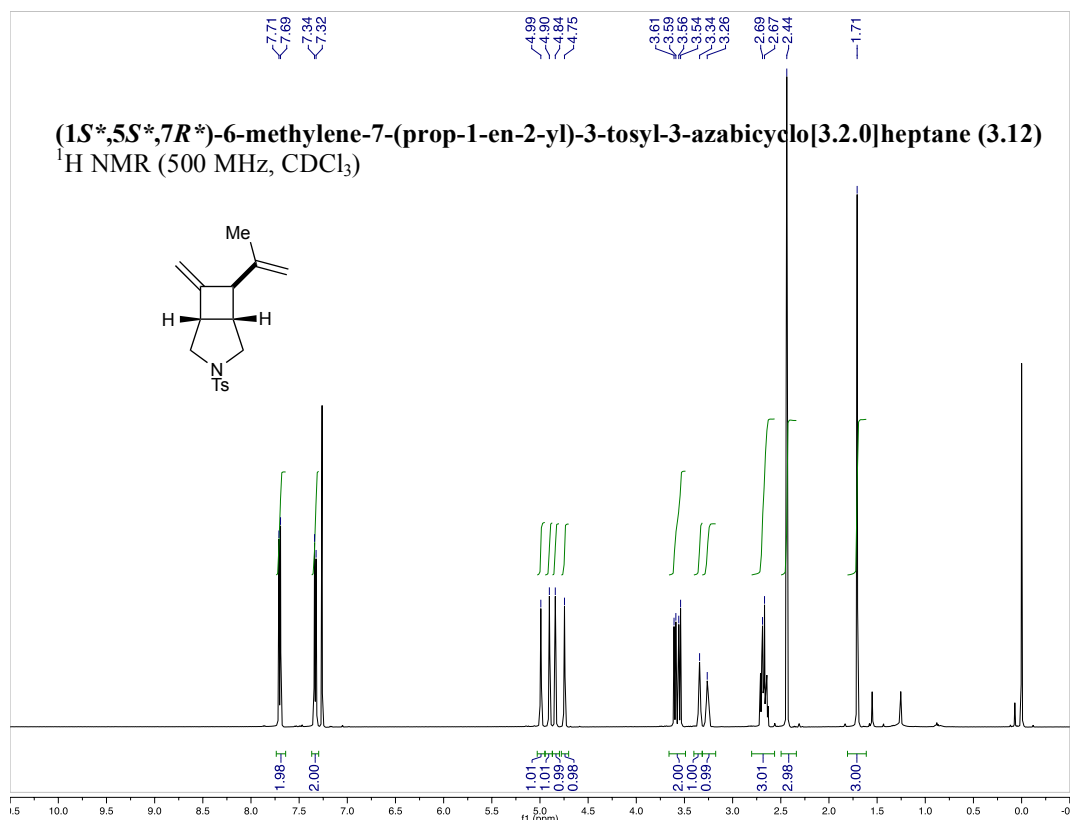


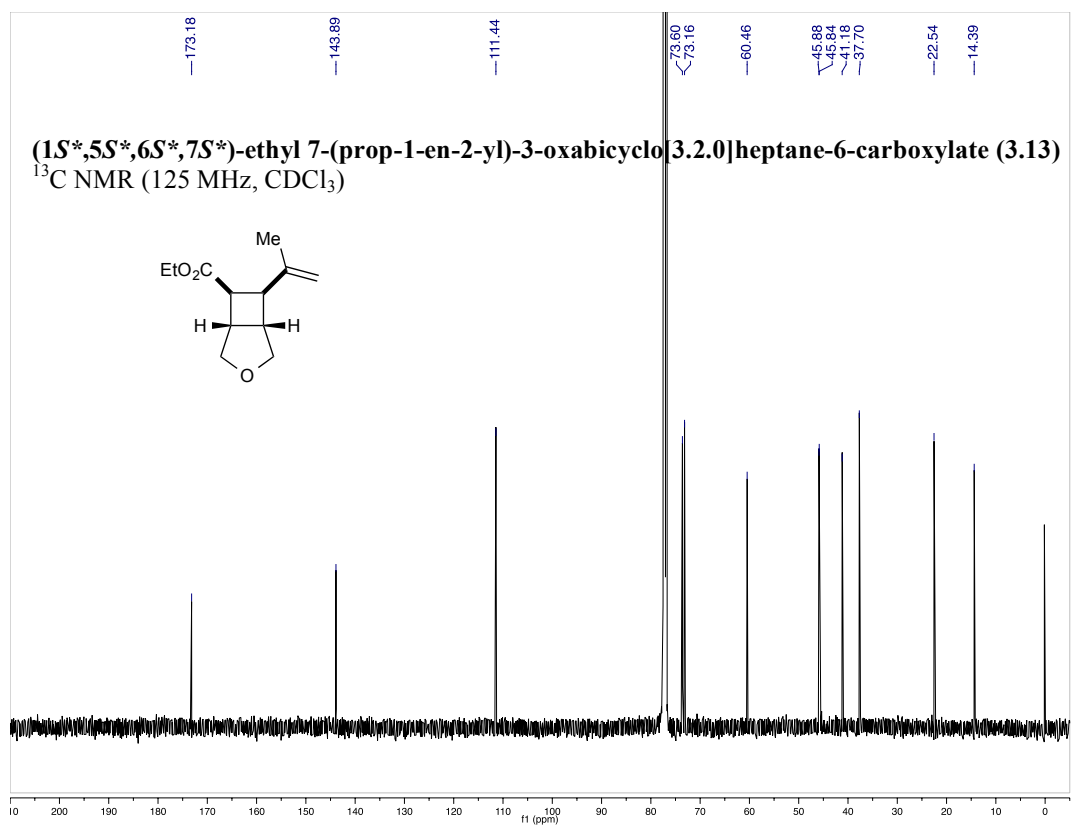
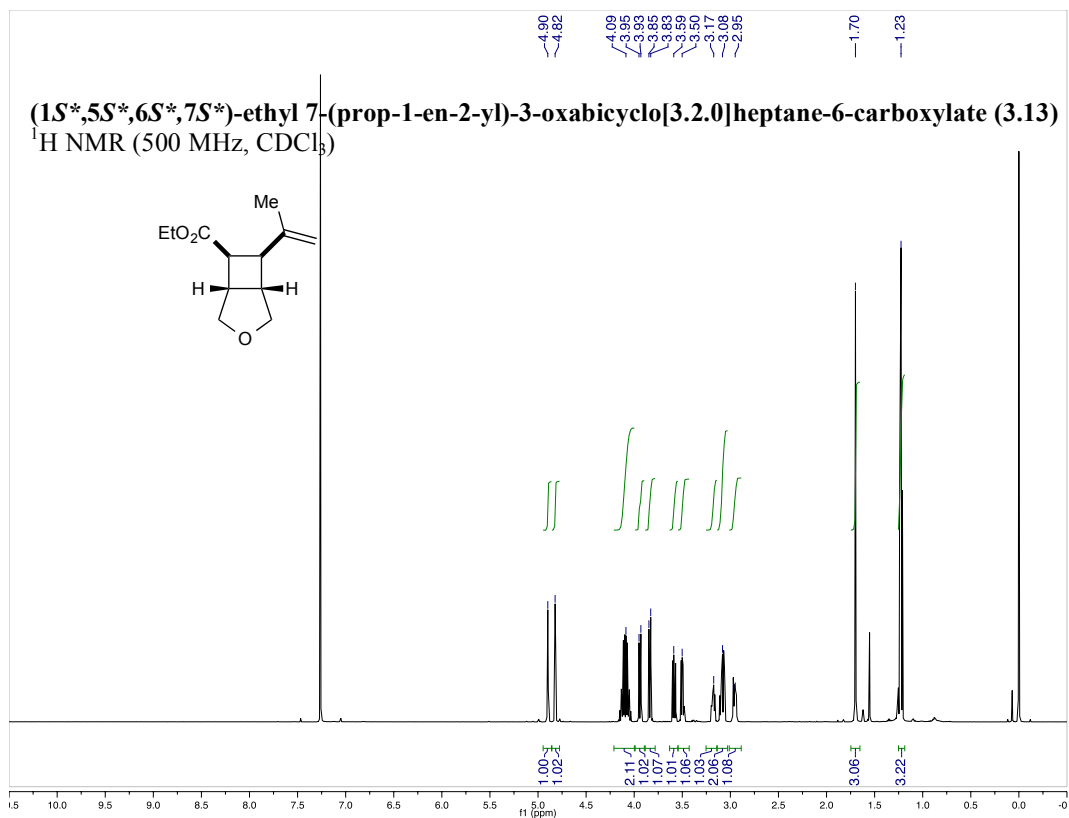




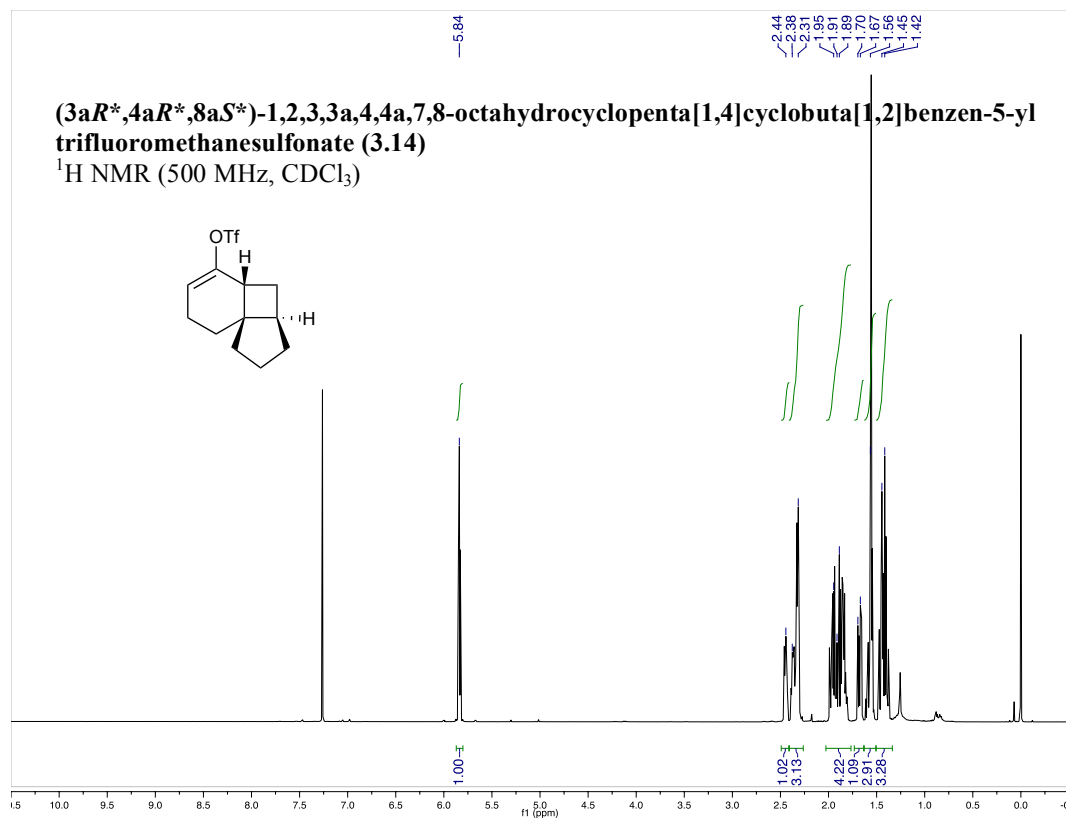




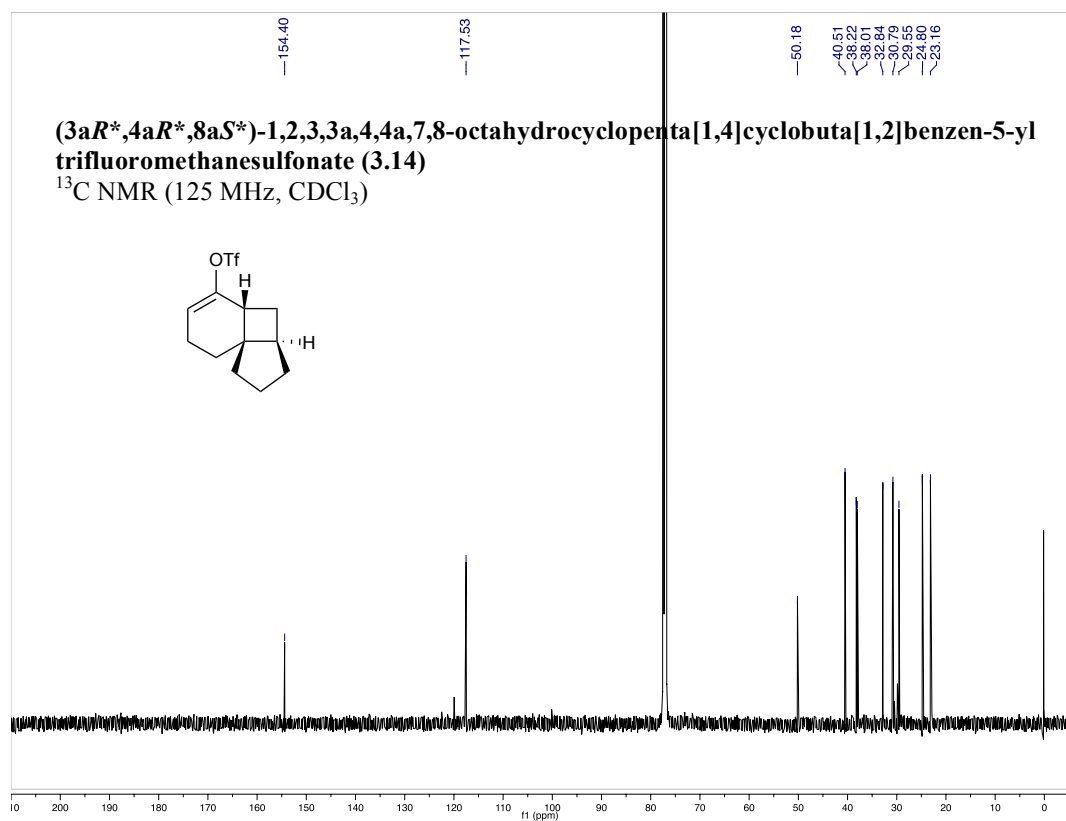


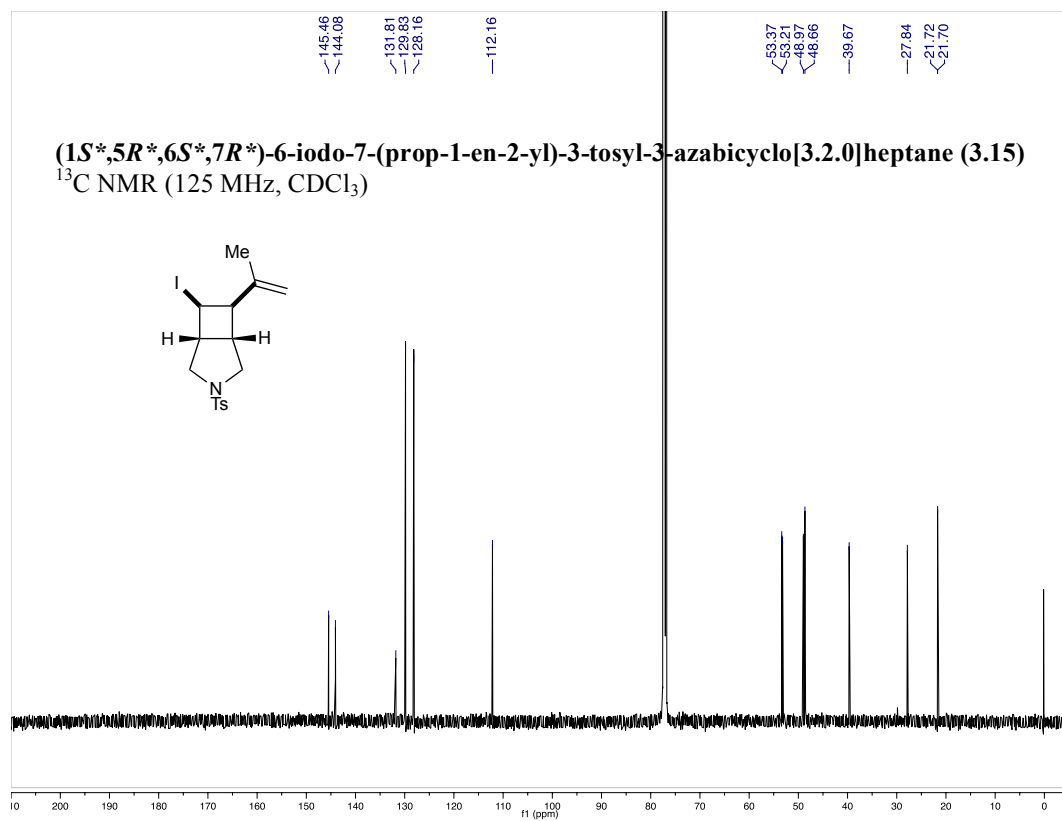
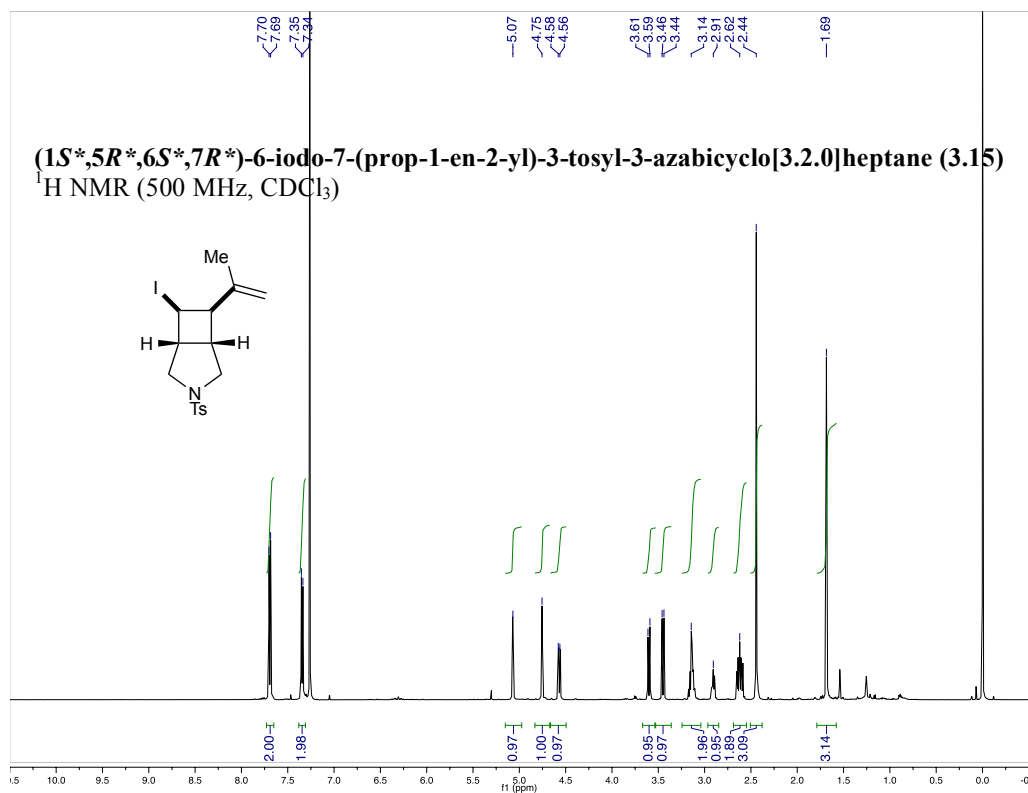


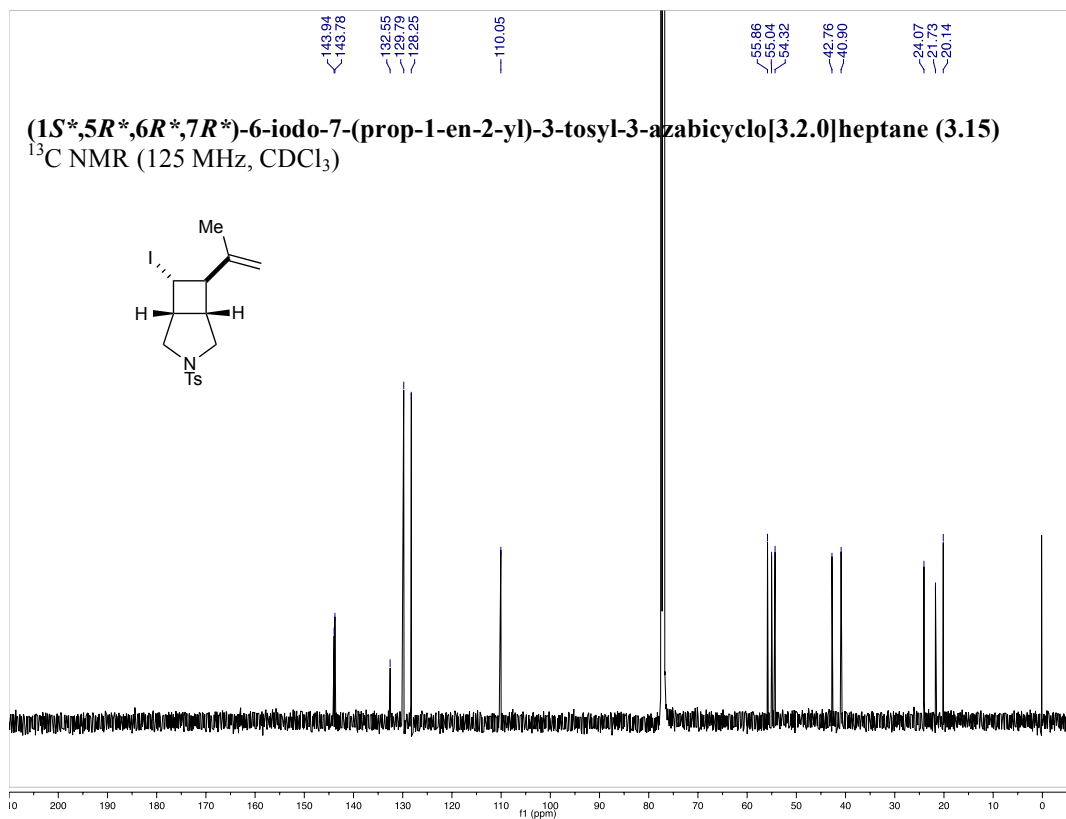
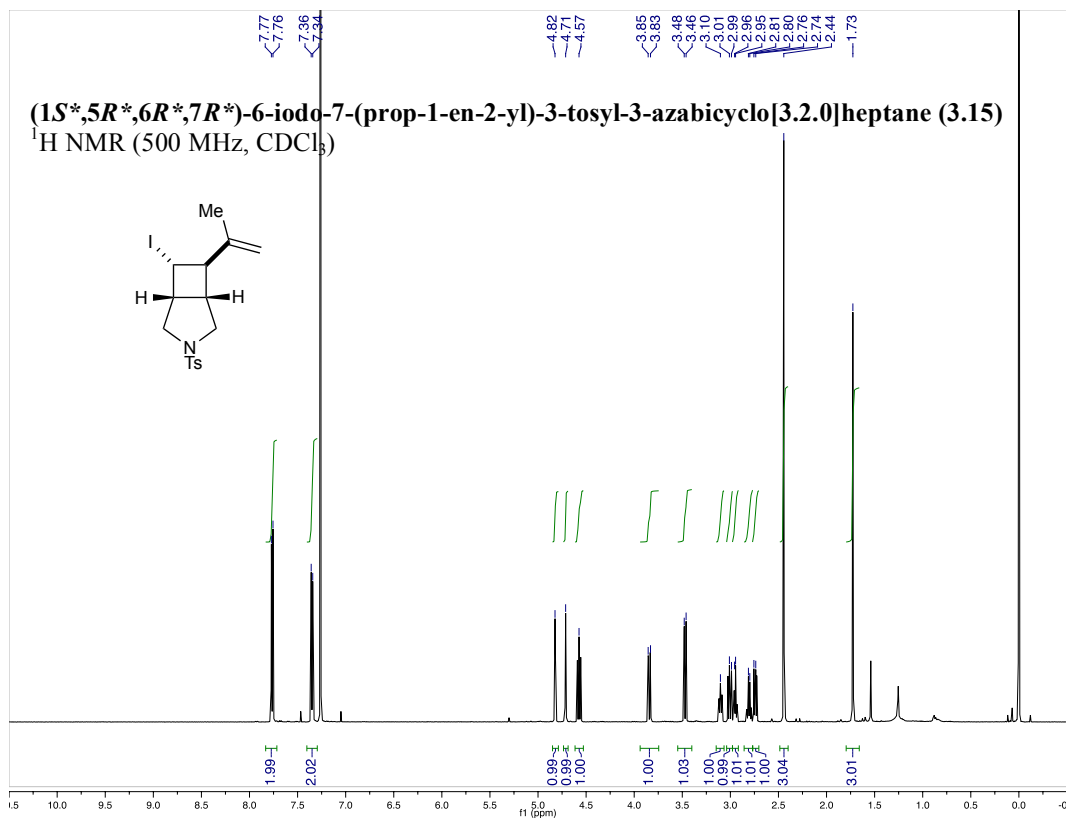
(3a*R,4a*R**,8a*S**)-1,2,3,3a,4,4a,7,8-octahydrocyclopenta[1,4]cyclobuta[1,2]benzen-5-yl trifluoromethanesulfonate (3.14)**
¹H NMR (500 MHz, CDCl₃)

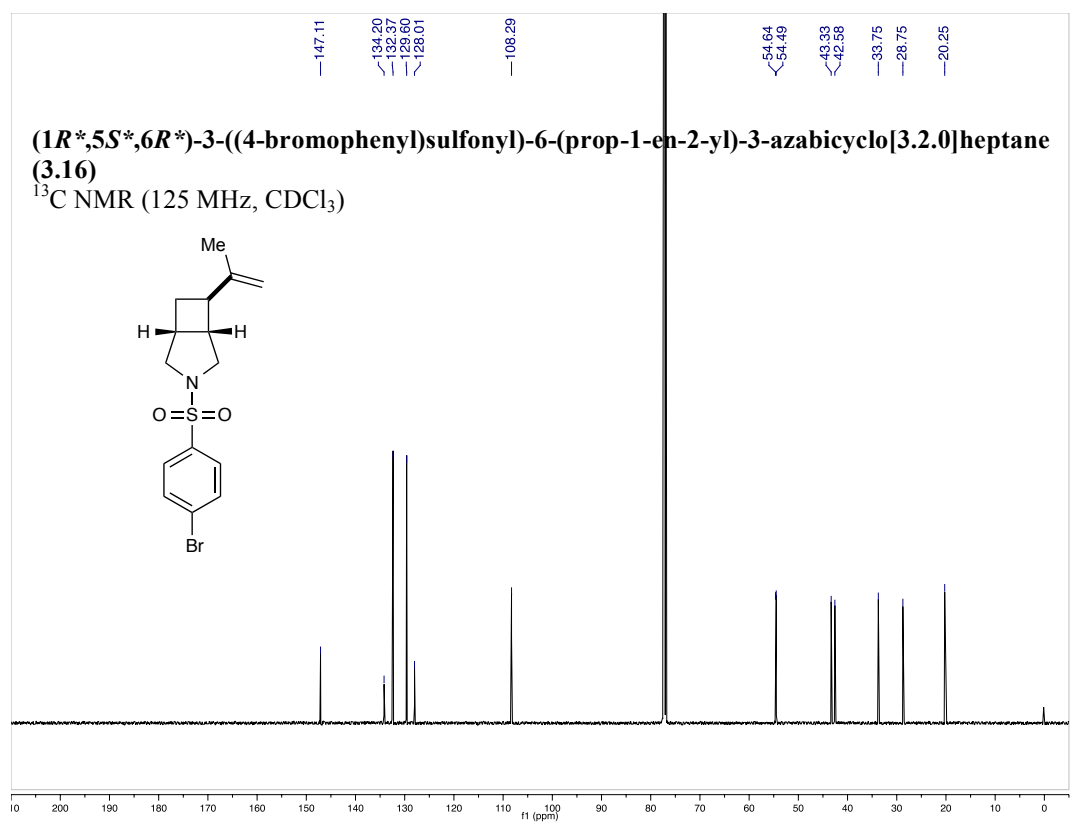
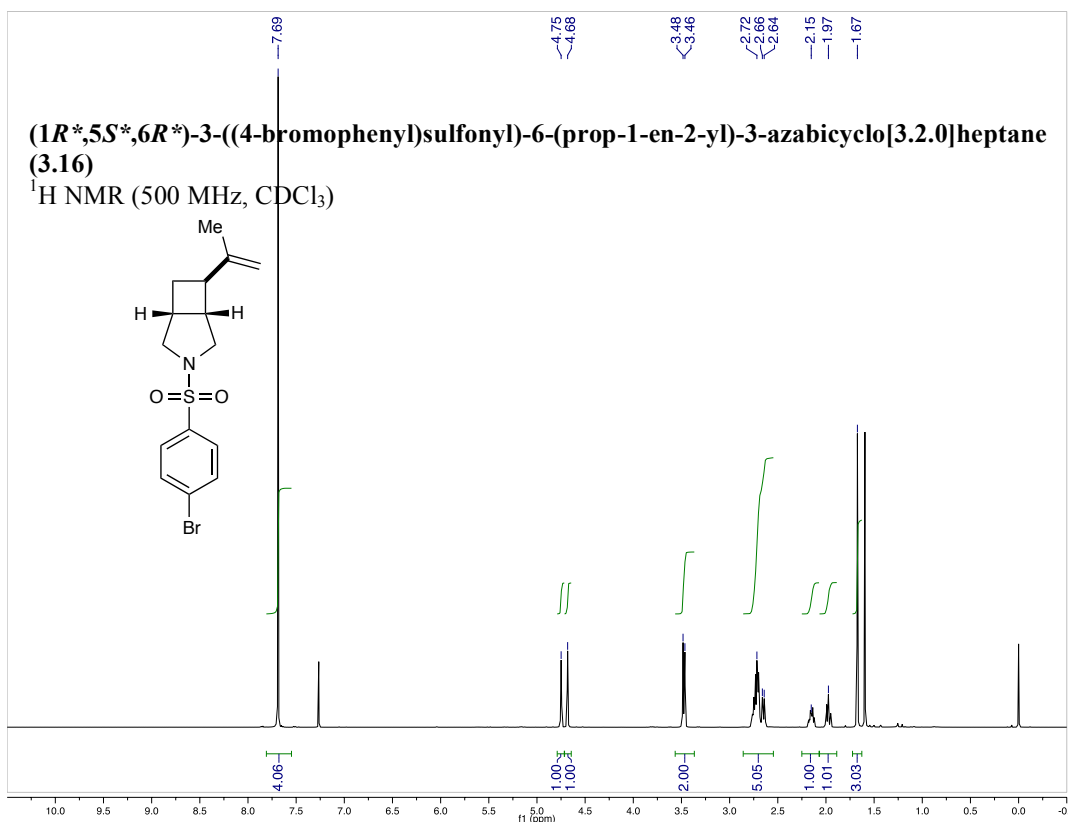


(3a*R,4a*R**,8a*S**)-1,2,3,3a,4,4a,7,8-octahydrocyclopenta[1,4]cyclobuta[1,2]benzen-5-yl trifluoromethanesulfonate (3.14)**
¹³C NMR (125 MHz, CDCl₃)

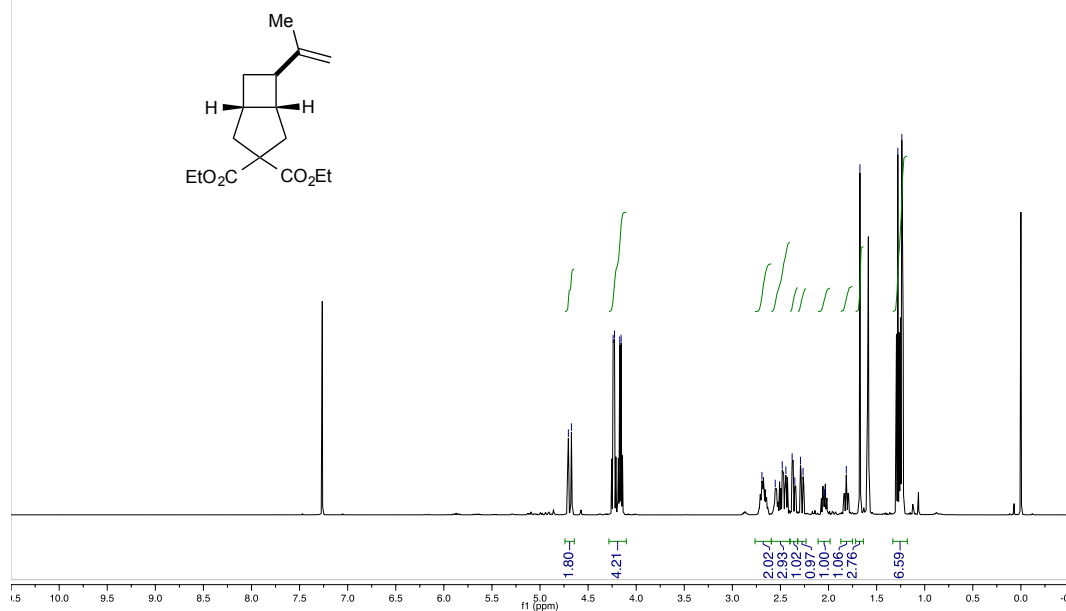




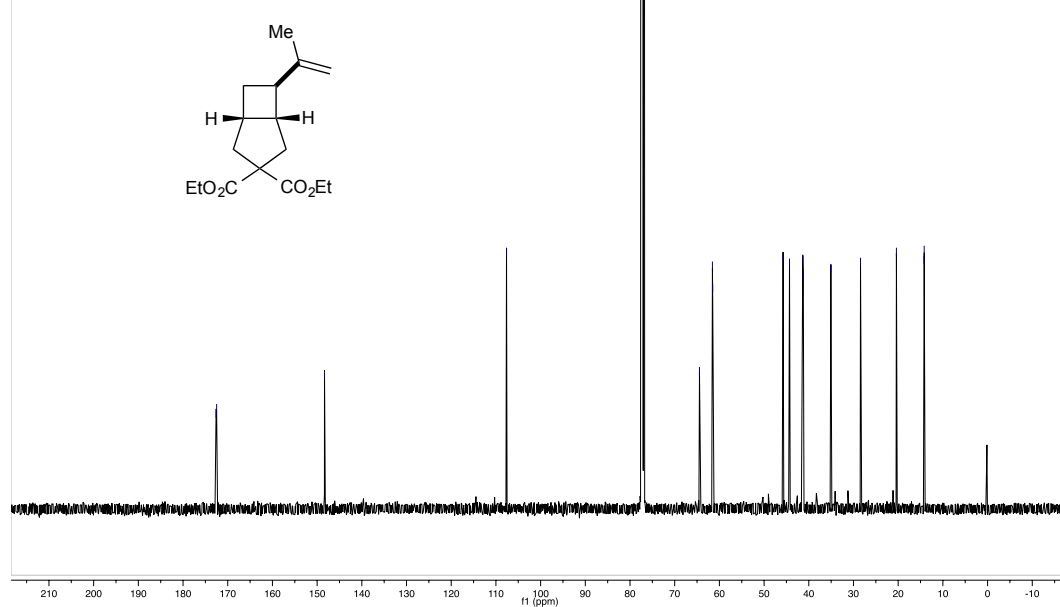


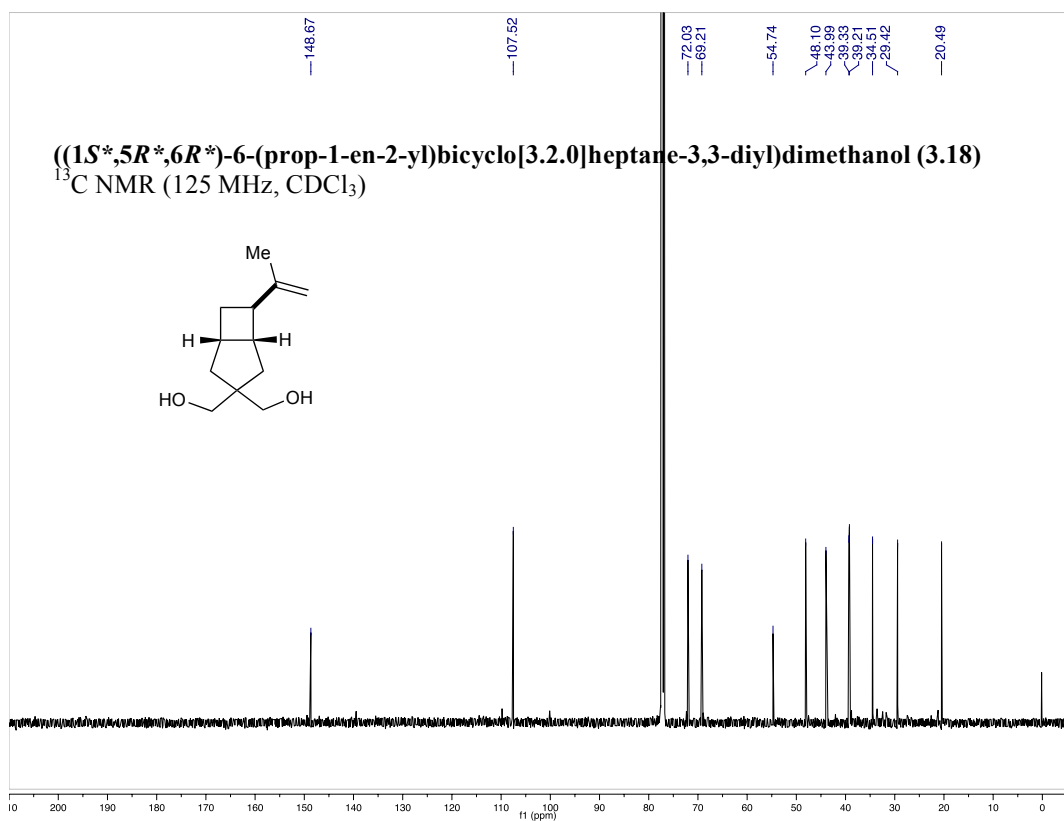
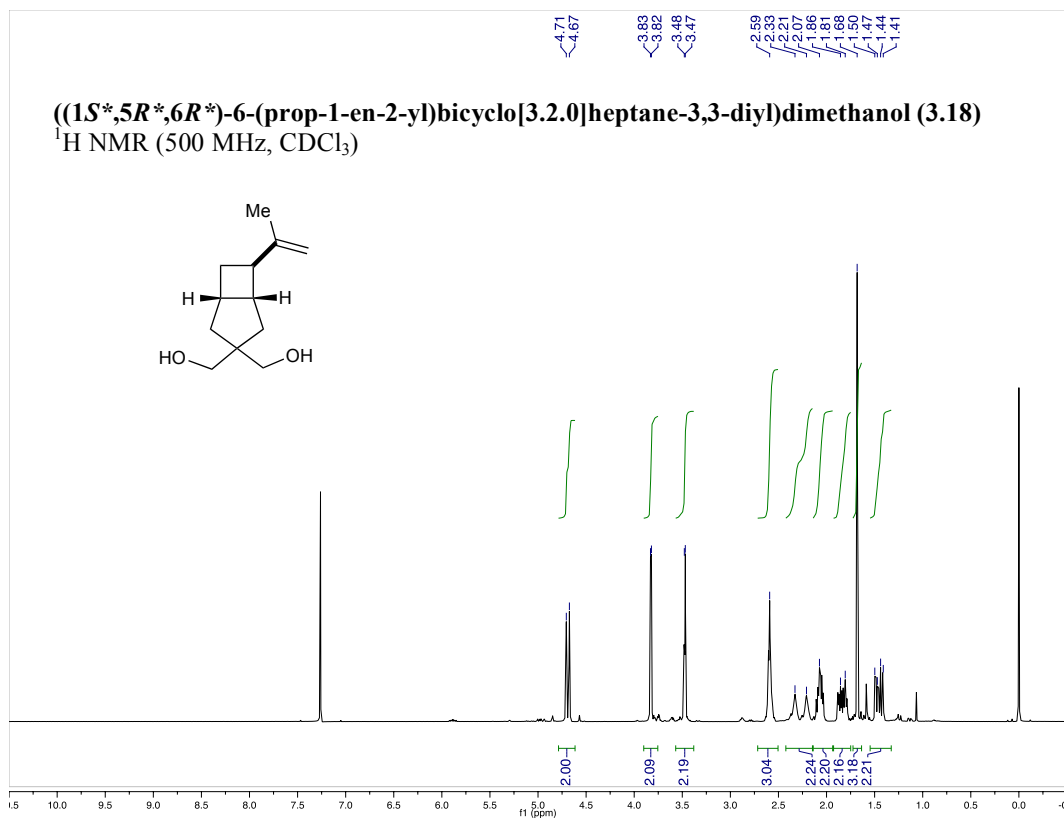


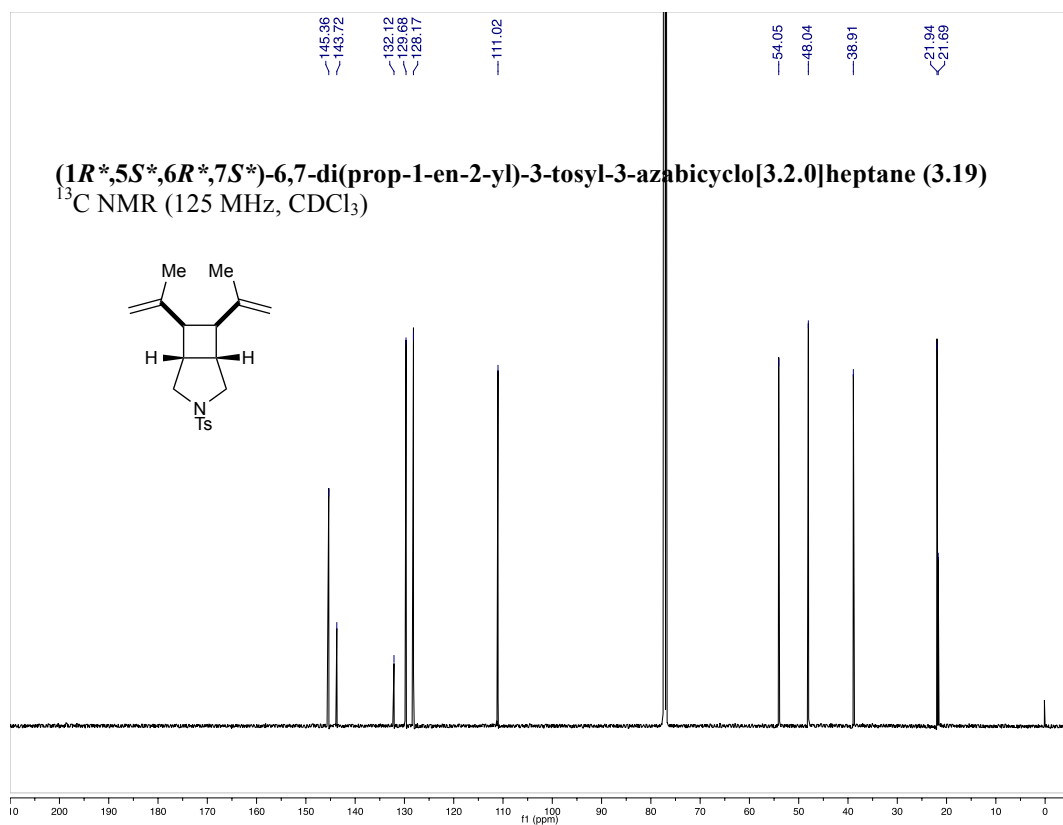
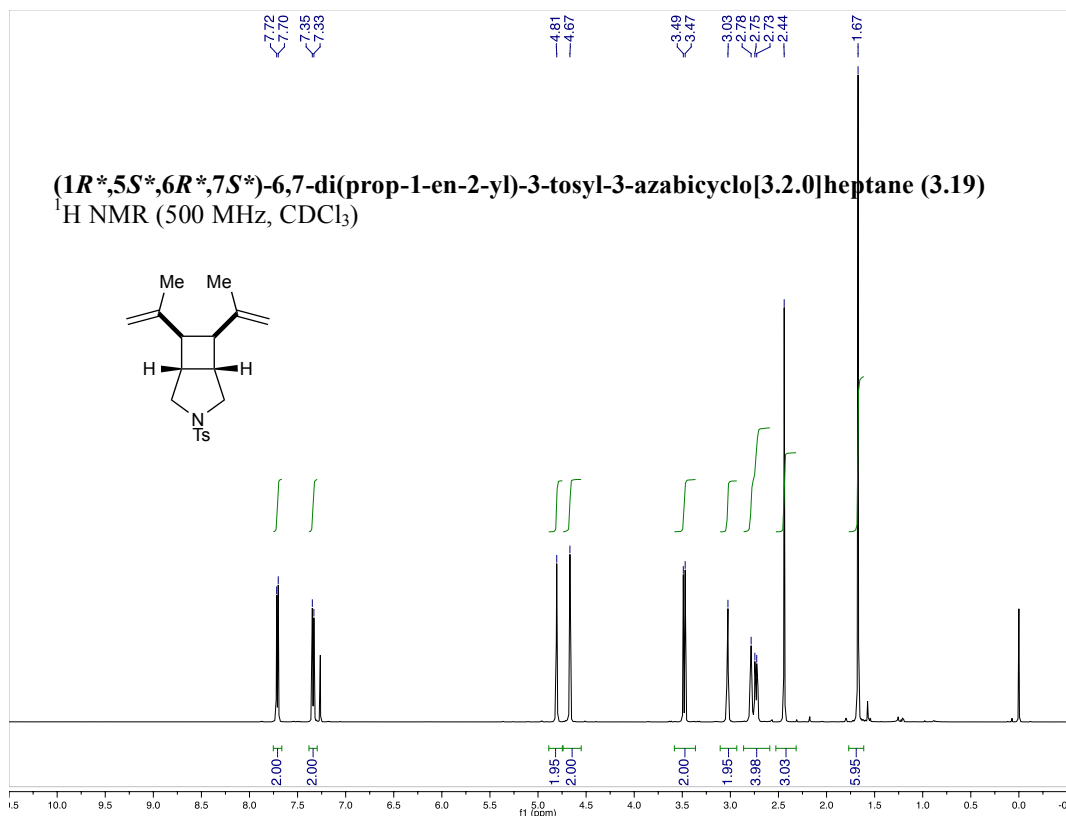
(1*S,5*R**,6*R**)-diethyl 6-(prop-1-en-2-yl)bicyclo[3.2.0]heptane-3,3-dicarboxylate (3.17)**
¹H NMR (500 MHz, CDCl₃)

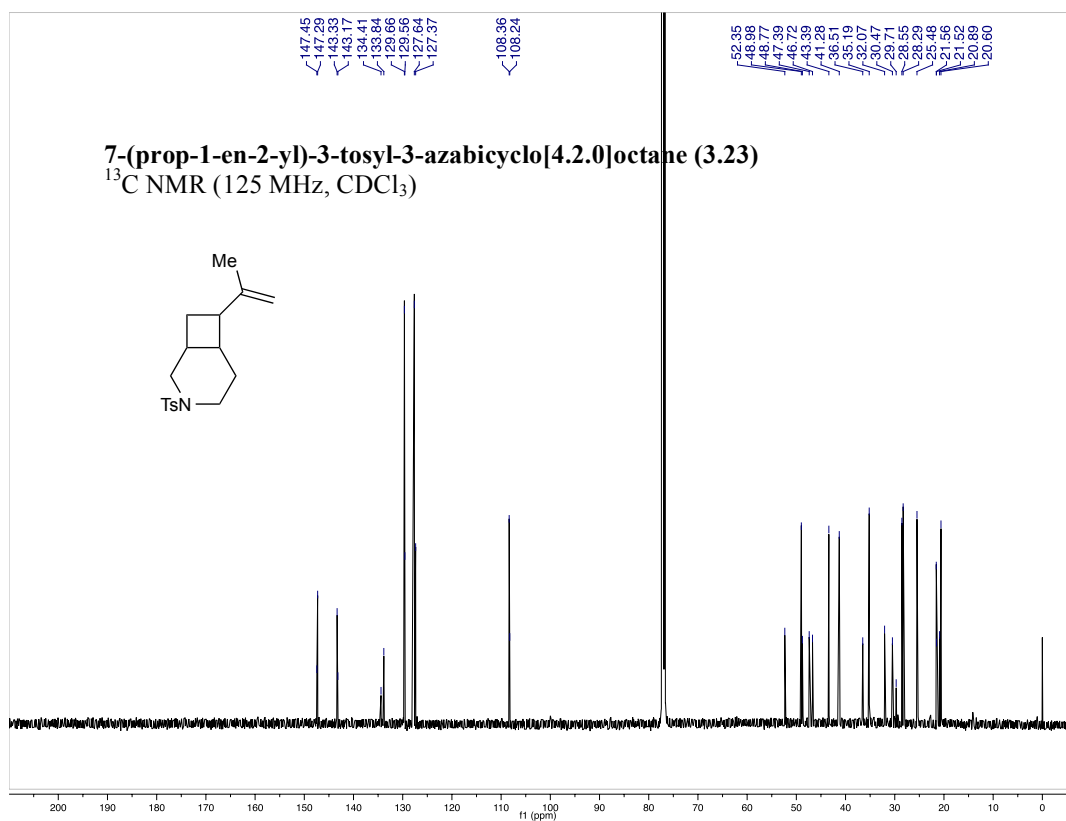
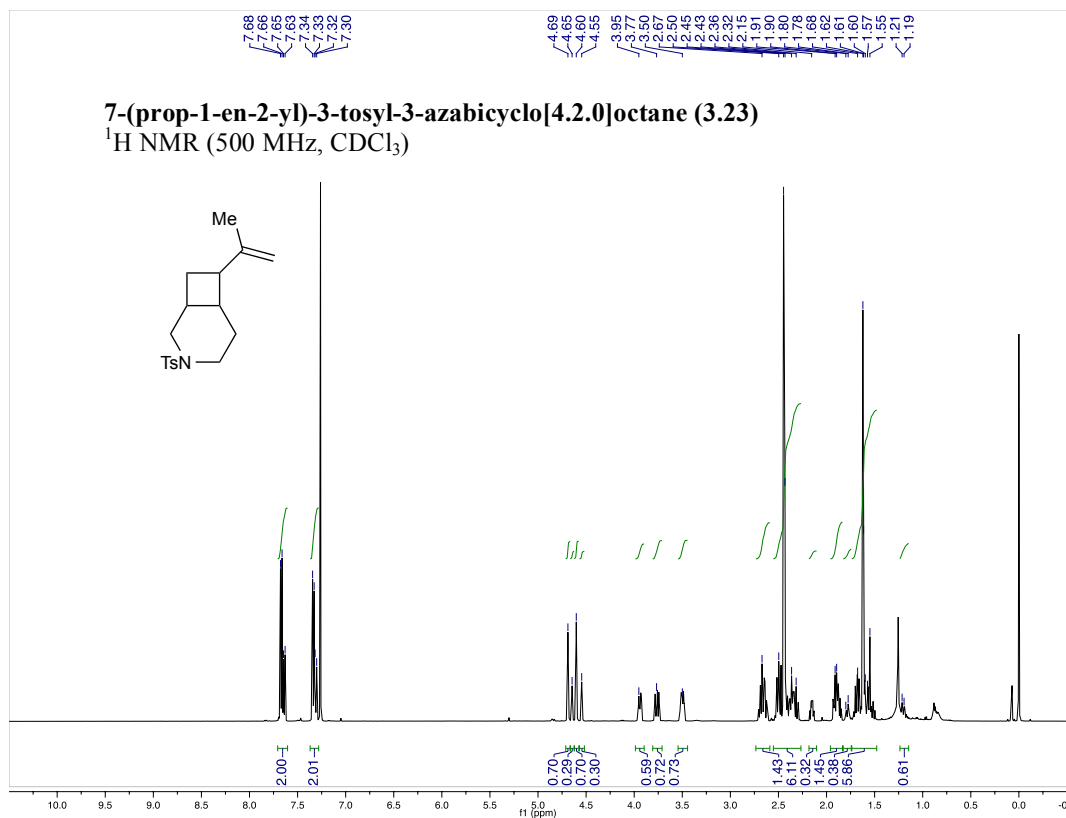


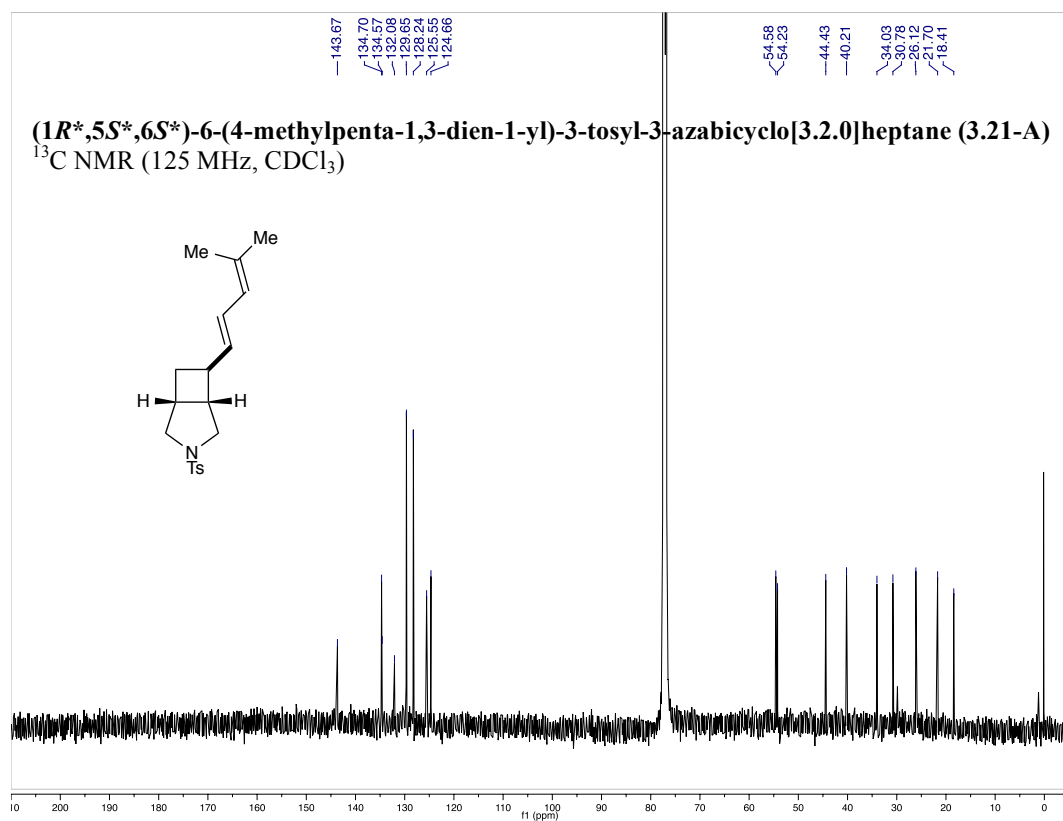
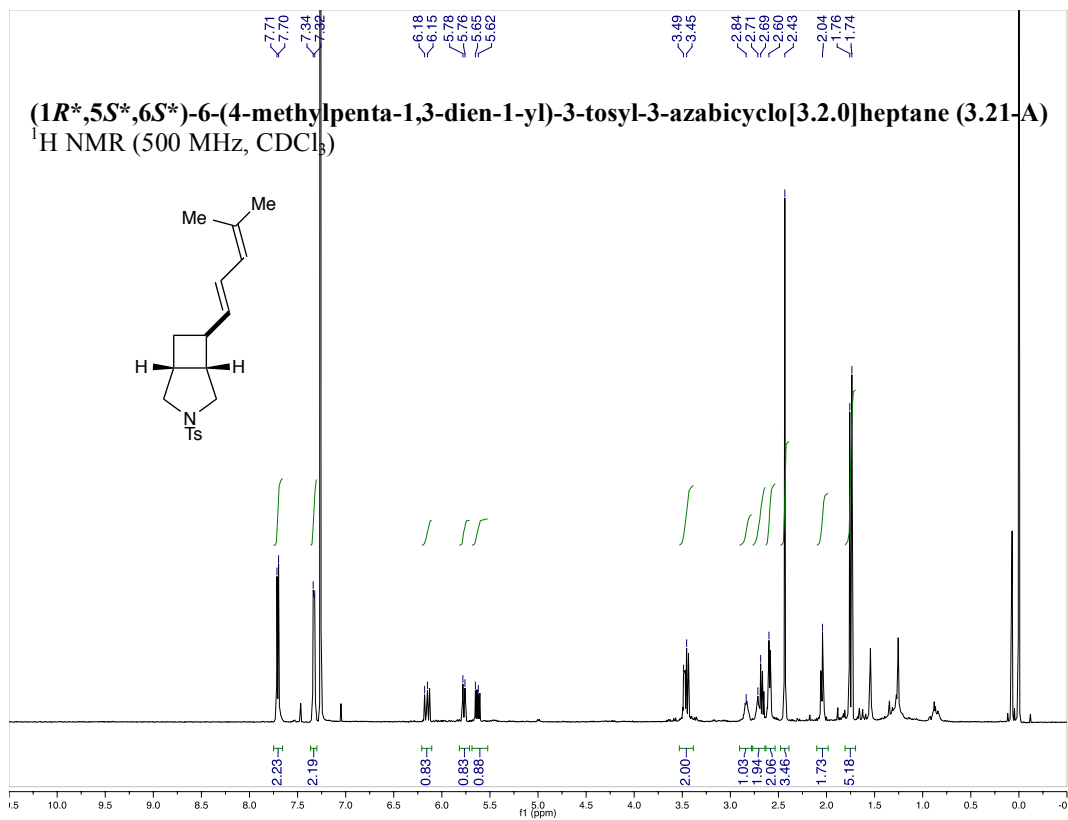
(1*S,5*R**,6*R**)-diethyl 6-(prop-1-en-2-yl)bicyclo[3.2.0]heptane-3,3-dicarboxylate (3.17)**
¹³C NMR (125 MHz, CDCl₃)

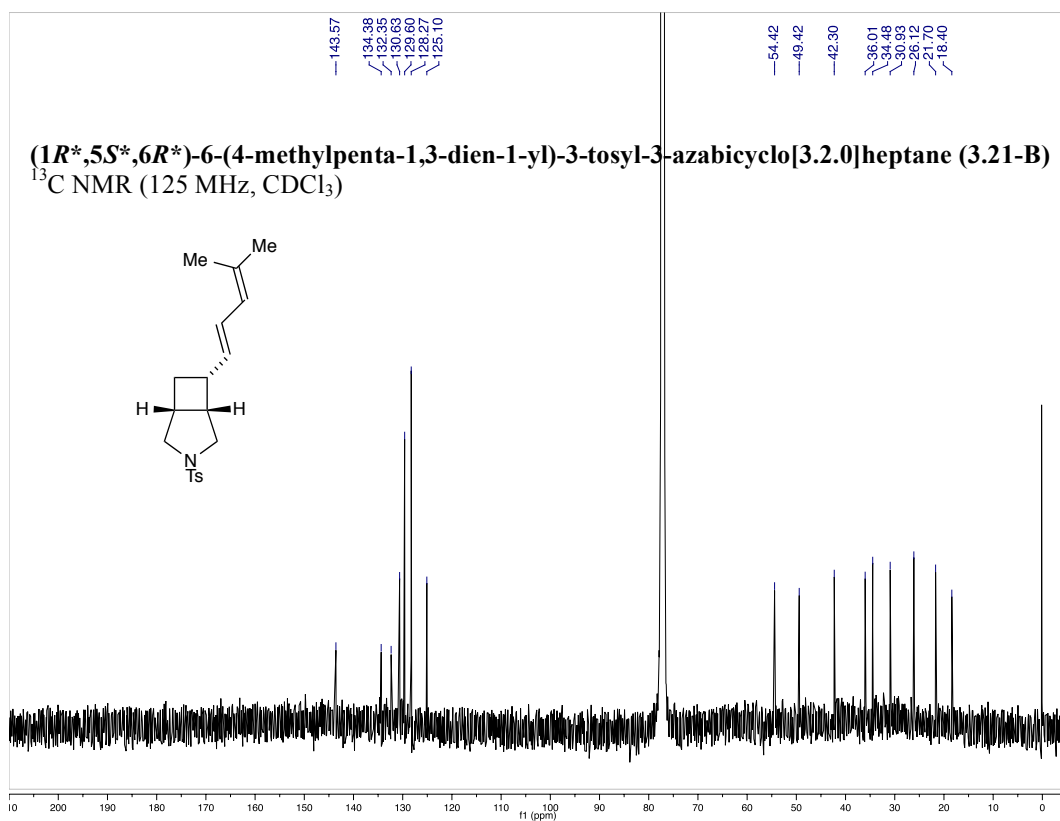
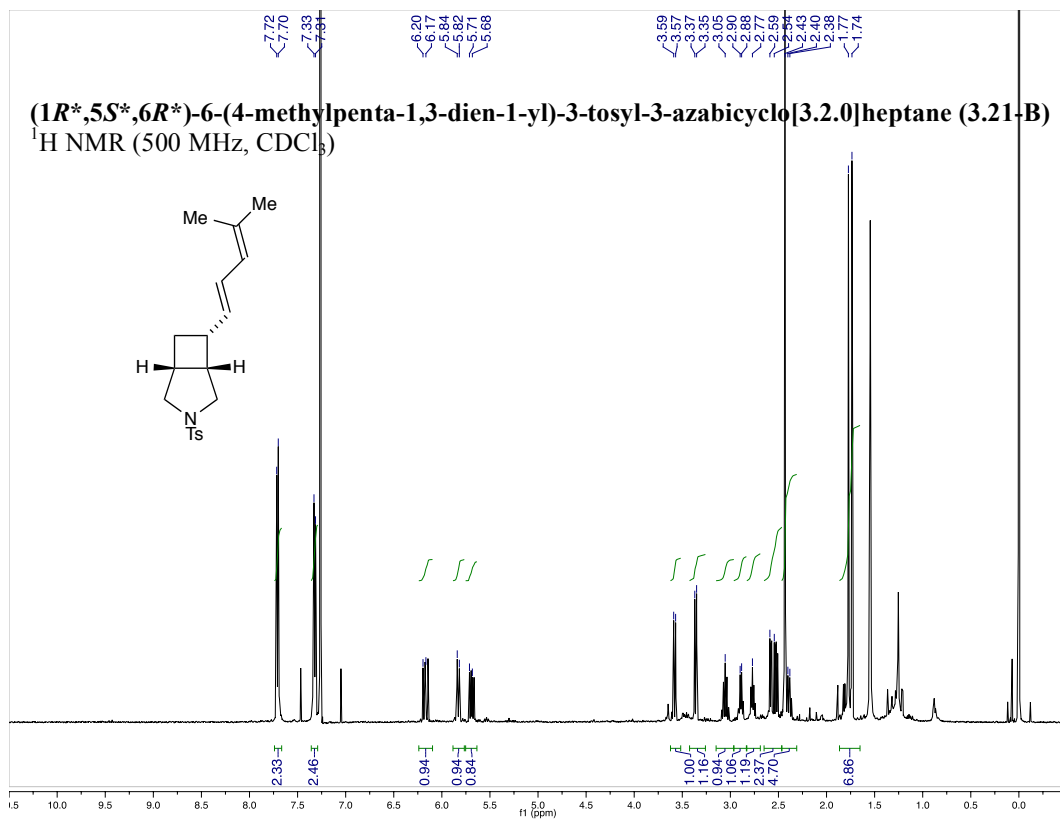


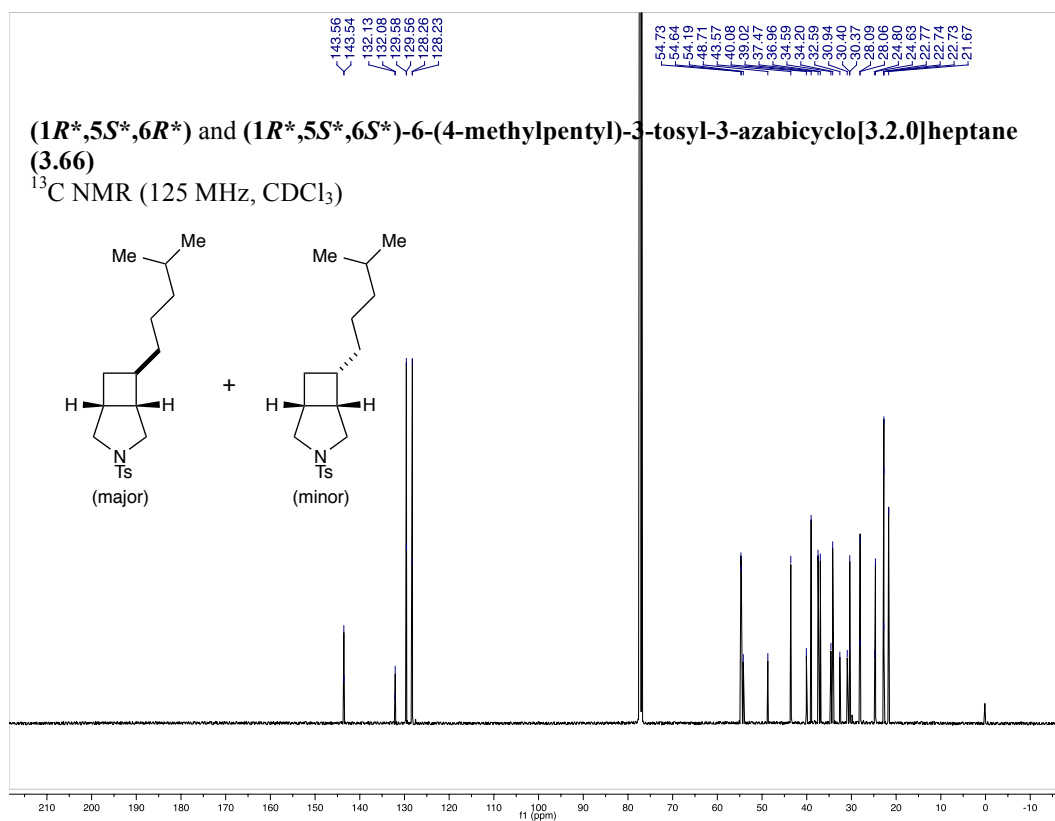
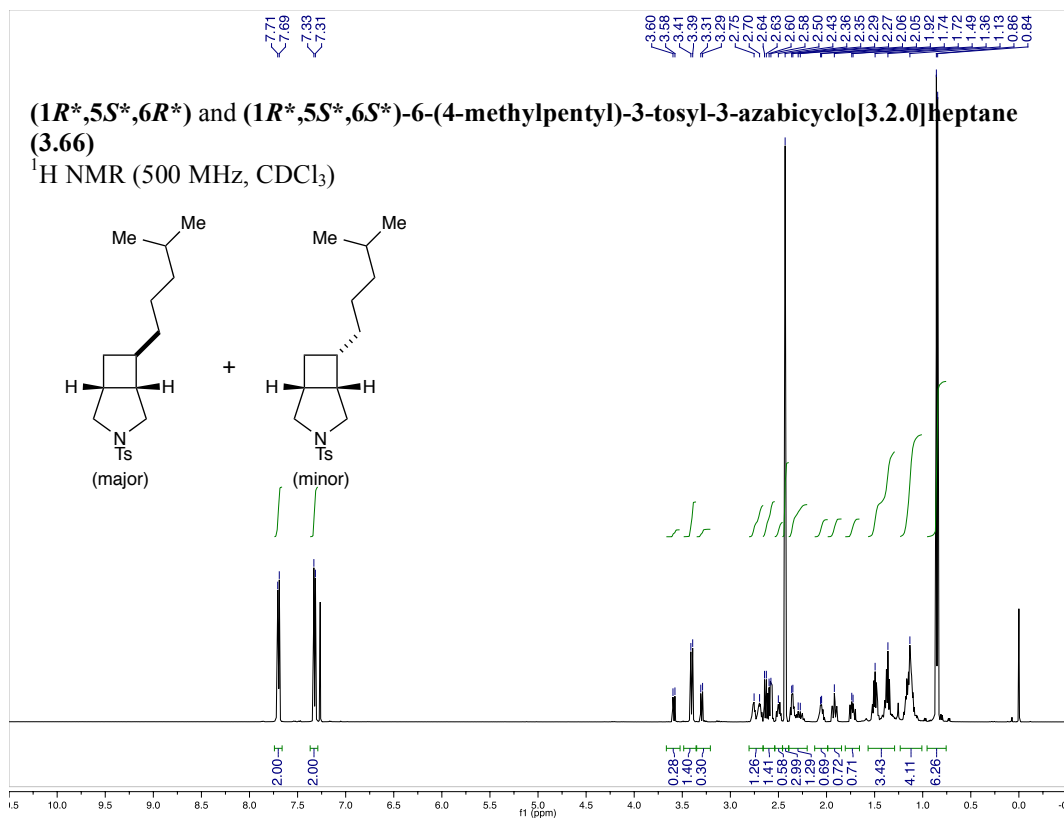


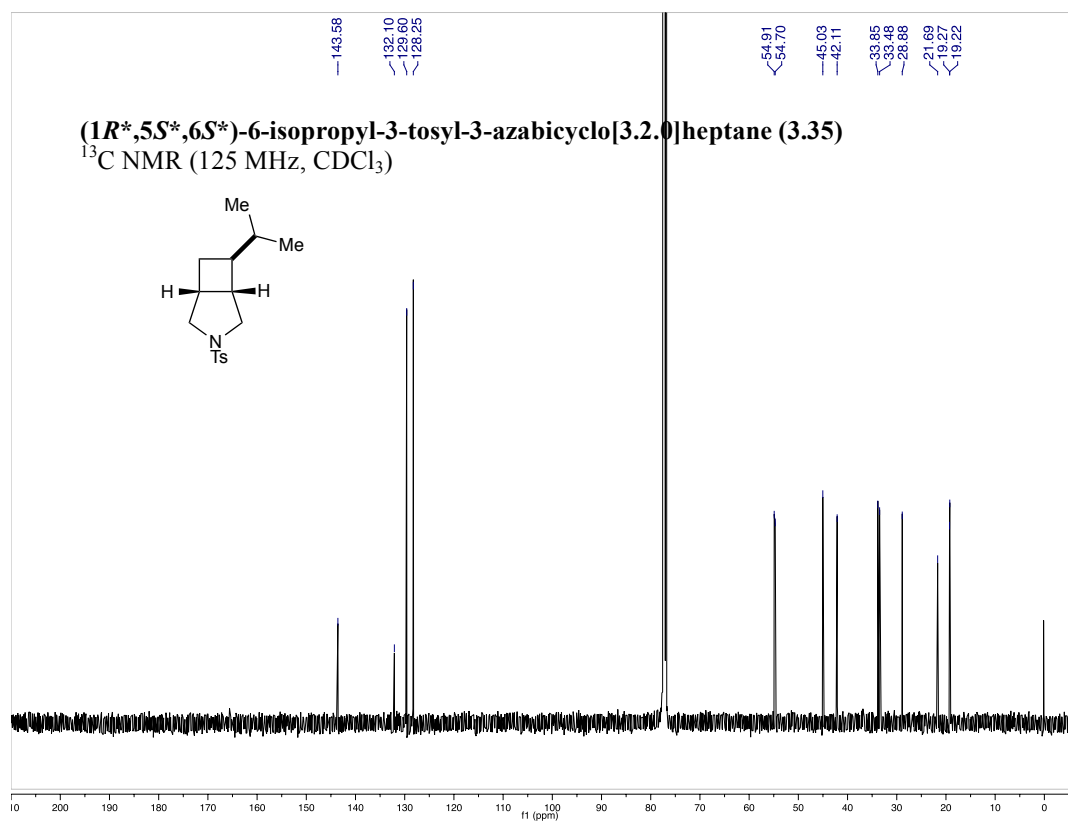
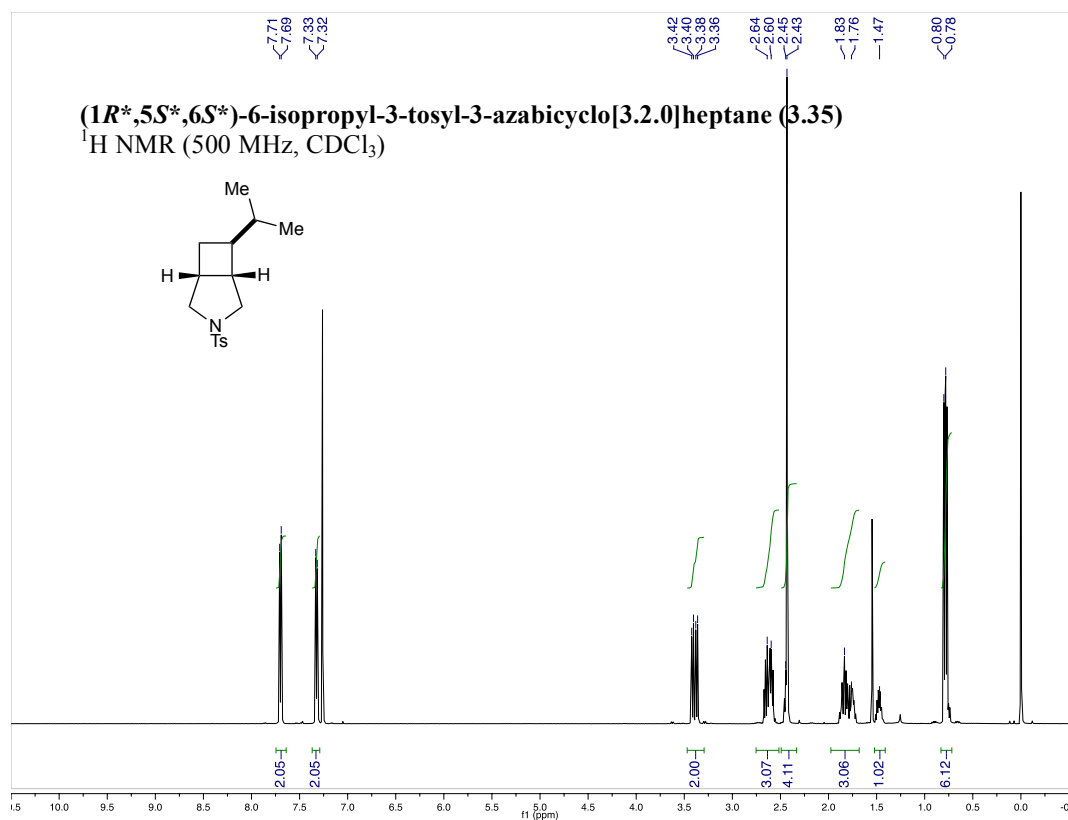


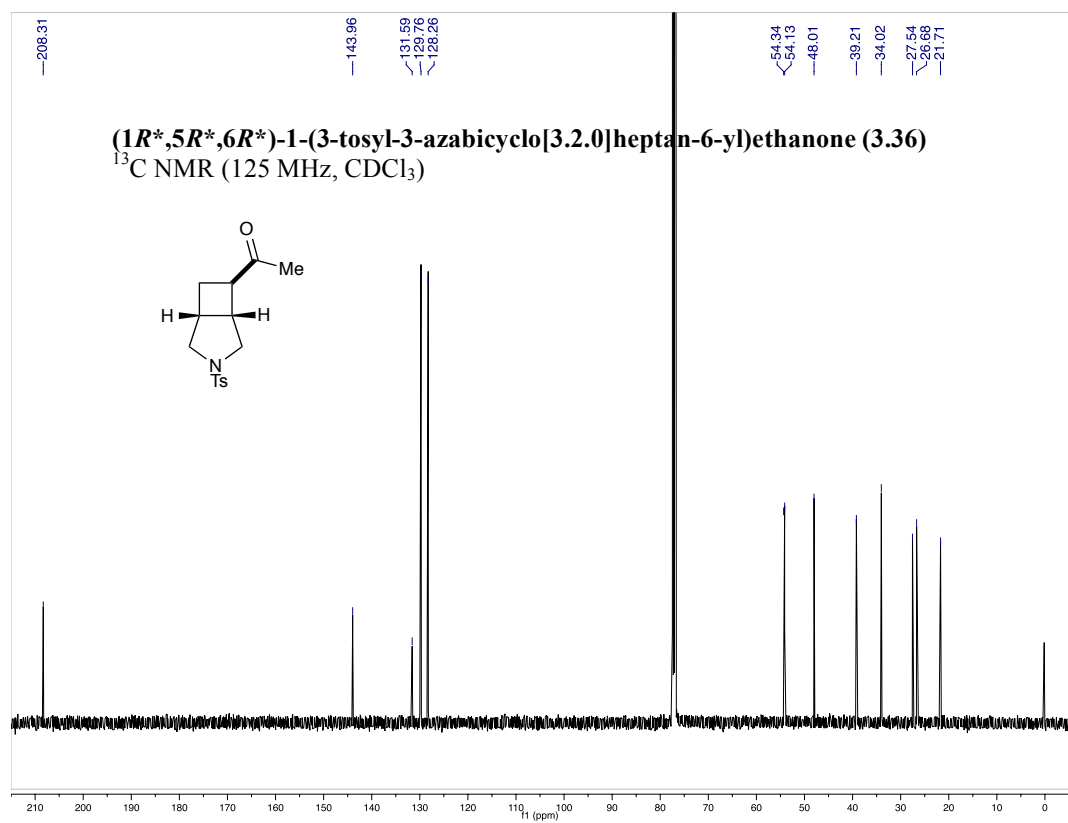
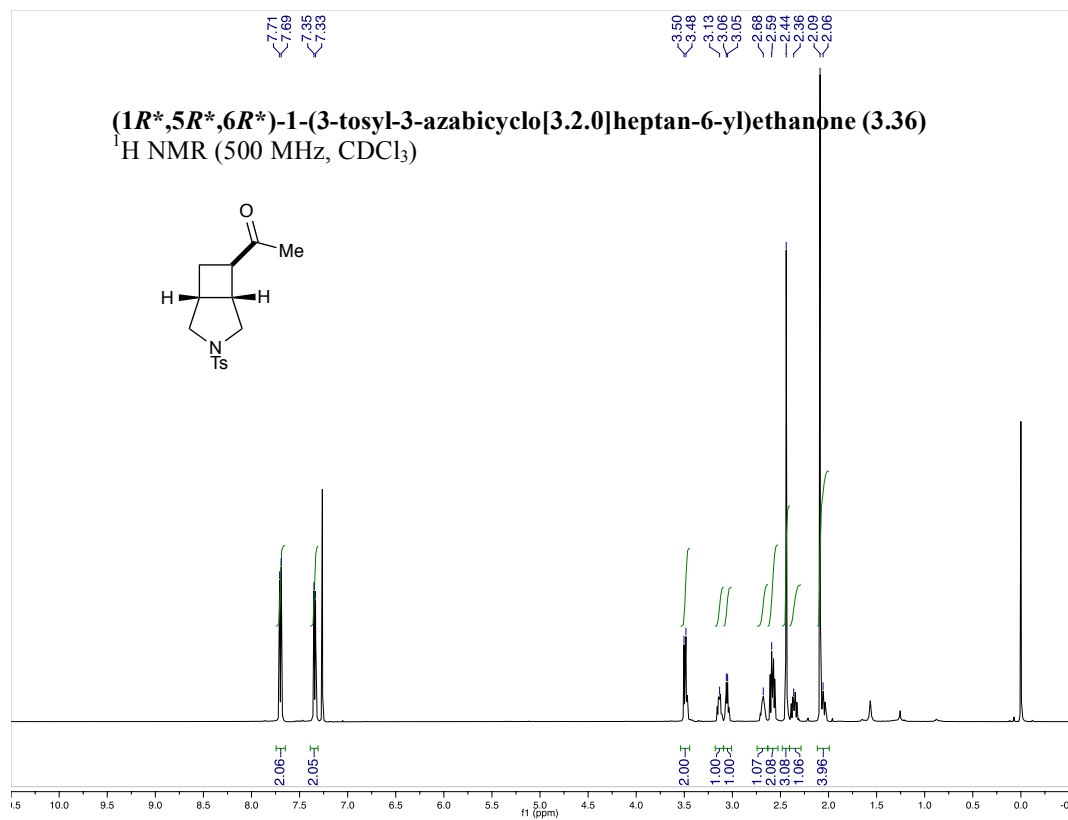


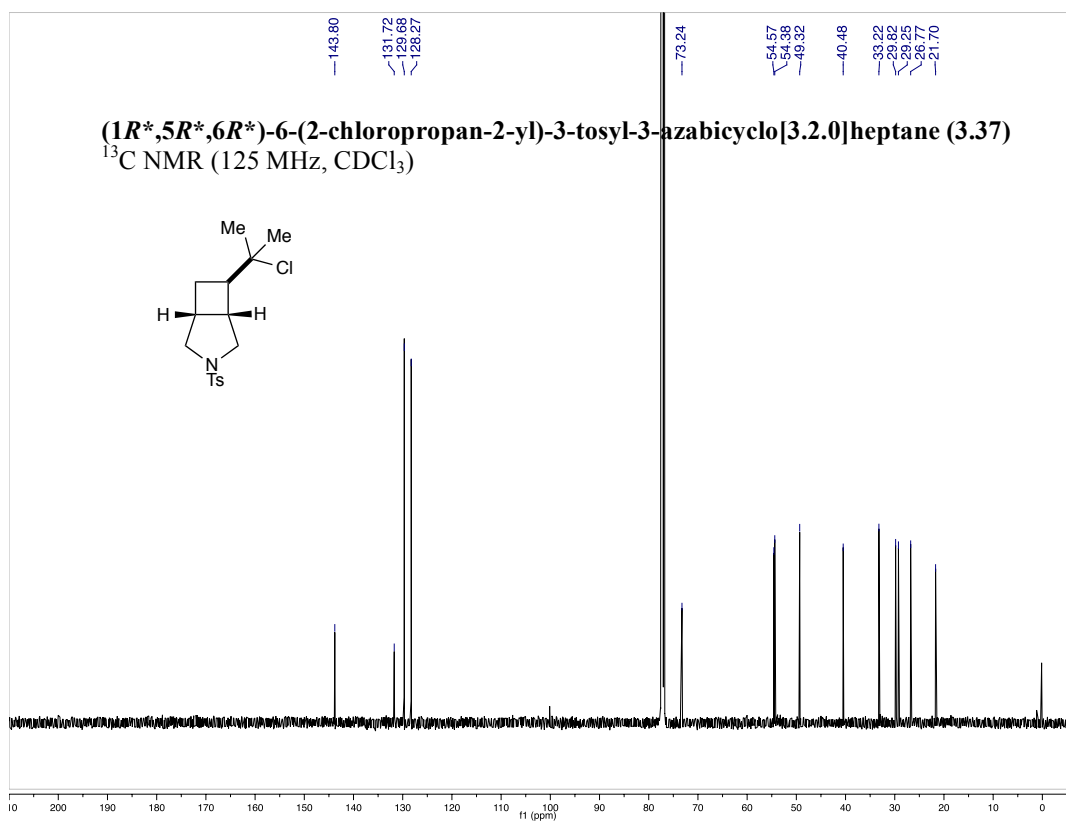
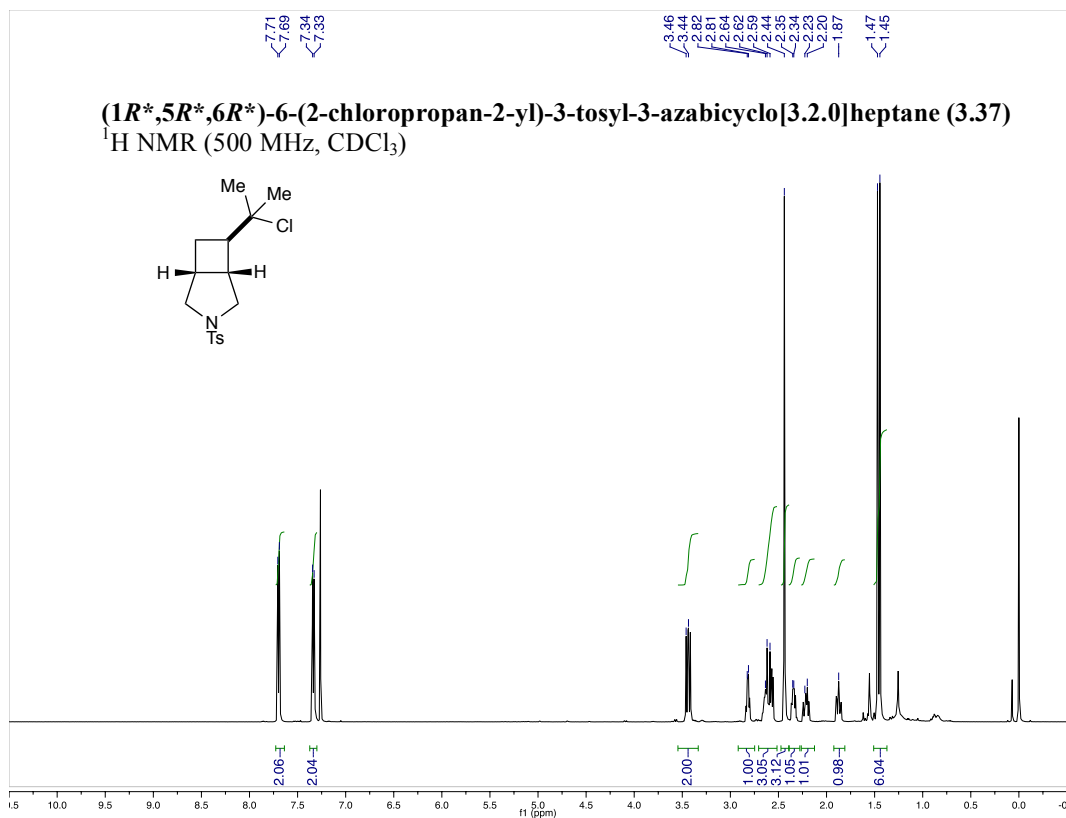


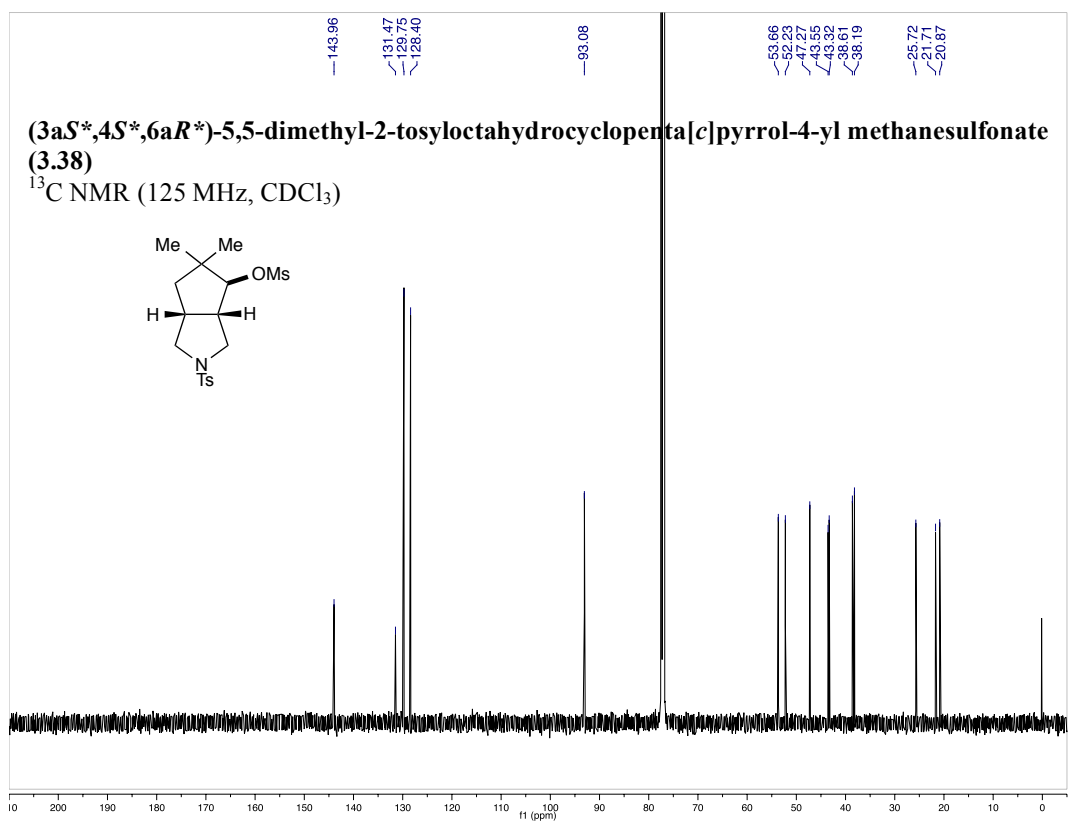
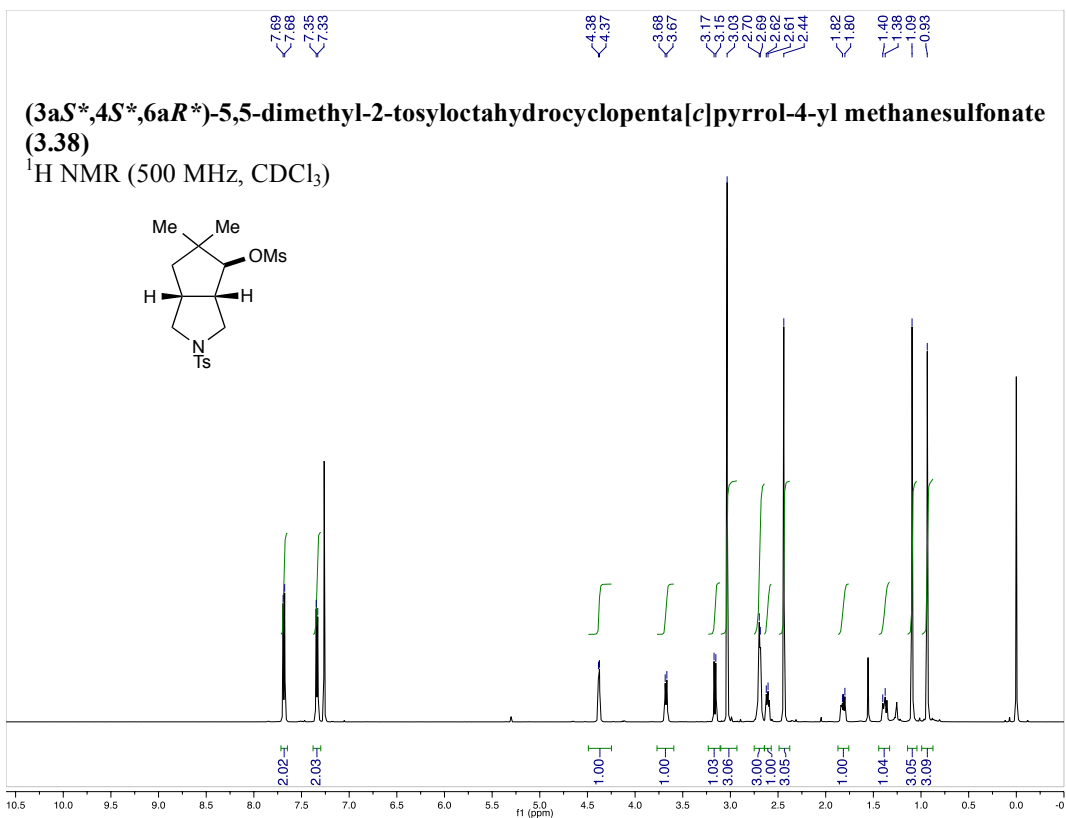


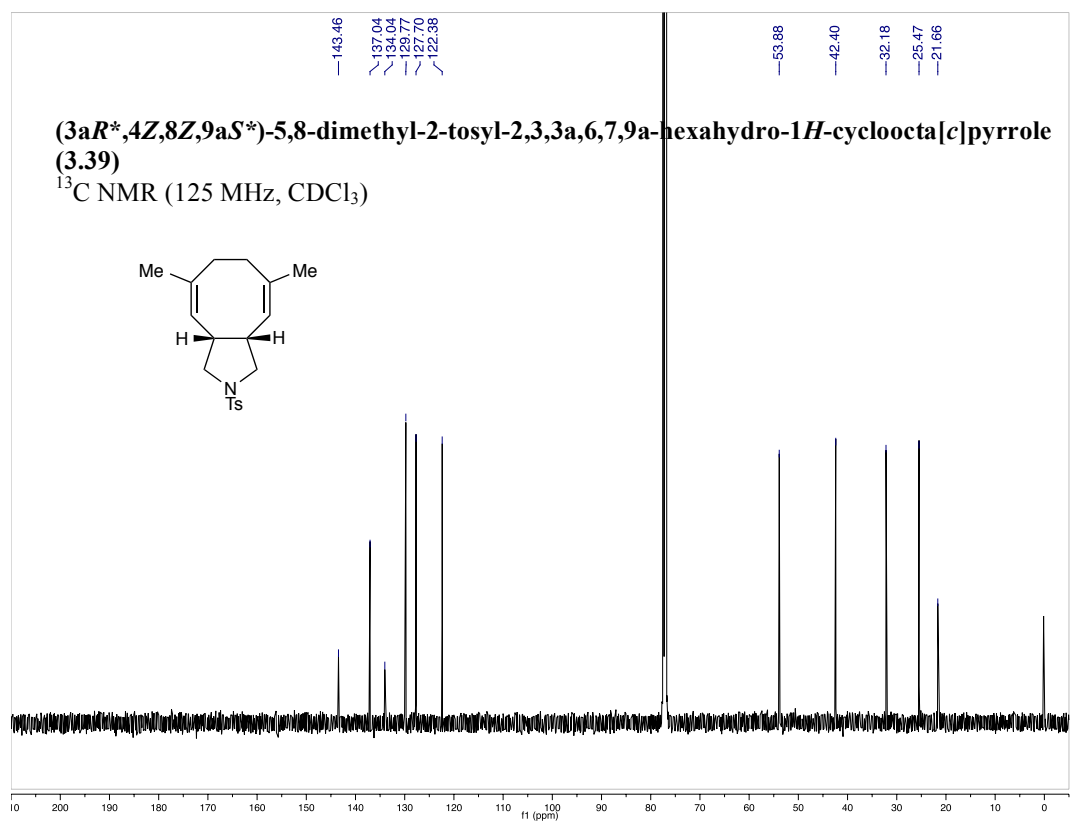
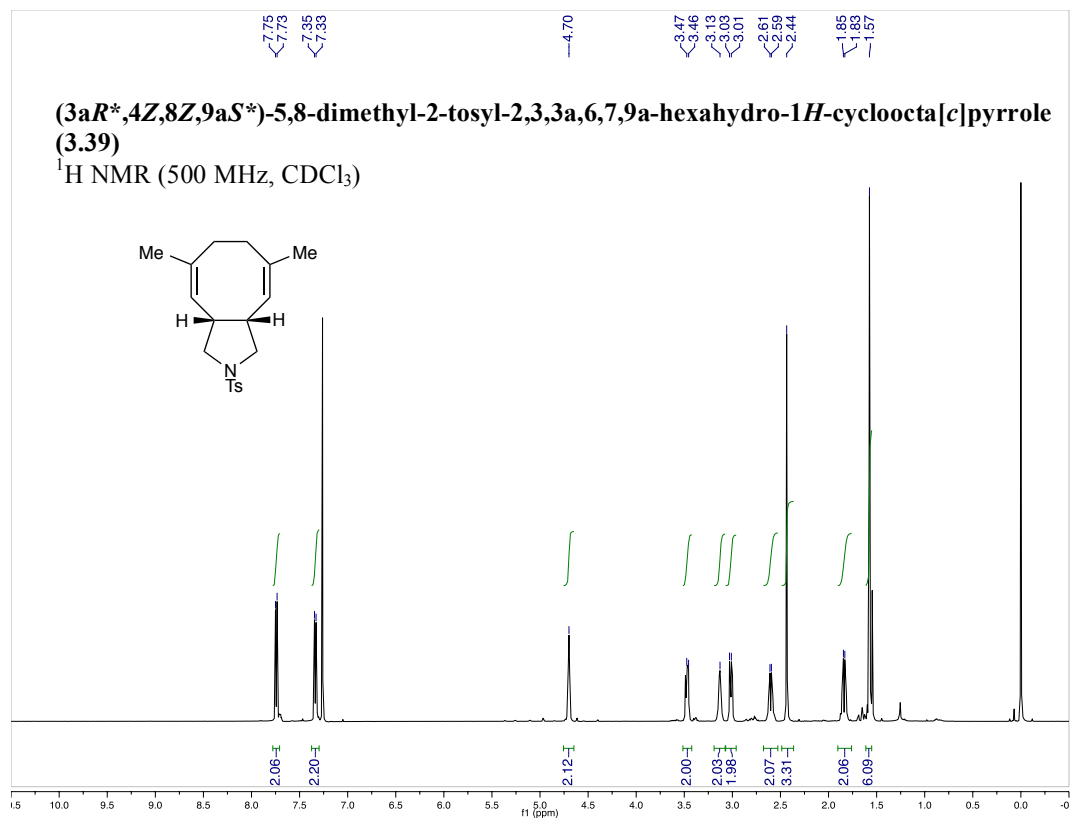


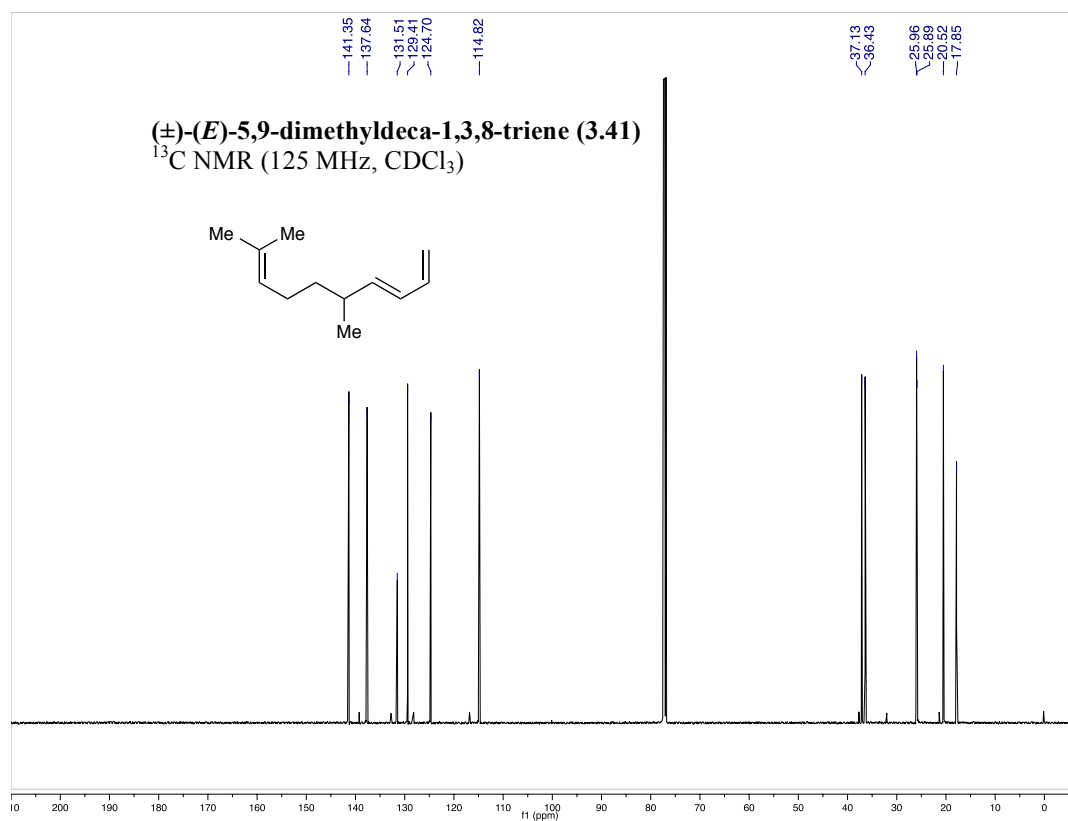
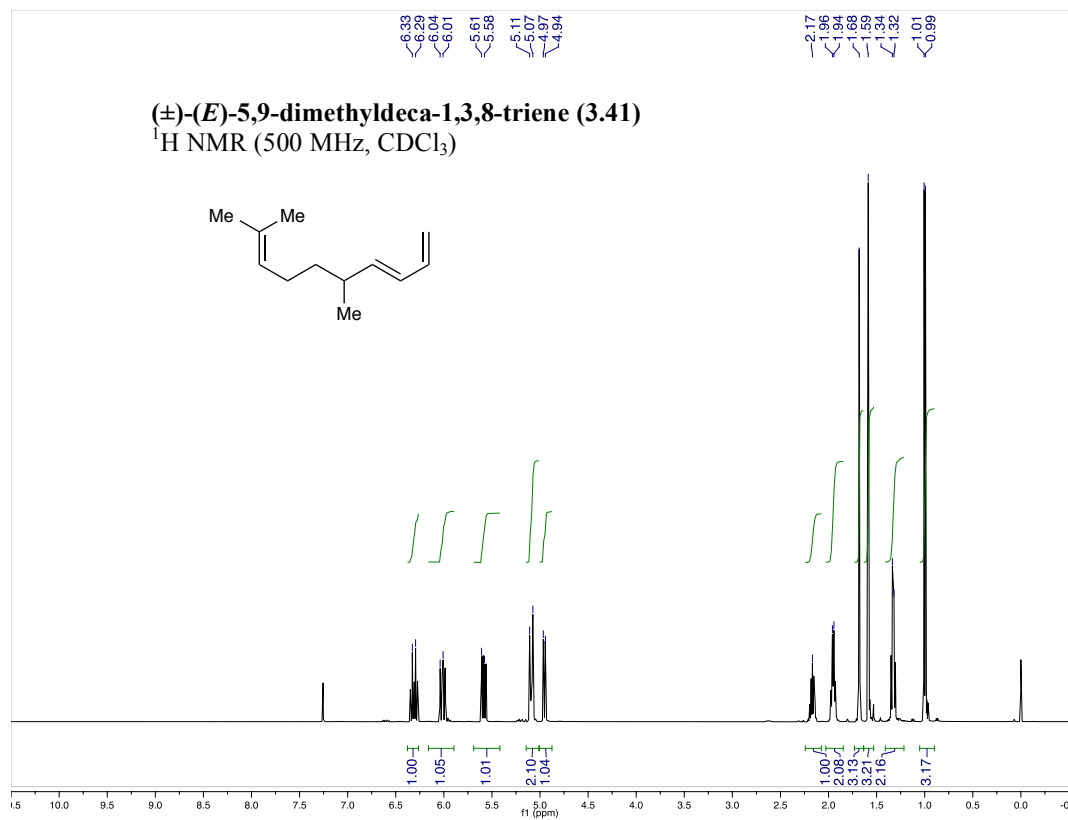


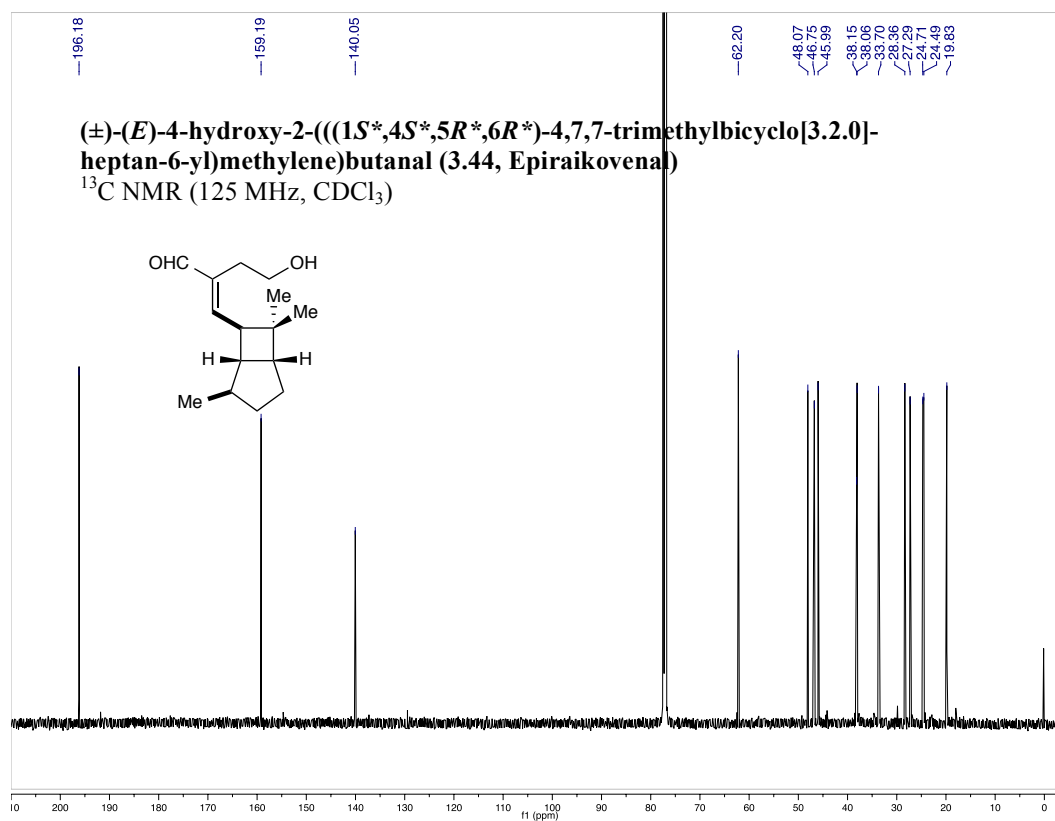
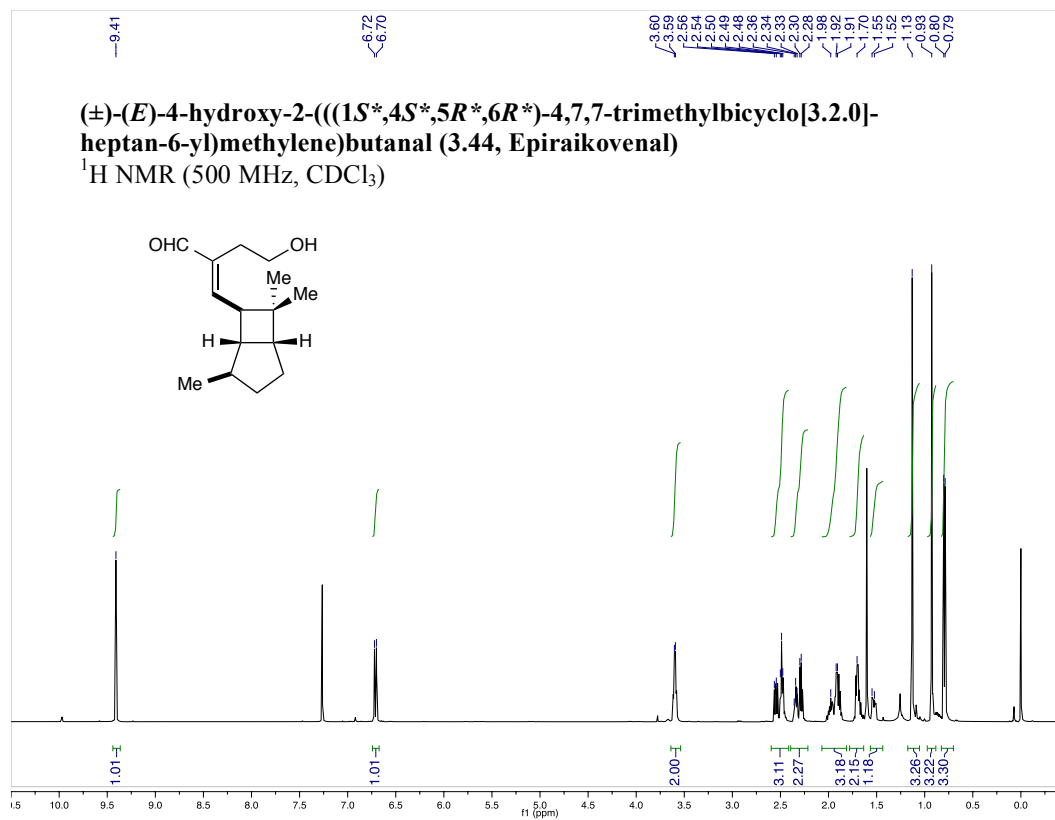


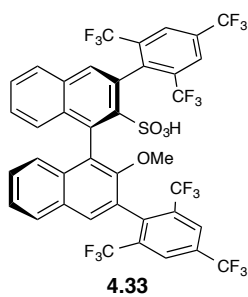
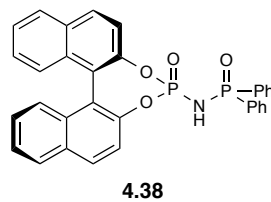
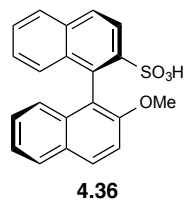


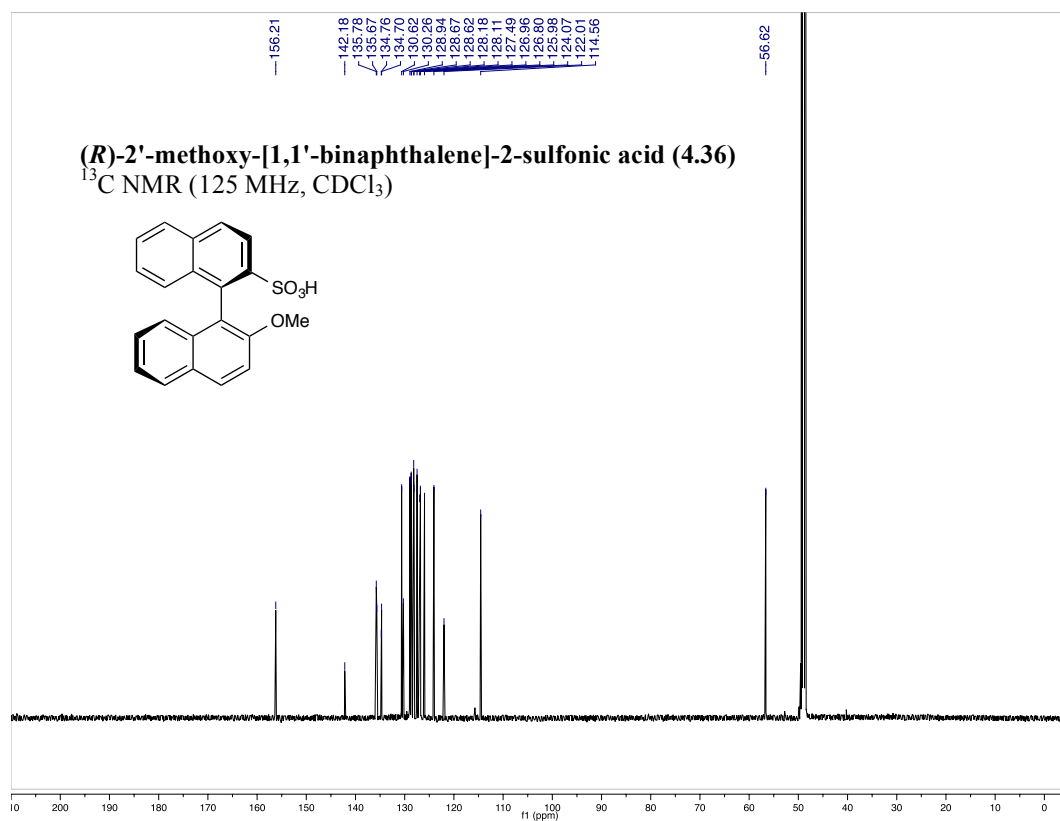
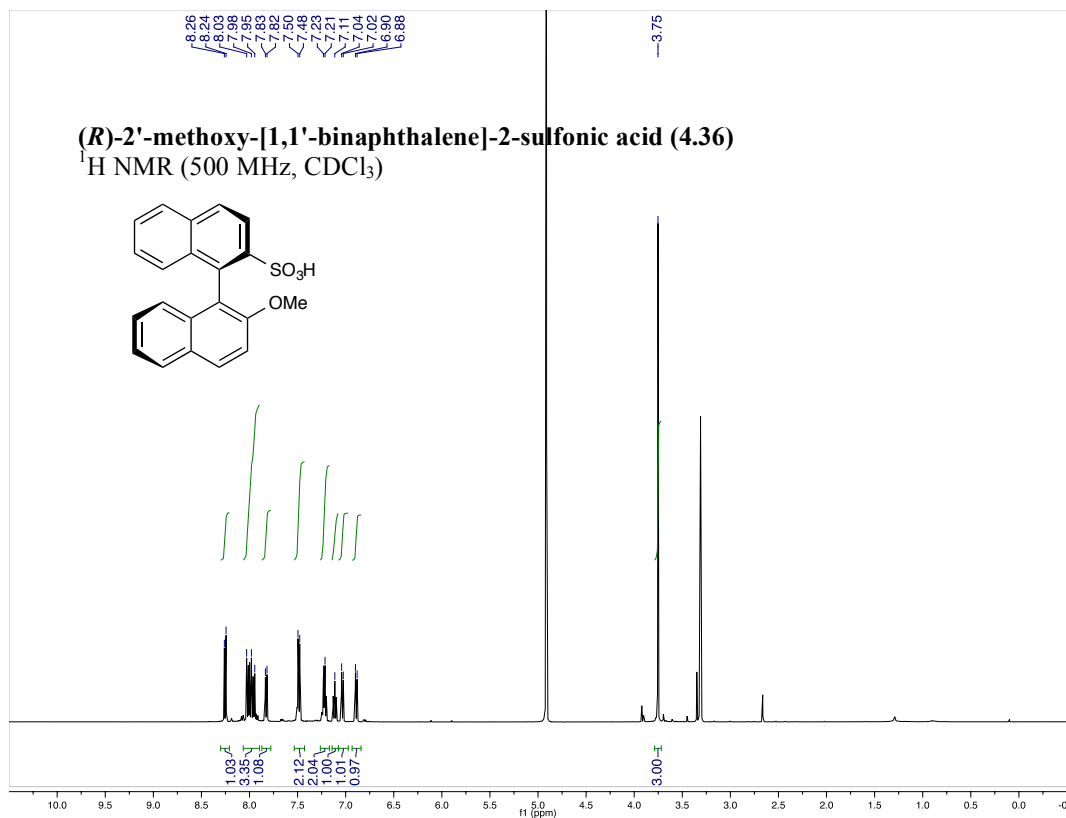


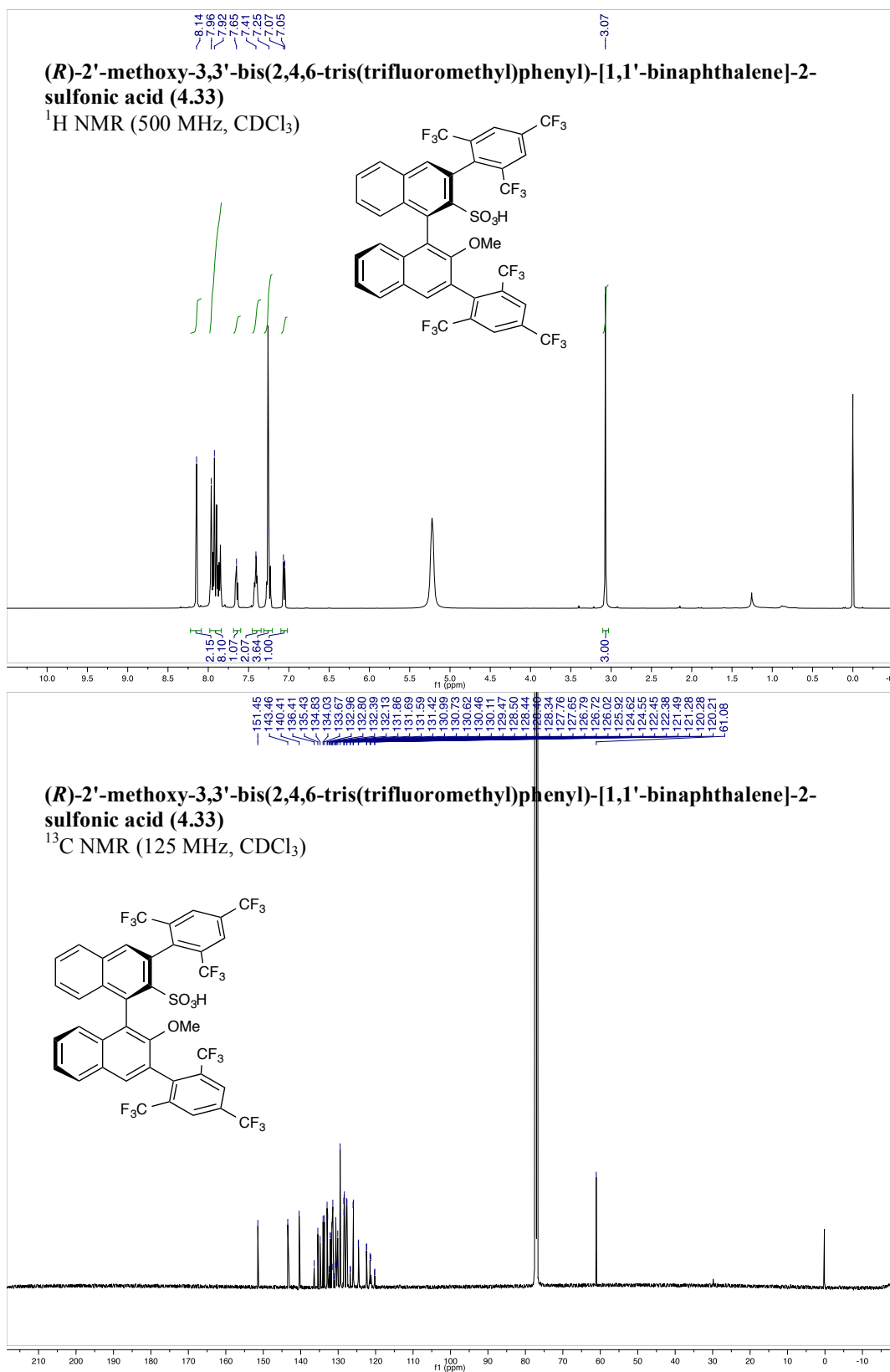


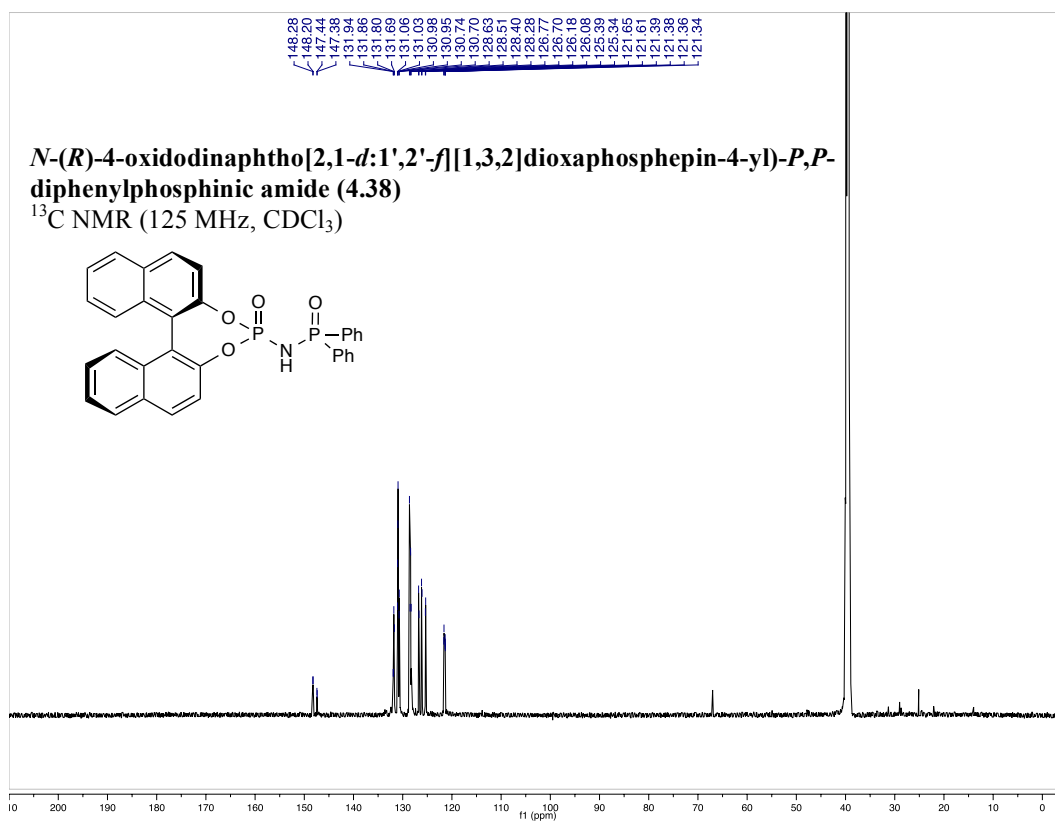




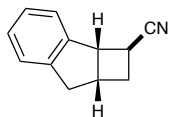
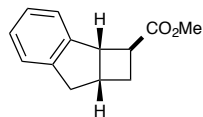
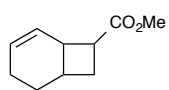
List of Compounds for Chapter 4

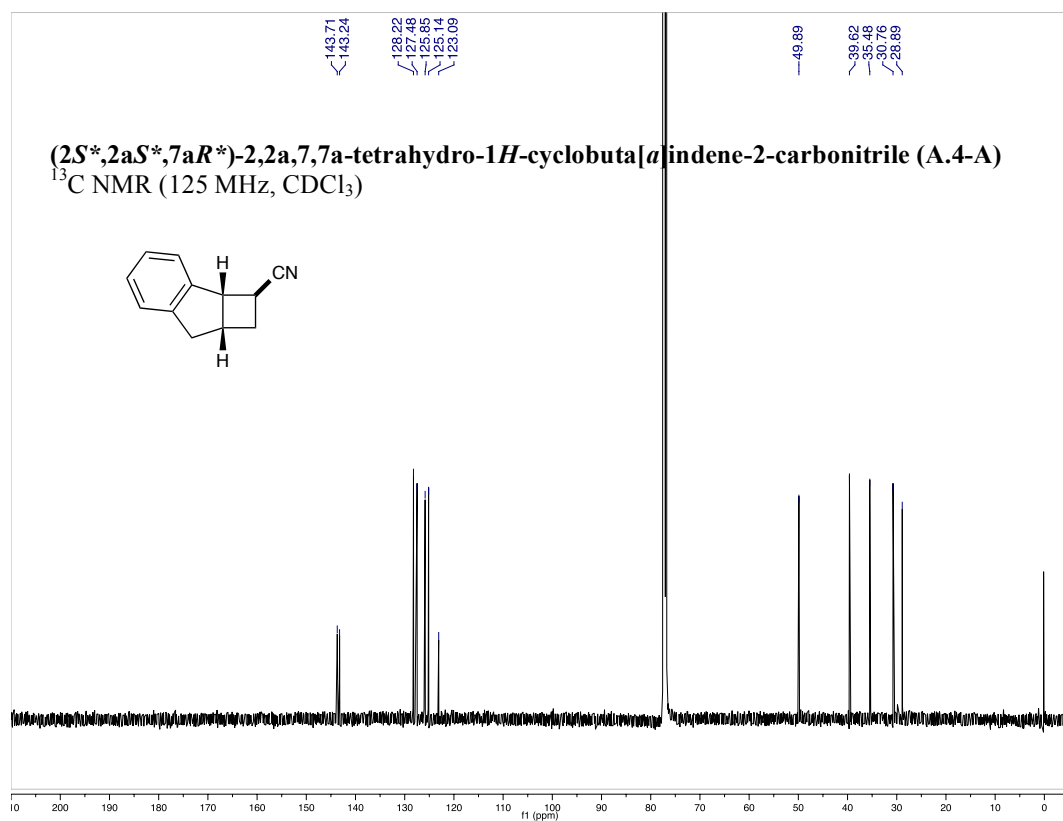
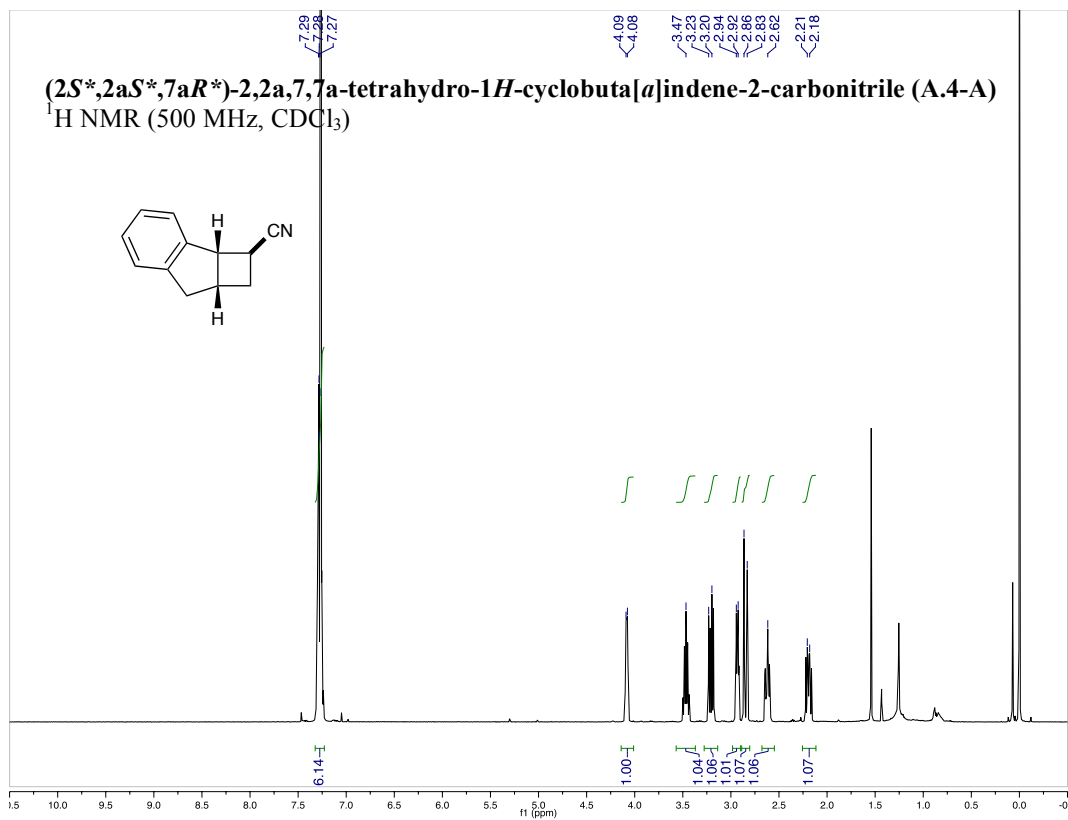


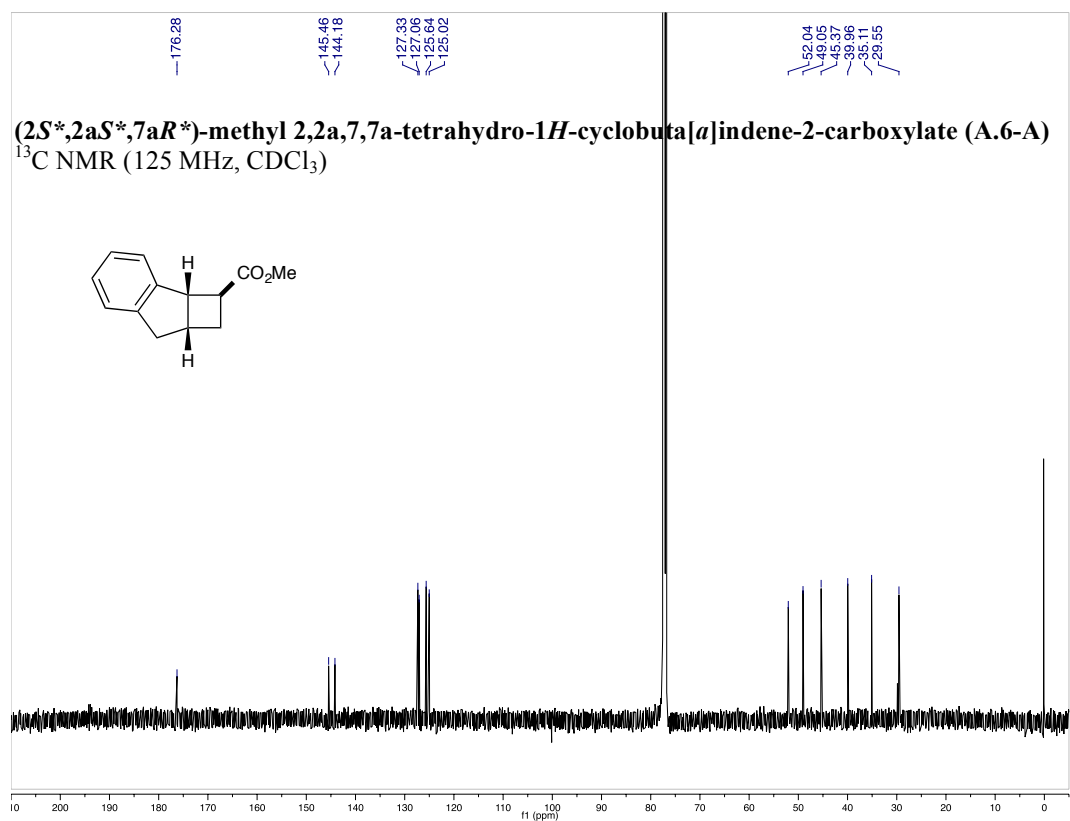
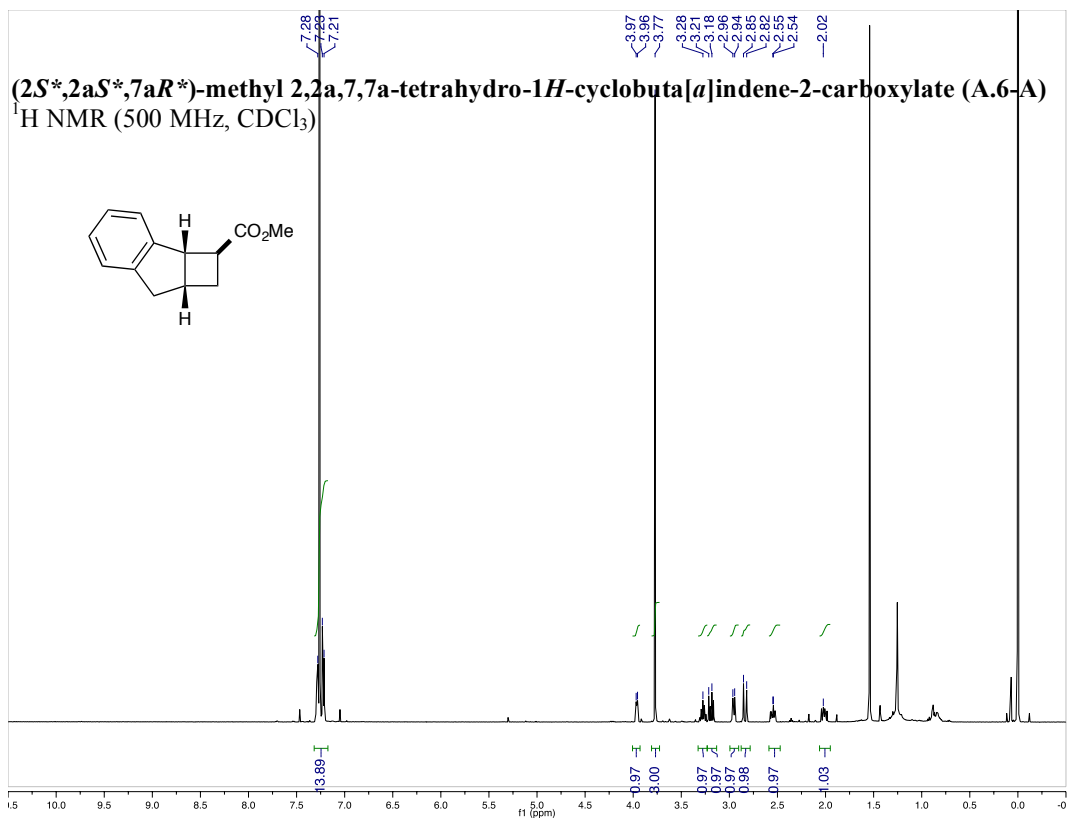


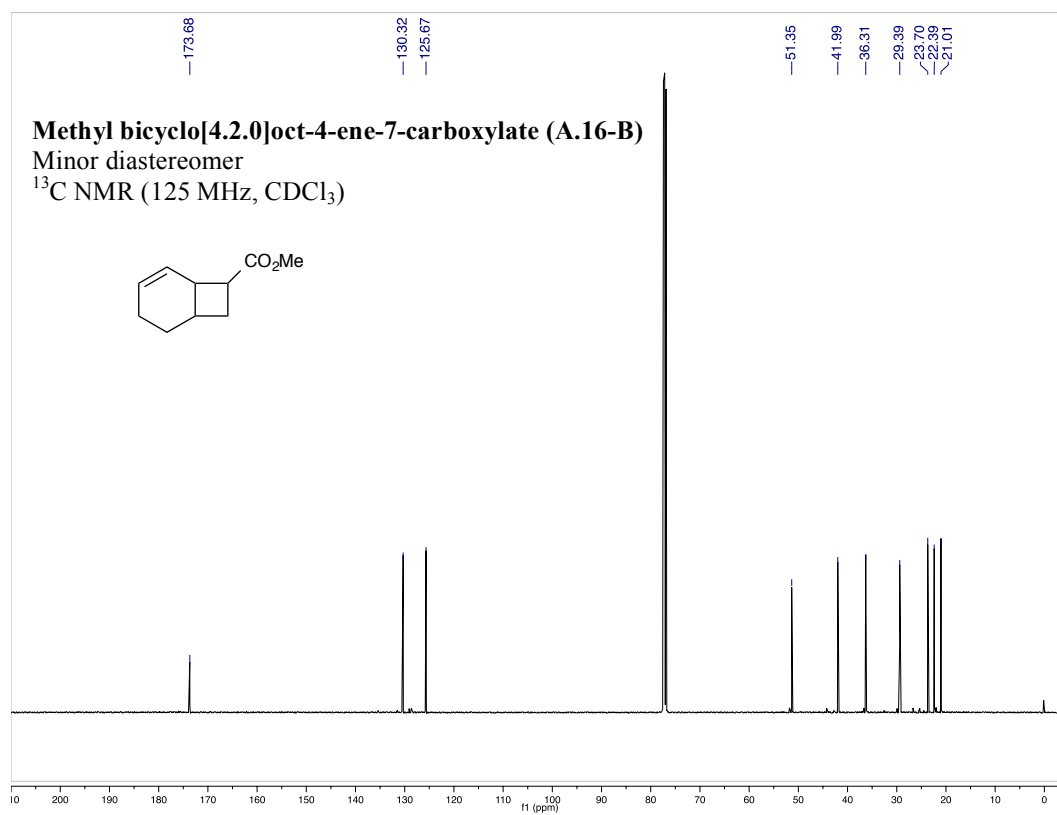
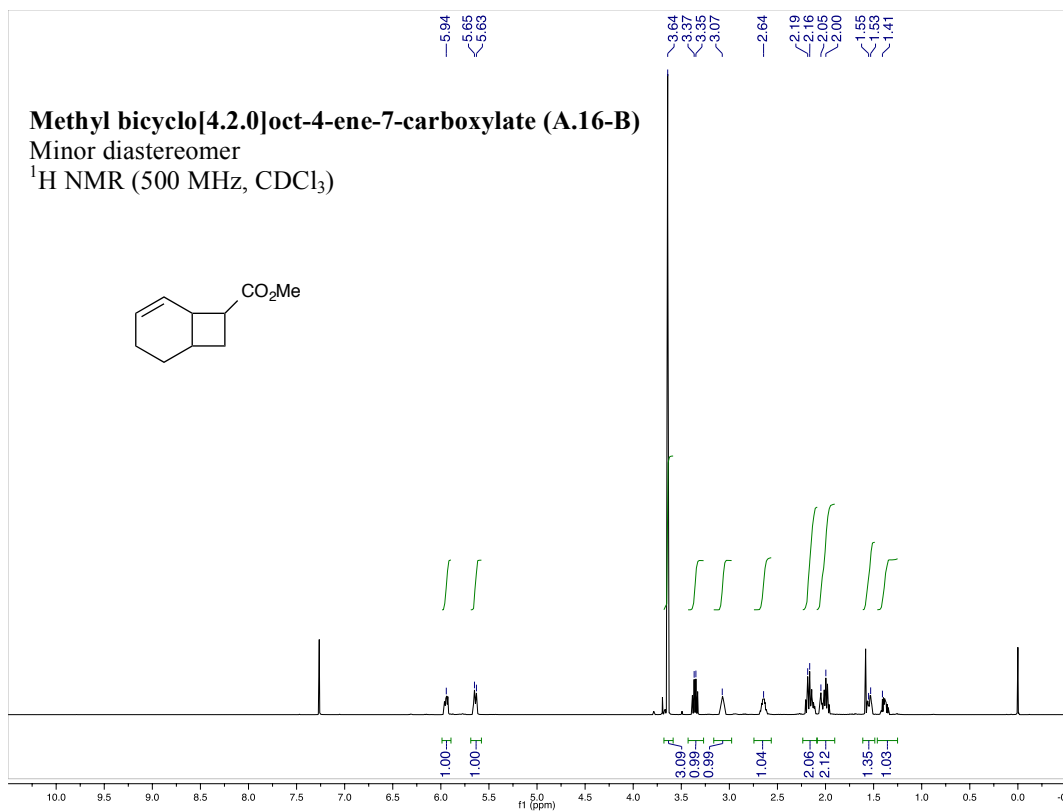


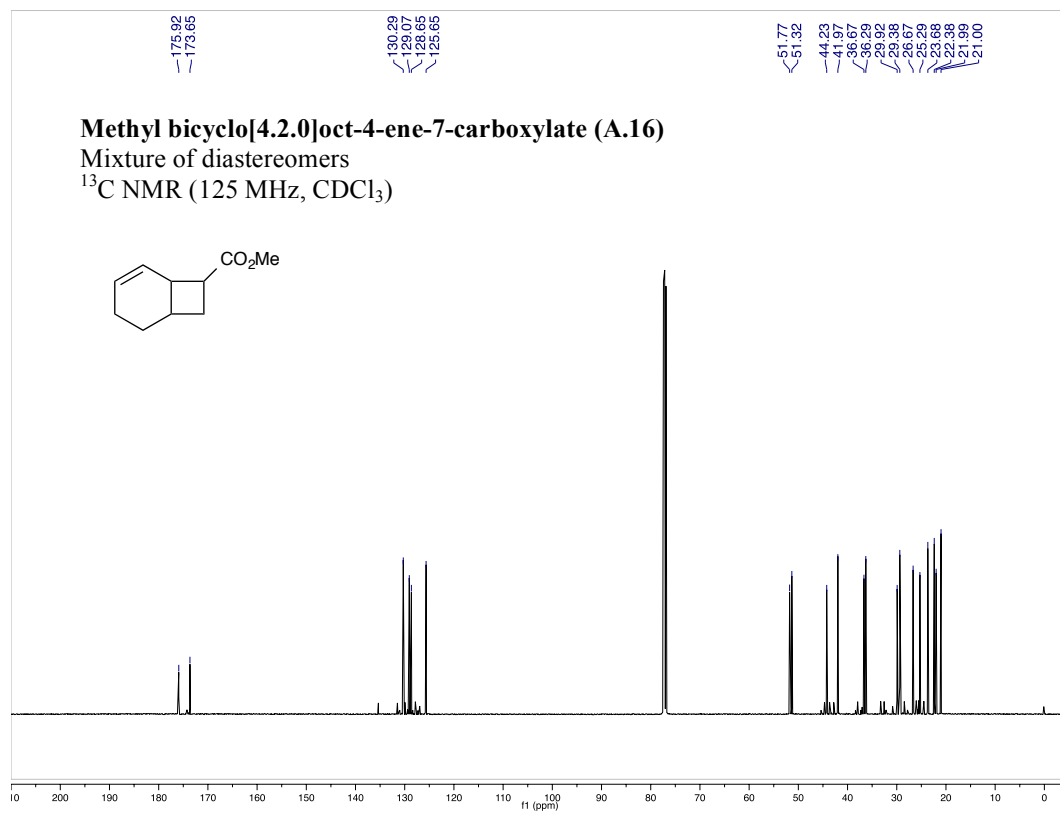
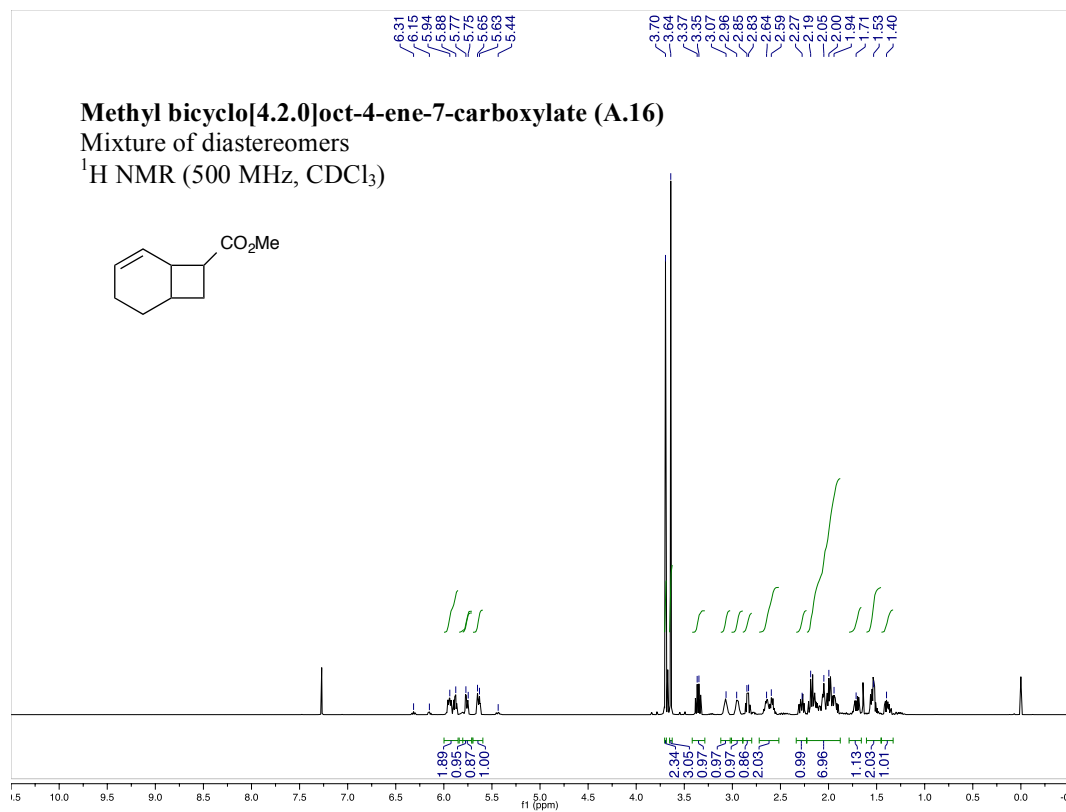
List of Compounds for Appendix A

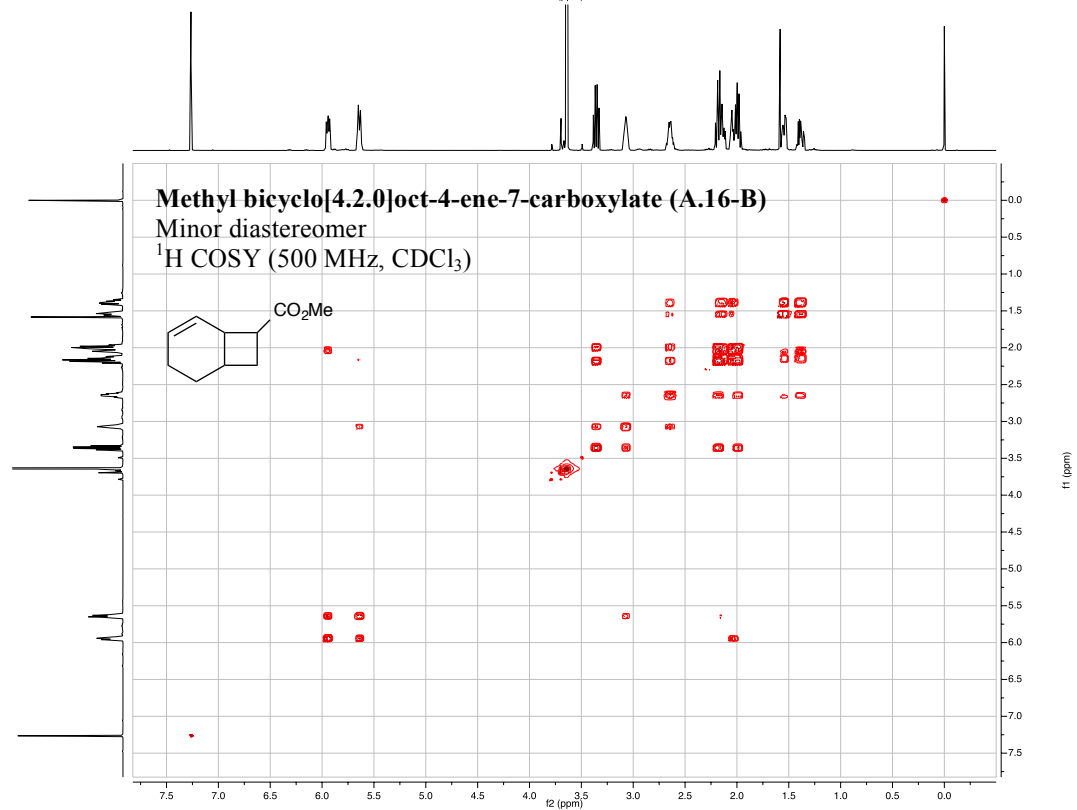
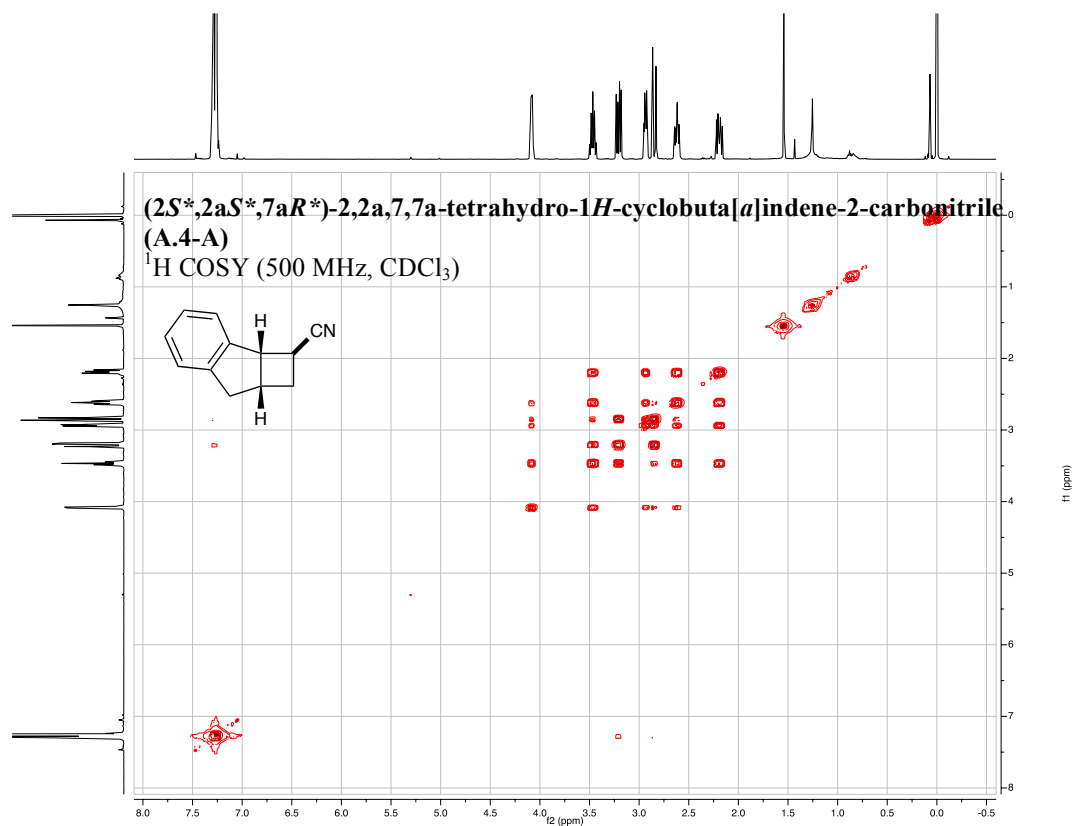
**A.4-A****A.6-A****A.16**



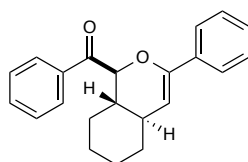




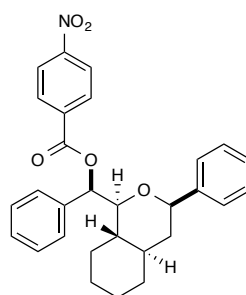




Appendix C. X-ray Crystallographic Data

Compounds characterized by X-ray diffraction analysis

3.14
(Yoon 15)



C.1
(Yoon27)

C. 1 Characterization of cycloadduct 3.4 (Yoon15)

Data Collection

A colorless crystal with approximate dimensions $0.54 \times 0.22 \times 0.12 \text{ mm}^3$ was selected under oil under ambient conditions and attached to the tip of a MiTeGen MicroMount©. The crystal was mounted in a stream of cold nitrogen at 100(2) K and centered in the X-ray beam by using a video camera.

The crystal evaluation and data collection were performed on a Bruker SMART APEXII diffractometer with Cu K_α ($\lambda = 1.54178 \text{ \AA}$) radiation and the diffractometer to crystal distance of 4.03 cm.

The initial cell constants were obtained from three series of ω scans at different starting angles. Each series consisted of 50 frames collected at intervals of 0.5° in a 25° range about ω with the exposure time of 5 seconds per frame. The reflections were successfully indexed by an automated indexing routine built in the APEXII program. The final cell constants were calculated from a set of 9941 strong reflections from the actual data collection.

The data were collected by using the full sphere data collection routine to survey the reciprocal space to the extent of a full sphere to a resolution of 0.82 \AA . A total of 43215 data were harvested by collecting 15 sets of frames with 0.7° scans in ω with an exposure time 6-12 sec per frame. These highly redundant datasets were corrected for Lorentz and polarization effects. The absorption correction was based on fitting a function to the empirical transmission surface as sampled by multiple equivalent measurements. [1]

Structure Solution and Refinement

The systematic absences in the diffraction data were uniquely consistent for the space groups $P2_1/n$ that yielded chemically reasonable and computationally stable results of refinement [2].

A successful solution by the direct methods provided most non-hydrogen atoms from the E -map. The remaining non-hydrogen atoms were located in an alternating series of least-squares cycles and difference Fourier maps. All non-hydrogen atoms were refined with anisotropic displacement coefficients. All hydrogen atoms were refined with independent isotropic displacement coefficients.

There are two symmetry independent molecules (mirror-image-related stereoisomers) in the asymmetric unit.

The final least-squares refinement of 565 parameters against 6146 data resulted in residuals R (based on F^2 for $I \geq 2\sigma$) and wR (based on F^2 for all data) of 0.0543 and 0.1574, respectively. The final difference Fourier map was featureless.

The molecular diagrams are drawn with 50% probability ellipsoids.

References

- [1] Bruker-AXS. (2007) APEX2, SADABS, and SAINT Software Reference Manuals. Bruker-AXS, Madison, Wisconsin, USA.
- [2] Sheldrick, G. M. (2008) SHELXL. *Acta Cryst.* **A64**, 112-122.
- [3] Pennington, W.T. (1999) Diamond. *J. Appl. Cryst.* **32**(5), 1028-1029.
- [4] Dolomanov, O.V.; Bourhis, L.J.; Gildea, R.J.; Howard, J.A.K.; Puschmann, H. "OLEX2: a complete structure solution, refinement and analysis program". *J. Appl. Cryst.* (2009) **42**, *in print*.

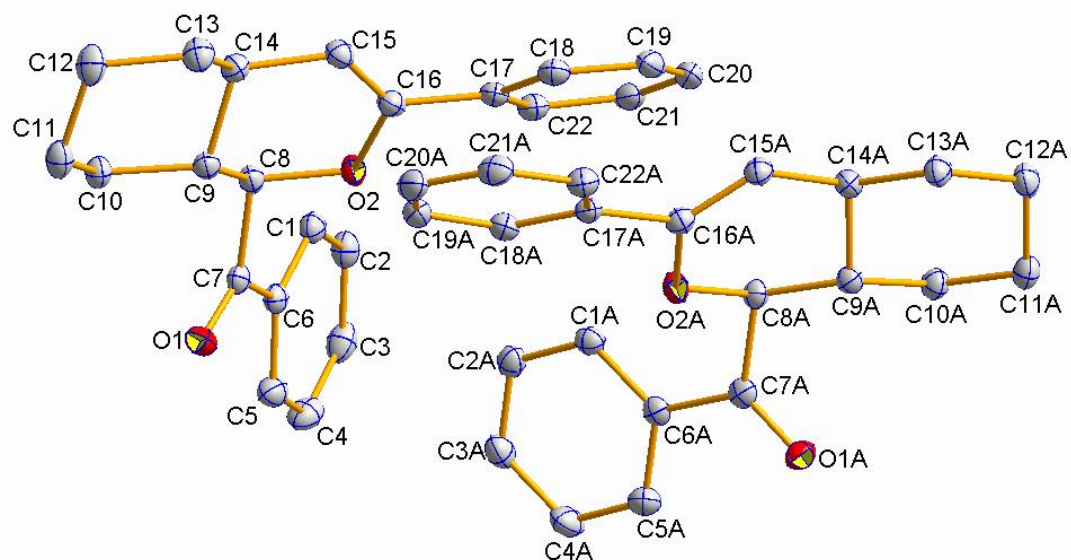


Figure C-1. A molecular drawing of Yoon15. All H atoms are omitted [3].

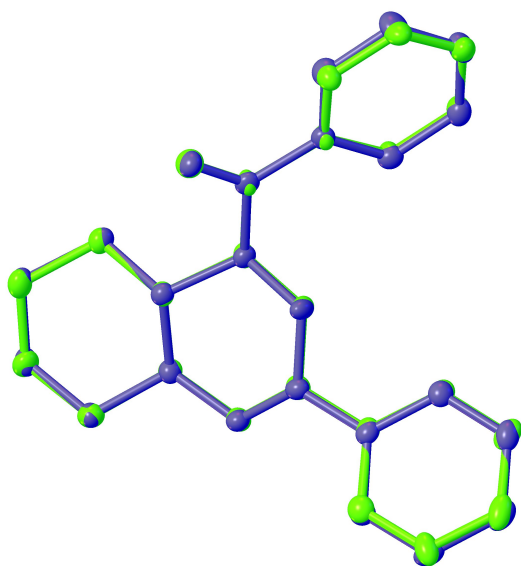


Figure C-2. The two stereoisomers of Yoon15 superimposed (one molecule had to be inverted). All H atoms are omitted [4].

Table C-1. Crystal data and structure refinement for yoon15.

Identification code	yoon15	
Empirical formula	C ₂₂ H ₂₂ O ₂	
Formula weight	318.40	
Temperature	100(2) K	
Wavelength	1.54178 Å	
Crystal system	Monoclinic	
Space group	P2 ₁ /n	
Unit cell dimensions	a = 9.6022(3) Å	$\alpha = 90^\circ$.
	b = 18.1549(6) Å	$\beta = 97.663(2)^\circ$.
	c = 19.5359(6) Å	$\gamma = 90^\circ$.
Volume	3375.22(19) Å ³	
Z	8	
Density (calculated)	1.253 Mg/m ³	
Absorption coefficient	0.616 mm ⁻¹	
F(000)	1360	
Crystal size	0.54 x 0.22 x 0.12 mm ³	
Theta range for data collection	3.34 to 69.72°.	
Index ranges	-11 ≤ h ≤ 11, -21 ≤ k ≤ 21, -23 ≤ l ≤ 23	
Reflections collected	43215	
Independent reflections	6146 [R(int) = 0.0276]	
Completeness to theta = 67.00°	97.6 %	
Absorption correction	Empirical with SADABS	
Max. and min. transmission	0.9319 and 0.7304	
Refinement method	Full-matrix least-squares on F ²	
Data / restraints / parameters	6146 / 0 / 565	
Goodness-of-fit on F ²	1.034	
Final R indices [I > 2σ(I)]	R1 = 0.0543, wR2 = 0.1479	
R indices (all data)	R1 = 0.0613, wR2 = 0.1574	
Largest diff. peak and hole	0.703 and -0.227 e.Å ⁻³	

Table C-2. Atomic coordinates ($\times 10^4$) and equivalent isotropic displacement parameters ($\text{\AA}^2 \times 10^3$) for yoon15. U(eq) is defined as one third of the trace of the orthogonalized U^{ij} tensor.

x	y	z	U(eq)	
O(1)	7009(1)	8752(1)	1858(1)	22(1)
O(2)	7582(1)	7601(1)	3131(1)	19(1)
C(1)	9830(1)	7422(1)	2222(1)	19(1)
C(2)	10659(2)	6963(1)	1875(1)	22(1)
C(3)	10431(2)	6920(1)	1159(1)	26(1)
C(4)	9371(2)	7336(1)	786(1)	26(1)
C(5)	8547(2)	7796(1)	1131(1)	22(1)
C(6)	8768(1)	7844(1)	1852(1)	17(1)
C(7)	7857(1)	8354(1)	2195(1)	17(1)
C(8)	7980(1)	8350(1)	2989(1)	17(1)
C(9)	7065(1)	8919(1)	3287(1)	17(1)
C(10)	7488(2)	9717(1)	3162(1)	19(1)
C(11)	6501(2)	10248(1)	3467(1)	23(1)
C(12)	6484(2)	10110(1)	4239(1)	25(1)
C(13)	6142(2)	9307(1)	4379(1)	23(1)
C(14)	7151(1)	8790(1)	4068(1)	18(1)
C(15)	6934(2)	7991(1)	4214(1)	18(1)
C(16)	7140(1)	7463(1)	3762(1)	18(1)
C(17)	6954(1)	6664(1)	3862(1)	17(1)
C(18)	5917(2)	6402(1)	4240(1)	20(1)
C(19)	5748(2)	5650(1)	4330(1)	24(1)
C(20)	6623(2)	5150(1)	4058(1)	26(1)
C(21)	7661(2)	5406(1)	3689(1)	24(1)
C(22)	7818(2)	6157(1)	3582(1)	20(1)
O(1A)	1963(1)	4665(1)	1847(1)	22(1)
O(2A)	2493(1)	5799(1)	3133(1)	19(1)
C(1A)	4786(1)	5989(1)	2255(1)	18(1)
C(2A)	5659(2)	6435(1)	1922(1)	20(1)
C(3A)	5540(2)	6439(1)	1208(1)	24(1)
C(4A)	4547(2)	5993(1)	821(1)	27(1)
C(5A)	3664(2)	5554(1)	1151(1)	22(1)
C(6A)	3774(1)	5547(1)	1870(1)	17(1)
C(7A)	2812(1)	5052(1)	2197(1)	17(1)
C(8A)	2901(1)	5052(1)	2989(1)	16(1)
C(9A)	1980(1)	4476(1)	3274(1)	16(1)
C(10A)	2428(2)	3684(1)	3146(1)	19(1)
C(11A)	1424(2)	3144(1)	3430(1)	21(1)
C(12A)	1356(2)	3275(1)	4197(1)	22(1)
C(13A)	1014(2)	4078(1)	4350(1)	20(1)
C(14A)	2040(1)	4598(1)	4054(1)	17(1)
C(15A)	1827(1)	5396(1)	4208(1)	17(1)
C(16A)	2055(1)	5930(1)	3767(1)	17(1)
C(17A)	1922(1)	6730(1)	3890(1)	17(1)
C(18A)	2773(2)	7233(1)	3596(1)	19(1)
C(19A)	2689(2)	7984(1)	3734(1)	22(1)
C(20A)	1733(2)	8242(1)	4151(1)	25(1)
C(21A)	868(2)	7746(1)	4435(1)	24(1)
C(22A)	960(2)	6999(1)	4309(1)	20(1)

Table C-3. Bond lengths [Å] and angles [°] for yoon15.

O(1)-C(7)	1.2154(17)	O(1A)-C(7A)	1.2158(17)
O(2)-C(16)	1.3795(16)	O(2A)-C(16A)	1.3811(16)
O(2)-C(8)	1.4494(16)	O(2A)-C(8A)	1.4496(15)
C(1)-C(2)	1.390(2)	C(1A)-C(2A)	1.389(2)
C(1)-C(6)	1.3980(19)	C(1A)-C(6A)	1.3982(19)
C(1)-H(1)	1.003(17)	C(1A)-H(1A)	0.955(17)
C(2)-C(3)	1.389(2)	C(2A)-C(3A)	1.383(2)
C(2)-H(2)	0.972(19)	C(2A)-H(2A)	0.954(18)
C(3)-C(4)	1.392(2)	C(3A)-C(4A)	1.395(2)
C(3)-H(3)	1.017(19)	C(3A)-H(3A)	0.992(18)
C(4)-C(5)	1.385(2)	C(4A)-C(5A)	1.383(2)
C(4)-H(4)	0.945(19)	C(4A)-H(4A)	0.954(19)
C(5)-C(6)	1.3994(19)	C(5A)-C(6A)	1.3956(19)
C(5)-H(5)	0.974(18)	C(5A)-H(5A)	0.992(18)
C(6)-C(7)	1.4935(19)	C(6A)-C(7A)	1.4921(19)
C(7)-C(8)	1.5390(18)	C(7A)-C(8A)	1.5386(18)
C(8)-C(9)	1.5209(19)	C(8A)-C(9A)	1.5213(18)
C(8)-H(8)	0.977(17)	C(8A)-H(8A)	1.000(17)
C(9)-C(10)	1.5317(18)	C(9A)-C(10A)	1.5302(18)
C(9)-C(14)	1.5362(18)	C(9A)-C(14A)	1.5336(18)
C(9)-H(9)	0.961(17)	C(9A)-H(9A)	0.970(17)
C(10)-C(11)	1.5289(19)	C(10A)-C(11A)	1.5307(19)
C(10)-H(10B)	0.994(18)	C(10A)-H(10D)	1.000(17)
C(10)-H(10A)	0.995(17)	C(10A)-H(10C)	0.978(17)
C(11)-C(12)	1.531(2)	C(11A)-C(12A)	1.528(2)
C(11)-H(11A)	0.994(19)	C(11A)-H(11D)	0.988(18)
C(11)-H(11B)	0.991(19)	C(11A)-H(11C)	0.977(18)
C(12)-C(13)	1.527(2)	C(12A)-C(13A)	1.5326(19)
C(12)-H(12B)	0.997(19)	C(12A)-H(12D)	0.984(18)
C(12)-H(12A)	0.998(19)	C(12A)-H(12C)	0.997(18)
C(13)-C(14)	1.5311(19)	C(13A)-C(14A)	1.5316(19)
C(13)-H(13A)	0.994(18)	C(13A)-H(13C)	0.985(17)
C(13)-H(13B)	0.989(18)	C(13A)-H(13D)	0.965(18)
C(14)-C(15)	1.4992(19)	C(14A)-C(15A)	1.5001(18)
C(14)-H(14)	0.999(17)	C(14A)-H(14A)	0.985(17)
C(15)-C(16)	1.336(2)	C(15A)-C(16A)	1.334(2)
C(15)-H(15)	0.940(17)	C(15A)-H(15A)	0.941(17)
C(16)-C(17)	1.4774(18)	C(16A)-C(17A)	1.4803(18)
C(17)-C(22)	1.398(2)	C(17A)-C(18A)	1.3998(19)
C(17)-C(18)	1.400(2)	C(17A)-C(22A)	1.402(2)
C(18)-C(19)	1.389(2)	C(18A)-C(19A)	1.393(2)
C(18)-H(18)	0.957(18)	C(18A)-H(18A)	0.988(18)
C(19)-C(20)	1.390(2)	C(19A)-C(20A)	1.388(2)
C(19)-H(19)	0.920(19)	C(19A)-H(19A)	0.990(18)
C(20)-C(21)	1.386(2)	C(20A)-C(21A)	1.388(2)
C(20)-H(20)	0.990(19)	C(20A)-H(20A)	0.992(19)
C(21)-C(22)	1.391(2)	C(21A)-C(22A)	1.385(2)
C(21)-H(21)	0.980(19)	C(21A)-H(21A)	0.947(19)
C(22)-H(22)	0.981(18)	C(22A)-H(22A)	0.956(18)
C(16)-O(2)-C(8)	117.54(10)	C(3)-C(2)-C(1)	120.05(14)
C(2)-C(1)-C(6)	120.13(13)	C(3)-C(2)-H(2)	120.1(10)
C(2)-C(1)-H(1)	121.3(10)	C(1)-C(2)-H(2)	119.9(10)
C(6)-C(1)-H(1)	118.6(10)	C(2)-C(3)-C(4)	120.27(14)

C(2)-C(3)-H(3)	118.7(10)	C(16)-C(15)-C(14)	122.11(13)
C(4)-C(3)-H(3)	121.1(10)	C(16)-C(15)-H(15)	117.6(10)
C(5)-C(4)-C(3)	119.75(14)	C(14)-C(15)-H(15)	120.2(10)
C(5)-C(4)-H(4)	120.5(11)	C(15)-C(16)-O(2)	123.45(13)
C(3)-C(4)-H(4)	119.8(11)	C(15)-C(16)-C(17)	125.83(13)
C(4)-C(5)-C(6)	120.51(14)	O(2)-C(16)-C(17)	110.71(11)
C(4)-C(5)-H(5)	119.4(10)	C(22)-C(17)-C(18)	118.89(13)
C(6)-C(5)-H(5)	120.0(10)	C(22)-C(17)-C(16)	120.42(13)
C(1)-C(6)-C(5)	119.28(13)	C(18)-C(17)-C(16)	120.69(13)
C(1)-C(6)-C(7)	122.57(12)	C(19)-C(18)-C(17)	120.32(14)
C(5)-C(6)-C(7)	118.15(12)	C(19)-C(18)-H(18)	120.0(11)
O(1)-C(7)-C(6)	121.02(12)	C(17)-C(18)-H(18)	119.5(11)
O(1)-C(7)-C(8)	120.35(12)	C(18)-C(19)-C(20)	120.44(14)
C(6)-C(7)-C(8)	118.61(11)	C(18)-C(19)-H(19)	120.1(12)
O(2)-C(8)-C(9)	112.56(11)	C(20)-C(19)-H(19)	119.5(12)
O(2)-C(8)-C(7)	102.12(10)	C(21)-C(20)-C(19)	119.55(14)
C(9)-C(8)-C(7)	114.31(11)	C(21)-C(20)-H(20)	120.1(10)
O(2)-C(8)-H(8)	108.6(10)	C(19)-C(20)-H(20)	120.3(10)
C(9)-C(8)-H(8)	108.8(10)	C(20)-C(21)-C(22)	120.48(14)
C(7)-C(8)-H(8)	110.2(10)	C(20)-C(21)-H(21)	122.0(11)
C(8)-C(9)-C(10)	113.69(11)	C(22)-C(21)-H(21)	117.5(11)
C(8)-C(9)-C(14)	108.64(11)	C(21)-C(22)-C(17)	120.29(14)
C(10)-C(9)-C(14)	108.84(11)	C(21)-C(22)-H(22)	119.9(10)
C(8)-C(9)-H(9)	107.8(10)	C(17)-C(22)-H(22)	119.8(10)
C(10)-C(9)-H(9)	109.4(10)	C(16A)-O(2A)-C(8A)	117.24(10)
C(14)-C(9)-H(9)	108.4(10)	C(2A)-C(1A)-C(6A)	120.15(13)
C(11)-C(10)-C(9)	110.07(12)	C(2A)-C(1A)-H(1A)	121.3(10)
C(11)-C(10)-H(10B)	109.9(10)	C(6A)-C(1A)-H(1A)	118.5(10)
C(9)-C(10)-H(10B)	108.0(10)	C(3A)-C(2A)-C(1A)	120.06(13)
C(11)-C(10)-H(10A)	111.6(10)	C(3A)-C(2A)-H(2A)	119.9(10)
C(9)-C(10)-H(10A)	111.1(10)	C(1A)-C(2A)-H(2A)	120.0(10)
H(10B)-C(10)-H(10A)	106.0(14)	C(2A)-C(3A)-C(4A)	120.20(14)
C(10)-C(11)-C(12)	111.67(12)	C(2A)-C(3A)-H(3A)	118.4(10)
C(10)-C(11)-H(11A)	108.0(10)	C(4A)-C(3A)-H(3A)	121.4(10)
C(12)-C(11)-H(11A)	108.8(10)	C(5A)-C(4A)-C(3A)	119.86(14)
C(10)-C(11)-H(11B)	111.3(10)	C(5A)-C(4A)-H(4A)	121.3(11)
C(12)-C(11)-H(11B)	108.2(10)	C(3A)-C(4A)-H(4A)	118.9(11)
H(11A)-C(11)-H(11B)	108.7(14)	C(4A)-C(5A)-C(6A)	120.41(13)
C(13)-C(12)-C(11)	111.32(12)	C(4A)-C(5A)-H(5A)	120.6(10)
C(13)-C(12)-H(12B)	108.6(11)	C(6A)-C(5A)-H(5A)	119.0(10)
C(11)-C(12)-H(12B)	110.5(11)	C(5A)-C(6A)-C(1A)	119.32(13)
C(13)-C(12)-H(12A)	109.6(11)	C(5A)-C(6A)-C(7A)	117.91(12)
C(11)-C(12)-H(12A)	110.7(10)	C(1A)-C(6A)-C(7A)	122.76(12)
H(12B)-C(12)-H(12A)	106.0(14)	O(1A)-C(7A)-C(6A)	121.04(12)
C(12)-C(13)-C(14)	110.56(12)	O(1A)-C(7A)-C(8A)	120.55(12)
C(12)-C(13)-H(13A)	110.7(10)	C(6A)-C(7A)-C(8A)	118.41(11)
C(14)-C(13)-H(13A)	109.6(10)	O(2A)-C(8A)-C(9A)	112.74(11)
C(12)-C(13)-H(13B)	112.2(10)	O(2A)-C(8A)-C(7A)	102.40(10)
C(14)-C(13)-H(13B)	108.5(10)	C(9A)-C(8A)-C(7A)	114.30(11)
H(13A)-C(13)-H(13B)	105.2(14)	O(2A)-C(8A)-H(8A)	107.9(9)
C(15)-C(14)-C(13)	113.98(12)	C(9A)-C(8A)-H(8A)	110.3(9)
C(15)-C(14)-C(9)	110.28(11)	C(7A)-C(8A)-H(8A)	108.8(10)
C(13)-C(14)-C(9)	110.34(11)	C(8A)-C(9A)-C(10A)	113.32(11)
C(15)-C(14)-H(14)	109.0(9)	C(8A)-C(9A)-C(14A)	108.57(11)
C(13)-C(14)-H(14)	105.6(9)	C(10A)-C(9A)-C(14A)	108.87(11)
C(9)-C(14)-H(14)	107.4(9)	C(8A)-C(9A)-H(9A)	108.4(10)

C(10A)-C(9A)-H(9A)	109.7(10)	C(13A)-C(14A)-C(9A)	110.24(11)
C(14A)-C(9A)-H(9A)	107.9(9)	C(15A)-C(14A)-H(14A)	107.8(10)
C(9A)-C(10A)-C(11A)	109.83(11)	C(13A)-C(14A)-H(14A)	106.5(10)
C(9A)-C(10A)-H(10D)	107.2(10)	C(9A)-C(14A)-H(14A)	107.5(9)
C(11A)-C(10A)-H(10D)	109.6(10)	C(16A)-C(15A)-C(14A)	122.21(13)
C(9A)-C(10A)-H(10C)	112.2(10)	C(16A)-C(15A)-H(15A)	118.1(10)
C(11A)-C(10A)-H(10C)	111.4(10)	C(14A)-C(15A)-H(15A)	119.6(10)
H(10D)-C(10A)-H(10C)	106.4(14)	C(15A)-C(16A)-O(2A)	123.41(12)
C(12A)-C(11A)-C(10A)	111.52(11)	C(15A)-C(16A)-C(17A)	125.63(13)
C(12A)-C(11A)-H(11D)	110.0(10)	O(2A)-C(16A)-C(17A)	110.94(11)
C(10A)-C(11A)-H(11D)	108.2(10)	C(18A)-C(17A)-C(22A)	118.60(13)
C(12A)-C(11A)-H(11C)	110.0(10)	C(18A)-C(17A)-C(16A)	120.45(12)
C(10A)-C(11A)-H(11C)	111.1(10)	C(22A)-C(17A)-C(16A)	120.95(12)
H(11D)-C(11A)-H(11C)	105.9(14)	C(19A)-C(18A)-C(17A)	120.45(14)
C(11A)-C(12A)-C(13A)	112.24(12)	C(19A)-C(18A)-H(18A)	119.7(10)
C(11A)-C(12A)-H(12D)	108.8(10)	C(17A)-C(18A)-H(18A)	119.9(10)
C(13A)-C(12A)-H(12D)	109.1(10)	C(20A)-C(19A)-C(18A)	120.27(14)
C(11A)-C(12A)-H(12C)	110.6(10)	C(20A)-C(19A)-H(19A)	122.3(10)
C(13A)-C(12A)-H(12C)	108.7(10)	C(18A)-C(19A)-H(19A)	117.4(10)
H(12D)-C(12A)-H(12C)	107.3(14)	C(19A)-C(20A)-C(21A)	119.59(13)
C(14A)-C(13A)-C(12A)	110.28(12)	C(19A)-C(20A)-H(20A)	118.5(11)
C(14A)-C(13A)-H(13C)	109.2(10)	C(21A)-C(20A)-H(20A)	121.8(10)
C(12A)-C(13A)-H(13C)	111.5(10)	C(22A)-C(21A)-C(20A)	120.55(14)
C(14A)-C(13A)-H(13D)	108.9(11)	C(22A)-C(21A)-H(21A)	120.0(11)
C(12A)-C(13A)-H(13D)	112.3(10)	C(20A)-C(21A)-H(21A)	119.5(11)
H(13C)-C(13A)-H(13D)	104.5(14)	C(21A)-C(22A)-C(17A)	120.52(14)
C(15A)-C(14A)-C(13A)	114.01(12)	C(21A)-C(22A)-H(22A)	120.7(11)
C(15A)-C(14A)-C(9A)	110.53(11)	C(17A)-C(22A)-H(22A)	118.7(11)

Symmetry transformations used to generate equivalent atoms:

Table C-4. Anisotropic displacement parameters ($\text{\AA}^2 \times 10^3$) for yoon15. The anisotropic displacement factor exponent takes the form: $-2p^2 [h^2 a^{*2} U^{11} + \dots + 2h k a^* b^* U^{12}]$

U^{11}	U^{22}	U^{33}	U^{23}	U^{13}	U^{12}	
O(1)	23(1)	22(1)	20(1)	3(1)	-1(1)	2(1)
O(2)	27(1)	14(1)	17(1)	0(1)	7(1)	-2(1)
C(1)	20(1)	17(1)	20(1)	1(1)	4(1)	-4(1)
C(2)	21(1)	19(1)	28(1)	0(1)	5(1)	-2(1)
C(3)	27(1)	22(1)	30(1)	-6(1)	11(1)	-4(1)
C(4)	29(1)	31(1)	19(1)	-5(1)	8(1)	-7(1)
C(5)	23(1)	25(1)	19(1)	1(1)	2(1)	-5(1)
C(6)	16(1)	17(1)	18(1)	1(1)	3(1)	-4(1)
C(7)	16(1)	15(1)	19(1)	2(1)	2(1)	-5(1)
C(8)	17(1)	15(1)	18(1)	2(1)	1(1)	-1(1)
C(9)	16(1)	16(1)	18(1)	1(1)	1(1)	0(1)
C(10)	20(1)	15(1)	22(1)	1(1)	3(1)	0(1)
C(11)	22(1)	16(1)	31(1)	1(1)	5(1)	1(1)
C(12)	28(1)	17(1)	32(1)	-3(1)	10(1)	2(1)
C(13)	26(1)	21(1)	22(1)	-1(1)	7(1)	1(1)
C(14)	19(1)	18(1)	17(1)	-1(1)	2(1)	0(1)
C(15)	20(1)	19(1)	16(1)	2(1)	3(1)	0(1)
C(16)	18(1)	19(1)	16(1)	2(1)	1(1)	0(1)
C(17)	19(1)	17(1)	14(1)	2(1)	-2(1)	0(1)
C(18)	20(1)	22(1)	18(1)	2(1)	-2(1)	0(1)
C(19)	25(1)	26(1)	20(1)	7(1)	-4(1)	-8(1)
C(20)	34(1)	18(1)	22(1)	4(1)	-9(1)	-5(1)
C(21)	30(1)	19(1)	19(1)	-2(1)	-6(1)	2(1)
C(22)	23(1)	20(1)	16(1)	0(1)	-2(1)	-1(1)
O(1A)	22(1)	22(1)	20(1)	-3(1)	1(1)	-4(1)
O(2A)	27(1)	14(1)	17(1)	0(1)	8(1)	2(1)
C(1A)	19(1)	18(1)	17(1)	0(1)	2(1)	3(1)
C(2A)	19(1)	18(1)	24(1)	1(1)	1(1)	0(1)
C(3A)	24(1)	22(1)	26(1)	7(1)	4(1)	-1(1)
C(4A)	30(1)	31(1)	19(1)	7(1)	2(1)	-4(1)
C(5A)	23(1)	24(1)	19(1)	1(1)	-1(1)	0(1)
C(6A)	16(1)	16(1)	19(1)	0(1)	2(1)	3(1)
C(7A)	15(1)	15(1)	19(1)	-1(1)	2(1)	4(1)
C(8A)	18(1)	14(1)	18(1)	-1(1)	3(1)	1(1)
C(9A)	16(1)	16(1)	17(1)	0(1)	1(1)	1(1)
C(10A)	20(1)	16(1)	21(1)	-1(1)	3(1)	1(1)
C(11A)	21(1)	15(1)	26(1)	-1(1)	3(1)	-1(1)
C(12A)	26(1)	17(1)	25(1)	3(1)	5(1)	-3(1)
C(13A)	24(1)	18(1)	19(1)	0(1)	5(1)	-4(1)
C(14A)	19(1)	16(1)	16(1)	2(1)	2(1)	0(1)
C(15A)	20(1)	17(1)	16(1)	-1(1)	4(1)	0(1)
C(16A)	16(1)	18(1)	16(1)	-2(1)	2(1)	0(1)
C(17A)	19(1)	16(1)	14(1)	-1(1)	-1(1)	0(1)
C(18A)	21(1)	19(1)	16(1)	2(1)	0(1)	0(1)
C(19A)	25(1)	18(1)	21(1)	3(1)	-3(1)	-3(1)
C(20A)	32(1)	18(1)	23(1)	-2(1)	-3(1)	2(1)
C(21A)	27(1)	23(1)	20(1)	-4(1)	2(1)	5(1)
C(22A)	20(1)	21(1)	18(1)	-1(1)	2(1)	0(1)

Table C-5. Hydrogen coordinates ($\times 10^4$) and isotropic displacement parameters ($\text{\AA}^2 \times 10^3$) for yoon15.

x	y	z	U(eq)	
H(1)	9973(17)	7457(9)	2739(9)	23
H(2)	11398(19)	6671(10)	2135(9)	27
H(3)	11037(18)	6573(10)	917(9)	31
H(4)	9224(19)	7306(10)	299(10)	31
H(5)	7809(19)	8086(10)	867(9)	27
H(8)	8956(18)	8427(9)	3190(8)	20
H(9)	6111(18)	8841(9)	3081(8)	20
H(10B)	8467(19)	9789(9)	3390(9)	23
H(10A)	7509(18)	9812(9)	2661(9)	23
H(11A)	5540(20)	10173(10)	3221(9)	27
H(11B)	6779(18)	10768(10)	3407(9)	27
H(12B)	7420(20)	10232(10)	4505(9)	30
H(12A)	5789(19)	10438(11)	4424(9)	30
H(13A)	5158(19)	9189(10)	4184(9)	27
H(13B)	6199(18)	9201(10)	4878(9)	27
H(14)	8113(18)	8938(9)	4283(8)	22
H(15)	6687(18)	7843(9)	4644(9)	22
H(18)	5283(19)	6742(10)	4409(9)	25
H(19)	5057(19)	5479(10)	4574(9)	29
H(20)	6519(18)	4615(10)	4135(9)	31
H(21)	8296(19)	5071(10)	3487(9)	28
H(22)	8552(18)	6332(9)	3317(9)	24
H(1A)	4886(17)	5958(9)	2747(9)	22
H(2A)	6358(19)	6731(10)	2185(9)	24
H(3A)	6177(18)	6762(10)	984(9)	29
H(4A)	4497(19)	5995(10)	329(10)	32
H(5A)	2953(19)	5235(10)	881(9)	26
H(8A)	3904(18)	4984(9)	3192(9)	20
H(9A)	1018(18)	4552(9)	3064(8)	19
H(10D)	3397(18)	3618(9)	3397(9)	23
H(10C)	2490(18)	3591(9)	2658(9)	23
H(11D)	483(19)	3206(9)	3164(9)	25
H(11C)	1695(18)	2634(10)	3356(9)	25
H(12D)	2269(19)	3145(10)	4460(9)	27
H(12C)	634(19)	2951(10)	4365(9)	27
H(13C)	45(18)	4207(10)	4155(9)	24
H(13D)	1052(18)	4172(10)	4838(9)	24
H(14A)	2989(17)	4458(9)	4271(8)	21
H(15A)	1562(17)	5533(9)	4637(9)	21
H(18A)	3463(18)	7055(9)	3302(9)	23
H(19A)	3340(18)	8315(10)	3530(9)	26
H(20A)	1723(19)	8776(11)	4257(9)	30
H(21A)	222(19)	7923(10)	4723(9)	28
H(22A)	332(18)	6659(10)	4484(9)	24

Table C-6. Torsion angles [°] for yoon15.

C(6)-C(1)-C(2)-C(3)	-0.3(2)	C(6A)-C(1A)-C(2A)-C(3A)	-0.6(2)
C(1)-C(2)-C(3)-C(4)	0.0(2)	C(1A)-C(2A)-C(3A)-C(4A)	-0.3(2)
C(2)-C(3)-C(4)-C(5)	0.3(2)	C(2A)-C(3A)-C(4A)-C(5A)	1.1(2)
C(3)-C(4)-C(5)-C(6)	-0.3(2)	C(3A)-C(4A)-C(5A)-C(6A)	-1.0(2)
C(2)-C(1)-C(6)-C(5)	0.3(2)	C(4A)-C(5A)-C(6A)-C(1A)	0.1(2)
C(2)-C(1)-C(6)-C(7)	-179.13(12)	C(4A)-C(5A)-C(6A)-C(7A)	-178.79(13)
C(4)-C(5)-C(6)-C(1)	0.0(2)	C(2A)-C(1A)-C(6A)-C(5A)	0.7(2)
C(4)-C(5)-C(6)-C(7)	179.43(13)	C(2A)-C(1A)-C(6A)-C(7A)	179.51(12)
C(1)-C(6)-C(7)-O(1)	174.78(13)	C(5A)-C(6A)-C(7A)-O(1A)	0.27(19)
C(5)-C(6)-C(7)-O(1)	-4.63(19)	C(1A)-C(6A)-C(7A)-O(1A)	-178.55(13)
C(1)-C(6)-C(7)-C(8)	-7.08(18)	C(5A)-C(6A)-C(7A)-C(8A)	-178.68(11)
C(5)-C(6)-C(7)-C(8)	173.52(12)	C(1A)-C(6A)-C(7A)-C(8A)	2.51(18)
C(16)-O(2)-C(8)-C(9)	-36.52(15)	C(16A)-O(2A)-C(8A)-C(9A)	37.74(15)
C(16)-O(2)-C(8)-C(7)	-159.56(10)	C(16A)-O(2A)-C(8A)-C(7A)	161.04(10)
O(1)-C(7)-C(8)-O(2)	116.84(13)	O(1A)-C(7A)-C(8A)-O(2A)	-115.56(13)
C(6)-C(7)-C(8)-O(2)	-61.31(14)	C(6A)-C(7A)-C(8A)-O(2A)	63.39(13)
O(1)-C(7)-C(8)-C(9)	-5.01(17)	O(1A)-C(7A)-C(8A)-C(9A)	6.69(17)
C(6)-C(7)-C(8)-C(9)	176.83(11)	C(6A)-C(7A)-C(8A)-C(9A)	-174.36(11)
O(2)-C(8)-C(9)-C(10)	178.42(10)	O(2A)-C(8A)-C(9A)-C(10A)	-178.15(10)
C(7)-C(8)-C(9)-C(10)	-65.65(14)	C(7A)-C(8A)-C(9A)-C(10A)	65.44(14)
O(2)-C(8)-C(9)-C(14)	57.08(14)	O(2A)-C(8A)-C(9A)-C(14A)	-57.06(14)
C(7)-C(8)-C(9)-C(14)	173.01(10)	C(7A)-C(8A)-C(9A)-C(14A)	-173.47(10)
C(8)-C(9)-C(10)-C(11)	179.08(11)	C(8A)-C(9A)-C(10A)-C(11A)	-178.41(11)
C(14)-C(9)-C(10)-C(11)	-59.69(14)	C(14A)-C(9A)-C(10A)-C(11A)	60.68(14)
C(9)-C(10)-C(11)-C(12)	56.88(15)	C(9A)-C(10A)-C(11A)-C(12A)	-56.61(15)
C(10)-C(11)-C(12)-C(13)	-54.10(16)	C(10A)-C(11A)-C(12A)-C(13A)	53.11(16)
C(11)-C(12)-C(13)-C(14)	54.40(16)	C(11A)-C(12A)-C(13A)-C(14A)	-53.27(16)
C(12)-C(13)-C(14)-C(15)	176.99(12)	C(12A)-C(13A)-C(14A)-C(15A)	-177.28(11)
C(12)-C(13)-C(14)-C(9)	-58.29(15)	C(12A)-C(13A)-C(14A)-C(9A)	57.73(15)
C(8)-C(9)-C(14)-C(15)	-48.12(14)	C(8A)-C(9A)-C(14A)-C(15A)	47.46(14)
C(10)-C(9)-C(14)-C(15)	-172.39(11)	C(10A)-C(9A)-C(14A)-C(15A)	171.25(11)
C(8)-C(9)-C(14)-C(13)	-174.92(11)	C(8A)-C(9A)-C(14A)-C(13A)	174.42(11)
C(10)-C(9)-C(14)-C(13)	60.81(14)	C(10A)-C(9A)-C(14A)-C(13A)	-61.80(14)
C(13)-C(14)-C(15)-C(16)	146.18(14)	C(13A)-C(14A)-C(15A)-C(16A)	-146.33(13)
C(9)-C(14)-C(15)-C(16)	21.43(18)	C(9A)-C(14A)-C(15A)-C(16A)	-21.50(18)
C(14)-C(15)-C(16)-O(2)	0.9(2)	C(14A)-C(15A)-C(16A)-O(2A)	0.5(2)
C(14)-C(15)-C(16)-C(17)	179.90(12)	C(14A)-C(15A)-C(16A)-C(17A)	-177.56(12)
C(8)-O(2)-C(16)-C(15)	6.61(18)	C(8A)-O(2A)-C(16A)-C(15A)	-8.50(18)
C(8)-O(2)-C(16)-C(17)	-172.57(10)	C(8A)-O(2A)-C(16A)-C(17A)	169.78(10)
C(15)-C(16)-C(17)-C(22)	-146.37(14)	C(15A)-C(16A)-C(17A)-C(18A)	148.82(14)
O(2)-C(16)-C(17)-C(22)	32.78(16)	O(2A)-C(16A)-C(17A)-C(18A)	-29.42(16)
C(15)-C(16)-C(17)-C(18)	33.3(2)	C(15A)-C(16A)-C(17A)-C(22A)	-30.3(2)
O(2)-C(16)-C(17)-C(18)	-147.52(12)	O(2A)-C(16A)-C(17A)-C(22A)	151.49(12)
C(22)-C(17)-C(18)-C(19)	-0.44(19)	C(22A)-C(17A)-C(18A)-C(19A)	1.74(19)
C(16)-C(17)-C(18)-C(19)	179.85(12)	C(16A)-C(17A)-C(18A)-C(19A)	-177.37(12)
C(17)-C(18)-C(19)-C(20)	1.3(2)	C(17A)-C(18A)-C(19A)-C(20A)	-1.6(2)
C(18)-C(19)-C(20)-C(21)	-0.7(2)	C(18A)-C(19A)-C(20A)-C(21A)	0.5(2)
C(19)-C(20)-C(21)-C(22)	-0.8(2)	C(19A)-C(20A)-C(21A)-C(22A)	0.6(2)
C(20)-C(21)-C(22)-C(17)	1.7(2)	C(20A)-C(21A)-C(22A)-C(17A)	-0.4(2)
C(18)-C(17)-C(22)-C(21)	-1.06(19)	C(18A)-C(17A)-C(22A)-C(21A)	-0.72(19)
C(16)-C(17)-C(22)-C(21)	178.65(12)	C(16A)-C(17A)-C(22A)-C(21A)	178.38(12)

Symmetry transformations used to generate equivalent atoms:

C.2 Characterization of C.1 (Yoon27)

Data Collection

A colorless crystal with approximate dimensions $0.68 \times 0.51 \times 0.48 \text{ mm}^3$ was selected under oil under ambient conditions and attached to the tip of a MiTeGen MicroMount©. The crystal was mounted in a stream of cold nitrogen at 100(1) K and centered in the X-ray beam by using a video camera.

The crystal evaluation and data collection were performed on a Bruker SMART APEXII diffractometer with Cu K_α ($\lambda = 1.54178 \text{ \AA}$) radiation and the diffractometer to crystal distance of 4.02 cm.

The initial cell constants were obtained from three series of ω scans at different starting angles. Each series consisted of 41 frames collected at intervals of 0.6° in a 25° range about ω with the exposure time of 2 seconds per frame. The reflections were successfully indexed by an automated indexing routine built in the APEXII program. The final cell constants were calculated from a set of 9982 strong reflections from the actual data collection.

The data were collected by using the full sphere data collection routine to survey the reciprocal space to the extent of a full sphere to a resolution of 0.81 \AA . A total of 26521 data were harvested by collecting 27 sets of frames with 0.7° scans in ω with an exposure time 3-7 sec per frame. These highly redundant datasets were corrected for Lorentz and polarization effects. The absorption correction was based on fitting a function to the empirical transmission surface as sampled by multiple equivalent measurements. [1]

Structure Solution and Refinement

The systematic absences in the diffraction data were consistent for the space groups *Ia* and *I2/a*. The *E*-statistics suggested the non-centrosymmetric space group *Ia* that yielded chemically reasonable and computationally stable results of refinement [2-4].

A successful solution by the direct methods provided most non-hydrogen atoms from the *E*-map. The remaining non-hydrogen atoms were located in an alternating series of least-squares cycles and difference Fourier maps. All non-hydrogen atoms were refined with anisotropic displacement coefficients. All hydrogen atoms were included in the structure factor calculation at idealized positions and were allowed to ride on the neighboring atoms with relative isotropic displacement coefficients.

The final least-squares refinement of 318 parameters against 4270 data resulted in residuals *R* (based on F^2 for $I \geq 2\sigma$) and *wR* (based on F^2 for all data) of 0.0284 and 0.0759, respectively. The final difference Fourier map was featureless.

The molecular diagram is drawn with 50% probability ellipsoids.

References

- [1] Bruker-AXS. (2007) APEX2, SADABS, and SAINT Software Reference Manuals. Bruker-AXS, Madison, Wisconsin, USA.
- [2] Sheldrick, G. M. (2008) SHELXL. *Acta Cryst.* **A64**, 112-122.
- [3] Dolomanov, O.V.; Bourhis, L.J.; Gildea, R.J.; Howard, J.A.K.; Puschmann, H. "OLEX2: a complete structure solution, refinement and analysis program". *J. Appl. Cryst.* (2009) **42**, 339-341.
- [4] Guzei, I.A. (2006-2008). Internal laboratory computer programs "Inserter", "FCF_filter", "Modicifer".

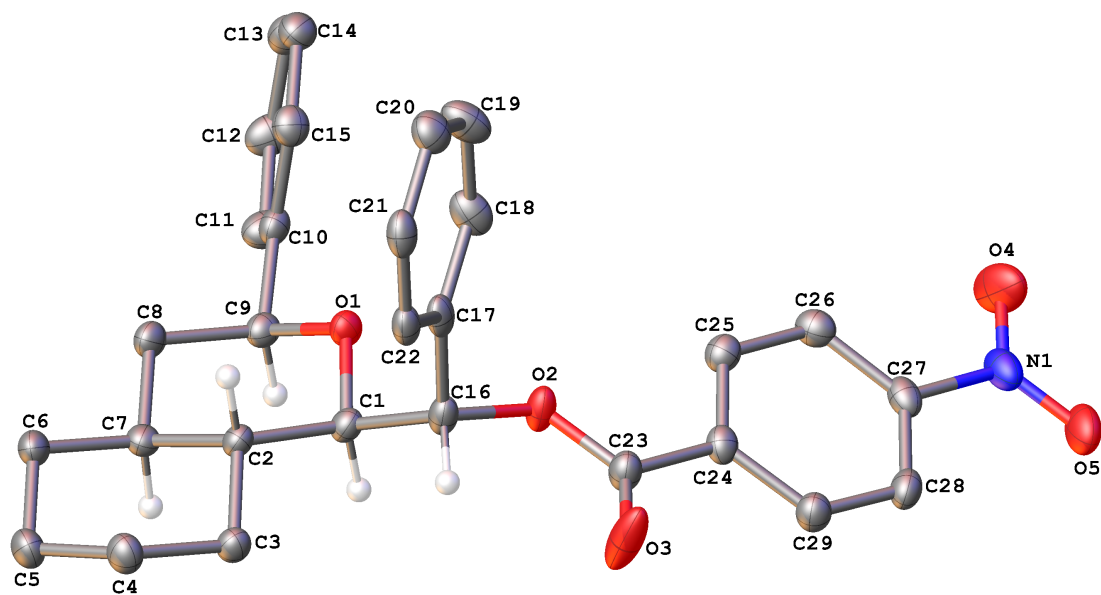


Figure C-3. A molecular drawing of Yoon27. The H atoms on the non- chiral C atoms are omitted.

Table C-7. Crystal data and structure refinement for yoon27.

Identification code	yoona27	
Empirical formula	C ₂₉ H ₂₉ N O ₅	
Formula weight	471.53	
Temperature	100(2) K	
Wavelength	1.54178 Å	
Crystal system	Monoclinic	
Space group	Ia	
Unit cell dimensions	a = 8.7727(2) Å	$\alpha = 90^\circ$.
	b = 27.9624(7) Å	$\beta = 91.8390(10)^\circ$.
	c = 9.8321(4) Å	$\gamma = 90^\circ$.
Volume	2410.63(13) Å ³	
Z	4	
Density (calculated)	1.299 Mg/m ³	
Absorption coefficient	0.717 mm ⁻¹	
F(000)	1000	
Crystal size	0.68 x 0.51 x 0.48 mm ³	
Theta range for data collection	3.16 to 71.67°.	
Index ranges	-10 ≤ h ≤ 10, -34 ≤ k ≤ 33, -11 ≤ l ≤ 12	
Reflections collected	26521	
Independent reflections	4270 [R(int) = 0.0237]	
Completeness to theta = 67.00°	99.8 %	
Absorption correction	Numerical with SADABS	
Max. and min. transmission	0.7257 and 0.6426	
Refinement method	Full-matrix least-squares on F ²	
Data / restraints / parameters	4270 / 2 / 318	
Goodness-of-fit on F ²	1.051	
Final R indices [I > 2σ(I)]	R1 = 0.0284, wR2 = 0.0758	
R indices (all data)	R1 = 0.0285, wR2 = 0.0759	
Absolute structure parameter Flack x	-0.08(12)	
Absolute structure parameter Hoof y	-0.02(3)	
Extinction coefficient	0.00075(10)	
Largest diff. peak and hole	0.193 and -0.182 e.Å ⁻³	

Table C-8. Atomic coordinates ($\times 10^4$) and equivalent isotropic displacement parameters ($\text{\AA}^2 \times 10^3$) for yoon27. U(eq) is defined as one third of the trace of the orthogonalized U^{ij} tensor.

x	y	z	U(eq)	
O(1)	8132(1)	3644(1)	5502(1)	20(1)
O(2)	5462(1)	3717(1)	6859(1)	25(1)
O(3)	3763(2)	3352(1)	8160(2)	52(1)
O(4)	3220(2)	5917(1)	8909(1)	50(1)
O(5)	1843(1)	5608(1)	10463(1)	37(1)
N(1)	2716(2)	5577(1)	9520(1)	29(1)
C(1)	7593(2)	3241(1)	6234(1)	20(1)
C(2)	8181(2)	2771(1)	5646(1)	18(1)
C(3)	7660(2)	2327(1)	6418(1)	22(1)
C(4)	8235(2)	1870(1)	5750(2)	25(1)
C(5)	9968(2)	1874(1)	5641(2)	27(1)
C(6)	10521(2)	2327(1)	4942(1)	24(1)
C(7)	9934(2)	2782(1)	5616(1)	20(1)
C(8)	10461(2)	3235(1)	4911(1)	22(1)
C(9)	9760(1)	3679(1)	5545(1)	20(1)
C(10)	10176(2)	4130(1)	4798(1)	21(1)
C(11)	11327(2)	4427(1)	5318(1)	28(1)
C(12)	11771(2)	4833(1)	4619(2)	31(1)
C(13)	11049(2)	4950(1)	3387(2)	28(1)
C(14)	9902(2)	4657(1)	2868(2)	26(1)
C(15)	9466(2)	4248(1)	3558(1)	24(1)
C(16)	5853(2)	3270(1)	6182(1)	21(1)
C(17)	5133(1)	3274(1)	4767(2)	22(1)
C(18)	5099(2)	3691(1)	3980(2)	28(1)
C(19)	4467(2)	3687(1)	2674(2)	33(1)
C(20)	3840(2)	3270(1)	2130(2)	28(1)
C(21)	3849(2)	2856(1)	2902(2)	25(1)
C(22)	4500(2)	2858(1)	4210(1)	22(1)
C(23)	4385(2)	3705(1)	7768(1)	23(1)
C(24)	4007(2)	4201(1)	8240(1)	20(1)
C(25)	4558(2)	4603(1)	7582(1)	22(1)
C(26)	4130(2)	5055(1)	7999(2)	24(1)
C(27)	3175(2)	5092(1)	9083(1)	23(1)
C(28)	2618(2)	4700(1)	9764(1)	24(1)
C(29)	3035(2)	4249(1)	9325(1)	24(1)

Table C-9. Bond lengths [Å] and angles [°] for yoon27.

O(1)-C(1)	1.4258(15)	C(10)-C(11)	1.3918(19)
O(1)-C(9)	1.4315(15)	C(11)-C(12)	1.389(2)
O(2)-C(23)	1.3216(17)	C(11)-H(11)	0.9500
O(2)-C(16)	1.4603(15)	C(12)-C(13)	1.387(2)
O(3)-C(23)	1.1976(18)	C(12)-H(12)	0.9500
O(4)-N(1)	1.2159(19)	C(13)-C(14)	1.381(2)
O(5)-N(1)	1.2250(18)	C(13)-H(13)	0.9500
N(1)-C(27)	1.4821(16)	C(14)-C(15)	1.3899(19)
C(1)-C(16)	1.5275(19)	C(14)-H(14)	0.9500
C(1)-C(2)	1.5311(17)	C(15)-H(15)	0.9500
C(1)-H(1)	1.0000	C(16)-C(17)	1.5100(19)
C(2)-C(3)	1.5337(17)	C(16)-H(16)	1.0000
C(2)-C(7)	1.5398(17)	C(17)-C(22)	1.3931(19)
C(2)-H(2)	1.0000	C(17)-C(18)	1.3990(19)
C(3)-C(4)	1.5288(18)	C(18)-C(19)	1.382(2)
C(3)-H(3A)	0.9900	C(18)-H(18)	0.9500
C(3)-H(3B)	0.9900	C(19)-C(20)	1.388(2)
C(4)-C(5)	1.527(2)	C(19)-H(19)	0.9500
C(4)-H(4A)	0.9900	C(20)-C(21)	1.385(2)
C(4)-H(4B)	0.9900	C(20)-H(20)	0.9500
C(5)-C(6)	1.5283(19)	C(21)-C(22)	1.391(2)
C(5)-H(5A)	0.9900	C(21)-H(21)	0.9500
C(5)-H(5B)	0.9900	C(22)-H(22)	0.9500
C(6)-C(7)	1.5301(18)	C(23)-C(24)	1.5009(18)
C(6)-H(6A)	0.9900	C(24)-C(25)	1.3913(19)
C(6)-H(6B)	0.9900	C(24)-C(29)	1.394(2)
C(7)-C(8)	1.5231(18)	C(25)-C(26)	1.3855(18)
C(7)-H(7)	1.0000	C(25)-H(25)	0.9500
C(8)-C(9)	1.5272(18)	C(26)-C(27)	1.380(2)
C(8)-H(8A)	0.9900	C(26)-H(26)	0.9500
C(8)-H(8B)	0.9900	C(27)-C(28)	1.383(2)
C(9)-C(10)	1.5098(17)	C(28)-C(29)	1.3843(19)
C(9)-H(9)	1.0000	C(28)-H(28)	0.9500
C(10)-C(15)	1.3902(19)	C(29)-H(29)	0.9500
C(1)-O(1)-C(9)	112.77(10)	C(2)-C(3)-H(3A)	109.5
C(23)-O(2)-C(16)	118.11(10)	C(4)-C(3)-H(3B)	109.5
O(4)-N(1)-O(5)	124.42(12)	C(2)-C(3)-H(3B)	109.5
O(4)-N(1)-C(27)	117.78(13)	H(3A)-C(3)-H(3B)	108.0
O(5)-N(1)-C(27)	117.80(12)	C(5)-C(4)-C(3)	111.51(12)
O(1)-C(1)-C(16)	106.73(10)	C(5)-C(4)-H(4A)	109.3
O(1)-C(1)-C(2)	111.48(10)	C(3)-C(4)-H(4A)	109.3
C(16)-C(1)-C(2)	112.45(10)	C(5)-C(4)-H(4B)	109.3
O(1)-C(1)-H(1)	108.7	C(3)-C(4)-H(4B)	109.3
C(16)-C(1)-H(1)	108.7	H(4A)-C(4)-H(4B)	108.0
C(2)-C(1)-H(1)	108.7	C(4)-C(5)-C(6)	111.69(11)
C(1)-C(2)-C(3)	113.53(10)	C(4)-C(5)-H(5A)	109.3
C(1)-C(2)-C(7)	109.85(10)	C(6)-C(5)-H(5A)	109.3
C(3)-C(2)-C(7)	109.83(10)	C(4)-C(5)-H(5B)	109.3
C(1)-C(2)-H(2)	107.8	C(6)-C(5)-H(5B)	109.3
C(3)-C(2)-H(2)	107.8	H(5A)-C(5)-H(5B)	107.9
C(7)-C(2)-H(2)	107.8	C(5)-C(6)-C(7)	112.23(11)
C(4)-C(3)-C(2)	110.93(11)	C(5)-C(6)-H(6A)	109.2
C(4)-C(3)-H(3A)	109.5	C(7)-C(6)-H(6A)	109.2

C(5)-C(6)-H(6B)	109.2	O(2)-C(16)-H(16)	109.1
C(7)-C(6)-H(6B)	109.2	C(17)-C(16)-H(16)	109.1
H(6A)-C(6)-H(6B)	107.9	C(1)-C(16)-H(16)	109.1
C(8)-C(7)-C(6)	112.54(10)	C(22)-C(17)-C(18)	118.52(13)
C(8)-C(7)-C(2)	110.07(10)	C(22)-C(17)-C(16)	120.37(12)
C(6)-C(7)-C(2)	110.05(10)	C(18)-C(17)-C(16)	121.11(12)
C(8)-C(7)-H(7)	108.0	C(19)-C(18)-C(17)	120.50(13)
C(6)-C(7)-H(7)	108.0	C(19)-C(18)-H(18)	119.7
C(2)-C(7)-H(7)	108.0	C(17)-C(18)-H(18)	119.7
C(7)-C(8)-C(9)	111.04(11)	C(18)-C(19)-C(20)	120.48(13)
C(7)-C(8)-H(8A)	109.4	C(18)-C(19)-H(19)	119.8
C(9)-C(8)-H(8A)	109.4	C(20)-C(19)-H(19)	119.8
C(7)-C(8)-H(8B)	109.4	C(21)-C(20)-C(19)	119.70(14)
C(9)-C(8)-H(8B)	109.4	C(21)-C(20)-H(20)	120.2
H(8A)-C(8)-H(8B)	108.0	C(19)-C(20)-H(20)	120.2
O(1)-C(9)-C(10)	107.46(10)	C(20)-C(21)-C(22)	119.90(13)
O(1)-C(9)-C(8)	110.27(10)	C(20)-C(21)-H(21)	120.1
C(10)-C(9)-C(8)	111.97(10)	C(22)-C(21)-H(21)	120.1
O(1)-C(9)-H(9)	109.0	C(21)-C(22)-C(17)	120.90(13)
C(10)-C(9)-H(9)	109.0	C(21)-C(22)-H(22)	119.6
C(8)-C(9)-H(9)	109.0	C(17)-C(22)-H(22)	119.6
C(15)-C(10)-C(11)	118.68(12)	O(3)-C(23)-O(2)	125.46(12)
C(15)-C(10)-C(9)	121.07(11)	O(3)-C(23)-C(24)	123.61(13)
C(11)-C(10)-C(9)	120.21(12)	O(2)-C(23)-C(24)	110.92(11)
C(12)-C(11)-C(10)	121.14(12)	C(25)-C(24)-C(29)	120.44(12)
C(12)-C(11)-H(11)	119.4	C(25)-C(24)-C(23)	121.24(12)
C(10)-C(11)-H(11)	119.4	C(29)-C(24)-C(23)	118.27(12)
C(13)-C(12)-C(11)	119.77(13)	C(26)-C(25)-C(24)	119.95(13)
C(13)-C(12)-H(12)	120.1	C(26)-C(25)-H(25)	120.0
C(11)-C(12)-H(12)	120.1	C(24)-C(25)-H(25)	120.0
C(14)-C(13)-C(12)	119.34(13)	C(27)-C(26)-C(25)	118.26(13)
C(14)-C(13)-H(13)	120.3	C(27)-C(26)-H(26)	120.9
C(12)-C(13)-H(13)	120.3	C(25)-C(26)-H(26)	120.9
C(13)-C(14)-C(15)	121.02(13)	C(26)-C(27)-C(28)	123.17(12)
C(13)-C(14)-H(14)	119.5	C(26)-C(27)-N(1)	118.00(12)
C(15)-C(14)-H(14)	119.5	C(28)-C(27)-N(1)	118.82(12)
C(14)-C(15)-C(10)	120.04(12)	C(27)-C(28)-C(29)	118.03(13)
C(14)-C(15)-H(15)	120.0	C(27)-C(28)-H(28)	121.0
C(10)-C(15)-H(15)	120.0	C(29)-C(28)-H(28)	121.0
O(2)-C(16)-C(17)	108.45(10)	C(28)-C(29)-C(24)	120.13(13)
O(2)-C(16)-C(1)	106.24(10)	C(28)-C(29)-H(29)	119.9
C(17)-C(16)-C(1)	114.76(11)	C(24)-C(29)-H(29)	119.9

Symmetry transformations used to generate equivalent atoms:

Table C-10. Anisotropic displacement parameters ($\text{\AA}^2 \times 10^3$) for yoon27. The anisotropic displacement factor exponent takes the form: $-2p^2 [h^2 a^{*2} U^{11} + \dots + 2h k a^* b^* U^{12}]$

	U^{11}	U^{22}	U^{33}	U^{23}	U^{13}	U^{12}
O(1)	17(1)	20(1)	24(1)	2(1)	4(1)	0(1)
O(2)	24(1)	18(1)	34(1)	-4(1)	13(1)	0(1)
O(3)	71(1)	21(1)	68(1)	-6(1)	52(1)	-6(1)
O(4)	85(1)	21(1)	45(1)	-2(1)	15(1)	7(1)
O(5)	44(1)	34(1)	33(1)	-10(1)	3(1)	15(1)
N(1)	38(1)	24(1)	25(1)	-6(1)	-5(1)	10(1)
C(1)	21(1)	20(1)	18(1)	-1(1)	4(1)	0(1)
C(2)	18(1)	20(1)	16(1)	0(1)	4(1)	1(1)
C(3)	22(1)	21(1)	22(1)	2(1)	5(1)	1(1)
C(4)	26(1)	21(1)	30(1)	0(1)	3(1)	2(1)
C(5)	27(1)	24(1)	30(1)	2(1)	4(1)	8(1)
C(6)	21(1)	26(1)	23(1)	3(1)	4(1)	7(1)
C(7)	20(1)	24(1)	18(1)	2(1)	0(1)	3(1)
C(8)	17(1)	26(1)	23(1)	2(1)	4(1)	2(1)
C(9)	17(1)	25(1)	19(1)	1(1)	1(1)	0(1)
C(10)	17(1)	24(1)	21(1)	-2(1)	4(1)	1(1)
C(11)	26(1)	35(1)	23(1)	2(1)	-2(1)	-5(1)
C(12)	29(1)	36(1)	28(1)	0(1)	0(1)	-13(1)
C(13)	29(1)	25(1)	30(1)	3(1)	8(1)	-1(1)
C(14)	24(1)	30(1)	25(1)	3(1)	1(1)	3(1)
C(15)	19(1)	26(1)	27(1)	-2(1)	0(1)	-1(1)
C(16)	20(1)	16(1)	27(1)	-1(1)	9(1)	0(1)
C(17)	13(1)	21(1)	32(1)	0(1)	7(1)	2(1)
C(18)	25(1)	20(1)	40(1)	1(1)	-3(1)	-3(1)
C(19)	30(1)	26(1)	44(1)	10(1)	-6(1)	-3(1)
C(20)	22(1)	31(1)	32(1)	1(1)	-1(1)	2(1)
C(21)	16(1)	22(1)	37(1)	-6(1)	5(1)	1(1)
C(22)	17(1)	19(1)	30(1)	0(1)	8(1)	3(1)
C(23)	23(1)	21(1)	27(1)	-2(1)	6(1)	1(1)
C(24)	17(1)	22(1)	23(1)	-4(1)	0(1)	2(1)
C(25)	21(1)	24(1)	21(1)	-3(1)	1(1)	-1(1)
C(26)	27(1)	21(1)	24(1)	0(1)	-2(1)	-1(1)
C(27)	23(1)	22(1)	24(1)	-5(1)	-6(1)	6(1)
C(28)	22(1)	29(1)	22(1)	-4(1)	3(1)	5(1)
C(29)	23(1)	22(1)	26(1)	0(1)	4(1)	1(1)

Table C-11. Hydrogen coordinates ($\times 10^4$) and isotropic displacement parameters ($\text{\AA}^2 \times 10^3$) for yoon27.

	x	y	z	U(eq)
H(1)	7962	3267	7204	23
H(2)	7778	2745	4686	22
H(3A)	8054	2342	7372	26
H(3B)	6532	2320	6428	26
H(4A)	7930	1590	6294	30
H(4B)	7755	1838	4830	30
H(5A)	10288	1591	5118	32
H(5B)	10448	1852	6564	32
H(6A)	10173	2323	3975	28
H(6B)	11650	2331	4973	28
H(7)	10342	2789	6577	25
H(8A)	10162	3220	3932	26
H(8B)	11587	3257	4988	26
H(9)	10131	3706	6514	24
H(11)	11817	4351	6166	34
H(12)	12566	5030	4983	37
H(13)	11340	5228	2905	33
H(14)	9405	4737	2026	31
H(15)	8682	4049	3183	29
H(16)	5432	2996	6703	25
H(18)	5514	3979	4346	34
H(19)	4461	3972	2146	40
H(20)	3408	3270	1231	34
H(21)	3411	2571	2538	30
H(22)	4512	2572	4732	26
H(25)	5226	4567	6848	26
H(26)	4485	5333	7551	29
H(28)	1969	4738	10511	29
H(29)	2657	3973	9764	29

Table C-12. Torsion angles [°] for yoon27.

C(9)-O(1)-C(1)-C(16)	176.13(10)	O(1)-C(1)-C(16)-O(2)	-61.44(12)
C(9)-O(1)-C(1)-C(2)	-60.72(13)	C(2)-C(1)-C(16)-O(2)	176.02(10)
O(1)-C(1)-C(2)-C(3)	178.77(10)	O(1)-C(1)-C(16)-C(17)	58.38(13)
C(16)-C(1)-C(2)-C(3)	-61.41(14)	C(2)-C(1)-C(16)-C(17)	-64.16(14)
O(1)-C(1)-C(2)-C(7)	55.36(13)	O(2)-C(16)-C(17)-C(22)	-140.96(12)
C(16)-C(1)-C(2)-C(7)	175.19(10)	C(1)-C(16)-C(17)-C(22)	100.46(14)
C(1)-C(2)-C(3)-C(4)	177.91(10)	O(2)-C(16)-C(17)-C(18)	39.67(17)
C(7)-C(2)-C(3)-C(4)	-58.67(14)	C(1)-C(16)-C(17)-C(18)	-78.92(16)
C(2)-C(3)-C(4)-C(5)	56.08(15)	C(22)-C(17)-C(18)-C(19)	-0.8(2)
C(3)-C(4)-C(5)-C(6)	-52.91(15)	C(16)-C(17)-C(18)-C(19)	178.57(14)
C(4)-C(5)-C(6)-C(7)	53.33(15)	C(17)-C(18)-C(19)-C(20)	0.7(2)
C(5)-C(6)-C(7)-C(8)	-179.10(11)	C(18)-C(19)-C(20)-C(21)	0.1(2)
C(5)-C(6)-C(7)-C(2)	-55.94(13)	C(19)-C(20)-C(21)-C(22)	-0.7(2)
C(1)-C(2)-C(7)-C(8)	-51.69(13)	C(20)-C(21)-C(22)-C(17)	0.7(2)
C(3)-C(2)-C(7)-C(8)	-177.24(10)	C(18)-C(17)-C(22)-C(21)	0.12(19)
C(1)-C(2)-C(7)-C(6)	-176.28(10)	C(16)-C(17)-C(22)-C(21)	-179.27(12)
C(3)-C(2)-C(7)-C(6)	58.17(13)	C(16)-O(2)-C(23)-O(3)	5.4(2)
C(6)-C(7)-C(8)-C(9)	175.88(10)	C(16)-O(2)-C(23)-C(24)	-173.47(10)
C(2)-C(7)-C(8)-C(9)	52.73(13)	O(3)-C(23)-C(24)-C(25)	-168.25(15)
C(1)-O(1)-C(9)-C(10)	-177.25(10)	O(2)-C(23)-C(24)-C(25)	10.62(17)
C(1)-O(1)-C(9)-C(8)	60.46(13)	O(3)-C(23)-C(24)-C(29)	9.2(2)
C(7)-C(8)-C(9)-O(1)	-56.28(13)	O(2)-C(23)-C(24)-C(29)	-171.94(12)
C(7)-C(8)-C(9)-C(10)	-175.88(10)	C(29)-C(24)-C(25)-C(26)	-0.47(18)
O(1)-C(9)-C(10)-C(15)	-44.53(16)	C(23)-C(24)-C(25)-C(26)	176.92(11)
C(8)-C(9)-C(10)-C(15)	76.70(15)	C(24)-C(25)-C(26)-C(27)	0.94(18)
O(1)-C(9)-C(10)-C(11)	137.97(13)	C(25)-C(26)-C(27)-C(28)	-0.45(19)
C(8)-C(9)-C(10)-C(11)	-100.80(15)	C(25)-C(26)-C(27)-N(1)	-179.69(11)
C(15)-C(10)-C(11)-C(12)	-0.3(2)	O(4)-N(1)-C(27)-C(26)	-0.83(19)
C(9)-C(10)-C(11)-C(12)	177.27(13)	O(5)-N(1)-C(27)-C(26)	178.48(12)
C(10)-C(11)-C(12)-C(13)	0.7(2)	O(4)-N(1)-C(27)-C(28)	179.89(13)
C(11)-C(12)-C(13)-C(14)	-0.5(2)	O(5)-N(1)-C(27)-C(28)	-0.79(18)
C(12)-C(13)-C(14)-C(15)	-0.2(2)	C(26)-C(27)-C(28)-C(29)	-0.51(19)
C(13)-C(14)-C(15)-C(10)	0.6(2)	N(1)-C(27)-C(28)-C(29)	178.72(12)
C(11)-C(10)-C(15)-C(14)	-0.4(2)	C(27)-C(28)-C(29)-C(24)	1.0(2)
C(9)-C(10)-C(15)-C(14)	-177.89(12)	C(25)-C(24)-C(29)-C(28)	-0.51(19)
C(23)-O(2)-C(16)-C(17)	102.98(13)	C(23)-C(24)-C(29)-C(28)	-177.98(12)
C(23)-O(2)-C(16)-C(1)	-133.17(12)		

Symmetry transformations used to generate equivalent atoms: